

INFLUENCE OF DURABILITY PROPERTIES ON PERFORMANCE OF BITUMEN STABILIZED MATERIALS

By

ELIAS MATHANIYA TWAGIRA M.Sc. (Eng)



A Dissertation

Presented for the degree of **Doctor of Philosophy (Engineering)** at the
Stellenbosch University, South Africa

Promoter

Professor Kim J. JENKINS Ph.D.
SANRAL Chair of Pavement Engineering

External examiners:
Prof. M. F. C van de Ven
Prof. A. A. A Molenaar

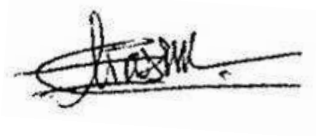
Internal examiner:
Dr. M. de Wet

Stellenbosch University
January 2010

DECLARATION

I, the undersigned, hereby declare that the work contained in this dissertation is my own original work, and that I have not previously in its entirety or in part submitted it at any other University for a degree.

Done at ...Stellenboschon the ...25th January 2010.....

A handwritten signature in black ink, appearing to read 'E.M. Twagira', written over a horizontal line.

Signature.....

Elias M. Twagira

SUMMARY

In both developing and developed countries, to ensure sustained economic growth the quest for optimal roads performance is an extremely high priority. A global increase in the use of foamed bitumen and bitumen emulsion materials (BSMs) as a solution to roads maintenance, rehabilitation, and upgrading has become evident. This is driven by environmental policies aimed at conserving energy and limiting the exploitation of new borrows pits. It has therefore become imperative that BSMs are used optimally, and, in order to achieve this, practitioners need to understand the mechanisms that influence durability and long-term performance.

The changes in the behaviour of materials and the failure mechanisms of BSM mixes are long-term phenomena. This implies that the study of the physicochemical and mechanical properties of the mixes is vital. Therefore, a fundamental understanding of the moisture damage and age-hardening characteristics, which are related to materials' properties, is required. The main objective of this study is to advance BSM technology by assessing the influence of the selected materials on durability behaviour and long-term performance in all phases of application (i.e. mix design, construction, and in-service condition).

This study begins with a comprehensive literature review of research dealing with the interactions of binder and mineral aggregates. The properties of bitumen (foamed bitumen or bitumen emulsion) and mineral aggregates were reviewed. This was followed by review into the colloidal behaviour of foam and emulsion and physicochemical and mechanical interaction with mineral aggregates. Factors influencing the interaction of BSMs were then identified. Finally, the fundamental theories on thermodynamics, hydrodynamics, and electrokinetics were used to describe the step-by-step process by which adhesive bonding and cohesion occur in BSMs.

The mixture durability in terms of moisture damage was investigated. To achieve this aim, the physical and mechanical moisture-induced damage process was analysed. The test control parameters were established and a laboratory device to quantify these parameters designed. New moisture conditioning procedures were developed and demonstrated in this study. From the moisture induction simulation test (MIST) procedure, it became evident that pulsing water pressures into compacted and cured BSM mixes simulates the hydrodynamic effect that occurs in the field due to dynamic traffic loading. The different mix matrices typically applicable to the recycling processes – such as Hornfels-RAP and Quartzite crushed stone, stabilised with either foamed bitumen or bitumen emulsion and the addition of active filler (cement or lime) – were investigated. It was found that a new moisture-conditioning procedure using the MIST device and monotonic triaxial testing can distinguish those BSM mixes that are resistant to moisture damage from those that are less resistant. The validation of the MIST and monotonic test results was done using the APT device, which is the MMLS3 wet trafficking test. The results on both tests showed good correlations in evaluating and screening BSMs in terms of moisture susceptibility.

Field temperature data was collected and a model to accurately simulate the curing of BSMs was identified and proposed for further investigation and validation. It was found from the field temperature data collected in this study that the temperature gradient on the study site varied according to the depth of the BSMs (that is, 10°C-17°C during winter and 17°C– 47°C during summer). Understanding the influence of the temperature conductivity and rate of evaporation is important for inferring moisture damage and age-hardening behaviour and proper selection of BSMs.

The age-hardening behaviour of BSMs is linked to the durability properties and long-term performance of these materials. The fundamental characteristics associated with short- and long-term age hardening were investigated in this study. The short-term dimension involved assessing the age-hardening characteristics of the binder (foamed bitumen colloids and bitumen

emulsion droplets) prior to the production of BSMs. The long-term study involved extracting and recovering the binder from the briquettes (made from different mixes) compacted in the laboratory and cores extracted from different field pavement sections which were in service for 8-10 years. The study found that the length of time bitumen is kept in circulation in the laboratory plant at elevated temperature (170°C–180°C) before making BSM-foam contributes to the ageing of the binder, especially after eight hours. The foaming process in itself was found not to alter the bitumen properties. It is recommended that a temperature range between 160°C-165°C be used for the production of foamed bitumen with softer bitumen. This will not compromise its quality. In addition, the time of circulation of bitumen in laboratory plant should not be longer than three (3) hours.

The rheological properties of the bitumen recovered from laboratory briquettes and cores from field pavement show that age hardening on foamed bitumen and bitumen emulsion during in-service life occurred. The ageing also seemed to be dependent on the effect of traffic, with trafficked areas (i.e. on-wheel path and inner-wheel path) experiencing more ageing than untrafficked areas (i.e. between-wheel path). However, the extraction and recovery process was found to be complex, and produce uncertain results. Although the results show that binders in BSMs undergo age hardening, its distinct behaviour in BSM performance was not obvious from the extensive tests carried out in this study.

The last part of the study contains its conclusions and recommendations. The study provides an insight into fundamental material durability properties, and this will assist in improving the current procedure for selection, combining and formulation of the mix matrices for BSMs. In addition, the study provides guidelines that will enable practitioners to confidently apply a mix that is durable and long-lasting. The specific durability-related issues addressed in this study are substance for future research. This novel solution to the application of BSMs will benefit all parties involved in the development of pavement recycling technology.

OPSOMMING

Om volgehoue ekonomiese groei te verseker in beide ontwikkelende en ontwikkelde lande, geniet die soeke na die optimale werkverrigting van paaie 'n baie hoë prioriteit. 'n Wêreldwye toename in die gebruik van skuimbitumen en bitumen-emulsiemateriale (BSMs) as 'n oplossing vir padonderhoud, rehabilitasie en opgradering is merkbaar. Dit word meegebring deur die omgewingsbeleide wat die ontginning van nuwe leengroewe beperk en besparing van energie bevorder. Die korrekte gebruik van hierdie materiale vereis dat die meganismes wat die duursaamheid en langtermyn-werkverrigting daarvan beïnvloed, deeglik verstaan word.

Die verandering in materiaalgedrag en falingsmeganismes van BSM materiale is langtermynverskynsels. Dit impliseer dat bestudering van die fisiochemiese en meganiese eienskappe van die mengsels uiters belangrik is. Dis dus voor die hand liggend hoe belangrik vogbeskadiging en verharding met tyd, wat verwant is aan materiaaleienskappe, is. Die hoofdoelwit met hierdie studie is om die vooruitgang van BSM tegnologie te versnel deur dit moontlik te maak om gekose materiale te evalueer op grond van hulle invloed op duursaamheid en langtermyn-werkverrigting in alle toepassingsfasies (naamlik mengontwerp, konstruksie en dienstoestand).

Hierdie studie begin met 'n uitgebreide literatuuroorsig oor fundamentele begrippe van die karakterisering van interaksie van die bindstof en die minerale-aggregate. Inligting oor bitumen (skuimbitumen en bitumen emulsies) en eienskappe van minerale aggregate is bestudeer. Dit is gevolg deur 'n studie van die fundamentele begrip van die kolloïdale gedrag van skuim en emulsie, asook fisiochemiese en meganiese interaksie met minerale aggregate. Faktore wat die interaksie van BSM-materiale beïnvloed is geïdentifiseer. Die basiese teorie van termodinamika, hidrodinamika en elektrokinetika is daarna gebruik om stap vir stap die proses en formulering van adhesie-binding en kohesie in die BSMs, wat in hierdie studie aangebied word, te beskryf.

Die kwantifisering van mengsel-duursaamheid in terme van vogbeskadiging is ontwikkel. Om hierdie doel te bereik, is die fisiese en meganiese proses van beskadiging deur vogindringing geïdentifiseer. Die gekontroleerde parameters is bepaal en 'n laboratoriumapparaat is ontwerp om hierdie parameters te kwantifiseer. Nuwe vogkondisioneringsprosedures is ontwikkel en in hierdie studie gedemonstreer. Van prosedures van voggeïnduseerde sensitiwiteitstoetsing (Engels: moisture induction simulation test (MIST)) was dit duidelik dat pulsering van waterdruk in BSM materiale die hidrodinamiese effek naboots wat in die veld bestaan as gevolg van dinamiese verkeerslaste. Verskillende mengselmatrikse wat tipies is van hergebruik, soos byvoorbeeld hoornfels-hersiklerde asfalt produk (Engels: recycled asphalt product (RAP)) en vergruisde granietklip, met skuimbitumen of bitumen-emulsie gestabiliseer en met byvoeging van aktiewe vulmateriaal (sement of kalksteen), is ondersoek. Daar is bevind dat nuwe vogkondisioneringsprosedures (soos bepaal deur MIST apparaat en drie-assige toets) kan onderskei tussen BSM materiale wat weerstandig is teen vogbeskadiging en dié wat minder weerstandig (vatbaar) is. Die geldigheid van die MIST en monotone toetsresultate is bepaal deur gebruik van die APT apparaat wat 'n MMLS3 nat verkeerstoets is. Die resultate van beide toetse toon goeie korrelasie in die keuring van BM materiale in terme van vogvatbaarheid.

In hierdie ondersoek is veldtemperatuurdata versamel en die toepaslike model om verouderende BM lae akkuraat te simuleer is geïdentifiseer en voorgelê vir verdere ondersoek en verifikasie. Daar is uit veldtemperatuurdata bevind dat temperatuurgradiënt op die betrokke terrein gewissel het met die dikte van die BSM, naamlik 10°C-17°C gedurende die winter en 17°C-47°C gedurende die somer. Begrip vir die invloed van temperatuuroordragkoëffisiënt en verdampingstempo is belangrik by die afleiding van vogbeskadiging en verharding met ouderdom en die korrekte keuse van BSM materiale.

Verouderingsverhardingsgedrag van BSMs is verwant aan die duursaamheidseienskappe en langtermynwerkverrigting van hierdie materiale. Die basiese karakteristieke wat met kort- en langtermyn verouderingsverharding geassosieer word, is in hierdie studie ondersoek. Die klem op die kort termyn is geplaas op die verouderingsverhardingsgedrag van die bindstof (skuimbitumen kolloïdes en bitumen-emulsiedruppels) voordat BSMs vervaardig word. In die lang termyn evaluasie het die studie ekstraksie en herwinning van bindstof uit brikette wat in die laboratorium gekompakteer is (van verskillende mengsels) en uit kerns verkry vanaf verskeie plaveiselgedeeltes na 8-10 jaar diens ingesluit. Die ondersoek het bevind dat die tydsverloop waarin bitumen in sirkulasie gehou is by verhoogde temperatuur (170°C-180°C) in die laboratorium-aanleg voordat BSMs vervaardig is, veral indien na 8 uur, bydra tot die veroudering van die bindstof. Die skuimproses op sigself verander nie die bitumeneienskappe nie. Daar word aanbeveel dat temperature tussen die grense 160°C-165°C gehandhaaf word vir produksie van skuimbitumen met sagter bitumen sonder dat die kwaliteit benadeel word en dat die sirkulasietyd nie 2 tot 3 ure behoort te oorskry nie.

Die reologiese eienskappe van die herwinde bitumen vanuit laboratoriumbrikette en kerns van plaveisels toon dat ouderdomsverharding van skuimbitumen en bitumen-emulsie tydens die diensleeftyd plaasvind. Die veroudering is skynbaar ook afhanklik van verkeerseffekte, met belaste areas (in wielspoor of binne wielspoor) wat 'n hoër mate van veroudering toon as onbelaste areas (tussen wielspore). Die ekstraksie- en herwinningsproses op sigself was egter bevind as baie kompleks met uiters onseker resultate. Dit het gelei tot onsekere gedrag in terme van ouderdomsverharding van die BSM bindmiddel (skuim of emulsie). Alhoewel resultate toon dat die bindmiddels ouderdomsverharding ondergaan het, is die BSM werkverrigting nie duidelik uit die uitgebreide toetse wat in hierdie studie uitgevoer is nie.

Die laaste deel van die studie bevat gevolgtrekkings en aanbevelings. Die studie lewer insig in die fundamentele duursaamheidseienskappe van die materiaal, wat bydra tot verbetering van die huidige prosedure van seleksie, saamstelling en formulering van die mengmatriks vir BSMs. Verder voorsien dit 'n metode wat in die praktyk gebruik kan word om met vertrouwe duursame mengsels met lang diensbaarheidsleeftyte te vervaardig. 'n Nuwe oplossing en vooruitgang in die toepassing van BSMs is daargestel tot voordeel van alle partye betrokke by die ontwikkeling van herwinningstechnologie.

ACKNOWLEDGMENTS

Working toward my PhD was a blessing and beyond my normal understanding. I'm very grateful to the Almighty Father, who provides me with health, forbearance, wisdom and endurance during my studies. Through His grace, different people come into play. It started with a professor, who offered me to work on an interesting and challenging project on cold stabilised materials. It developed and turned out to offer me more challenges than expected and finally revealed the unknown behaviour of pavement recycling technology. The point I want to make though is that one can never tell in advance how a research project will turn out, how its outcome will be perceived by the industry and, on a personal note, whether one will benefit from doing doctorate research.

With regard to research outcomes, this dissertation serves as a testimony for the time and resources utilised on the work done. As far as the personal benefit is concerned, apart from the scientific insight on pavement recycling technology gained, what has made the entire experience very rewarding was the exposure to the South African (SA) pavement practitioners and to different seminars and conferences supported by Stellenbosch University. Having defined the achievement, I would like to acknowledge the soldiers who came out of it, and without whom this doctoral research would have been a different story.

First and foremost to Prof. Kim Jenkins, who not only offered me a wonderful opportunity to tackle an interesting, timely wanted topic, "durability" in pavement recycling technology, but allowed me to get exposure in the SA pavement industry. Prof. Kim made me interact and network with practitioners. He also helped me to organise all the necessary materials, gave me visibility and a solid technical background and the tools to further develop myself as a researcher. Kim always talked about being critical and smart in reviewing things, and I thank you Kim for being a real promoter and mentor. Without your support, my effort would not have reached where I am today. Apart from the academic support, Kim was concerned with my family livelihood. Without your financial facilitation support and generously intervening during my financial crisis, my study would not have been possible. I cannot emphasise enough how important I feel from your sincere assistance that you showed to me and my family during my duration of stay here at Stellenbosch. Probably, it is an investment for a long-term working relationship.

Secondly, I would like to express my gratitude to Mr Johan Muller, senior electro-mechanical engineer in Stellenbosch University. His selfless time and creative thinking has made possible the research work being presented in this dissertation. He has been timely maintaining the MTS equipment and foam-plant, which were at the core of my research. His creative ideas on the designing of the dynamic system of the MIST device as well as membrane-making devices are greatly appreciated. Teaching on the features and operation of the MMLS3 was essential for simulating the real field moisture damage phenomenon in BSMs. Johan, your skill is an asset and your contribution will never be forgotten. Design and manufacturing go hand in hand. In that respect, I wish to thank Mr Dion Viljoen and Louis Fredericks and later Johan van der Merwe from the Civil Engineering workshop for their timely manufacturing of the these important devices and always assisting on day-to-day maintenance of equipment.

I owe a lot of gratitude to Kaviti Musango for various aspects, particularly for the selfless time spent reviewing the write-up of my chapters and your general comments on my material presentation and the interest in my thesis. Your contribution to my success will never be forgotten. Regarding data collections, I would like to thank the following 4th year students for their assistance in collecting valuable data in various tests: Jacobous van Riet and Jaco Bruwer,

for carrying out some MMLS3 tests and Sindie van der Linde, for carrying out some ageing tests. Your inputs into this thesis are greatly appreciated.

This research would not be complete without the generous support of the external laboratories. Firstly, is Soil Lab in Kraaifontain. Willie Venter and Joseph, I thank you very much for providing access to your facilities and for the selfless help of your laboratory staff, particularly Dion in the extraction and recovery of bitumen from BSMs. It was challenging and time-consuming work, but success was recorded. Secondly, is MUCH Asphalt central laboratory in Eersterivier. Alec Rippenaar and Henry for providing access to the facilities and the use of the new installed rotary recovery device. Your allocation of laboratory staff, particularly Jonathan, in assisting the extraction and recovery is very much appreciated. Thirdly, is COLAS in Cape Town. I thank Morne for providing me with emulsion and assisting in recovery and rheological testing of bitumen emulsion. Your co-operation and interest in my research is very much appreciated. Fourthly, is Madeleine Frazenburg from the Department of Geology, Stellenbosch University, who was responsible for running scanning electron microscopy (SEM) testing. I thank you very much for your assistance in carrying out microstructure analysis on BSM specimens. Your input has provided meaningful results into understanding the fundamental behaviour of BSMs. Last but not least is CSIR Laboratory in Pretoria. Dave Ventura, your permission for me to use the durability mill index (DMI) device and allowing Moosa Sekatane to help me in the entire testing procedure is greatly appreciated. I owe Dr. Phil Paige-Green a lot of gratitude for his comments on the DMI results and sharing the knowledge of the behaviour and DMI classification of different rock types. Your continual co-operation is very much appreciated.

Our research in Stellenbosch has been well received, both nationally and internationally, which is a result of fruitful collaboration. In this light, I would like to thank my fellow postgraduate students who were involved in the big TGX project. These are Percy Moloto, Rex Kelfkens, William Mulusa and Lucas Ebels. My special thanks goes to Ebels for his selfless time in explaining the MTS operation, testing procedure and analysis of triaxial test data. Your input will never be forgotten. The achievement in intensive laboratory experiment would not have been possible without the help of the Lab assistants. My great appreciation goes to Colin Isaacs and Gaven Williams. I thank you very much for working long hours during laboratory and field experimentations. I owe a lot of gratitude to Colin for not only helping me on laboratory works but facilitating the procurements of various materials, as well as assisting me and my family personally. Colin, your selfless style is a grace.

Administratively, my studies would not have gone smoothly without the assistance and facilitation of the following: Janine Myburgh, Dr. Marius De Wet, Alett Slabbert, Amanda de Wet, Rodney Davides and Ruth Sedeman. My special thanks go to Janine. Your quick response to all my requests and timely facilitation of my financial assistance is greatly appreciated. My sincere thanks also go to Kate Jenkins for the time spent in editing the entire thesis. Prof. Craig MacKenzie for additional editing to enhance language quality, Dr. Marius De Wet and Louis Roodt spent time in writing the Afrikaans abstract. Your help is greatly appreciated.

I would further like to acknowledge the individuals and institutions whose support impacted significantly on my career. Prof. Fred Hugo, I thank you very much for giving me the opportunity to undertake prestigious managerial training as a CMP delegate. Your acceptance and financial support is greatly appreciated. I thank SABITA and GAUTRANS for financing the big TGX project, which formed part of my study. I also thank the Republic of Rwanda for financial support and the Institute of Science and Technology for allowing me to pursue my PhD study.

My spiritual growth, which has enabled me to succeed in my studies, is dedicated to the following: Rev. Lee Marshall of St. Paul's Church. Your Bible teaching was precious and made me and my family grow widely and deeply in understanding the Lord Jesus correctly. Your talent in teaching the Bible is a grace. I also thank Rev. Jurie Goosen and his wife Maggie for being

the first family in Stellenbosch giving a warm welcome and fellowship. Your further assistance in various aspects for me and my family is greatly appreciated. Prof. Eric Strauss, I thank you for accepting me to your house as a colleague and for the fellowship we shared together during Bible study. Kate Jenkins, I thank you very much for offering your time to Diana for her advancement on school performance. Your inspiration in the Afrikaans language will never be forgotten. I also thank Prof. Anton Basson, his wife Erna, Mimi and Jan for inviting me as a member of their Bible study group, Nathan and his family and Prince Kalem and his family for the fellowship and for being good neighbours at Die Rand Estate. Hellen Marshall, thanks for the fellowship and acceptance of Derrick at Montessori School in Newberry House; your assistance will not be forgotten.

Finally, I would like to thank my wife Annonciata and my children, Diana and Derrick for their love and patience. Derrick was discouraged with my career, seeing as Dad had no opportunity to relax, was always working late in the laboratory and writing a thick book. Thank you for understanding the objective of us being in Stellenbosch and cheering me all along to be able to meet the deadlines. I also thank my mother Elizabeth for laying a solid foundation.

TABLE OF CONTENTS

INFLUENCE OF DURABILITY PROPERTIES ON PERFORMANCE OF BITUMEN STABILIZED MATERIALS

DECLARATION	2
SUMMARY	3
OPSOMMING	5
ACKNOWLEDGMENTS.....	7
LIST OF TABLES.....	13
LIST OF FIGURES	15
LIST OF ABBREVIATION AND SYMBOLS.....	21
CHAPTER 1: INTRODUCTION.....	23
1.1 BACKGROUND.....	23
1.2. THE NEED FOR DURABILITY PROPERTIES OF BSMs.....	25
1.3 OBJECTIVES AND SCOPE OF DISSERTATION	30
1.4 LAYOUT OF DISSERTATION.....	34
REFERENCES.....	35
CHAPTER 2: LITERATURE REVIEW ON DURABILITY PROPERTIES OF MATERIALS AND MIXTURE COMPOSITION OF BITUMEN STABILISED MATERIALS	36
2.1 INTRODUCTION.....	36
2.2 MINERAL AGGREGATES DURABILITY.....	38
2.3 BITUMEN BINDER DURABILITY	60
2.4 MIXTURE COMPOSITION DURABILITY	80
2.5 ENGINEERING PROPERTIES AND DURABILITY OF BSMs LAYER	94
2.6 SUMMARY ON DURABILITY ISSUES IN BSMs.....	103
REFERENCE.....	106
CHAPTER 3: MOISTURE SUSCEPTIBILITY AND DAMAGE MECHANISMS	114
3.1 INTRODUCTION.....	114
3.2 GOVERNING PROCESSES AND FORMULATIONS.....	114
3.4 LABORATORY SIMULATION OF MOISTURE SUSCEPTIBILITY	126
3.5 DEVELOPMENT OF A NEW MOISTURE CONDITIONING PROCEDURE.....	129
3.6 ANALYSIS AND DISCUSSION OF RESULTS	141
3.7 VALIDATION OF MIST TEST RESULTS	149
3.8 MOISTURE EFFECT ON DISINTEGRATION OF MINERAL AGGREGATES	154
3.9 CONCLUSIONS AND RECOMMENDATION	156
REFERENCES.....	158

CHAPTER 4: THE ROLE OF MMLS3 IN VALIDATION OF MOISTURE DAMAGE	
CLASSIFICATIONS OF BSMs	159
4.1 INTRODUCTION	159
4.2 SELECTION OF TEST VARIABLES AND TEST SETUP	160
4.3 EXPERIMENTAL PROGRAM	165
4.4 MMLS3 AND ITS TESTING	168
4.5 ANALYSIS AND DISCUSSION OF RESULTS	171
4.6 CONCLUSIONS	181
REFERENCES	182
CHAPTER 5: ADVANCED CHARACTERISATION OF MOISTURE DAMAGE	183
5.1 INTRODUCTION	183
5.2 DETERMINATION OF MOISTURE DAMAGE THROUGH TRIAXIAL TESTS	184
5.3 MOISTURE DAMAGE CHARACTERISATION USING TRIAXIAL PROPERTIES	189
5.4 ANALYSIS OF MOISTURE DAMAGE TO BSM LAYER IN PAVEMENT	197
STRUCTURES	197
5.5 CONCLUSIONS	204
REFERENCES	205
CHAPTER 6: INFLUENCE OF TEMPERATURE DISTRIBUTION AND VOID	
CHARACTERISTICS ON DURABILITY BEHAVIOUR OF BSMs	206
6.1 INTRODUCTION	206
6.2 TEMPERATURE MONITORING AND EVALUATION	208
6.3 TEMPERATURE DISTRIBUTION PREDICTION MODEL (Burger Model)	216
6.4 RELATIVE HUMIDITY DISTRIBUTION IN THE BSM-EMULSION LAYER	218
6.5 VOID CHARACTERISTICS IN THE MIX MATRIX	221
6.6 CONCLUSIONS	232
REFERENCES	233
CHAPTER 7: AGE HARDENING AND ENGINEERING PROPERTIES	234
7.1 INTRODUCTION	234
7.2 METHODOLOGY AND EXPERIMENTAL PROGRAM	236
7.3 EVALUATION AND ANALYSIS OF RESULTS	243
7.5 ENGINEERING PROPERTIES	259
7.6 CONCLUSIONS	262
REFERENCES	264
CHAPTER 8: CONCLUSIONS AND RECOMMENDATIONS	265
8.1 MINERAL AGGREGATES DURABILITY	265
8.4 CHARACTERISATION OF MOISTURE DAMAGE	266
8.5 AGEING BEHAVIOUR OF BSMs	267
8.6 CLIMATE AND ENGINEERING PROPERTIES	268
8.7 RECOMMENDATIONS FOR FURTHER STUDY	269
APPENDIX A: NEW MOISTURE CONDITIONING PROCEDURE FOR BITUMEN	
STABILISED MATERIALS (BSMs), USING MIST DEVICE	271
APPENDIX B: MONOTONIC TRIAXIAL RESULTS FOR DRY AND MOISTURE	
CONDITIONED SPECIMENS USING MIST DEVICE	274

APPENDIX C: TRIAXIAL RESILIENT MODULUS RESULTS FOR DRY AND MOISTURE CONDITIONED SPECIMENS USING MIST DEVICE	276
APPENDIX D: RAVELLING RESULTS AFTER WET MMLS3 TRAFFICKING	277
APPENDIX E: SHEAR PROPERTIES RESULTS FOR THE DRY AND CONDITIONED (WET) MIXES	281
APPENDIX F: TRIAXIAL PERMANENT DEFORMATION TEST RESULTS	284

LIST OF TABLES

Table 1: Summary of comparative materials and long-term durability of different pavement materials	28
Table 2: Grouping of rock type based on presence or absence of quartz and weathering potential, TRH 14 (CSIR, 1985).....	47
Table 3: Climatic Index on different region using Weinert's N-value, (Weinert,1980).....	49
Table 4: Aggregate properties related to pavement performance (Dukatz, 1989).....	51
Table 5: Comparison of results from sound and distressed outer wheel path areas of basecourse materials (Sampson and Netterberg, 1989).....	54
Table 6: Durability Mill Index, limit for rocks and soils, (Sampson, 1991).....	55
Table 7: Erosion test results on different rock type (Paige-Green <i>et al.</i> , 2004 and Long <i>et al.</i> , 2004)	57
Table 8: The difference between foamed bitumen and bitumen emulsion on age hardening characteristics	74
Table 9: Difference in bitumen recovery from HMA and BSMs using conventional methods	75
Table 10: Phase description for bitumen, aggregates and water interaction applicable to BSMs.	80
Table 11: Classification of void in term of permeability (k) Caro <i>et al.</i> (2008)	89
Table 12: Methods used to quantify moisture damage in BSMs through the loss of surface materials.....	92
Table 13: Test methods that stem from Asphalt Institute to test BSMs moisture sensitivity	93
Table 14: Test methods for engineering and performance properties on BSMs	94
Table 15: Step-by-step governing process for bond formation in BSMs until full strength is achieved	115
Table 16: Constituted mix type and testing matrix for moisture susceptibility	131
Table 17: Aggregates type and grading of Hornfels-RAP and Quartzite crushed stone.....	132
Table 18: Summary of optimum moisture contents and maximum dry densities of blends	133
Table 19: Scale settings for measuring, loading and displacement in the MTS	138
Table 20: Compaction density achieved on BSMs using BOSCH® compactor	141
Table 21: MIST conditioning time and related retained cohesion and retained stiffness on different BSM mixes	143
Table 22: Recommended retained cohesion after MIST conditioning and static triaxial test....	146
Table 23: Durability Mill Index (DMI) results for the selected mineral aggregates.....	155
Table 24: The axial loading, tyre pressure and contact length applicable to MMLS3 setting ...	162
Table 25: Comparison of shear failure parameters of unconditioned (dry) and conditioned (wet) specimens of different studied BSMs mixes	193
Table 26: BSM-emulsion layer, material properties for BISAR analysis.....	197
Table 27: Material properties of layers analysed using BISAR 3.0 program.	198
Table 28: Extract of the hottest maximum daily temperatures in the BSM-emulsion layer at 2/3 depth during summer.....	213
Table 29: Temperature gradient in the BSM-emulsion at different solar time	215
Table 30: Bulk relative density, RICE density and void content in BSMs.....	222
Table 31: Volumetric properties of the field extracted cores from P243.....	223
Table 32: The average rutting, bitumen content and percentage voids of the cores extracted from different stations and locations of Shedgum Road.....	224
Table 33: Source and type of binder for short-term ageing study	238
Table 34: Mix matrix for the laboratory prepared specimen.....	238
Table 35: List of pavement section selected for field ageing studies	238
Table 36: Summary of cores sourced for investigating BSMs field age hardening behaviour ..	239

Table 37: Separated filler collected after each cycle on different cup.	240
Table 38: Difference in bitumen recovery from HMA and BSMs using conventional methods .	242
Table 39: Specification for road bitumen in South Africa, SABS 307	244
Table 40: Base bitumen and foamed bitumen rheological properties of 80/100 pen grade from NATREF refinery with lab conditioning.....	245
Table 41: Base bitumen and foamed bitumen rheological properties of 80/100 pen from CALTEX refinery with lab conditioning.....	245
Table 42: Base bitumen and foamed bitumen rheological properties of 60/100 pen from NATREF refinery with lab conditioning	246
Table 43: Base bitumen and foamed bitumen rheological properties of 60/70 pen from CALTEX refinery with lab conditioning.....	246
Table 44: Recovered bitumen rheological properties from Emulsion, ANi B SS-60	250
Table 45: Summary of the laboratory and field cores material type, binder type, content and pavement age	252
Table 46: Recovered bitumen properties from Grassy Park BSM-foam and BSM-emulsion section (Abson method).....	253
Table 47: Recovered bitumen properties from P243/1 Vereeniging BSM-foam and BSM-emulsion section (Abson or rotary vapour method).....	254
Table 48: Recovered bitumen properties from Shedgum Road BSM-foam section (Abson method).....	254
Table 49: Recovered bitumen properties of Shedgum Road BSM-foam section from different laboratories for comparison	255
Table 50: Recovered bitumen properties of laboratory-prepared specimens.....	256
Table 51: Shear properties of BSM-emulsion at dry and wet (conditioned) state, tested at 25°C.	274
Table 52: Shear properties of BSM-emulsion at dry and wet (conditioned) state, tested at 25°C.	275
Table 53: Resilient modulus of BSM-emulsion and BSM-foam at dry and wet (conditioned) state, tested at a confinement of 50kPa and SR of 10% at 25°C.	276
Table 54: Number of load application and ravelling depth after wet MMLS3 trafficking at 25°C on H1CE and H1LE trafficked together.....	277
Table 55: Number of load application and ravelling depth after wet MMLS3 trafficking at 25°C on Q1LE and Q1CE trafficked together.	278
Table 56: Number of load application and ravelling depth after wet MMLS3 trafficking at 25°C on H0CE and Q0CE trafficked together	278
Table 57: Number of load application and ravelling depth after wet MMLS3 trafficking at 25°C on Q0CF and H0CF trafficked together	279
Table 58: Number of load application and ravelling depth after wet MMLS3 trafficking at 25°C on Q1LF and H1LF trafficked together	279
Table 59: Number of load application and ravelling depth after wet MMLS3 trafficking at 25°C on Q1CF and H1CF trafficked together	280
Table 60: Number of load application and ravelling depth after wet MMLS3 trafficking at 25°C on F2CF and S2CE trafficked together	280

LIST OF FIGURES

Figure 1: Conceptual illustration of engineering durability, (van de Ven, 1998)	24
Figure 2: Moisture diffusion on aggregates-mastic interface resulting in cohesive and adhesive failure (Erkens, 2002).....	25
Figure 3: Durability of weathered crystalline rocks in pavement, depending on the N-value and the percentage of secondary minerals (Weinert, 1980).	28
Figure 4: Conceptual reliability versus completeness on pavement materials evaluation (Jooste <i>et al.</i> , 2007)	29
Figure 5: Key elements determining the durability properties of BSMs	30
Figure 6: General overview of the research approach	33
Figure 7: Conceptual performance properties of BSMs in different phases	36
Figure 8: Main variables influencing durability properties and long-term performance of BSMs	37
Figure 9: Crystal chemistry of silicate rock and soil type (After Michell, 1993).....	41
Figure 10: Crystal chemistry of silicates rock and soil type (Michell, 1993).....	42
Figure 11: Changes in pH of water in which aggregates were immersed (Yoon and Tarrer, 1988).....	43
Figure 12: Classification of mineral aggregates (Mertens and Wright, 1959).....	44
Figure 13: Order of mineral crystallisation stability (Mitchell, 1993)	46
Figure 14: Source of moisture infiltration and suction to the pavement layers (Jenkins, 2007) ..	48
Figure 15: Moisture condition on different region in South Africa according to Thornthwaite's moisture index (Paige-Green, 2009).....	50
Figure 16: South African LTPP base materials for the BSMs pavement layer (Long, 2007)	52
Figure 17: Mineral aggregate durability testing devices ACV vs. DMI.....	55
Figure 18: Wet/dry durability test: Hand brush vs. Mechanical brush	56
Figure 19: Wheel-trafficking erosion testing device (Long, 2003)	57
Figure 20: Comparative Erosion Index for BSM-foam with different rock type	58
Figure 21: Example of typical colloidal nature of foam and emulsion in microscopic scale	60
Figure 22: Schematic representation of a SOL and GEL type bitumen (Hagos, 2008)	62
Figure 23: Oxidation pathways for sulfoxide formation (SHARP A-368, Vol.2, 1993).....	63
Figure 24: Schematic diagram of chemical compositional change toward more polar fraction bitumen (oxidative ageing).....	63
Figure 25: Examples of important chemical functional groups [1] naturally occurring and [2] formed on oxidative ageing (source: SHARP A-368, Vol.2, 1993)	64
Figure 26: FTIR spectrum showing increase in carbonyl/ketone (1700 cm^{-1}) and Sulfoxide (1030 cm^{-1}) formation with ageing (Hagos, 2008).	64
Figure 27: Variation in binder adsorption in a RAP-aggregate surface (aged bitumen).....	66
Figure 28: Simplistic diffusion process of the free atmospheric oxygen into the BSM layer	69
Figure 29: Comparison of stiffening potential versus percentage bulk volume of mastic for the BSM- foam and HMA (Jenkins, 2000)	70
Figure 30: Aging potential of foamed bitumen mastic as a function of bulk volume for Hornfels-RAP dust and 150/200 Calref bitumen (Jenkins 2000).....	71
Figure 31: Hydrophobic nature of the surface due to the addition of active filler	73
Figure 32: Effect of short and long-term ageing of the binder on viscosity ratio with ageing period for general trend of the HMA (Shell Bitumen 2003).....	77
Figure 33: Change in functional groups of bitumen during ageing (Hagos, 2008).....	78
Figure 34: Typical viscosity depth relationship as a function of time at a given temperature.....	79
Figure 35: Three-phase boundary of a liquid drop on a solid surface in vapour.....	83

Figure 36: Formulation of the three-phase boundary relationship of a liquid drop on a solid surface in vapour (Adamson, 1990)	83
Figure 37: Structure of equilibrium emulsion droplets (James, 2006)	85
Figure 38: Mix composition and possible moisture transport into BSMs	88
Figure 39: Categories of static moisture (water) (Grobler, 1995)	90
Figure 40: BSM moisture damage classification system.....	91
Figure 41: Time-temperature superimposition for BSMs, HMA and HW-STAB ($T_{ref}=20^{\circ}C$) (Ebels, 2008)	95
Figure 42: Fatigue behaviour of BSM-emulsion and BSM-foam with higher percentage of RAP materials (Twagira, 2006).....	96
Figure 43: Permanent axial strain of BSM-foam mixes at different curing conditions, and confinement of 68.9kPa, loading rate of 0.1s, and 0.2s rest period at 20°C (Fu <i>et al.</i> , 2009)	97
Figure 44: Schematic illustration of seal type common in South Africa (SANRAL, TRH 3, 2007)	98
Figure 45: Dynamic hydroplaning simulation using MSC Dytran at 80km/h (Okano <i>et al.</i> 2008).....	99
Figure 46: Three-zone concept and schematic figure of dynamic of hydroplaning (Nikajima <i>et al.</i> , 2000).....	99
Figure 47: (a) Pressure on pavement under rolling tyre, (b) velocity dependence on hydrodynamic force (Nikajima <i>et al.</i> , 2000).....	100
Figure 48: Minimum and Maximum pavement temperature in different regions of South Africa, (HMA guideline, 2000)	101
Figure 49: Permanent deformation on emulsion and foam test section using HVS (Steyn, 2001)	102
Figure 50: The influence of diffused water on the bonding formation at the mastic-aggregates interface	117
Figure 51: Typical South African pavement structure with boundary condition for BSMs.....	121
Figure 52: Illustration of pore pressure effect on void structures for the moisture damage	121
Figure 53: Erosion behaviour of laboratory-compacted and cured specimen made from Quartzite crushed stone stabilised with foamed bitumen and exposed to cyclic pulsing of water pressure.....	122
Figure 54: Selected triaxial resilient modulus results for different foamed mixes cured at different conditions and applied deviator stress of 62.1kPa and 103.4kPa, at Hz of 0.1s (Fu <i>et al.</i> 2009)	124
Figure 55: The influence of density and retained moisture on mixes with different foamed bitumen and cement contents (Long and Ventura, 2003).....	126
Figure 56: Illustration on approach to laboratory simulation of moisture susceptibility	127
Figure 57: The ITS and UCS testing configuration and analysis.....	128
Figure 58: Monotonic triaxial test and mechanical evaluation of critical parameter of BSMs....	129
Figure 59: Short time dynamic (resilient modulus) triaxial test evaluation at different saturation levels in BSMs.	129
Figure 60: Grading curves of Hornfels-RAP and Quartzite aggregates in envelop of the BSMs limits	132
Figure 61: a) Modified BOSCH® compactor b): specimen in the mould	134
Figure 62: Designed MIST device features and setup.....	135
Figure 63: Heating unit for hot water simulation connected to the MIST device.....	135
Figure 64: Oscilloscope device used for calibration of water pressure, cyclic loading time and rest period during trials on the MIST device.....	136
Figure 65: MTS loading system and triaxial specimen with membrane fitting tool	138
Figure 66: Rotary membrane device and membrane product 127mm x 500mm.....	139
Figure 67: Illustration of MMLS3 test setup including details of vinite installation	140

Figure 68: CT scan analysis at the interface (scarified surface) of the vibratory compacted specimen, BSM (emulsion or foam)	142
Figure 69: Mathematical model of the 80% saturation level at OMC of the mixes (Savage, 2006)	144
Figure 70: Saturation levels after MIST conditioning on different BSMs	144
Figure 71: Retained cohesion of different BSMs and proposed limits	145
Figure 72: Resilient modulus versus saturation level of BSM-foam and BSM-emulsion	147
Figure 73: The relationship between retained cohesion and retained modulus ratio of BSMs ..	148
Figure 74: Example of inconsistency results captured by LVDT's during short dynamic test...	148
Figure 75: Correlation tests for moisture susceptibility of BSMs	149
Figure 76: Correlation between ravelling depth, retained cohesion, and tensile strength retained on moisture damage sensitivity in a) H1CE & H1LE and b) Q1LE & Q1CE BSM mixes.....	151
Figure 77: Correlation between ravelling depth, retained cohesion, and tensile strength retained on moisture damage sensitivity of: H0CE & Q0CE and Q0CF & H0CF BSM mixes.....	151
Figure 78: Correlation between ravelling depth, retained cohesion, and tensile strength retained on moisture damage sensitivity in e) Q1LF & H1LF and f) Q1CF & H1CF BSM mixes.....	152
Figure 79: Correlation between ravelling depth, retained cohesion, and tensile strength retained on moisture damage sensitivity in F2CF & S2CE BSM cores extracted from the field.....	153
Figure 80: Extracted cores from existing pavement and erosion behaviour.....	153
Figure 81: DMI test setup for dry and wet simulation of Hornfels-RAP materials	154
Figure 82: Schematic load-time hydrodynamic effect on BSMs due to distressed surface layer	160
Figure 83: MMLS3 illustration of the four re-circulating wheel axles and tyre	161
Figure 84: The calibration unit for the wheel load in the MMLS3	161
Figure 85: Illustration of cyclic loading time and rest period on MMLS3 for the moisture damage simulation	163
Figure 86: Ravelling versus rutting on the foamed bitumen section tested with MMLS3 after three days of compaction (Jenkins and van de Ven, 1999)	163
Figure 87: Typical pavement structure with BSMs (base layer) and surface loading	164
Figure 88: The design of vinite layer to protect direct wheel load abrasion on BSMs	164
Figure 89: Plan view of the vinite protective layer on the briquettes and its discolouring during trafficking	165
Figure 90: Flow diagram illustrating moisture damage classification of BSMs using MMLS3 and ITS tests	166
Figure 91: The top view of briquettes measurements and the double saw cutting setup	167
Figure 92: The side view of briquette measurement after trimming of the sides	168
Figure 93: Comparable surface finish after sawcutting for MMLS3 testing	168
Figure 94: Overview of the MMLS3 test bed setup and profilometer guide.....	169
Figure 95: Non-linear pattern of ravelling growth during MMLS3 trafficking of BSMs.....	170
Figure 96: ITS test setup on specimen after MMLS3 testing tested at 25±1°C	170
Figure 97: Cumulative number of load applications to failure of BSMs in wet condition at 25°C, 420kPa, 1.8kN and speed of 7 200 wheels per hour.....	172
Figure 98: Application of wet MMLS3 trafficking on screening mixes that are susceptible to moisture damage.....	173
Figure 99: Disintegration behaviour of H1CE during MMLS3 wet trafficking at 25°C	174
Figure 100: Ravelling depth of Hornfels-RAP material stabilised with emulsion and additional 1% cement or lime after 45 000 cycles of wet MMLS3	

trafficking at 25°C	174
Figure 101: Ravelling behaviour of BSM-foam and BSM-emulsion without the addition of active filler, under wet MMLS3 trafficking at 25°C	175
Figure 102: Ravelling behaviour of BSMs, which are less resistant to moisture damage under dry MMLS3 trafficking at 25°C	176
Figure 103: ITS values of BSMs after wet MMLS3 and dry trafficking	177
Figure 104: Superimposed values of wet ITS and dry ITS of different BSM mixes.	177
Figure 105: Tensile Strength Retained values for the BSMs after MMLS3 wet and dry trafficking at 25°C.....	178
Figure 106: Ravelling behaviour of different BSM mixes (H1LE and H1CE) under wet MMLS3 trafficking after 45 000 load applications at 25°C	179
Figure 107: Potential classification of BSMs using ravelling depth after wet MMLS3 trafficking at 25°C	180
Figure 108: Ravelling model for wet MMLS3 trafficked BSMs at different number of MMLS3 wheel load applications at 25°C.....	180
Figure 109: Flows diagram illustrating the triaxial testing methods for moisture susceptibility .	184
Figure 110: Stress (Mohr-Coulomb) circles at failure and determination of shear parameters.	186
Figure 111: Descriptions of the resilient deformation test, showing seating axial strain	187
Figure 112: Typical LVD's displacement data captured at 800 Hz with 10% stress ratio and 50 kPa confining pressure at 25°C	188
Figure 113: Typical loading data captured at 800 Hz with 10% stress ratio and 50 kPa confining pressure at 25°C	188
Figure 114: Sequence of deviator stress ratio in multi-stage permanent deformation testing at constant confining stress 100 kPa.....	189
Figure 115: Comparison of moisture sensitivity of BSMs between retained cohesion (RC) and deviator stress ($\sigma_{d-dry}/\sigma_{d-wet}$) at 50kPa and 100kPa.....	190
Figure 116: Comparison of moisture sensitivity of BSMs between retained cohesion (RC) and deviator stress at failure ($\sigma_{d,f-dry}/\sigma_{d,f-wet}$) at 50kPa or 100kPa	190
Figure 117: Effects of moisture damage on shear properties of BSM-emulsion mixes of Hornfels-RAP without the addition of cement (H0CE)	191
Figure 118: Effects of moisture damage on shear properties of BSM-emulsion mixes of Hornfels-RAP with 1% cement (H1CE)	192
Figure 119: Permanent axial strain of H1CE and H0CE tested wet and dry at various parameters (i.e. havesine wave, square wave, 25°C, 40°C, 40% SR, multi-stage stresses 40%– 80% SR) at 100kPa and frequency of 2Hz.....	195
Figure 120: Permanent axial strain of field extracted cores (BSM-foam) with 100% RAP from Shedgum Road, tested at 40% SR, 100kPa and different temperatures of 40°C, 50°C and 60°C.....	196
Figure 121: Comparative pavement structure comprising a BSM-emulsion layer at equilibrium state and in a saturated state, used in BISAR analysis	198
Figure 122: Comparison of vertical stress distribution in BSM-emulsion at equilibrium and in a saturated sate, in a pavement structure	199
Figure 123: Comparison of vertical and horizontal stresses distribution in BSM-emulsion at equilibrium and in a saturated state, in a pavement structure.....	200
Figure 124: Comparison of vertical stain distribution in a BSM layer, at equilibrium and in saturated condition, in a pavement structure.....	201
Figure 125: Comparison of horizontal strain distribution in BSM-emulsion, at equilibrium and in saturated condition, in a pavement structure	201
Figure 126: Comparison of deviator stress distribution in BSM-emulsion, at equilibrium and in saturated condition, in a pavement structure	202

Figure 127: Comparison of deviator stress ratio in BSM-emulsion, at equilibrium and in saturated condition, in a pavement structure.....	203
Figure 128: Temperature distribution of distressed pavement structure including BSM-foam as a base layer (Loudon International, 2008)	207
Figure 129: Flow diagram illustrating focus area of temperature distribution and void characteristics of BSMs	208
Figure 130: The section of N7 pavement structures after recycling with BSM-emulsion.....	209
Figure 131: iButtton, blue dots, USB and ClimaStats software used for retrieving temperature and RH measured in the BSM-emulsion layer.....	209
Figure 132: Layout and location of the installed iButtons in a BSM-emulsion pavement section of the N7 expressway	210
Figure 133: Daily temperature data near the inner lane (IL) at 1/3 depth of the BSM-emulsion layer of the N7 expressway near Cape Town.....	212
Figure 134: Daily temperature data near the yellow line at 2/3 depth of the BSM-emulsion layer of the N7 expressway near Cape Town.....	213
Figure 135: Daily temperature data near the yellow line at 2/3 depth of the BSM-emulsion layer of the N7 expressway near Cape Town.....	214
Figure 136: Temperature gradient through of N7 BSM-emulsion layer, with surface layer extrapolated.....	215
Figure 137: Models parameters on control volume for a unit layer of pavement surface exposed to the natural environmental conditions (Berger <i>et al.</i> , 2005)	217
Figure 138: Daily RH data near the yellow line at 1/3 depth of the BSM-emulsion layer of the N7 expressway near Cape Town	219
Figure 139: Daily RH data near the yellow line at 2/3 depth of the BSM-emulsion layer of the N7 expressway near Cape Town	219
Figure 140: Daily RH data near the yellow line at 2/3 depth of the BSM-emulsion layer of the N7 expressway near Cape Town	220
Figure 141: Void properties of BSMs and influence of mineral aggregates type.....	222
Figure 142: The different mode of voids structure present in BSMs	223
Figure 143: The relationship between void content, binder content and rutting behaviour in BSM mixes from Shedgum Road	225
Figure 144: The CT-scan (x-ray tomography) technique, (Hagos, 2008).....	226
Figure 145: CT-scan analysis of the distribution of foamed bitumen mix composition of vibratory compacted specimens S3b and S3a	227
Figure 146: CT-scan analysis on the distribution of bitumen emulsion mix composition on vibratory compacted specimen S2 and S1	227
Figure 147: The Scanning Electron Microscopy, SEM, device system and prepared polished samples	228
Figure 148: SEM analysis and magnification (200µm) of a selected part of Quartzite aggregates stabilised with foamed bitumen and added of cement (Q1CF).....	229
Figure 149: SEM analysis and magnification of selected parts of Hornfels-RAP aggregates stabilised with foamed bitumen and no cement (H0CF), further elemental analysis on the whitish part of the mastic was done by EDS.....	230
Figure 150: EDS elemental analysis of the thread structure of the mastic composition.	231
Figure 151: Flow chart describing the procedure for the study on binder ageing on the BSMs.....	236
Figure 152: Locations of the field cores extracted from the pavement section.....	237
Figure 153: Laboratory- prepared specimen and cores extracted from the existing pavement sections for both emulsion and foam mixes	239
Figure 154: Cold centrifuge for washing bitumen from mineral aggregates	240
Figure 155: Abson method of bitumen recovery from the solvent (done at Soil Lab. Kraaifontein).....	241

Figure 156: A rotary vapour recovery system for separation of solvent from bitumen (done at MUCH Asphalt Eersterivier).....	242
Figure 157: Penetration and softening point test setup.....	243
Figure 158: Dynamic viscosity test setup	244
Figure 159: Penetration versus ageing time (hr) of base bitumen and foamed bitumen at 170°C–180°C.....	245
Figure 160: Penetration versus ageing time (hr) of base bitumen and foamed bitumen at 170°C-180°C.....	247
Figure 161: Penetration versus softening point of base bitumen and foamed bitumen at circulation temperature of 170°C -180°C for the 80/100 penetration.....	247
Figure 162: Penetration versus softening point of base bitumen and foamed bitumen at 170°C-180°C for 60/70 penetration	248
Figure 163: Viscosity versus mixing time (hr) of base bitumen and foamed bitumen at temp 170°C-180°C.....	248
Figure 164: Viscosity versus mixing time (hr) of base bitumen and foamed bitumen at 170°C-180°C.....	249
Figure 165: Penetration Index (PI) of base bitumen versus foamed bitumen and bitumen emulsion for 80/100 penetration bitumen	251
Figure 166: Penetration Index (PI) of base bitumen versus foamed bitumen and bitumen emulsion for 60/70 penetration bitumen	251
Figure 167: Comparison of age hardening behaviour of trafficked and untrafficked location on the pavement layer	257
Figure 168: The combined (short and long-term) age hardening behaviour of BSMs.....	258
Figure 169: Comparison between air void content and age hardening behaviour in BSMs	259
Figure 170: Comparison between age hardening and rutting behaviour of BSMs in the field ..	260
Figure 171: Comparison of age hardening and ravelling behaviour of BSM mixtures.....	261
Figure 172: Effects of moisture damage on shear properties of BSM-emulsion mixes of Quartzite crushed stone without the addition of cement (Q0CE)	281
Figure 173: Effects of moisture damage on shear properties of BSM-emulsion mixes of Quartzite crushed stone with 1% cement (Q1CE).....	281
Figure 174: Effects of moisture damage on shear properties of BSM-foam mixes of Hornfels-RAP without the addition of cement (H0CF)	282
Figure 175: Effects of moisture damage on shear properties of BSM-foam mixes of Hornfels-RAP with 1% cement (H1CF)	282
Figure 176: Effects of moisture damage on shear properties of BSM-foam mixes of Quarzites crushed stone without the addition of cement (Q0CF).....	283
Figure 177: Effects of moisture damage on shear properties of BSM-foam mixes of Quartzite crushed stone with 1% cement (Q1CF)	283
Figure 178: Multistage permanent deformation results on wet BSM-emulsion (H1CE) at 40°C and confinement of 100kPa and varying stress ratios.....	284
Figure 179: Multistage permanent deformation on dry BSM-emulsion (H0CE) at 40°C and confinement of 100kPa and varying stress ratios.....	284
Figure 180: Permanent deformation results on wet and dry BSM-emulsion (H1CE) at 25°C and confinement of 100kPa at SR= 0.4.....	285
Figure 181: Comparison of square wave and haversine wave permanent deformation results on wet BSM-emulsion (H1CE) at 40°C and confinement of 100kPa at SR=0.4	285

LIST OF ABBREVIATION AND SYMBOLS

Abbreviations

AC	Asphalt concrete
ACV	Aggregates crushing value
APT	Accelerated pavement tester
BRD	Bulk relative density
BSM-emulsion	Bitumen stabilised materials-with bitumen emulsion as a binder.
BSM-foam	Bitumen stabilised material- with foamed bitumen as binder
BSMs	Bitumen stabilised materials
BWP	Between-wheel-path
CTMs	Cement treated materials
CT-scan	Collimator (x-ray) tomography
DMI	Durability mill index
EMC	Equilibrium moisture content
GPC	Gel permeation chromatography
FACT	Fine aggregates after crushing test
FTIR	Fourier transformation infra red
HMA	Hot mix asphalt
HVS	Heavy vehicle simulator
ICL	Initial consumption of lime
IL	Inner lane
ITT	Indirect tensile test
ITS	Indirect tensile strength
IWP	Inner-wheel-path
LVDT	Linear variable displacement transducer
MDR	Moisture damage ratio
MIST	Moisture induction simulation test
MMLS3	Model mobile load simulator 3 scale.
MTS	Material testing system
OMC	Optimum moisture content
OWP	On-wheel-path
PAV	Pressure ageing vessel
PI	Plasticity index.
RAP	Reclaimed asphalt pavement
RC	Retained cohesion
RDm	Relative maximum theoretical density
RH	Relative humidity
RM	Residual modulus
RTFOT	Rolling thin film oven test
RvD	Ravelling depth
SEM	Scanning electron microscopy
TRH	Transport research highway
TSR	Tensile strength retained
UCS	Unconfined compression strength
YL	Yellow-line
N7	National road 7 or expressway in South Africa

Symbols

Σ	Normal stress
ε	Strain
E	Elastic
μ	Friction
V	Velocity/speed
P	Density
ν	Viscosity
C	Cohesion
Φ	Angle of internal friction
Δ	Small increment
τ	Shear stress
T	Time
K	Coefficient
Q	Rate
Θ	Angle
L	Liquid
S	Solid
V	Volume, Vapour/gas
O	Oxygen
H	Hydrogen
C	Carbon
N	Nitrogen
S_r	Saturation
M_r	Resilient modulus
T	Temperature

Symbols for temperature distribution

A	Solar absorptivity
ε	Emissivity
$\Delta\varepsilon$	Emissivity correction
Ω	Hour angle
A	Ambient air
Dp	Dew point
Lw	Long wave
P	Pressure
S	Surface or solar
Sky	Sky
W	Wind
Z	Zenith
G	Ground
C_f	Friction coefficient
H	Conventional heat transfer coefficient
I	Solar radiation
Q	Heat flux

CHAPTER 1

INTRODUCTION

1.1 BACKGROUND

In both developing and developed countries, to ensure sustained economic growth the quest for optimal performance of roads is an extremely high priority. A global increase in the use of foamed bitumen and bitumen emulsion as a solution to roads maintenance, rehabilitation and upgrading, has become important to pavement engineers. This has created a need for practitioners to understand the mechanisms that influence the durability and long-term performance of these materials.

Like conventional hot mix asphalt (HMA) and cement treated materials (CTMs), the use of bitumen stabilised materials (BSMs) for road construction, rehabilitation and upgrading needs proper design. The mix design procedures for BSMs have advanced and this has opening an avenue for the understanding behavioural and failure characteristics of BSM mixes. The research on BSMs, however, has been limited to permanent deformation, bearing strength, shear strength and fatigue failure (Jenkins, 2000; Long, 2003; Twagira, 2006; Ebels, 2008) and little is known about durability properties. Therefore, there is potential for the development of new or improved mechanisms of failure that influence long-term performance of BSMs.

The global trend in the use of reclaimed asphalt pavement (RAP) materials in pavement construction is increasing. Similarly, the South African environmental and resource conservation Act of 2004 limits exploitation of new borrow pits for road construction and rehabilitation. Currently in South Africa, the use of RAP in pavement rehabilitation is less than 15%; nevertheless, the incorporation of higher percentages of RAP in BSMs is the objective. However, the challenge is to understanding the long-term performance and durability properties of BSM mixes incorporating the higher percentages of RAP materials.

Unlike HMA and CTMs, the durability properties of BSMs are not well understood and a sound guideline for mix design is lacking. The materials durability, mechanism of moisture failure, binder ageing and critical mechanical properties that influence durability of BSMs require clarification. This will enable reliable and cost-effective pavement structure construction. The parent mineral aggregates and binders used in BSMs are natural and found in different sources. Since the utilisation of locally available materials must be efficient and cost-effective, the selection of materials for BSMs should focus on their durability properties. Durability properties influence other mechanical performances under different environmental and traffic conditions. This is applicable to both new construction and road rehabilitation works, with the latter placing emphasis on in-place or in-plant recycling of existing pavements materials. This study therefore, focuses on the understanding of durability properties of BSMs with the aim of providing a better decision in all stages of application that is mix design, construction, and in-service condition.

1.1.2 What is durability?

Durability is a time dependent parameter or behaviour. In general terms, it is defined as enduringness, lastingness, persistence, changelessness, or everlasting (Houghton, 2000). Therefore, durability is a measure of the useful life of physical phenomena. In an engineering context, durability is defined as lastingness of structures and materials for the ability to maintain the initial performance properties through time above a certain threshold level. The illustration of durability by van de Ven (1998) is shown in Figure 1. Durability is achieved by resisting stresses and strains or withstanding destructive agents with which the materials come in contact. The

destructive agents can include air, water, light, temperature, chemicals, and traffic loading over a long period of time.

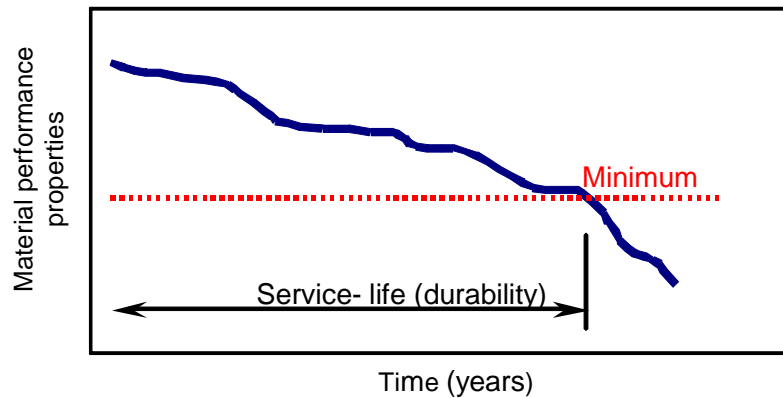


Figure 1: Conceptual illustration of engineering durability, (van de Ven, 1998)

It is clear from the definition that durability is a time-related issue and that durability has multidimensional parameters and is not a single property. Therefore as a word of caution, there is no single measure of durability of pavement materials. For BSMs, the durability has commonly been referred to only as the measure of moisture resistance. In fact, moisture damage often manifests early in a BSM's life. However, in long-term performance, other environmental factors can influence a BSM's durability. In comparison with other pavement materials, durability of CTMs is measured as resistance to disintegration and degradation of parent aggregates and carbonation effects on stabiliser e.g. lime (TRH 14, 1985). For HMA, durability is measured as resistance of binders to stripping, ageing and degeneration of modifiers in specific application, knowing that parent aggregates in HMA are adequately durable (Asphalt Academy TG1, 2007, Shell Bitumen, 2003). The fact that BSM is applicable in a wide range of aggregates (including RAP) and varying bitumen contents, its durability are based on materials durability, as well as mixture durability. Although moisture damage is considered a major factor influencing durability of BSMs, the durability of parent aggregates and bitumen are found to play a significant role (Øverby *et al.*, 2004; Jenkins, 2000; Paige-Green, 2004). Therefore, the focus of this thesis is in the understanding of the durability behaviour¹ of materials and mixture composition making the BSMs.

1.1.3 Benefit of durability properties

For any product to have a sustainable performance, it must have certain qualities that make it suitable for its intended function. The benefits of understanding the durability properties of materials and mixture composition of BSMs can lead to improvement on:

- Mix design procedure
- Defining failure mechanisms
- Pavement modelling and design procedure
- Short-term strength characteristics
- Long-term performance prediction
- Life cycle for maintenance and rehabilitation and,
- Life-cost benefit analysis

¹ Durability behaviour and durability properties are used interchangeably in this thesis

The author believes that these benefits can be realised through an understanding of the physicochemical and mechanical properties of materials and mixes constituting the BSMs. To this end, a clear objective of materials' properties evaluation and mechanisms of failure manifested in BSMs can provide a reliable and distinctive qualitative measure of the BSMs' engineering properties in long-term performance.

1.1.4 Modelling of pavement materials' durability

Pavement modelling is used in the design and analysis in order to provide safe and economical pavement structures. The behaviour of a pavement structure depends solely on its geometry, environmental condition, applied loads and the material(s) used (Erkens, 2002). To arrive at a good design method, both material behaviour and pavement structure must be modelled with sufficient accuracy. The least researched and documented aspect of BSMs is durability properties. This is evident from the literature review indicated in the forthcoming chapter.

Most studies on the long-term performance of BSMs provide procedures for pavement design based on permanent deformation and fatigue behaviour. There is no cognisance of or an attempt to account for the mode of failure based on durability properties. The need to develop a methodology for modelling the durability properties of BSMs and prediction of long-term performance is therefore vital. However, modelling durability properties is complicated due to the diversity of materials. BSM is applicable on a wide range of materials from marginal at lower binder content to high-quality granular materials at high binder content. Therefore, development of a unified model that satisfies this range of mixes is ambitious and probably unrealistic. For this reason, in this study, the focus is on mixes particularly pertinent to high-quality granular and RAP content commonly used in South Africa.

Modelling of durability behaviour is not the prime focus in this thesis and therefore receives only a short analysis. Figure 2 shows the influence of load, binder and moisture on durability behaviour of HMA. HMA is a top layer in South African pavement structures, therefore the effects of stripping (moisture damage) in HMA influence the durability behaviour of the underlying base layer, such as BSMs.

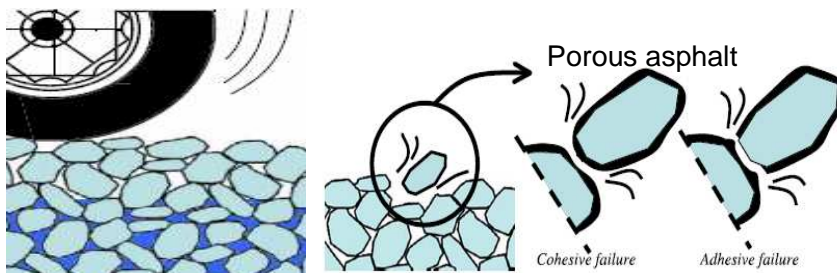


Figure 2: Moisture diffusion on aggregates-mastic interface resulting in cohesive and adhesive failure (Erkens, 2002)

1.2. THE NEED FOR DURABILITY PROPERTIES OF BSMs

1.2.1 Purpose and usefulness

Pavement engineers clearly understand that pavement materials are predominantly natural and variable. Therefore, the area of application influences their variability, suitability and the behaviour of the composite materials. Pavement materials are often a combination of numerous ingredients formulated, combined, and processed to provide a composite product for a specific purpose. In order to produce construction materials with the necessary quality and consistency to fulfil their intended function, adequate mix design procedures need to be established. This will

assist in identifying durability properties for optimal formulation, blending, and production of pavement materials. Durability properties are particularly pertinent for the mix design procedure of BSMs.

The long-term performance models developed for the BSM mix design focuses on rutting as a function of stress ratio and flexibility. Of all the aspects of mix design, durability is one of the most difficult to address. This is due to a number of factors, explained below:

- The diversity of ways in which the durability of materials is measured, e.g. resistance of aggregates to wear and tear, resistance of binder to age hardening and resistance of mixture to moisture damage.
- Difficulties in the identifying unified durability mode of failure of BSMs and mechanisms contributing to this failure.
- The variety of mix properties and intrinsic materials' properties that can influence durability, e.g. gradation of mineral aggregate, aggregate properties, binder type and content, use of active filler, etc.
- The varieties of external factors on BSMs e.g. climate, traffic load, including speed, magnitude, configuration and their variability.
- The difficulties in simulating durability effects in a manner that does not negatively effect selection of different mix properties.
- Time and cost involved in modelling durability behaviour of materials simulating field conditions accurately through research.

Notwithstanding these difficulties, studies by Jenkins, (2000); Collings, (2007); Long, (2001); Øverby *et al.*, (2004); and Paige-Green and Ventura, (2004), have indicated that the fundamental durability on materials and mixes requires consideration during mix design of BSMs. In particular, material durability needs to be characterized in terms of its suitability prior to its application. Although moisture susceptibility is the prime factor in addressing durability requirements of BSMs mixes, the entire definition outlined above is at the core issue under consideration.

1.2.2. Materials and mixture behaviour

The main materials composing BSMs is bitumen binder (foamed bitumen or bitumen emulsion), virgin aggregates and/or RAP and addition of active filler (lime or cement). The use of bitumen emulsion and foamed bitumen in stabilisation of the pavement materials is the technology which has been around globally for many years (Ebels *et al.*, 2005; 2007). In South Africa, the use of bitumen emulsion started in the 1960s and foamed bitumen become famous in the 1990s after the expiration of certain patents on foamed bitumen production (Ebels *et al.*, 2005).

The development and invention of different bitumen emulsions since the 1950s (anionic or cationic) has significantly improved the use of cold bitumen technology. In South Africa, the use of Cape seal, texture slurries and an emulsion-treated base, contributed to the popularity of anionic stable emulsion over cationic due to climatic influence on anionic emulsion. The stability of bitumen emulsion however depends on the type and quantity of emulsifier used (Louw, 1997). In most cases 80/100 penetration grade bitumen is used to produce bitumen emulsions, although in different requirements 60/70 penetration grade bitumen may also be used. Jenkins (2000) provides a comprehensive literature on the development of foamed bitumen globally and the advances in the mix design of foamed bitumen in BSMs. The production of foamed bitumen is commonly uses standard 80/100 penetration grade bitumen, although softer base bitumen 150/200 or hard base bitumen 60/70 may also be used. Researchers have raised concern about the long-term performance and durability of the standard bitumen on stabilised materials. It is obvious that bitumen undergoes physical and chemical change during its service life (Shell Bitumen, 2003). However, little has been done towards understanding the ageing behaviour of

BSM-emulsion or BSM-foam. Therefore, it is apparent that a study of short-term and long-term performance and durability properties of BSMs in term of age hardening is vital.

Mineral aggregates constitute the largest part (both in mass and volume) of BSMs. Crushed stone, natural gravel, RAP and natural sand are amongst the mineral aggregates used to produce BSMs. When in-situ recycling is applied, the selection of aggregates is limited and one has to work with the materials present in the pavement. Weinert (1980) states that materials placed in the pavement layers normally have specific properties at the time of testing or construction that need to be retained over the service life of the layer; hence, mineral aggregates need to be durable. Durable aggregates are able to resist deterioration or disintegration and so retain their original grading, shape and physicochemical properties during the service life of the pavement.

Disintegration of poor aggregates can occur during construction and/or during in service condition. Disintegration during construction is a result of hauling, damping, spreading, mixing, and compaction. Whereas during in-service condition, it is a result of compression/deflection, abrasion/erosion under loading and/or physical disintegration by salt, freezing and thawing. The effect of disintegration is the addition of fines into the materials. This may results in changes to specific surface of the mix permeability, and engineering properties such as shear properties, and stiffness. Decomposition of poor aggregates may result in the release of secondary minerals (i.e. change in mineralogy of materials), increase in the Plasticity Index (PI) and reduction in bearing strength of the pavement layer.

Physicochemical properties of mineral aggregates have a significant influence on adhesion behaviour with the binder and water, among other factors. *Adhesion* is a Latin word which means 'to stick to'. ASTM D097 gives its scientific context as "the state in which two surfaces are held together by valence forces or interlocking forces, or both". The fundamental of adhesion with the emphasis on surface free energy have extensively been studies for HMA (Hefer *et al.*, 2005). Since adhesion between bitumen (mastic) and aggregates is one of the important prerequisites for obtaining durable BSMs, the fundamental of the surface free energy theory and its potential for understanding mechanism of failure and long-term performance need to be explored for BSMs.

Due to the inherent variability in durability conditions of rocks and natural gravel, it is essential also to have a good understanding of:

- Mineralogical composition
- The stage of weathering of the materials
- Secondary mineral type and content
- The expected in-place weathering process

Weinert (1980) indicates that suitable materials can be found everywhere in South Africa, but particular care is required when selecting weathering crystalline rocks or diamictites for use in a pavement layer. Based on "N-values"² and percentage content of secondary mineral produced during decomposition of rock type, Weinert defined limits for durable and non-durable material as indicated in Figure 3.

² N-value, numerical value describing the different climatic environment, see formula in chapter 2

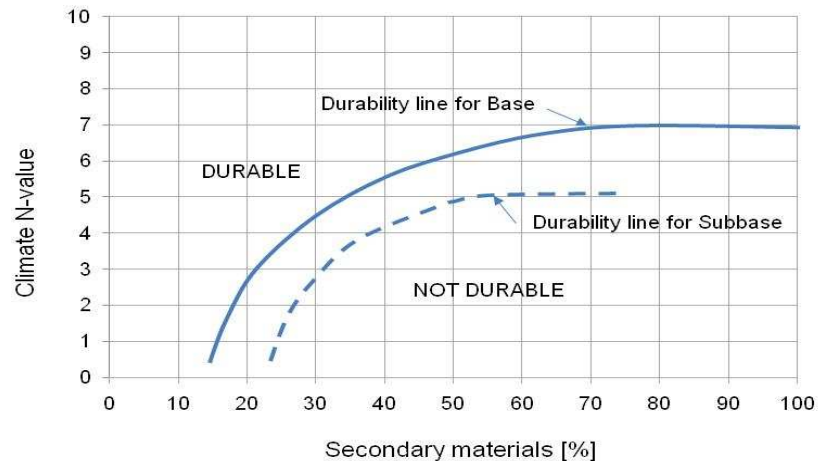


Figure 3: Durability of weathered crystalline rocks in pavement, depending on the N-value and the percentage of secondary minerals (Weinert, 1980)

1.2.3 Comparison of BSMs durability with other mixes

Table 1 highlights some of the differences between BSMs and other pavement mixtures (HMA and CTMs): It compares the material behaviour in terms of mixtures and long-term durability.

Table 1: Summary of comparative materials and long-term durability of different pavement mixtures

Factor	BSMs	HMA (AC)*	CTMs
Aggregate type applicable	Durable to less durable	Durable	Durable to less durable
Binder content	1.5%-3.5% residual bitumen foam or emulsion	5%-7% bitumen	3%-8% cement or lime
Void content	12%-15%	4%-5%	< 10%
Strength gain	Slow	Fast	Medium
Failure	Permanent deformation, shear, bearing	Permanent deformation, shear, creep, fatigue, cracks	Compression, carbonation, cracks
Moisture damage	Ravelling, erosion, pumping	Stripping, polishing	Erosion, pumping

*Note AC refers to dense asphalt concrete

The purpose of a mix design procedure is to produce combined construction materials with the necessary quality and consistency to fulfil their intended function. The poor long-term performance of pavement materials has been in many instances attributed to insufficient understanding of durability properties of the mixture and constituent materials. It is evident from Table 1 that, although some of the aspects of the mix design process, such as material selection, are shared by BSMs, HMA and CTMs, some fundamental difference in the composition and preparation of these mixes occur. In particular, the binder characteristics differ markedly between HMA and BSMs. Similarly, addition of cement in BSMs and CTMs differs significantly. Furthermore, the inclusion of a water phase in BSMs introduces more complicated durability properties. These and other factors require consideration in the development of an improved determination method of durability properties of BSMs.

1.2.4 Statistical requirement for material classification

The durability of BSMs is relatively unknown, and therefore faces with a wide array of test parameters and condition indicators. These parameters can be quantitative or qualitative and subjectively or objectively determined. Therefore, no single test is able to quantify durability properties and the sample sizes for different indicator types may vary significantly.

It is imperative however, in pavement engineering that due to the number of variables for material characterisation, holistic assessment is given preference to aid classification and the understanding of performance behaviour. Jooste *et al.*, (2007) indicates that quantifying uncertainty is related to the sample taken, but assessment of data to draw a conclusion is often more complex and sample size is just one of many factors to consider. Minimisation of uncertainty in mix and pavement design is not often as simple as just taking more samples. Rather, it largely depends on the engineer's judgment and background of the limited collected samples. Statistical reliability requires a sufficient number of test specimens to analyse average, standard deviation, and confidence interval. A medium sample size of 3-10 and a large sample size of greater than 30 are required to minimise uncertainty of one indicator. However, this is only possible when limited variables are involved or sufficient time and money is available. In this study, small samples were used to provide wide range on durability assessment rather than focusing on the reliability of a single indicator. The reliability versus completeness concept is provided in Figure 4 as an indicator of the importance of a small sample for the characterising of pavement materials.

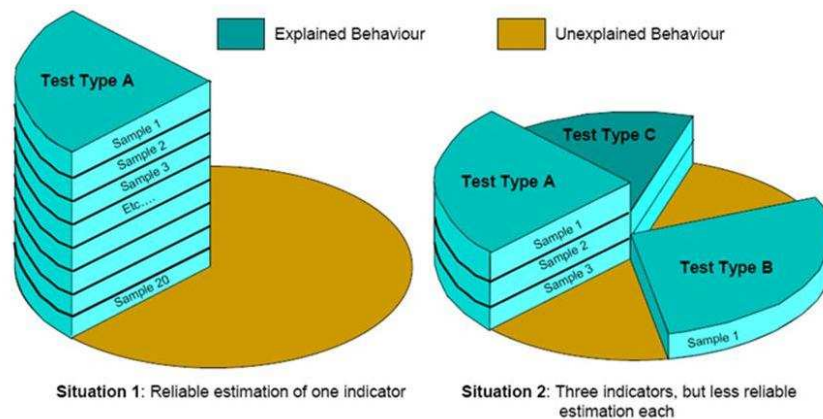


Figure 4: Conceptual reliability versus completeness on pavement materials evaluation (Jooste *et al.*, 2007)

An important aspect of evaluation of durability properties is that each test must provide a single valuable information of the materials evaluation. In a holistic evaluation approach, what is needed is not more of the same information, but many different information, as indicated in Figure 4. Given the fact that most test parameters provide incomplete information, the approach would be to regard each evaluation as an additional information of evidence. Based on a holistic evaluation approach, a problem statement was formulated to assess the durability properties and long-term performance of BSMs as described in section 1.2.5.

1.2.5 Problem statement

From the background information, it is evident that practitioners globally are faced with the challenge of understanding proper manifestation of BSM durability. The fundamental durability problem can be categorised as aggregate durability, binder durability, and their interaction, including other components such as water and active filler. To this end, understanding of BSM durability requires manifestation of three main components all working at the same time that is

binder (bitumen) durability, aggregate durability and their interaction. The latter demonstrate mastic durability, which is a combination of bitumen, filler fraction and moisture and the addition of an active filler. The author abbreviates these key components as “BAMD” as described in Figure 5.

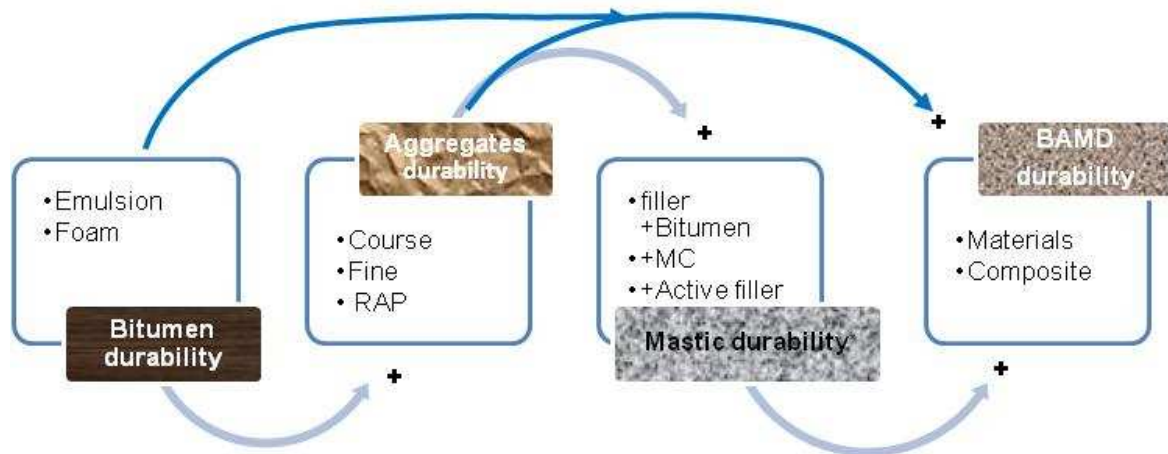


Figure 5: Key elements determining the durability properties of BSMs

The pertinent problems of BAMD are resistance of the binder to age hardening, resistance of aggregates to wear and tear and resistance of mixture (mastic) to detrimental effects e.g. moisture ingress, temperature effect and loading effect. The identification and understanding of physicochemical and mechanical factors and the mechanisms contributing to failure of BAMD, through external factors such as climate, traffic and their variability, is the centre of the problem. Therefore, these parameters will be addressed throughout this study. The study will try to determine durability properties in a manner that is unique to different mix properties, whilst applying laboratory and field conditions accurately.

1.3 OBJECTIVES AND SCOPE OF DISSERTATION

In the light of the shortcoming in existing design guidelines and manuals and the ongoing development of the unifying guideline for BSM-emulsion and BSM-foam, understanding of the fundamental durability behaviour and long-term performance of these materials requires further research. In a broader perspective, the aims invariably include requirements set by sponsors of the research to extend the existing knowledge of BSMs with a view to improving the mix design and structural design of pavement. These requirements are refined into objectives and scope of this research as detailed below:

Critically review and analyse durability-related issues of BSM constituent materials and mixtures. At present, only spatial compositions and engineering properties for monitoring mineral aggregates suitability of BSMs are documented. In the same way, limited studies have been documented on the fundamentals of mineral aggregates durability, binder durability and behaviour of BSMs. Therefore, identification of main factors contributing to BSMs durability on mix design criteria requires development. In particular, mineral aggregates and binder interaction, binder and filler fraction behaviour as well as the influence of active filler and moisture on the mix characteristics require clarity. Therefore, the objective of the research is to

recognise of factors that influence the durability behaviour of BSMs and establish well-founded boundaries within which these factors should be approached for mix design proposal.

Developing the fundamental understanding of mechanisms that govern durability behaviour of BSMs, with emphasis on moisture sensitivity. Current understanding of BSMs moisture sensitivity is limited and based on empirical relationships. Several laboratory procedures have been developed for the identification of BSM mixes with unacceptable moisture sensitivity. Nevertheless, optimisation of BSMs durability properties was not possible. The identification of a relevant method that simulates field conditions and the development of a laboratory moisture conditioning device to effectively optimise the mix design is an objective of this study. If possible, such device should be structured to suite the needs of the road construction industry.

Validation of a newly developed laboratory device for moisture conditioning (Moisture Induced Simulation Test, MIST) of BSMs. A known Accelerated Pavement Tester (APT) device, that is Model Mobile Load Simulator (MMLS3,) is used for validation purposes. As part of the development of a newly designed experimental device for laboratory moisture conditioning, validation of the test results with a known device is necessary. APT devices such as MMLS3 are known for simulating pavement performance in terms of moisture damage. This simulation takes into account the material's durability under the influences of traffic and environmental conditions. An objective of the research is to perform parallel tests of similar mix types conducted in a newly developed laboratory device (MIST) and in the MMLS3 device. The correlated test results will provide reliability for applicability of the new device. In addition to validation, the test results may provide understanding of the moisture failure mechanisms related to field performance of BSMs.

Identification of triaxial test parameters that advances the investigation into mechanisms that influence moisture damage in BSMs. It is essential to classify BSMs into representative groupings with similar behavioural characteristics followed by the selection of the pertinent performance criteria for the mix and pavement design. The objective of this research is to investigate mechanisms that influence durability properties and long-term performance through triaxial tests including advanced parameters such as square wave loading and different temperatures on specific selected materials.

Demonstration of moisture-induced damage and its influence on pavement performance. This links laboratory test results with the performance of the BSM pavement layer with respect to moisture damage. The mechanisms that influence moisture sensitivity in BSMs should preferably be measurable through mix design and utilised in pavement design by incorporating the relevant mix properties. The objective of this research is to demonstrate the relevance of pavement models to sufficiently capture moisture sensitivity of BSMs as determined in the laboratory.

Identification of the influence of temperature and voids distribution in the BSM mixes particularly in the field condition. Temperature distribution in pavement layers plays a significant role in both the ultimate gains of mix engineering properties and the exhibition of premature distress. Void content distribution in the mix influences moisture transport into the BSM layer as well as enhancing age hardening of the binder. The objective of this research is to identify temperature distribution behaviour and its magnitude in the BSMs layer under field environmental conditions. The temperature distribution can be linked to void content characteristics in the mix to provide a better understanding of the influence of curing or evaporation of moisture from the BSM layer. In addition, the mechanism of age hardening as well as moisture damage potential can be accurately defined.

Establishing the age hardening characteristics of binders in BSMs, that is emulsion and foamed bitumen. Current understanding of BSMs binder age hardening behaviour is limited. While significant advances have been made in the use of BSMs in pavement construction and rehabilitation, the problem of binder hardening is a concern for practitioners globally particularly

its performance during in-service conditions. The identification of relevant mechanisms influencing the binders age hardening behaviour of BSMs is an objective in this study. As such, the study investigates the differential laboratory and field ageing (if any) for the foamed bitumen and bitumen emulsion and establishes the knowledge base for the mix design of BSMs.

The scope of this study is described in the overall research approach presented in Figure 6. It encompasses, first, the critical review and analysis of past studies on the durability-related issues pertaining to mineral aggregates and binders in BSMs. The focus is on durability properties of the materials constituting BSMs and their interactions. Second is the development of a laboratory moisture conditioning device and related procedures by performing limited tests for effectively optimising mix design procedures of BSMs. The applicability of the developed MIST device is validated using the APT laboratory MMLS3 device. The test matrixes involved in the studies are indicated in Chapters 3,4,5 and 6. From the matrices, it can be seen that the BSM study is limited to two granular material types (Hornfels-RAP from N7 near Cape Town and Quartzite crushed stone from Prima quarry in Western Cape Province), one type of bitumen (80/100) for foamed bitumen, one type of emulsion (ANiB SS-60), one grading for each aggregate, one compaction method, standard curing, and mechanical testing i.e. triaxial testing and ITS test. In addition limited triaxial tests are performed for advance classification of BSMs. Third is the collection of field temperature and relative humidity data from selected pavement sections and a demonstration of their distribution in the BSM layer. Last, but not least is binder age hardening behaviour. The investigation on binder ageing is limited to laboratory prepared specimens i.e. Hornfels-RAP and Quartzite materials, as well as field extracted cores. Extracted field cores came from selected existing pavement sections of N7 near Cape Town, P243 in Vereeniging Gauteng, Grassy park roads in Cape Town as well as Shedgum Road in Saudi Arabia.

Finally, significant conclusions are highlighted and recommendations for the future studies are provided.

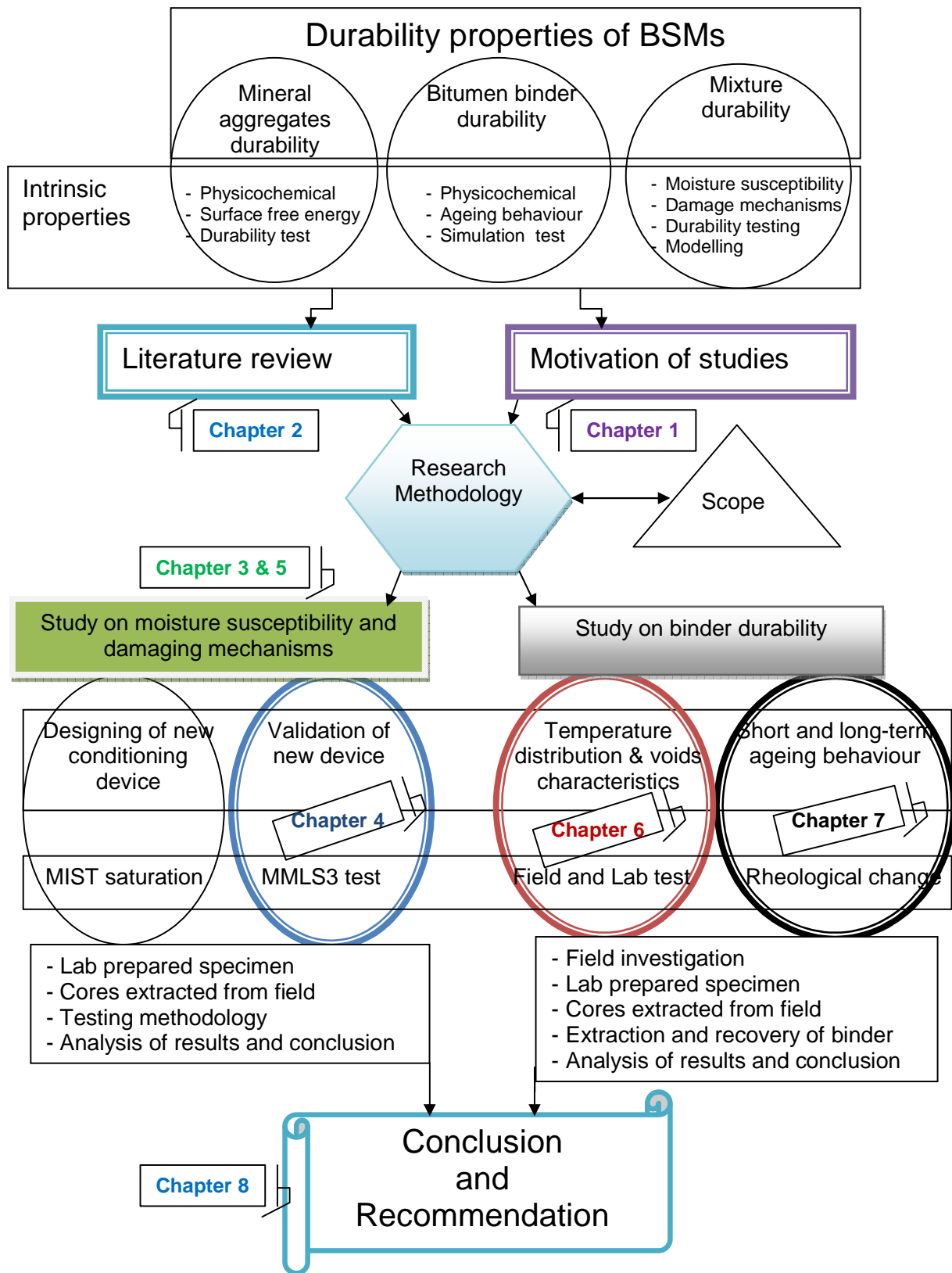
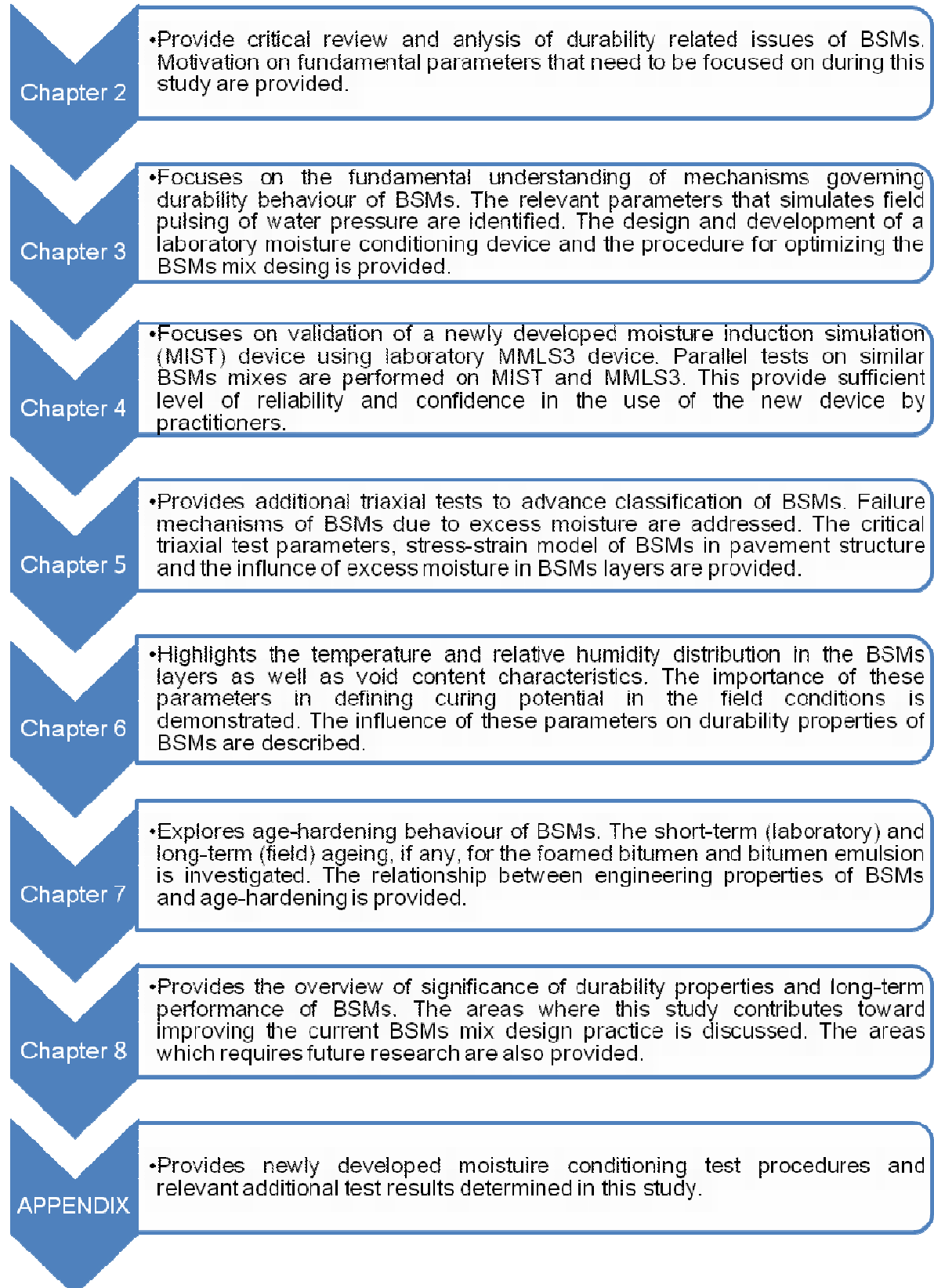


Figure 6: General overview of the research approach

1.4 LAYOUT OF DISSERTATION



REFERENCES

- Asphalt Academy TG1. 2007. The use of modified bituminous binder in road construction. 2nd edition. Technical guideline. Pretoria. South Africa.
- AASHTO, 2002. Standard test method for resistance of coarse aggregates to degradation by abrasion in the Micro-Deval Apparatus. AASHTO Designation: TP 58-02.
- Collings D. and Thompson H. 2007. A critical appraisal of the performance of foamed bitumen and bitumen emulsion treated materials. 9th conference on asphalt pavement in Southern Africa. Gaborane, Botswana.
- Ebels L, Jenkins K. and Collings D. 2005. Cold mix (Bitumen stabilisation) technology in Southern Africa into the 21st Century. International symposium on pavement recycling. Sao Paul, Brazil.
- Ebels L, and Jenkins K. 2007. Mix design of bitumen stabilised materials: Best practice and considerations for classification. Proceedings of the 9th conference on asphalt pavements for Southern Africa (CPSA), Gaborone, Botswana.
- Ebels L.J. 2008. Characterisation of materials properties and rehabilitation of cold bituminous mixture for road pavements. PhD dissertation, published at the University of Stellenbosch, South Africa.
- Erkens S. 2002. Asphalt concrete response (ACRe): Determination, modelling, prediction. PhD dissertation, published in Delft University of Technology, The Netherlands
- Houghton Mifflin Company, 2000. Dictionary of English language, 4th edition. Princeton University, USA.
- Hefer A. and Little D. 2005. Adhesion in bitumen-aggregate systems and quantification of the effects of water on the adhesive bond. PhD dissertation, Texas A&M University, College Station, Texas.
- Jenkins K.J. 2000. Mix design consideration for the cold and half-warm bituminous mixes with emphasis on fomed bitumen. PhD dissertation, published at the University of Stellenbosch, South Africa.
- Jooste F., Long F. and Hefer A. 2007. A method for consistent classification of materials for pavement rehabilitation design. Technical memorandum CSIR/BE/IE/ER/2007/0005/B. Pretoria.
- Long F. 2001. The development of structural design models for bitumen treated pavement layers. Contract report CR-2001/76. CSIR Transportek. Pretoria.
- Louw L. 1997. ETB mix design. Summary for the best practice. Contract report CR96/079. Transportek, CSIR. Pretoria. South Africa
- van de Ven M.F. 1998. Pavement material III, Module 3 bitumen type and composition. Presentation for postgraduate course, at Stellenbosch University, South Africa.
- Paige-Green P. and Ventura D.F.C, 2004. Durability of foamed bitumen treated basalt base course. CSIR report CR 2004/8. Pretoria. South Africa.
- Øverby, C., Johanson, R. and Mataka, M., 2004. *Bitumen foaming*: An innovative technique used on a large scale for pavement rehabilitation in Africa. Case study: Same-Himo monitored pilot project. Proceedings of the 8th Conference on Asphalt Pavements for Southern Africa (CAPSA'04). Sun City, South Africa
- Shell Bitumen, 2003. Shell Bitumen Handbook. Shell Bitumen UK.
- TRH 14, 1985. Guideline for road construction materials, Department of Transport, Pretoria, South Africa.
- Twagira M.E. 2006. Characterisation of fatigue performance of selected cold bituminous mixes. MSc. thesis. University of Stellenbosch, South Africa.
- Weinert H.H. 1980. The natural road construction materials of Southern Africa. Academia. Cape Town. South Africa.

CHAPTER 2

LITERATURE REVIEW ON DURABILITY PROPERTIES OF MATERIALS AND MIXTURE COMPOSITION OF BITUMEN STABILISED MATERIALS

2.1 INTRODUCTION

Material and mixture durability plays a significant role during the selection of combined, formulated and processed BSMs for mix design. The mix design should maintain its initial performance properties through time above a certain threshold level by resisting stresses and strains or withstanding destructive agents within which the materials come in contact, such as traffic and environment. This extends material performance for the intended design period, so that performance prediction can be predicted as shown in Figure 7. It is important that the factors influencing failure in selected materials be clearly defined. Failure mechanism in BSMs cannot be determined through mechanical evaluation alone, but studies at micro and macro levels of binder and mineral aggregate interaction need to be analysed. Thus, the constraints and restrictions in terms of durability behaviour, scope and time, need to be fully understood. In this way, the mix design can be optimised by addressing certain aspects of investigations that ensure that the collected data is sufficient and appropriate to result in the correct decision in the application of BSMs.

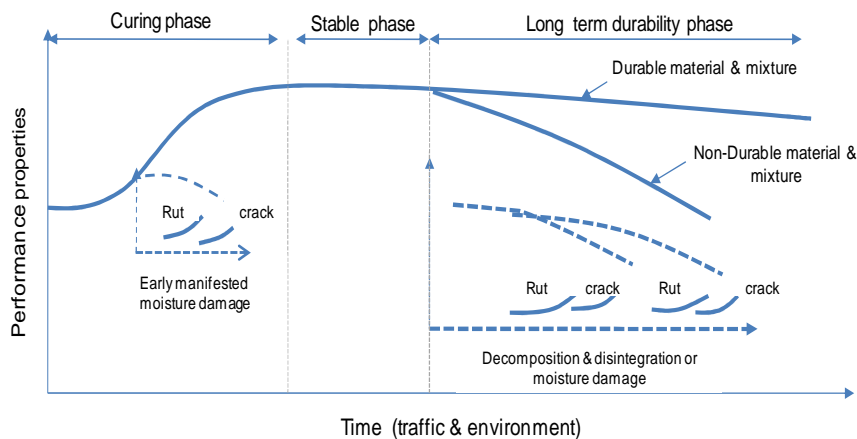


Figure 7: Conceptual performance properties of BSMs in different phases

In this study, a distinction is made between material durability requirements and mixture composition requirements for the durability properties and long-term performance of BSMs. Material durability relates to characteristics of mineral aggregate and binder (foamed bitumen or bitumen emulsion) requirements in fulfilling the intended function. The mixture composition requirements relate to the mix design performance necessary to guarantee the functional and structural capacity of the pavement layer. To highlight these requirements, a critical review and analysis of durability-related issues of BSMs will be discussed according to the main variables constituting BSMs and fundamental engineering properties. Figure 8 presents compositional

variables, which characterise the BSMs durability properties and long-term performance in the field.

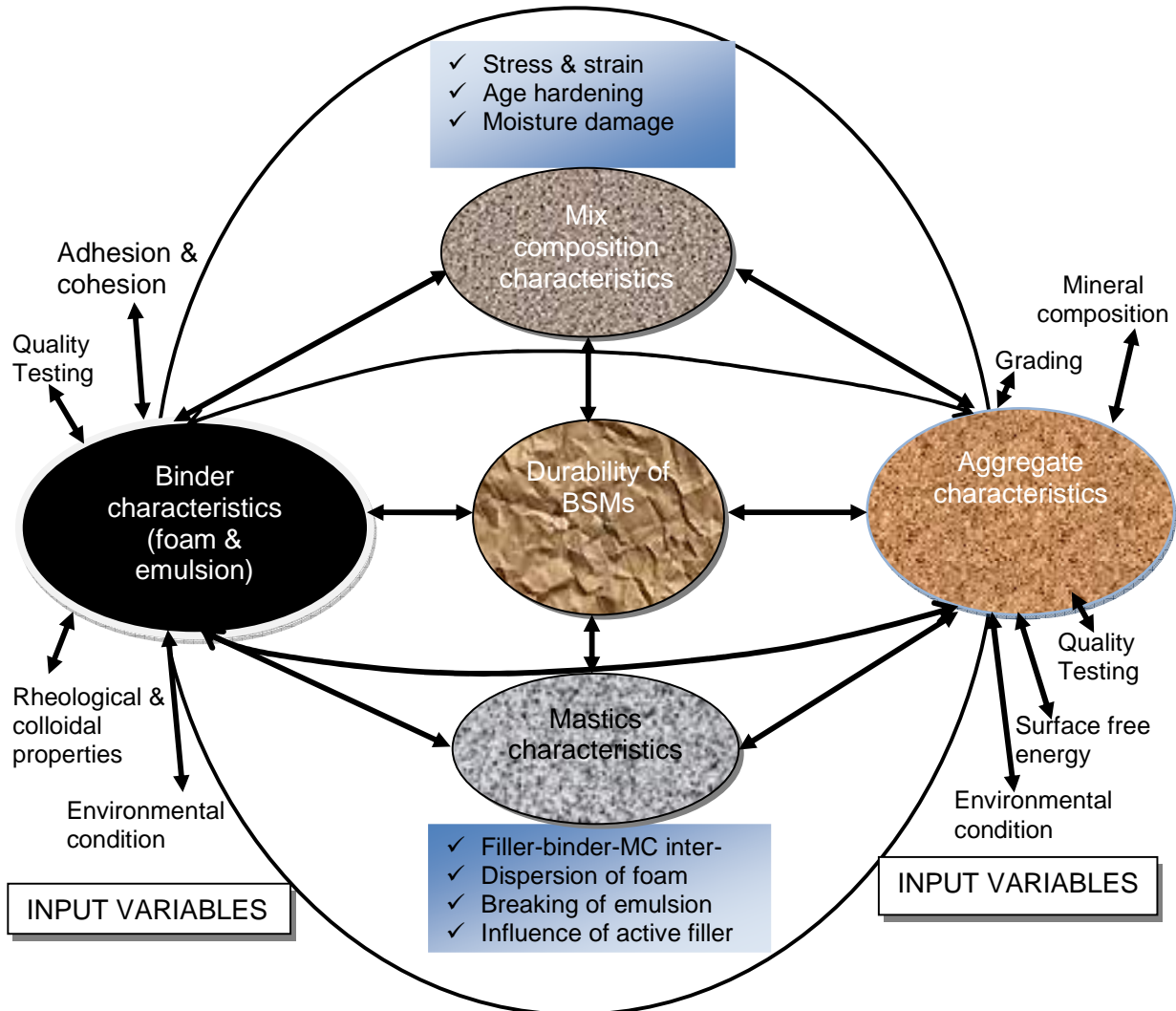


Figure 8: Main variables influencing durability properties and long-term performance of BSMs

This chapter reviews the important factors that influence the durability properties and long-term performance of BSMs. The review provide substantial understanding of the mechanisms related to BSMs durability behaviour and compiles the research to investigate some of the more important, but less understood variables, with the emphasis on:

- Characterising durability properties in terms of physicochemical, mechanical and electrokinetic properties of aggregates and binder. These aspects, put emphasis on the use of surface free energy techniques to determine the relationship between binder and mineral aggregates properties and bonding.
- Interaction between mastic (filler: binder: MC) and aggregates surface during adhesion. In addition, reviewing the factors that influence failure mechanisms due to moisture ingress and age hardening in mixes composition.

- Analysing the effects of the application of active filler (cement or lime) on the properties of binder-aggregate interaction, dissolution behaviour, kinetic effect, binder bonding energy and type and engineering performance.

Further research is recommended into the pertinent issue of binder-aggregates surface free energy characterisation. Here follows a review of the main variables presented in Figure 8, which influence durability properties and long-term performance of BSMs.

2.2 MINERAL AGGREGATES DURABILITY

2.2.1 Background

The durability behaviour of mineral aggregates is primarily controlled by the mineralogical composition and physicochemical characteristics of the parent rock or soil. The properties such as morphology, electrokinetic and mineral composition play a significant role in the interactions among aggregates, binder and water (Tarrer and Wagh, 1991). Therefore understanding these properties is important, especially for BSMs whose mineral aggregates constitute the largest part, both in mass and volume. Unlike HMA, where mineral aggregate durability plays a key role in the selection during mix design, BSM mineral aggregates are selected based on PI and grading requirements. To this end, BSM technology has been successfully applied to a wide range of natural aggregates of sound and marginal quality, from both virgin and recycled sources (Jenkins, 2000). In contrast to artificial materials, natural rock and soil cannot be artificially controlled for intended use and so their behaviour during in-service life cannot easily be predicted over time, Dukatz (1989).

As a result of the ubiquitous nature of suitable aggregates for BSMs, research in the past focussed on specific types of materials. Ruckel *et al.*, (1983) list suitable materials for foam treatment such as crushed stone, natural gravel, sand, silty sand, sandy gravel, slag, reclaimed aggregate and ore tailing. Other researchers investigated the performance of these materials, these are; Acott (1979, 1980) researched sands stabilised with foamed bitumen, including aeolian sand, river sand, mine sand and blends of these materials. Jenkins (2000) investigated crushed Hornfels-RAP stone, Philippi sand and Dolerate gravel. Lee (1981), Ebels (2008), Twagira (2006) investigated recycled materials (combination of RAP and virgin aggregates) and Dijkink (1992) investigated slag residual and ashes from zinc production. Paige-Green and Ventura (2004) investigated weathered basaltic treated with foamed bitumen. Furthermore, SABITA (1993, 1999) recommends that the selection of aggregate for bitumen emulsion should take into account charges compatibility.

It is apparent from the mentioned studies that the influence of parent soil and rock durability on the performance of BSMs was not investigated. However, extensive research on rock and soil reported by Weinert (1980) indicates that when rock is exposed to the surface (excavated from its natural state) it changes its properties gradually change. During this transformation process, many intermediate stages occur during which the rock's physicochemical properties may be very different. Weinert further commented that it is important during selection of natural aggregates for mix design, to first consider durability properties. Thus testing durability of mineral aggregates assesses the following:

- Suitability for its intended function
- Variability during service life (weathering process)
- Initial quality during construction
- Limitation to specification
- Comparison with different sources

The review in this study will focus more on the less understood aspects of rock type or soil (physicochemical properties) that control the interaction of mineral aggregates, binder, and water in BSMs. The emphasis is on intrinsic aggregate surface properties, environmental and processing in-situ or in plant that can significantly alter the physical chemical state of aggregate

surface and in turn influence the aggregate-binder bond strength. Studies conducted in South Africa by Sampson *et al.*, (1989), and Sampson (1991) indicate that various granular materials used in base layers, and cover of seal layers, disintegrated and/or decomposed with the formation of excessive plastic and non-plastic fines under traffic and environmental conditions. Paige-Green (1989a, 1989b) researched granular materials placed in base layers and recommends that granular material suitability for use in a base layer depends on particle sizes distribution, cohesion, adequate strength and hardness. Weinert (1980) reports that suitable materials can be found everywhere in South Africa, but particular care is required when selecting weathering crystalline rocks or diamictites for use in pavement layers. Mineral aggregate being dynamic systems are affected far more by traffic, environment, and state of material conditions. The durability aspect is probably the principal component of the total system affecting long-term performance and durability behaviour of BSMs. Therefore, a method for classifying mineral aggregates durability is vital during a BSM mix design process. Due to inherent variability of durability of rocks and natural gravel, it is essential to have good understanding of:

- Mineralogical composition
- The stage and expected in-place weathering of the materials
- Climatic effect and
- Aggregates properties

This section critically analyses the components of mineral aggregates that influence the durability behaviour of BSMs. Mineral composition of aggregates has significant influence on binder-aggregates bond characteristics. However, the stage and expected in-place weathering together with production of secondary mineral type and content is unknown for BSMs. The in-place weathering might influence the Plasticity Index (PI) and the grading of the mix. Moreover, the change in aggregate physicochemical properties has influence on the interlocking properties and bonding in the BSM mix matrices. All these factors have a significant effect on contribution to engineering properties and the consequent durability behaviour of the BSM layer. Additionally, a property such as surface free energy of mineral aggregates is of significant importance and needs to be analysed as to its relevance and applicability to the correct selection of aggregates during mix design. The investigations on typical BSMs used in South African pavement structures are recorded in the Long Term Pavement Performance (LTPP) database (Long, 2007). The extracted information from LTPP is discussed. Lastly, the testing methods applicable for classifying granular and sand minerals and possible mix design limits for BSMs are described. Recommendations for further research in this area are also discussed.

2.2.2 Mineralogical composition

The mineralogical and chemical composition of mineral aggregates is known to be important factors in the understanding of binder-aggregate interaction. The knowledge of bonding, crystal structure, surface characteristics and weathering behaviour of mineral aggregates is the most important aspect in understanding the durability of mineralogical composition and interaction with other phases i.e. gas and liquid (Mitchell, 1993). The bonding in rock minerals influences the surface adsorption and desorption properties (porosity), which in turn determine the flow and attenuation of various substances through soil. The properties of pavement construction materials therefore depend primarily on mineral composition and secondarily on the size, shape and arrangement of and bond between the minerals (Weinert, 1980; Mitchell, 1993). Large numbers of rock-forming minerals are present on the earth; they are grouped according to similarities for easy durability assessment. Most rock-forming minerals are composed of silicates (SiO_2), carbonate (CO_2 or CO_3) and sulphur. The silicate minerals are the most abundant constituents of the mineral aggregates and soils in the earth's crust. Mitchell, (1993) indicates that mineral aggregates composed of an assemblage of one or more minerals that have definite chemical compositions and order of atomic arrangement. The arrangement of the

atomic lattice is such that each atom is bound by neighbouring atoms through electrostatic coordination bonds. The coordination bonds of silicate polyhedral groups are described in Figure 9 and Figure 10.

When aggregates are crushed or cleaved in the quarry or during construction or in-service condition the new surface atoms are unbalanced due to some of their neighbouring atoms and some of the coordination bonds are broken. These atoms seek to form new coordination bonds to replace the broken ones (Thelen, 1958). This molecular activity serves as the basis for the development of surface charge, literarily described as the concept of surface free energy. This concept recommends the study of thermodynamic theory. New coordination bonds can be formed by directing some of the forces inward with consequent orientation adjustment of the crystal lattice as the atoms are pulled closer. Another way to satisfy the broken bonds is to attract to the surface contaminants such as water and organics (clay) to serve as bonding sites for the functional group of bitumen (binder mastic) in the bituminous mixture composition.

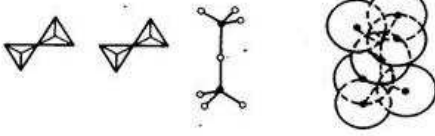
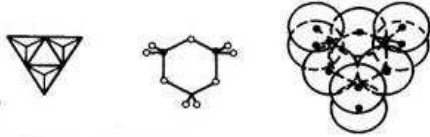
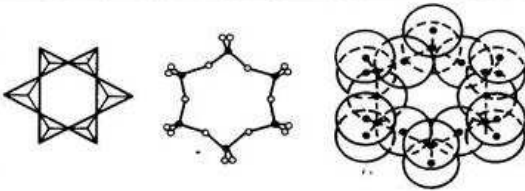
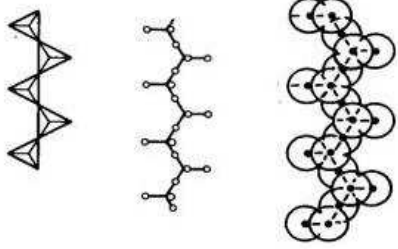
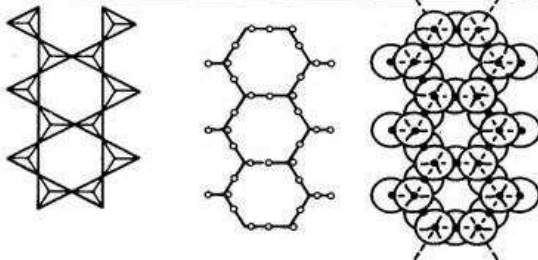
Combination of Tetrahedra	Diagrammatic Representation of Structure	Si-O Group and Negative Charge	Oxygen to Silicon Ratio	Example
Island Independent		$(Si_4O_4)^{4-}$	4 : 1	Olivines $(Mg, Fe)_2SiO_4$
Double		$(Si_2O_7)^{6-}$	7 : 2	Amermanite $Ca_2Mg_2Si_2O_7$
Rings		$(Si_3O_9)^{6-}$	3 : 1	Benitoite $BaTiSi_3O_9$
		$(Si_6O_{18})^{12-}$		Beryl $Be_3Al_2Si_6O_{18}$
Chains		$(Si_nO_{3n})_n^{2-}$	3 : 1	Pyroxenes
Bands		$(Si_nO_{3n})_n^{6-}$	11 : 4	Amphiboles

Figure 9: Crystal chemistry of silicate rock and soil type (After Michell, 1993)

Combination of Tetrahedra	Diagrammatic Representation of Structure	Si-O Group and Negative Charge	Oxygen to Silicon Ratio	Example
Sheets		$(\text{Si}_4\text{O}_{10})_n^{4-}$	5 : 2	Micas
Frameworks		$(\text{SiO}_2)_n^0$ Also feldspars, for example, orthoclase, KAlSi_3O_8	2 : 1	Quartz SiO_2

(b)

Figure 10: Crystal chemistry of silicates rock and soil type (Michell, 1993)

Michell further indicates that the interatomic bond in silica (Si-O) is about half-covalent and half-ionic. The covalent and ionic are directional primary strong atomic and interparticle bonds and influence the structural properties of mineral aggregates. Nevertheless, the coordination of silicate polyhedral is seldom electrically neutral; in such case, a secondary bond holds some units together. Secondary bonds, which are relatively weak compared with primary bonds (i.e. hydrogen and van der Waals), are the source of attraction between very small particles (clay) and liquid and solid particles. Secondary bonds such as hydrogen bonds influence the interaction between mineral aggregate surface and water, while van der Waals bonds which are nondirectional, have significant influence on cohesion and adhesion of the mineral aggregate surface. The importance of van der Waals forces, in the study of durability of the BSM mixture, is described further in section 2.4.

It is evident from mineralogical composition that the structure of mineral aggregates tells a great deal about their surface characteristics and their potential interaction with adjacent phases (binder and water). Rocks with high silicate content are acidic (low pH). Acidic aggregates exhibit a hydrophilic (water loving) chemical nature, whilst rocks with high carbonate content are alkaline (high pH) and exhibit a hydrophobic (water hating) chemical nature. These

characteristics have been applied in the studies of BSMs. Louw (1997) and SABITA (1999) indicate that the selection of bitumen emulsion (anionic or cationic) for mix design should be compatible with the proper charges of the mineral aggregates. However, Jenkins (2000) indicates that aggregate charges are not a requirement for compatibility with foamed bitumen. Nevertheless, both studies did not investigate the influence of the chemical nature on the susceptibility of binder-aggregate bond durability in terms of moisture and age hardening.

Yoon and Tarrer (1988), Labib (1992), Scott (1978), and Huang *et al.* (2000) report that the chemical nature of the aggregate surface influences the pH value of water at the bitumen-aggregate interface. The pH of water, which affects the binder-aggregate bond durability, differs depending on environmental conditions. The pattern of the change in pH values after aggregate filler is added to water is presented in Figure 11.

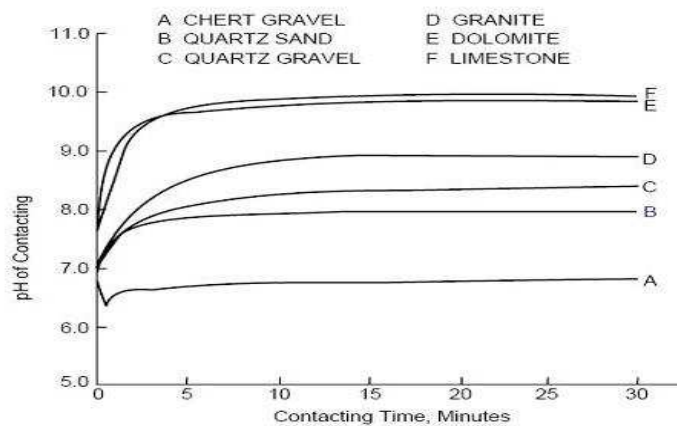
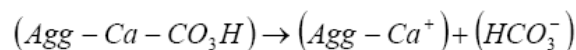


Figure 11: Changes in pH of water in which aggregates were immersed (Yoon and Tarrer, 1988)

Figure 11 reveals that the chemical nature of the aggregate surface tends to increase the pH of the contacting water. This is common to both basic rocks (e.g. limestone) and acidic rocks (e.g. granite). Mertens and Wright (1959) reported the phenomenon of the pH influence on the aggregate surface charge of different rock and soil types. The mechanism of charge development in different rock types and soils serves as a molecular description for the concept of surface free energy. This phenomenon (pH change) can have significant influence on the wettability and bonding behaviour of colloidal particles of foam and emulsion in the mix.

2.2.2.1 Carbonate mineral aggregates

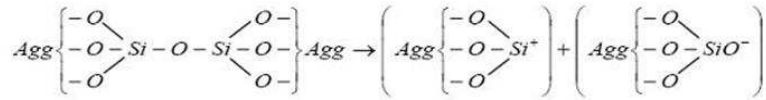
Carbonate mineral aggregates generally have electropositive surface characteristics. When these aggregates fracture, electrostatic bonds break and unsatisfied charges of calcium and carbonate ions occur in the newly formed surfaces (Mertens and Wright, 1959). The simplified reaction describing the fracturing process with the consequent formation of the countless unsatisfied charges is shown as follows:



where *Agg* represents the bulk aggregate structure, with the atomic lattice consisting of the $CaCO_3$ rhombohedral unit cell the intermolecular bonds are represented by a “-” sign. Water vapour or clay particles are normally adsorbed instantaneously into the aggregate to satisfy broken bonds. Therefore, the free charges are the determinant for bond formation with interaction in the different binder function group.

2.2.2.2 Silicate mineral aggregate

Silicate mineralogical rocks generally have electronegative and positive charge characteristics. Upon fracturing, the creation of unsatisfied charges occurs. See the following elemental compositional below:



Agg represents the bulk aggregate structure, with the atomic lattice consisting of a silicate tetrahedron (Si coordinated with four oxygen atoms) unit cell. As water adsorbs, the hydration process occurs (i.e. H₂O dissociated into H⁺ and OH⁻) in response to the unsatisfied charges.

From the description of silicate and carbonate reactions, it is evident that mineral aggregate surfaces generally contain elements that cause both electropositive and electronegative features. Figure 12 classifies mineral aggregates according to surface charges, based on silica and alkaline or alkaline earth oxide content.

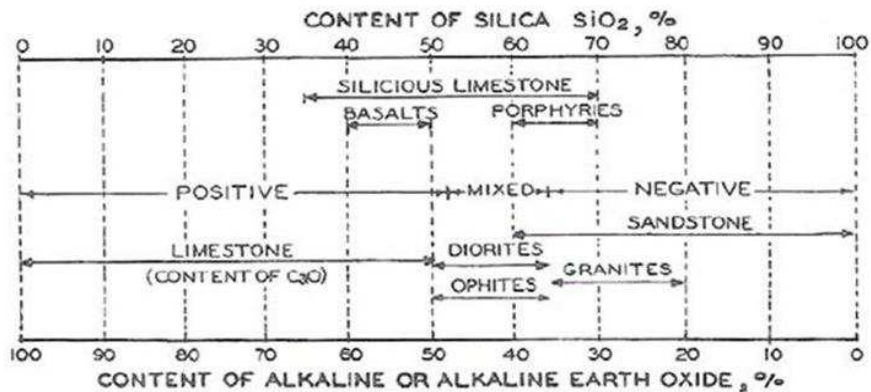


Figure 12: Classification of mineral aggregates (Mertens and Wright, 1959)

2.2.2.3 Clay mineral particles

Clay minerals show different mechanisms of charge development. The charge in mica, for example, comes from structural imperfections due to ion substitution (called isomorphous substitution). From the literature survey, it is evident that functional group, bonding, aggregate reactivity, and aggregate surfaces in the field of BSM technology have not received as much attention as binder characteristics (foam or emulsion). The importance of surface characteristics on the mineral aggregates is phase boundary (Petersen *et al.*, 1982). Phase boundary produces unsatisfactory force fields, which may be balanced in any of the following ways:

- Attraction (adhesion) and adsorption of molecules from the adjacent phase,
- Cohesion with the surface of another mass of the same substance,
- Structural adjustment due to different environmental conditions.

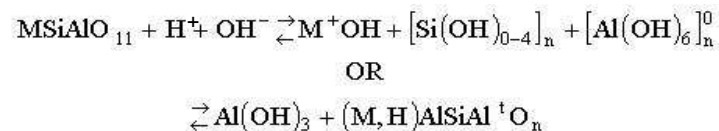
The influence of filler particles charges on the mastic and bond formation in mineral aggregates will be presented in this study. Thus, physicochemical change (structural adjustment) of mineral aggregates due to weathering is a factor to be considered during selection of mineral aggregates for BSMs. Previous studies have indicated that the phase boundary of many mineral aggregates changes by producing fine particles (Sampson 1989). Most of these fine particles, plastic (clay) or non-plastic, behave like colloids, both because of their small particles and unbalanced surface charges. This phenomenon of weathering might have significant influence

on the durability behaviour and long-term performance of mineral aggregates in the pavement layer. The effect of weathering of different mineral aggregates in a pavement layer is discussed in the next section.

2.2.3 Weathering effects on aggregates durability

Weathering, according to Weinert (1980), is a general term describing the disintegration or decomposition of rock and soil, or natural road-building materials. Disintegration refers to mere physical break down of mineral aggregates into small particles while minerals properties remain unaltered. This can occur in all types of road-building material in any environmental condition. Decomposition, on the other hand, is referred to as chemical alteration of the mineral aggregates properties, predominantly applicable to acidic and basic crystalline minerals, with the influence of the presence of water (i.e. condition where N-value is less than 5).

There are thus two principal groups of rock-forming minerals, distinguished by i) their prominent occurrence in different types of rock and ii) the differences in their mode of weathering which must be considered when assessing the durability and quality of natural road construction materials (Weinert, 1980). Crystalline rock such as syenite, diorite, norite, dolerite, felsite may decompose if environmental conditions are suitable. However, chemical decomposition is not affected by static water. Instead, continuous hydrolysis (introduction of H+) is required for mineral reactivity, in turn is resulting in erosion under water. This phenomenon supports the concept of applying cyclic pore water for evaluating moisture susceptibility of BSMS. Hydrolysis is typical chemical weathering where the H+ ion from the water molecule destroy the polyhedron's silicate structure by cation exchange. The general expression for hydrolysis of a silicate mineral is indicated in the reaction below;



where, M=metal cations; n= unspecified atomic ratio; o and t = silicate structure co-ordinations. Depending on the pH value of the system, solubility of SiO₂ and Al₂(OH)₃ may result in different types of clay mineral being formed. The formations of clay mineral will inturn adversely influence the aggregates' properties.

The predominant sedimentary rocks, such as sandstone, shale, tillite, limestone, and dolomite conglomerate hardly decompose, but physical breakdown is the dominant change they experience. Quartzitic rock-forming minerals, such as Quartzite, Granite, Gnesis, Mica, Hornfels, Marble are more stable minerals in any environment. However, these aggregates are seldom available minerals for road construction. Bowen's mineral stability sequences in Figure 13, indicates that Quartz is the most stable non-clay mineral in the earth's crust.

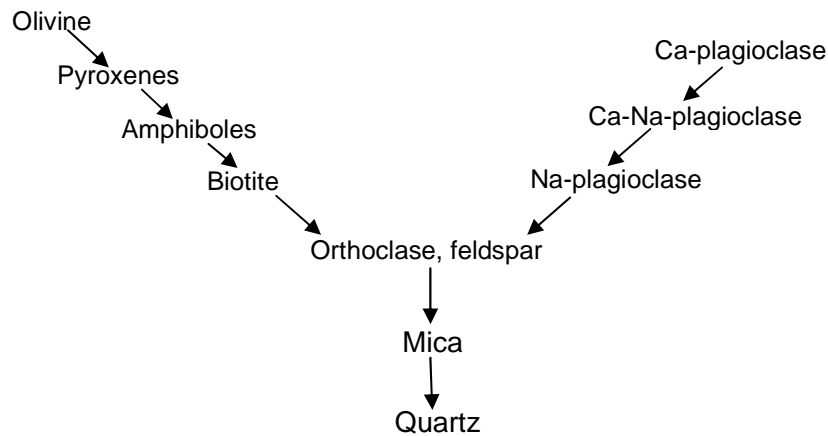


Figure 13: Order of mineral crystallisation stability (Mitchell, 1993)

The rock types with high silica content are Quartz, Feldspar, Mica, Pyroxene, Amphibole and Olivine. Weinert (1980) indicates that these minerals, with the exception of Quartz are sensitive to decompose (chemical change) and give rise to the development of secondary minerals, e.g. clay. The second group such as Calcite, Dolomites, Gypsum sulphate salt, rock slat and clay, according to Weinert are final products of some form of weathering, and they therefore do not decompose further. However, they dissolve in water and hence they are susceptible to durability failure. The sulphur minerals such as Pyrites and Opal, decompose easily and fast once exposed to air and water, and are therefore, less durable or not suitable for road construction.

Rock-forming minerals therefore have a significant role in durability and long-term performance of the pavement layer. The rock types that are used in Southern Africa road construction were grouped based on the presence or absence of Quartz and its weathering potential. These nine groups are described in TRH14, as indicated in Table 2, (CSIR, 1985).

Table 2: Grouping of rock type based on presence or absence of quartz and weathering potential, TRH 14 (CSIR, 1985)

Rocky type	Mineral group	Quartz content	Weathering potential	Remarks
Basic crystalline	Basalt, Dolerite, Gabbro	Very little or None	Decompose	Produce montmorillonite (expansive clay) when $N < 5$
Acid crystalline	Granite, Felsite, Gneiss	High, except on Syenites and Felsites	Less Quartzite decomposed	Produce kaolinite (non-expansive clay) when $N < 5$ or sand
High- silica	Quartzite & Hornfels-RAP	Very high	Disintegrate	Produce gravel or sand
Arenaceous	Sandstone, Mica, Conglomerates	High	Disintegrate	Produce various sand with cementing matrix
Argillaceous	Shale, Mudstone Slate	High	Easily absorb water and disintegrate	Produce sand clay
Carbonates	Dolomite, Limestone, Calcite	Low	Disintegrate	Produce sand
Diamictites	Tillite, & Greywacke	High to little	May disintegrate or decompose	Produce clay (when $N < 5$) depending on the quartz composition
Metalliferous	Ironstone, Magnetite	High	Disintegrate	Produce gravel or sandy
Pedogenic	Calcrete, Ferricrete and Silcrete	Different composition	Final stage of weathering	Produce soil with cementing properties.

Tarrer *et al.*, (1991) indicate that the effect of weathering on aggregate properties is predictable from surface energy considerations. As an aggregate ages and is exposed to a cycle of varying temperature and humidity, its outermost adsorbed water molecules are partially replaced or covered by fine clays or fatty acids (organic material). This in turn reduces the spreading coefficient or free energy of the system. The durability of mineral aggregates is a natural property and the tendency to change is inherent from the parent rock. The rate of change varies. There are rocks, which change faster and others changes that occur so slowly that none are viable during the lifespan of a road.

The rate of weathering, decomposition in particular, depends on the local climate the materials are exposed to within the pavement structure and the stage of weathering at the time the materials were removed from their natural source. To assess durability therefore is to assess how and at what rate changes in mineral aggregates occur after a material is placed in the pavement layer.

2.2.4 Climatic effect on aggregate durability

The environment, in which each road is built has greater influence on its durability behaviour and long-term performance, than is often realised. The road environment has to be accepted as it is and the design and method of construction must be suitably adapted. The climatic influence on the quality of mineral aggregate durability, as well as the general performance of roads, has been studied. Weinert (1980) indicates that the climatic effects are more pronounced in large countries where climate variation regionally and seasonally is wide, e.g. South Africa. The mechanism by which moisture can infiltrate the pavement layers i.e. subgrade, subbase, base and surface, has been studied and reported on (Jenkins, 2007; Pinard, 2006). It is apparent from Figure 14 that moisture movement into pavement layers is a complicated phenomenon, although proper design of pavement geometry, the drainage system and pavement structure seems to get rid of moisture problems. Material characteristics and mix design also play a significant role in moisture movement and, in turn, durability behaviour of different rock and soil types in pavement layers. The mode of moisture transport within the mixture is discussed further in this study.

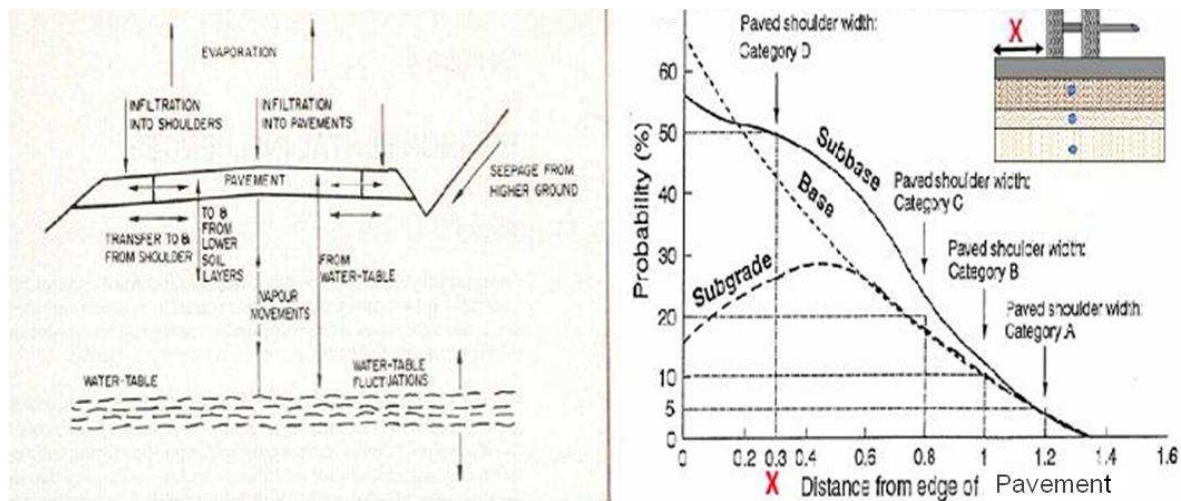


Figure 14: Source of moisture infiltration and suction to the pavement layers (Jenkins, 2007)

Rock minerals such as weathered basic igneous or decomposed dolerite are widely used as base materials in South Africa. However, their durability behaviour was seen to be different when used in different parts of the country (east to west). Clauss, (1967) indicates that roads constructed using these materials only lasted a few months after being opened to traffic. When the trial pit was opened and the base materials compared to the original materials in the borrow pit, the deterioration in the quality and condition was significant. However, performance of similar materials was deemed to be satisfactory when they were used as base materials in the east. Paige-Green and Ventura, (2004) similarly report premature failure on problematic basalt in Zambia, with formation of plastic smectite clays due to climatic weathering. These deteriorations were linked to climate influence and high moisture content. Weinert (1959, 1961) indicates that climatic indices from Thornthwaite's moisture index were used in South Africa for the road design. However, these indices did not satisfactorily distinguish the deference performance that existed in South Africa rock minerals.

Therefore, Weinert further investigated all climatic factors, including those, which were unlikely to have an effect on weathering. The investigation was extended to include January, the warmest month, and July, the coldest, in the Cape peninsular region. The month of January, is

dry in winter rainfall areas with consequently high evaporation (E_j) and low precipitation (P_j). In July, evaporation is low (coldest month) while precipitation is high. The rainwater during this season is cold and its effectiveness as a chemical agent is lower than during the warm season. Glasstone (1956) indicates that the rate of water reactivity increases with temperature. Within the range of water temperatures found in South Africa, a rise in temperature of 10°C usually doubles the speed of chemical reaction. Therefore, Weinert investigation found January agreed satisfactorily with the performance and weathering boundary in summer rainfall areas. Thus, the correlation of the month for evaporation and the whole year's precipitation was developed. The relationship indicated that 12 times the computed evaporation of the warmest month, mostly January in South Africa, divided by the total annual precipitation gives a numerical value called N-value. The N-value can be used to describe the different climatic environments in which rock weathering might perform differently in pavement layers. The correlations of climatic parameters are shown in Equation 1.

$$N = \frac{12E_j}{P_a} \quad \text{Equation 1}$$

where P_a = total annual precipitation; E_j = evaporation for the month of January. Therefore, $N=1$, $N=2$, $N=5$ and $N=10$ are important indices for road engineering. No climatic region was identified with and N value greater than 10. Table 3 indicates the summary of the Weinert values adopted for the South African climatic index. These values have been used in South African TG2 (Asphalt Academy, 2002 and 2009) guideline to define the influence of moisture damage on mix design.

Table 3: Climatic Index on different region using Weinert's N-value, (Weinert,1980)

Environmental/climate	Wet	Moderate	Dry
Weinert's N-value	$N < 2$	$2 < N < 5$	$N > 5$

Although Weinert's climatic index is applicable in pavement design, the regions classifications are relative wide than Thornthwaite's moisture index. Therefore, Paige-Green (2009) indicates that Thornthwaite's moisture index covers are realistic for the climatic condition in South African regions. The description of contour map illustrating the different Thornthwaite's moisture index is presented in Figure 15. And Thornthwaite formula based on monthly evaporation is indicated in Equation 2.

$$PE_m = 16 N_m \left(\frac{10 T_m^-}{I} \right)^a \quad \text{Equation 2}$$

where m = months 1, 2, 3...12, N_m = monthly adjustment factor related to hours of daylight, T_m =

monthly mean temperature ($^\circ\text{C}$), I = heat index for the year, given by: $I = \sum i_m = \sum \left(\frac{T_m^-}{5} \right)^{1.5}$ for

$m = 1 \dots 12$ and: $a = 6.7 \cdot 10^{-7} \cdot I^3 - 7.7 \cdot 10^{-5} \cdot I^2 + 1.8 \cdot 10^{-2} \cdot I + 0.49$

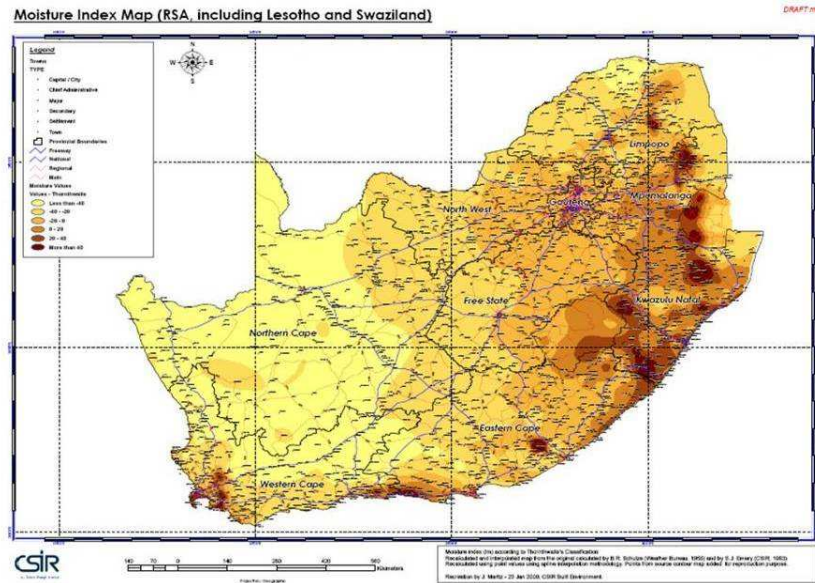


Figure 15: Moisture condition on different region in South Africa according to Thornthwaite's moisture index (Paige-Green, 2009)

2.2.5 Aggregate properties

The aggregate properties, such as particle size distribution or grading, are the most influential characteristics in BSM mix design (i.e. classifying suitable material and identifying optimum binder content). Grading generally has been used to optimise almost every important property of pavement materials including stiffness, stability, durability, compactability, permeability, workability, fatigue resistance frictional resistance, and resistance to moisture damage (Roberts *et al.*, 1996; Jenkins, 2000). Because of this, gradation is a primary concern in pavement mix design for HMA, CTMs and BSMs. The types of materials suitable for BSMs have been referred to in the literature by gradation rather than characteristics of parent material type (Akeroyd and Hicks, 1988; SABITA, 1993; Jenkins, 2000; Asphalt Academy, 2002; Wirtgen, 2007).

Spatial composition technique (3-dimensional volumetric structure of a material) has earlier been utilised for volumetric composition of HMA Jenkins, (2000) adopt this technique to determine optimum mix design for foamed bitumen. The emphasis is on the importance of the filler fractions and sand fractions based on the unique nature of binder dispersion, particularly foamed bitumen in an aggregate skeleton. It is evident from the literature that optimisation of the BSM mix performance is related to more continuous grading close to the maximum density curve where $n=0.45$ (Nijboer, 1943). Cooper *et al.*, (1985) extended the work of Nijboer by introducing varying equivalent fines contents after fixing the filler content at a predetermined level, as shown in Equation 3;

$$P = \frac{(100 - F)(d^n - 0.075^n)}{(D^n - 0.075^n)} + F \quad \text{Equation 3}$$

where: P= percentage by mass passing a sieve of size [dmm], D= maximum aggregate size [mm], F= percentage filler content, n= variable dependent on aggregate packing characteristics.

The aggregate grading and its influence on the performance of BSMs have extensively been researched in past studies. Therefore, the objective of this study is to explore other parameters of aggregate properties, i.e. physicochemical properties (aggregates surface characteristic) and their influence on durability and long-term performance of BSMs. Dukatz (1989) addresses the properties of mineral aggregates that influence pavement performance,

against the background of the: i) physical, ii) chemical, and iii) mechanical properties as indicated in Table 4.

Table 4: Aggregate properties related to pavement performance (Dukatz, 1989)

Property	Permanent deformation	Fatigue	Low temp. cracking	Moisture damage
<u>Physical</u>				
Shape	5	4	3	2
Surface	3	1	3	4
Absorption	3	3	1	4
Specific gravity	3	3	3	1
Morphology	3	4	3	4
Gradation	5	4	3	4
<u>Chemical</u>				
Composition	3	3	2	5
Solubility	3	3	1	5
Surface charge	1	2	2	5
<u>Mechanical</u>				
Strength	3	4	2	1
Durability	5	5	2	1
Toughness	5	5	2	1
Hardness	3	5	1	1

Note: 5 denotes significant influence and 1 denotes minor influence

It can be seen from the relative performance of aggregate properties in Table 4 that physicochemical property (e.g. aggregate surface) plays a significant role in moisture susceptibility. Therefore, fundamental understanding of the interfacial cohesion and adhesion of bitumen (mastic) and aggregates bonding vital for BSMs. Tarrer (1991) indicates that adhesion of bitumen to aggregates is a surface phenomenon and depends on close contact between the two phases and the mutual attraction of their surfaces. Surface texture, porosity and adsorption properties affect adhesion to bitumen. That means rough or smooth aggregates surface influences adhesion of bitumen film or mastic. Because of surface characteristics, carbonaceous aggregates tend to be more moisture resistant and siliceous aggregates tend to be the most moisture sensitive. This in turn affects other properties such as shear, stiffness and fatigue.

The literature on mineral aggregate durability shows that a fundamental understanding of adhesion, surface chemistry and their influence on performance and durability of BSMs is vital. The objective of section 2.4 is to review fundamental theories and associated mechanisms of binder (mastic)–aggregates adhesion, and to provide supporting evidence for these mechanisms. Adhesion theories place bitumen-aggregates interaction and moisture susceptibility on a comparative basis. This may enable the analysis of the practical implication for the materials and structural design of BSMs.

2.2.6 The use of rock and soil in BSMs

The purpose of introducing this section is to bring to attention the importance of considering mineral aggregate durability consideration during the mixing of BSMs. It is evident from the literature survey that the use of rock and soils typically depends on mineralogical composition and physicochemical properties. BSM technology in South Africa is predominantly in-situ recycling of the base layer. The extract from the LTPP database on BSMs projects in South Africa prepared by Long (2007) is converted into a pie chart and presented in Figure 16. The composite materials of RAP plus cement-treated granular materials and natural gravel were

mainly applied in the recycling process. Because recycled materials were in the pavement layer for long periods, it is evident from the literature review that some deficiency in engineering properties is expected compared with virgin materials.

2.2.6.1 Base layer

The base layer in pavement structure is predominantly important due to its ability to spread the applied stresses. South African pavement structures incorporate BSMs as a base layer. This requires proper selection of materials, which must also be durable to fulfil the intended function. Weinert (1980) indicates that, up until 1960s, South African base materials were obtained from sources of weathered rock or pedocretes, e.g. Dolerite, Calcrete, and Ferricrete. Crushed stone bases were used in exceptional cases in the base layer for provinces and municipality areas and later commonly used in the freeways. The quality requirements for the crushed stone e.g. Quartzitic sandstone and Hornfels for the base, were relatively similar to aggregates used in surface layer, however, accepting the compromising strength, freshness and cleanliness. The weathered rock or pedocretes for the base in most mix designs were stabilised with cement (4-8%) to improve engineering properties.

Due to high application of cement, field investigation shows that structural distress frequently occurs in pavement structure. This results in the introduction of a more flexible base layer by recycling the cracked base layer and stabilising with bitumen emulsion. Reclaimed asphalt pavement (RAP) plus cemented weathered base materials (CTB) are recycled and become a new composite material for the pavement base layer. The use of bitumen emulsion for treating recycled moist granular materials (composite material) for base layer have been successfully applied for the past 40 years. In the mid 1990s, foamed bitumen entered the market offering similar benefits to bitumen emulsion. The database of typical base materials used for the construction and rehabilitation using bitumen emulsion and foamed bitumen was compiled and summarised in a long-term pavement performance (LTPP) database by Long (2007). Figure 16 provides an extract of typical rock types and soil used for the base in the BSM layer.

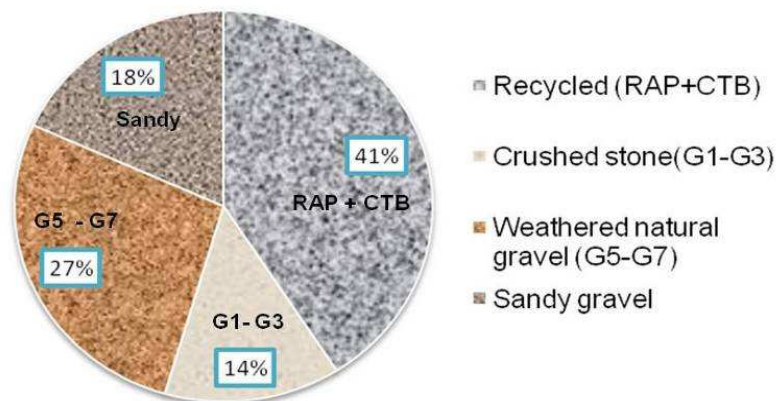


Figure 16: South African LTPP base materials for the BSMs pavement layer (Long, 2007)

From the extract of the LTPP database, it is evident that BSMs are mainly applied on the recycled materials compared to virgin mineral aggregates. Nevertheless, most of the recycled RAP comprises aggregates of good quality e.g. crushed stone from Hornfels, Granite, and Quartzite rock type. Whereas, recycled CTB comprises low-quality aggregates e.g. weathered

Dolerite, Ferricrete, and Calcrete. However, the percentage of RAP content in a recycled layer is relatively small compared to CTB. Therefore, due to a large percentage of low-quality aggregates in a recycled layer it is important that quality and durability of composite materials be evaluated. The current guidelines i.e. TRH14 (1985) and TG2 (2002), provide quality and durability of mineral aggregate requirements for the HMA, CTB and granular layers. No cognisance of quality and durability is indicated for the recycled composite materials for BSMs. Therefore, classification of recycled materials based on quality and durability requirements for BSMs is an area, which needs more investigation. The author's personal discussion with geology expert Dr Phil Paige-Green of CSIR indicated that the most recycled (composite) materials include cement and old bitumen. That means that their CBR and shear parameters are equivalent to material with G4 classification (see TRH14, 1985). However, in order to assign material classes with certainty, since the recycled materials have been in service for some time, assessment of the composite-wearing potential and residual parameters such as strength and grading need further investigation through laboratory testing. The initial laboratory investigation, based on DMI testing of known properties of the composite materials compared to the virgin materials of known properties, was carried out and the results will be discussed in Chapter 3.

2.2.6.2 Performance classification

According to TRH 14, performance classification of different mineral aggregates in newly constructed layers is G1, C1, BT1, etc. However, this type of classification becomes more complex if these materials have been in service for sometime. If the plasticity index (PI) of mineral aggregates, G1 changes and conforms to G4, while the grading or CBR conforms say to G3, then what is the new class? Based on the complexity of the classification of recycled materials for pavement rehabilitation, Jooste (2007) introduces a new classification system called "design equivalent materials". This classification indicates that:

"when a design equivalent class is assigned to a material, it implies that the materials exhibit in-situ shear strength, stiffness and flexibility properties similar to newly constructed materials of the same class as in TRH14".

It is apparent from a new proposed classification that additional information on the aggregate properties are required to ensure consistent application of recycled materials for the BSM mix design. Apart from strength properties of the mineral aggregates indicated above, surface characteristics also need to be evaluated and included in the classification as they play a significant role in the bitumen-aggregate-water interaction (bonding).

2.2.7 Testing of aggregates durability

2.2.7.1 Background

The durability of mineral aggregates has been a subject of great concern for the performance of HMA, CTB and granular base layers, and a number of durability tests have been developed and are in use. Unfortunately, because of the ubiquitous nature of suitable aggregates for BSMs and their better performance, the durability of mineral aggregates for both virgin and recycled, seems to have been largely overlooked until fairly recently (Jenkins *et al.*, 2006). This is true because a number of field investigations showing premature distresses or failure have been linked to mixture properties and not directly to mineral aggregates durability. Jenkins *et al.*, (2006) prepared a research proposal on improving mix design for BSMs, with the focus on moisture susceptibility as a prime factor in addressing durability requirements of BSMs. However, the core issue was to outline the mix composition including binder and aggregates durability. Natural aggregates durability has been addressed by many researchers including

Weinert (1989), Sampson and Netterberg (1989) and Sampson and Paige-Green (2004), whilst De Beer (1989) and Sampson and Paige-Green (1990) address CTB.

Sampson and Netterberg (1989) reported a number of field investigations into different untreated basecourses covered with a seal layer. The investigation was done on the basecourses of the distressed area under the outer wheel path (heavily trafficked) and under the less distressed centreline (less trafficked) area. The change in the material properties of the base layer was reported as indicated in Table 5.

Table 5: Comparison of results from sound and distressed outer wheel path areas of basecourse materials (Sampson and Netterberg, 1989)

Site	Road	Material	Condition	PI	P425	P075	Finesse product	Soaked CBR	FMC/OMC
Hanover to Richmond	9/8	Sandstone	Sound	5	17	9	85	91	0.62
			Distressed	8	25	17	200	74	0.90
Hanover to De Aar	17/2	Dolerite	Sound	6	20	8	120	107	0.62
			Distressed	10	30	15	300	60	0.71
Port Alfred to East London	45/3	Tillite	Sound	4	21	7	84	89	0.60
			Distressed	8	21	8	168	62	0.85

The investigation reveals that:

- PI in the wheel path was either similar to or higher than under the centreline. The PI under the centreline was found to compare well with the record during construction, whilst, high PI under the wheel path suggests that it was generated in-situ.
- Sieve analysis shows percentage fines passing 0.425mm and 0.075mm, higher in distressed areas than in sound areas in the same wheel path in most cases and exceeding the specified limits. The centreline values were within the specified limits.
- The ratio of field moisture content (FMC) to optimum moisture content (OMC) was always higher in wheel path area than the centreline. Emery (1984) recommends that a FCM/OMC ratio of 0.6 is expected for the base layer under normal climatic conditions. The higher ratio in the wheel path (Table 5) is an indication of excessive moisture and/or lower-grade materials.

It is evident, from the results that the base material was either initially unsuitable or underwent degradation during in-service life. This also confirms the finding reported by Land Transport New Zealand (2000) of the effect of hydroplaning, the forcing water through the seal to the base layer, resulting in detrimental moisture damage or erosion. The hydroplaning effect on moisture damage will be presented in detail in section 2.5.6. The experience of Sampson working with base granular materials under the seal shows that degradation on the top 20mm to 30mm can occur, leading to a loose layer of fine just under the seal. Ball *et al.* (1999) and Seta *et al.* (2000) report on similar studies of distress caused by pore water exerted under the seal by tyre pressures. Disintegration of BSMS under the seal has not extensively been studied, therefore, this type of distress and failure is likely to occur depending on binder content and type of materials coupled with environmental conditions. Paige-Green and Ventura (2004) report on a study of basaltic material from Zambia, which was known for degradation during in-service, leading to premature failure. However, when stabilised with foamed bitumen and lime, these materials performed impressively. The reason for the improved performance was linked to the influence of bitumen and lime on the physicochemical properties of the basaltic materials. However, the durability and long-term performance of the basaltic stabilised mixes was not certain. This prompted Paige-Green and Ventura to identify whether the existing durability test techniques could provide an adequate solution to assessing the durability of foamed bitumen-basaltic treated materials, instead of developing a new test. Tests techniques identified were durability mill index, accelerated carbonation, wet/dry cycling, erosion and SEM for microscopic

study of bitumen-filler-aggregate interaction. These conventional durability tests methods are described as follows;

2.2.7.2 Conventional durability tests methods

2.2.7.2.1 Durability Mill Index (DMI)

The durability testing carried out on the raw materials, such as ACV, Los Angles or 10%FACT, are commonly used to determine the degree of disintegration of the crushed aggregate. Sampson (1989) indicates that these tests are done on a fraction of the materials and do not simulate field conditions. Again, neither of these methods is suitable for the natural gravels. Sampson further develops the Durability Mill test to simulate field conditions using the abrasion method to determine the degree of disintegration and decomposition by the testing entire mix gradation in dry and wet conditions. Figure 17 depicts the ACV and DMI devices respectively, for testing aggregate durability.

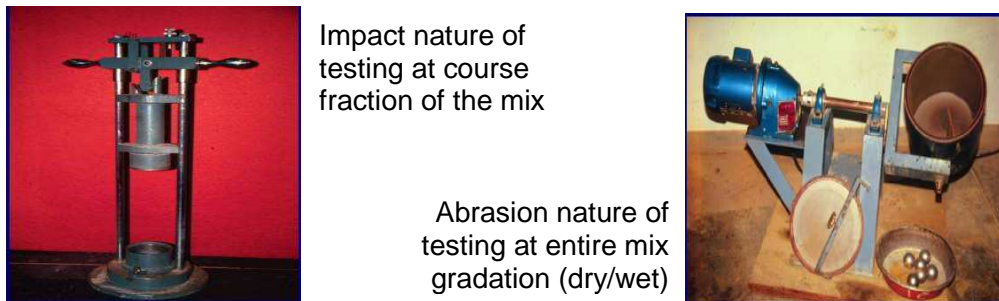


Figure 17: Mineral aggregate durability testing devices ACV vs. DMI

Further to the development of the DMI device, Sampson classifies rock type based on potential use as base materials using the following Durability Mill Index limits indicated in Table 6.

Table 6: Durability Mill Index, limit for rocks and soils, (Sampson, 1991)

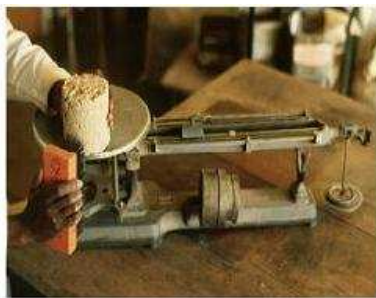
Aggregates type	Rock and soil group	DMI, limit
Granites, gneiss, granite	Acid crystalline	
Hornfels-RAP, Quartzite	High silica	< 420
Dolomite, limestone,	Carbonate	
Calcrete, ferricrete, silcrete	Pedogenic materials	< 480
Sandstone, siltstone, conglomerate	Sandstone	< 125
Grey wacke, Tillite	Diamictite	
Mudrock, phillites, shale	Mudrock	
Basalt, Dolerite, Babbro	Basic crystalline	
Ironstone, magnesite, magnetite	Metalliferous	< 90

These limits were adopted in South African pavement material specification as presented in the COLTO document (1993). Although these devices were developed for crushed natural gravels, their simplistic nature and applicability in CTMs and granular mixes can also be adopted to classify mineral aggregates for BSMs. However, due to a wide range of applicable material for BSMs (i.e. marginal, high-quality and recycled), modification of the testing method and the consequent limit is apparent.

2.2.7.2.2 Wet / dry durability test

Paige-Green and Ventura (2004) indicate that marginal quality materials such as basaltic materials shouldn't be used as a base layer with its natural properties. However, after stabilisation with bitumen and active filler they performed well in practice. Due to the fact that bitumen stabilisation with the addition of an active filler changes the physicochemical properties of mineral aggregates, they recommend that it is appropriate to quantify the effect on long-term durability by looking at the binder-aggregates system and not only at aggregates or bitumen materials. The conventional test applicable for assessing the durability of cement- or lime-treated materials is the wet/dry test or erosion test.

The wet/dry test is commonly performed to identify the susceptibility of cement/lime-stabilised materials to degradation (disintegration or decomposition) in the presence of adverse conditions of cyclical wetting and drying and/or carbonation. The wet/dry test on compacted and cured specimens was done using a hand brush. This method was later modified to use a mechanical brush as shown in Figure 18. Paige-Green and Ventura applied a mechanical test to identify potential degradation or long-term durability of the foamed bitumen-treated basaltic materials. The mechanical brushing test measures the loss of materials from the specimen surface resulting from soaking, drying and carbonation. The loss of materials is a result of chemical alteration (decomposition) or physical weakening (disintegration) of cementitious bonds developed during cement hydration. The early failure in their study suggests that the use of the brush test might be too harsh for the foam mix. Therefore, the brush component was removed in a repeat test, but specimens still failed at the first and fourth cycles. The premature failure was explained to be caused by the high temperature (105°C) of the curing specimen, which might have resulted in the flow of bitumen and softening of the cohesion of the mix. Wet/dry mechanical testing is not a relevant test for BSMs. Firstly, it might be harsh on the adhesive bond due to the dispersion nature of the bitumen into the mix (spot welding of the foam to the coarse aggregates or thin film coating of bitumen emulsion in the large aggregate). Secondly, its applicability does not simulate the mode of moisture failure (erodability or mass loss) that BSMs experience in field conditions.



Repeatability and reproducibility is poor

Brushing mechanism too harsh



Figure 18: Wet/dry durability test: Hand brush vs. Mechanical brush

2.2.7.2.3 Erosion durability test

The erosion test was developed to assess the mass loss of cement- or lime-stabilised materials and is more likely to simulate field conditions. The procedure came from observation and findings during HVS testing on flexible pavements. The mass loss due to disintegration and decomposition is assessed according to the influence of hydraulic or mechanical abrasion applied by a wheel-trucking device (De Beer, 1989).

The objective of the erosion test (Figure 19) is to provide erodibility that simulates flexible pavement behaviour in a wet state. This incorporates the aggregate-to-aggregate contact stresses that may contribute to surface crushing and allows for quick assessment of

material, whilst minimising fraught inconsistencies in weight-loss measurement by applying linear measurement of the depth.

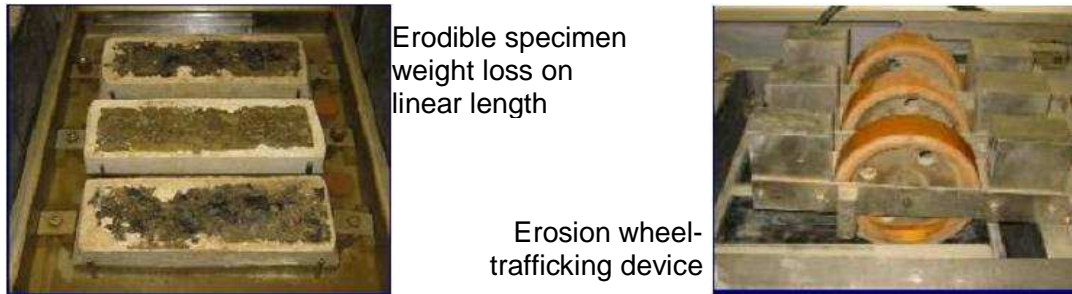


Figure 19: Wheel-trafficking erosion testing device (Long, 2003)

The inconsistent results from the wet/dry brushing test prompted Paige-Green *et al.* (2004) to apply the erosion test to assess the durability of basaltic foamed bitumen-treated materials. The materials were treated with 1.5% foamed bitumen and 3% hydrated lime. The mean erosion of the linear depth is summarised in Table 7. The comparisons of similar erosion tests on different rock types studied by Long *et al.* (2004) are also included in Table 7 for the critical analysis of the applicability of the test to BSM durability.

Table 7: Erosion test results on different rock type (Paige-Green *et al.*, 2004 and Long *et al.*, 2004)

Rock type	Treatment	Binder content [%]	Erosion [mm]	Index	Tested by
Basaltic	Natural	0	6.0		Paige-Green <i>et al.</i> , 2004
	Lime only	3	0.4		
	Foam only	1.5	3.7		
	Lime + foam	3+1.5	0.2		
Hornfels-RAP	Natural	0	18		Long <i>et al.</i> ,2004
	Cement only	1	8		
	Foam only	2.25	1		
	Cement +foam	1+1.5	1.6		
	Cement +foam	1+2.25	1.3		
	Cement +foam	1+3.0	1.3		
	Cement +foam	2+1.8	1.5		
	Cement +foam	2+2.25	1.6		
Lateritic	Natural	0	12		Long <i>et al.</i> ,2004
	Cement +foam	1+3.0	4.5		
	Cement +foam	2+1.8	0.8		

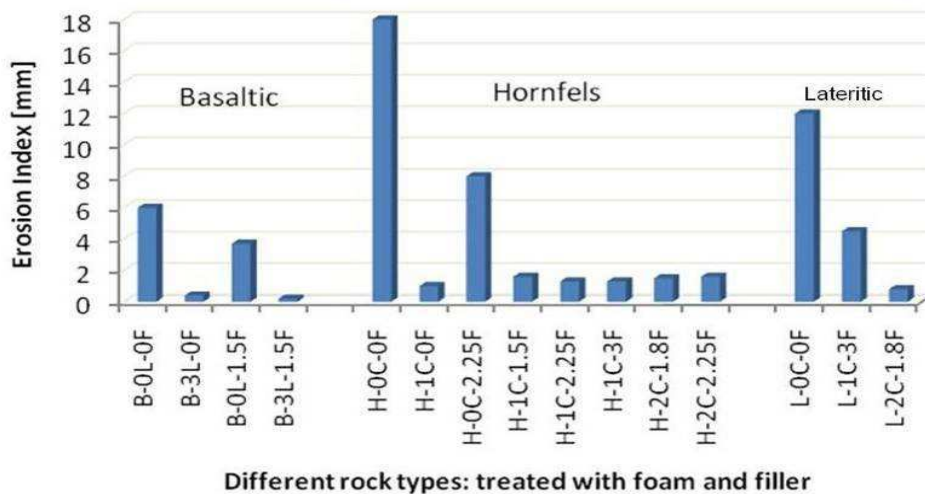


Figure 20: Comparative Erosion Index for BSM-foam with different rock type

Looking at the results of stabilised basaltic rock type, Figure 20, Paige-Green *et al.*, indicate that the erosion test relies more on physical attrition (i.e. disintegration of mix in wet state) than chemical change occurring for example in the wet/dry brushing test. Whilst Long *et al.*, discuss the influence of cement and/or binder content in terms of propensity loss of materials in the stabilised mix. Critical observation of the erosion results for different rock types as shown in Figure 19, gives more insight on the following:

- The mass loss after wet/dry brushing is not merely influenced by the quantity of binder and/or active filler applied in the mix. Instead, comparison should also look at the physicochemical properties of the rock and the interaction with other phases (i.e. bitumen and active filler). It can be seen from the results that untreated basaltic material (low quality) has relatively low mass loss compared to Hornfels (high quality) and lateritic (low quality) materials. This is attributable to the fact that filler particles of weathered basalt might have equilibrated the surface energy of the aggregates with better adhesion even after intrusion of the water phase compared to Hornfels and lateritic.
- Further analysis, shows that Basaltic material, with the addition of 3% lime and 1.5% foamed bitumen has significant adhesion to the mineral aggregates (low mass loss) compared to, for example Hornfels, with addition of 1% cement and 2.25% or 3% foamed bitumen. Likewise, Lateritic materials with the addition of 2% cement and 1.8% foamed bitumen, has higher adhesion (low mass loss) compared to, for example Hornfels with 2% cement and 1.8% foamed bitumen. We would expect high-quality material to have relatively low mass loss compared to low quality rock types. However, these differences confirm that BSMs mix composition should not be designed only for the binder and active filler content; instead, emphasis should be placed on the understanding of the theory of adhesion in mix composition. In this study, the moisture sensitivity and damaging mechanism is discussed based on the theory of adhesion as presented in Chapters 3 and 4.
- Determination of initial consumption of lime (ICL) is an important aspect when applied to adhesion behaviour in BSMs. This can be seen from low mass loss of Basaltic material with the addition of 3% lime and 1.5% foamed bitumen compared to similar mix with no addition of lime, or Hornfels with addition of 2% cement and 2.25% of foamed bitumen. The literature has indicated that a change in the pH of the water at the binder-aggregate interface due to the addition of active filler has an influence on the durability of a mix in a wet state.

- If the durability mill index, for example is used to characterise rock types to be selected for the BSM mix design, Hornfels-RAP would be given preference due to its high quality. However, looking from a surface free energy perspective at the binder-aggregate system, fundamentals of the BSMs durability might be explored.

Although erosion or MMLS3 tests give an insight into the physical disintegration of adhesion and/or cohesion of the BSMs mixes in a wet state and a reduction in strength, understanding of the physicochemical properties of the surface of mineral aggregates is vital in exploring the long-term durability of BSMs under different adverse conditions. Bhasin *et al.* (2006), Cheng (2002), Hefer *et al.* (2006) and Bhasin and Little (2006) apply different techniques to quantify surface characteristics of asphalt binder and mineral aggregates to understand adhesion and cohesion behaviour in HMA. These techniques, using the universal approach of thermodynamic theory are described in section 2.4.2.3. Although not investigated in this study, the universal approach of thermodynamic theory has potential to be explored for fundamental understanding of the durability and long-term performance of BSMs.

2.2.7.2.4. Adhesive durability tests

1. Contact angles.

The contact angles concept has been used to measure the hydrophobicity of bitumen (colloidal) surfaces (Liu *et al.*, 2005). Work of adhesion can be quantified from the contact angle (θ) which forms when a liquid (colloid) is in contact with a solid surface. This aspect is of paramount importance due to the nature of foamed bitumen or bitumen emulsion (colloidal) dispersion in mineral aggregates. The Wilhelmy plate technique (Elphinstone, 1997; Cheng, 2002, and Hefer, 2004) and Sessile Drop technique (Bose, 2002) are both techniques that have been used to measure contact angles of different liquids on bitumen surfaces. The former measures dynamic contact angles while the latter produces static contact angles. In both techniques a thin film of bitumen is coated onto a micro cover glass slide and allowed to cool before angle measurement.

2. Force microscopy

While most techniques characterise adhesion indirectly through parameters such as contact angles, equilibrium spreading pressure, and retention time, Konitpong and Bahia (2003) suggest the use of the modified Pneumatic Adhesion Tensile Testing Instrument (PATTI) device for the evaluation of the adhesion properties of binders in binder-aggregates systems in different adverse conditions. The PATTI apparatus applies pressure to pull off a thin film of bitumen from between the aggregate surface and the pull stub. When the applied pressure exceeds the work of adhesion or cohesion between binder-aggregate, interface failure occurs. Failure might occur due to cohesive failure of the binder or due to adhesion at the interface of the binder-aggregate system.

3. Electrophoresis

Electrophoresis is a study of charge particles in motion in an electric field. This technique has been applied to bitumen-aggregate systems in HMA to explain moisture damage (Labib, 1992). Zeta potential, essentially surface charges, is the main property derived from these experiments. Hefer *et al.*, (2005) comment that this approach is valuable and perhaps one of a few fundamental approaches for the study of the effect of pH (of the interface water) on binder-aggregate adhesion. Change in pH due to a high application of active filler in the BSMs, is an essential parameter for quantifying the durability of a mix after the addition of an active filler like lime.

2.3 BITUMEN BINDER DURABILITY

2.3.1 Introduction

Foamed bitumen and bitumen emulsion exhibit a colloidal nature when produced from paving asphalt (Figure 21). *Colloids* are particles that have a high ratio of surface area to volume, compared with bulk materials (i.e. paving asphalt). Special characteristics of colloids are size, shape, surface area and surface charge density (Birdi, 2002).

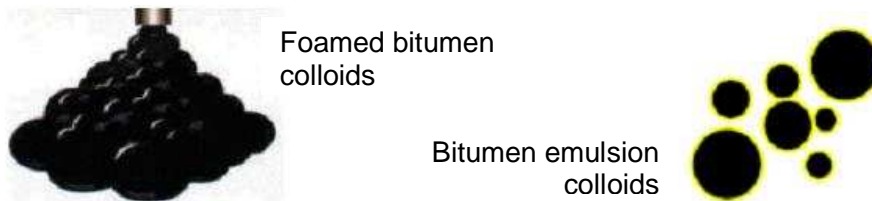


Figure 21: Example of typical colloidal nature of foam and emulsion in microscopic scale

The dispersion of colloidal or coagulation (break or collapse) is largely determined by the charges and surface films at the interfaces. Therefore, stability of colloids depends on surface free energy or interfacial free energy (Adamson, 1990). Due to thermodynamic and hydrodynamic effects, when mixing with aggregates, colloidal free energy dissipates; that leads to an unstable drop or bubble film and consequently rupture and coalescence. The coalescence rate (breaking of emulsion) might be fast or slow depending on the attractive (electrostatic) interaction across the film. Dispersion and coating of foam bubbles depends on the filler content, aggregate temperature and moist surface on the coarse particles. These phenomena might explain the influence of active filler on the acceleration of the phase separation, i.e. breaking of emulsion or dispersion of foam in the mix, and the influence on the locking of the polar function group of a bituminous binder onto a mineral aggregate surface. As a result of the breaking of the emulsion or collapse of the foam, an apparent thin film of bituminous binder is formed on and between mineral aggregates. The overall process is complete when setting or curing is finished, with the build-up of the cohesion and adhesion on the mix matrix.

The durability of the thin film coating the aggregates and mastics has significant influence on the durability behaviour and long-term performance of BSMs. Therefore, understanding binder durability in term of age hardening is vital. However, from the literature survey, it is apparent that little has been done in understanding the age hardening characteristic of the binder in BSMs. This section explores the binder durability of BSMs to provide a better understanding of the mechanisms that influence age hardening behaviour and consequently long-term performance of BSMs.

2.3.2 Physicochemical change in binder durability

Bitumen is a complex compound manufactured from different oil sources (Marais, 1979). Marais reports different sources of crude oil used in South Africa, while SABITA (1998) recommends a distillation process for straight bitumen for road pavement in South Africa. This indicates that bitumen characteristics differ from different sources and different methods of manufacture. Chemistry and composition of bitumen have extensively been reported; Robert *et al.* (1990) emphasise that the chemistry of bitumen can be considered at two levels: molecular and intermolecular. At molecular level, bitumen is a complex mixture of organic molecules that range in molecular weight from a few hundred to several thousand. These molecules also range from no polarity to highly polar or polarisable. At intermolecular levels, the different molecule types exhibit behavioural characteristics ranging from polar to non-polar. van de Ven *et al.* (1999)

summarise the various methods of separating bitumen into the generic functionally related groups of compounds; these methods are based on chemical precipitation, adsorption chromatography and size exclusion. Shell Bitumen (2003) and Hoiberg (1965) give detailed descriptions of the types of molecular structure within bitumen, indicating that intermolecular forces between hydrocarbon are Van der Waal's forces, polarisation forces and electron forces. These forces play a significant role in the bitumen interface.

It is believed that a durable binder can be described as having acceptable initial properties to contribute to BSM performance and good ageing behaviour during in-service conditions. When a thin binder film in a BSM is exposed to atmospheric air (oxygen), an oxidation reaction takes place which changes the chemical composition of the binder. Oxidation is an irreversible chemical reaction and is considered to be the dominant ageing process during in-service life (Branthaver *et al.*, 1993; Kandal and Chakraborty, 1996).

An important mechanism of age hardening is the change in the chemical composition of binder molecules because of a reaction with the atmospheric oxygen. This may occur during foam production (observed in this study) and during the in-service life. Oxidation influences the durability properties of the binder, which is a function of the chemical composition. The rate of chemical compositional change for the thick film asphalt (HMA) is different from the thin film on BSMs. The difference being that the thin film on a BSM is highly exposed to oxidation pathways due to a discrete coating of the colliding bubbles of the foamed bitumen or breaking of emulsion droplets on the mineral aggregates, leaving higher voids in the mix matrix. Therefore, an understanding of the chemical factors affecting physical properties is essential in describing the factors affecting BSM binder durability.

2.3.2.1 Colloidal and Rheological character of bituminous binder

The bitumen function groups are generally considered to be saturates, aromatics (non-polar), resins (polar aromatics), and asphaltenes. Girdler (1965) and Ishai *et al.* (1988) consider bitumen a colloidal system consisting of strongly associated polar molecules (high molecular weight asphaltenes), micelles, dispersed or dissolved in less polar bitumen molecules (lower molecular weight oily medium of continuous phase), maltenes. The micelles (electrically charged) are considered to be asphaltenes together with an absorbed sheath of high molecular weight aromatics and resins which act as a stabilising solvating layer. In the presence of sufficient quantities of resins and aromatics of adequate solvating power, the asphaltenes are fully peptised and the resulting micelles have good mobility within the bitumen (properly balanced chemical components) which determines the viscosity of the bitumen (Figure 22a). If the aromatics/resins component is not present in sufficient quantities or has insufficient solvating power, the asphaltene/micelle structure can alter to be irregular and open-packed (Figure 22b) which leads to an alteration in the state of dispersion, thus changing mobility. This behaviour significantly influences the chemical reactivity of the bitumen (Shell Bitumen, 2003). The phenomenon of colloidal behaviour of the asphaltenes in bitumen, resulting from aggregation and solvation, is a good departure point for understanding the chemical reactivity of binder molecules and their susceptibility to oxidation.

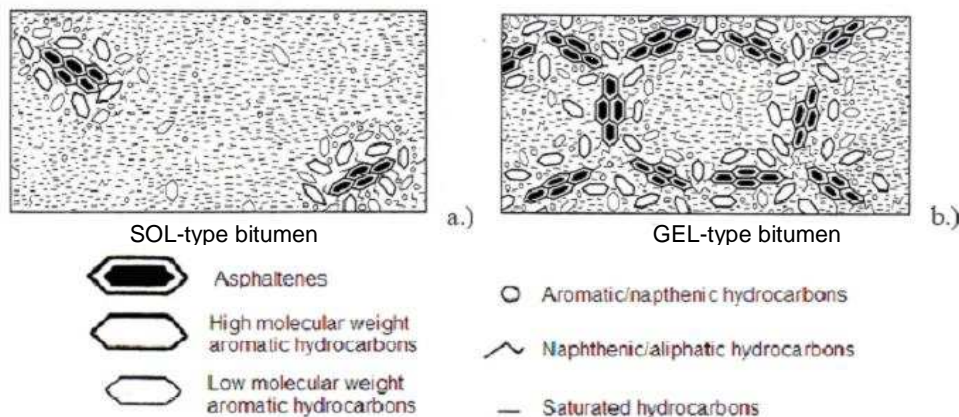


Figure 22: Schematic representation of a SOL and GEL type bitumen (Hagos, 2008)

Although bitumen molecules are composed of predominantly carbon and hydrogen, most molecules contain one or more of the so-called heteroatoms, i.e. nitrogen, sulphur and oxygen, together with a trace amount of metals, principally vanadium and nickel. The heteroatoms often impart functionality of polarity to the molecules; their presence may contribute significantly to the differences in physical properties of binders from different sources (Peterson, 2000). Compositional change of bitumen during oxidative ageing results in a development of polar fraction from non-polar components. Domke *et al.* (1999) reported that oxidation of bitumen causes naphthene (non-polar) aromatics to form polar aromatics (resins) and the polar aromatics to form asphaltenes; hence the asphaltenes content increased, while saturates are considered to be non-reactive (Figure 22). Similar observations are reported by Ishai *et al.* (1988) using a colloidal model (Gaestel index, IC) by characterising the chemical composition of the colloidal structure. They indicate that saturate fractions remain unchanged during oxidation while asphaltenes content increases significantly by comparison with both polar and naphthene aromatics which decrease thereby increasing viscosity or hardening.

The thin films of the binder formed by dispersed colloidal bubbles (foam) or droplets (emulsion) into another phase boundary (aggregates) can be explained using thermodynamic and hydrodynamic theory, described in section 2.4 below. Nevertheless, the adhesion of the thin film binder to the aggregates and the change in the rheological properties of bituminous binder might be related to three fundamental composition-related factors governing the changes that could cause binder ageing:

1. Oxidation reaction of binder molecules
2. Loss of oily components of the binder either by volatility (short-term ageing) or absorption by porous aggregates and
3. Molecular structure (isothermal viscosity change or steric hardening)

Since the isothermal reversible age hardening (point 3) is not peculiar to BSMs during in-service conditions the first two points will be discussed further.

1. Oxidation of bitumen

Oxidative ageing of bitumen is a physicochemical process. In a simplified description (Figure 23), oxygen from the environment has to diffuse physically into the asphalt before it reacts with the asphalt components to result in hardening. These phenomena might be critical for BSMs due to high void content as well as the presence of high equilibrium moisture (i.e. 50% OMC) in the mix in the pavement layer.

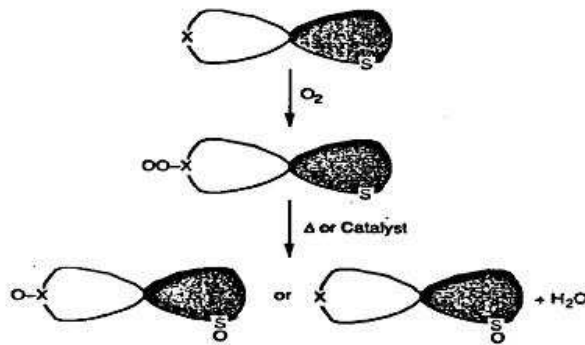


Figure 23: Oxidation pathways for sulfoxide formation (SHARP A-368, Vol.2, 1993)

Petersen (1984) indicates that no chemical changes are observed upon heating asphalt at 60°C–130°C in the absence of oxygen. However, small amounts of volatiles may be lost at an elevated temperature, causing viscosity increases. Above 150°C, non-oxidative (non-chain free radical oxidation) reaction may begin to cause chemical changes, even without oxygen. This aspect may influence the behaviour of foamed bitumen, which is produced at 160°C–180°C. Temperature is a powerful accelerating factor in ageing for two reasons: 1) it softens the bitumen and increases the diffusion rate and 2) it accelerates the chemical reaction. The complex composition of bitumen, with polar and non-polar aromatic hydrocarbon in the mixture, leads to a variety of reactions with atmospheric oxygen even at the moderately low temperatures encountered under the pavement service conditions (see Figure 24).

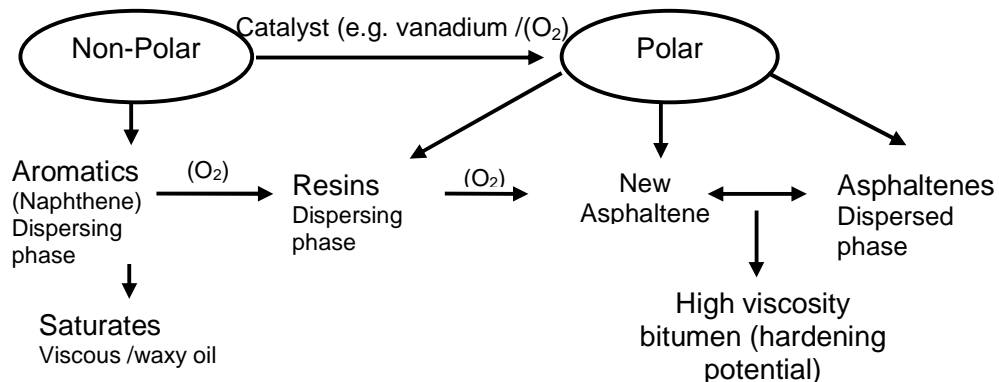


Figure 24: Schematic diagram of chemical compositional change toward more polar fraction bitumen (oxidative ageing)

The oxidation process is only a part of an explanation of the change in rheological properties, but it is not a single chemical process as illustrated in Figure 25. However, analysis of the functional groups of the binder indicates that ketone and sulfoxide are the two major oxidation products formed during oxidative ageing, while anhydrides and carboxylic acids are also formed but in smaller amounts (Plancher *et al.*, 1976).

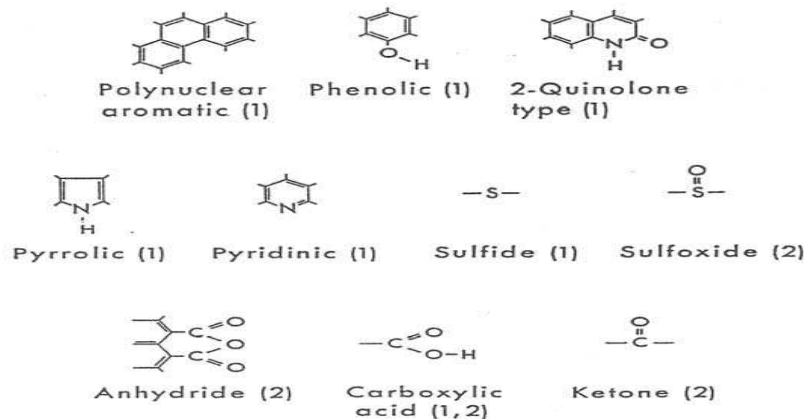


Figure 25: Examples of important chemical functional groups [1] naturally occurring and [2] formed on oxidative ageing (source: SHARP A-368, Vol.2, 1993)

Bell and Sosnovske (1994) indicated that bitumen ageing involves oxidation at the molecular level and structuring at the intermolecular level. The two products of oxidation are ketones/carbonyl (C=O) and sulfoxides (S=O) (Figure 26). These are formed by a slow oxidation reaction of the benzylic carbon during the chemical reaction. SHARP A-368 reported that sulfoxide is easily measured by a single band in the Fourier Transformation Infra Red (FTIR) spectrum near the wavelength of 1030 cm^{-1} (Figure 26). Because it is easy to measure sulfoxide formation, many researchers have used it as an indicator of the bitumen ageing but without clear evidence of the relationship with the other oxidative changes such it as carbonyl formation. The amount of hetroatoms of bitumen varies between less than 1% and 5% depending on the source of bitumen. High vanadium content is generally present in binders with high numbers of hetroatom. According to Bell and Sosnovske (1994), severe hardening occurs at high vanadium content. This is due to its role as a catalyst for the oxidation process.

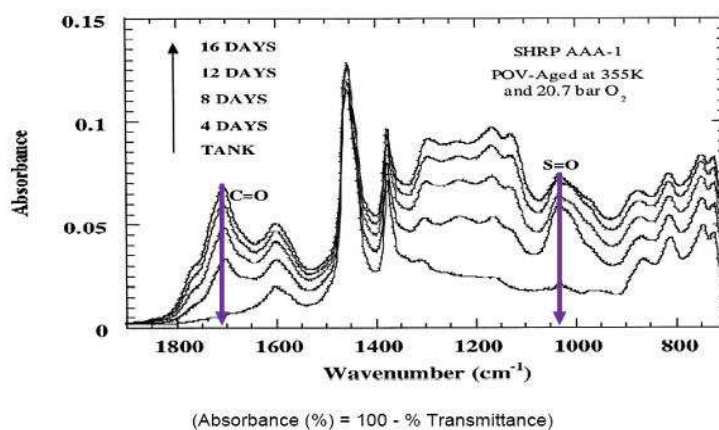


Figure 26: FTIR spectrum showing increase in carbonyl/ketone (1700 cm^{-1}) and Sulfoxide (1030 cm^{-1}) formation with ageing (Hagos, 2008)

2.3.2.2 . Influence of binder- mineral surfaces interaction with in age hardening

In the previous sections it was indicated that the physicochemical properties of mineral aggregates and the colloidal nature of bitumen play a significant role in binder-aggregate interactions. Mineral aggregates have the potential to adsorb (adhere) asphalt components on

their surfaces through thermodynamic, hydrodynamic and electrokinetic means. Therefore, the role of aggregates in influencing ageing mechanisms comes mainly from interaction with highly polar components of the binder. The differences in ageing performance of the same asphalts mixed with different aggregates are believed to be caused by the different adsorption properties (acidic or basic) mineral aggregates may have. This effect has received almost no attention in the literature on BSMs. Anderson *et al.* (1994) indicate that aggregates, depending on their mineral composition, may have a dual role in the binder oxidation: 1) they may work as catalysts promoting the formation of the oxidation products in the less polar generic fractions (saturate and naphthalene aromatics) or 2) they may adsorb the high polar fractions making them less oxidisable. Adsorption of the highly polar fractions is the potential of the aggregate surface to orient the polar molecules in the asphalt in the vicinity of the interface and isolate them by inhibiting their reaction with oxygen. At the same time, this reduces their catalytic effect in promoting the oxidation of saturate and naphthalene aromatics.

Although Anderson *et al.* (1984) investigated oxidation effects on HMA, these phenomena are more pronounced in BSMs due to the dispersion of thin film binder and inclusion of high filler content in the mixture. Person *et al.*, (1974), after experimenting with four different asphalt and four different aggregates, indicate that the rate and degree of catalytic or oxidation reaction between the binder and the aggregates depends not only on the type of binder, but also on the surface charge of the aggregates. Siliceous aggregates (acidic, such as Quartz, Granite, and Hornfels etc) are negatively charged at the surface, while calcareous aggregates (basic, such as calcite, basalt, limestone etc) are positively charged at the surface. Therefore, the aggregates with the least adsorption of high polar fractions (e.g. Quartzite) exhibited the greatest catalytic effect in asphalt oxidation, while those showing the largest adsorption (e.g. Limestone) exhibited the smallest catalytic effects. Similar effects on oxidation of asphalt resulting from charged aggregate surface were reported by Anderson *et al.*, (1994) and Read and Whiteoak (2003). The difference in the diffusion process of the polar fraction between bulk bitumen and bitumen-aggregates interface may also contribute to the viscosity build-up. This phenomenon gives an insight into analysing the interaction of the binder-RAP aggregate interface. The influence of temperature on RAP reactivity and BSM performance from field temperature gradient is presented in subsequent sections.

2.3.3 Influence temperature on RAP and age hardening

Due to the fact that RAP aggregate has an existing strong, adhered, old bitumen, its surface characteristic might be regarded as “inert or dull” due to the equilibrium of interfacial charges. The inert surface has minimal potential to adsorb/diffuse the high polar fractions at ambient temperature. Instead it may work as a catalyst in promoting the formation of the oxidation products in the less polar generic fractions (saturate and naphthalene aromatics). Therefore, depending on the RAP contents in the mix, durability and long-term performance of BSMs will be affected. Twagira (2006) and Ebels (2008) indicate that BSMs with a higher percentage of RAP show inferior performance in terms of mechanical properties (such as shear, stiffness and fatigue) compared to virgin aggregates or mixes with a lower percentage of RAP aggregates. It is apparent from these performances that an understanding of the interfacial interaction between binder and RAP aggregates will give insight into the usage of higher RAP percentages in BSM technology.

Previous discussion shows that diffusion or adsorption of high polar fractions reduces oxidation reaction and improves adhesion between the binder-aggregate interfaces. Cussler, (1997) indicates that the diffusion rate is influenced by 1) size and shape of molecules, 2) intermolecular forces, 3) temperature, 4) structural rigidity of the diffusing molecules and 5) macroscopic structure of a relative stationary phase. The stationary phase is considered to be the continuous phase of bitumen (maltenes) and the viscosity enhancing phase (asphaltenes) becoming less mobile. The effect of the stationary (inert) phase in a gels molecular network is a

physical obstacle in diffusion of polar and non-polar molecules and surface lowering of mobility and phase adhesion. However, rising the temperature activates the stationary phase and consequently increases mobility and adsorption/diffusion of the new binder. The conceptual adsorption/diffusion of new binder into old bitumen (stationary phase) upon increase of temperature is indicated in Figure 27.

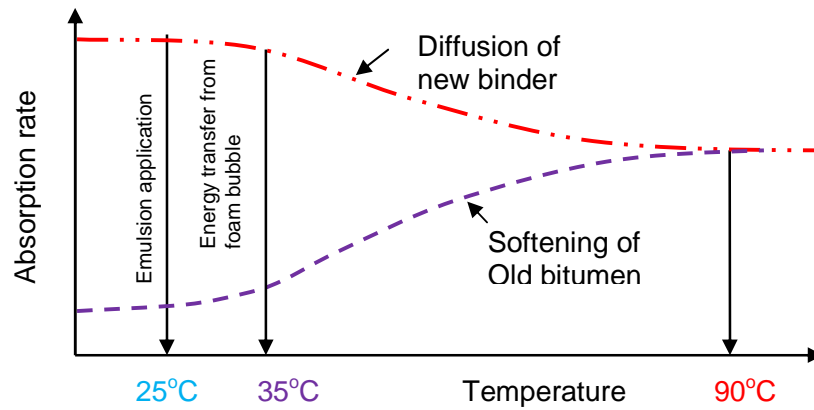


Figure 27: Variation in binder adsorption in a RAP-aggregate surface (aged bitumen)

Oliver (1975) indicates that diffusion rates could be increased and concludes that the diffusion coefficient depends on the temperature in an Arrhenius-type relationship as indicated in Equation 3.

$$D(T) = D_o e^{(k_1/T)+k_2} \quad \text{Equation 4}$$

where, the rate of diffusion $\log D(T)$ is directly proportional to the reciprocal of the absolute temperature, $1/T$ with K_1 and K_2 being constant.

Jenkins (2000), in his research into half-warm foamed bitumen, indicates that heating aggregates before foaming improves particle coating or binder dispersion. At microscopic levels, this might imply better adsorption/diffusion of the binder into aggregate surfaces, both filler and coarse fractions. The aggregates were heated above ambient temperature but below 100°C . Jenkins further indicates that in cold mix the effect of a lower temperature gradient between the aggregates and the foamed bitumen might influence the rate of collapse of the foam. This might occur even though the bitumen has relatively poor thermal conductivity. Since, at foam state, the surface area of the bitumen that makes contact with the aggregates is high and the film thickness of the bubbles is thin, the rate of heat transfer is rapid. This makes the rate of collapse of the foam and rate of viscosity increase in the binder during mixing rapid as well. Moreover, if the aggregates are preheated, the equilibrium temperature of the mix will be marginally lower than 100°C , therefore the bitumen will have lower viscosity for a longer time during mixing, consequently increasing the particle coating “better adsorption/diffusion” of the binder in the mix.

The rate of heat transfer from foamed bitumen to the aggregates, even at lower temperatures of aggregates, may explain the better performance of foamed bitumen compared with bitumen emulsion. This has been reported for BSMs with a higher percentage of RAP content. It has been recognised in various studies that the oxidation susceptibility of binders depends not only on the source of the base binder and the mixture variables, such as voids content, but also on temperature variation, moisture content, UV light, etc. Anderson *et al.* (1994) report that seasonal and daily pavement temperature strongly affects the ageing rate of the binder. Sensitivity of binder ageing rate to temperature is binder specific – that is binders

from different sources could have different ageing dependencies – and the degree of ageing can also be related to the energy of the solar influx at different angles of solar radiation. The models for predicting heat transfer in pavement layers are discussed in the following section and validation of the model for the prediction of heat transfer in BSMs is presented in Chapter 4.

2.3.4 Influence of temperature distribution on BSMs durability

As pointed out in the previous sections, temperature is a powerful accelerating factor in ageing because it causes softening of the bitumen and increases the diffusion rate or accelerates chemical reaction in the presence of oxygen. It is evident from the literature that moderate temperature in the pavement layer plays a key role in age hardening of BSMs in a pavement during its service life. Therefore, an understanding of the thermal properties of the BSM layer will give an insight into the mechanism influencing not only age hardening but also the evolution of adhesion and cohesion in the mix through evaporation and the curing potential of the mix which enhances its durability.

In a pavement structure, BSMs are incorporated as a base layer particularly in in-situ recycling technology. Therefore, understanding the thermal properties of BSMs requires a good knowledge of the thermal properties of the surface layer (i.e. AC or seals). From literature surveys, it is clear that the thermal property of HMA has been extensively studied. Highter *et al.* (1984) studied the thermal conductivity of different limestone mixes in HMA with different asphalt contents (i.e. 3.5 to 6.5%). They found that the thermal conductivity of the mix increases as binder content increases. This is due to the fact that an increase in binder content replaces the air in the voids in the mix and because the conductivity of bitumen is higher than air this results in a higher mix conductivity. The general conclusion shows that the dominant mechanism for thermal conductivity depends on the asphalt content and mix properties such as percentage coarse fraction, gradation and the specific surface of the mix (percentage of filler content).

Solaimanian *et al.* (1993) extend the work of Barber (1957) on heat diffusion theory. They propose the mathematical method for predicting maximum pavement surface temperature using maximum air temperature and hourly solar radiation. Their method was developed based on heat transfer theory and takes into account the effect of latitude on solar radiation. Jia *et al.* (2007) improve this work by indicating that the method focuses on calculating maximum higher temperature, while assuming wind speed remains constant; this is different from actual field conditions. Therefore, Jia *et al.* incorporate the effect of wind speed and develop a numerical temperature prediction model for the thermal properties of asphalt pavement applicable to Chinese weather conditions. Burger (2005) indicates that most of the existing simplified numerical models that predict pavement temperature are in part based on equations that do not adequately describe actual heat transfer rates in the pavement layer. Starting from the deficiencies in the SHARP model reported by Evaritt *et al.* (1999) and Selaimanian *et al.*, he further improves the temperature distribution and prediction model for HMA. The sensitivity test in the model was based on South African environmental conditions. Although the model was designed for HMA, its applicability, and usefulness can be extended to BSMs.

The advantages of predicting temperature distribution in the BSMs layer from local environmental conditions have twofold:

1. Ability to understand the mechanism of binder ageing and/or mastic stiffening during curing process of the compacted mix.
2. Ability to predict water evaporation from the material during the curing period. This is an important aspect for the contractor/designer to be able to predict the early opening of the BSMs layer for traffic.

To this end, the model is presented in Chapter 6 and its usefulness will be discussed based on the temperature and relative humidity of the BSMs layer as presented in this study.

2.3.5 Age hardening characteristics

2.3.5.1 Background

Very limited studies have been reported on age hardening characteristics and/or its influence on the engineering performance on BSMs. Studies in the past indicated that BSMs can age significantly during in-service pavement life (Jenkins, 2000; Øverby *et al.*, 2004; Gueit *et al.*, 2007 and Serfass *et al.*, 2008). Jenkins's research on foamed bitumen mastic indicates that the thin film binder thickness and high surface area of bitumen in BSM foam can render it susceptible to premature ageing if not properly compacted or sealed on surface. The investigation by Øverby *et al.* into the field performance of foamed bitumen, indicates that bitumen properties reduced from 80/100 penetration to approximately 3–10dmm penetration after 10 years of pavement life. However, despite severe ageing, they report that the pavement was still in very good service condition in terms of rutting, IRI and E-Modulus. Guites *et al.* recognised the need for investigating the age hardening behaviour of bitumen emulsion. However, their emphasis was on finding the appropriate method for binder extraction, which is a challenge in determining ageing characteristics of BSM mixtures. Serfass *et al.* investigate age hardening behaviour of emulsion mixes in laboratory-prepared samples and field-constructed sections. Their results found that bitumen penetration decreases from 88dmm to 42dmm in 90 days under accelerated curing at 35°C and 20% relative humidity. However, field age hardening results show a change of penetration from 82dmm to 7dmm for unsealed and 14dmm for sealed (single seal) sections. For this reason, binder ageing of BSMs has been of concern to practitioners globally, hence the need for further investigation into this behaviour.

It is apparent from the literature that understanding the age hardening characteristics of BSMs requires microscopic analysis. In this literature survey, fundamental ageing characteristics of BSMs during formulation, combination and production are discussed, with emphasis on the influence of binder thickness, mastic filler, addition of active filler and binder-aggregate interaction (adhesion and cohesion). Further, validations of these factors are studies and presented in Chapter 6.

The oxidation process, even at moderate temperatures, encountered under pavement service conditions might be a part of an explanation for the change in rheological properties of binder in BSMs. The oxidation pathway to the binder can be explained by the diffusion process. *Diffusion* is a process by which matter is transported from one part of a system to another as a result of random molecular motions under the influence of a concentration gradient (Burger and Kröger, 2006 and Tuffour *et al.*, 1990). The transfer of molecules takes place from a region of high to one of low concentration. Surface layer (AC or seal) is exposed to a high concentration of atmospheric oxygen. Therefore, depending on the void content in the mix, oxygen might diffuse through to the underlying BSM layer. The diffused oxygen might further penetrate the BSM mix due to its high void content, and subsequently react with the binder film.

In order to apply the diffusion model to binder oxidation in a long-term scenario and to make the complex reaction kinetics amenable to mathematical formulation, some assumptions were made regarding the process of oxidation absorption into and subsequent reaction with the binder film (Burger and Kröger, 2006 and Tuffour *et al.*, 1990). The possible flow of air in the surface layer might also imply possible flow of moisture through the same pathway into the underlying BSM layer.

- Free atmospheric oxygen dissolves in the surface layer contiguous with the atmosphere. Because of concentration build-up, some of the oxygen is transported through diffusion to underlying layer.

- Figure 28 shows that the rate at which diffusion occurs depends on the concentration gradient and the diffusion coefficient of the oxygen in the surface layer under the given exposure conditions.
- The diffusion coefficient for oxygen in the binder is dependent on the local viscosity condition, under activation temperature.
- As soon as free oxygen is present in a given layer, the oxygen will react with the binder at a rate determined by the concentration of oxygen and the reactivity of the polar and non-polar molecules of the binder. The reaction however, is considered to be of a first order.
- The reactive component of the binder has a specified amount so that the reaction is retarded as the amount of this component is used up.

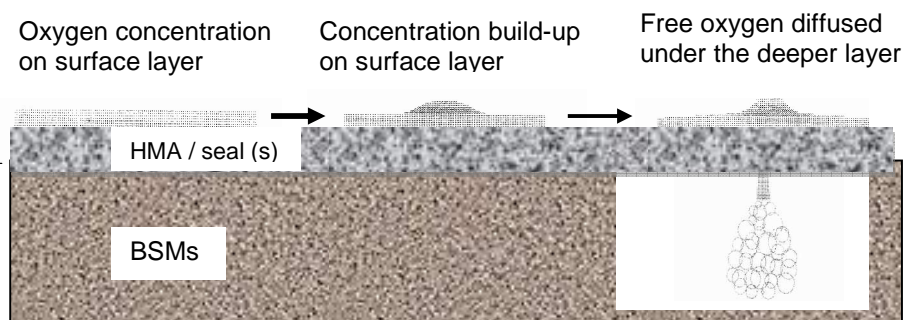


Figure 28: Simplistic diffusion process of the free atmospheric oxygen into the BSM layer

2.3.5.2 Effect of binder film thickness on ageing

Unlike HMA, where binder smears the fine and coarse fraction on the entire surface, binder particle coating in BSMs is complex because it involves filler content, moisture content, aggregate temperature and foam or emulsion characteristics. Jenkins (2000) indicates that temperature gradient between the aggregates and the foamed bitumen significantly influences the rate of collapse of the foam. This is because, in a foam state, the surface area of bitumen that makes contact with the aggregates is high and the film thickness of bubbles is extremely thin, making the rate of heat transfer rapid. The rate of collapse of the foam, and hence the rate of viscosity increase, in the binder during mixing will therefore be rapid. As particles of mineral aggregates make contact with foamed bitumen they acquire heat from the foam bubbles; in turn the following occurs:

- If the particle penetrates the foam bubble, it may be burst mechanically leaving bitumen droplets either attached to or separate from the particle.
- If a large particle makes contact with a foam bubble, high energy transfer occurs. This , reduces the steam pressure in the bubble causing it to collapse, which reduces the temperature and hence increases the viscosity of the bitumen. Thus there is less coating of the particle as mixing continues.
- If a small particle makes contact with the foam bubble, less heat is transferred, leaving the bubble either intact or deflated but allowing the bitumen to retain more heat and hence remain at a lower viscosity. This allows bitumen to displace the water around the particle and encourage coating on the smaller surface area as mixing continues (before equilibrium temperature of the entire mix is reached).

Unlike foamed bitumen, the coagulation and dispersion of bitumen emulsion droplets are relatively uniformly distributed within mineral aggregate fractions. However, due to the high surface area of filler particles and more reactivity with droplets, thin film will coat the large fraction but the higher binder concentration will be attached to the filler content.

It is apparent from the mechanisms of coating of foamed bitumen and bitumen emulsion into mineral aggregates that the mix will have higher voids content. Therefore, the access of oxygen diffused into the thin film of the binder in BSM-foam or BSM-emulsion might result in premature ageing. Oxidation might occur faster if a mix is not adequately compacted or sealed at the surface or if it is allowed to dry out without seal. However, the probable difference of the binder hardening for coarse and fine fractions in the mix matrix needs investigation. Another factor that might influence ageing is densification of the mix (reduction of void in the mix) under traffic, this also needs to be investigated.

2.3.5.3 Effect of bitumen mastic

It is widely accepted that the mixture of filler and bitumen (i.e. the mastic) is an important component that binds the large particles together. During its metastable life, foamed bitumen is mixed with cold, moist mineral aggregates agitated in a mixer. The colloidal mass, which collapses very quickly during mixing with the erupted bitumen, provides globules at low viscosity that favour the particle with the highest surface-to-mass ratio, i.e. finest fraction. Similarly, the coagulation and dispersion nature of the emulsion droplets favour filler particles the most. The stiffening potential of the mastics both in foamed bitumen and bitumen emulsion has significant influence on BSM performance, including failure behaviour and resistance to permanent deformation (Fu *et al.*, 2007 and Jenkins, 2000).

Jenkins studied the stiffening behaviour of mastics with water and foamed bitumen or bitumen emulsion with a variety of filler types. His study reveals that the percentage of bulk volume for the mastic is a primary factor influencing the stiffening of foam or emulsion mix. Using a softening point temperature approach, mastics produced by 150/200 pen-grade foamed bitumen with different filler types at different percentages of bulk volume were tested and compared with HMA as indicated in Figure 29.

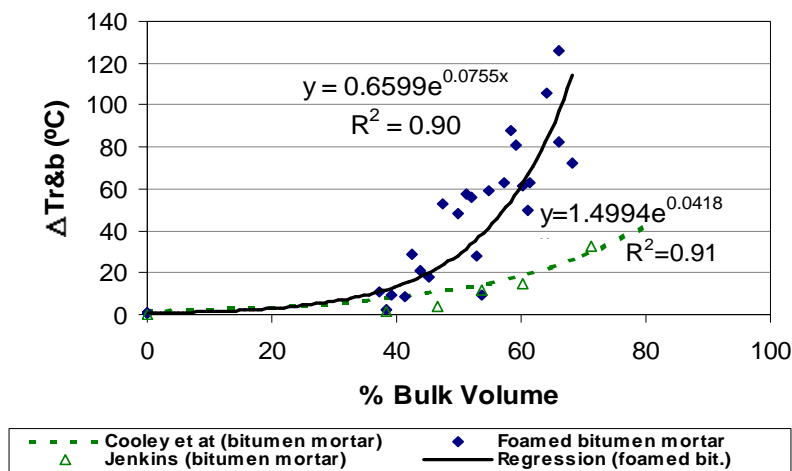


Figure 29: Comparison of stiffening potential versus percentage bulk volume of mastic for the BSM- foam and HMA (Jenkins, 2000)

It is evident from Figure 29 that foamed bitumen stiffens at lower %Vdb (40%) and stiffens more rapidly as %Vdb increases, compared to HMA. The best explanation for the stiffening behaviour of mastic is the physicochemical properties of filler-binder interaction. The high affinity (reactivity) of filler fraction to the polar and non-polar molecules of the dispersed foamed bubbles influences the faster stiffening potential compared to the interaction of thick film dispersed in the HMA. Nevertheless, studies on the stiffening behaviour of the bitumen emulsion mastics compared to foamed bitumen conducted by Jenkins indicates that emulsion

mastic has a quicker initial stiffening at the same %Vdb (40%) compared to foamed bitumen. Due to the coagulation and dispersion nature of emulsion droplets in the mix, it is evident that a higher percentage of bulk volume (filler to binder ratio) impedes the binder-filler reactivity, resulting in no significant stiffening potential with a higher filler content due to unreactive or free polar molecules in the mixture. This phenomenon might be an explanation for the easy oxidation of free polar molecules with oxygen present in the emulsion mix, which results in higher ageing compared to foamed bitumen.

A SHARP report (SHARP-A-341) indicates that filler content has two effects: 1) they decrease the temperature susceptibility of the binder and 2) they increase resistance to cracking by retarding binder oxidation. The interaction of the binder with mineral filler might delay the increase in the viscosity of binders upon ageing compared to bulk bitumen ageing for equivalent ageing times. This difference in viscosity is thought to have been caused by filler particles holding some of the oxidative functional groups that prevent formation of viscosity build-up. This phenomenon is an important factor describing the lower risk of ageing in the early life of BSMs. However, in the long-term age hardening might occur at a minimal rate. The improvement in the resistance to oxidation of binders varies widely depending on the type of filler (acidic or basic) and the bitumen composition or source. Nevertheless, no study has been conducted on filler properties and their influence on ageing. Jenkins (2000) conducted a study using filler mastics for ageing. He was probably the first author to try this approach in a study of the durability of foamed bitumen. Jenkins used the rolling thin film oven test at 163°C as per the ASTM D 175-97 method and tested the change in softening point as indicated in Figure 30.

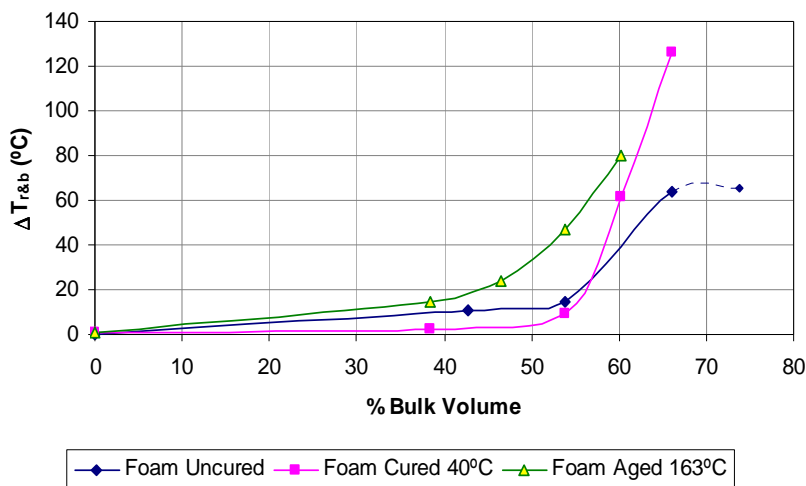


Figure 30: Aging potential of foamed bitumen mastic as a function of bulk volume for Hornfels-RAP dust and 150/200 Calref bitumen (Jenkins 2000)

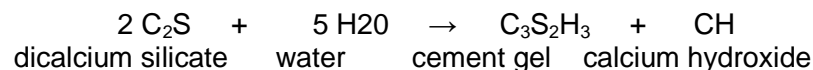
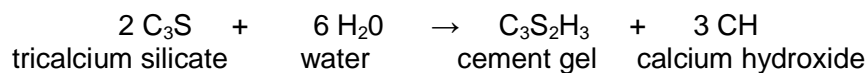
Although a laboratory ageing temperature of 163°C was used in the simulation, this temperature does not simulate the ageing potential of BSMs under field conditions. The raising of the softening point temperature by 20°C at 163°C, with %Vdb of 60%, may be partly due to the stiffening potential at higher curing temperatures coupled with the ageing of the binder. Since the actual ageing of the binder in the mastics was not extracted and tested ($\Delta T_{RB-mastic}$ vs. $\Delta T_{RB-binder}$), the indication of the rate of age hardening is inconclusive and therefore further research is required in this area.

2.3.5.4 Influence of active filler

In South Africa, cement-treated materials are used extensively, particularly as subbase materials. Because of this, a proper guideline was established (TRH13). Due to its suitability for modification or stabilisation of natural gravel and crushed aggregates, cement and lime were applied in BSMs to achieve the same improvement in engineering performance. Extensive studies have been done globally on the application of active filler in BSMs, and the results indicate that small dosages of active filler (i.e. 1%) have significantly improved the durability and mechanical properties of BSMs. This improvement is linked to active filler acting as an agent for dispersing foam and emulsion in the mix, faster curing and the early development of cohesive bonding between binder and aggregate. However, aside from these improvements, little study has been made of the influence of the active filler (cement or lime) on the age hardening characteristics of BSMs. The role of the active filler on dispersion, curing and cohesive bonds is due to its physicochemical properties. Looking at a microscopic level, the physicochemical interaction of active filler, mineral aggregates and binder might influence age hardening as described below:

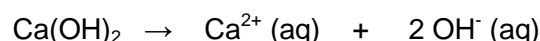
Cement

Cement consists mainly of tricalcium silicate, Ca_3SiO_5 ($\equiv \text{C}_3\text{S}$), and dicalcium silicate, Ca_2SiO_4 ($\equiv \text{C}_2\text{S}$). The hydration of cement takes places as follows:



where $\text{C}_3\text{S}_2\text{H}_3$ stands for calcium silicate hydrate ($3\text{CaO} \cdot 2\text{SiO}_2 \cdot 4\text{H}_2\text{O}$) also referred to as cement gel or paste. CH is the notation for calcium hydroxide, $\text{Ca}(\text{OH})_2$, also referred to as hydrated lime. Both of the above reactions generate heat, which is beneficial for the dispersion of foam or breaking of emulsion. The cement gel crystallises or sets into an interlocking matrix causing a cementing action. This phenomenon will be discussed further in moisture susceptibility in section 2.4.

However, the calcium hydroxide that comes free during the hydration of the calcium silicates is partly soluble and ionised. The calcium ion and ionised hydroxide become freely available as shown in the reaction below:



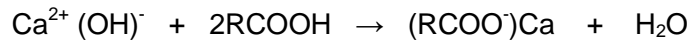
when a small dosage of cement is added to the mineral aggregates, two reactions might take place, 1) it coats large particle by reacting with dust/filler, covering the aggregates surface, or 2) cationic exchange takes place between cement and fine/filler particles. The calcium (Ca^{2+}) ion (with high valences) can replace hydrogen (H^+), sodium (Na^+) and potassium (K^+) (with low valence) from fine particle (clay) or dust on coarse fraction. The replacing ions (Ca^{2+}) can hold substantially fewer water molecules than the ions being replaced. This results in a reduction of the thickness of the bond water layer around the clay particle, which promotes the development of a flocculent structure.

However, the cement or lime is added and mixed in the BSMs (laboratory) for shorter time (1 min) prior to the addition of foam or emulsion. Therefore due to the incomplete hydration process during mixing, cement or lime has the following benefits:

1. Acts as a mineral filler to favourably assist dispersion of foam or breaking of emulsion and in turn stiffens the binder and the mix matrix

2. Improves resistance to permanent deformation (i.e. improves shear property) at low temperatures
3. Favourably alters oxidation kinetics and interacts with products of oxidation to reduce their deleterious effects, and
4. Alters the plastic properties of clay fines to improve moisture susceptibility and durability.
5. Facilitates reactivity of the surfactant to the mineral aggregates surface (locking mechanism of the bond at binder-aggregate interface).

The discussion of point 1, 2, 4 and 5 can be found elsewhere in this chapter. However, according to point 3, Little *et al.*, (2001) indicate that free calcium ions (Ca⁺) and ionised hydroxide (OH⁻) have two main influences on oxidation: 1) they react with the bitumen and 2) the released alkaline hydroxide (OH⁻) can raise the pH level (above 8) of surface water and increase positive charges which is beneficial for the mineral adsorption of polar and non-polar fractions of the bitumen as shown in the reaction below.



Lime

Various types of lime exist, i.e. hydrated lime (Ca(OH)₂), calcitic quick lime (CaO), dolomite lime (CaO, MgO), and agricultural lime (CaCO₃-limestone). The commonly used lime for BSMS stabilisation is hydrated lime. The physicochemical characteristic of lime is similar to the reactivity of cement described above. However, the cationic exchange between lime and clay in the mineral aggregates take place more rapidly than in cement, resulting in quick reduction of the liquid limit and plastic limit index (Jenkins 2007). Because of the reduction of bound water on the surface of the mineral aggregate due to the exchange ion (electrokinetics process), it alters the oxidation process by improving adsorption of bitumen fraction and changes the surface from hydrophilic to hydrophobic which facilitates the evaporation of water from the mix and/or workability during mixing (see Figure 31).

Surfactants displace water from the surface of the filler due to the high reactivity of the cation exchange between the filler and the surfactants from the binder (Admson, 1990).

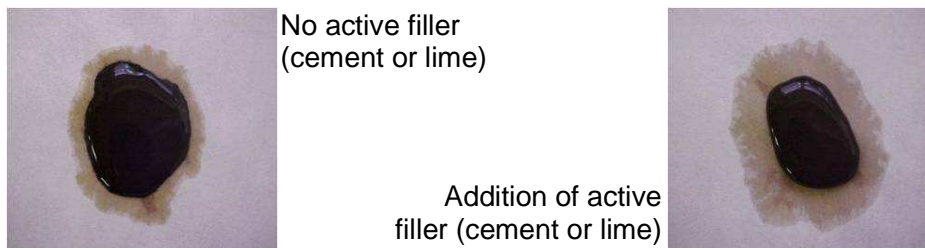


Figure 31: Hydrophobic nature of the surface due to the addition of active filler

Little *et al.* (2001) indicate that as HMA ages due to oxidation, the addition of hydrated lime reduces not only the rate of oxidation but also the harm created by the products of oxidation. This effect keeps the asphalt from hardening excessively and from becoming highly susceptible to cracking. Jenkins (2007) notes that lime is usually a better modifier than cement, whereas cement is a much better binding agent (i.e. quick setting of CSH gel, because production of such gel in lime takes much longer and only if sufficient lime is available after the rapid reaction has been completed). Tarrer (1996) indicates that hydrated lime cures rapidly (within 15 to 30 minutes) and forms water insoluble compounds. Hydrated lime creates a very strong bond between the bitumen and the aggregate, in turn preventing moisture susceptibility at all pH

levels. The benefit and influence of lime in BSMs will be discussed further in section 2.4 and Chapter 3 of this study.

2.3.5.5 Influence of ageing on cohesion and adhesion

It is evident from the literature study that depending on the surface layer covering BSMs, ageing of the binder in BSMs can be a long-term phenomenon and therefore to ascertaining the influence of the ageing on the cohesion and adhesion and performance of BSMs is a complex matter. This is particularly due to the following reasons:

1. The physicochemical interaction of the mineral aggregate, filler and the binder (foam or emulsion) provides a basis to explain the multifunctional effects in BSMs as discussed in the previous sections above.
2. Depending on the filler/binder ratio in the mix, the fillers have an effect on graduated temperature sensitivity. This positive characteristic allows the bitumen to resist softening at relatively moderate temperatures in the pavement layer, in turn minimising the oxidation reaction.
3. Difficulties in quantifying binder compositional change (rheological properties) due to ageing in the BSMs. This point will be discussed further and validated in the results presented in Chapter 7.

2.3.5.6 Foamed bitumen vs. bitumen emulsion ageing characteristics

It is apparent from the discussion on the literature study that the ageing characteristics of BSM foam and BSM-emulsion are different, which means different durability behaviour in long-term performance. The effect of the differences in foamed bitumen and bitumen emulsion age hardening characteristics is elucidated in Table 8.

Table 8: The difference between foamed bitumen and bitumen emulsion on age hardening characteristics

Factor	BSM-foam	BSM-emulsion
Production temp	Higher temp (160°C-180°C) is required for production of foam: this influence the initial ageing of binder	Lower temp (< 95°C) is required for manufacturing of emulsion this has less influence on initial ageing of binder
Binder thickness	Lower concentration of bubbles dispersed on coarse fraction: thin film on mastic is less prone to oxidation	Large drops smear the coarse fraction during coagulation, thin film on larger fraction is prone to oxidation
Filler content	5-20% is suitable for reactivity with dispersed bubbles: the higher mastic content retards temperature sensitivity, in turn less oxidation reaction	>10% impends reactivity of some bitumen components, which becomes free for oxidation (but the effect can be rectified by addition of lime or cement); less mastic content might allow temperature sensitivity, in turn oxidation reaction
Aggregate temp	Foam bubble dissipates energy to the aggregate surface, hence influences reactivity	No dissipation of energy from emulsion droplet

2.3.6 Indicator of binder compositional change

2.3.6.1 Recovery of bitumen from mixes

The change in binder characteristics in the mixture cannot easily be examined without full separation of bitumen from aggregates. Full extraction therefore, is performed to recover the bitumen from the mix or RAP to enable examination of its rheological properties. Full extraction implies the use of a particular solvent and equipment to separate bitumen from aggregates. The extraction of bitumen from HMA or BSMs differs. The differences are presented in Table 9.

Table 9: Difference in bitumen recovery from HMA and BSMs using conventional methods

Properties	HMA	BSMs
Binder content	Usually higher (4-5%)	Usually lower (1.5% -3%)
Binder dispersion	Coats all aggregates fractions	Selectively coats aggregates fractions, particularly filler fractions
Mineral aggregates	Clean and dry, with minimum size of sand fractions	Mist & coated with clays, minimum size fractions, supper filler
Extraction with cold centrifuge	Possible to separate bitumen from sand fraction	Number of repetitions is required to separate bitumen from supper filler, some bitumen fractions might be discarded with the filler
Dissolving solvent	Little quantities required to wash bitumen from aggregates	Large quantity is required to wash a little bitumen in the mix
Recovery method		
○ ABSON (ASTM D 1856-95a)	Applicable for distillation of the solvent, care should be taken not to overheat the bitumen content	Applicable for distillation of solvent, due to large quantity of solvent, trace of solvent might stay with bitumen. Possible overheating due to longer distillation.
○ Rotary vapour (DIN En 126997/3)	Applicable for distillation of the solvent	Applicable for distillation of the solvent, longer time is required with use of heavy oil.

Conventional methods for qualitative extraction and recovery of asphalt from paving mixture are done by centrifuge extraction, vacuum extraction, reflux extraction etc. (ASTM 2003). Different common solvents have been used in the binder extraction and recovery procedures, i.e. trichloroethylene (TCE), methylene chloride, benzene, 1-trichloroethane (TCA), etc. However, due to the carcinogenic and environmental hazardous nature of all chlorinated solvents, the use of these solvents is being phased out (EPA, 2003; Collins-Garcia *et al.*, 2000).

The extraction and recovery of bitumen has an important influence on the binder characteristics. Many tests have been performed to define the most suitable extraction method and solvent, sometimes with contradictory conclusions. There is no consensus (Okan *et al.*, 2003). It is clear that there are several extraction-recovery methods and solvent choices for both binder content determination and binder performance characterisation. In Europe, two main extraction methods are used for the extraction of bitumen i.e. centrifuge and the reflux (Soxhlet) method. Centrifuge is generally a cold process; this process is preferred because of lower temperature than reflux, which appears to age the bitumen (Burr *et al.*, 1993). There is

consensus in Europe for the removal of solvent by use of rotary vapour distillation. The alternative is using the Abson method (ASTM 2003). However, studies have indicated that the standard Abson recovery method may leave an amount of solvent in the recovered binder or over-heat the bitumen if not done with care, which might result in a change of viscosity properties (Burr *et al.*, 1990, 1993; Peterson *et al.*, 2000 and NCHRP, 2000).

Since the 1970s many USA laboratories have adopted the use of rotary vapour in the recovery process. The rotary vapour method for distilling solvent needs less heat, thus resulting in a lower risk of ageing of binder during recovery. The selection of solvent can also influence the final binder properties. Peterson *et al.* (1994) found that both the extraction and recovery process as well as chlorinated solvent could age the binder. The use of EnSolv and reclaimed EnSolv for the extraction and recovery of binder has been studied as an alternative to TCE. Studies conducted by the NCHRP (2000) found that there are no significant differences between samples recovered using TCE, EnSolv n-PB and reclaimed EnSolv. Hence, the use of EnSolv and modified rotary vapour, which have the advantage of less time in the recovery process and are less toxic, has been recommended.

In this study, the extraction and recovery of the bitumen from foamed bitumen or bitumen emulsion mixes (i.e. the compacted specimens and cores extracted field) was done using the standard Abson method according to ASTM D 1856-95a and rotary vapour method according to DIN En 126997/3. The cold centrifuge with minimum force of 3000 time gravity was used together with trichloroethylene (TCE) solvent to separate the binder from the mineral aggregates.

Recovery of bitumen from Emulsion

Several methods exist for the recovery of bitumen from emulsion. These methods are divided into two types. 1) Thin film oven method, 2) evaporation method "heating en mass" or a chemical reaction under defined operation conditions. The thin film method consists of storing a small amount of emulsion, 1mm thick for 24 hours at ambient temperature and for 24 hour at 50°C in the oven (EN 14895). Heating en mass, Belgium procedure (08-34) consists of heating 50g of emulsion for 2 hours at 163°C in a 600ml beaker of specified shape to prevent foaming of the emulsion. The same principles apply for ASTM D 244–A in the evaporation method. A chemical method developed by Colas France, namely the Ethanol Precipitation method, can be used to separate the aqueous phase and partial or complete separation of the emulsifier. It is believed that this is the only method, which can recover bitumen with identical properties to that of the base bitumen, with regard to not only consistency but also chemical properties (Geit *et al.*, 2006).

2.3.6.2 Short and long-term ageing indicator

The ageing characteristics of the bituminous mixture can be classified into two major groups; short and long-term ageing (Roberts *et al.*, 1996). The age hardening process of the BSMs might be affected by several factors, all operating at the same time. In assessing these factors, Serfass *et al.* (2008), noted that the most critical variables to consider are the characteristics of the mixes themselves. Hardening of the original bitumen for HMA is different from BSMs. High temperatures and the presence of air during plant mixing, mixing time and construction are the variables that can cause age hardening of the HMA. These phenomena do not occur during BSM mixing process because mixing and lay down are done at ambient temperature; however researchers have indicated concern at the high binder temperature required during the foaming process, i.e. where bitumen is heated at 170°C–180°C and combined with hot moisture. For bitumen emulsion no elevated temperature is used for mixing and lay down. Therefore, short-term hardening due to high temperature will not play a key role.

Figure 32 shows the general trend of the effect of ageing during production and mixing (short term) and in-service period (long term) on the viscosity ratio (ratio of aged to unaged

binder) of HMA. However, the general trend line for BSMs obviously will take different path due to different exposure conditions. The trend line for BSMs is discussed further in Chapter 7.

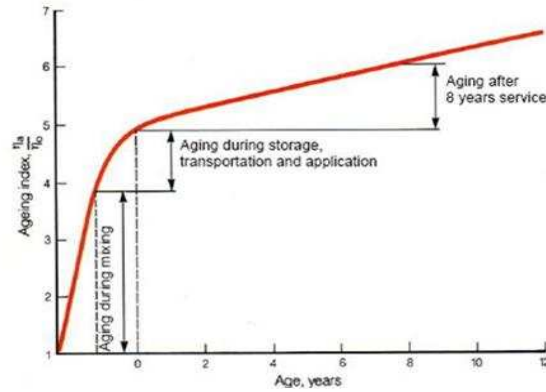


Figure 32: Effect of short and long-term ageing of the binder on viscosity ratio with ageing period for general trend of the HMA (Shell Bitumen 2003)

A number of relationships to predict the composition change in the binder properties during long-term performance have been developed and reported by different researchers.

2.3.6.2.1 Ageing Indicators

The extent of age hardening of base bitumen can be quantified in terms of an empirical relationship. Shell Bitumen (2003) use Penetration Index (PI) and Ageing Index (AI) to determine viscosity change with change in temperature. The ageing behaviour is defined by the PI of greater than -1 or less than 1. Ishai *et al.* (1988) explain the chemical composition change of the binder using the Gaestel Index (IC), an expression of the internal colloidal structural change, as shown in Equation 5.

$$IC = \frac{\text{Asphaltene} + \text{Saturates}}{\text{NaphtheleneAromatics} + \text{Resines}} \quad \text{Equation 5}$$

The use of the colloidal structure model for compositional analysis is believed to provide a meaningful explanation of the long-term ageing behaviour of the binder better than an empirical expression. The major change to the initial rheological properties and ageing properties is expressed by the creation of a new level of colloidal stability compared to the structure of the base binder. An increase in IC after ageing results in an increase in polar functional groups (the asphaltenes content) and a decrease in the polar aromatics (resins) and non-polar (naphthene) aromatic function groups (see Figure 33). This ageing indicator might be useful for BSMs because there is strong adsorption in polar fractions of colloidal particles of the bitumen with electrically charged filler fraction of mineral aggregates. Therefore, identification of true ageing in BSMs requires the quantification of the presence of all compositional fractions of bitumen after recovery, prior to the testing of bitumen rheological properties.

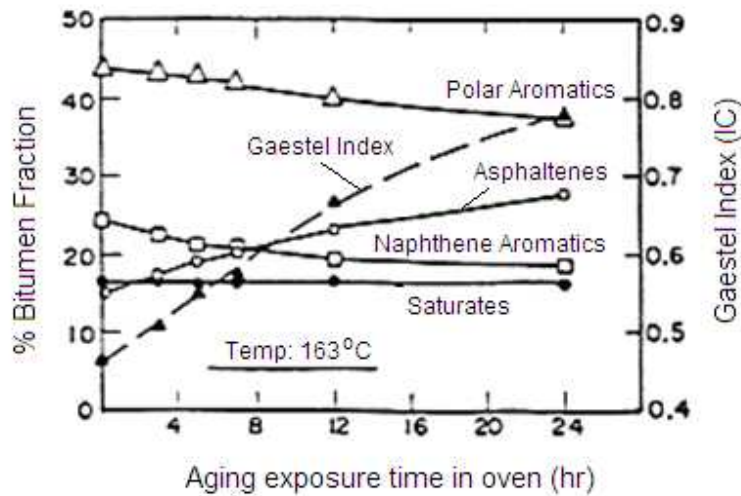


Figure 33: Change in functional groups of bitumen during ageing (Hagos, 2008)

The formation of sulfoxide and carbonyl and a change in molecular weight distribution as a result of binder oxidation can be determined using the Fourier Transformation Infrared (FTIR) spectroscopy test and Gel-Permeation Chromatography (GPC) test respectively. These methods are widely used by researchers to explain the ageing characteristic of the binder. Sulphur oxidation to sulfoxide and formation of carbonyl (ketone) function groups can easily be measured in bitumen by a single band in the IR (SHARP-368). The peak at $1\ 030\text{cm}^{-1}$ represents sulfoxide formation ($\text{S}=\text{O}$) and the one at $1\ 700\text{cm}^{-1}$ represents carbonyl formation ($\text{C}=\text{O}$) as discussed previously.

2.3.7 Simulation of age hardening

The age hardening process in BSMs may be affected by several factors. In assessing these factors, one should note that the most critical variables to consider are the characteristics of the BSMs themselves. BSM-foam hardening may start to occur during mix production (longer circulation time, at a higher temperature) and later during in-service life. This might be different for the BSM-emulsion, where ageing is more pronounced during in-service life.

In the field, climatic effects are the influencing variables in BSMs. The rate of age hardening is dictated by the severity of the environmental temperature levels, time and the access of oxygen into the binder and the intrinsic reactivity of the binder. The access of oxygen into the binder film in the BSM layer is tied to the air-void content in the mixture as well as the presence of high humidity (moisture content). However, only binder molecules accessible to oxygen (either diffused from surface or hygroscopic moisture in the mineral aggregates) will harden. It has however been indicated that due to higher surface area of the filler in the mix and the higher adsorption of the colloidal (foam or emulsion) to the filler, accessible molecules for oxidation reaction might be minimal, depending on the nature of reactivity of the aggregate. Although large air-voids content is found in the mix, the oxidised non-polar molecules (aromatics) to polar (asphaltenes) might not accumulate due to inaccessible existing asphaltene molecules that have strongly adhered to the filler particles. However, the factor that might influence severe ageing in BSMs is the thickness of the film binder. It is general that a thick binder film presents a long diffusion oxidation pathway, which slows down rate of ageing (Tuffour *et al.*, 1990). While in BSMs with predominantly thin film binder, particularly coarse fractions might oxidise faster in the presence of air and moderate pavement temperature.

The laboratory Rolling Thin-film Oven Test (RTFOT) and the pressure ageing vessel (PAV) test are commonly used to simulate short-term (mixing and construction) and long-term

(in-service pavement condition) ageing for HMA. RTFOT is done on a thin film binder tested at 163°C for 75-85 minutes and 5-20kg/m² air pressure. The PAV test is done at different ageing time (typically 20 hours) at temperatures between 60°C and 90°C and pressure of 2.1MPa (Hagos, 2008). These conditions are not applicable for simulating ageing characteristics of BSMs. The higher filler/binder ratio thin film in the coarse aggregates lower temperature gradient and presence of higher relative humidity in these mixes during in-service conditions, cannot be simulated following HMA procedure. The rate of viscosity change varies with depth during pavement life, while at the construction time (t=0) the full depth binder viscosity is considered uniform as indicated in Figure 34. Field ageing is mainly due to the oxidation process. The higher concentration of oxygen occurs at the surface i.e. on HMA before diffusing deeper into the BSM layer. The circulating air and higher surface temperature from solar radiation when diffused in a layer means the effect normally decreases with depth and becomes negligible deeper below the pavement surface.

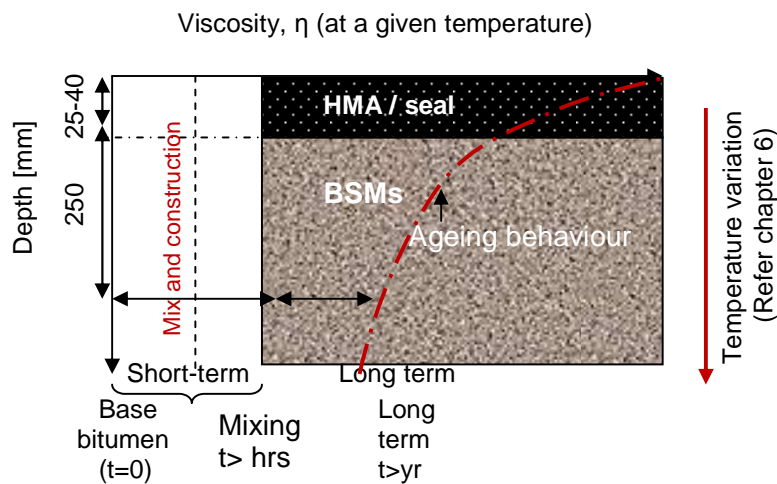


Figure 34: Typical viscosity depth relationship as a function of time at a given temperature

It is generally accepted that the Rolling Thin Film Oven Test (RTFOT) simulates the changes that occur in the binder during mixing, transportation and lying of HMA (British Standard, 2000). This testing at higher temperatures will not simulate BSM ageing as low temperatures are common applied during mixing and construction. In the same way, a test to simulate long-term changes (hardening) acceptable in HMA is Pressures Ageing Vessel (PVA) (AASHTO, 1993). However, the use of elevated temperature and pressure on a thin film of binder might not simulate the ageing effect occurring in BSMs under field conditions. It is apparent from the existing accelerated ageing that the simulation test for the HMA needs refurbishment to be applicable for simulating ageing hardening in BSMs. Serfass *et al.* (2008) studied the age hardening of grave-emulsion, through accelerated curing at 35°C and 20% RH for 90 days. This kind of ageing needs to be simulated for BSMs. However, short time of simulation and the accelerating device need development.

2.4 MIXTURE COMPOSITION DURABILITY

2.4.1 Introduction

The central role of the mixture compositional design and performance in BSMs is illustrated in Figure 7 above. Figure 7 formulates a more detailed approach to mixture compositional durability by relating to binder and mineral aggregate durability. In material science, the mixture computational durability is the study of the structure of the material or its surface, at micro and macro levels, in order to develop a fundamental understanding of the durability properties and/or a model that can be used to explain material behaviour. This might assist in predicting long-term performance. Clearly, the mixture compositional durability is of paramount importance to the mix design of BSMs, and should be considered at all phases of application, i.e. mixing, compaction, curing and opening to traffic.

Based on physicochemical interaction between binder (foam or emulsion) and mineral aggregates as discussed in the material characteristics, mixture composition durability requires fresh investigation. The approach utilised to analyse mixture composition durability of HMA, i.e. surface free energy, binder characteristics and mechanism of moisture damage, can certainly to a large extent be applied to research on mixture composition durability of BSMs. However, the adoption needs to take cognisance of the specific aspects peculiar to BSM mixes such as aqueous phase, colloidal nature of binder, grading of aggregates and changes in durability as a consequence of curing. Due to the unique nature of dispersion of foam and breaking of emulsion on the filler fractions, mastic behaviour and the manner in which it combines with the larger aggregates require special attention in the mixture composition durability studies.

2.4.2 Bitumen, mineral aggregates and water interaction

The interaction between bitumen, mineral aggregates and water is a physicochemical phenomenon and, as such, deals with interfaces. Because there are three types of bulk phases (i.e. solid, liquid and gas), it is possible to classify interfaces based on the nature of the bulk phases that lie on either side of the interface. Thus there are five types of interfaces. Table 10 shows these interfaces and some relevant references of particular interest to BSM mixtures.

Table 10: Phase description for bitumen, aggregates and water interaction applicable to BSMs.

No	Phase type	Abbreviation	Definition	Reference
1	Gas – Liquid	G - L	air-bitumen interface (foamed bitumen, bubbles)	Jenkins (2000); Schramm (2005)
2	Liquid 1- Liquid 2	L – L2	bitumen –water interface (bitumen emulsion, droplets)	James <i>et al.</i> (2004); Salomon <i>et al.</i> (2006) etc
3	Gas-Solid	G - S	air-mineral aggregates interface	Mitchell (1993); and Weinert (1980)
4	Liquid –Solid	L - S	binder/ or water –mineral aggregates interface	*Relatively unknown
5	Solid-Solid	S1 – S2	bulk mineral aggregates interface	Highly researched

Note: * The focus in this study

Systems involving interfaces are often metastable, that is, a state of equilibrium behaviour exhibited in certain aspects, although the system as a whole may be unstable in other aspects. Several mechanisms governing the durability of interfaces on the mixture composition exist. These mechanisms can be largely attributed to different physicochemical properties at the surfaces of these materials. Evidence from the literature suggests that thermodynamic and/or hydrodynamic parameters are linked to adhesion and cohesion of mixture composition and can

be derived by measuring the surface free energy of the binder and mineral aggregates (Bhasin *et al.*, 2006; Cheng, 2002).

The adhesion and cohesion bonding between binder and aggregates in BSM mixtures is one of the most important bonds that differentiate BSMs from granular materials. However, it is also one of the least understood bonds, partly due to the complexity of the binder characteristics and partly due to the variety of surfaces of aggregates with which the binder comes into contact. Most researchers attempt to describe cohesion and adhesion in the binder-aggregates system in BSMs using mechanical means. But in the HMA, the work of adhesion and cohesion using thermodynamic theory has extensively been studied by measuring the surface free energy of the asphalt and aggregates with four advantages (Elphingstone, 1997):

- The mechanical work required to crack an asphalt-aggregate interface is related to the free energy of the adhesion, and cohesion in a certain limiting case.
- Crack propagation models have shown to be a function of the surface free energy of materials. By measuring the surface free energy of the asphalt and aggregates the cracking parameters can be calculated.
- The asphalt-aggregate system can be evaluated for the propensity to be water susceptible (stripping potential).
- Ability to relate asphalt healing after cracking to the surface free energy of the asphalt and aggregates.

Part of the objective of this section is to establish a theoretical framework, based on previous studies on HMA, to predict and analyse adhesion and cohesion in BSMs using fundamentals of the surface free energy of the binder (foam or emulsion) and mineral aggregates. The goals of the framework are::

- To establish if a link exists among in the theoretical work of adhesion and cohesion between surface free energy and durability properties of BSMs.
- To establish if a link exists between the theoretical adhesions and cohesions in BSMs and moisture susceptibility
- To evaluate influence of various binder-mineral aggregate systems in BSMs on shear properties, stiffness and water damage.

2.4.3 Thermodynamic concept on adhesive

The thermodynamic concept is a widely used approach in the adsorption theory or adhesion science, as indicated by most references on this subject (Schramm, 2005; Adamson, 1990; Birdi, 2003; Ensley *et al.*, 1984). The theory indicates that the adhesive will adhere to substrate due to established intermolecular forces at the interface, provided that intimate contact is achieved. The magnitude of these fundamental forces can generally be related to thermodynamic quantities, such as surface free energies of the materials involved in the adhesive bond. The orientation of polar molecules in bitumen, for example as part of minimisation of free energy and consequent adhesion at the interface, has been extensively studied for HMA (Elphingstone, 1997; Goebel *et al.*, 2004; Caro *et al.*, 2007; Hefer *et al.*, 2005).

This section discusses a framework supporting incorporation of surface free energy into the thermodynamic and/or hydrodynamic theory of adhesion and cohesion for understanding durability properties of BSMs. Based on this approach, it is demonstrated that the overall durability behaviour of mixture composition elements (such as mineral particles, foam and emulsion) is physicochemically dependent. Although such dependency is negligible for conventional structural elements, it becomes significant when colloidal particles interact with free energy on the mineral aggregate surfaces.

2.4.3.1 Surface free energy

The properties of surface can be defined in different ways, i.e. bulk phases and inter-phase. Gibbs (1928) introduces the concept of dividing surface into phases using surface free energy (or surface tension). The Gibbs density of surface free energy, γ , is defined as the reversible work involved in creating a unit area of new surface at constant temperature, volume and total number of moles, as indicated in Equation 6.

$$G = \gamma.A \quad \text{Equation 6}$$

$$\Delta G' = 2\gamma$$

where $\Delta G'$ is the Gibbs free energy of adhesion per unit area, and γ is surface free energy of phase. When two dissimilar materials form an interface by being in intimate contact, Dupré postulates the following relationship, which plays a central role in the study of adhesion (Elphinstone, 1997):

$$\Delta G_{12}^a = \gamma_1 + \gamma_2 - \gamma_{12} \quad \text{Equation 7}$$

where ΔG_{12}^a is Gibbs free energy of adhesion per unit area and γ_i is surface energy of i^{th} material and γ_{12} is the interfacial surface free energy of phases 1 and 2.

2.4.3.1.1 Wettability and Contact angle

Hydrodynamic is the change of energy due to wettability. Wettability of the mineral aggregates in BSMs is an important factor influencing the adsorption process or adhesion of different interfacial surfaces. According to Goebel *et al.* (2004), wettability is the ability of a liquid (e.g. bitumen) to spread/coat on a solid surface. Wettability is related to liquid contact angles, which in turn depends on solid surface free energy. When a drop of liquid is placed on a solid surface the liquid may form a bead on the surface or it may spread to form a film. A liquid having a strong affinity (wettability) for the solid, i.e. if its surface energy is less than the critical surface energy of the surface, γ_c will seek to minimise its contact (interfacial area) and spread to form a film. A liquid with much weaker affinity i.e. its surface tension is above γ_c will form a bead. To account for the degree of spreading, the contact angle, θ is defined as an angle, measured through the liquid, which is formed at the junction of three phases, i.e. solid-liquid-vapour (S-L-V) as indicated in Figure 35.

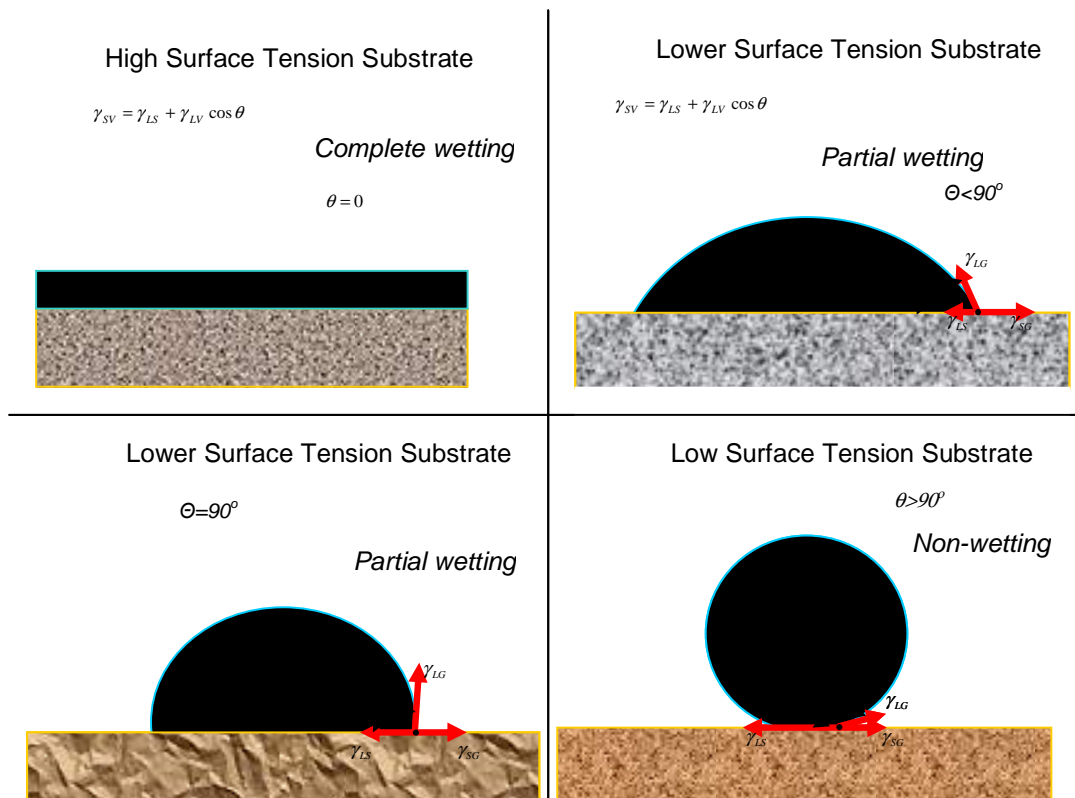


Figure 35: Three-phase boundary of a liquid drop on a solid surface in vapour

According to Young's equation (Adamson, 1990), the mathematic formulation on the interaction of S-L(G or V) interface Figure 36, was developed with the concept that as the drop spreads, the change in surface energy ΔG_s as a result of change in area of solid covered ΔA can expressed as follows:

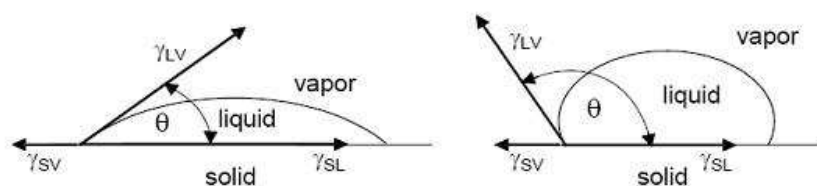


Figure 36: Formulation of the three-phase boundary relationship of a liquid drop on a solid surface in vapour (Adamson, 1990)

$$\gamma_{SV} = \gamma_{SL} + \gamma_{LV} \cos \theta_{SL}$$

if $\gamma_{SV} - \gamma_{SL} > \gamma_{LV}$ then $\cos \theta_{SL} = 1$ perfect wetting

Equation 8

The combination of the Dupré's and Young's equations above, the work of adhesion or Gibbs free energy of adhesion per unit at the solid-liquid interface is expressed as follows:

$$\Delta G_{SL}^a = \gamma_{LV} (1 + \cos \theta_{SL})$$

Equation 9

2.4.3.1.2 Surface free energy measurements

Different techniques are widely used to characterise the surface free energy of binder and mineral aggregate interaction. Hefer *et al.* (2005) describes these techniques as follows:

- Contact angle approach, which includes Wilhelmy plate and sessile drop
- Vapour sorption
- Inverse gas chromatography
- Atomic force microscopy
- Microcalorimetry and
- Electrophoresis

Several researchers have used these techniques to quantify the surface energy of colloidal bitumen (i.e. emulsion droplets and foamed bitumen bubbles). Liu *et al.* (2005) apply atomic force microscopy (AFM) to determine the contact angle due to colloidal force between the bitumen surface in the aqueous phase and the effect of pH on the interaction with filler particles. Laroche *et al.* (2002) apply hydrodynamic force balance to define the dynamic and static repulsion energy between emulsion droplets in the water and the influence of pH on the adhesion or coalescence of the droplets in a different process. Rodríguez *et al.* (2008) apply imaging techniques (sessile drop) to elucidate the mechanism of breaking and curing of bituminous emulsion after the drops of emulsion were deposited in different substrates (Figure 39, section 2.4.3.1.1). Binks *et al.* (2002) apply the Owens and Wendt method to predict contact angle (surface energy) and wettability behaviour of Pickering emulsions. Fortes *et al.* (2001) apply plateau border and liquid pool to determine the contact angle and surface energy of the foam bubbles. All of the above-mentioned techniques have the potential to characterise binder-mineral aggregate interaction and consequently aid in understanding the durability properties and predicting long-term mechanical performances. Although not investigated in this study, the application of these techniques might provide insight into the durability properties of BSMs and so provide an avenue for further research on improving mix design of BSMs as well as the recycling technology as a whole.

2.4.4 Influence on adhesion during dispersion and breaking

During dispersion of foam bubbles with cold, moist, mineral aggregates, that are being agitated, the bubble meta-stable life is curtailed. The bubbles then collapse leaving a structure of binder that is dispersed throughout the mineral aggregate with high affinity to filler reaction leading to the formation of a black spot. The dispersion of binder and the formation of mastic and consequently adhesion to the mineral aggregates depends on a number of factors (Jenkins, 2000):

- Viscosity (expansion) and stability (half-life) of foamed bitumen. The dispersion and wettability potential during mixing is influenced by the foam properties. Lower viscosity reduces dispersion, resulting in balling on collapsed bubbles, in turn resulting in no coating.
- Percentage of filler fraction. The higher affinity of dispersed bubbles on filler fraction results in mastic formation, providing glue for bonding large fractions.
- Mixing method. The mixing energy and duration are important factors for short meta-stable life bubbles. A mixing device, such as a twin-shaft pumill, has significant influence on dispersion and coating of mineral aggregates i.e. production of quality mix matrix.
- Additional moisture before mixing. The dispersed energy of bubbles to the moist surface has significant influence in the wide dispersion and particle coating on filler fractions. Upon complete release of water from the mastic, further bond development occurs.
- Aggregates temperature. Higher temperature in the mix significantly improves wettability and adsorption of binder into the aggregates surfaces.

Microscopic analysis of the compacted mixes indicates that some of the dispersed bubbles are drawn into thin thread like mastic. The formation of these threads within the mix, in the presence

of active filler might result in improved durability properties of foamed bitumen mixes. The formation of thread mastic will be discussed further in Chapter 6.

Breaking of emulsion droplets in the mineral aggregate skeleton must revert to continuous film in order to enhance the development of adhesive bonds. The breaking of droplets involves flocculation coalescence and the removal of the water. The speed of this breaking process depends on a number of factors:

- Reactivity of the emulsion. The use of surfactant in the aqueous phase determines the charges on the droplets. Anionic or cationic surfactant influences the breaking of emulsion when in contact with mineral aggregates.
- Environmental temperature, humidity and wind speed, influence the rate of evaporation. which Influences phase separation (flocculation and coalescence).
- Reactivity of mineral aggregates. The eletrokinetic effect occurs when aggregates attract the surface charge of droplets in water. Cationic emulsifiers droplets contain positively-charged nitrogen (N) atoms in the head group, while anionic emulsifiers contain negatively-charged (O) atoms. These charges are balanced by counterion, which diffuses away from the droplets. Depending on the nature of the mineral aggregates, pH value and the presence of soluble salts, cationic emulsions react faster with an aggregate with a negative surface charge and vice versa for anionic emulsion. The structure of equilibrium emulsion droplets is indicated in the Figure 37.

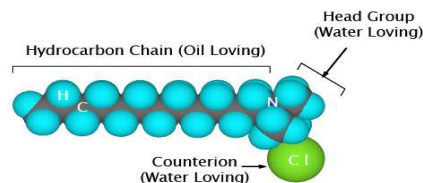


Figure 37: Structure of equilibrium emulsion droplets (James, 2006)

- Mechanical action, during compaction or traffic densification, squeezes the droplets together, promoting coalescence and squeezing water out of the coalesced film.
- Setting of emulsion during breaking is a complex phenomenon Rodríguez *et al.*, (2008) indicated that through imaging techniques, breaking of emulsion in mineral aggregates can be analysed through the contact angle approach. Full spreading or wettability of droplets occurs at a contact angle equal to zero.
- Adamson (1990) indicated that depending on the interaction between binder and mineral aggregate, wetting potential is more than just the contact angle. The advantage of surfactant during breaking of droplets is that it displaces the dust or adhered water from the mineral aggregate surface and enhances the polar fraction of the function group to penetrate between dust particles and adhere to or interact with mineral aggregate surface charges. The bond development occurs in full water evaporation.

2.4.5 Influence of compaction

The compaction method and level of BSMs plays a significant role, in both the laboratory-prepared specimens and in the field construction, to achieve the intended durability properties. The dispersion of foam bubbles and breaking of emulsion droplets favourably coat the filler fraction and partly coat the coarse fraction. During mixing, the mineral aggregates are in a conglomerate state which means the binder-aggregate interaction is incomplete. It is therefore through compaction that the following advantages might occur:

- Improvement in adhesion and cohesion of mastic and mineral aggregates,
- Compression of bitumen or mastic (spot glue) between large fractions,

- Moisture squeezes out of the mineral aggregates and mastic to the surface,
- Enhanced parking of mineral aggregates, skeleton.

The compaction method of BSMs in a laboratory-prepared specimen is a primary factor in producing mix designs which simulate durability behaviour in field conditions. Previous research on compaction methods of BSMs conducted by Weston *et al.*, (2002) uses Marshall, Hugo, Kango, Superpave Gyratory and pedestrian roller. The research indicates that the modified Kango Hammer® could be a useful tool in the compaction of BSMs. The advantages of the Kango hammer® is that it requires low compaction energy to obtain equivalent level of compaction compared to other method. Secondly, it is relatively cheap, easy to use and simulates field compaction.

The current research in Stellenbosch develops a more robust compaction method for the BSMs using a BOSCH® vibratory hammer (Kelfkens, 2008). This device was extensively used in preparing laboratory specimens designed in this study, for the reasons indicated above. The compaction technique will further be discussed in Chapter 3 of this thesis.

2.4.6 Influence of curing

Curing of BSMs is the main influential process for the development of bonding between binder-mineral aggregate interfaces and consequently the building of durability properties. It has been indicated in the literature that failure manifestation in these mixes might occur at an early age of service life due to insufficient curing. However, the challenge still remains on how the curing process in the laboratory can simulate the real field conditions. On the other hand, the curing mechanism in field conditions has not been sufficiently studied by looking at all key elements playing a role in curing mechanisms..

Curing of BSMs is a process which entirely depends on the mechanism of moisture evaporation. Literature reviews have indicated that in field conditions the evaporation process is linked to the temperature gradient in the layer, wind speed, relative humidity and boundary conditions surrounding BSMs. A model that sufficiently addresses these parameters has not been studied. It is apparent, therefore, that in order to understand and accurately predict the curing mechanism, particularly in the field conditions, a model needs to be established to encompass all these parameters. The developed model will be able to assist the simulation of laboratory-accelerated conditions. In this study, based on an extensive literature survey, the empirical evaporation model will be discussed in Chapter 6. This highlights the important features responsible for the mechanism of evaporation based on field conditions and provides an avenue for further research.

Currently, the curing process in laboratory conditions is focused on achieving equilibrium moisture content (i.e. 40–50% OMC). This process stems from the model established by Jenkins (2000). The Jenkins model is a modification of a model developed by Emery (1988) who studied equilibrium moisture content of granular base layers in South Africa using the Weinert climatic Index. Malubira (2005) indicates that the model developed by Jenkins is not sufficient to encounter or predict the actual moisture content measured in field conditions. During Malubira's studies, he further extends Jenkins model by including constant parameters established from the acquired field data. However, these extended constant parameters still do not address the fundamental environmentally related conditions occurring in the pavement layers in field environmental conditions. The study on the curing mechanism of BSMs by Jenkins *et al.* (2008) tries to focus on the fundamental environmental conditions occurring in the pavement layer during the curing process. In this study, temperature and humidity in the BSM layer are investigated by installation of the DS1923 iButton. The data from this field investigation will be presented and discussed in Chapter 6 of this thesis.

2.4.7 Moisture damage mechanism

2.4.7.1 Background

Moisture damage contributes significantly to the premature deterioration of pavement materials, HMA, CTMs, BSMs or granular. The deterioration process is the degradation of the mechanical properties of the materials due to the infiltration of excess moisture into the microstructure. Microstructure moisture damage is a complex phenomenon that involves thermodynamic, chemical, physical and mechanical processes. Unlike HMA where the effect of the infiltration of water at the binder-aggregate interface and consequential damage has extensively been studied, little has been reported about moisture damage, particularly in field conditions, in BSMs (Twagira and Jenkins, 2009). Although moisture damage in the field has been reported, little is known about the mechanism of moisture damage at the microstructure level in BSMs. This section explores the context in which the developed adhesive and cohesive bond in the mix might be affected by infiltrated excess moisture in the microstructure of BSMs and hence influence the durability behaviour. Thus covers the following:

- Mode of moisture infiltration and influence on moisture damage
- Describing the process occurring at the binder-mineral aggregate interface and the theories that explain the nature of the adhesive bond and its resistance to moisture damage

The studies on HMA by Kringos *et al*, (2008) at Delft University on moisture damage, provide an intrinsic analysis and related factors for insight into understanding the mechanism of moisture damage in BSMs.

2.4.7.2 Definition of moisture damage

A generalised definition of the term damage is the degree of loss of functionality of a system (Caro *et al*, 2008). Within this context, moisture damage in BSMs is broadly defined as the degradation of physicochemical and mechanical properties of materials due to infiltrated excess moisture or vapour state. However, the most comprehensive definition of moisture damage in the literature is provided by Kiggundu and Robert (1988). They state that moisture damage is the progressive functional deterioration of pavement mixture by loss of the adhesive bond between the binder and mineral aggregate surface and/or loss of cohesive resistance within the mixture from the action of water. However, the loss of adhesion and cohesion is the last step, as the process starts with different modes of moisture transport and in turn generation of moisture damage.

2.4.7.3 Moisture damage mechanism

Damage mechanism is a process that leads to change in the internal or external conditions of a system producing a new state or condition (Caro *et al*, 2008). When the final state of the system represents a reduction in its original integrity, the process is considered a damaged mechanism. Moisture damage mechanism consists of the following steps:

- Moisture transport: process by which moisture or vapour infiltrate the pavement materials and reach binder (mastic) and aggregate interface
- The response of the system: change in the microstructure properties that lead to a loss of engineering properties

The materials and system formulations (mixture composition) that influence moisture transportation are illustrated in Figure 38 and comprise the following:

- The binder in BSMs is thin film and does not completely cover the larger particles of aggregate,
- Binder contents utilised in the mix are generally lower than equivalent HMA, which lives more isolated and interconnects void in the mix.
- The mineral aggregate is moist at the time of mixing which reduces adhesion

- The air void content of the mix is usually relatively higher than HMA.

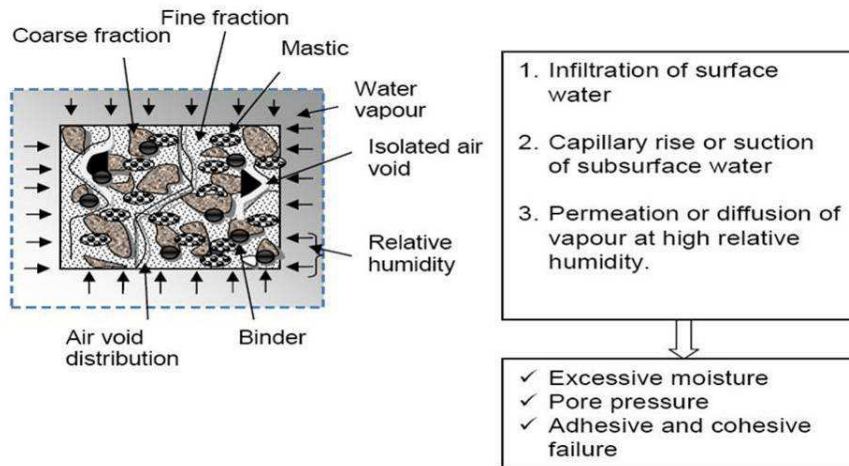


Figure 38: Mix composition and possible moisture transport into BSMs

Figure 38 illustrates intrinsic mixture composition with partial coating of aggregates with binder-mastic and parameters influencing transportation of excessive moisture to the bulk material. The high void content, external environmental conditions (infiltrated moisture and high relative humidity) influence the diffusion process, while spot welding of binder and thin film influence adhesive failure when exposed to high pore pressure. A detailed analysis of bond formulation and failure mechanism is provided in Chapter 3 of this thesis

The possible moisture mechanism portrayed in Figure 38 above is twofold: 1) high percentage of air void with low connectivity. This allows development of pore pressure in a saturated flow condition and can cause erosion upon dynamic loading causing mechanical failure. 2) Infiltrated excessive moisture can also diffuse through the mastic and displace the binder from the aggregate surface resulting in poor adhesive bond strength at the interface. Past research indicates that the common moisture damage mechanisms are related to 1) ravelling- distress manifestation due to dislodgement of aggregate particles in the mixture from the surface and 2) hydraulic scour/erosion of saturated surface due to dynamic action of tyre in the presence of water. It is certain that adverse environmental conditions play a significant role: high relative humidity in the material, intense rainfall period and temperature variation in the materials increase the damaging potential. Other factors that influence moisture damage are intense traffic loading and ageing of the binder. However, the quantification of the latter is not obvious.

2.4.7.4 Mode of moisture transport

Depending on the boundary condition surrounding the BSM layer (i.e. surface layer (AC or seals) or subbase layer, i.e. CTMs or granular), the modes by which moisture can reach the mixture in the BSM are as follows: 1) infiltration of surface water 2) capillary rise of subsurface water and 3) permeation or diffusion of water vapour.

Infiltration of surface water is regarded as the main source of moisture in the pavement and directly related to rainfall, dynamic loading and cracking or voids on the surface. However, in regions with low levels of annual rainfall, studies indicate that severe moisture damage on pavements is linked to poor drainage, capillary rises or suction of subsurface water due to material properties. The sources of moisture transport to the BSM layer are described as follows:

Permeability

Permeability is defined as the ability of materials to transmit fluid. According to Darcy's law, permeability is the rate of water flow and is proportional to the hydraulic gradient. The mathematical relationship in Darcy's law can be written as follows (Kanitpong *et al.*, 2001):

$$Q = k.i.A \Rightarrow k = \frac{\Delta H}{L}.A \quad \text{Equation 10}$$

where Q = rate of flow; k = coefficient of permeability; i = hydraulic gradient; ΔH = head loss across specimen; L= length of specimen; A = cross section area of specimen perpendicular to the direction of flow. Factors influencing permeability are compaction level, air voids structure (size and connectivity), mineral aggregates (size, shape and grading), binder content and degree of saturation (Caro *et al.*, 2008 and Kuvhanganani, 2008). Terrel *et al.* (1994) categorise effectiveness of air void permeability in the mixture based in percentage voids content, while Caro *et al.* describe effectiveness of void permeability based on the coefficient of mixture permeability as indicated in Table 11.

Table 11: Classification of void in term of permeability (k) Caro *et al.* (2008)

Void [%]	K [cm/s]	Permeability condition	Void structure	Mixture
6 or lower	10 ⁻⁴ or lower	Impervious	Impervious	Dense (typical HMA)
6 – 15	10 ⁻⁴ – 10 ⁻²	Poor drainage	Semi-effective	Dense* (typical BSM)
15 or more	10 ⁻² or more	Free drainage	Effective	Porous asphalt

*Study on BSMs was done by Kuvhanganani (2008)

Terrel *et al.* further indicate that mixtures with very low and very high void contents are not affected detrimentally by exposure to water. In the intermediate range, where water enters into the mixture and does not readily escape, the retained moisture contributes to the damage on the mixture coupled with dynamic loading.

Unlike HMA, where permeability and its influence on moisture damage has extensively been studied (Huang *et al.*, 1999; Terrel *et al.*, 1994; Choubane *et al.*, 1998 and Caro *et al.*, 2008), the permeability of BSMs has been little reported. Kuvhanganani (2008) and Ventura (2001) studied permeability of foamed bitumen mixes, with different binder contents and percentage of active filler (cement). Their results indicate poor correlation between density and permeability. In addition, there is no clear trend on the effect of the addition of cement and binder content on permeability. The cause of variability was the testing method applied. The UCS type of specimen was used for saturation while in compaction mould. This type of method has been reported to influence the coefficient of permeability due to sidewall flow effect. Kanitpong *et al.* (2001), Head (1986), and Kanitpong (2008) recommend a triaxial permeability test, where the flow of water through a sample can be maintained under a known pressure. The rate of flow can be measured while the sample is subjected to a known confining stress. The method was found to produce a more reliable coefficient of permeability than the traditional method. This shows that the permeability test using triaxial cells with application of confinement might be applicable to determining the permeability properties of BSMs.

Since the air void in BSMs is relatively high compared to HMA, it might be seen to be more effective in permeability. However, this relationship is neither simple nor evident. Densely compacted BSM mixtures might have significantly different air void size distributions and connectivity in the mix, with the same percentage air voids. It is apparent therefore that understanding moisture damage requires good knowledge of the void structure in BSM

mixtures. In this study, void microstructure was observed using CT-Scan and SEM as discussed further in Chapter 6.

Capillary rise and suction

Capillary rise is defined as the rise in liquid above the level of zero pressure due to a total upward force produced by the attraction of liquid molecules to a solid surface (Caro *et al.*, 2008). In BSMs, depending of support conditions and degree of saturation, capillary rise might allow subsurface water to be transported into the bulk though the capillaries formed by the interconnected voids. The final column of water above the saturation surface, h , as well as rate of rise, depends on: 1) geometry of the capillaries, i.e. tube-like voids with assumed radius r , 2) the surface tension of water, T_s , 3) the density of water, ρ and 4) the contact angle between the liquid and the solid, α . The general equation describing capillary rise in free drain mixture is found by the equilibrium of forces acting on the system.

$$2\pi.r.T_s.\cos\alpha = \pi.r^2.h.g.\rho \tag{Equation 11}$$

Vapour diffusion

The amount of water vapour and the rate at which it accumulates in the bulk of BSMs depends on three primary factors: 1) relative humidity, 2) diffusion coefficient and 3) water-holding potential within the bulk. The relative humidity depends on environmental conditions, whereas diffusion coefficients and water-holding potential and capacity depends on the chemical and thermodynamic properties of the materials. Grobler (1995) indicates that the water present in a soil mass can be divided into water in motion and static water. The static water is subdivided into four categories as shown in Figure 39. The categories of static water show that moisture content and movement is a complex phenomenon which contributes significantly to the performance of the soil. The four categories are: 1) chemical water, water bounded in crystal structure of soil, 2) adsorbed water, water held by the magnitude of the electric charges of soil particles or water held by surface tension, 3) thermodynamic surface free energy and contact angle between liquid and solid and 4) capillary water, tubing or seepage, which evaporates easily. These categories of water can also be found in BSMs at equilibrium state. It is therefore important to understand their behaviour and contribution to bonds formation and possible contribution to moisture accumulation and resulting damage.

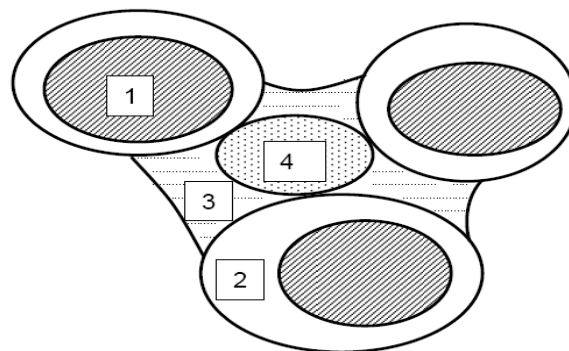


Figure 39: Categories of static moisture (water) (Grobler, 1995)

2.4.8 Characterisation of moisture damage

Deterioration of the pavement structure due to the action of moisture rarely occurs in isolation. The distress such as permanent deformation (shear failure) and fatigue cracking (loss in stiffness) is often aggravated by the detrimental effect of moisture on the internal structure of the pavement materials. Therefore characterisation of moisture damage is essential to quantify the loss of functionality of the BSMs mixture by considering variable parameters, such as shear, strength, stiffness etc. These parameters allow the determination of the thresholds that can be used in the form of specification to separate acceptable from unacceptable materials or mixtures in terms of moisture damage resistance.

Although problems of moisture susceptibility on BSMs has been identified in various studies (Jenkins, 2000; Long *et al.*, 2004; Liebenberg, 2004 and Paige *et al.*, 2004), its complexity has made it difficult to find a unique test or analytical method to comprehensively quantify damage and accurately predict the material performance in the field. The various test methods used to assess moisture damage can be classified based on the generic nature of each test method.

Figure 40 presents two main classification approaches applied to moisture sensitivity on pavement materials e.g. BSMs.

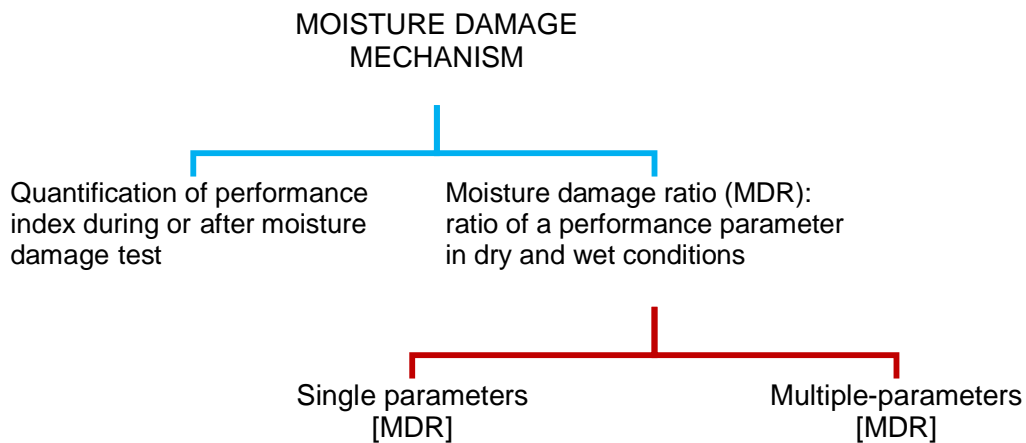


Figure 40: BSM moisture damage classification system

2.4.8.1 Quantification of performance index

The current qualitative method to assess moisture damage in BSMs is the related test method designed for cement-treated material. This test is like the mechanical brushing or erosion test method and is conducted on compacted and cured specimens with or without loading. The assessment of the quality of adhesion and cohesion with the influence of moisture is done by determining the loss of surface material. These tests, however, do not identify or explain the fundamental failure mechanism due to moisture damage. Table 12 presents all test methods in this category, along with a brief explanation of performance criteria.

Table 12: Methods used to quantify moisture damage in BSMs through the loss of surface materials

Test method	Performance index (damage parameter)	Reference
Erosion test (wheel-trafficking)	Loss of surface materials, after 5000 application of wheel abrasion in wet conditions, measure difference in height before and after the test	Long, Thyese and Ventura (2004)
Mechanical brushing	Mass loss, measured as percentage of the original mass of sample, after soaking –drying and brushing at 50 revolutions repeated 12 times.	Long, Thyese and Ventura (2004)
Water jet erosion	Mass loss, measured as percentage of the original mass of sample, after 9 jet of water spraying at low pressure, at angle 35° from horizontal, jetting 10mm to the specimen at constant intensity	Jones and Ventura (2002); Van Wijk and Lovell (1985)
Rotating a cylindrical specimen in water	Mass loss, measured as percentage of original mass of sample	Van Wijk and Lovell (1986)

Although quantification of mixture performance is possible, these test methods might be unrealistically severe for the evaluation of BSMs. In addition, to a large extent, they are not simulate moisture damage in BSMs during in-service pavement conditions.

2.4.8.2 Moisture damage ratio (MDR) on dry and moisture-conditioned specimens

A widely used approach for quantifying moisture damage is the comparison of a parameter (or parameters) derived by testing dry or control specimens with the same parameter(s) derived by testing moisture-conditioned specimens. The goal of the moisture conditioning process is to simulate the detrimental effect of moisture on materials during short periods of time. Moisture conditioning is considered an accelerated damage process. The ratio of affected parameters after moisture conditioning to the control state is expressed as a percentage. The relationship of MDR is expressed as follows (Caro *et al.*, 2008).

$$\text{MDR} = \frac{(\text{material properties in wet condition})}{(\text{material properties in dry condition})} \times 100\% \quad \text{Equation 12}$$

The relationship can be used to evaluate single parameters or multiple parameter properties of *MDR*. Single parameters are traditionally used to evaluate the influence of moisture damage using mechanical tests in a dry and wet state. These parameters include stiffness, strength, shear properties and fatigue. The advancement of moisture damage quantification using multiple parameters is in the ability to quantify moisture damage by combining more than one material property, while considering both dry and wet states. This approach allows the evaluation of physical, chemical and mechanical properties of materials which are fundamental in moisture damage.

Single parameter is achieved by conducting mechanical tests on both dry and moisture conditioned states. For BSMS, several laboratory procedures in the past have been applied for the identification of a mix's moisture sensitivity. Generally, these procedures stem from early findings of the Asphalt Institute (1992), which entailed moisture conditioning of a compacted, cured BSM specimen and mechanical testing. The moisture conditioning is carried out using vacuum saturation of the specimen in order to accelerate any possible moisture damage. Although this method provides an empirical measure of moisture damage, it yields both variable and unreliable results. Table 13 enumerates some of the test methods within this category.

Table 13: Test methods that stem from Asphalt Institute to test BSMS moisture sensitivity

Test	Moisture conditioning method	Material properties	Reference
Marshal stability test	Vacuum saturation at 23°C	Marshal stability	Ruckel <i>et al.</i> (1983); Van Wijlk and Wood (1983)
Marshal stability test	1 hour vacuum soaking and 4 days soaking	Retain Marshal stability	Hotte (1995)
UCS and CBR	4 days soaking	Strength and cohesive value	Bowering and Curie (1973)
Triaxial test	Vacuum and saturation at 60%	Resilient Modulus after 1000 cycles	Shackel <i>et al.</i> (1974)
Triaxial test	Soaking 24 hours at 60°C	Resilient Modulus after 1000 cycles	Lancaster <i>et al.</i> (1994)
Indirect Tensile test (ITS)	24 hours at 64°C	Tensile strength	Maccaronne <i>et al.</i> (1994)
Duriez test	Fresh and cured specimen	Immersion compressive strength	Serfass <i>et al.</i> (2004)

Walubita *et al.* (2002) showed that the dynamic test on asphaltic materials subjected to traffic and moisture damage is more reliable than static tests. There is a strong correlation between APT performance in the laboratory and in the field, if a dynamic test is carried out on the materials after conditioning. In this study, the key issues in moisture damage that have created significant discrepancies in previous test results, such as the saturation method, degree of saturation and evaluation parameters after conditioning (residual strength ratio versus retained stiffness), were observed. Subsequently, a simple device was developed to assess moisture-induced damage based on pulsing moisture into triaxial specimens. Different saturation levels were investigated in a developed device with experimental determination of stiffness ratio (M_r) and shear parameters (C and ϕ). These parameters are known to be critical parameters for the performance of BSMS.

2.5 ENGINEERING PROPERTIES AND DURABILITY OF BSMs LAYER

2.5.1 Introduction

Demand for better-performing, long-lasting, safer, more economical and more environmentally friendly pavement materials and structures are constantly pushing the boundaries of technological capability and engineering practice globally. As a result, there are relentless moves toward close tolerances and the use of realistic life cycle design, condition-based maintenance, and performance-based designs. Nevertheless, pavement engineers are faced with the problem of finding useful and relevant material durability property data for use in the mix and structures design to provide top performance pavement for an extended period of time (i.e. pavement design life).

The engineering properties of BSMs have extensively been studied in the past. As a result, numerous tests have been utilised to characterise the properties of the BSM mix durability. However, testing procedures for BSMs have undergone major transformation in recent times, with a shift from ITS, UCS and dynamic creep to the fundamental tests such as triaxial testing (i.e. resilient modulus, permanent deformation, and shear property), fatigue testing, and APT (field related simulation) testing. Nevertheless, the limiting values of these tests on BSMs are still uncertain, as the mechanisms of failure are not yet clearly defined.

In this section, an overview of the types of tests utilised for the BSM research and the performance properties that influence the durability behaviour of BSMs will be discussed as indicated in Table 14.

Table 14: Test methods for engineering and performance properties on BSMs

Test method	Engineering properties	Performance properties
4PB or 3PB fatigue test	Tensile strain (fracture) and stiffness	Flexibility or fatigue resistance
Indirect Tensile Strength (ITS)/split test	Tensile strength, failure energy, cohesion	Resistance to crack formation/fracture resistance
Dynamic Triaxial (short-term loading), ITT	Resilient modulus, Mr, or stiffness	Stress distribution or load carrying capacity
Dynamic triaxial (long-term loading)	Plastic strain or rutting and shear strength	Rutting resistance or resistance to permanent deformation
Unconfined compressive strength (UCS)	Compressive strength	Resistance to crushing and disintegration
Erosion test, wet brushing, ITS and Triaxial (soaked) Soaking condition stemmed from Asphalt institute method	Retained surface material, retained strength after moisture exposure	Resistance to moisture damage or moisture susceptibility (cohesion and adhesion durability)

2.5.2 Fatigue behaviour

Stiffness of bituminous mixture is closely related to its fatigue behaviour. Most materials bound by cement and/or bitumen show fatigue resistance properties that will resist the formation of tensile failure (cracks) when subjected to tensile stress or strain. Fatigue cracking, therefore, is one of the major load-related distresses experienced in bituminous layers and it occurs when a pavement is subjected to repeated application of induced traffic. The ability of mixes to resist fatigue failure will therefore enhance durability and long-term performance. The mixture variables that affect stiffness also affect fatigue life. Mixture variables such as binder content, binder type, aggregate type and grading and addition of active filler directly influence fatigue

performance. Dukatz (1989) indicates that physicochemical properties, such as morphology, grading and mineralogy contribute significantly to fatigue performance by affecting cohesivity of the mixture. Loizos *et al.* (2007) indicate that fatigue behaviour in BSMs is not a dominant failure mechanism. The field investigation on BSM foam conducted after Cold In-Place Recycling (CIRP) indicates that stiffness of the foamed bitumen layer increases with time. This behaviour is contrary to fatigue failure mechanism known for HMA. Jenkins (2000) comments that foamed bitumen with relatively high binder content (>3.5%) is considered to behave in a manner similar to HMA. Twagira *et al.* (2006) tested fatigue behaviour of BSMs at varying binder content from 2.4%-3.6% and varying percentage of RAP content. Their results show that fatigue stiffness behaviour is time and temperature dependent (i.e. if loading rate increases, stiffness increases and if testing temperature increases, stiffness reduces). This trend is typical for HMA; however because BSMs have much lower temperature susceptibility compared to HMA, the stiffness results were relatively small compared with HMA and half-warm STAB as indicated in Figure 41. From Figure 41 it can also be seen that time-temperature superimposition for BSMs is much flatter (lower) than HMA and half-warm, particularly at a higher loading rate. This is partly contributed to by the lower binder content as well as stiffening behaviour of the mastics in the BSM mixture.

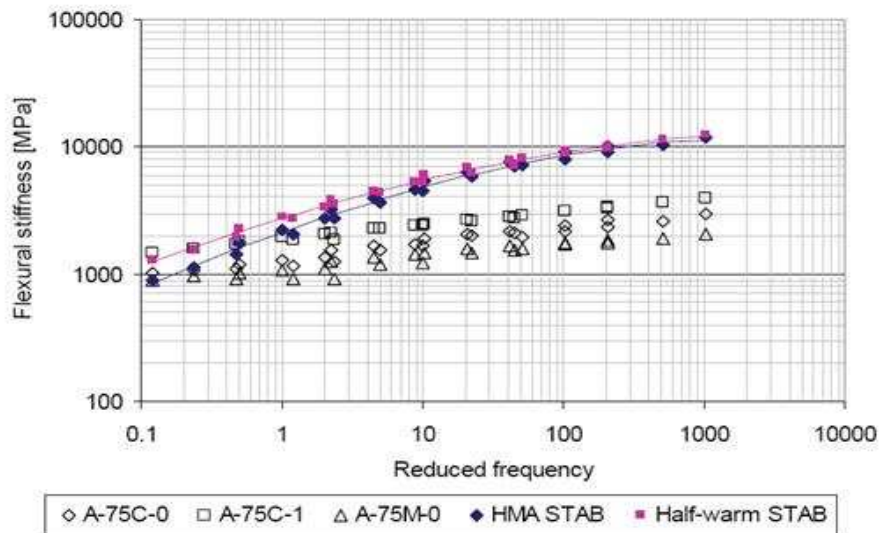


Figure 41: Time-temperature superimposition for BSMs, HMA and HW-STAB ($T_{ref}=20^{\circ}\text{C}$) (Ebels, 2008)

Further analysis of Figure 41 shows that flexural stiffness is influenced by the percentage of RAP in the mix, the addition of active filler and the type of binder. It can be seen that emulsion mix (A-75C-1%) with 1% cement has higher flexural stiffness compared to emulsion mix with no cement (A-75C-0%) and higher percentage of RAP content (A-75M-0%). A similar fatigue property of BSMs was reported by Twagira (2006); he reports that the fatigue life of emulsion mix with higher RAP content (B-75M-0%) without cement has a relatively lower fatigue life compared to the same mix treated with foamed bitumen (C-75M-0%) as indicated in Figure 42.

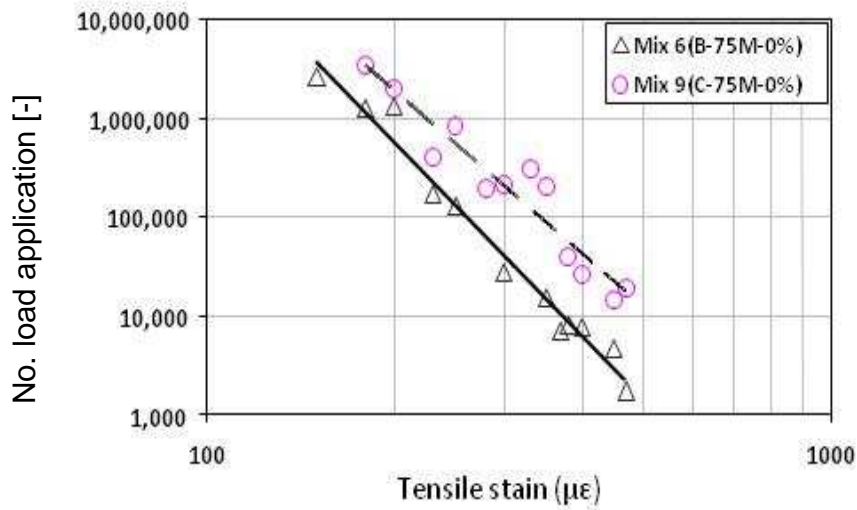


Figure 42: Fatigue behaviour of BSM-emulsion and BSM-foam with higher percentage of RAP materials (Twagira, 2006)

The better performance of the foam mix with higher RAP content seems to agree with the concept of binder diffusion previously discussed in section 2.3.3. Jenkins (2000) indicates that the rate of heat transfer from foamed bubbles to the aggregate surface, even at lower temperatures of aggregate, may contribute to comparative performance of the foamed bitumen and bitumen emulsion. This is because the heat transfer dissipated from the bubble might soften the old bitumen (both in the filler and in coarse fraction) and enhance adhesion of new bitumen. While, because emulsion is applied at ambient temperature, the old coated bitumen in mineral aggregates is inactive, reactivity, and adhesion of new bitumen will be retarded. However, depending on the type of surfactant, different emulsions might behave differently in adhesion and cohesion with a higher addition of RAP content in a mix.

5.2.3 Permanent deformation behaviour

Permanent deformation is an engineering property used to classify material durability properties in terms of resistance to rutting. It can also be used for better classification of materials which are moisture susceptible. This is done through long dynamic tests of the mixes at excess moisture content. This behaviour is investigated further in this study and will be discussed in Chapter 5.

Recent research on permanent axial strain due to the effect of moisture on BSM-foam, was carried out by Fu *et al.* (2009). Their objective was to determine the influence of cement on different curing conditions and shear strength development. Permanent triaxial testing was performed on different mixes with different moisture contents. The observed permanent axial strain at applied multi-stage deviator stresses is presented in Figure 43.

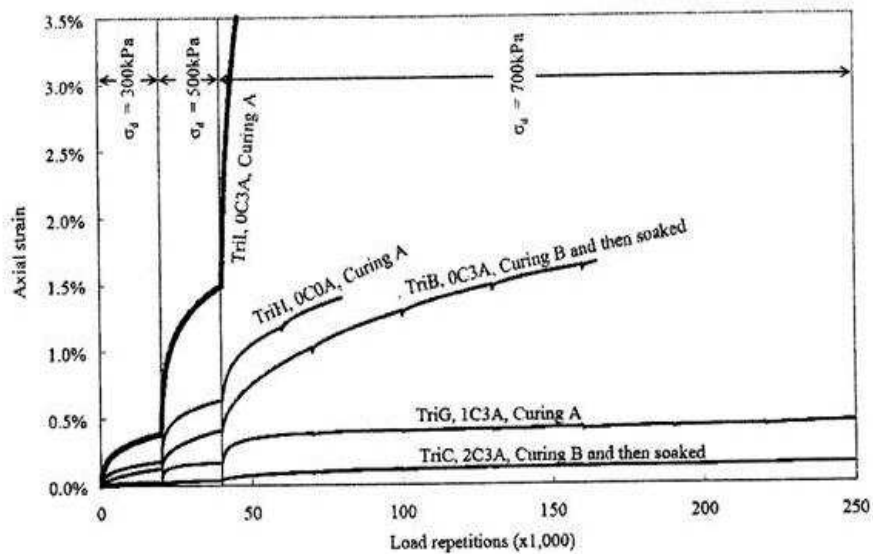


Figure 43: Permanent axial strain of BSM-foam mixes at different curing conditions, and confinement of 68.9kPa, loading rate of 0.1s, and 0.2s rest period at 20°C (Fu *et al.*, 2009)

The results in Figure 43 show that mixes with the addition of cement (1C3A) and curing conditions A (i.e. 7 days at ambient temperature) have permanent axial strain of less than 0.5% after 250×10^3 load application compared to a similar mix with no cement (0C3A) but cured at condition B (i.e. 38 days at 40°C and then soaked before tested). The difference is the influence of the added cement. Ebels (2008) indicates that the critical stress ratio's for the BSMs range from 0.4 to 0.6 for the tertiary flow to occur. More interesting to note from Ebels results, is that an increase in the RAP content of the mix stabilised with foamed bitumen has better initial permanent strain accumulation even with higher stress ratios compared to similar mix stabilised with bitumen emulsion. The reason for the better performance of foam with RAP is the same as the one given in fatigue behaviour.

Shackel *et al.* (1974) carried out numerous triaxial tests on Sydney breccia in Australia treated with foamed bitumen. He reported that the resistance to permanent deformation is a function of the binder content and the degree of saturation (% voids filled with water by volume) of foam-treated material. The ratio of axial strain to peak axial strain ($\epsilon_{axial} / \epsilon_{peak\ axial}$) decreases with the increase in binder content and degree of saturation.

2.5.4 Tensile and compressive strength

Tensile strength (ITS) or unconfined compressive strength (UCS) engineering properties are considered as an indicator for the initial mix design of BSMs, TG2 (Asphalt Academy, 2009). This is because they do not model the performance of BSMs accurately (Ebels and Jenkins, 2007). Past studies have investigated the relationship between the ITS and UCS tests and posed the question whether the ITS (splitting) test is an appropriate test to determine the flexibility of BSMs. This is due to the complex nature of stress distribution at the centre of the specimen. Houston *et al.* (2004) and Bondietti *et al.*, (2004) found that a linear relation with a good level of confidence exists between the ITS and UCS tests over a range of bitumen and cement content ratios. Houston *et al.*, concluded that an ITS or a UCS test alone on 150mm briquettes at equilibrium moisture content can be used for materials classification and determination of optimum binder content. However, It was further recommended that performing a second test (either ITS or UCS test) will not lead to a more accurate classification of BSMs.

2.5.5 Moisture susceptibility

Durability of BSMs depends on, among other factors, resistance to moisture-induced damage. The consequences of moisture damage on BSMs in the field have been reported. Chen *et al.* (2006) report failure on full-depth recycling (FDR) foamed asphalt on Highway 82 in Texas, Ramanujan and Jones (2007) report failure of FDR foamed asphalt on Cunningham Highway in Australia and Fu *et al.* (2007) report failure of FDR foamed asphalt in California. According to Fu *et al.*, all reported failures resulted from poor drainage and infiltration/suction of subgrade moisture to the BSM layer. Similar distress due to suction of seepage ditch water, patched water tables and unpaved shoulders has been modelled by Birgisson and Bryon (2003). The saturated condition of the BSM layer slightly above optimum moisture content (OMC) resulted in severe alligator cracking and rutting of the surface layer.

The mechanism of moisture damage in BSMs is complex and difficult to model. Different mechanisms are involved in saturating BSMs. One of the causes of moisture induction to BSMs in a pavement layer is traffic related. This section presents the mechanism of moisture induction to BSMs through pulsing pressure exerted by loading stress on the pavement surface, particularly surface seals. However, a similar phenomenon might occur in thin HMA which has higher void content or stripping or cracking or both.

Typical flexible pavement components in South Africa consist of a surface layer, base layer (granular or BSM), subbase (granular or CTM) and subgrade (natural or selected materials). Surface design consists of the selection of two types of wearing course, either thin asphalt concrete or surface seals. With the modern trend of increased traffic loading and contact stresses, seal performance criteria have been designed to avoid certain failure parameters (Milne, 2004). These are: 1) permanent deformation (punching, rotation of stone, reducing void), 2) early rutting or ponding, 3) fatigue cracking, 4) moisture damage and 5) adhesive failure. Typical schematic illustration of different types of surface seal is indicated in Figure 44 (SANRAL, 2007).

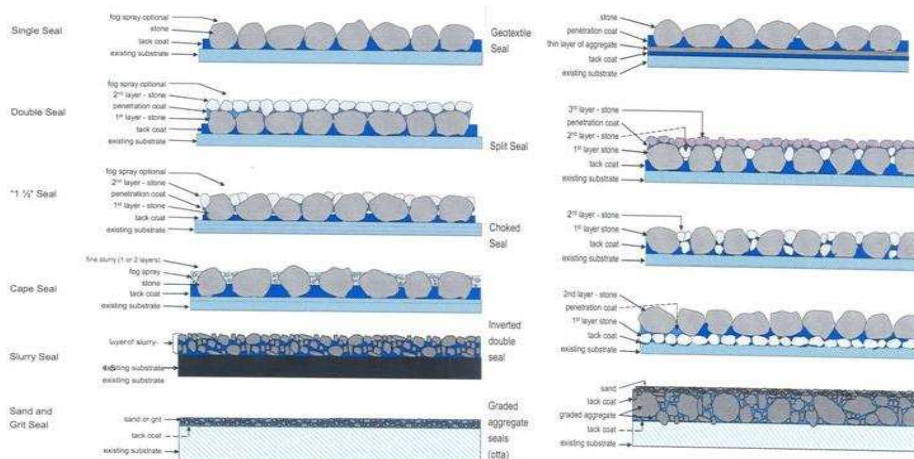


Figure 44: Schematic illustration of seal type common in South Africa (SANRAL, TRH 3, 2007)

Seal design has extensively been studied in New Zealand, South Africa and Australia. The research conducted by Land Transport New Zealand (2005) confirms that at high vehicle speed, surface water can be forced through the cheap seal that does not show signs of cracking. The penetrated water to the base layer may in turn result in detrimental moisture damage. Ball *et al.* (1999) report a similar behaviour. They studied the effect of water on the flushing process in cheap seal and observed that under tyre pressure water can penetrate through the cheap seal.

The study involved tyre deformation and the surrounding fluid in the pavement is referred to as *hydroplaning phenomenon*. The hydroplaning characteristic is widely covered in the tyre science and technology industry, for safe driving on wet roads.

Mechanism of hydroplaning

Hydroplaning is a hydrodynamic phenomenon caused by the collision of water with a tyre at high speed. Hydroplaning is usually explained by the well-known three-zone concept as shown in Figure 45 and Figure 46 (Nikajima *et al.*, 2000; Okano *et al.*, 2008).

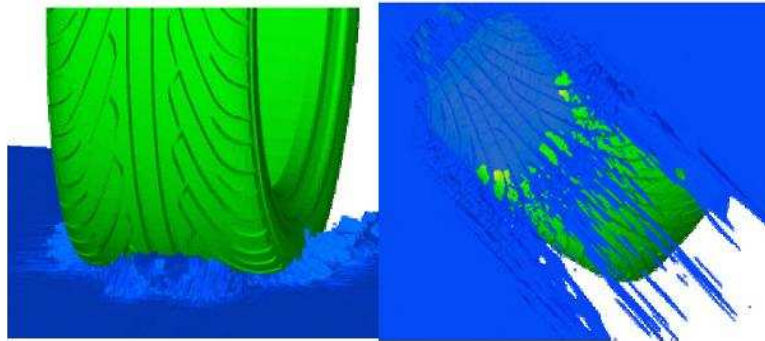


Figure 45: Dynamic hydroplaning simulation using MSC Dytran at 80km/h (Okano *et al.*, 2008)

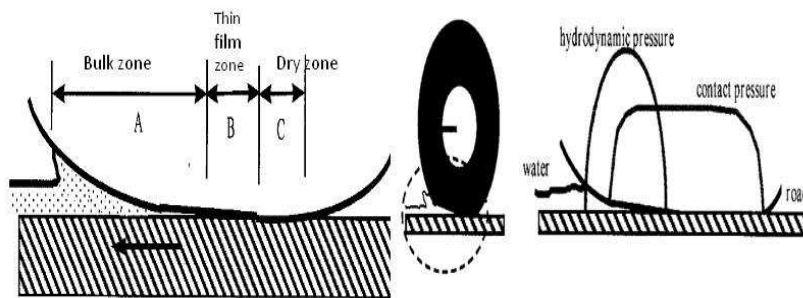


Figure 46: Three-zone concept and schematic figure of dynamic of hydroplaning (Nikajima *et al.*, 2000)

The three regions of tyre-road interaction are defined as: region A, dynamic pressure of water colliding with tyre, resulting in full separation of tyre from the road surface; region B, thin film water layer exists and due to influence of viscosity lubrication of water, tyre is partially separated; region C, no water film exists and tyre adheres to road completely. When the vehicle drives at slow speeds, region C dominates the contact patch; as the vehicle speed increases, the dynamic pressure of the water tends to lift the tyre and region A becomes dominant. This is a zone of interest in understanding the mechanisms of water infiltration through surface layers. The viscosity lubrication of the thin film of water (zone B) is considered less important because the surface property of micro-texture may be considered effective in thin film penetration for ground contact.

Nikajima *et al.* indicate that a 10mm depth of water film on road surface is thick enough for dynamic hydroplaning (zone A) to dominate. The schematic illustration of hydrodynamic pressure is shown in Figure 46 and the mechanism of hydrodynamic pressure on thick water film is described as follows:

1. Water collides with tyre at high speed,

2. Hydrodynamic pressure is generated by the inertia of the water,
3. When the hydrodynamic pressure exceeds the contact pressure at the leading edge, the tyre starts to float on water,
4. The tyre deformation due to hydrodynamics pressure increases progressively.

From the mechanism of hydrodynamic pressure, it can be seen that at high speed, generation of hydrodynamic pressures increases and when the contact pressure (loading condition) at the leading edge, exceeds the hydrodynamic pressure, the water film penetrated into the contact patch is forced through the pavement layer. However, the water infiltration depth depends on: 1) tread pattern of the tyre, 2) velocity of the tyre, 3) size of the tyre, 4) inflation pressure, 5) loading of the tyre and 6) surface condition between the tyre and the road.

Nikajima *et al.* modelled the water flow under a tyre as it went through a 10mm deep water film. Their results show that the contact pressure on the pavement with and without water is different in the area noted as rolling, and the difference between these pressures is considered hydrodynamic uplift force caused by water not being removed from under the tyre. The effect of vehicle speed and tyre tread was also modelled, and the results, in Figure 47, show that the hydrodynamic force of the rolling tyre, with tread pattern or blank tread, increases with vehicle speed. The forces can double from approximately. 0.7kN at 60km/h to 1.4kN at 80km/h. An estimate of the pressure in terms of kPa is approximating 1 kN force to a pressure of 100kPa.

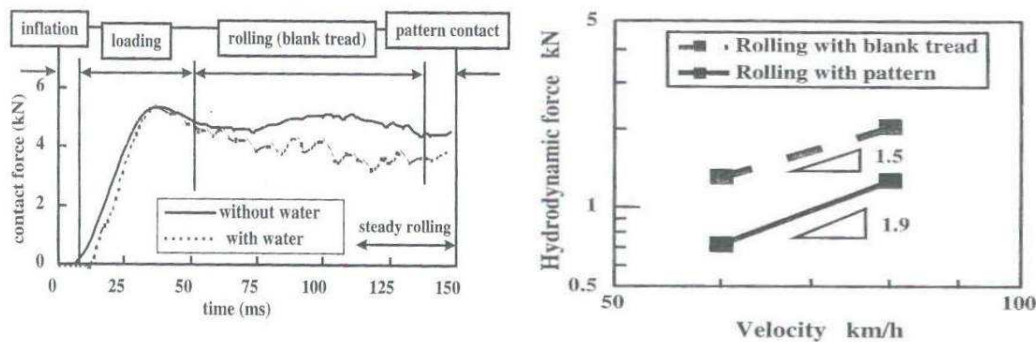


Figure 47: (a) Pressure on pavement under rolling tyre, (b) velocity dependence on hydrodynamic force (Nikajima *et al.*, 2000)

The finding on hydrodynamic pressure between tyre-road interactions is considered an avenue for hydrodynamic simulation of moisture susceptibility of the underlying surface layer. The variables determined in hydrodynamic studies were taken further in this study for the development of the new conditioning system for BSM moisture susceptibility. The development can be found in Chapter 3. The research in New Zealand on multiple seals shows that the measurable flow rate under the surface course was a pressure of around 100kPa, with potholing observed to appear where water had ponded. That means rutting and stagnant water on pavement surfaces may result in high hydrodynamic pressure under dynamic loading.

2.5.6 Equilibrium moisture content

Durability behaviour of BSMs is closely related to the equilibrium moisture content (EMC). Past research indicates that BSMs might reach equilibrium moisture in two to three years after a full curing process (Malubila, 2005 and Jenkins *et al.*, 2007). The level of moisture content at the equilibrium state ranges from 40–50% (Jenkins, 2007 and 2008). However, the understanding or prediction of equilibrium moisture content in the pavement layer is a complex task because many variables play a significant role in determining equilibrium moisture content of the layer.

These variables can be divided into three parts: 1) materials 2) constructability and 3) environmental conditions. Materials are related to physicochemical interaction between mineral aggregates and binder, including addition active filler; constructability is related to the compaction, layer thickness, supporting layer and drainage condition, while the environment is related to rainfall, temperature, wind and ground water level. Although an empirical relationship exists (Emery, 1988; Jenkins, 2000; Malubila, 2005) for predicting equilibrium moisture in pavement layers under long-term field conditions, factors such as the coefficient of heat transfer in the pavement layer and evaporation coefficient were not considered.

Øverby *et al* (2004) report the results from Same-Himo road after monitoring for a number of years. They indicate that E-modulus derived from field cores increased rapidly in the first three years and then tapered down from a peak of over 5 000 to lower values over 3000MPa. Øverby *et al*. show that E-modulus was higher in the top 60mm than in the bottom half of the base due to better compaction effect. Though temperature gradient in the layer was not considered, the evaporation coefficient in the top layer is much higher than below the layer. Therefore, this shows that top E-modulus will be higher than deeper in the BSM layer due to the effect of temperature. In the HMA design guide, (2000), the temperatures to which pavements in South Africa are subjected are reported as shown in Figure 48. The availability of this type of data might make it possible to model or predict EMC accurately using local environmental conditions. In light of this, EMC might be determined as temperature distribution and moisture evaporation or diffusion of water vapour over long-time seasonal variation in the BSM layer. However, good knowledge of thermodynamics and heat transfer is required.

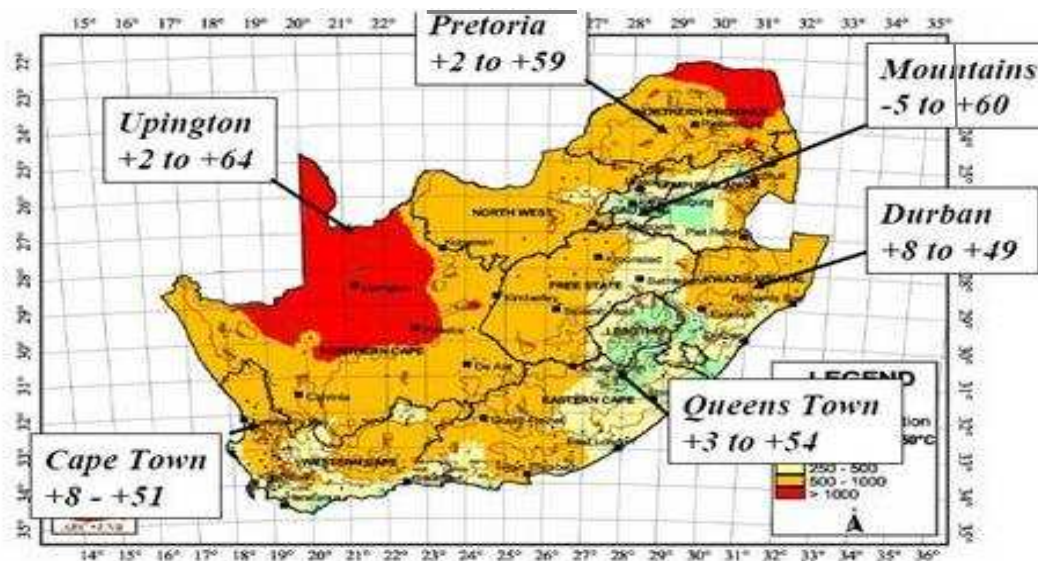


Figure 48: Minimum and Maximum pavement temperature in different regions of South Africa, (HMA guideline, 2000)

2.5.7 Pavement structure consideration

The measurement of surface deformation or rutting of a pavement, under load application on the surface layer, is a method of analysing interaction of different layers in the entire pavement structure. Through application of accelerated pavement testing (APT), i.e. HVS or scaled load mobile simulators MMLS3, useful information on the durability behaviour or long-term performance of BSM layers can be obtained. Research conducted by Steyn (2001) in emulsion and in foam using HVS, shows fundamental evaluation of moisture damage when water was introduced as a result of permanent deformation (rutting development) or stiffness reduction.

Figure 49 indicates sharp reduction in shear behaviour of emulsion and foam mix after the introduction of water in different numbers of load applications. This behaviour agrees with the hydrodynamic concept discussed in section 2.4 above.

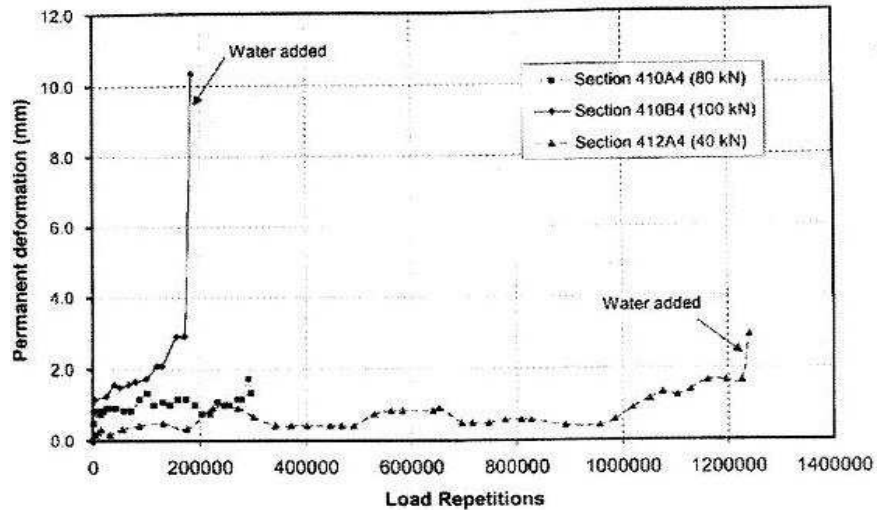


Figure 49: Permanent deformation on emulsion and foam test section using HVS (Steyn, 2001)

The use of the MMLS3 test device was adopted in this study with a threefold advantage:

- Well developed and widely used for simulating the effect of long-term service conditions in short period of time
- Evaluation of wide range of variables, this is particularly applicable to BSMs
- Validation of mixture behaviour under different test conditions that is the ability to link laboratory test results to field simulation conditions.

In this study, MMLS3 was adopted due to the reasons mentioned for correlation with the newly developed moisture simulation device (MIST) for screening BSM mixtures that are susceptible to moisture damage.

The background on MMLS3, including features, sample preparation and testing procedures has extensively been reported in various studies: Jooste *et al.* (1997); Hugo and Epps (2004); Walubita *et al.* (2002); Ebels *et al.* (2003) and Smit *et al.* (2003). Therefore, they are not repeated in this literature survey. However, most of the MMLS3 tests on BSMs were done in field investigation and little has been reported on laboratory testing conditions. The current testing procedure for laboratory conditions available is for HMA. During the MMLS3 validation testing for the MIST device, the HMA testing procedure GPG1-draft protocol guideline 1 for rutting and moisture damage ITT (2008), was slightly adjusted to simulate the possible moisture damage a BSM layer is exposed to in a real pavement structure. The tests setup limits and improvements on the current HMA testing procedure are presented in Chapter 4 of this thesis.

2.6 SUMMARY ON DURABILITY ISSUES IN BSMs

In this section, the conclusions on the literature review are summarised. The findings on mineral aggregate durability, bitumen durability, mixture durability and engineering aspects of BSMs are presented. The knowledge gained from the comprehensive literature review provides an insight into the unique durability properties of BSMs, creating a platform from which new development was established.

2.6.1 Mineral aggregate durability

Mechanisms associated with adhesion and cohesion of mineral aggregates were reviewed and presented. Specific reference was on mineralogical composition, physicochemical and mechanical properties. The theories identified in mineral aggregate adhesion and the advancement in the durability of BSMs include weak bond or van de Waal forces, mechanical, electrokinetics, chemical bond and thermodynamic concepts.

A review on adsorption-desorption studies indicates that the surface chemistry theory of aggregates dominates the bitumen-aggregate adhesive bond strength. This confirms that adhesion in bitumen-mineral aggregate systems cannot be adequately addressed without special assessment of the bonds in dry and wet states. In Chapter 3, the theories of adhesion are applied to discussing BSM durability, particularly in moisture sensitivity and damaging mechanisms. However, surface free energy is not experimentally investigated.

As aggregates age and are exposed to the cycles of varying temperature, humidity and dynamic loading, their physicochemical properties might change. This in turn influences bonding characteristics or durability behaviour. To assess durability is to assess how and at what rate those changes in physicochemical properties may occur after the materials are placed in a pavement layer. Therefore, because in-situ recycling largely uses aged aggregates, their durability properties prior to pavement maintenance, rehabilitation or upgrading need evaluation.

The standard laboratory methods of testing mineral aggregate durability are ACV, Los Angeles and/or 10% FACT. These tests are used to determine the degree of disintegration of the crushed aggregates on a fraction of combined materials. Nevertheless, they are not suitable for natural gravel, where secondary smectite is the major component within the soil matrix. In addition, these tests do not account for decomposition of mineral aggregates due to the effect of water. In this respect, a DMI test that combines the effect disintegration and decomposition of the combined mineral aggregates is more realistic for evaluation of mineral aggregate durability for BSMs with simulation of field conditions. In Chapter 3, a DMI test procedure is used to investigate the durability of selected mineral aggregates.

2.6.2 Bituminous binder durability

The most important mechanism of age hardening is the change in chemical composition of binder molecules because of the reaction with atmospheric oxygen both during production and during in-service life. The physicochemical properties of mineral aggregates and the colloidal nature of bitumen play a significant role in binder-aggregate interactions. During production of foamed bitumen, short-term ageing might be critical for bond formations. Therefore, this area requires evaluation. The presence of heteroatoms in bitumen contributes to the difference in physical properties and their ageing behaviour. Binders from different sources have different ageing behaviour. Because of this, short-term ageing of different bitumen used for production of foamed bitumen can be distinguished by a sensitivity test simulating circulation time at respective temperatures. In Chapter 7, short-term age hardening during production of foamed bitumen and bitumen emulsion are investigated and reported.

Unlike HMA, chemical composition change in BSMs is predominantly during in-service life. This is because a thin film on BSMs is highly exposed to oxidation pathways due to discrete coating on the mineral aggregates, leaving a higher void in the mix matrix. The addition of active filler (cement or lime) into BSMs serves not only to enhance the long-term performance, but also

favourably alters the oxidation kinetics and interacts with products of oxidation to reduce their ageing effects. Therefore, determination of long-term ageing requires extraction and recovery of bitumen from BSM mixes which were exposed to environment and loading conditions for a number of years. In Chapter 7, several existing pavement sections are investigated and ageing behaviour of the binders is discussed.

The quantification of binder chemical composition change and/or determination of change in rheological properties after age hardening are complex issues. Several methods for qualitative extraction and recovery of asphalt from paving mixtures exist. Conventional methods used for extraction and recovery procedures for HMA are applied for the recovery of BSMs. In Chapter 7, cold centrifuge and solvents such as trichloroethylene (TCE) are used in dissolving bitumen from mineral aggregates. Absorption and rotary vapour are used for the recovery of bitumen through a distillation process.

It is evident from the interaction of the filler and colloidal characteristics of the binder (foam and emulsion) that depending, on the filler/binder ratio in the mix, the filler has an effect on graduating temperature sensitivity. This positive characteristic allows the bitumen to resist softening at relatively moderate temperatures in the pavement layer, in turn minimising oxidation. The influence of mastic stiffening might suitably define the age hardening behaviour of BSMs; although mastic stiffening is not investigated in this study, it is an area which requires future study.

2.6.3 Mixture composition durability

The theory of material science and the study of mixture composition structure and/or its surface at micro and macro levels develop a fundamental understanding on durability properties. The use of material performance models can be used to explain material behaviour and assist in the prediction of long-term performance of BSMs.

The adhesion and cohesion bonding between binder and aggregates in BSMs is one of the most important bonds that differentiate BSMs and granular material. However, it is one of the least understood bonds. This is partly due to the complexity of the binder characteristics and partly due to the variety of surfaces of aggregates with which the binder comes into contact. Theory of adhesion science, which has been extensively studied for HMA, is applied in understanding the binder-aggregate interaction in BSMs, taking cognisance of the specific aspects peculiar to BSM mixes, such as acquire phase, the colloidal nature of the binder, grading of aggregates, additional of active filler and bond development as a result of the curing process. In Chapter 3, conceptual bond formation and governing process in BSM mix matrices is developed based on an understanding of the thermodynamics, hydrodynamics, and electrokinetics of the material.

Curing of mixture composition in BSMs remains an influential process for bond development within the mix matrix. However, the curing process is entirely dependent on the mechanisms of moisture evaporation. Review shows that in field conditions the evaporation process is linked to the temperature gradient in the layer, wind speed, relative humidity and boundary conditions surrounding the BSMs. The model that sufficiently addresses these parameters has not been studied. In Chapter 6, a proposed model adopted from HMA is presented. It is believed that further investigation into the model will accurately predict the curing mechanism, particularly under the field conditions, by encompass all evaporation parameters.

Moisture damage contributes significantly to the premature deterioration of pavement materials. The moisture transport mechanisms, coupled with adverse environmental conditions and dynamic loading, have been found to influence moisture damage mechanisms of BSMs. A wide approach for quantification of moisture damage is derived by testing a dry or control specimen and moisture-conditioned specimens using the same variable parameters. Although the methods provide an empirical measure of moisture damage, they also provide both variable and unreliable results. Therefore, there is a need to develop new moisture conditioning

procedures, which accurately simulate the field moisture infiltration conditions and consequently performing a mechanical test peculiar to BSM properties such as shear and stiffness. In Chapter 3, a device, which simulates more realistic pulsing of water pressured into mix matrix to determine the consequential adhesion and cohesion deterioration, is developed. In addition, the threshold values to separate acceptable from unacceptable moisture susceptibility of materials or mixtures is established.

2.6.4 Engineering properties durability

The engineering properties of BSMs have extensively been studied in the past. As a result, numerous tests have been utilised to classify the properties of BSM mix durability. However, in recent times there has been a shift from ITS, UCS and dynamic creep to more fundamental tests related to principle material behaviour in BSMs. Such tests are triaxial testing (i.e. resilient modulus, permanent deformation and shear properties), fatigue testing, and APT (field-related simulation). Nevertheless, the limiting values of the various tests are still uncertain as the mechanism of failure is not yet clearly defined. In Chapter 5, advanced triaxial testing on moisture damage is performed and discussed. In addition, in Chapter 4 the APT device is used to validate the moisture damage threshold values determined by the new device for moisture conditioning of BSM specimens.

The mechanism of moisture damage in BSMs is complex and difficult to model. Different mechanisms are involved in saturating BSMs. One of the causes of moisture induction to the BSMs in a pavement layer is traffic related. The review of the hydroplaning phenomenon shows that at a high vehicle speed of 80km/h, the film of water infiltrated into tyre patches may be forced through the voids in the pavement layer at a magnitude of 1.4kN (140kPa). In Chapter 3, such magnitude of water pressure is adopted for conditioning BSM specimens to simulated field moisture damage, prior to mechanical triaxial (monotonic) testing.

2.7 Conclusive remark

The findings on the literature review have defined the pertinent durability issues to be research on BSMs. In this light, research methodology of this study was designed. The overview of the research approach is presented in Figure 6, see Chapter 1.

REFERENCE

- Adamson A.W. 1990. A Textbook of physical Chemistry of Surface, 5th Edition, John Wiley and Sons, Inc. USA.
- Asphalt Institute, 1992. A Basic Asphalt. Emulsion Manual. Manual Series No 19, Second Edition. Lexington, USA. Pp 87
- Akzo Nobel Chemical, 1997. Bitumen Emulsifier, Technical paper presented in 24th AEMA meeting, Concu, Mexico.
- American Standard Test Method, 2003. Standard Test for Recovery of Asphalt from Solution by Absorb Method. ASTM Designation D 1856-95a,
- American Association of State Highway and Transportation Official. 1993. Standard practice for Accelerated Ageing of Asphalt Binder using a Pressure Aging Vessel (PVA), AASHTO Designation PPI, Edition 1A.
- Barber E.S 1957. Calculation of maximum pavement temperature from weather report. TRB no.168, pg 1-8.
- Ball G.F.A, Logan T.C, and Patrick J.E. 1999. Flushing process in chip-seals: Effects of water. Transfund NZ research report, no. 156.
- Bell C.A. and Sosnovske D. 1994. Ageing: binder validation. Report no. SHARP-A-384, National Research Council, Washington DC
- Birdi K.S. 2002. Handbook of surface and colloid chemistry. 2nd Edition, CRC press, USA.
- Binks B.P, and Clint J.H. 2002 Solid Wettability from Surface Energy Components: Relevance to Pickering Emulsions. Langmuir is published by the American Chemical Society. Washington, DC Vol. 18, pg.1270-1273
- Bose A. 2002. Measurement of work of adhesion between asphalt and rock. Unpublished report, Department of chemical engineering, University of Rhode Island, Rhode Island.
- Bowering, R. H., 1970. Upgrading Marginal Road Building Materials with Foamed Asphalt. Highway Engineering in Australia. Mobil Oil of Australia, Melbourne South.
- Burger, M. and Kröger D.G. 2006. Experimental convection heat transfer coefficient between a horizontal surface and the natural environment, proc. 17th international congress of chemical and process engineering, Prague, Czech Rep. pp. 1523 – 1524,
- Burger M. 2005. Prediction of the temperature distribution in asphalt pavement samples. Master thesis, Department of mechanical engineering, Stellenbosch University, South Africa.
- Butt H.J Graf K. and Kappl M. 2003. Physics and chemistry of interfaces. Weinheim. WILEY-VCH Verlag GmbH & Co. KgaA.
- Burr B. L., Davidson R. R., Glover C.J., and Bullin J.A., 1990. Solvent removal from Asphalt. Transport Research records TRR, 1269. Washington DC.
- Burr B. L., Glover C.J., Davidson R. R., and Bullin J.A., 1993. New Apparatus and Procedure for the Extraction and Recovery of Asphalt Binder from pavement Mixtures. Transport Research records TRR, 1391. Washington DC.
- Blakely, J.M., 1973. Introduction to the Properties of Crystal Surfaces. Pergamon Press, New York.
- Branthaver J.F., Petersen J.C., Robertson R.E., Duvall J.J., Kim S.S, Harnsberger, P.M. Mill T., Ensley E.K., Barbour F.A., Schabron J.F. 1993. Binder Characterization and Evaluation Volume 2: Chemistry. Report- SHARP-A-368, National research Council Washington, DC.
- Brennen M., Tia M., Altschaefl, A. and Wood L. E., 1983. Laboratory Investigation of the Use of Foamed Bitumen for Recycled Bituminous Pavements. Transportation Research Record 911. Pp 80-87
- British Standard Institution, 2000. Petroleum and its products, determination of the resistance to hardening under the influence of heat and air. British standard EN 12607-1.

- Caro S., Masad E., Bhasin A., Little D. N. 2008. Moisture susceptibility of asphalt mixtures, Part 1: mechanisms, Part 2: Characterisation and modelling. *International Journal of Pavement Engineering*. Vol. 9, No. 2, pg81–98
- Cooper K. E. Brown S.F. and Pooley G. R. 1985. The design of aggregate grading for asphalt base courses, *Proceedings of Association of Asphalt Paving Technologists*, Vol.54.
- Collins-Garcia H., Mang T., Roque R., and Choubane D., 2000. An evaluation of Alternative Solvent for Extraction of Asphalt to Reduce Health and Environmental Hazards. *TRB Annual Meeting*, Washington DC.
- Cussler E.L. 1997. *Diffusion-Mass transfer in fluid systems*. 2nd Ed. Cambridge University Press London.
- Chen J.S and Huang L.S. 2000. Developing an ageing model to evaluate engineering properties of asphalt paving binders. *Journal of material and structure* vol. 33,pg 559-565.
- Cheng D. 2002. Surface free energy of asphalt-aggregates systems and performance analysis of asphalt concrete based on surface free energy. PhD dissertation, Texas A&M, University College, station. Texas.
- Choubane, B., Page G. C., and Musselman J. A., 1998. Investigation of Water Permeability of Coarse Graded Superpave Pavements. *Association of Asphalt Paving Technologists*, Vol. 67.
- Csanyi L.H. 1957. Bituminous Mixes Prepared with Foamed Asphalt. Ames, IA: Iowa State University, Iowa Engineering Experiment Station. (Bulletin; 189).
- CSIR. TRH 14. 1985. Guidelines for road construction materials. Technical recommendation for highway. Pretoria.
- De Beer M. 1989. Aspect of erodability of light cementitious materials. Pretoria Division of road and transport technology. CSIR Research report DPVT 39, Pretoria.
- Dingrevillea R., Qua J., and Cherkaoui M.. 2005. Surface free energy and its effect on the elastic behavior of nano-sized particles, wires and films. *Journal of the Mechanics and Physics of Solids*. Vol. 53 pg. 1827–1854.
- Domke C.H, Davison R.R. and Glover C.J. (1999). Effect of oxidation pressure on asphalt hardening susceptibility. *TRB*. Issue no. 1661. Pg 114-121.
- Domke C.H, Liu M, Davison R.R, Bullin J.A, and Grover C.J, 1997. Study of strategic highway research program pressure ageing vessel procedure using low-temperature aging experiments and asphalt kinetics. *TRR* No. 1586, pg 10-15.
- Dukat, L.E. 1989. Aggregate properties related to pavement performance. *Proceedings of Association of Asphalt Paving Technologist*, Nashville, Tennessee, Vol.58 pp 492-502
- Dron R.P. 1964. In *Contact Angle Wettability and Adhesion*, *Adv. Chem. Ser.*, No. 43, American Chemical Society, Washington, DC, p. 310.
- Ebels L.J, Jenkins K.J, and Sadzik. E. 2003. Investigation into the correlation of the MMLS3 and HVS APT devices. Technical report ITT/2003. Stellenbosch University, South Africa.
- Ebels. L.J. 2008. Characterisation of materials properties and rehabilitation of cold bituminous mixture for road pavements. PhD dissertation, published at the University of Stellenbosch, South Africa
- Emery S.J, 1988. The prediction of moisture content in untreated pavement layers and an application to design in Southern Africa. CSIR research report no.644. Division of Roads and Transport Technology. *DRTT Bulletin* 20. Pretoria
- Emery S. J. and Zacharias M. P., 1994. Temperature Susceptibility of South African Bitumen. 6th Conference on Asphalt Pavement for Southern Africa, CAPSA, Cape Town.
- Emery, S.J. 1984. Prediction of pavement moisture content in south Africa, 8th Proceeding Regional conference in Africa for soil mechanics and foundation engineering, Harare, Vol.1 pp 239-251

- Environmental Protection Agency United State, 2003. EPA's Proposed Regulation of n-Propyl Bromide. Air and radiation regulation. EPA-430-F-039 Washington DC
- Elphinstone G.M 1997. Adhesion and cohesion in asphalt-aggregate systems. PhD dissertation, Texas A&M University, College station, Texas.
- Ensley E.K., Petersen J.C and Robertson R.E. 1984. asphalt-aggregate bonding energy measurements by microcalorimetric methods. *Thermochimica Acta*, 77 (1984) 95-107 Elsevier Science Publishers B.V., Amsterdam - Printed in The Netherlands
- Fowkes F.M. 1964. Attractive forces at interfaces. *Industrial engineering and Chemistry* vol. 56(12) pg 40-52.
- Fu P.,Harvey J.T., Jones D., Chao Y.C. 2007. Understanding internal structure characteristics of foamed asphalt mixes with fracture face image analyses. *Journal of transportation research board*.TRB.Resubmitted for publication. Washington DC.
- Gast R. 1977. Surface and colloidal chemistry. In J.B Dixon and S.B. Weed (Eds), *Minerals in soils environments*. Soil Science of America. Madison Wisconsin. Pg 27-73
- Gibbs, J.W., 1928. *The Collected Works of J. Willard Gibbs*. Longmans, New York
- Girdler R.B 1965. *Proc. AAPT*. Vol. 34 pg 45, Settle. USA
- Good R.J and van Oss C.J. 1991. The modern theory of contact angles and the hydrogen bond component of surface energies. In M.E Schrader and G.Loeb (Eds), *Modern approach to wettability: Theory and applications*. New York. Plenum Press, pg 1-27.
- Goebel M. O, Bachmann J. Woche S.K Fischer W.R. and Harton R. 2004. Water potential and aggregate size effects on contact angle and surface energy. *Soil science of America journal*. ProQuest Agriculture journal pg 383-393.
- Grobler, J.A. 1995. The influence of compaction moisture on shrinkage in stabilised materials. Masters dissertation (M Eng). University of Pretoria. Pretoria: South Africa.\
- Gueit C., Robert M., and Durand G., 2006. Characterisation of Different Phases in the Life Cycle of the Binder in Bitumen Emulsion. *Recovery Method*. Eurasphalt and Eurobitume General review no. 849.
- Hagos E.T. 2008. The effect of ageing on binder properties of porous asphalt concrete. PhD dissertation published at the Technical University of Delft. The Netherlands.
- Head, K. 1981. *Manual of soil laboratory testing volume 1*. Engineering laboratory equipment ltd: London.
- Heukelom W., 1973. An Improved Method of Characterising Asphaltic Bitumen with Aid of their Mechanical Properties. *Proceeding of Association of Asphalt Paving Technologist*. Vol. 42, pg 67-84
- Hefer A.W 2004. Adhesion in bitumen-aggregates system and quantification of the effects of water on the adhesive bond. PhD dissertation, Texas A&M university, College station, Texas.
- Herfer A.W., and Little D.N 2005. Toward quantification of adhesion and water stripping in bitumen materials using modern surface energy theory. 24th proceeding of the South African Transport conference (SATC) Pretoria, South Africa pg 115-122
- Herfer A.W. Little D.N. and Lytton R.L 2005a. A synthesis of theories and mechanism of bitumen-aggregates adhesion including recent advances in quantifying the effect of water. *AAPT* vol 74 pg.
- Hefer A. 2005. Adhesion in bitumen-aggregate systems and quantification of the effects of water on the adhesive bond. *Research report ICAR –505-1*. Springfield, Virginia
- Highter W.H and Wall D.J 1984. Thermal properties of some asphaltic concrete mixes. *TRB* no. 969 pg. 38-45.
- Hoiberg A.J. 1965. *Bituminous materials, Asphalt, Tars, Pitches*. Vol 1, 2 and 3. Interscience publishers.
- Houston M., and Long F. 2004. Correlation between different ITS and UCS test protocol for foamed bitumen treated materials. 8th Conference on asphalt pavements for Southern Africa. Sun City, South Africa.

- Hotte P. 1995. Six years of Recycling with Foam Bitumen. Proceedings ARRA. San Diego, USA
- Huang S.C Branthaver J.F and Robertson R.E. 2000. Effects of aggregates on asphalt-aggregate interaction. 8th Annual Symposium of the international Centre for aggregates research. Denver, Colorado pg 1-20.
- Ishai I., Brule B., Vaniscote J.C. and Ramond G. 1988. Some rheological and physio-chemical aspects of long-term asphalt durability. AAPT, vol 57 pg 65-93.
- Israelachvili J.!1992. Intermolecular and surface forces, 2nd ed. Academic press, San Diengo,CA
- James A. 2006. Overview of asphalt emulsion. Transporation research circular E-C102, asphalt emulsion technology. TRB Washington DC.
- Jenkins KJ. 2007. Moisture in subgrade, session 8 presentation on postgraduate course, at Stellenbosch University, South Africa. "Hitchhiker's Guide to Pavement Engineering."
- Jenkins K.J., Ebels L.J. and Twagira M.E. 2006. Updating bituminous stabilised materials guideline: Mix design inception study. First draft. Pav. Eng.cc, Stellenbosch, South Africa.
- Jenkins K.J. 2000. Mix design consideration for the cold and half-warm bituminous mixes wirh emphasis on famed bitumen. PhD dissertation, published at the University of Stellenbosch, South Africa
- Jenkins K.J, Ebels L.J, Twagira M.E, Kelfkens R.W, Moloto P and Mulusa W.K 2008. Updating bituminous stabilised materials guideline: Mix design report, phase II. Research report, prepared for SABITA and Gautrans, Pritoria. South Africa.
- Jia L and Sun L. 2007. Numerical prediction model and thermal properties for asphalt pavement. Journal of advanced characterisation of pavement and soil engineering materials. Taylor & Francis Group. London.
- Jones D and Ventura D.F.C. 2002. Development of cerification test for unsealed road additives-Phase I. CR 2002/32. CSIR. Pretoria.
- Jooste F. Kekwick S.V Sadzik E and Rohde G, 1997. Comparison of accelerated pavement test results with long-term pavement behaviour and performance. 8th international conference on asphalt pavement, Seattle, USA.
- Kandhal P.S and Chakraborty S. 1996. Effect of asphalt film thickness on short-term and long-term ageing of asphalt paving mixtures. TRB, Vol no. 1535 pg 83.
- Karlsson, R., and Isacson, U. _2003_. "Investigations on bitumen rejuvenator diffusion and structural stability." *J. Association of Asphalt Paving Technologists*, 72 463–501
- Karlsson, R., and Isacson, U. _2002_. "Bitumen rejuvenator diffusion as influenced by aging." *Int. J. Road Materials and Pavement Design*, 3_2_, 167–182.
- Kelfkens R.W.C 2008. Vibratory hammer compaction of bitumen stabilised materials. MSc. Thesis. University of Stellenbosch. South Africa.
- Kiggundu B.M and Robert F.L. 1988. Stripping in HMA mixtures: state of art and critical review of test methods. Report 88-02. National centre for asphalt technology . Auburn University, Alabama.
- Konitpong K, Bensons C.H. and Bahia H.U. 2001. Hydraulic conductivity (permeability) of laboratory compacted asphalt mixtures. TRB no. 1767. Washington DC, pg 25-32
- Konitpong, K., Benson C. H., and Bahia H. U., 2001. Hydraulic Conductivity (Permeability) of Laboratory Compacted Asphalt Mixtures. Transportation Research Record, no. 1767, Transportation Research Board, Washington DC, p25 – 32,
- Konitpong K. and Bahia H.U. 2003. Role of adhesion and thin Film Tackness of Asphalt Binders on Moisture Damage of HMA. Association of Asphalt Paving Technologists (AAPT) Vol. 72 pg 502-528.
- Kuvhanganani L. T. 2008. Moisture sensitivity of selected foamed bitumen-treated Materials. Master's degree in technology, Pavement Engineering. Tshwane University of technology. Pretoria, South Africa.

- Kringos N. Scarpas T. Kasbergen C. and Selvadurai P. 2008. Modelling of combined physical-mechanical moisture-induced damage in asphaltic mixes, Part 1: governing processes and formulations. Part 2 Moisture damage parameters. *International Journal of Pavement Engineering*. Vol. 9, No. 2, pg 115–128.
- Lancaster, J., McArthur, L. and Warwick, R., 1994. VICROADS Experience with Foamed Bitumen Stabilisation. *Proceedings 17th ARRB conference Part 3*. Australia. Pg 193-211
- Labib M.E. 1992. Asphalt-aggregate interactions and mechanisms of water stripping. *American Chemistry Society, Fuel*, 37, pg 1472-1481
- Land Transport New Zealand. 2005. The waterproofness of first coat chipseals. Research report style guide. Report xxx. Pg 35.
- Laroche I. Wu X. Masliyah J.H and Czarnecki J. 2002. Dynamic and Static Interactions between Bitumen Droplets in Water. *Journal of Colloid and Interface Science* 250, pg. 316–326
- Liu J., Xu Z. and Masliyah J. 2005. Colloidal forces between bitumen surfaces in aqueous solutions measured with atomic force microscope. *Colloids and Surfaces A: physicochem. Eng. Aspects* 260 pg. 217–228
- Li. W. 1997. Evaluation of the surface energy using the Chan balance. Unpublished manuscript, Texas A&M University, Department of chemical engineering College station, Texas.
- Liebenberg JJE. 2002. The Influence of Various Emulsion and Cement Contents on an Emulsion Treated Ferricrete from the HVS Test Sections on Road P243/1. Contract Report CR-2001/77, CSIR-Pretoria.
- Litte D.N and Epps J. A. 2001. the benefits of hydrated lime in hot mix asphalt. Report prepared for National Lime Association, The versatile chemical, USA.
- Loizos A and Papavasiliou V. 2007. Assessment of in-situ cold in-place recycling performance using the foam asphalt technique. Workshop on pavement recycling. Athens, Greece.
- Long F and Jooste F., 2007. Summary of LTPP Emulsion and Foamed Bitumen Treated Sections. Technical Memorandum Modelling and Analysis Systems, Cullinan, South Africa.
- Long. F, Thyese H. and Ventura D.F.C. 2004. Characterisation of foamed bitumen treated materials from HVS test sections.
- Louw L. 1997. ETB mix design. Summary for the best practice. Contract report CR96/079. Transportek, CSIR. Pretoria.
- Maccarrone, S., Holleran G., Leonard, D. J. and Hey, S., 1994. Pavement Recycling using Foamed Bitumen. *Proceedings 17th ARRB Conference Part 3*. Australia. Pp 349-365
- Malubila S.M. 2005. Curing of foamed bitumen mixes. Masters thesis. University of Stellenbosch. South Africa.
- Mertens, E.W. and Wright, J.R. (1959). Cationic emulsions: How they differ from conventional emulsions in theory and practice. *Highway Research Board Proceedings*, 38, 386-397
- Milne T. I. (2004). Towards a Performance Related Seal Design Method for Bitumen and Modified Bitumen Seal Binders. PhD Thesis, University of Stellenbosch. South Africa.
- Mitchell, J.K. 1993. Fundamentals of soil behaviour, *second edition*, John Wiley & sons, inc. USA
- Myers, D., (2002). Some general concepts about interfaces. *Interfaces and colloids (Part 1)*, retrieved from T. Cheresources, Inc <http://www.cheresources.com/interfaces2.shtml>
- National Cooperative Highway Research Program, 2000. Recommended Use of Reclaimed Asphalt pavement in the Superpave Mix Design Method. NHC Final Report D9-12, USA
- Nijboer L W, 1943, Plasticity as a factor in the design of dense bituminous road carpets, Amsterdam Laboratory of the N.V. DeBataafsche Petroleum Maatschappij (Royal Dutch Shell Group), Published by Elsevier Publishing Company, Inc
- Nikajima Y., Seta E., Kamegawa T. and Ogawa H. 2000. Hydroplaning analysis by FEM and FVM: Effect of the rolling and tire pattern on hydroplaning. *International journal of automotive technology*, Vol. 1 no.1 pp 26-34.

- Okan S. and Mang T., 2003. Investigation of Problem in Binder Extraction from Conventional and Rubber Modified Asphalt Mixture. 6th Rilem Symposium, Zurich, Pg 212-219
- Oliver J.W.H and Tredrea P.F. 1997. The change in properties of polymer modified binders with simulated filed exposure. Association of Asphalt Paving technologists (AAPT) vol. 66.
- Oliver J.W.H. 1984. An interim Model for predicting bitumen hardening in Australian sprayed seals. Australian Road Research Board conf vol. 12. Part 2.
- Oliver, J. W. H. _1975_. "Diffusion of oils in asphalts." *Rep. No. 9*, Australian Road Research Board, Vermont South, Victoria, Australia
- Overby, C., Johanson, R. and Mataka, M., 2004. Bitumen foaming: An innovative technique used on a large scale for pavement rehabilitation in Africa. Case study: Same-Himo monitored pilot project. Proceedings of the 8th Conference on Asphalt Pavements for Southern Africa (CAPSA'04). Sun City, South Africa
- Paige-Green P. 2009. Personal communication on durability of mineral aggregates. CSIR-Transportec. Pretoria
- Paige-Green P. and Ventura D.F.C, 2004. Durability of foamed bitumen treated basalt base course. CSIR report CR 2004/8. Preoria.
- Paige-Green P. 1989a, 1989b. New performance-related specification for upaved roads. Proceeding annual transportation convention, Pretoria. Vol 3A pg 3A/12.
- Peterson G. D., Soleymani H. R., Anderson R. M., and McDaniel R.S., 2000. Recovery and Testing of RAP Binder from Recycled Asphalt Pavement, Proceedings of the Association of Asphalt Pavement Technologist
- Petersen J.C. Plancher H., Ensley E.K., Miyake G and Venable R.L. 1982. Chemistry of asphalt-aggregate interaction: Relationship with moisture damage prediction test. Transportation Research Record, 843,95.
- Peterson J.C. 2000. Chemical composition of asphalt as related to asphalt durability, included in series of Asphaltenes and Asphalts, 2. Developments in Petroleum Science. 40B. Elsevier, USA
- Petersen, J. C. _1984_. "Chemical composition of asphalt as related to asphalt durability: State of the art." *Transportation Research Record 999*, Transportation Research Board, Washington, D.C., 13–30.
- Petersen, J. C. _2000_. "Chemical composition of asphalt as related to asphalt durability." *Asphaltenes and asphalts, developments in petroleum science 40B*, Elsevier, New York.
- Peterson, G. D., Davison, R. R., Glover, C. J., and Bullin, J. A. _1994_. "Effect of composition on asphalt recycling agent performance." *Transportation Research Record 1436*, Transporation Research Board, Washington, D.C., 38–46.
- Pinard M. 2006. Alternative materials and pavement design technologies for low-volume sealed roads +case studies. International workshop, Bamako mali.
- Plancher H.m Green E.L. and Peterson J.C. 1976. Reduction of oxidative hardening of asphalts by treatment with hydrated lime-a mechanistic study. AAPT vol. 45 pg 1-24.
- Ramanujam, J.M & Jones, J.V. 2000. Characterisation of foamed bitumen stabilization. Queensland Department of Main Roads: Australia
- Roberts F.L, Kandhal P.S., Ray B.E, Lee D.Y, Kennedy T.W. 1996. Hot mix asphalt materials, mixture design and construction. NAPA, Research and Education Faoundation, Lanham, Maryland
- Rodríguez-Valverde M.A., Ramón-Torregrosa P. Páez-Dueñas A., Cabrerizo-Vílchez M.A, Hidalgo-Álvare R. 2008. Imaging techniques applied to characterize bitumen and bituminous emulsions. Advances in Colloid and Interface Science 136 pg.93–108
- Ruckel, P. J., Acott, S. M. and Bowering, R. H., 1983. Foamed-Asphalt Paving Mixtures: Preparation of Design Mixes and Treatment of Test Specimens. Transportation Research Record 911. Pp 88-95

- SABS 307 (1993). Standard Specification for the Bitumen Rheological Properties for Road Construction. South Africa.
- SABITA , ETB Manual 21. 1999. The design and use of emulsion-treated bases.
- SABITA, GEMS Manual 14. 1993. The design and use of granular emulsion mixes, ETB.
- Sampson, L.R. and Netterberg, F. 1989. The durability mill: A new performance-related durability test for base course aggregates. *Journal of civil engineer in South Africa*, Vol. 31 no.9 pp 287-294
- Sampson, L.R. Emery, S.J. and Rose, D.A. 1985. Investigation into premature distress at four sites in the Cape Province. *Proceeding annual transport convention*, Pretoria
- Sampson L.S. and Paige-Green P. 1990. Recommendation for suitable durability limits for lime and cement stabilised materials. Pretoria Division of Roads and Transport Technology, CSIR research report DPVT 130, Pretoria.
- Sampson L.S and Netterberg F. 1989. The durability mill: A new performance related test for base course aggregates. *The civil engineer in South Africa*, pg 287-294.
- Seta E., Nakaima Y, Kamegawa T, and Ogawa. 2000. Hydroplaning Analysis by FEM and FVM: Effect of Tire Rolling and Tire Pattern on Hydroplaning, *Journal of Tire Science and Technology*, Vol. 28, No3, pg140-155.
- Serfass, J. P., Carbonneau X., Delfosse F., Triquigneaux J.P., and Verhee F. 2008. Mix Design Method and Field Performance of Emulsion Cold Mixes. 4th Eurobitume and Eurasphalt Congress, Copenhagen.
- Serfass, J. P., Poirier, J. E., Henrat, J. P. and Carbonneau, X. 2003. Influence of Curing on Cold Mix Mechanical Performance. *Performance Testing and Evaluation of Bituminous Materials PTEBM'03*, 6th International Rilem Symposium, Zurich, Switzerland
- Serfass, J. P., Henrat, J. P. and Carbonneau, X. 2004. Evaluation of the Cold Mixes Performance in the Short and Long Term. Eurobitume and Eurasphalt Congress, Vienna. Paper 113.
- Solaimanian M. and Kennedy T.W. 1993. Predicting maximum pavement surface temperature using maximum air temperature and hourly solar radiation. *TRB no. 1417* pg. 1-11.
- South Africa National Road Agency. 2007. Technical Recommendation for Highways (TRH3). Design and construction of surface seals. Pretoria, South Africa.
- Scott J.A.N 1978. Adhesion and disbanding mechanisms of asphalt used in highway construction and maintenance. *AAPT 47* pg 19-48.
- Schramm L.L 2005. Emulsion, foams and suspension: fundamentals and applications. Wiley-VCH Verlag GmbH & Co. KGaA. Germany
- Shackel B., Makiuchi K. and Derbyshire J.R. 1974. The response of foamed bitumen stabilised soil to repeated triaxial loading. 7th ARRB conference. Vol. 7 part 7 Australia pg 74-89.
- Shell Bitumen, 2003. Shell Bitumen Handbook. Shell bitumen UK.
- Smit A.F, Hugo F., Rand D. Powell.B, 2003. Model mobile load simulator testing at the national centre for asphalt technology test track, *TRB no. 1832*, Washington DC. report CR-2001/5. CSIR transportek, Pretoria.
- Stellenbosch University Institute of Transport Technology. 2008. Method for evaluation of permanent deformation and susceptibility to moisture damage of bituminous road paving mixtures using the *Model Mobile Load Simulator (MMLS3)*. DPG1-drapft protocol guideline. First Draft Version 3 Rev1. South Africa.
- Strategic Highway Research Program (SHRP). 1993. Binder Characterization and Evaluation Volume 2: Chemistry. National Research Council, Washington, DC.
- Stroup-Gardiner M., Nelson J. W., 2000. Use of Normal Propyl Bromide Solvent for Extraction and Recovery of Asphalt Cements. NCAT Report, Auburn University.
- Styne W.JvdM. 2001. First level data analysis of HVS tests on foam treated gravel and emulsion treated gravel on road P243-1 at 80kN and 100kN test sections.

- Tarrer A.R. and Wagh V. 1991. The effect of the physical and chemical characteristics of the aggregate on bonding. SHARP-A/UIR-91-507, contract A-003B.
- Tarrer R. 1996. Use of Hydrated Lime to Reduce Hardening and Stripping in Asphalt Mixes. 4th Annual ICAR Symposium, Atlanta, Georgia.
- Terrel R.L and Al-Swailmi S. 1994. Water Sensitivity of Asphalt-Aggregate Mixes, Test Development. Report No. SHRP-A-403, USA.
- Tuffour Y. A. and Ishai I., 1990. The Diffusion Model and Asphalt Age-Hardening. Proceedings of Association of Asphalt Paving Technologists. Pg 73-92.
- Thelen, E 1958. Surface energy and adhesion properties in asphalt-aggregate systems, HRB vol 192, pg 63-74.
- Twagira M.E. 2006. Characterisation of fatigue performance of selected cold bituminous mixes. MSc Thesis. University of Stellenbosch, South Africa.
- Twagira ME and Jenkins KJ. 2009. Moisture damage on bituminous stabilised material using a MIST device. 7th RILEM international symposium at Rhodes, Greece.
- van de Ven M.F.C and van Assen E.J. 1999. South African bitumen specifications and compositional balance, 7th conference of asphalt pavements for Southern Africa, Zimbabwe.
- Van Oss C.J. Chaudhury MK. And Good R.J. 1988. Interfacial Lifshitz-van-der Waals and polar interaction in macroscopic systems. Chemical review 88 pg 927.
- Van Wijk, A. and Wood, L. E., 1983. Use of Foamed Asphalt in Recycling of an Asphalt Pavement. Transportation Research Record 911. Pp96-103
- Van Wijk A. J. and Lovell, C. W. 1986. Prediction of subbase erosion caused by pavement pumping. Transportation Research Record, 1099, pp 45-57
- Van Wijk A. J. and Lovell, C. W. 1985. Erosion of subbase materials under rigid pavements. Proc. 3rd Int. conference on concrete pavement design. Perdue University
- Ventura, D. 2001. Durability aspects of the ferricrete from the HVS sections on Road P243/1. CSIR Transportek. Pretoria: South Africa. (CR-2001/81).
- Verhasselt A.F. and Choquet F.S. 1997. Field ageing of bituminous binders: Simulation and kinetics approach. 5th RILEM Symposium on Mechanical Test Method for bituminous materials. Lyon, France.
- Walubita, L. F., Hugo, F., Epps-Martin, A. L., 2002. Indirect tensile fatigue performance of asphalt after MMLS trafficking under different environmental conditions. Journal of the SA Institution of Civil Engineering, Vol. 44, Number 3. Johannesburg, South Africa
- Weston C., Van Amsterdam and Jenkins K., 2002. A Study into the Mechanical Properties of Foamed Bitumen Stabilised Materials. 21st Annual South Africa Transportation Conference.
- Weinert H.H. 1980. The natural road construction materials of Southern Africa. Academia. Cape Town.
- Wisconsin department of transport, 2004. effect of pavement thickness on superpave mix permeability and density. WisDOT Highway Research Study 0092-02-14, Madison, WI 53704.
- Yoon H.H and Tarrer A. 1988. Effect of aggregate properties on stripping. Transportation Research Record, 1171 pg 37-43.

CHAPTER 3

MOISTURE SUSCEPTIBILITY AND DAMAGE MECHANISMS

3.1 INTRODUCTION

Moisture susceptibility and consequential damage manifestation in BSMs is the phenomenon that describes the effect of the presence of excess moisture in the microstructure of the binder and mineral aggregates. Moisture susceptibility is a measure of how susceptible the mixture's internal system is to weakening in the presence of moisture. The weakening should be severe enough to result in stripping, ravelling, or the loss of adhesion and cohesion in the system. Due to the dispersion and coagulation nature of the binder (foam and emulsion respectively) in the mineral aggregates, coating of the thin film of binder in the mineral aggregates is non-uniform. Whereas the dispersion of foamed bitumen bubbles has high affinity to filler fractions resulting in mastic formation, the bitumen emulsion to a large extent coats the large aggregates as well as forming mastic within the mixes. Because dispersion and coagulation during mixing is not completely uniform, large percentages of filler and coarse fractions are left uncoated by the bitumen.

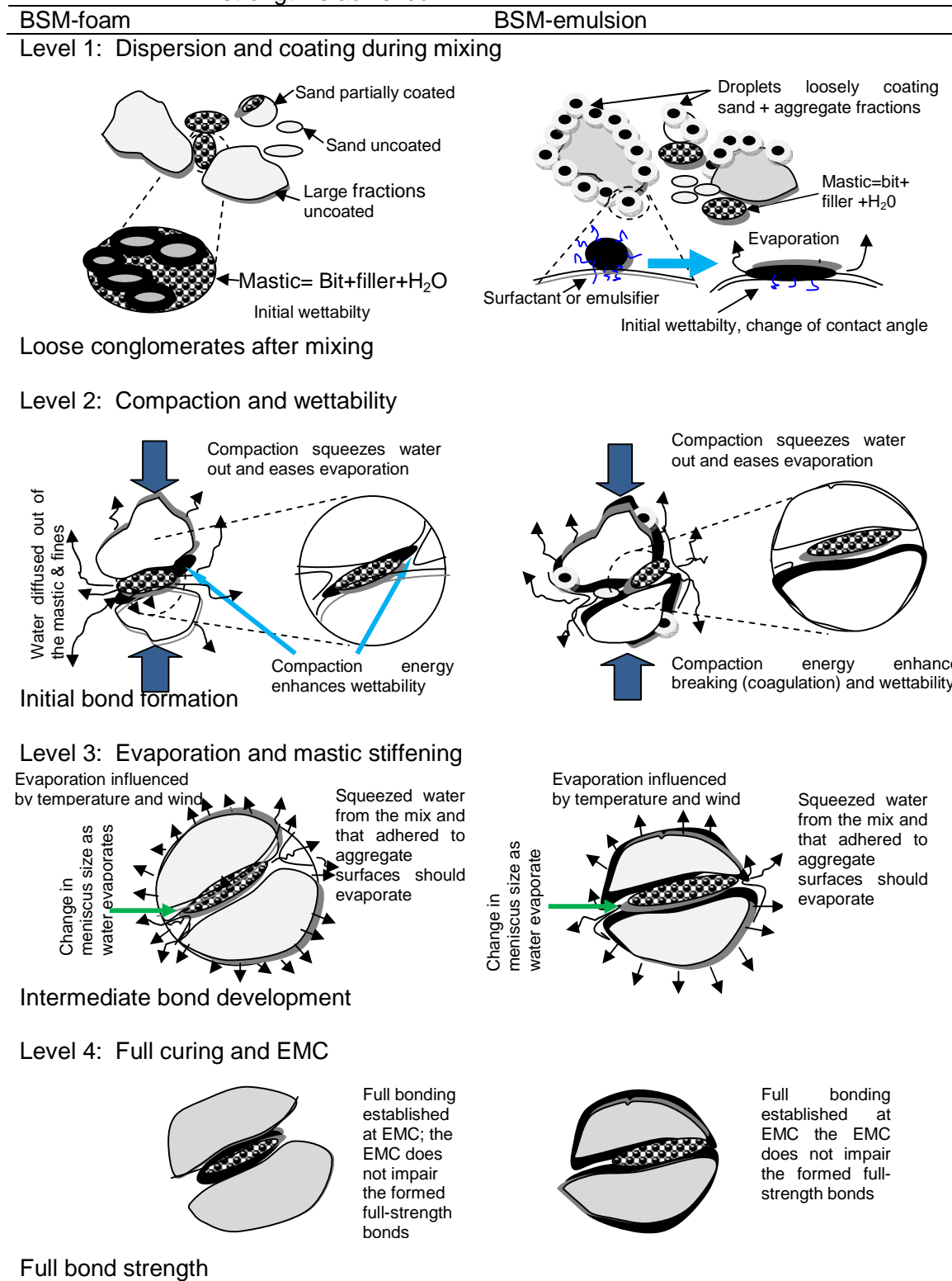
Partial coating of thin film binder in the mineral aggregates results in the formation of high void content in the mixture. The presence of moisture in the interconnected and isolated voids between the mix matrixes significantly influences moisture susceptibility and plays a major role in the damage mechanisms. The objectives of this chapter are firstly to establish a theoretical framework for bond evolution in the BSM mix matrix and analyse the adhesion and cohesion using fundamentals of physicochemical interaction between the binder and the mineral aggregates. Secondly, to establish if a link exists between bonding (adhesion and cohesion) and moisture susceptibility in the mixture. Thirdly, to evaluate the damage mechanism on various formulated and combined mix matrix in terms of mechanical properties. This implies the study of the influence of moisture damage on reductions in stiffness, shear properties, and strength of BSMs.

3.2 GOVERNING PROCESSES AND FORMULATIONS

The adhesive and cohesive bonding between binder and mineral aggregates in BSM mixtures is an important bond that differentiates BSMs from granular materials. Therefore, understanding the governing process and formulation of the bonds between binder and mineral aggregates gives an insight into the fundamentals of mixture performance and failure mechanisms, which is essential for all phases of application of BSM technology (i.e. mix design, construction and in-service condition).

The evolution of bonding in BSMs begins during mixing, continues during compaction and fully develops after curing. The interaction between bitumen, mineral aggregates and water is a physicochemical phenomenon. As such, it deals with the interfaces because there are three types of bulk phase (i.e. binder, mineral aggregates and water). Therefore, it is possible to determine the governing process toward formulation of bonding in the mix matrix based on the nature of the interaction between different phases at the interfaces. Table 15 conceptually shows the step-by-step governing process of bond formation for both BSM-foam and BSM-emulsion, as they show differences and similarities in achieving full bond formation.

Table 15: Step-by-step governing process for bond formation in BSMs until full strength is achieved



3.2.1 Bond evolution and susceptibility to moisture damage (or durability)

The objective of the diagrams in Table 15 is to provide perspective on the descriptions of the mechanisms of bond formation in BSMs. Although they do not portray a clear image of the micro process of bond formation, they clarify the general concept at micro level, the actual thermodynamic and hydrodynamic properties occurring during bond formation. A possible formulation in 3D or a finite element is able provide a clear perspective of these images. From these diagrams it is possible to confidently describe the factors influencing durability behaviour as well as providing an insight into the mechanisms of failure in BSMs. Bond evolution and susceptibility to moisture damage can be described in the different levels as follows:

3.2.1.1 Level 1 diagrams

Level 1 depicts the dispersion and coagulation nature of BSM-foam and BSM-emulsion. During dispersion of foamed bubbles, several concepts affect the production of a quality mix matrix. These are: 1) viscosity (expansion) and stability (half-life) influence dispersion and initial wettability of the filler during mixing; 2) percentage of filler fractions influences mastic formation, which is the glue for bounding large fractions. During dispersion, foamed bubbles have a higher affinity to filler fractions than coarse fractions, therefore excess bitumen might result in balling during collapse, which in turn impairs durability due to poor bonding; 3) mixing method and speed influence dispersion and coating. Time of mixing is an important element. Longer mixing might break or cause thread-like behaviour in the mastic resulting in a reduction in the wettability of bitumen on coarse fractions during compaction (gluing behaviour); 4) additional moisture influences the dispersed energy of the bubbles to the moist surface for better spread and coating on filler; and 5) aggregate temperature influences dispersion, wettability and bonding during compaction.

For bitumen emulsion, the breaking of droplets in the mineral aggregate skeleton must revert to continuous film in order to enhance bonding. The breaking of droplets involves flocculation and coalescence. The speed of the breaking process depends on a number of factors: 1) reactivity of emulsion depends on the surfactant in the aqueous phase, which determines the charges on the droplets. Anionic or cationic surfactant influences the wettability of droplets (i.e. breaking) when they come into contact with the surface of the mineral aggregates. Wettability is a measure of the spreadability of the droplets on the surface of the coarse fraction by changing the shape (angle) from a drop (90°) to flat (0° or film) (see diagram 1); 2) the temperature of the aggregates has significant influence on the wettability of the droplets, i.e. influencing electrokinetics. Electrokinetics is the reactivity of the mineral aggregates to taking up the surface charge of the droplets in water. Cationic emulsifier in the droplets contains positively-charged nitrogen (N) atoms in the head group, while anionic emulsifier contains negatively-charged oxygen (O) atoms. The charges are balanced by a counterion, which diffuses away from droplets into the continuous phase. Depending on the pH value of the mineral aggregates and the presence of soluble salts, cationic emulsion might react faster with aggregates with a negative charge and anionic emulsion with positively-charged aggregates. Therefore, selection of the right emulsion is important to ensure breaking and wettability of emulsion for bond formation; 4) an additional advantage of surfactant in the droplets is the ability to displace water or dust in the aggregate surface and adhere the polar fraction (asphaltenes) to the aggregates surface; and 5) mixing method influences coating and breaking of emulsion. The time of mixing is also important, that is longer mixing might enhance breaking and consequently stripping off of the coagulated film on the surface of the coarse fraction. Stripping will significantly impair bond formation during mix compaction. Therefore, it is recommended that a short mixing time be applied and compaction be done prior to significant breaking of droplets.

3.2.1.2 Level 2 diagrams

In level 2, compaction plays a significant role in bond formation in BSMs, both in the laboratory and in the field. The dispersion or breaking of foam or emulsion during mixing results in the formation of mastic and the partial coating of the mineral aggregates respectively. As such, the binder-aggregate interaction is incomplete during mixing. Therefore, the initial bonding is significantly influenced by compaction. The benefits of compaction are the following: 1) squeezing water out of the mastic and mineral aggregates to the surface. The exposed surface water can easily be evaporated in a conducive environment; 2) compaction energy significantly influences the wettability of the mastic to the coarse fraction surface, thus squeezing the bitumen polar fraction to react (interact) with the mineral aggregate surface charges. However, the entrapped water in the mastic impairs the binder-aggregate interaction. The entrapped water needs to diffuse out of the mastic before bonding. Because water has a higher affinity to the aggregates, the diffused water from mastic through the bitumen film adheres to aggregates before evaporation. This process therefore delays the bonding process. Figure 50 present the movement of water out of mix matrices through evaporation process; 3) packing of mineral aggregates during compaction results in an increase in cohesion and a reduction in the voids content or the conduit of water infiltration back to the cured mix matrices.

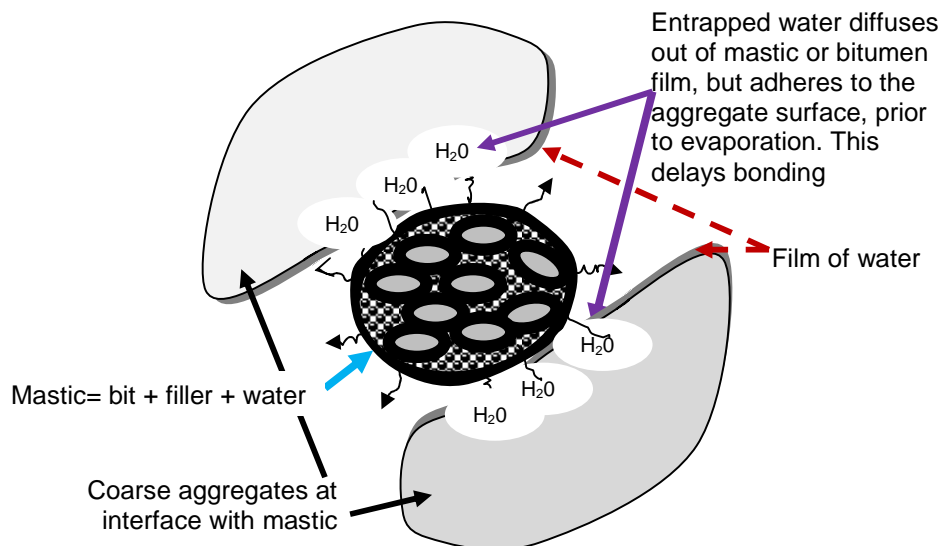


Figure 50: The influence of diffused water on the bonding formation at the mastic-aggregate interface

3.2.1.3 Level 3 diagrams

In level 3, evaporation of the moisture content, or curing, is a primary process for bonding. Without the expulsion of moisture in the mix matrix, BSMs might behave like granular material, or much worse, due to the lubrication behaviour of the unbound mastic or emulsion. Therefore, a mechanism to ensure sufficient reduction of water is vital in BSM bond formation. The reduction of moisture in the mix matrices, particularly in the filler particles, will result in meniscus change (see diagram in level 3). The change of the water film meniscus creates greater capillary suction between the mix matrixes, which is similar to pores fluid suction pressure. This phenomenon has significant influence on the adhesion of the mastic to the coarse fraction and the entire cohesion behaviour of the mix matrices. Moisture loss is an environmental phenomenon; different climatic regions exhibit different behaviour, therefore a sufficient curing period needs to be accurately predicted. The model for evaporation should take into account all the factors contributing to evaporation in particular climatic environments. As such, the use of

ambient temperature, wind speed, relative humidity and temperature distribution coefficient in the layer of interest is essential to the understanding of evaporation behaviour. The model predicting evaporation is briefly presented in this study. Although not validated, it might give a better understanding of the curing duration and prediction of the EMC in BSMs compared to the current oversimplified models described in the literature review. Therefore, further study of the evaporation model might contribute not only to the curing method for BSMs, but also to the long-term durability.

3.2.1.4 Level 4 diagrams

In level 4, the diagram indicates bonding conditions which have achieved full strength. However, due to the partial coating of the binder by the mineral aggregates, BSMs might absorb moisture from a relatively high humidity environment and therefore reside with some amount of moisture during in-service life. Previous studies have indicated that BSM mix matrices have EMC which lies between 40–50% of the OMC. After full evolution of the bonds, any addition of moisture to the mix cannot easily diffuse into the interface. This is due to the hydrophobic nature of the binder, particularly at EMC, and whether the temperature and loading conditions are maintained at the acceptable designed level. However, any change in these parameters might be detrimental to the EMC or any increase in the concentration of moisture. The excess diffused moisture might reach the interface through thin film binder to the filler entrapped in the mastic and later to the mineral aggregate surface. Hence stripping of mastic occurs. This stripping process might be faster in the mastic without the presence of active filler than where active filler is present.

Past researchers have validated the above governing process. Nevertheless, it is further validated in this study and discussed along with the whole structure of moisture damage mechanisms and durability behaviour. The addition of active filler has proved to improve the resistance to moisture damage in BSMs, even with a small dosage (typically 1% of cement). The explanation on the behaviour of active filler in the mechanism of moisture resistance in BSMs is discussed below.

3.2.2 Influence of active filler

The addition of active filler in small percentage (< 2%) has been observed to perform a significant role in the improvement of BSMs, both in resistance to moisture damage as well as mechanical properties (Long *et al.* 2003; Fu *et al.*, 2008; Ebels, 2008; Twagira, 2009; Gonzalez, 2009). However, the mechanism of improvement in these properties by the active filler is not properly explained. It is the objective of this section to describe at microscopic level the vital role of the addition of cement in BSMs.

As previously described in the literature review, the addition of active filler has a significant influence on the physicochemical interaction between binder-aggregate and water. When cement or lime is added to BSMs, the following key behaviour in the mixture occurs: 1) due to finer characteristics of cement, it has high affinity to filler particles and therefore gets entrapped into the mastic (Figure 50). The entrapped water hydrates the entrapped cement, drying the water entrapped in the mastic. The benefits of hydration are firstly, limiting the diffusion of water through the bitumen to delay the bonding as described in Figure 50. Secondly, the cementation action of the gel ($C_3S_2H_3$) is vital for the stiffening of the mastic, which in turn plays a significant role in resisting moisture damage and mechanical performance of the mastic after hydration; 2) during hydration of the cement by water in the mastic, heat is generated. The heat energy influences the adsorption of the polar fraction of the bitumen with filler particles through thermodynamic and electrokinetic action. This phenomenon influences the locking of the polar fraction of the binder from being exposed to oxidation (less temperature susceptible). The locking behaviour also causes separation (recovery) of all bitumen components from the filler relatively complex; 3) the added cement also coats large aggregates by reacting with

dust/filler adhering to the surface. The benefit of cement coating the large aggregates is that cationic exchange might take place between cement or lime and filler/dust particles. The calcium (Ca^{2+}) ion with higher valences can replace hydrogen (H^+), sodium (Na^+) and potassium (K^+) with low valences from clay or silt coating on the coarse fraction. The replacing ions (Ca^{2+}) can hold fewer water molecules than the ions being replaced, resulting in reduction of water at the binder-aggregate interface. In this regard, from Figure 50, the water diffused from the mastic and adhering to the aggregate surface will not be an issue with the addition of cement. Therefore, no delay in bond strengthening between the mastic and the aggregate surface will occur. This means the mechanism of displacing water is beneficial to BSM foam because less moisture at the mastic–aggregate interface occurs. Thus, early strength (cohesive and adhesive) gained from the mix can influence opening of the layer to traffic within the shortest possible time compared to BSM emulsion.

In BSM-emulsion, similar reactions to those mentioned above take place. However, due to significant binder coverage on the coarse fraction, the bonding of the mixes also improves from the catalytic action of the cement. This results in BSM-emulsion having relatively better resistance to moisture damage compared to BSM-foam. Nevertheless, the displaced water needs to be evaporated for bond strengthening, which takes longer for emulsion due to the high amount of water.

It is apparent from the catalytic nature of cement that high addition of cement might not improve further these reactions. Instead, it will result in cementing the whole mix matrix, which in turn will influence crack formation. Likewise, a high addition of binder (foam or emulsion) with a deficit of filler in the BSM-foam will cause the bitumen to ball and less stiffening will occur due to the lack of entrapped filler and cement. The unstiffened bitumen will then become more susceptible to temperature. Similarly, a higher content of emulsion will excessively cover the mix and not all will be effective in bond formation. The higher binder reduces voids in the mix, but makes it more susceptible to temperature.

For BSMs with a higher RAP content, the catalytic behaviour of cement might not significantly influence binder-aggregate interaction. The inactive nature of the RAP-aggregate surface and filler fraction impairs wettability and adsorption of the new binder into the mineral aggregates at ambient temperature. In addition, cement, which is entrapped in the RAP mastic, will hydrate the entrapped water and stiffen the mastic. However, the RAP filler, which is coated with old bitumen, will not fully interact with (adsorb) the new bitumen fractions due to its inactive nature. Nevertheless, dispersed energy of the bubbles to the filler fractions coated with old bitumen might have better adsorption properties compared to cold dispersed emulsion droplets. On the other hand, cement which covers coarse aggregates will hydrate the surface water, but electrokinetics will not take place due to the inactive surface. Instead, compaction energy might enhance the binder wettability and in turn bond development. Curing is also important to ensure bond strengthening. The weak bonding between binder and RAP mineral aggregate surface will be more susceptible to moisture damage than virgin mineral aggregates, and damage mechanisms might be more significant for BSM-emulsion than BSM-foam due to the influence of temperature.

3.2.3 Evaporation prediction model

Depending on the moisture content in the mix after mixing and compaction, it is common practice during construction to delay the application of surfacing, to allow significant moisture loss through evaporation. In the field, this is done empirically by allowing the compacted or wetted surface (materials) to remain untrafficked for three to five days, depending on the field environmental condition. This method of curing is subjective and is done without any guideline. It is important that moisture evaporation is predicted accurately to ensure proper bond development in the BSM mix matrix, according to predominant climatic conditions, prior to surfacing or opening to traffic. Burger and Kröger (2004) developed a model to determine water

evaporation that emulates the natural environment. Their model deduces the approximate equation that predicts turbulent convection of mass transfer or the evaporation rate where water surface concentration is measurably higher than air temperature. However, if thermals become relatively weak and the transfer process is largely determined by the degree of turbulence or eddies in the atmosphere, Burger and Kröger (2004) recommend the following mode.

$$m_{vom} = 6.43 \times 10^{-8} \left[(\rho_{avi} - \rho_{avom})^{\frac{1}{3}} + 0.451 v_w \right] x (p_{vo} - p_{vi}) \quad \text{Equation 13}$$

where m_{vom} = rate of mass transfer or evaporation from a horizontal wetted surface (z) at uniform concentration (m) on $z = 0$; ρ_{avi} = the density of the air-vapour (av) at ambient air temperature; ρ_{avom} = the density of saturated air at the wetted surface; v_w = wind speed; P_{vo} = vapour pressure at the wetted surface; and P_{vi} = vapour pressure in the air. Empirical relations exist for the density of air vapour and vapour pressure at the air and wetted surface. These parameters takes into account location of pavement construction in respect to air temperature, wind speed, air pressure and relative humidity as well as heat transfer coefficient of pavement layers.

The model in equation 12 only considers the evaporation of water at the wetted surface ($z = 0$). Evaporation through diffusion of vapour below the wetted surface (e.g. $z = a$) requires further investigation. The relation of the mass transfer or evaporation and coefficient of heat distribution in the layer, particularly in BSMs, might provide long-term prediction of vapour diffusion and/or curing behaviour. This might occur under varying climatic conditions throughout the year. This kind of model is very important for providing insight into durability behaviour and prediction of long-term performance in pavement recycling technology. However, development of such a relationship requires multi-disciplinary knowledge of heat transfer and thermal conductivity of these materials.

3.3 MOISTURE DAMAGE MECHANISMS

Based on the physicochemical interaction between the binder (foam or emulsion) and mineral aggregates as described in the different levels in Table 15, mixture composition in BSMs will have different moisture susceptibility behaviour as well as moisture damage mechanisms. The presence of excess moisture in the microstructure of the mix is the key player in moisture damage mechanisms. The moisture damage in cured and in-service pavements is a long-term phenomenon. The excess moisture residing in the voids coupled with dynamic loading may result in progressive moisture damage. This section covers the context by which the developed adhesive and cohesive bonds in the mix might be affected by the ingress of excess water. The key factors describing moisture damage mechanisms in the microstructure level are discussed as follows:

3.3.1 Moisture infiltration

The various modes of moisture infiltration into BSMs have been described in detail in the literature review. However, depending on the boundary layers in BSM, sources of moisture which have been reported to significantly influence the damage mechanisms, particularly in the field are: firstly, the infiltration of surface water (i.e. stagnant water from high precipitation) might be forced through the porous surface layer into the BSM by applied dynamic loading, especially if the surface layer has high void content or cracking; secondly, capillary rise of subsurface water, from a high water table or poor side drainage.

Figure 51 presents typical boundary layers in BSMs for South African pavement structures. The top layer is typically 40mm AC, or single or double seals; BSMs (foam or emulsion) form a base layer 250–300mm thick; the subbase is granular or CTMs 100–150mm thick and subgrade is the natural material or foundation.

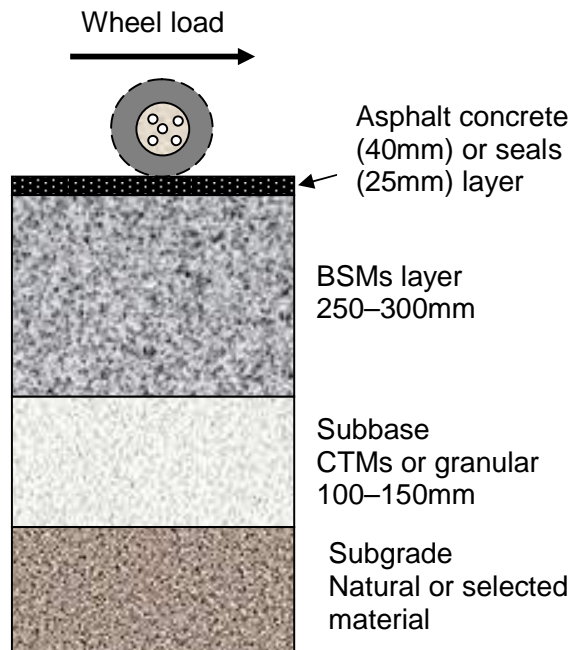


Figure 51: Typical South African pavement structure with boundary condition for BSMs

Moisture damage is a process that leads to change in the internal structure of a mixture by a reduction in adhesion and cohesion. The damaging mechanisms consist of moisture transport, which largely depends on the voids structure. Localised voids are prone to severe damage because the residing moisture generates higher pore pressure during dynamic loading, whilst interconnected voids might result in severe erosion under high dynamic loading. The BSM mix matrix is generally characterised by large localised voids and few interconnected voids. Therefore, pore pressure is characteristic of moisture damage mechanisms in BSMs. The voids structures in BSMs are discussed at micro level, from the results of CT scan images and SEM images, in Chapter 6 of this study. The characteristics of voids and moisture damage are illustrated in Figure 52.

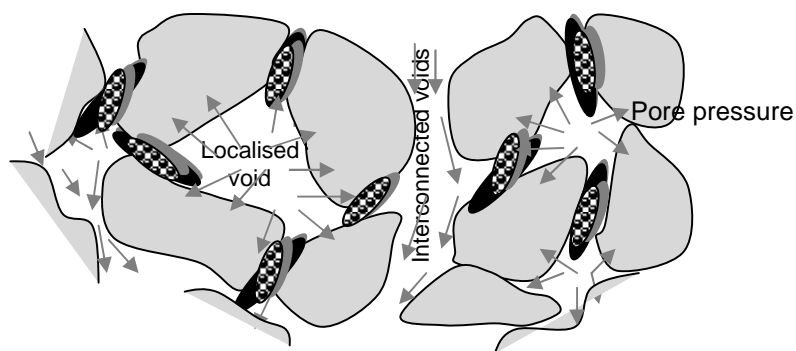


Figure 52: Illustration of pore pressure effect on void structures for the moisture damage

As illustrated in Figure 52, infiltration of moisture to the microstructure can result in pore pressure and erosion due to dynamic loading. Pore pressure and erosion result in disintegrations, which progressively degrade the physical integrity of cohesion and adhesion in the mixture. Adhesion and cohesion (i.e. ravelling or stripping of mastic) in BSMs is a failure

pattern which undoubtedly relates to a combined action of mechanical failure and moisture infiltration. Weakening of the interlock bonds of the mineral aggregates promotes a cohesive failure, while weakening of the binder-aggregates promotes a pronounced adhesive failure. In the following subsection, the process that results in weakening of the BSM mix matrix is identified.

3.3.2 Weakening of the cohesion and mastic-aggregate bonds

The interlocking properties of mineral aggregates (densely packed) play a crucial role in the load transfer performance of the mix matrix, while the addition of binder improves the cohesion by selectively binding or gluing the fine and large aggregates together. The presence of a large percentage of unbound mineral aggregates in the mix matrix makes BSMs behave to some extent like granular materials. However, the addition of binder in BSMs certainly gives different performance in terms of moisture damage mechanisms compared to granular materials.

The adhesion between mastic-aggregate improves with curing. However, due to the dispersive nature of the binder and the coating of thin film on moist aggregates, the bonding in the mixture will clearly be very fragile with the infiltration of water. The stripping of mastic or binder due to insufficient bonding is closely related to the texture of the mineral aggregates. A smooth aggregate surface (e.g. 90–100% quartz contents) bonds poorly with mastic. This is more pronounced in foamed bitumen mastic, because the interlocking of foam-mastic with the aggregate surfaces is mainly influenced by physical adhesion. On the other hand, for bitumen emulsion, a rough aggregate surface can be a problem, because it can affect initial wettability potential during mixing. This implies that compaction of bitumen emulsion needs to be done prior to the full breaking of emulsion for better adhesion. Figure 53 shows severe erosion of quartzite material from a lab-compacted and cured specimen, exposed to cyclic pulsing of water pressure.

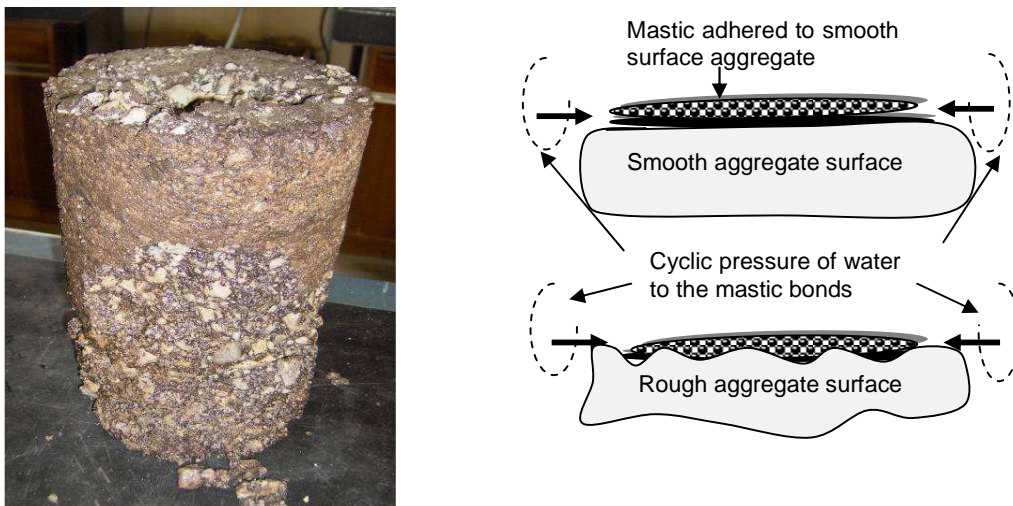


Figure 53: Erosion behaviour of laboratory-compacted and cured specimen made from Quartzite crushed stone stabilised with foamed bitumen and exposed to cyclic pulsing of water pressure

The presence of moisture in the micro-pores of the mix does not necessarily weaken the bonding; the moisture must be able to reach the binder-aggregate interface. However, the presence of excessive moisture (>EMC) in the mineral aggregates which surrounding the mastic film can result in water diffusion. However, water diffusion depends on the moisture diffusion coefficient of the mastic, thickness of the mastic film and porosity or cracks in the

mastic. The moisture diffusion coefficient of mastic can be higher for the mixes without the addition of active filler (cement or lime) coupled with softening of the bitumen, due to moderate temperature within the pavement layer. For mixes with added cement, cracks can result due to shrinkage of cement in the mastic. However, the cementing action might curtail the diffusion rate of moisture to the mastic; this can explain why weakening of the adhesive bond is more predominant in mixes without active filler (cement or lime). However, this phenomenon needs further research to determine different diffusion coefficients of BSM mastic film. Moisture diffusion through the mastic film continues with moisture gradient diminishing as a significant amount of water reaches the binder-aggregate interface. Since aggregates have a high affinity to water, progressive debonding of the mastic film from aggregates will occur and eventually exhibit predominantly adhesive failure when exposed to moisture for a long time.

Depending on the sensitivity of the mastic film to moisture, the stripping action of mastic film from the aggregate surface will occur due to mechanical abrasion of the aggregates from dynamic loading. Because of weakening of bonds, mixes will slowly lose their strength, hence becoming more prone to cohesive failure. Due to the higher percentage of uncoated fines in BSMs, a saturated mix will initially destroy cohesiveness of the uncoated fine and filler particles, which become significantly susceptible to the pumping action. The dislodging of fine particles in the mix will accelerate the weakening of the binder-aggregate bonding, and this affects the integrity of the mix.

3.3.3 Pumping action due to traffic loading

The pumping action results from moisture damage, when the mix matrix is exposed to traffic loading and micro-pores in the mix matrix are saturated. The fast traffic load will locally cause high water pressure in the pores. These excess pore pressures might even be generated away from the actual wheel path. Since the water has no time to redistribute itself within the voids, the pore pressure contributes to extra stresses within the mixes (see Figure 52). The filler fractions in the mix matrix, in large percentages, are normally not bounded by the binder during mixing. Nevertheless, the unbound mineral filler in the mineral aggregates skeleton can have relatively high strength when dry. However, they become loose when saturated with water. The pumping action will progressively remove the fine fraction and filler progressively, resulting in severe exposure of the binder-aggregate bonds and eventually ravelling (loss of large particles).

Pumping action of fine fraction and filler is a moisture damage process that is directly related to the application of dynamic loading. However, this process does not have any effect on the physicochemical process described above in the moisture damage mechanisms. Nevertheless, pore pressures certainly accelerate damaging mechanisms. It is apparent from the pumping action that factors influencing moisture susceptibility and damaging mechanisms can be analytically determined for prediction of BSM durability in terms of moisture damage. The coefficients, which are functions of moisture damage in BSMs, are presented in following relationship.

$$\text{MDC} = f(S_r, C, W_a, P, H_T) \quad \text{Equation 14}$$

where MDC = moisture damage coefficient; S_r = degree of saturation [%]; C = cohesion of material; W_a = work of adhesion; P = dynamic pore pressure; H_T = temperature distribution coefficient on full layer thickness. The numerical formulation using this relationship can be used to define the moisture damage mechanisms in BSMs. Therefore, the numerical formulation is an area which can be taken further in future studies.

3.3.4 Microscopic analysis on the influence of cement from previous results

Past studies on moisture susceptibility are compared for BSM mixes, with or without the addition of active filler, as presented by Long and Ventura (2003), Ebels (2008), Fu *et al.* (2009), Gonzalez (2009) and Twagira and Jenkins (2009). Most studies confirm that BSM mixes with added active filler (cement) have shown a significant improvement in performance without clearly defining the mechanism of the influence of cement dosage on the durability properties of the mixes. This section serves to substantiate the discussions on moisture susceptibility and damage mechanisms explained in this chapter using the results found from past studies on BSMs.

Fu *et al.* (2009) investigate the curing mechanisms for the different phases in foamed bitumen mixes in order to understand the bond development between mastic and the aggregate skeleton. Different percentages of cement (0%, 1% and 2%) and foamed bitumen (0% and 3%) were added to the recycled aggregates with compositions of 25% granite and 75% RAP. The laboratory-prepared specimens were cured differently: curing condition A involves a sealed specimen oven-dried at 20°C for 24 hours and curing condition B involves an unsealed specimen oven-dried at 40°C for 7 days. The specimens cured at condition B were soaked for a period ranging from 1 to 38 days prior to mechanical testing while specimens cured under condition A were tested immediately after curing. The triaxial resilient modulus results on these different methods of curing are presented in Figure 54.

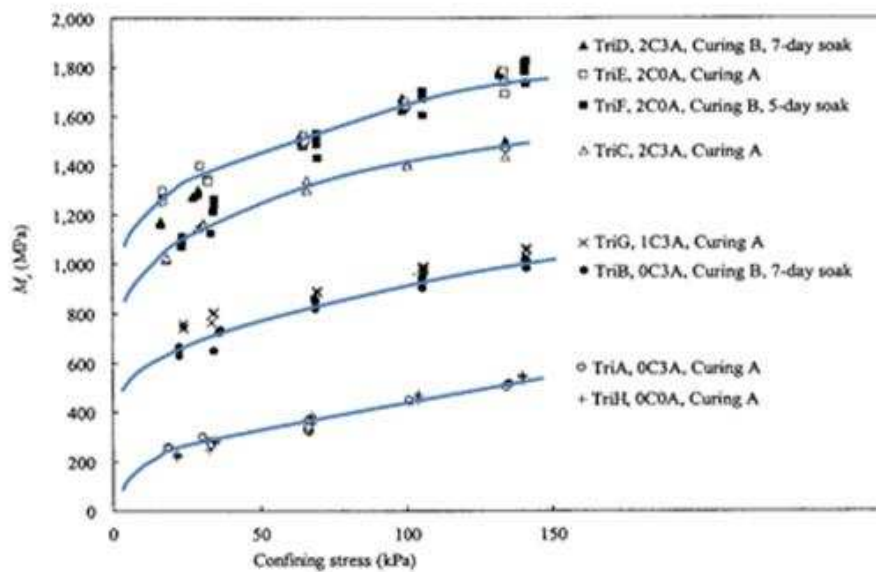


Figure 54: Selected triaxial resilient modulus results for different foamed mixes cured at different conditions and applied deviator stress of 62.1kPa and 103.4kPa, at Hz of 0.1s (Fu *et al.* 2009)

The triaxial resilient modulus was performed on a 150mm x 305mm specimen size. The results show that the mixes with added cement show significantly improvement in stiffness behaviour under different curing conditions. Although the study indicates that mixes with cement show improvement in bond development and resistance to moisture damage, there is no explanation of the fundamental cause of bond evolution between binder and mineral aggregates by the addition of active filler (cement) at different curing conditions.

The results in Figure 54 indicate that at curing condition A, the foam mix 0C3A (with no cement) has relatively lower stiffness compared to the mix 1C3A (with 1% cement). At curing

condition A, a substantial amount of moisture was still present in 0C3A. In that case, the diffused moisture entrapped in the mastic and the moisture at the aggregate interface impairs the bonding between binder and aggregate, resulting in a reduction in the stiffness of the mix. In 1C3A, the entrapped cement in the mastic hydrates the entrapped water and displaces water from the aggregate surface, which significantly improves the bonding and stiffness. The influence of long curing (significant evaporation of moisture) is noted in the stiffness results. The stiffness of 1C3A at curing condition A is similar to the stiffness of 0C3A at curing condition B.

The comparison between mixes with the addition of 2% cement, 2C0A (without foamed bitumen) and 2C3A (with 3% foamed bitumen) shows that a mix without the binder cured under condition A has higher stiffness compared to a mix stabilised with foamed bitumen. The lower stiffness of 2C3A was influenced by the higher RAP content. This shows that the unadhered binder in mix 2C3A acts as a lubricant in the presence of moisture and decreases the stiffness. This reduction will affect the shear properties as well. Thus, the addition of more cement in a BSM mix increases tensile strength but does not benefit adhesion development. Instead, the mix composition becomes prone to crack formation.

The influence of additional cement in Hornfels-RAP aggregates was presented by Long and Ventura (2003). They performed comprehensive monotonic triaxial testing on foamed bitumen stabilised recycled materials from the N7 expressway. The RAP content in the mix was not more than 15%. The effects of density, saturation, foamed bitumen content and cement content on shear and internal angle of friction in the mixes were studied. They conclude that the addition of cement improves the cohesion of materials, regardless of the foamed bitumen content, but reduces the friction angle. Nevertheless, no founding reason was established on the effect of cohesion by the addition of foamed bitumen into the mix with 1% cement. However, from the discussion presented in section 3.2.1, governing process, and formulation bonding, it is possible to explain with confidence the adhesion and cohesion behaviour in BSM mixes. The specimens in this study were cured for 28 days at ambient temperature (20°C–25°C). The saturation condition, indicated in Figure 55, (high saturation and low saturation) is the amount of moisture remaining after the curing period in different mixes; variability in the compaction level is indicated as low and high density. Triaxial test was performed in a group of specimens with similar volumetric properties. The presented results show that mixes with low compaction and high retained moisture content (>EMC) have lower cohesion. This is as expected, as compaction is the factor that influences voids content and the adhesion of the mastic on the coarse fractions, whilst, high saturation indicates poor bond development. The trend shows that mixes with high density have higher cohesion. However, due to variability in retained moisture content after curing, the trend of high or low saturation with cohesion results also varies. Therefore, the nature of the variability in results can be addressed statistically.

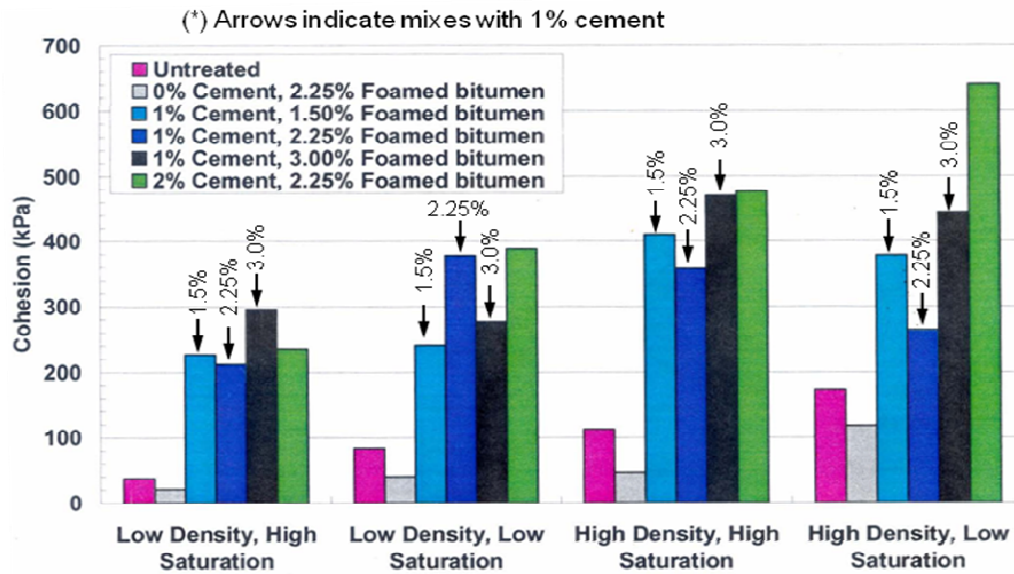


Figure 55: The influence of density and retained moisture on mixes with different foamed bitumen and cement contents (Long and Ventura, 2003)

It is evident from the discussion that understanding the performance of BSMs at a microstructure level provides insight into the fundamental failure mechanisms, to the point that durability and long-term performance of BSMs can be determined with confidence. Although past studies' results show comparable performances of mixes with respect to moisture influence, the method of saturation (conditioning) in those studies do not simulate field conditions. Therefore, damaging mechanisms due to high pore water pressure were underestimated. Infiltration of moisture by soaking to mixes such as 0C3A, discussed above, resulted in shear properties, which could probably be differently if infiltration of water (saturation) is done by pulsing water pressure into the mix, i.e. simulating field conditions. In the literature review, it was indicated that several laboratory test procedures for determining moisture susceptibility of pavement materials are used globally. However, saturation followed by mechanical evaluation after conditioning for BSMs does not simulate field conditions, hence yields unreliable classification. It is the objective of this chapter to present a newly developed simple device, called a moisture induction simulation test (MIST), to assess moisture-induced damage based upon cyclic pulsing of water pressure into a compacted and cured specimen. The study investigates different saturation levels with experimental determination of a stiffness ratio (M_r) and shear parameters (c and ϕ) of BSMs. These parameters are critical for BSMs due to their stress dependent nature.

3.4 LABORATORY SIMULATION OF MOISTURE SUSCEPTIBILITY

Excess moisture in the mix matrix is a major factor contributing to poor adhesion and cohesion in BSMs. The focus in this section is to develop a moisture conditioning procedure (i.e. design of a new device) which realistically simulates pulsing moisture into BSM mixes. In addition, experimental investigation on different BSM mixes is performed and the results obtained from the new device are validated with known laboratory device, e.g. MMLS3. The approach to this laboratory simulation of moisture susceptibility is illustrated in the flow diagram shown in Figure 55.

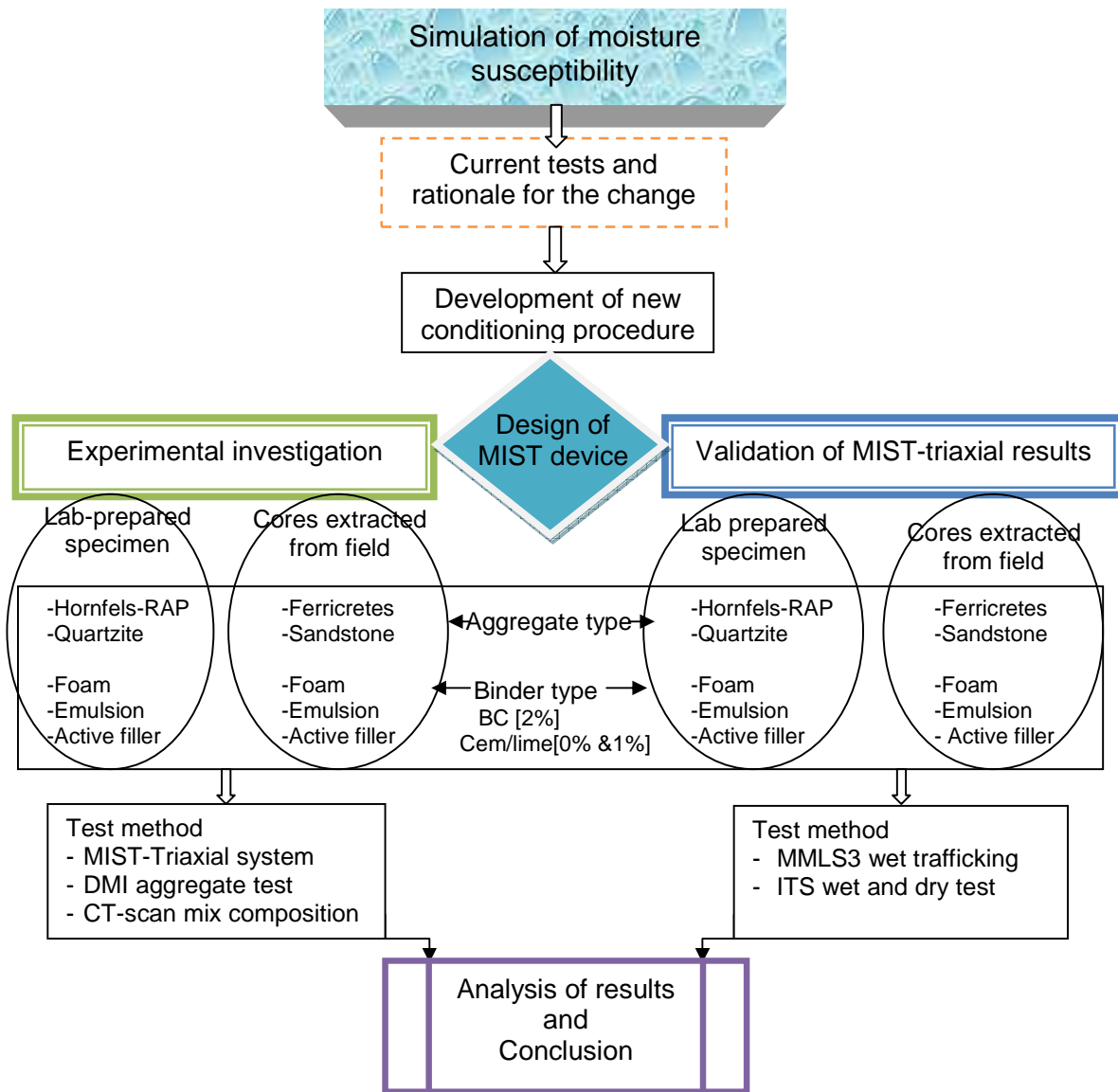


Figure 56: Illustration on approach to laboratory simulation of moisture susceptibility

3.4.1 Available lab tests simulating field moisture susceptibility.

The current test procedures, of saturation followed by mechanical evaluation after conditioning of BSMs, stem from early findings by the Asphalt Institute (1992). In this procedure, moisture conditioning for mix assessment is carried out using vacuum saturation of the compacted and cured specimen, in order to accelerate any possible moisture damage. The conditioned and unconditioned specimens are then compared in terms of retained strength, e.g. TSR obtained after Indirect Tensile Strength (ITS) or from Unconfined Compressive Strength (UCS) or Indirect Tension Test (ITT). This approach cannot provide moisture susceptibility of BSMs with high certainty ratio compared with static and dynamic test results of a triaxial-size specimen.

3.4.2 Ratio of parameters derived from tests

ITS and UCS tests (Figure 57) are standard tests that involve monotonic displacement controlled loading of specimens up to a maximum stress or failure. The dimensions of a specimen for ITS are normally 100 or 150mm in diameter and 65mm (± 5 mm) in height, while a UCS specimen is 150mm diameter and 125mm (± 5 mm) in height. An ITS specimen is diametrically loaded, inducing a horizontal tensile stress at the centre of the specimen caused by the shape of the specimen, which is estimated using linear elastic theory. A UCS specimen is axially loaded and the compressive stress is calculated using the force-force quotient. The ITS and UCS values are defined as the maximum stress applied to the specimen during the tests. The test setups and determined ultimate stresses are presented in Figure 57.

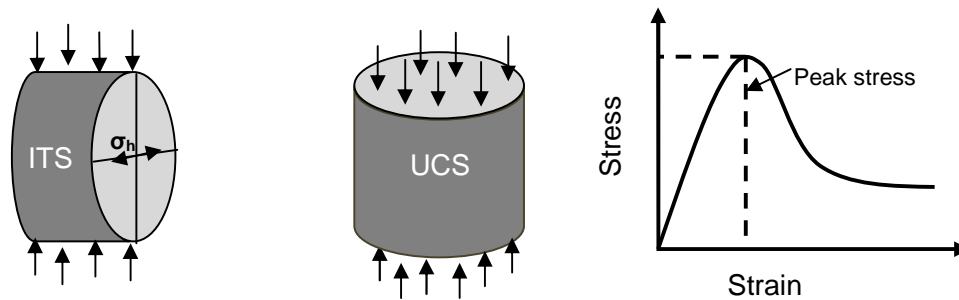


Figure 57: The ITS and UCS testing configuration and analysis

In TG2 (Asphalt Academy, 2009), ITS or UCS test method is recommended for initial screening of BSMs for the mix design. Ultimately, triaxial test is preferable method for the final mix design. This is because, as discussed in the literature review, the ITS test does not accurately represent the failure mode occurring in BSMs. This is due to specimen size and stress distribution at the centre of the specimen and the unconfined nature of the test. BSMs are stress-dependent materials; therefore, strength or stiffness and shear behaviours are sufficiently determined through triaxial testing using triaxial-size specimens with a diameter/height ratio of 1:2. The triaxial test method was adapted in this study for ultimate screening and classification of BSM mixes in moisture susceptibility with high certainty.

3.4.3 Rationale for a new laboratory test simulating moisture susceptibility

The new laboratory-based testing procedure and analysis protocol for the evaluation of moisture sensitivity and damage mechanisms considers more aspects of field conditions. Although the laboratory simulation cannot provide exact replication of mechanisms that are manifested in service, it should represent the fundamental or key failure mechanisms for BSMs. At the same time, a simplified, reliable and cost-effective procedure is required for classification test of moisture susceptibility. In this study, a testing and evaluation framework was based on the new MIST device that was developed. The saturation condition of MIST is designed to replicate the field condition of pulsing of cyclic water pressure by dynamic means. The moisture conditioning and mechanical testing (static or monotonic and short dynamic or resilient modulus) were applied on triaxial-size specimens for determining the level of moisture damage in BSMs (see Figure 58). The influence of saturation level on stiffness ratio (M_r) and shear parameters (c and ϕ) were investigated as shown in Figure 59. These parameters are critical for the prediction of durability properties and long-term performance of BSMs. Past study, however, has indicated that although short dynamic test is more sensitive to change in material properties, but it is a complex test. Therefore, in South Africa this test will remain at research level and not a requirement for mix design purpose in the commercial laboratories. The application of short dynamic triaxial testing for moisture susceptibility and complexity nature will be discussed further in this study.

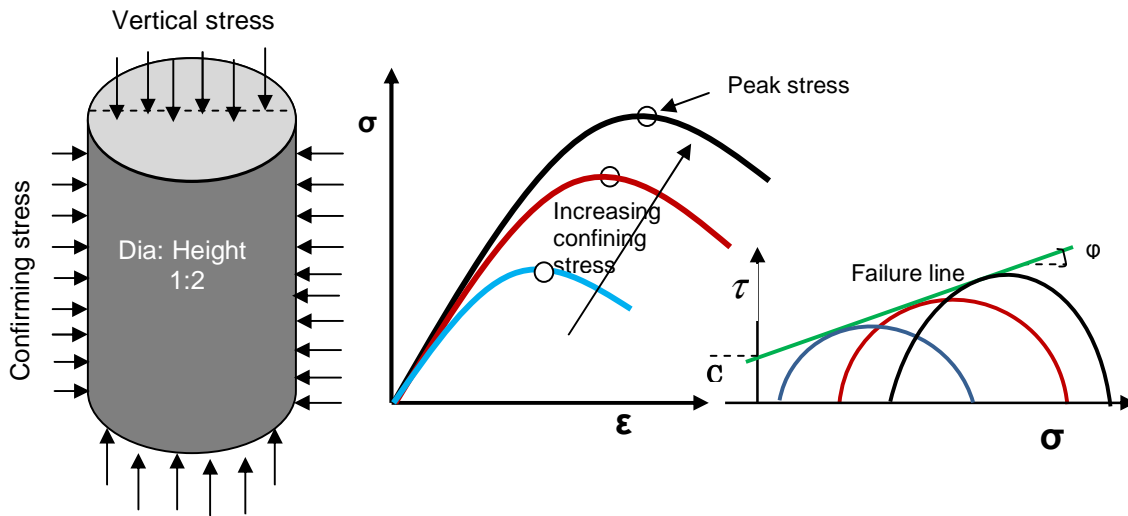


Figure 58: Monotonic triaxial test and mechanical evaluation of critical parameter of BSMs

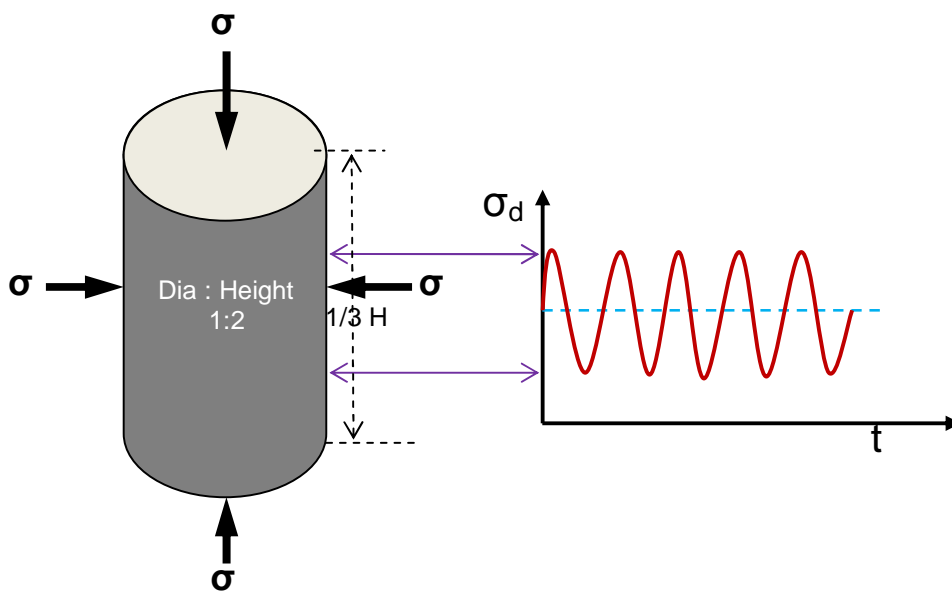


Figure 59: Short time dynamic (resilient modulus) triaxial test evaluation at different saturation levels in BSMs.

3.5 DEVELOPMENT OF A NEW MOISTURE CONDITIONING PROCEDURE

3.5.1 INTRODUCTION

The presence of excess pore water in the BSM mix matrix can result in rapid deterioration due to moisture damage. The process typically associated with moisture ingress and damage is mechanism occurs over long periods of time under field conditions. In the absence of a method that simulates all of the possible mechanisms of moisture damage, a surrogate, laboratory-based moisture conditioning method should accelerate the ingress of moisture into the mix and evaluate its effect on stiffness (M_r) and shear parameters (C & ϕ). In essence, the laboratory conditioning procedure should adopt the following:

- Applicable to field conditions: evaluate material behaviour under expected field conditions by testing the materials under more controllable laboratory conditions.
- Appropriateness to material characteristics: the dispersion nature of the binder and voids content in the mix matrix, has significant influence on the conditioning and/or saturation to simulate the accelerated moisture damage mechanisms. Therefore, due to ambiguous materials in BSMs, there is a need for standardisation of conditioning procedures to be able to screen materials for moisture susceptibility.
- Repeatability and reproducibility: the ability to produce the same results if the same material is tested following the same procedure, by the same operator in the same laboratory, or by a different operator in a different laboratory of the same standard. However, there are inevitably some factors not directly controlled in the procedure. The effect of these factors should be well understood to ensure that they do not significantly bias or dominate the testing results.
- Simplicity: generally complex devices and testing procedure increase the chances for operational error, thereby impairing repeatability and reproducibility. Complex devices are always expensive and require specialised skill, therefore, not suitable for use at the mix design level.

This section presents the results of an experiment aimed at determining whether cyclic pulses of water pressure into BSMs induces sufficient damage to the triaxial specimen. This enabled a distinction between different levels of resistance to moisture damage in BSMs. However, the constraints on the simulation procedure were the allocated time and budget: the conditioning had to be accomplished within a reasonable length of time and simple and cost-effective laboratory equipment had to be used. The evaluation of moisture damage in this study was carried out using the newly developed Moisture Induction Simulation Test (MIST) device and triaxial test. Mixed compositions of aggregate blends with and without RAP, with different bitumen binder types (foamed bitumen or bitumen emulsion), active filler types (cement or lime) and contents were investigated. In order to test the validity of the moisture damage prediction using the MIST device, the influence of traffic on the laboratory-prepared specimen with similar mix composition was simulated using the known Model Mobile Load Simulator (MMLS3), a scaled APT device. The results obtained by the MIST and triaxial tests and MMLS3 wet trafficking on the control and conditioned specimens are also presented in this section. The comparison and conclusion are made in terms of the ranking of moisture damage susceptibility. In this light, the main objectives include:

- The development of upgraded or new laboratory-based representative testing procedures and analysis protocols for the evaluation of moisture-related damage as distinguished from current over-simplified procedures
- Evaluation of MIST conditioning system by using BSM-foam and BSM-emulsion with varying aggregate and active filler types
- If warranted from findings, make appropriate recommendations regarding the use of the new moisture conditioning for screening BSM mixtures based on moisture-related damage for mix design

3.5.2 EXPERIMENTAL PROGRAM

3.5.2.1 Materials

Two selected material types were used in this study: first, reclaimed asphalt pavement (RAP) combined with hornfels base material, i.e. Hornfels-RAP. The RAP content was not more than 15%. These materials were used during the in-place recycling project on the National expressway, N7, near Cape Town. Second, the crushed virgin Quartzites (G4)³, procured from the Prima quarry in the Western Cape. Quartzite aggregates are known to be moisture susceptible with bitumen, particularly foamed bitumen, in the field. These aggregates are graded according to a maximum size of 19mm and percent passing 0.075mm of 10% and 6%, respectively. Selected materials were stabilised in the laboratory with either foamed bitumen or bitumen emulsion. 2% net bitumen content was applied on both Hornfels-RAP and Quartzite materials. 0% or 1% active filler (cement or lime) was added to the stabilised materials. The total number of laboratory-prepared and tested mixes was 12. Table 16 shows the matrices of the mixes used in this study. In addition, cores extracted from existing pavement, P243/1 in Vereeniging, were included in the study, in order to determine moisture susceptibility on field-cured materials. These cores were taken from pavement sections stabilised with foamed bitumen and from sections stabilised with bitumen emulsion. The objective of including a wide range of variables (materials and mixture) in the study was to ensure completeness of the investigation into BSM moisture susceptibility. This is as opposed to the selection of a few variables for the purposes of statistical evaluation.

Table 16: Constituted mix type and testing matrix for moisture susceptibility

Binder type	Lab prepared mix		Cores extracted from Field	
	Aggregates type			
	Hornfels-RAP [+] 2% net bitumen*	Quartzite [+] 2% net bitumen	Ferricrete [+] 1.8% net bit	Sandstone [+] 1.8% net bit
A- Bitumen	Mix 1: 0% cement	Mix 7: 0% cement		Mix 14: 2% cem
Emulsion	Mix 2: 1% cement	Mix 8: 1% cement		
	Mix 3: 1% lime	Mix 9: 1% lime		
B- Foamed	Mix 4: 0% cement	Mix 10: 0% cement	Mix 13: 2% cem	
Bitumen	Mix 5: 1% cement	Mix 11: 1% cement		
	Mix 6: 1% lime	Mix 12: 1% lime		

*Net bitumen is residual binder after evaporation of water from foamed bitumen and bitumen emulsion

The materials required for making the triaxial specimen were constituted from a percentage of dry weight from the actual grading, indicated in Figure 60. 12kg of materials was measured from combined batches of sieves: first batch consisted of material passing a 19mm sieve, retained on 13.2mm; second batch passing 13.2mm, retained on 4.75mm; third batch retained on 2.36mm; fourth batch passing 2.26mm. These materials were combined as fine and filler. The constituted weights of different batches for the both Hornfels-RAP and Quartzite are presented in Table 17.

The active filler used in the mix matrix for this study are cement and lime. Cement brand type is Surebuild 42.5 (CEM II-B/M L/S according to South African specification), whilst the lime brand type is hydrated lime (Ca(OH)₂) which is obtained from local hardware stores.

³ G4 is the South African classification system for crushed or natural gravel (TRH14, 1985)

Table 17: Aggregates type and grading of Hornfels-RAP and Quartzite crushed stone
Aggregates type and grading

Hornfels-RAP			Quartzite(virgin crushed aggregates)		
MDD	2177.3	(Kg/m ³)	MDD	2240	(Kg/m ³)
OMC	5.12	(%)	OMC	6.0	(%)
Total Mass	12	(Kg)	Total Mass	12	(Kg)
Stockpile	Ratio in Blend	Mass in Blend (Kg)	Stockpile	Ratio in Blend	Mass in Blend (Kg)
19.0– 13.2	6.90%	0.828	19.0–13.2	14.92%	1.790
4.75–13.2	40.60%	4.872	4.75–13.2	32.95%	3.954
2.36	16.00%	1.920	2.36	12.87%	1.544
<0.075–2.36	36.49%	4.379	<0.075–2.36	39.26%	4.711
Total	100.0%	12.00	Total	100.0%	12.00

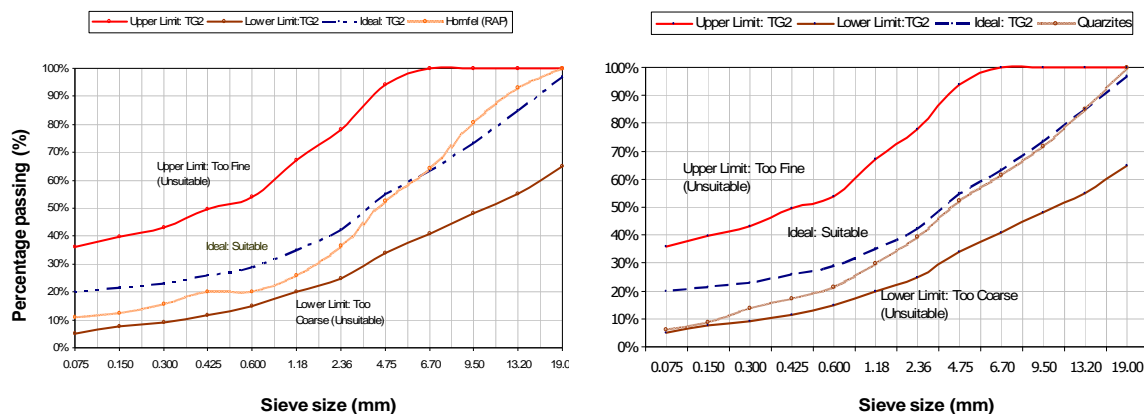


Figure 60: Grading curves of Hornfels-RAP and Quartzite aggregates in envelop of the BSMs limits

3.5.2.2 Binder type

The bitumen emulsion was procured from COLAS (SA) in Cape Town. The emulsion type ANiB The bitumen emulsion, type ANiB SS-60 stable grade anionic emulsion (60% residual binder and 40% emulsion water), used in this study was procured from COLAS (SA) in Cape Town. A bitumen emulsion content of 3.33% (i.e. 2% residual binder) was applied for stabilisation of both Hornfels-RAP and Quartzite materials.

Bitumen from CALTEX, 80/100 pen grade, was used for the foaming process. 2% residual binder content of foam bitumen was applied for stabilisation of the virgin Quartzite crushed aggregates and Hornfels-RAP materials. Before production of foam bitumen, the foaming properties of bitumen viscosity (expansion ratio) and stability (half-life) are determined using 3% foamant water, by mass percentage of the bitumen. The bitumen was found to have an expansion ratio of 12 times and a half-life of 18 seconds. The bitumen procured from NATREF was found to produce relatively inferior foam characteristics with a half-life of 5 seconds and an expansion ratio of 18 times. Similar behaviour presented at different foamant water application rates. The short half-life of foamed bitumen can negatively influence the durability properties of BSM mix.

3.5.2.3 Moisture content and mixing process

The optimum moisture content (OMC) and maximum dry density (MDD) of the selected materials was determined by Modified AASHTO compaction. The summarised results are given in Table 18 for the two selected materials. The hygroscopic moisture in the mineral aggregates was 0.75% for the Quartzite and 0.5% for the Hornfels-RAP.

Table 18: Summary of optimum moisture contents and maximum dry densities of blends

Blend	Compaction	OMC (%)	MDD (Kg/m ³)
Hornfels-RAP	Mod AASHTO	5.12	2177.3 (field comp)
Quartzite	Mod AASHTO	6.0	2240

The mixing processes for bitumen emulsion and foamed bitumen mixes differ. The BSM-emulsion was mixed in a standard laboratory vertical shaft mixer and the BSM-foam mixed in a twin-shaft pugmill placed in front of the spraying nozzle of the WLB-10 foam plant. The influence and effect of the mixing method on bond formation has been discussed in section 3.2.1. The vertical shaft mixer is used to mix emulsion uniformly without the effect of stripping the binder from the aggregate surface, while the twin-shaft pugmill is suitable for foamed bitumen dispersion and mixing.

The moisture content added during mixing was 65%–80% of OMC in the bitumen emulsion and 80%–90% of OMC in the foamed bitumen. These moisture content was found to be optimal for the vibratory BOSCH® compaction. The initial mixing moisture, 60% of the total mixing moisture, is added to the material and mixed for one minute. After mixing, the aggregates are sealed in a bag and left for 2–3 hours to allow the aggregates to moisten and to fill any pores. After that period, the remaining 40% of the moisture is added and mixed for one minute. Thereafter, while mixing continues, cement or lime (active filler) is added, then bitumen emulsion or foamed bitumen is added. After addition of bitumen emulsion in the vertical shaft mixer, mixing continues for one more minute. After addition of foamed bitumen in the pugmill mixer, mixing continues for only 30 seconds. Finally, after stabilization, the mixture is sealed in a bag to prevent moisture loss. Minimal initial breaking of bitumen emulsion normally takes place before compaction. For foamed bitumen, compaction is done immediately after stabilisation.

3.5.2.4 Compaction and curing

The compaction of BSM-foam and BSM-emulsion was carried out using a vibratory BOSCH® compactor. The advantages of using a vibratory hammer are discussed in detail in the literature review and elsewhere in this study (Chapters 3 and 6). The conclusion drawn was that the modified BOSCH® compactor is a useful tool for the compaction of BSMS: it has higher point energy, which requires low compaction effort to obtain an equivalent level of compaction compared to other methods. Secondly, the higher point energy significantly influences the wettability (coating) of the binder (mastic) into the aggregate surface. Lastly, it is relatively cheap, easy to use and simulates field compaction. The modified BOSCH® compactor used for compaction in this study is shown in Figure 61. The complete compaction protocol is reported in TG2 Asphalt Academy (2009) and Kelfkens (2008). The prepared triaxial specimen was compacted in five layers of 50mm thick, each layer compacted to target density. The target density was achieved by measuring the amount of material required to achieve 100% of the Mod. AASHTO compaction or the density achieved in the field condition. The density achieved on each specimen is indicated in the discussion of results, section 3.5.



Figure 61: a) Modified BOSCH® compactor b): specimen in the mould

The curing technique used in this study involved placing the compacted specimens in a draft oven at 30°C for 20 hours unsealed, followed by sealing and raising the temperature to 40°C for 48 hours. The same curing protocol was followed for both bitumen emulsion and foamed bitumen mixes. After curing, the specimens were sealed in a different bag and left to cool at ambient temperature for storage prior to conditioning and testing.

3.5.2.5 The design of the MIST device and testing

The MIST device designed in this study was applied to evaluate the effect of moisture damage in BSMs, simulating the field pulsing conditions under controlled laboratory condition. The MIST apparatus features, presented in Figure 62, consist of:

- A water tank with capacity of 20 litres of compressed water to a maximum of 600kPa
- Water inlet to the tanks, connected to the water source (cold water) or heating unit (hot water)
- A water pump to fill the tank at required pressure
- Pressure control and pressure gauge ranging from 0–400kPa to regulate the pulsing water pressure in the triaxial cell
- Solenoid valves controlling water pulsing application, connected with timer ranging from 0-60seconds
- Cyclic water pressure IN/OUT of the triaxial cell
- Triaxial cell which can accommodate 150mm diameter and 300mm height specimen
- Container for keeping overflows of water at the end of conditioning
- Heating unit used to simulate different temperature conditioning, presented in Figure 63

The testing control variables applicable during the MIST conditioning procedure include:

- Temperature level,
- Saturation level,
- Water pressure level and
- Pulsing cycle time or number,

The MIST testing procedure has the following major subsystems: 1) fluid saturation subsystem by pulsing moisture into triaxial specimen; 2) loading sub-system using material testing system (MTS) for determination of retained properties. Fluid saturation (conditioning) and mechanical testing are described in section 3.5.2.7 and 3.5.2.8 respectively.

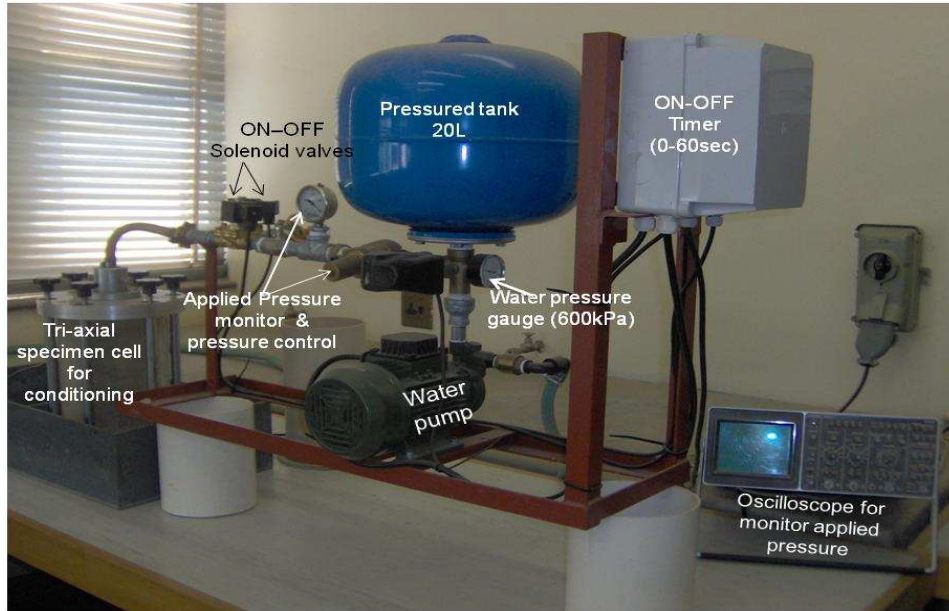


Figure 62: Designed MIST device features and setup

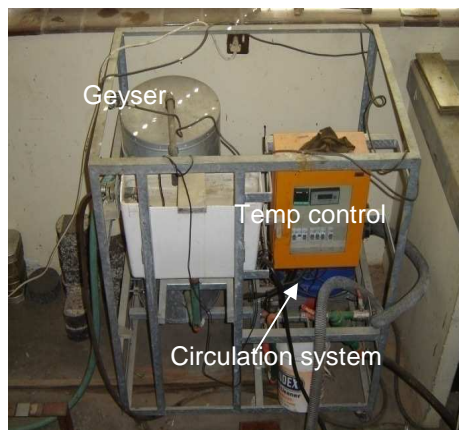


Figure 63: Heating unit for hot water simulation connected to the MIST device

3.5.2.6 Trials of the MIST design features

After identification of all necessary parameters applicable to the design of the MIST device, it was necessary to conduct trials prior to full-scale implementation of the device as a moisture-conditioning tool. The desing considerations and limitations were found to be:

- The ON/OFF timer connected to the solenoid valves. The minimum setting of loading time (ON) is limited to 0.54 seconds and rest period (OFF) at 1.4 seconds to generate

maximum pressure on the triaxial cell of 140kPa. Shorter times than the ones prescribed were found to generate insufficient pressure into the cell due to linear momentum of water. In other words, the change in velocity over change in time over a distance of 800mm (centre of the tank to the inlet of the triaxial cell) requires a certain time to realise a change in force or impulse of 140kPa. The coupling connections (Figure 62) applied to accommodate all necessary designed elements had a total length of 800mm, i.e. seven main coupling joints were used from the centre of the water tank to the inlet on the triaxial cell.

- The effect of the momentum of water requires a pressure regulator to be set higher (170kPa) than the pressures applied in the triaxial cell (140kPa). This was done in order to accommodate the pressure loss of $\pm 15\text{kPa}$ accrued during the loading momentum.
- Calibration of the MIST setting for the actual application of pulsing water pressured in the triaxial cell. In this study, the oscilloscope device was used to set the pressure regulator and an ON/OFF timer for the loading and rest period, which are critical for MIST conditioning. The Oscilloscope is a digital device with a real-time play screen to monitor applied frequency (see Figure 64).



Figure 64: Oscilloscope device used for calibration of water pressure, cyclic loading time and rest period during trials on the MIST device.

3.5.2.7 Fluid conditioning

Six triaxial specimens (150mm x 250mm) were prepared for each mix. Preparation of triaxial specimens is done by compacting 50mm layers in a mould of 150mm diameter, using a BOSCH® vibratory compactor. After compaction and curing, the specimens are grouped into set of two with approximately equal compaction levels or void contents (P_a). The void contents are calculated after determining the specimen bulk relative density (BRD) and mix maximum theoretical relative density (Rice). The BRD and Rice tests are standard tests, done according to the THM1 test methods C3 and C4 respectively. The first set comprises three specimens for wet conditioning and static (monotonic) tests and the second set comprises three specimens for dry (unconditioning) and static (monotonic) tests.

The test variables for the MIST device are set at 0.54 seconds load time, 1.40 seconds rest period, 140kPa pulsing water pressure. Fluid conditioning for MIST is done in the triaxial cell after placing and assembling the specimen as shown in Figure 62. The conditioning variables selected for MIST were related to MMLS3 scaled APT device. The MMLS3 settings are referred to in Chapter 4, where BSMs were tested under dry and wet trafficking conditions. After MMLS3 testing, the selected variables were at a level with those from MIST conditioning and triaxial testing. The validation results are presented in a subsequent section and the detailed procedure for MIST conditioning and triaxial testing is presented in Appendix A.

After MIST conditioning, the following specimen volumetric properties are determined.

- Volume of air voids (V_a) in specimen [cm^3],

$$V_a = \frac{P_a \times E}{100} \quad \text{Equation 15}$$

- Volume of water absorbed (V_w) in specimen [cm^3],

$$V_w = B - A \quad \text{Equation 16}$$

- Degree of saturation (S_r) in specimen [%],

$$S_r = \frac{V_w}{V_a} \times 100 \quad \text{Equation 17}$$

where B = weight of saturated-surface dry specimen [g]; A = weight of dry specimen in air after curing [g]; P_a = air void content in specimen [%]; E = volume of specimen [cm^3]. The degree of saturation during conditioning should be at least 80% for the accurate screening of BSMS. If the setup results in insufficient saturation levels, then selected parameters should be re-evaluated.

The MIST conditioning procedure can be widely used in moisture susceptibility of pavement material such as HMA, and CTMs and other related construction materials. However, simulation parameters for fluid saturation would require re-evaluation. In the light of further experimentation after the design of MIST device, Wehlitz, (2009) used MIST conditioning procedure to determine the moisture sensitivity of unbaked clay bricks used for low-income housing projects. The settings were adjusted and able to screen clay-mixes for moisture susceptibility and moisture resistance in long-term exposure to the detrimental environmental conditions of heavy downpours.

3.5.2.8 Loading or triaxial testing

A mechanical test on a prepared specimen is done after MIST conditioning. Mechanical triaxial testing is performed using the material testing system (MTS) equipment. The MTS is a closed loop servo-hydraulic testing system operated and controlled by the MTS controller. The loading and displacement test data of the load cell, MTS actuator (in-built LVDT) and external LVDTs are captured by a Spider 8 device, an amplifier that converts analogue voltage data to digital using a 12-bit A/D converter and displays the data in real-time on a computer. The captured data is stored in a computer and further analysed using an Excel spreadsheet. The loading capacity of the MTS is 10 metric tonnes (or 98.1kN) for the load cell and 80mm stroke (up/down) of the actuator. The measuring range of the load cell and MTS in-built LVDT can be adjusted to suit the testing range. This is done by increasing or decreasing the gain for either of the measuring devices. Increasing the gain results in a smaller measuring range and therefore a higher accuracy is achieved. The measuring scale settings of the load cell and MTS LVDT for triaxial testing in this study are shown in Table 19.

Testing mode	Scale settings	
	Load cell (10t =98.1kN)	MTS in-built LVDT (80mm)
Monotonic testing setup	100% = ± 98.1kN	50% =± 40mm
Short duration dynamic testing	20% = ± 19.6 kN	10% = ± 8mm
Long duration dynamic testing	20% = ± 19.6 kN	10% = ± 8mm

The triaxial cell has a maximum rating pressure of 1700kPa. A sample with a maximum diameter of 150mm and a height of 280 mm can be accommodated in the cell. However, due to clearance of the loading plate in the cell, the specimen height was reduced to a range of 250–260mm. The MTS is situated in a climate chamber, where temperature can be controlled between 0°C and 60°C. The temperature variable in this study was between 25°C and 40°C. These temperatures were found to be common in the BSM base layer. Figure 65 presents the MTS in a climate chamber, MTS controller and triaxial cell as well as a prepared specimen and membrane dressing device.

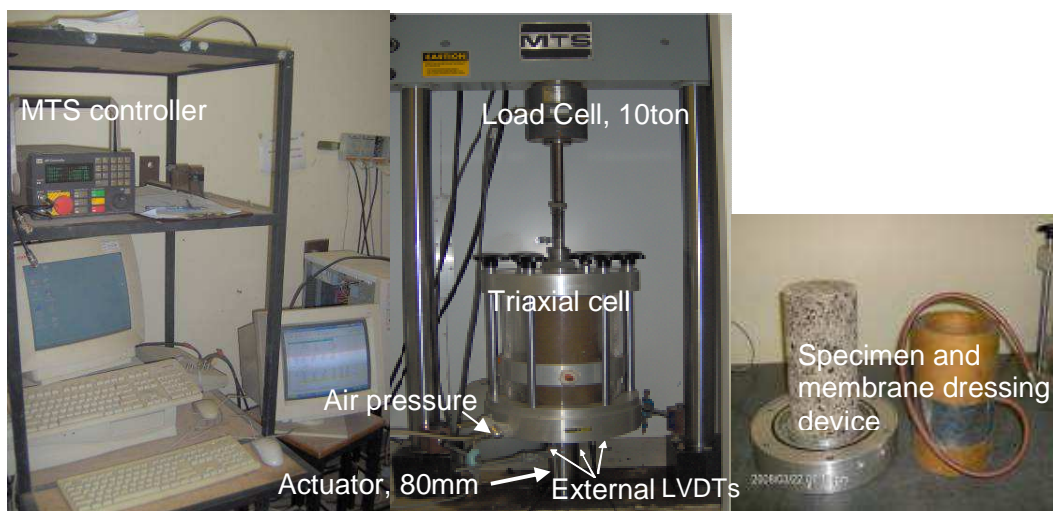


Figure 65: MTS loading system and triaxial specimen with membrane fitting tool

The rubberised membrane has been found to provide appropriate confinement on a triaxial specimen with applied air during MTS testing. However, the cost and availability of these membranes in South Africa is a major concern. Intensive research with triaxial testing at the University of Stellenbosch was impeded due to the scarcity of quality membranes. As part of my study, an innovative method was adapted to manufacture triaxial membrane devices to overcome this setback. Since the invention of the rotary membrane device, different membranes of natural latex with variable diameters and heights have been manufactured and successfully applied for triaxial testing. The natural latex type Mouldtex was supplied by Davidsons Fibreglass Company. The rotary membrane device designed in this study is indicated in Figure 66.

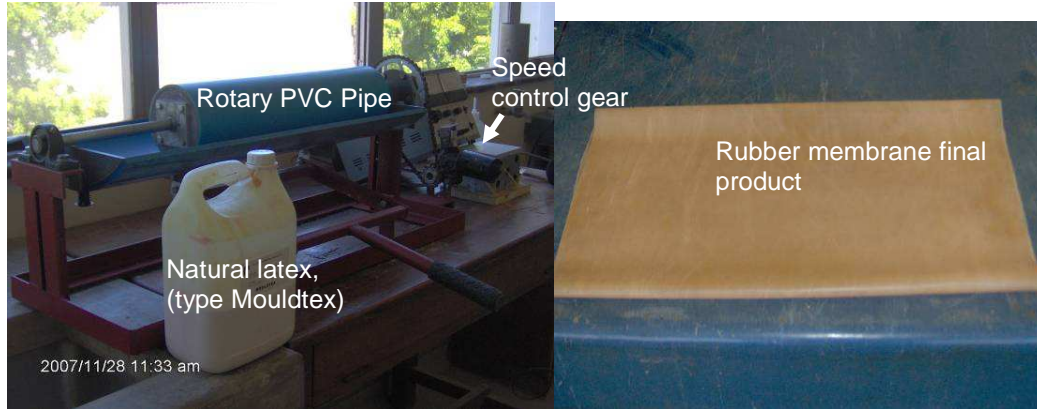


Figure 66: Rotary membrane device and membrane product 127mm x 500mm

3.5.2.9 Determination of retained cohesion and residual modulus ratio

The shear parameters (c and ϕ) and stiffness properties (M_r) are determined after the triaxial test. The triaxial testing is performed in accordance with the procedure developed by Stellenbosch University (2005). Therefore, a description of testing procedure is not repeated here.

The testing procedure involved one set of three specimens of predetermined height and approximately equal void content. These specimens are tested after MIST conditioning. Three different confining pressures are applied during the triaxial static (monotonic) test to determine failure mode. These confining pressures are 50kPa, 100kPa and 200kPa. Another set of three specimens are tested unconditioned also at 50kPa 100kPa, and 200kPa confinements. The applied rate of loading is 2.1%mm/min and the retained cohesion ratio is calculated as follows:

$$\text{Retained Cohesion}(RC) = \frac{\text{Cohesion of wet mix, (CoW)}}{\text{Cohesion of dry mix, (CoD)}} \times 100 \quad \text{Equation 18}$$

The cohesion of wet mixes (conditioned specimens) and dry mixes (unconditioned specimens) is calculated using the relationship in Equation 19 established from Mohr-Coulomb cycle.

$$\sigma_{1f} = \left(\frac{1 + \sin \phi}{1 - \sin \phi} \right) \sigma_3 + 2.C \cdot \left(\frac{\cos \phi}{1 - \sin \phi} \right) \quad \text{Equation 19}$$

where, σ_{1f} = Maximum principal stress at failure [kPa]; σ_3 = confining pressure [kPa]; ϕ = internal angle of friction of the mix [deg]; C = cohesion of the mix [kPa].

One set of six specimens grouped as described in section 3.4.2.3 was tested using short dynamic (resilient) loading. The short dynamic (resilient) test was performed in accordance with the procedure developed at Stellenbosch University (2005). Conditioned and unconditioned sets of specimens were tested at a stress ratio of 10% and a confining pressure of 50kPa at ambient temperature (25°C). Stress ratio was calculated from failure load determined during monotonic test at a confining pressure of 50kPa. The lower values of stress ratio and confining pressure were selected to minimise the effect of pore water pressure on the conditioned specimens. A higher external pressure can influence the dynamic response of the wet mix compared to dry mixes. Three external LVDTs were mounted at the bottom of the triaxial cell (Figure 65) to measure recovered displacement. After the application of 5 000 load cycles in dry conditions, the specimen was conditioned in the MIST device at different saturation levels, that is 50%, 80% and 100%, and the resilient modulus was determined. For unconditioned specimens, the dry

resilient modulus was also determined after application of 5 000 load cycles. After resilient modulus tests, static (monotonic) tests were carried out on the same specimen at a confining pressure of 100kPa to determine the shear properties (c and ϕ) of the conditioned and unconditioned sets of specimens. Residual modulus ratio is calculated as follows:

$$\text{Residual Modulus Ratio, (RM)} = \frac{\text{Resilient modulus at } S_r(100\%)}{\text{Resilient modulus of dry mix}} \times 100 \quad \text{Equation 20}$$

where, S_r = degree of saturation [%]; dry mix = mix at equilibrium moisture content.

Ranking of mixtures in term of moisture damage severity is determined from the calculated ratios. BSMs with high ratios show good resistance to moisture damage and BSMs with lower ratios show poor resistance. A ratio in between can be ranked as medium. These ranking results on BSMs were validated with MMLS3, which is set up at corresponding variables of 1.8kN axial load, 420kPa tyre pressure and full speed of 7 200 wheel loads/hr. These variables are equivalent to a light truck. Hence, there is minimal damage to BSMs and a possible extension of the test duration to a reasonable comparative range. In addition, to these variables, a thin vinite layer was introduced at the interface of tyre and BSM surface for the same purpose of minimising tyre damage during wet trafficking, while maintaining the stress influence on the surface of briquettes. MMLS3 test setup is indicated in Figure 67. The detailed procedure on the role of the MMLS3 in the validation of the MIST test results is presented and discussed in Chapter 4. Further characterisation of moisture damage using shear parameters and stiffness is presented and discussed in Chapter 5.



Figure 67: Illustration of MMLS3 test setup including details of vinite installation

3.6 ANALYSIS AND DISCUSSION OF RESULTS

3.6.1 Compaction level and moisture in BSMs mixes.

The Modified AASHTO compaction was used to determine the maximum dry density and optimum moisture content of the mixes. The compaction levels achieved using the vibratory BOSCH® compactor from the target density is presented in Table 20.

Table 20: Compaction density achieved on BSMs using BOSCH® compactor

BSM mix type	Compaction moisture content (5.12%OMC-H, 6%OMC-Q)	Weight after compaction [g]	Weight after curing [g]	Density [kg/m ³] after curing	Percentage MoD AASHTO (Target density 2177.3 kg/m ³ -H, 2240kg/m ³ -Q)
H0CF	4.5 (88%)	10 047.6	9 856.0	2 230.9	102
H1CF	4.7 (90%)	10 007.0	9 746.8	2 225.6	102
H1LF	4.9 (95%)	9 949.1	9 785.7	2 215.0	102
Q0CF	4.0 (70%)	10 250.7	9 959.1	2 254.0	101
Q1CF	4.3 (72%)	10 190.4	9 929.3	2 246.4	100
Q1LF	4.5 (75%)	10 224.0	9 955.7	2 253.4	101
H0CE	4.4 (85%)	10 130.2	9 899.0	2 240.4	103
H1CE	3.7 (72%)	10 014.8	9 864.0	2 232.7	103
H1LE	5.12 (100%)	10 151.3	9 921.7	2 245.9	103
Q0CE	3.6 (60%)	10 262.1	10 101.6	2 286.2	102
Q1CE	3.2 (53%)	10 328.6	10 156.3	2 300.1	103
Q1LE	4.3 (72%)	10 247.5	10 035.3	2 271.3	101

Note: Bracket values is (% OMC) of moisture in the mixture during compaction

The compaction level of laboratory-prepared specimens is vital for mechanical evaluation. To ensure consistency in screening mix performance, 100% target density was the objective for all mixes. The relative density to the Mod AASHTO, presented in Table 20, shows that all mixes were compacted at more than 100% of maximum target density. The advantage of higher compaction levels is proper packing of aggregates skeleton and minimise the influence of the void in moisture damage.

The effect of the layers interface and voids distribution during vibratory compaction (i.e. 50mm layer lift of 250mm triaxial specimen) was analysed through the CT scan. The CT scan's detailed analysis and devices are presented in Chapter 6. The scanning images indicated that at the layer interface higher void content dominates. The cause of high void is due to non-homogeneity of scarified materials between the layers (Figure 68). The effect of non-homogeneity is critical during moisture conditioning of pulsing water pressure. The high voids area can be more susceptible to moisture damage. Therefore, 100% compaction level at individual layer is necessary to minimise the high voids at the joints.

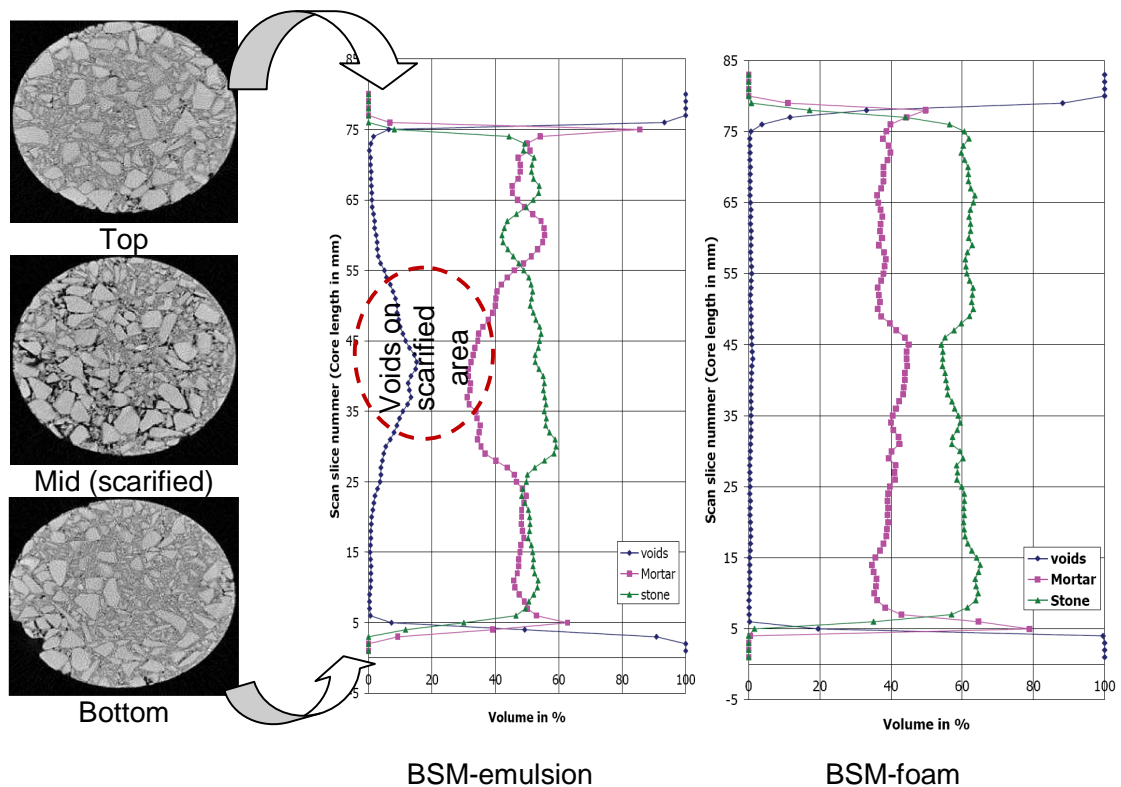


Figure 68: CT scan analysis at the interface (scarified surface) of the vibratory compacted specimen, BSM (emulsion or foam)

It is evident from the CT scanning that improper (deeper) scarification or inadequate compaction at each lift interface might influence the higher void content in the mix matrix. Due to different moisture contents during mixing in emulsion and foam mixes, less compaction time is applied to emulsion mix than foam mix. From the image analysis, shorter compaction time and inhomogeneity of the mix at the layer interface show an increase in voids from the bottom to the middle and a decrease again to the top, particularly in the bitumen emulsion mix. This behaviour is not observed in foamed bitumen mixes. It could be because of the high level of compaction applied on each layer and synergy of mastic-aggregate after scarification. The disturbed conglomerates of the emulsion mix after scarification do not heal to the same homogeneity at the one of foamed bitumen. To minimise the in-homogeneity effect at the layer interface, bitumen emulsion mixes need to be compacted at lower levels of breaking (or coagulation) to avoid stripping of mastic during scarification. More results of CT scan, and the resulting values are presented in detail in Chapter 6 of this study.

3.6.2 MIST conditioning and saturation level

The particle interlock, particle type and binder content determine the steady state saturation level of BSMS. Steady state saturation is regarded as non-time-dependent change in water content on the materials with the addition of pulsing water pressure. Mixes with high void contents show higher damage due to excess of moisture during pulsing time. Table 21 shows the pulsing time and void content to achieve steady state saturation level. The saturation level can be related to the OMC of the mixes. From the results in Table 21, it can be seen that void content varies from 16% to 10%. The mixes with relative higher voids (H0CF and Q0CF) suffered erosion during saturation or conditioning, with less pulsing time.

Table 21: MIST conditioning time and related retained cohesion and retained stiffness on different BSM mixes

BSM-foam and BSM-emulsion	Pulsing time [min]	Void content [%]	Saturation level relative to %OMC	Steady saturation level [%]	Retained cohesion ratio [%]	Residual modulus ratio [%]
H0CF	1.1	16.0	73	73	29	46
H1CF	3.6	13.9	102	90	68	62
H1LF	3.2	13.5	109	99	51	77
Q0CF	1.3	15.3	48	48	31	50
Q1CF	1.6	14.6	62	62	66	68
Q1LF	1.6	14.5	61	61	60	86
H0CE	4.6	12.5	109	88	50	52
H1CE	9.7	10.8	114	100	78	76
H1LE	6.5	13.0	112	100	69	79
Q0CE	1.3	11.4	60	60	50	53
Q1CE	9.7	12.5	78	78	82	78
Q1LE	5.5	12.0	87	87	74	71

Note: H = Hornfels-RAP Q = Quartzite L = lime C = cement F = foam E = emulsion

The steady state of saturation in this study was determined by checking that there was no change in bulk mass of the specimen in consecutive pulsing cycles (i.e. prohibiting more moisture ingress in a specimen) or whether severe damage occurred in the specimen. The specimens with lower steady-state saturation (less pulsing time) experienced erosion during MIST conditioning, particularly those mixes without the addition of active filler. However, quartzite with added cement or lime showed lower saturation, but this is due to particle type: quartzitic aggregates have smooth (glassy type) surfaces which are less able to retain moisture after conditioning. This is because, at the end of conditioning when materials were taken for moisture content determination, most of the water induced during condition drained out of the specimen upon removal from the cell. The Atterberg limit test showed no clay or plastic limit in quartzitic aggregates. For the Hornfels-RAP aggregates, the retention of moisture was approximately at OMC for both moisture-susceptible mixes and less moisture-susceptible mixes. After full conditioning, the moisture content determination was done by breaking the specimen, keeping the wet material in the oven at 110°C for 24 hours and measuring the MC the following day. The calculation of the degree of steady-state saturation was compared with the OMC of the compacted BSM mixes. Savage (2006) provides a mathematical formulation indicating different legs of granular material saturation (Figure 69). He concludes that steady-state saturation occurs when the degree of saturation is 80%. After 80% of saturation level, any addition of water pushes the particle apart or destroys the interlocking behaviour, hence decreased cohesivity and integrity of the mixes occur.

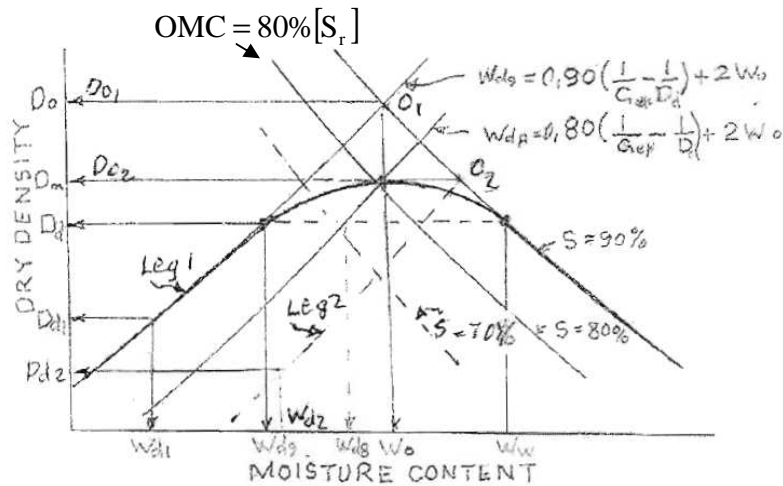


Figure 69: Mathematical model of the 80% saturation level at OMC of the mixes (Savage, 2006)

The steady state saturation of different BSMs mixes after MIST conditioning is superimposed in Figure 70. Steady state saturation was used to determine the critical pulsing time that is applicable to a wide range of mix compositions stabilised with either foamed bitumen or bitumen emulsion.

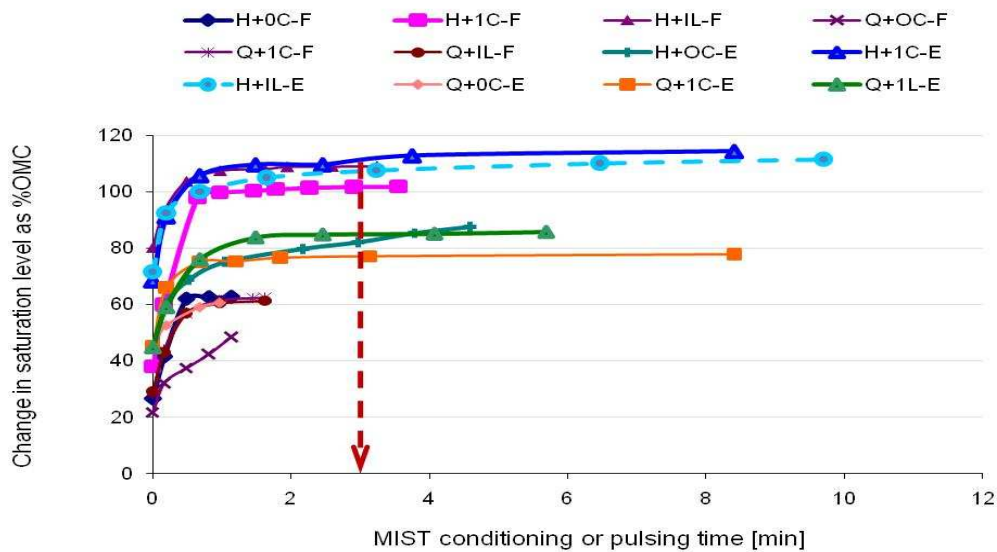


Figure 70: Saturation levels after MIST conditioning on different BSMs

From Figure 70, it can be seen that most BSMs will attain steady moisture saturation after 3.2min pulsing time or 100 pulsing cycles. Although saturation graphs begin to plateau after 2min pulsing time, this could be regarded as the threshold (pulsing time limit) for highly moisture-susceptible mixes. This is because high spalling in specimens occurs and signs of severe erosion are observed. However, to ensure reliable screening of BSM moisture susceptibility, a threshold of 3.2min pulsing time or 100 pulsing cycles was identified. BSMs that cannot withstand the threshold are regarded as highly susceptible to moisture damage.

Therefore, their selection in mix design needs proper consideration. On the other hand, BSMs that can withstand the threshold value justify their selection in mix design.

3.6.3 Analysis on moisture susceptibility and damage potential

3.6.3.1 Steady state saturation and retained cohesion

The steady-state saturation condition, coupled with the mechanical response of the mixes, is one of the indicators of moisture durability behaviour and long-term performance in field conditions. The difference in MIST pulsing cycles (time) of BSMs relates well with the retained cohesion and retained stiffness determined by triaxial tests. The results of the retained cohesion (determined from Mohr-Coulomb relationship) indicate that BSMs that withstand higher numbers of pulsing cycles show high retained cohesion while BSM mixes that withstand lower pulsing cycles show lower cohesion values. This is expected due to the fact that cyclic water pressure weakens the cohesion properties of the mixes that are susceptible to moisture damage. The influence and effect of the addition of active filler (cement or lime) is apparent. BSMs with the addition of active filler show higher retained cohesion or moisture resistance compared to mixes without the addition of active filler. Figure 71 summarises the results of retained cohesion after MIST conditioning and static triaxial testing.

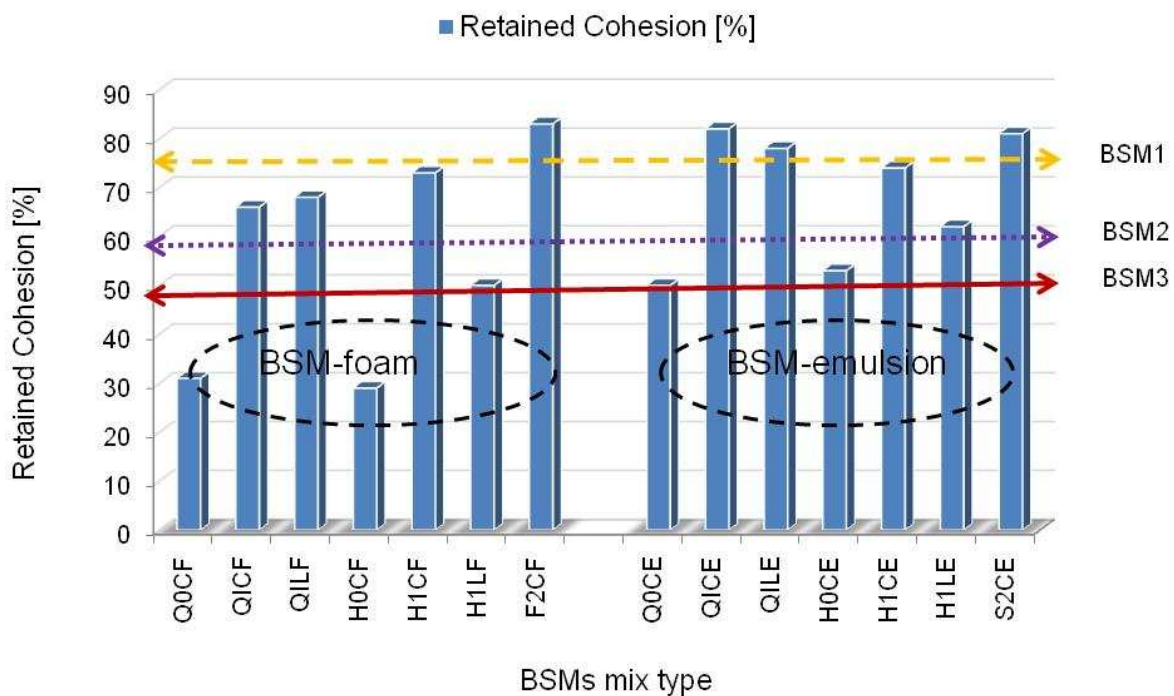


Figure 71: Retained cohesion of different BSMs and proposed limits

The results in Figure 71 show that Quartzite crushed stone and Hornfels-RAP, stabilised with foamed bitumen and without added cement, are susceptible to moisture damage (show significant reduction in cohesion under cyclic water pressure), relative to the same materials stabilised with bitumen emulsion. The BSM mixes with added cement or lime are less susceptible to moisture damage. Nevertheless, the addition of cement seems to be more effective than the addition of lime. However, from the literature review, lime is known to react quicker with the presence of clay (filler) than cement when added to the mineral aggregate. Therefore, the benefit of the addition of lime in terms of dispersion and bond development is

influenced by lower percentages of lime application. This lead to the conclusion that the addition of 1% lime cannot be generalised for its application in BSMs to improve durability in terms of moisture damage. To obtain similar benefits to cement, the initial consumption of lime (ICL) of the material needs to be analysed prior to the addition of the lime to BSMs. The overall performance of the tested mixes shows that BSM-emulsion has minimum retained cohesion of 50% on steady state saturation compared 30% retained cohesion of BSM-foam.

The differences in the retained cohesion in BSM mixes show ranking of mixes after conditioning using the MIST device. That means the ranking of BSM mixes with less or higher moisture susceptibility can be determined by the pulsing of cyclic water pressure using MIST and triaxial tests. To this end, the above analysis can establish the MIST threshold (limiting) values for pulsing cyclic water pressures into the triaxial cell. The ranking criteria (Table 22) are proposed for BSM mix design in relation to moisture damage. The classification of three different types of BSM is consistent with the new guidelines currently being published in South Africa, where BSM1 material is able to withstand the highest levels of traffic patterns in the network.

Table 22: Recommended retained cohesion after MIST conditioning and static triaxial test

MIST pulsing cycle [no.]	MIST pulsing time [min]	Equivalent residual cohesion percentage [%]	Possible equivalent design material
100	3.2	≥ 75	BSM 1
		≥ 60	BSM 2
		≥ 50	BSM 3

The influence of climatic regions plays a significant role in moisture damage. The performance and durability behaviour of BSMs will differ depending on the dominant climatic condition. Larger countries are characterised with different climatic zones. In South Africa, three main climatic zones were defined by Weinert (1980), these zones include Wet (Weinert $N < 2$), Moderate (Weinert $N = 2$ to 5) and Dry (Weinert $N > 5$). The defined zones can be linked to the three moisture damage evaluations established using the MIST-triaxial test, e.g. mix with high retained cohesion values ($\geq 75\%$) should be designed for the wet climatic zone at Weinert, $N < 2$.

3.6.3.2 Steady state saturation and resilient modulus

Another critical parameter investigated to determine moisture susceptibility in BSMs is stiffness reduction. From the discussion in section 3.5.4.1, it is evident that the progressive loss of cohesion and adhesion in the mix matrix results in reduction in stiffness properties. Progressive reduction in stiffness properties may result in erosion, pumping and finally formation of potholes. Figure 72 shows the comparison of BSM-foam and BSM-emulsion stiffness reduction due to the pulsing ingress of water in the mix. The ingress of water into BSM-foam has more effect on stiffness reduction than in BSM-emulsion. A similar trend occurs in the mixes with added active filler, with BSM-emulsion significantly retaining its stiffness after a number of pulses of water into the mix. The addition of lime to BSM-foam and BSM-emulsion shows different trend: It can be noted that an increase in resilient modulus occurs as saturation levels of the mixes increase. However, the effect on stiffness reduction occurs at high saturation levels, above the OMC of the mixes. Although this does not apply to all of the mixes with lime, it is a phenomenon that needs to be recognised when either cement or lime is selected for BSM mix design, particular for moderate or dry climatic conditions.

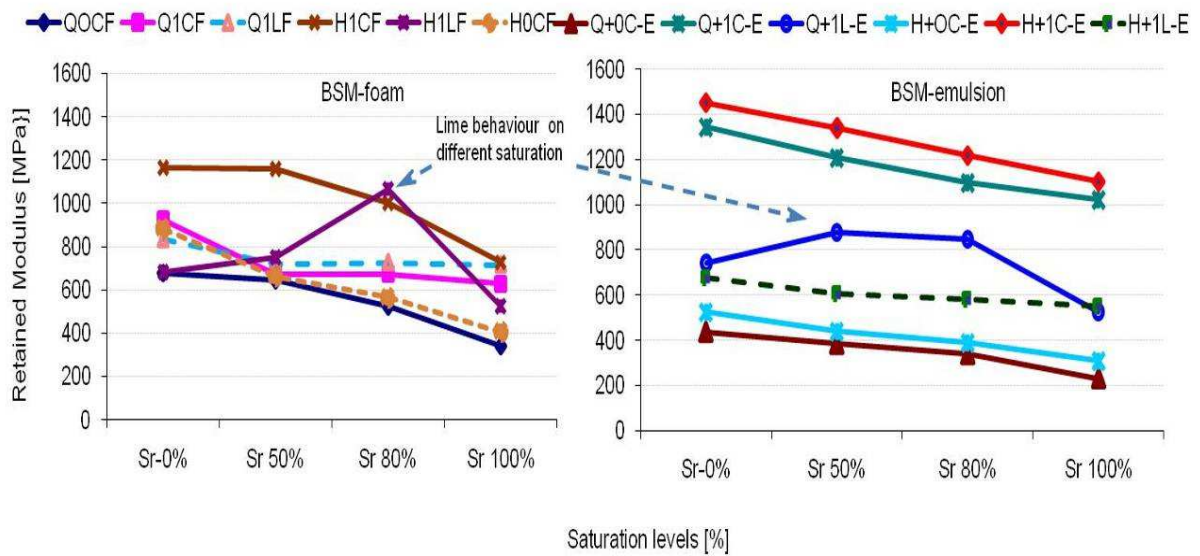


Figure 72: Resilient modulus versus saturation level of BSM-foam and BSM-emulsion

The short dynamic (resilient) triaxial test was performed to determine the retained modulus (M_r) ratio. The retained modulus ratio was calculated as a ratio of resilient modulus of wet mixes to resilient modulus of similar dry mixes. The short dynamic test was performed at a confining pressure of 50kPa to reduce the effect of pore water pressure in the specimen. In Figure 72, the results of resilient modulus at different saturation levels and retained modulus at 50kPa confining pressure are also shown (see data in Appendix C). It is evident from the results that resilient modulus decreases as saturation level increases. This behaviour indicates that progressive pulsing of water in BSMs reduces cohesion and adhesion in the mix and results in deterioration of stiffness properties. BSM-emulsion experiences a consistent drop in resilient modulus as the saturation level increases. On the other hand, BSM-foam seems to be sensitive in resilient modulus as the saturation level increases. On average, BSMs with quartzite and with hornfels-RAP, without the addition of active filler, in dry or wet conditions have lower resilient modulus compared to the mixes with additional active filler. The influence of active filler (cement or lime) on the increase of resilient modulus is evident for both BSM-foam and BSM-emulsion in all types of aggregates. Nevertheless, the healing effect on the stiffness reduction after the ingress and evaporation of moisture was not investigated in this study. However, it is an interesting area for further research.

Figure 73 shows the relationship between the retain cohesion (RC) and retained modulus (RM) of BSMs of the materials investigated in this study. These two parameters seem to have good correlation. However, significant variability can be noted for BSM-foam without active filler (Q0CF and H0CF) and BSM-foam with the addition of lime (Q1LF and H1LF). The reason for variability is not obvious, but it can be attributed to the sensitivity of the stiffness test method.

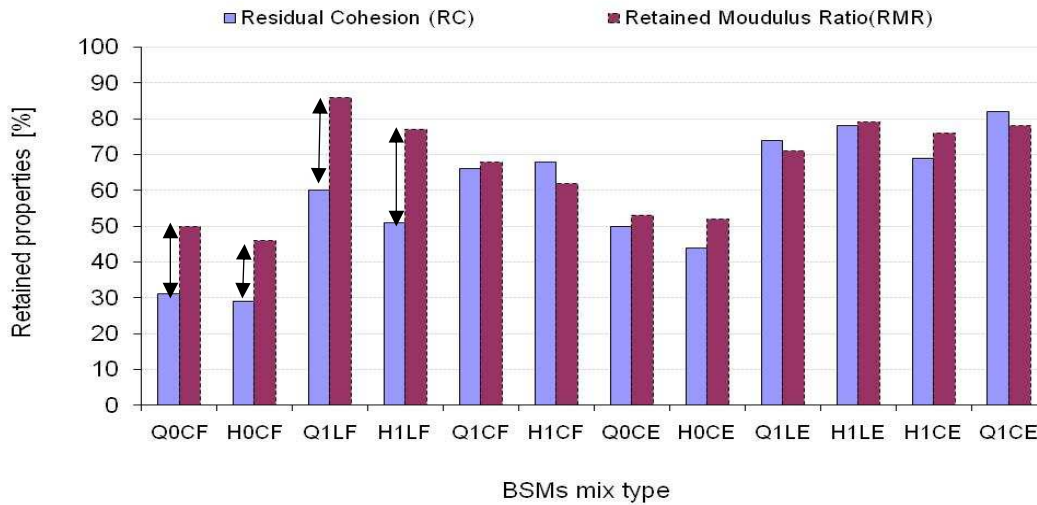


Figure 73: The relationship between retained cohesion and retained modulus ratio of BSMs

During short dynamic tests (resilient modulus), three external Linear Variable Displacement Transducers (LVDTs) were used to improve statistics of the captured results. The result of these LVDTs however, showed significant variability during a single repeated test. This was attributed to the sensitivity of the LVDTs since they were externally placed, touching bottom of the triaxial cell. That means, they were capturing not only the resilient response of the materials, but to some extent the movement of the cell itself. Angle of contact to the triaxial cell also seemed to influence the capturing of the results from different LVDTs. However, care was taken during placing the LVDTs and it was possible to analyse the data promptly before changing the test setup. In case of any discrepancies in the data captured from the three LVDTs, the test was repeated.

An example of inconsistency in the results of the external three LVDTs during capturing of the resilient response of the material is shown in Figure 73.

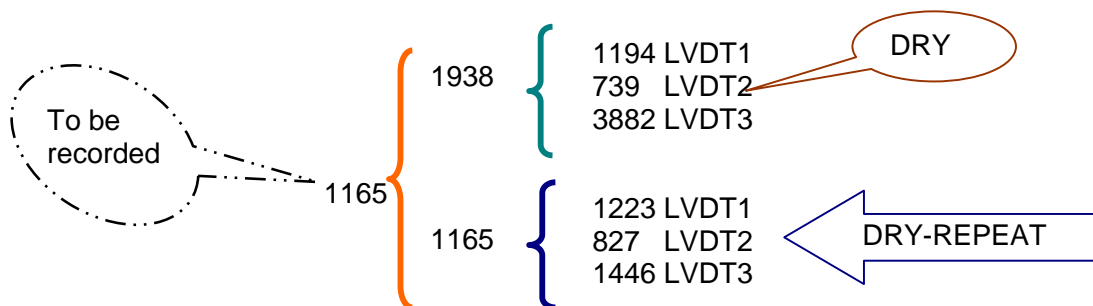


Figure 74: Example of inconsistency results captured by LVDT's during short dynamic test

It is obvious from the results indicated in Figure 74 that the resilient modulus of BSMs captured by LVDTs mounted externally is variable and unreliable. Therefore, if external LVDT's are used for stiffness testing spontaneously counter-checking of results is necessary during testing. A better result of the LVDTs is usually obtained from mounting the LVDTs on-specimen at one third of the height. However, this method is not applicable for the full saturated specimen with the current test-set-up in Stellenbosch University. The on-specimen mounting requires gluing on the LVDT components, which has to be left to dry before testing, that will not be applicable for

wet test. For these reasons, stiffness results from external LVDT's cannot rank moisture susceptibility accurately. It is therefore recommended that screening of BSMs should be carried out with MIST and static (monotonic) triaxial tests.

The use of MIST device has provided some insights into the failure behaviour of BSMs with the ingress of water. The retained cohesion and retained modulus determined after MIST saturation yield results that are consistent with the mechanical performance of BSM mixes under different moisture conditions.

3.7 VALIDATION OF MIST-TRIAXIAL TEST RESULTS

The applicability of the MIST device for conditioning BSM mixes could not be adopted without a validation test. The selection of the MMLS3 scaled accelerated pavement testing device for validation tests takes into account its known performance and ability to simulate field conditions. A similar testing matrix to that presented in Table 16 was prepared for the MMLS3 testing. Sample preparation and a test procedure using MMLS3 and ITS tests are reported in detail in Chapter 4. Wet and dry MMLS3 trafficking was carried out to determine the ravelling behaviour of different combinations of BSMs. ITS tests after wet and dry trafficking were carried out in order to determine tensile strength retained (TSR). This was done in order to find relationships that are comparable in terms of the durability of BSM mix composition. The validation was done between ravelling depth (RvD), retained cohesion (RC) and tensile strength retained (TSR) results established. The comparative mode of failure between these parameters and testing configuration is illustrated in Figure 75.

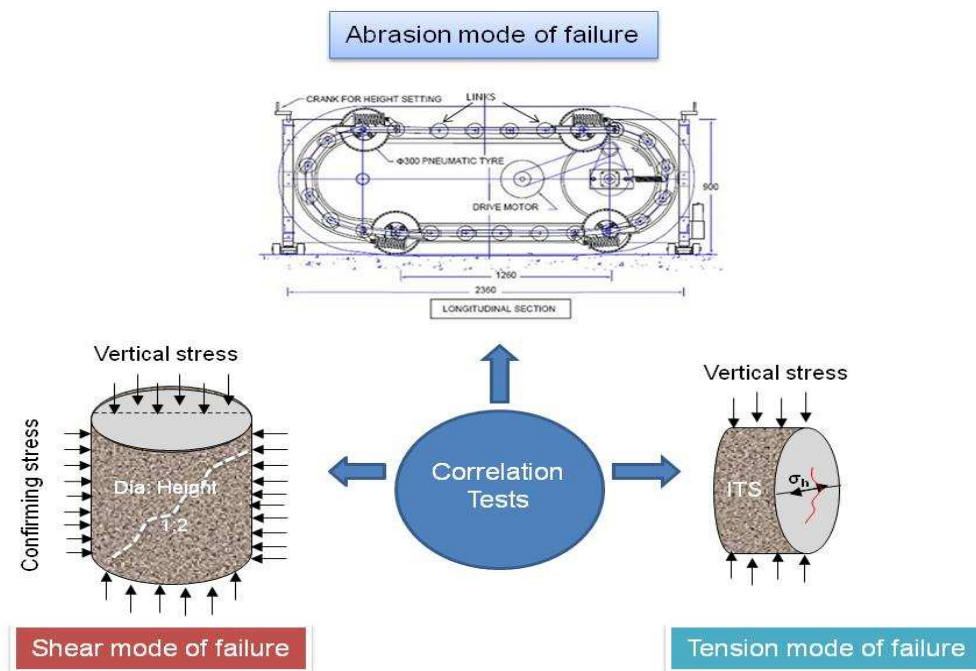


Figure 75: Correlation tests for moisture susceptibility of BSMs

The validation tests on moisture sensitivity using MIST/triaxial, MMLS3 and ITS were based on test configuration and the manner in which failure occurs. They all apply compression (vertical) stress; and, that the failure occurs because of progressive loss in adhesion and cohesion in a

mix matrix. Therefore, test results from these devices can be compared qualitatively. However, comparisons of retained properties should be done for similar state of distress conditions. In addition, the mechanisms of mode of failure for these devices need to be addressed. The dominant mode of failure in MIST/triaxial testing is shear failure, in MMLS3 testing is abrasion and/or ravelling and in ITS testing is tensile cracking. In pavement structure, tensile cracks are not dominant failure of BSMs. Therefore, tensile cracking in the ITS test do not simulate the failure mechanism of BSMs accurately compared to MIST/triaxial and MMLS3 testing. The reason for this is that crack formation and development due to tensile stress in the centre of BSM specimens, as well as the unconfined nature of the test are not typical representations of the failure mechanisms occurring in BSMs during in-service condition. Loizos *et al.* (2007) reported that stiffness of the BSM-foam layer during in-service condition increases with time. This is opposite to the decreasing nature expected from tensile stress or fatigue failure. Nevertheless, the mechanisms of failure for the triaxial and MMLS3 tests compare well. This is due to the fact that the abrasive action of the wheel load causes stress reversal in the aggregate skeleton, in turn resulting in progressive loss in cohesion and adhesion followed by ravelling (aggregate loss). Similarly, in MIST-triaxial testing, shear failure occur as a result of deterioration of cohesion and adhesion, which represent the failure mechanism typical for BSM layer in pavement structures.

In this section, the results of MMLS3 and ITS tests are presented for the validation with MIST-triaxial test results. However, testing methods for MMLS3 and ITS, and the additional test results will be presented further in Chapter 4.

Figure 76 to Figure 79 presents the cumulative ravelling depth of different BSM mixes. A combination of mixes for wet MMLS3 trafficking was selected based on the results of retained cohesion observed from MIST/triaxial testing. In this regard, mixes, which are susceptible to moisture damage, were trafficked separate from the ones, which are resistant to moisture damage. However, no distinction was made on mineral aggregate type (Hornfels-RAP or Quartzite). The MMLS3 trafficking parameters are axle load (1.8kN), tyre pressure (420kPa) and trafficking speed (7 200 wheel loads per hour). All mixes were tested in water temperature of 25°C.

The effect of moisture damage is measured by the loss of aggregates or ravelling depth (RvD) during MMLS3 wet trafficking, by retained cohesion (RC) during MIST/triaxial testing and by the retained tensile strength (TSR) during ITS testing. All these parameters provide a comparative effect on the moisture damage mechanism. As such, they provide an insight into the effect of cohesion and adhesion failure of different BSM mixes, which is fundamental in durability behaviour and long-term performance. The comparisons of RvD, RC and TSR are based on average values of three briquettes tested on each parameter as presented in Figure 76 to Figure 79.

The results in Figure 76 compare the moisture damage behaviour predicted by the RvD, RC and TSR. The Hornfels-RAP and Quartzite crushed stone stabilised with emulsion and addition of cement or lime, were able to withstand wet MMLS3 trafficking of more than 40000 load applications with a ravelling depth of less than 2mm. However, after 40000 load applications, Hornfels-RAP mix stabilised with emulsion and additional of lime starts suffering severe moisture damage prior to termination of the test. The levels of loading applications and ravelling distress after wet trafficking justify that mixes H1CE, Q1LE and Q1CE be classified as less susceptible to moisture damage. Moisture damage classifications based on RvD are presented in Chapter 4. There is no standard load application of the wet trafficking for screening BSMs in terms of moisture susceptibility. Therefore, various load applications were applied and RvD was observed prior to termination of the test. The corresponding RC of these mixes after MIST conditioning and static triaxial testing indicates that mixes H1CE, Q1LE and Q1CE are resistant to moisture damage. According to ranking criteria established in Table 22 of the previous section 3.5.4.1, they can be classified as BSM1 (i.e. retained cohesion $\geq 75\%$), whilst

mix H1LE can be classified as BSM2. The ranking criteria using RC for these mixes, shows similarity with the ranking criteria based on the RvD. However, ranking of these mixes using TSR show some difference. According to TG2 (2002) BSM mix with TSR value $\geq 75\%$ is regarded as less susceptible to moisture damage. In this regard, the results presented in Figure 76 show that only mix Q1CE is considered to be good resistance or less susceptible to moisture damage. This might not be realistic, because mixes with RvD $\leq 2\text{mm}$ after 45000 load applications cannot be classified as less resistant or susceptible to moisture damage.

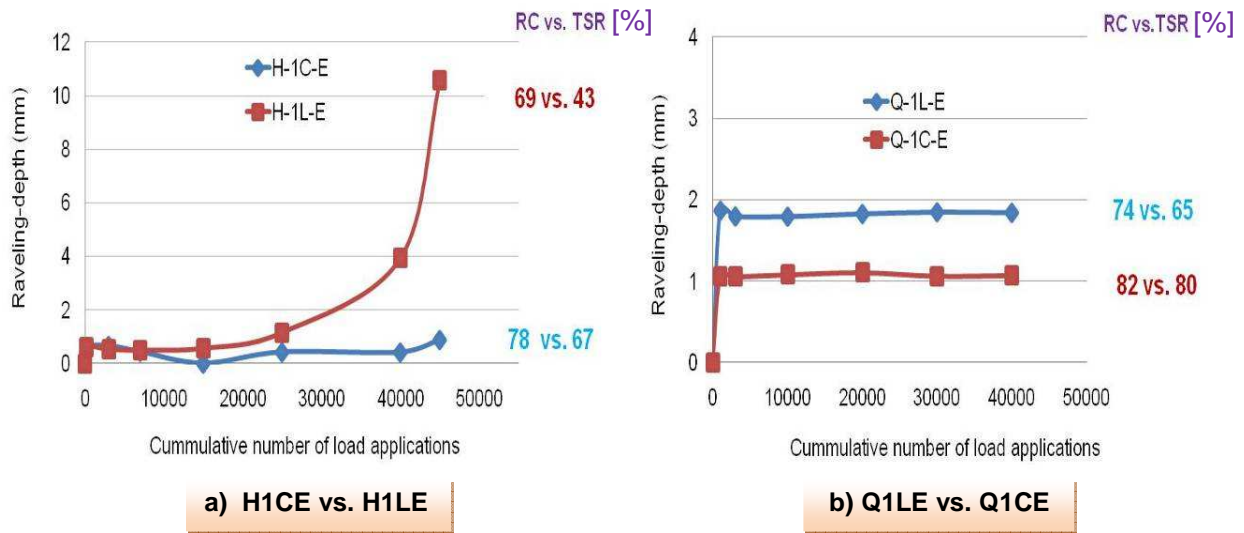


Figure 76: Validation between ravelling depth, retained cohesion, and tensile strength retained results on moisture damage sensitivity in a) H1CE & H1LE and b) Q1LE & Q1CE BSM mixes

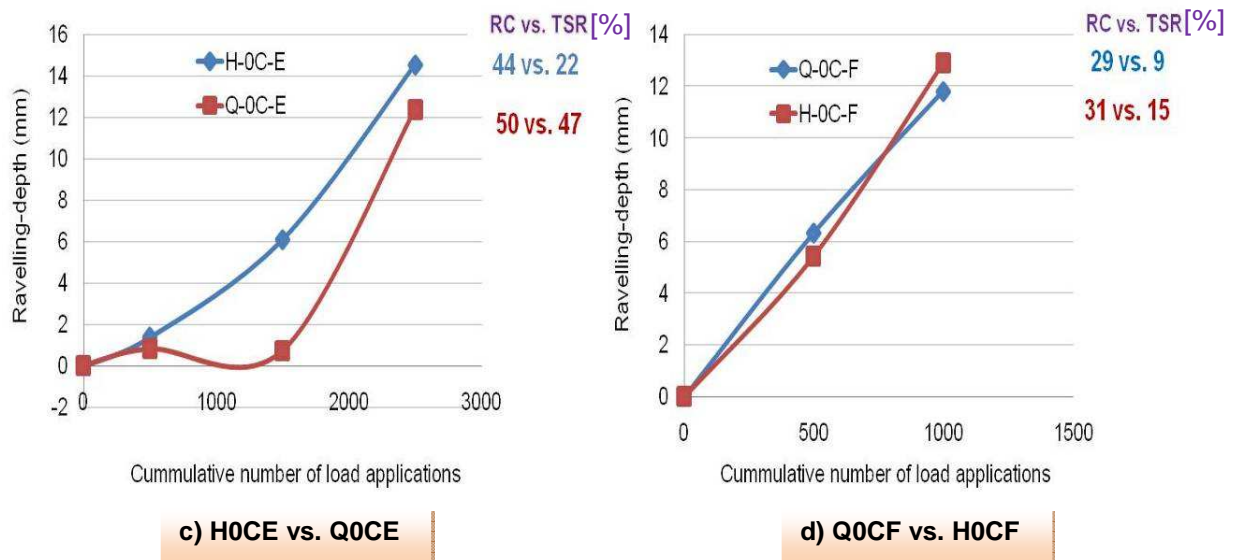


Figure 77: Validation between ravelling depth, retained cohesion, and tensile strength retained results on moisture damage sensitivity of: c) H0CE & Q0CE and d) Q0CF & H0CF BSM mixes

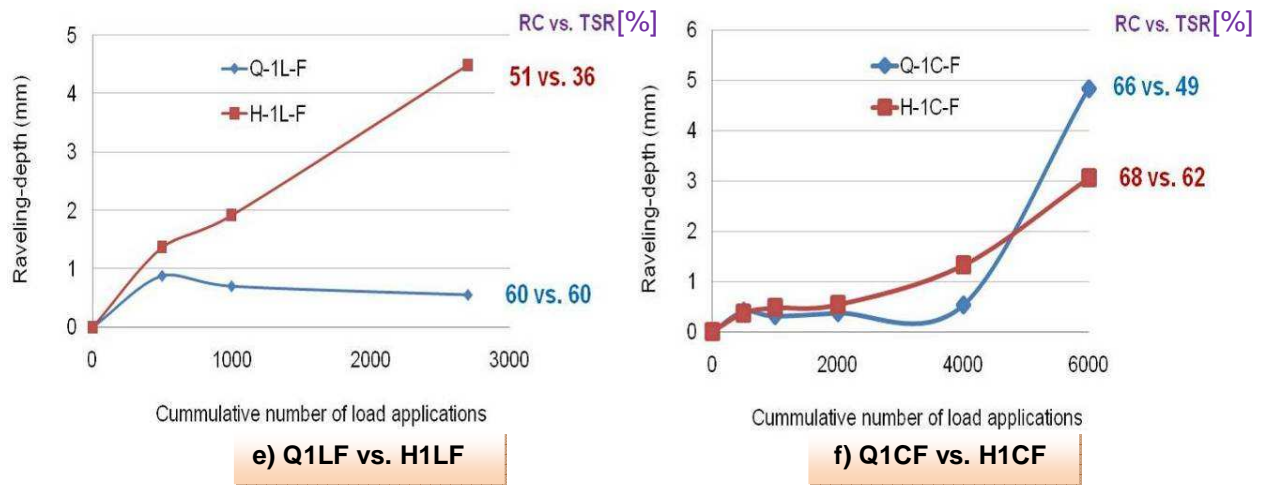


Figure 78: Validation between ravelling depth, retained cohesion, and tensile strength retained on moisture damage sensitivity in e) Q1LF & H1LF and f) Q1CF & H1CF BSM mixes

Figure 77 presents correlation results for BSM mixes without the addition of cement or lime (H0CE, Q0CE, Q0CF and H0CF). It can be seen from the result that these mixes suffered from severe ravelling during wet MMLS3 trafficking. For all ranking criteria, these mixes proved to be highly susceptible to moisture damage. However, the extent of severity differs for RC and TSR, with TSR showing much lower values. The poor performance of these mixes confirms the governing process and formulation of the bonds between binder and mineral aggregates postulated in section 3.2.

Figure 78 presents correlation results for mixes stabilised with foamed bitumen and with additional active filler (Q1IF, H1LF, Q1CF and H1CF). The results show that these mixes suffered aggregate loss at relatively lower numbers of load applications compared to bitumen emulsion (Figure 76). The addition of lime in the Hornfels-RAP stabilised with either foamed bitumen or bitumen emulsion, results in lower resistance to moisture damage compared to the addition of cement in similar materials. For all ranking criteria, mixes Q1IF, Q1CF and H1CF are classified as moderate resistant to moisture damage. While, mix H1LF is classified as susceptible to moisture damage. However, comparisons of number of load applications shows that bitumen emulsion mixes withstand higher wet MMLS3 trafficking of 40 000 compared to 6 000 for foamed bitumen. This behaviour can distinguish BSM-foam and BSM-emulsion in terms of bitumen mastic characteristics in the loss of adhesion and cohesion.

Figure 79 presents the results for cores extracted from existing pavement section, which was in service for eight years. These cores were extracted from P243 for the aim of investigating age hardening behaviour of the binder. However, the additional tests were carried out to gain an insight into moisture susceptibility of BSM mixes cured under field conditions. Mix F2CF is recycled material, comprising RAP (less than 20%) and cement-treated Ferricretes. The material was stabilised with 1.8% foamed bitumen and an additional 2% of cement. The mix S2CE is recycled material, comprising RAP and sandstone quartzite or dolomite natural gravel, stabilised with 1.8% bitumen emulsion and an additional 2% of cement.

Figure 80a depict the core types and their conditions. The physical evaluation of cores conditions after extraction from the pavement section shows that the top 100mm was heavily densified during in-service life, whereas the remaining 150mm seemed less dense. The less densified part result into losses of some materials from the recovered cores, especially in bitumen emulsion stabilisation section. The cores from the foamed bitumen stabilisation section were recovered in full and in good condition. The cores from both sections were tested for the

RvD, RC and TSR, the results are presented in Figure 79. It can be seen from the results that significant resistance to moisture damage was measured by higher values of RC and TSR. This is a result of higher degree of field densification and percentage of cement added. Nevertheless, in terms of wet MMLS3 trafficking, the RvD of 3mm to 6mm occurs at fewer load applications compared to the specimens prepared in the laboratory. The account for this behaviour is indicated in Figure 80b.

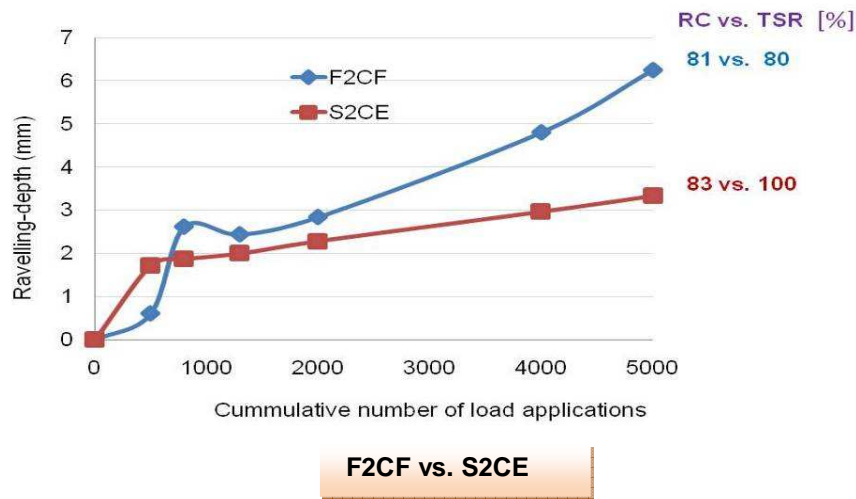


Figure 79: Validation between ravelling depth, retained cohesion, and tensile strength retained on moisture damage sensitivity in F2CF & S2CE BSM cores extracted from the field

From Figure 80b it can be seen that during MIST conditioning, moisture damage or erosion dominated in the RAP-gravel interface. This behaviour influences the rapid deterioration of the cores tested under wet MMLS3 trafficking. Therefore, poor adhesion and/or cohesion between RAP and granular material pose a challenge in the additional of higher percentage of RAP in BSMs and ensuring durability and long-term performance.

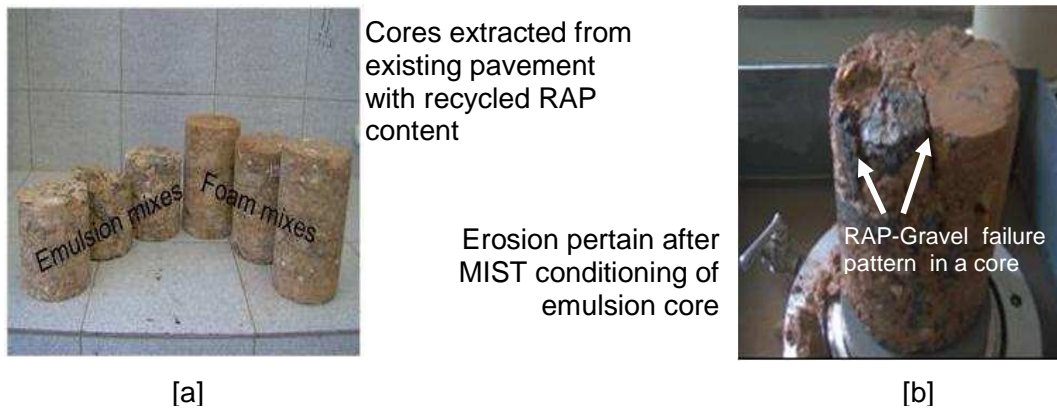


Figure 80: Extracted cores from existing pavement and erosion behaviour

3.8 MOISTURE EFFECT ON DISINTEGRATION OF MINERAL AGGREGATES

The disintegration and decomposition of mineral aggregates due to the moisture effect has been a concern for the performance of granular base layers. Unlike granular base material, durability of virgin and recycled materials used for BSMs have not been studied. Due to the ambiguous nature of suitable aggregates for BSMs, investigation on the effect of moisture in the disintegration and decomposition is vital. The mineral aggregates, which disintegrate under moisture absorption and dynamic loading, will have significant effects on adhesion and cohesion of the mix. In this section, the investigation of disintegration and decomposition behaviour of typical recycled, crushed stone and natural gravel used for BSM mix design were carried out using DMI device. The DMI device has been indicated to be a useful tool for determining the degree of disintegration and decomposition in mineral aggregates. It is in this light, the materials used in this study were studied, i.e. Hornfels-RAP, Quartzite and Ferricretes.

3.8.1 Material selection, testing and results

The selected materials were prepared according to the guideline prepared by Sampson *et al.*, (1987). That is four batches of materials of 3.65kg are required for each mix. The first batch is a control, for which standard Atterberg limits are determined for comparison with the limits determined after the DMI tests. The second batch is tested dry; six steel balls weighing 2.35kg each are added to the mix to simulate dry disintegration. The third batch is tested at fully saturation condition; six steel balls weighing 2.35kg each are also added to simulate disintegration and decomposition under 100% saturation. The last batch is tested fully saturated but without the addition of steel balls; this simulates the influence of moisture on disintegration and decomposition without the effect of dynamic loading. The full testing procedure can be found in the CSIR testing guideline. The author prepared the samples and went to CSIR laboratory in Pretoria to carry out the DMI tests. The test setup and photos of the device are presented in Figure 81.



Figure 81: DMI test setup for dry and wet simulation of Hornfels-RAP materials

After the DMI tests, the Atterberg test is performed on all the batches and the limits of the materials properties are determined. This involves determining the plastic limit (PL), liquid limit (LL), linear shrinkage (LS) and plasticity index (PI). According to the DMI procedure, the disintegration potential of the materials is reported as follows:

$$\text{DMI} = \% \text{ passing at } 0.425 \times \text{max. PI of the four treatments}$$

The Atterberg limits and the DMI results of the tested materials are presented in Table 23.

Table 23: Durability Mill Index (DMI) results for the selected mineral aggregates

Sample	Test	DMI treatment			
		A (control)	B(wet with*)	C(dry with)	D(wet w/out)
Hornfels-RAP	-0.425mm	22.3	26.6	21.9	23.0
	PI	5.8	5.8	4.8	7.1
	LS	2.3	2.6	2.6	2.6
	DMI	189 (26.6 x 7.1)			
Ferricretes	-0.425mm	30.5	41.9	34.4	35.1
	PI	6.0	5.3	4.0	5.3
	LS	3.2	2.7	2.6	2.7
	DMI	251 (41.9 x 6)			
Quartzite	-0.425mm	16.6	20.6	20.9	18.6
	PI	-	-	-	-
	LS	-	-	-	-
	DMI	N/A			

Note: with* means test with the addition of six steel ball

The DMI test results presented in Table 23 provide useful information pertaining to mineral aggregate disintegration and decomposition under different environmental and loading conditions. It can be seen from the results that Ferricrete have higher disintegration and decomposition under the influence of saturation and loading conditions. This is because the rock type is weak and contains higher amount of smectite clay in the materials. Both tested materials meet the required limit set for use as base material for the granular layer. Nevertheless, the limits set for the granular materials in a base layer cannot be applied direct to mineral aggregates for BSMs. This is because the addition of binder in the granular materials has the benefit of reducing moisture exposure. Therefore, additional test need be carried out to establish the limits that are appropriate for BSM mix design. Further evaluation shows that, although Quartzite crushed stone had minimal disintegration during DMI test compared to Hornfels-RAP and Ferricrete, the index could not be calculated because the fines content generated from Quartzite did not have a PI value (i.e. non-plastic). This is a disadvantage of the current testing protocol, because durability of non-plastic material cannot be compared using DMI test Therefore, this require further investigation. In addition, the DMI result needs to be correlated with other durability tests results such as RvD, RC and TSR. The DMI test results indicated in Table 23 cannot be correlated with other parameters because it was limited to granular material. The influence of binder type (foam or emulsion) and the addition of active filler were not investigated. Therefore, it is recommended that more tests be conducted using DMI in a wide range of BSMs to establish more realistic limits for the better screening of mineral aggregates during BSM mix design.

3.9 CONCLUSIONS AND RECOMMENDATION

Insight into the fundamental characteristics of BSMs associated with moisture susceptibility and damage mechanisms has been presented in this study. Based on the data of the study, the following conclusions can be drawn:

- The governing process and bond formation in the BSM mix matrix reveals that adhesion and cohesion between binder and mineral aggregates begins with mixing, continues during compaction and is fully developed after curing. The evolution of bonding through the interaction of binder, mineral aggregates and water reflects physicochemical and mechanical phenomena. These phenomena, which involve thermodynamic, hydrodynamic, physical, chemical, and mechanical properties in the mix matrix, seem to play a key role in adhesion and cohesion. These differentiate BSMs from other pavement materials in the evolution of bonding and damaging mechanisms. Therefore, they should be considered during material selection for mix design.
- The influence of the addition of active filler in cohesion and adhesion in BSMs is evident. Cement or lime plays a significant role in the early stiffening of the mastic and bond formation, which is beneficial for early trafficking of the layer, particularly in BSM-foam. At the microstructure level, addition of active filler has the following influences: 1) accelerated hydration of water entrapped in the mastic and reduced moisture diffusion in and out of the mastic; 2) bond formation between binder and mineral aggregate interface; 3) adhesion and cohesion of the mix matrix, resulting in high resistance to moisture damage.
- The compaction method and level influence durability behaviour of BSMs significantly. Compaction squeezes water out of the mix matrix, where the compaction energy influences bond formation between binder and mineral aggregates. It also minimises voids and interconnected voids in the mix. In this regard, laboratory vibratory hammer seems to sufficiently compact BSMs in a fashion similar to field conditions.
- The excess moisture (> EMC) in BSMs influence mechanisms of moisture damage significantly. The infiltration of excess moisture is linked to the environment and dynamic loading. The main components of moisture damage mechanisms are identified as: 1) change in internal conditions due to moisture transport mechanisms and 2) the response of the materials and loss of integrity due to deterioration of the cohesive and adhesive bonding. The deterioration is linked to void properties (pore pressure), aggregates characteristics and change in moisture state (i.e. degree of saturation). The quantification of voids in the mixes cannot fully describe the performance of BSMs in terms of moisture damage mechanisms. However, understanding void structure and distribution (i.e. size, connectivity and isolation) is important in explaining their relationship to mode of moisture transport and damaging mechanisms.
- The MIST device and the development of a new conditioning protocol has demonstrated the following:
 - It can be used to condition BSMs and screen the mixes, that are moisture susceptible and resistant to moisture damage.
 - Established protocol can be utilised by practitioners for the selection of mix composition in terms of moisture damage durability during mix design.
 - It is simple to use (repeatability and reproducibility), cheap and simulates pulsing of water similar to field conditions.
 - The ratio of the performance parameters from MIST conditioning and static triaxial testing show potential to be used for screening BSM mix with level of certainty than the tensile strength retain.

- The ranking of BSM mixes based on retained cohesion (RC) shows good agreement with ranking of similar BSM mixes using wet MMLS3 trafficking and ravelling behaviour.
- The study of moisture damage characterisation presented in this thesis indicates that Hornfels-RAP and Quartzite crushed stone, stabilised with bitumen emulsion and with the addition of 1% cement were less susceptible to moisture damage than similar materials stabilised with foamed bitumen.

3.9.1 Recommendation

The MIST device shows potential to be used as a conditioning device for BSMs. However, in this study, limited numbers of mix compositions were investigated. It is recommended that the device be applied to a wide range of mix types to populate a database that can be used to accurately model moisture susceptibility of BSMs.

The developed and investigated testing protocol for the MIST/triaxial testing has established threshold values that can be used as ranking criteria for BSMs mix design in relation to moisture damage durability. The recommended threshold values are presented below. These values have been included in the South African technical guideline (TG2, 2009) for BSMs, with emphasis on three main equivalent design materials: BSM1, BSM2 and BSM3. BSM1 mix design is ranked good, with a load-bearing capacity of over 30 million standard axles, while BSM2 and BSM3 are designed for the capacity of carrying 6 million and 1 million standard axles, respectively.

MIST pulsing cycles	MIST pulsing time [min]	Equivalent retain cohesion [%]	Possible equivalent design materials
100	3.2	≥ 75	BSM1
		≥ 60	BSM2
		≥ 50	BSM3

The current method for predicting the curing period in the field is unreliable and subjective. To predict curing of BSMs and bond formation accurately, the local environmental conditions need to be incorporated in the evaporation model. The model should account for the heat transfer coefficient of a layer and thermal conductivity of the materials. Such a model has been presented and discussed in this study. Therefore, it is recommended that the model be tested for its applicability to BSMs. This will give confidence in predicting the curing period suitable for opening a design layer to traffic after sufficient evaporation and bond strengthening in the mix matrix, in lieu of the current oversimplified empirical methods.

The limited study on mineral aggregate durability (i.e. Hornfels-RAP, Ferricrete and Quartzite) has shown that the DMI has potential to be used for screening mineral aggregates for BSM mix design. However, the current limits for natural granular materials cannot be applied directly to BSMs. It is therefore, recommended that a wide range of BSMs be investigated to established realistic limits applicable to BSMs for mix design.

REFERENCES

- Asphalt Academy. 2009. A guideline for the design and construction of bitumen emulsion and foamed bitumen stabilised materials. 2nd edition technical guideline:. Pretoria, South Africa.
- Asphalt Institute. 1992. A Basic Asphalt. Emulsion Manual. Manual Series No 19, Second Edition. Lexington, USA. pg 87.
- Sampson and L.R. and Roux P.L. 1987. Durability mill test for the assessment of unstabilized aggregates. Technical note, TS/20/85.
- Ebels L.J 2008. Characterisation of materials properties and behaviour of cold bituminous mixture for road pavements. PhD dissertation. University of Stellenbosch, South Africa.
- Fu P., Jones D. Hervey J.T, Asce M., and Halles F. A. 2009. An investigation of the curing of foamed asphalt mixes based on micromechanics principles. Journal of materials in civil engineering. Submitted November 9, 2008; accepted May 8, 2009.
- Gonzalez A. 2009. An experimental study on deformational characteristic and performance of foam bitumen pavements. PhD dissertation. University of Canterbury. New Zealand.
- Kelfkens, R.W.C. 2008. Vibratory hemmer compactor of bitumen stabilised materials. MSc Thesis. University of Stellenbosch. South Africa.
- Long F. and Ventura D.G.C 2003. Laboratory testing for the HVS test section on the N7 (TR 11/1). Contract report CR-2003/56. Pretoria.
- Land Transport New Zealand. 2005. The waterproofness of first coat chipseals. Research report style guide. Report xxx. Pg 35.
- Savege P.F. 2006. Insight into pavement materials density and strength. Proceedings of the 25th Southern Africa Transport Conference, Pretoria, South Africa, pg 281-294.
- Stellenbosch University Institute of Transport. 2005. performance models of bitumen emulsion treated materials for koch pavement solutions. Technical report pg 1-41. Stellenbosch, South Africa.
- THM1.1986. Standard methods of testing road materials. Department of Transport 2nd edition technical methods for highways. Pretoria.
- TRH14. 1985. Guideline for road construction materials Department of Transport–Technical recommendations for highways. Pretoria. South Africa.
- Twagira M.E. and Jenkins K. J. 2009. Moisture damage on bituminous stabilised materials using a MIST device. 7th RILEM International symposium on advance testing and characterisation of bituminous materials. Rhodes. Greece.
- Wehlitz C. 2009. Durability of compressed unbaked clay bricks. Final year project V02, BSc. thesis. Department of Civil engineering. Stellenbosch University. South Africa.
- Weinert H.H. 1980. The natural road construction materials of Southern Africa. Academia. Cape Town. South Africa.

CHAPTER 4

THE ROLE OF MMLS3 IN VALIDATION OF MOISTURE DAMAGE CLASSIFICATIONS OF BSMs

4.1 INTRODUCTION

The influence of moisture damage on the BSM layer is predominantly a long-term phenomenon. Early moisture damage manifested in BSMs is usually linked to an inappropriate mix design, excessive in-situ moisture or an insufficient curing period before opening to traffic. In the pavement structure, the access of moisture into BSMs normally depends on the conditions of the boundary layers, i.e. the surfacing layer (either AC or seal), the supporting layer (cemented or granular) and subgrade. Moisture mitigation and damage is linked to dynamic loading. The infiltration of surface water through asphalt surfacing or seal is regarded as the main cause of moisture transport to BSMs.

4.1.1 Time-dependent hydrodynamic (moisture) effects

The hydrodynamic effect usually occurs progressively and time is an important variable. A distressed surface layer (AC or seal) with severe cracks, high void content or potholes significantly influences the hydrodynamic effect on the underlying layer, such as BSM. The effect of hydrodynamics has three main features: inertia of loading with rest period, material durability behaviour and applied stress-wave with a rest period. Inertia effects are important when load changes abruptly on a cracked or porous surface. This is because a portion of the work that is applied onto the material is converted to kinetic energy. Kinetic energy results in crack development and cohesion reduction due to stress reversal on the aggregate skeleton. Most BSM layers are not sensitive to moderate variation in strain rate under the top surface, but the flow stress can increase appreciably when the strain rate increases by several orders of magnitude on the surface layer. The effect of rapid loading is even more pronounced on poor material coupled with moisture sensitivity. A study on seal design by Land Transport in New Zealand (2005) confirms that under fast dynamic loading, surface water can be forced through the cheap seal without any visible signs of cracking, into the base layer. Nikajima *et al.* (2000) and Okano *et al.* (2008) modelled the water flow under a tyre travelling through a 10mm deep water film. Intuitively, their results indicated that at high vehicle speed the hydrodynamic pressure that is generated increases. Water penetrated into the surface, being forced through the pore or voids and into the base layer. The pressure of penetration was found to double from approximately 0.7kN at 60km/h to 1.4kN at 80km/h. Maree (1982) indicates that stress waves propagate hydrodynamic forces through the materials and are reflected through the surface, such as crack planes or voids. The reflective stress wave influences the localised failure of materials, which in turn influences moisture sensitivity of BSMs. It is apparent that these features occur progressively over a long time. Therefore, if localised failures in the surface layer are addressed in time (proper maintenance), moisture damage in BSMs might be reduced to an acceptable level. Figure 82 illustrates the progressive hydrodynamic effect on BSMs.

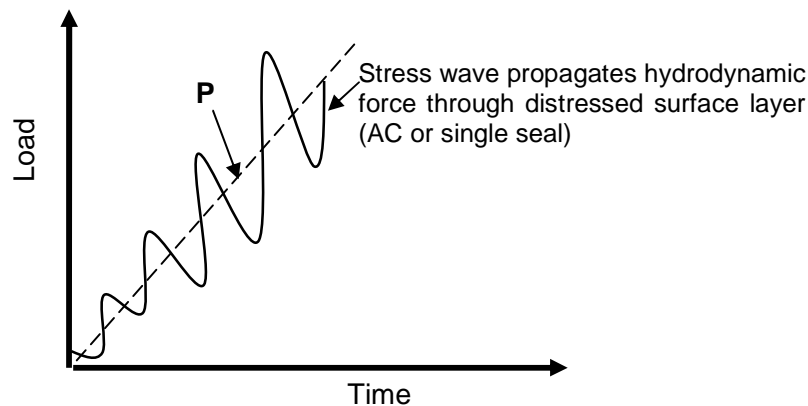


Figure 82: Schematic load-time hydrodynamic effect on BSMs due to distressed surface layer

In order to test the validity of the moisture damage prediction using the MIST/triaxial, the influence of traffic on laboratory-prepared specimens (compacted and cured) with similar mixture composition was simulated and analysed using an accelerated pavement tester (APT), i.e. Mobile Model Simulator MMLS3. Hugo and Epps (2004) define APT as “the controlled application of wheel loading to the pavement structure to determine pavement response and long-term in-service performance under controlled, accelerated, and accumulated damage in a compressed time period”. The role of the accelerated paving testing (APT) in this study was to simulate field moisture damage and compare the durability behaviour from MIST/triaxial monotonic testing. Further objectives in the application of the APT devices were as follows:

- Investigate accelerated testing procedures for MMLS3 on BSMs.
- Establish reliable limits for the MMLS3 test on BSMs exposed to moisture.
- Make recommendations regarding the appropriateness of the APT device for screening of BSMs on moisture related damage.

This chapter focuses on the determinations of validation parameters, which are RvD and TSR. These parameters were determined from the relevant factors applicable to BSMs under wet and dry MMLS3 trafficking. A comparison of moisture susceptibility in foamed bitumen and bitumen emulsion is made from different combined mineral aggregates. In addition, the influence of the addition of active filler (cement or lime) is also investigated.

4.2 SELECTION OF TEST VARIABLES AND TEST SETUP

MMLS3 is a unidirectional vehicle-load simulator used for the trafficking of a model wheel load on dry or wet pavements. The device consists of four wheels circulating in a closed loop. These wheels can be laterally displaced across 80mm to 150mm in a triangular distribution about the centre line to simulate traffic wandering, if desired. However, the lateral wander is only applicable when MMLS3 is tested on a laboratory slab or a field pavement and is, therefore, not applicable in a laboratory briquettes test setup. An illustration of distribution of the four circulating loading axles and tyres in the MMLS3 is presented in Figure 83.

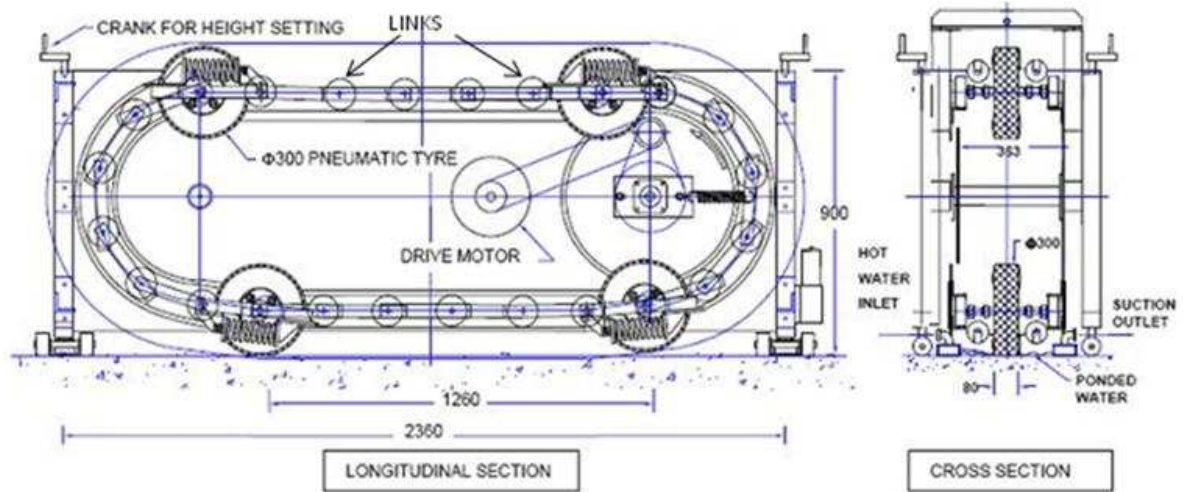


Figure 83: MMLS3 illustration of the four re-circulating wheel axles and tyre

The most applicable setting of the MMLS3 for the APT testing program is detailed as follows:

- The axle wheel loading can be set to 1.8kN, 2.1kN, 2.7kN and 2.9kN. The axial wheel loads are set using an electronic loading calibration unit indicated in Figure 84.

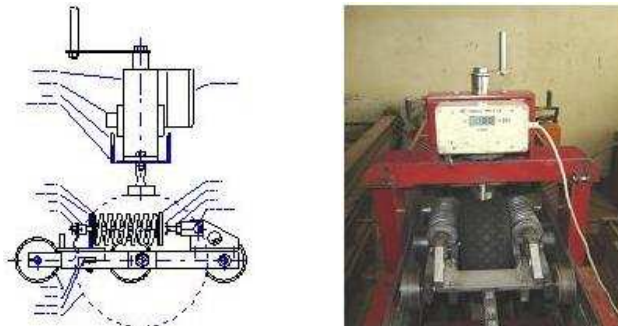


Figure 84: The calibration unit for the wheel load in the MMLS3

- The pneumatic wheel tyre diameter is 300mm with 70mm width of contact pressure.
- The tyre pressure range from 400kPa to 800kPa, inflated using a normal compressed air device
- The wheel speed varies from 0.2778m/s to 2.5m/s, with a nominal speed of 2.5m/s, which is equivalent to 9km/hr and frequency of 2Hz.
- The maximum applied wheel axial load per hour is 7200axle/hr, which is equivalent to 2wheel/sec.
- Distance between wheels (link distance, 210mm times number of links, 6) = 1.26m
- Rest period between wheel loading = $1.26m / 2.52m/sec = 0.5sec$
- Assuming circular shape of the tyre, the loading contact length can be calculated using the following relationship:

$$P = \frac{F}{A}$$

$$\text{contact length} = \frac{\text{Area, (A)}}{\text{width, (w)}}$$

where P = pressure [kPa]; F = axial load [kN]; A = contact area [mm²]; w = width of contact pressure (70mm).

The setting of the MMLS3 needs to be selected in terms of its appropriateness to the type of layer being tested. This is especially true for an applicable loading rate and rest period to simulate the pulsing of water pressure in the BSM layer. From the axial loadings and tyre pressure, the contact length applicable to MMLS3 can be summarised as shown in Table 24.

Table 24: The axial loading, tyre pressure and contact length applicable to MMLS3 settings

Range of axial load	Tyre pressure [kPa]			
	400	520	700	800
	Tyre contact length [mm]			
Maximum load (2.9kN)	104	80	59	52
Intermediate load (2.7kN)	96	74	55	48
Median load (2.1kN)	75	58	43	38
Lower load (1.8kN)	64	49	37	32

- In practice, the BSM layer is used in the base and seldom in the subbase, therefore some load distribution occurs in the overlying layers. This needs to be accounted for in laboratory testing. In the scaled model, the critical parameters are tyre pressure and axle load, as the viscous response of BSMs to loading time relative to the elastic component is not as acute as HMA (Jenkins, 2000). In this study, less severe variable values of the MMLS3 setting were selected to generate a similar magnitude of pulsing of water pressure observed in the base layer during hydrodynamic study by Land Transport New Zealand (2005). Likewise, to be able correlate the results of moisture damage determined with MIST/triaxial testing. Tyre pressure of 420kPa and wheel axial load of 1.8kN were used to determine the loading time and rest period applied on MMLS3. The damaging parameters, such as loading time and rest period, realised by MMLS3 for the selected variables were calculated as follows:

$$\text{Loading time} = \frac{\text{contact length, l}}{\text{velocity, v}}$$

- The loading time and rest period of MMLS3 trafficking is indicated in Figure 85. Similar mode of loading was applied in the MIST conditioning test setup using solenoid valves (with some adjustment). The ON/OFF timer was set to apply the cyclic pulsing water pressure in the triaxial specimen as indicated in the MIST test setup (see Chapter 3).

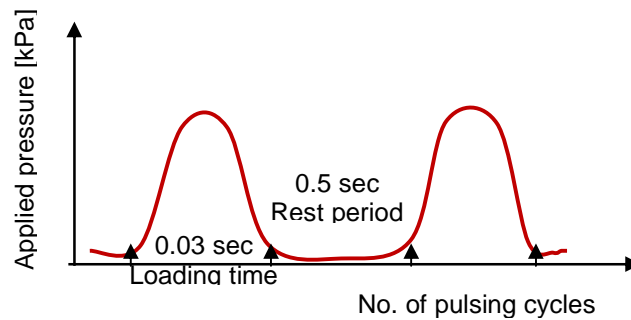


Figure 85: Illustration of cyclic loading time and rest period on MMLS3 for the moisture damage simulation

- The adverse environmental conditions are controlled by 1) a water supply unit with a heating condition to simulate water temperature on moisture damage; 2) a heating unit to simulate air temperature on dry testing. The air temperature can range from 0°C to 90°C.

4.2.1 Setup limits on the testing procedure for BSMs

Currently, the available testing procedure for MMLS3 on laboratory conditions is based on HMA. This document is known as GPG1, draft protocol guideline 1 for evaluation of permanent deformation and susceptibility to moisture damage on HMA (Institute of Transport Technology, 2008). This procedure was designed for HMA and cannot be entirely applied to BSMs. Previous research on BSMs using MMLS3 shows that one of the major challenges with wet trafficking of BSMs is the premature failure of the mixes after water exposure, compared with HMA (Van der Riet, 2007). The wet MMLS3 trafficking test was terminated at less than 500 wheel repetitions due to the disintegration of the specimens, compared with similar tests on HMA that endure for 20 times longer. Jenkins and van de Ven (1999) tested foamed bitumen mixes under field conditions; they indicate that foamed bitumen mixes are more susceptible to ravelling than rutting, as shown in Figure 86. Taking cognizance of this rate of failure, the development of a new laboratory test protocol that provides sufficient testing time, i.e. 50 000 to 100 000 wheel repetitions, was required. The challenges of realistically simulating the tyre-specimen surface interaction during MMLS3 testing need to be addressed in this study in order to develop sensitivity to mix performance during wet or dry trafficking.

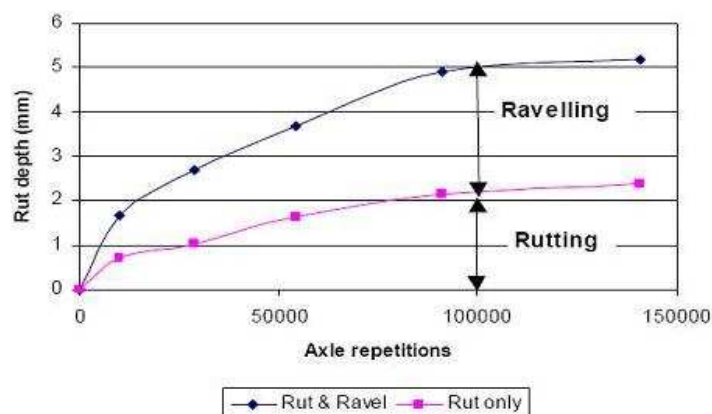


Figure 86: Ravelling versus rutting on the foamed bitumen section tested with MMLS3 after three days of compaction (Jenkins and van de Ven, 1999)

The location of BSMs in the pavement structure, as indicated in Figure 87, also necessitates the protection of the surface of BSM briquettes from ravelling during wet trafficking. The protection should not, however, reduce the pore pressure induction during wheel passages. To ensure simulation of realistic field pore pressure induction, the protective cover in the laboratory setup of the MMLS3 could not have a large thickness that would distribute the wheel stresses differently over the briquettes and convolute the moisture damage. To this end, a cover was selected to protect direct abrasion between tyres and briquette surface, as illustrated in Figure 88.

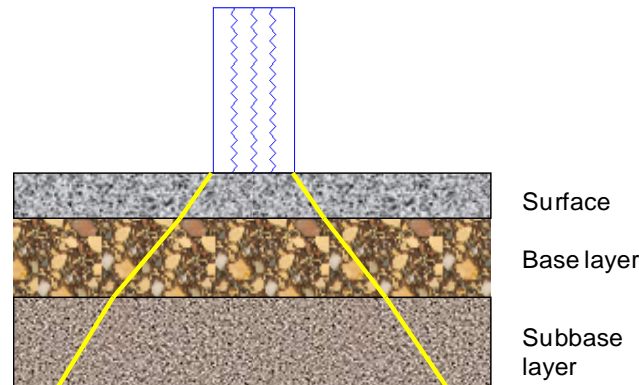


Figure 87: Typical pavement structure with BSMs (base layer) and surface loading

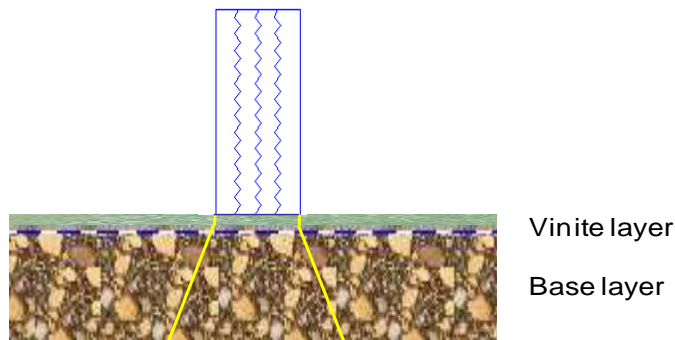


Figure 88: The design of vinite layer to protect direct wheel load abrasion on BSMs

The materials considered for the protection layer were vinite and a reinforced rubber mat, both exhibiting tough and flexible properties. The vinite layer is 3mm thick and green in colour, as shown in Figure 89. Prior to application of the selected covering layer, a trial test of MMLS3 wheel trafficking on a vinite layer covering the specimens (Hornfels, stabilised with bitumen emulsion, and cured at ambient temperature for nine months) was performed at 680kPa tyre pressure, 1.8kN wheel load and full speed of 7 200wheel/hr. The results show that after 100 000 load repetitions, the surface was still in sound condition. Similar behaviour occurred when the reinforced rubber mat was used as the protection layer. The grey path noted in Figure 89 is a result of the green discolouration from wheel abrasions. Following the trials, the vinite was selected for the MMLS3 testing protocol of BSMs. The installation of vinite layer on the test bed is done by securing the ends with metal brackets (see Figure 89). In this way, water in the bath freely infiltrates the specimens from top as well as through the sides. The water level above of the vinite layer is kept at 2mm during the entire test period.

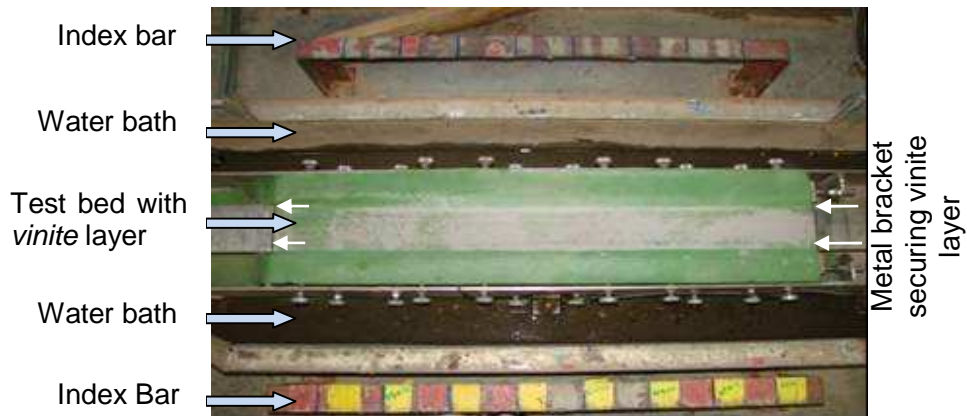


Figure 89: Plan view of the vinite protective layer on the briquettes and its discolouring during trafficking

The setup of the MMLS3 for BSMs included the following settings:

- Tyre pressure: 420kPa,
- Wheel axial load: 1.8kN for each of the four wheels,
- Wheel speed: 2.5m/s, equivalent to 7200 wheel per hour,
- Protecting layer (Vinite): 3.0mm thick,
- Water temperature: 25°C for wet test,
- Channelised trafficking (no lateral wander).

4.3 EXPERIMENTAL PROGRAM

In the experimental program, various BSM mix compositions from laboratory prepared specimens and the field extracted cores are investigated. The factors that influence moisture sensitivity for the MMLS3 trafficking under laboratory conditions are discussed. The limits for classification of moisture damage using MMLS3 and ITS tests are established and discussed. The determined limits are used to validate moisture susceptibility predicted by MIST-triaxial test presented in Chapter 3. To this end, the flow diagram illustrating testing methodology is presented in Figure 90.

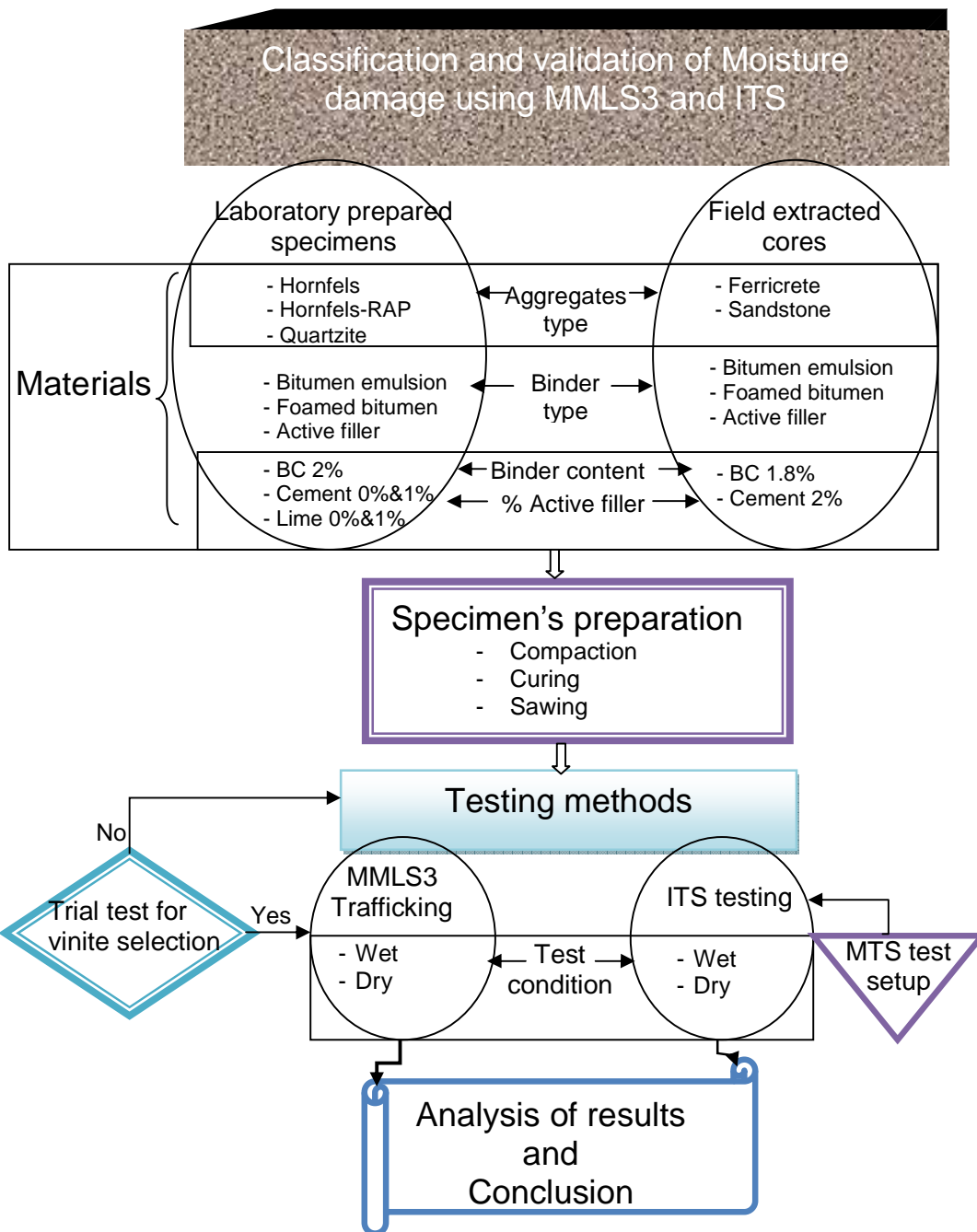


Figure 90: Flow diagram illustrating moisture damage classification of BSMs using MMLS3 and ITS tests

4.3.1 Material selection and specimen preparation

The selection of mineral aggregates was based on the validation of the MIST testing experimental program. Two representative base material types were selected for the MMLS3 study, namely recycled Hornfels and crushed stones. The blends of these two materials provide the basis of the mineral aggregates for the mixes, i.e. Hornfels-RAP and crushed virgin

Quartzite (85:15 percentage compositions). The grading of the aggregates was selected with a maximum aggregate size of 19mm and a percentage passing 0.075mm of 10% and 6% for Hornfels-RAP and Quartzite respectively. Selected mixes were stabilised in the laboratory with either foamed bitumen or bitumen emulsion binder. 2% net bitumen content was applied to both Hornfels-RAP and Quartzite materials, with the addition of active filler as variables. In addition, field cores extracted from pavement section P243 in Vereeniging, Gauteng, which has been in service for 8years, were included in the test mix.

4.3.2 Materials properties

The OMC and MDD of the selected materials are determined and reported in Chapter 3 of this study. In Chapter 3, the source of bitumen emulsion and bitumen for the production of foamed bitumen, as well as foamed bitumen properties, are presented. In addition, the type of active filler and mixing methods are described, therefore, they will not repeated in this chapter.

4.3.3 Compaction and curing

Compaction and curing of BSMs play a significant role in moisture damage simulation. Due to the dispersion nature of the binder in the mix, as explained in Chapter 2, all briquettes were compacted to achieve target density of 100% Mod AASHTO. The curing process for the MMLS3 briquettes was similar to the curing procedures for the triaxial specimens. The compaction and curing procedures are described in detail in Chapter 3 and therefore not repeated here.

4.3.4 Cutting of specimens

The cutting of a specimen is an important aspect in BSM testing, to ensure reliable results. Following curing and cooling to ambient temperature, the specimens are ready for cutting. The cutting process needs care and attention in order to minimise any damage to the specimen. Cutting BSMs with the addition of active filler seemed to be easier than cutting BSMs without active filler. The latter is less cohesive and rather brittle, so spalling of the aggregate occurs if the wrong cutting technique is applied. All prepared specimens are cut to a designed size to be able to fit into the MMLS3 test bed. The designed specimen size for the MMLS3 test is 110mm x 100mm. The cutting of specimens prior to installation into the test bed requires a trimming of 20mm from the sides as shown in Figure 91.

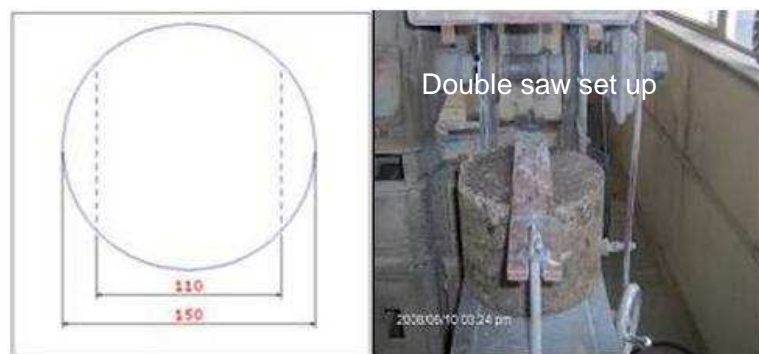


Figure 91: The top view of briquettes measurements and the double saw cutting setup

The cutting method involves sawing halfway using a double saw, turning the specimen and sawing the other halfway to avoid any spalling. The diameter of the specimen is reduced from 150mm to 110mm (see Figure 91 and Figure 92). Specimen thickness of 90mm–100mm can be installed into the MMLS3 test bed. The installations of briquettes in the test bed is done by

placing briquettes side by side on the trimmed faces, in this way stacked briquettes become a compact BSM layer (see Figure 94).

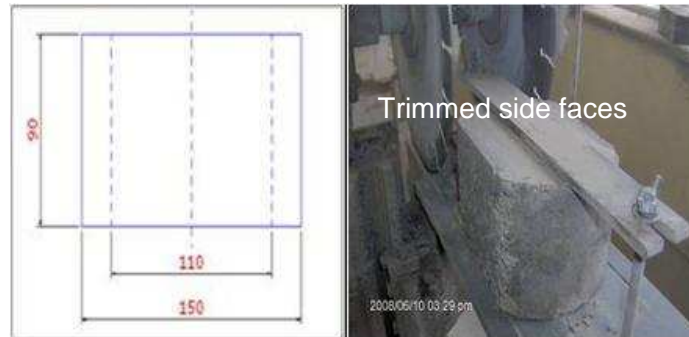


Figure 92: The side view of briquette measurement after trimming of the sides

BSM mixes that are less strongly bound can suffer severe spalling during cutting. This occurs especially where larger triaxial specimens are trimmed horizontally to produce MMLS3 size specimens. Surface finish with severe spalling is unacceptable for MMLS3 testing because tyre-surface interaction creates a dynamic loading effect, which in turn results in early damage. Such briquettes are discarded. Figure 93 shows a comparable surface finish after sawcutting for MMLS3 testing.



Figure 93: Comparable surface finish after sawcutting for MMLS3 testing

4.4 MMLS3 AND ITS TESTING

Two sets of similar mixes were prepared for MMLS3 testing. One set was tested in wet conditions and the other in dry conditions. After wet and dry MMLS3 trafficking, qualitative measurement of retained strength was done using ITS test. The ratio of ITS wet to ITS dry was calculated to determine tensile strength retained (TSR). The MMLS3 tests were carried out on laboratory-prepared specimens and cores extracted from the field pavement layer. The laboratory-prepared specimens were accelerated cured in the oven, while the extracted cores from the field pavement layer were in equilibrium moisture content after 8 years of field curing. An overview of the MMLS3 setup of the prepared specimens is provided in Figure 94. The setup can accommodate nine briquettes, of which seven are monitored during trafficking (two dummy specimens are placed at either end of the traffic path). The dummy specimens are made of HMA to withstand the dynamic loads during the transition. The overview of the MMLS3 test bed setup and the profilometer guide is indicated in Figure 94.

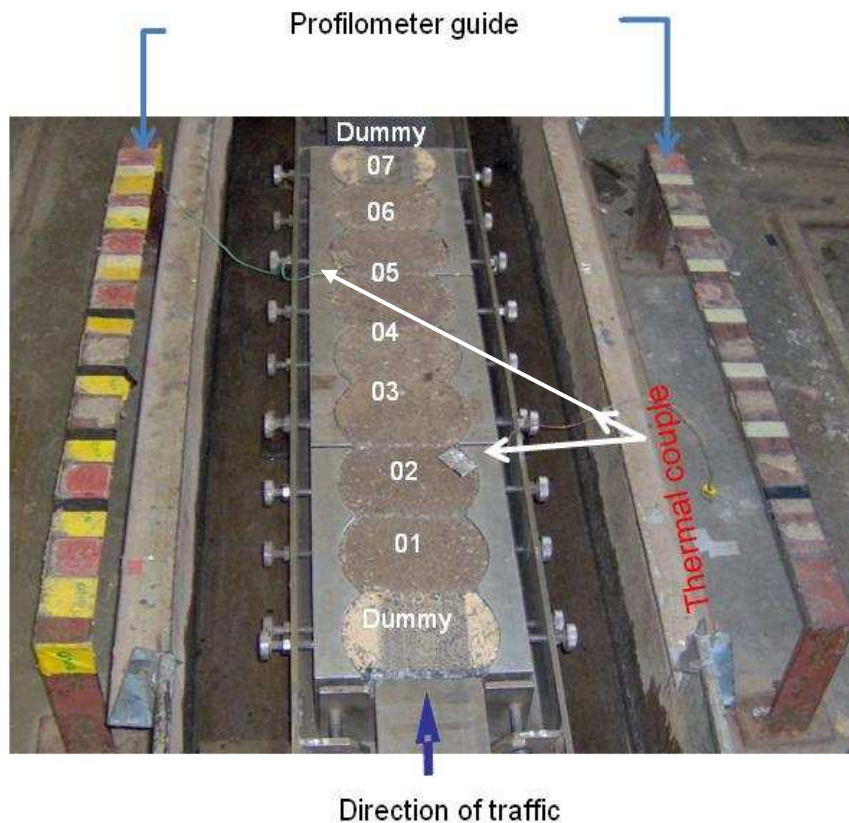


Figure 94: Overview of the MMLS3 test bed setup and profilometer guide

Typically, in one setup the seven specimens that are monitored could reflect two different variables, providing sufficient statistical data for analysis based on at least three specimens for each set of variables. The combination may monitor three briquettes of BSM-emulsion and four of BSM-foam or vice versa. In addition, the combination can be varied for BSMs with different aggregate types, with and without active filler. The transverse profile of the trafficked briquette is measured using an electronic profilometer. Readings are taken at exponential intervals of trafficking, given the non-linear form of the time function (see Figure 95). The profile of each briquette is measured, except the dummy specimens. The number of load repetitions at which profile measurements are taken differs according to the type of BSM. Generally, more measurements are made early on during the test, that is at shorter intervals. During profilometer reading, the MMLS3 is removed from the setup and reinstalled afterward; this makes the entire operation laborious and time-consuming.

Wet MMLS3 trafficking is undertaken with the water level in the bath filled to 2mm above the specimen's surface. The water depth is held steady by a weir at the end of the bath. The water is circulated through a geyser (heating unit) throughout the test to maintain constant temperature. The water temperature during testing is maintained at 25°C using a thermally adjustable water pump. The test temperature of the briquettes is monitored through a thermal couple, two thermal couple are installed at different location of the test bed (see Figure 94).

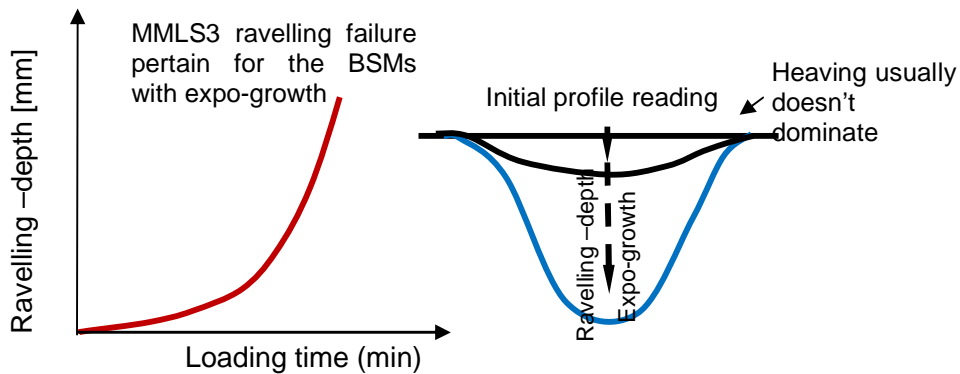


Figure 95: Non-linear pertain of ravelling growth during MMLS3 trafficking of BSMs

4.4.1 ITS testing

Subsequent to MMLS3 trafficking, an Indirect Tensile Strength (ITS) test was carried out on the specimens removed from the MMLS3 test setup. The ITS results on wet trafficking were compared with ITS results on dry trafficking, such that the TSR results that are related to moisture susceptibility can be assessed for the different BSM mixes.

The ITS test was performed using MTS equipment. The loading rate applied during ITS test was 50.8mm/min, according to TG2 (Asphalt Academy, 2009). The computation of ITS and tensile strength ratio are outlined in Equation 23 and Equation 24 respectively:

$$\text{Indirect Tensile Strength (ITS)} = \frac{2 \times P_{\max}}{\pi \times D \times t} \quad \text{Equation 23}$$

$$\text{Tensile Strength Ratio (TSR)} = \frac{ITS_{\text{wet}}}{ITS_{\text{dry}}} \times 100 \quad \text{Equation 24}$$

where P_{\max} = maximum applied load [N]; D = specimen diameter [mm]; t = average specimen height [mm]; ITS_{wet} = Indirect Tensile Strength at wet condition [kPa]; ITS_{dry} = Indirect Tensile Strength at dry condition [kPa].

Figure 96 shows the ITS setup in the MTS equipment, where the test was performed at ambient temperature of $25 \pm 1^\circ\text{C}$.

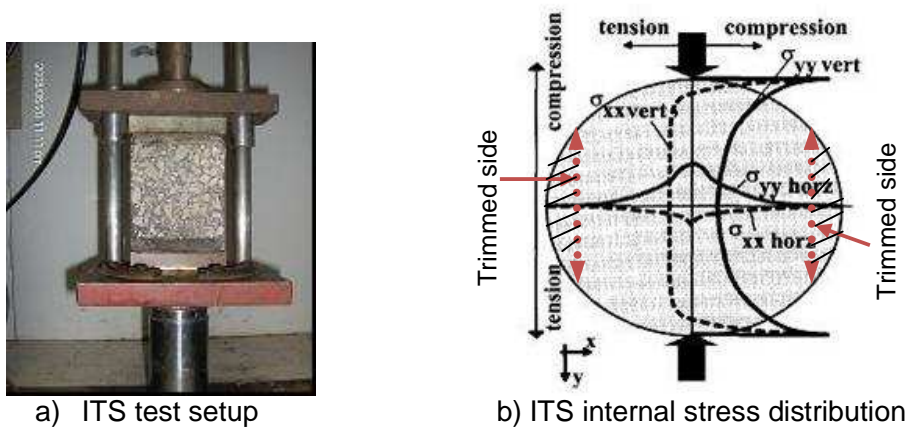


Figure 96: ITS test setup on specimen after MMLS3 testing tested at $25 \pm 1^\circ\text{C}$

The ITS test has been used to determine moisture susceptibility because of its simplicity compared to triaxial testing. However, internal stress distribution caused by indirect tensile splitting is extremely complex (see Figure 96b). In this case, oversimplified models are used to relate the applied force and the stress at the centre of the specimen (Erkens, 2002). Therefore, the use of the TSR in quantifying moisture damage in BSMs is rather an indicator, as it does not simulate the actual failure mechanisms predominant in BSMs. The ITS test was performed on briquettes that was trimmed on the sides. It can be seen from Figure 96b that trimming of the sides has small influence of stress distribution at the centre of briquette. Therefore, the qualitative measure of retained properties is similar to standard size specimen and can be used for validation.

4.5 ANALYSIS AND DISCUSSION OF RESULTS

The findings from the MMLS3 testing and subsequent ITS testing on wet and dry trafficked BSMs led to ranking of the different BSMs in terms of moisture susceptibility. The results obtained were used to establish a possible correlation or trend between deterioration under the MMLS3 and TSR results.

The settings selected for the MMLS3 testing allowed for an acceptable number of load applications of MMLS3 trafficking, i.e. in excess of 2 000 repetitions, for discerning the relative performance and thus classification of the BSMs. In the following sections, the different factors influencing moisture damage in BSMs are analysed.

4.5.1 Load application on BSMs

The impact of moisture on pavement performance is dependent on the type of pavement structure, loading condition, temperature, and degree of saturation, among other factors. There are three primary mechanisms in which dynamic loading and moisture interaction may degrade a BSMs mixture:

1. Failure of the adhesive bond between mastic and mineral aggregate,
2. Loss of cohesion within the matrix and
3. Degradation of the aggregate

The loss of adhesive or cohesive (i.e. bond) strength results in weakening in the BSMs matrix, which leads to a loss of stiffness and strength. The matrix strength loss because of moisture damage can lead to permanent deformation. The response of BSMs to the repeated loading of the MMLS3 is measured in terms of ravelling behaviour rather than rutting. The latter failure mechanism dominates in MMLS3 trafficking of HMA due to its higher binder content that promotes viscous behaviour.

The number of loading applications to reach severe depth of ravelling was determined, with a limit of 50 000 loading cycles. However, due to exponential deterioration after failure started, typically, tests were terminated at depths of ravelling between 10mm and 14mm. The maximum number of loading applications during wet trafficking of a particular mix was used to test the duplicate specimens in dry conditions. The wet and dry state of tested specimen was used for qualitative evaluation of the retained strength. The number of load applications in MMLS3 wet trafficking and corresponding ravelling depth of different BSM mixes are presented in Figure 97. The results in Figure 97 are sufficiently varied to discern the different levels of susceptibility to moisture damage for the range of materials. BSM-emulsion (G1CE) with a long curing condition (nine months) performed extremely well after 100 000 load applications, compared to other BSMs tested after standard accelerated curing. This indicates the durability properties of the long-term performance of BSMs are influenced by level of curing.

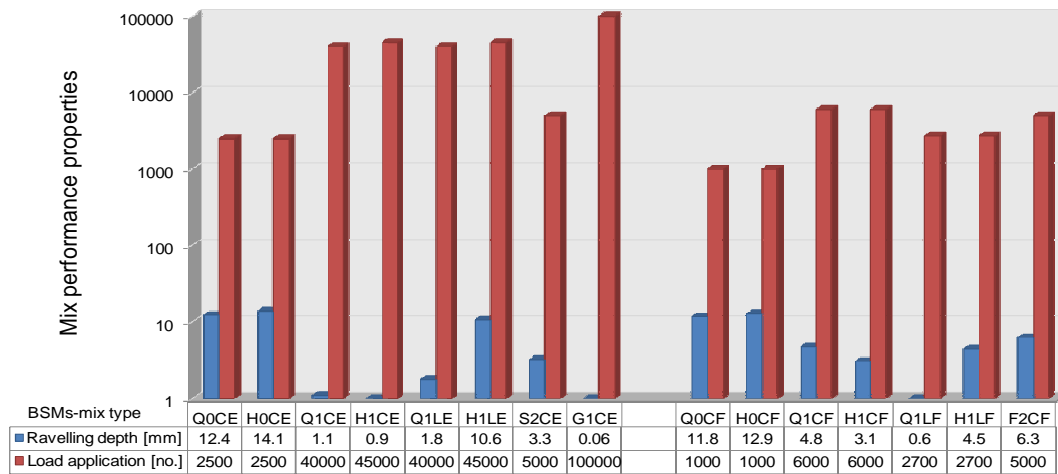


Figure 97: Cumulative number of load applications to failure of BSMs in wet condition at 25°C, 420kPa, 1.8kN and speed of 7 200 wheels per hour

In addition, Figure 97 shows that BSMs with less resistance to moisture damage can carry fewer load applications than BSMs with high resistance to moisture damage. In that case, the setting on MMLS3 with light wheel load and less tyre pressure shows an ability to screen mix susceptibility to moisture damage with considerable length of wheel load application. The impact of the addition of active filler on moisture resistance of the mix is significant. This is discussed in more detail in the following section.

4.5.2 Disintegration and ravelling of BSMs

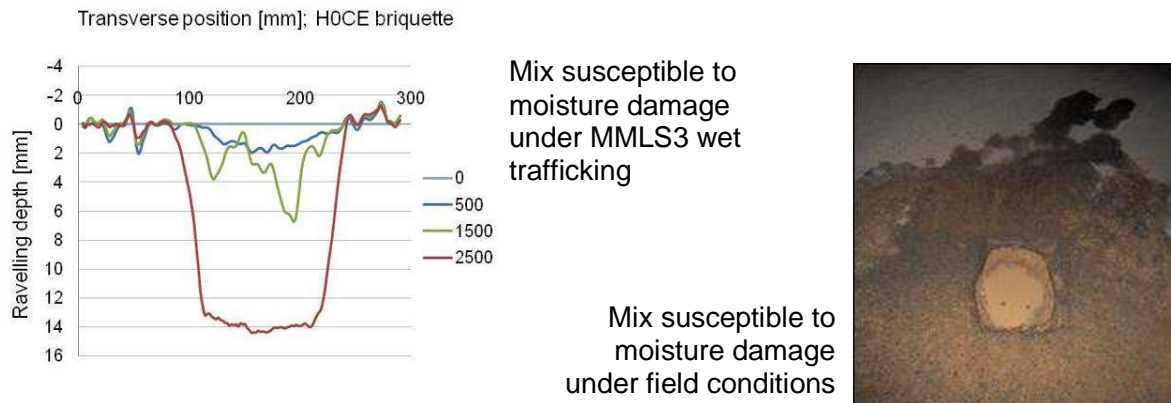
Disintegration of BSMs during wet trafficking can result from cohesive and/or adhesive failure. The consequence of this failure is accelerated ravelling potential under dynamic loading. The performance of BSMs is monitored during wet trafficking in the MMLS3 in two ways:

1. Surface disintegration through visual assessment for spalled aggregates at regular intervals and
2. Cohesion loss during wet trafficking; this is measured indirectly using a profilometer as the depth of ravelling accumulates.

Visual observation on the surface at intermittent times indicated no significant sign of cracks occurring, though micro cracks might develop in the matrix prior to ravelling. The profilometer readings on ravelling depth were taken transversely on each of the seven specimens and selected results are presented in Figure 99. The additional data on the profilometer readings of the studied BSM mixes is presented in Appendix D. The non-linear rate of ravelling is a dynamic process, that is once the ravelling begins, dynamic forces increase the wheel loads which accelerates the distress. Disintegration and ravelling are very sensitive to the surface finish at the start of the test.

The disintegration during MMLS3 testing shows that wet trafficking creates more damage in terms of cohesion loss or stiffness reduction than dry trafficking. This suggests that cohesion loss accrued under traffic and pore pressures in the presence of water aggravate the damage. Selected results on ravelling of BSM mixes with less resistance to moisture damage are presented in Figure 98. Figure 98a illustrates a transverse ravelling profile measured on wet trafficking after 2 500 cumulative wheel loads. The cohesion and adhesion loss observed in the field condition is explained in a similar manner. That means that upon widening of the micro cracks and surface water infiltration, the hydrodynamic effect on the moisture-susceptible base

materials will result in exponential erosion and ravelling. This consequently creates a pothole, as depicted in Figure 98b.



a) Transverse ravelling profile after MMLS3

b) Ravelling or pothole formation in the field after cracks and trafficking

Figure 98: Application of wet MMLS3 trafficking on screening mixes that are susceptible to moisture damage

4.5.3 The influence of active filler

The comparative results in Figure 98 and Figure 99 show that BSMs with no addition of active filler fail at a lower number of load applications (i.e. 2 500) compared to BSMs with additional active filler, which did not show sign of failure after 45 000 load applications. The influence of the addition of active filler in the form of cement is noted in Figure 99 where there is a significant reduction in ravelling e.g. for the Hornfels-RAP stabilised with emulsion and the addition of 1% cement (H1CE). A ravelling depth of 0.9mm after 45 000 wet MMLS3 trafficking cycles shows relatively good resistance to moisture damage compared to the same mix without the addition of active filler. The improvement of the adhesive behaviour with the addition of active filler has been apparent to mixes stabilised with either foamed bitumen or bitumen emulsion and with different types of mineral aggregates, that is Hornfels-RAP and Quartzite crushed stone.

The negative measurement observed in the transverse profile is not a heaving behaviour; instead, it indicates that profilometer measurement is sensitive to the surface levels and placement in the index bars. The peaks observed at 50mm in Figure 99 are the results of the un-even surface of exposed aggregates after compaction.

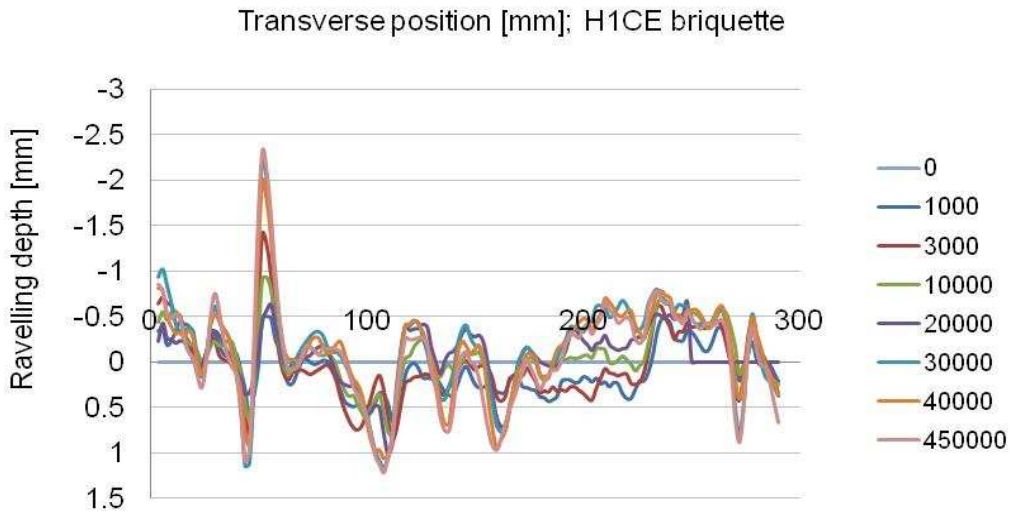


Figure 99: Disintegration behaviour of H1CE during MMLS3 wet trafficking at 25°C

It is evident from the results in this study that a link exists between the theoretical work of adhesion and cohesion on BSMs and moisture susceptibility. The bond formation mechanisms described in Chapter 3 clearly stipulate the influence of the addition of active filler in the adhesion behaviour of the binder and mineral aggregates. Thus, the addition of a small dosage of cement or lime (1%) is vital in improving moisture susceptibility. The improvement in adhesive behaviour with the addition of active filler has been apparent in both mixes with either foamed bitumen or bitumen emulsion and with different types of mineral aggregates, that is crushed stone and natural gravel.

Nevertheless, the addition of a small percentage of lime as an active filler in BSMs has shown a lower adhesive benefit compared to the addition of 1% cement in the same mix tested with wet MMLS3 trafficking. Figure 100 presents the deterioration model of BSM-emulsion of Hornfels-RAP with the addition of 1% lime or cement.

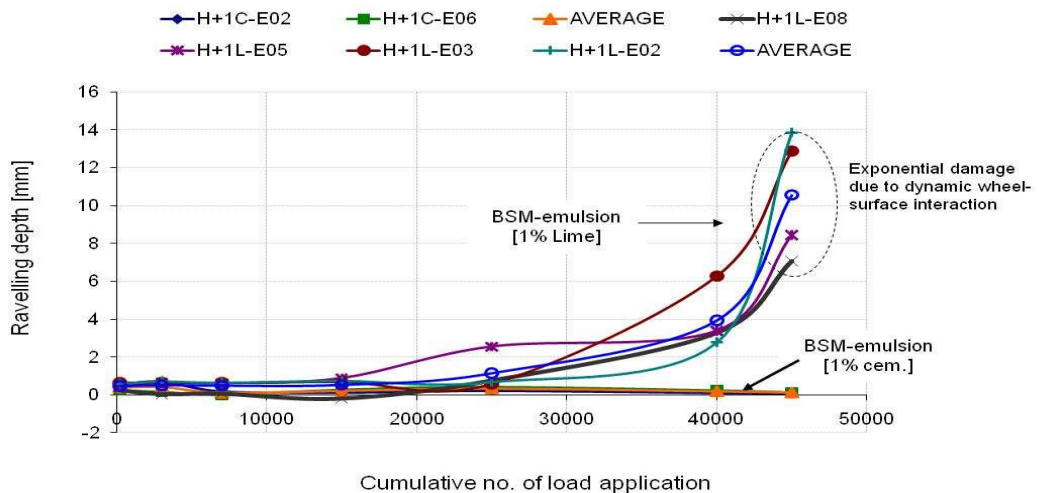


Figure 100: Ravelling depth of Hornfels-RAP material stabilised with emulsion and additional 1% cement or lime after 45 000 cycles of wet MMLS3 trafficking at 25°C

Based on the results of this study, it can be seen that arbitrary selection of a 1% lime has little benefit of improving the moisture resistance in BSMs. Therefore, it is recommended that initial consumption of lime (ICL) in the BSMs mixture is determined prior to application. In this way, the additional content of lime will provide similar adhesive behaviour to cement content.

4.5.4 Wet versus dry MMLS3 trafficking

Wet MMLS3 trafficking was done on a full saturated specimen (submerged in a water bath). Moisture ingress and saturation level of BSMs depends on particle interlock, particle type, binder content, compaction levels and permeability of the mix, among other factors. The disintegration during the MMLS3 tests shows that wet MMLS3 trafficking creates more damage in terms of cohesion loss or stiffness reduction than dry MMLS3 trafficking. Dry MMLS3 trafficking was done on specimens at equilibrium moisture content. Standard curing protocol of BSMs resulted in an equilibrium moisture content equal to 40%–50% OMC. Quartzite and Hornfels-RAP without the addition of active filler (lower cohesion) exhibit severe disintegration due to high void pore pressure under wet MMLS3 trafficking compared to similar mixes tested under dry conditions (see Figure 101 and Figure 102). Walubita *et al.* (2000) conducted MMLS3 tests in field conditions and indicate that much lighter wheel loads can cause more damage on the pavement through wet trafficking than could be achieved by full-scale trafficking under dry conditions.

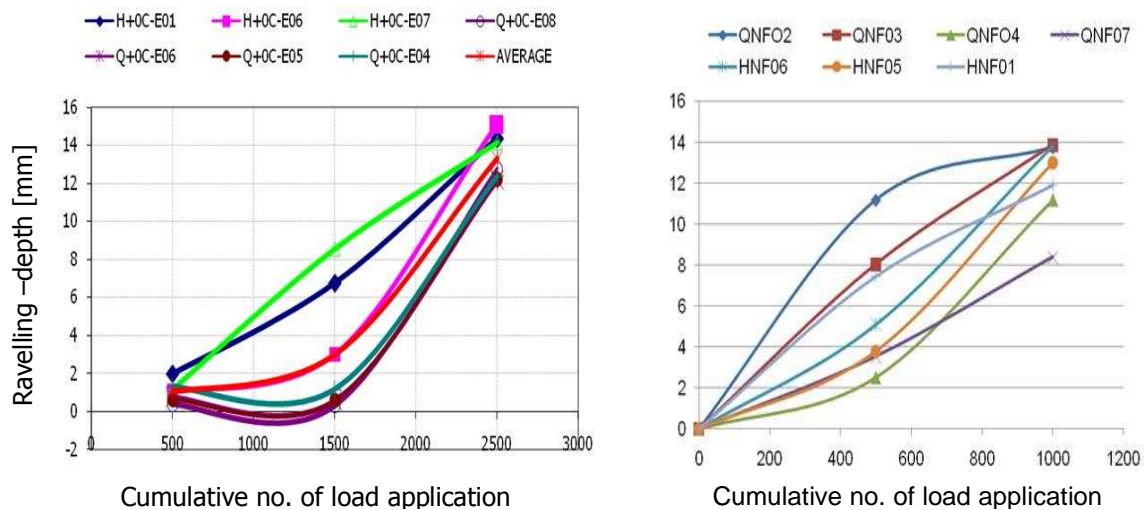


Figure 101: Ravelling behaviour of BSM-foam and BSM-emulsion without the addition of active filler, under wet MMLS3 trafficking at 25°C

BSM mixes without the addition of active filler have shown to be less resistant to moisture damage when tested under MMLS3 wet conditions. Hornfels-RAP and quartzite stabilised with bitumen emulsion and without additional active filler suffer 14mm ravelling depth at 2 500 load applications under wet trafficking (see Figure 101). Similar mixes tested under dry trafficking, at the same test conditions, show high resistance to ravelling with no sign of cracks observed (see Figure 102). The study of pavement deterioration using a Heavy Vehicle Simulator (HVS) reported by Maree *et al.* (1982) indicate that, when pavement structures are properly maintained (e.g. by crack sealing and proper surface drainage), moisture-susceptible materials, such as the one tested in Figure 101, might have a long remaining life in long-term durability performance. Therefore, selection of mix composition for BSMs highly depends on the climatic region.

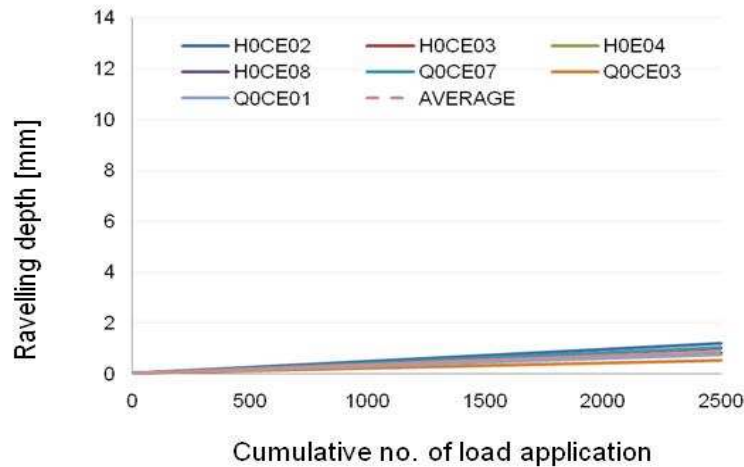


Figure 102: Ravelling behaviour of BSMs, which are less resistant to moisture damage under dry MMLS3 trafficking at 25°C

4.5.5 Influence of temperature

The wet MMLS3 trafficking and dry MMLS3 trafficking in this study was conducted at 25°C. However, field temperature in pavement layers can vary significantly, for instance from 5°C to 50°C (HMA guideline, 2001). The influence of a higher temperature might result in significant damaging effects in terms of cohesion loss or permanent deformation and stiffness reduction. In a broad range of climatic conditions of South Africa, moisture ingress and related damage can take place during winter rainfall or summer rainfall. However, during that period, the pavement surface temperature normally does not exceed 40°C. Therefore, due to the temperature gradient in BSM layers, as presented in Chapter 6, the effective temperature may not exceed 30°C. In this case, performing the wet MMLS3 trafficking at a temperatures ranging from 25°C–30°C can give a good indication of BSM mix susceptibility to moisture damage as it represents the prescribed field environmental conditions.

During MMLS3 trafficking, thermocouples were attached to the briquette to monitor the test temperature. The intermittently control of temperature from heating unit was necessary to ensure steady supply of heat.

4.5.6 Strength retained properties

After MMLS3 trafficking, the integrity of the specimens was further evaluated using an ITS test to determine the TSR from wet and dry wheel trafficking. The removal of briquettes needs to be done with precaution to avoid further damage. At least three specimens from every type of mix were tested. The ITS tests were performed at displacement controlled rate of 50.8mm/min and testing temperature of 25°C. The ITS wet and dry results from the tested matrix are summarised in Figure 103 while the additional test data is presented in Appendix D.

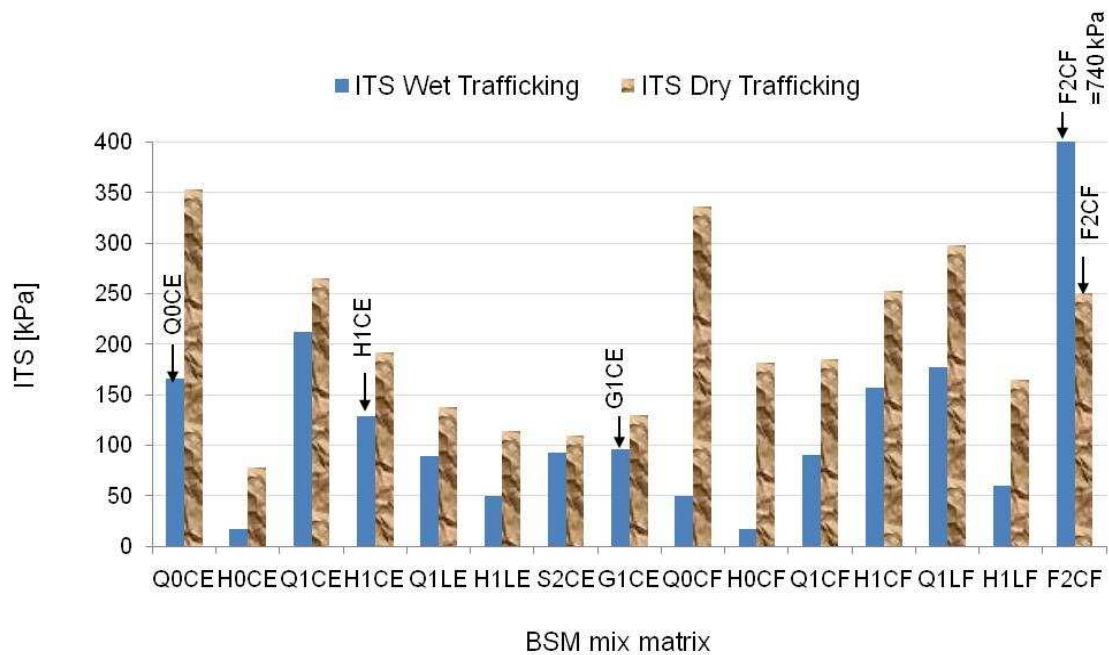


Figure 103: ITS values of BSMs after wet MMLS3 and dry trafficking

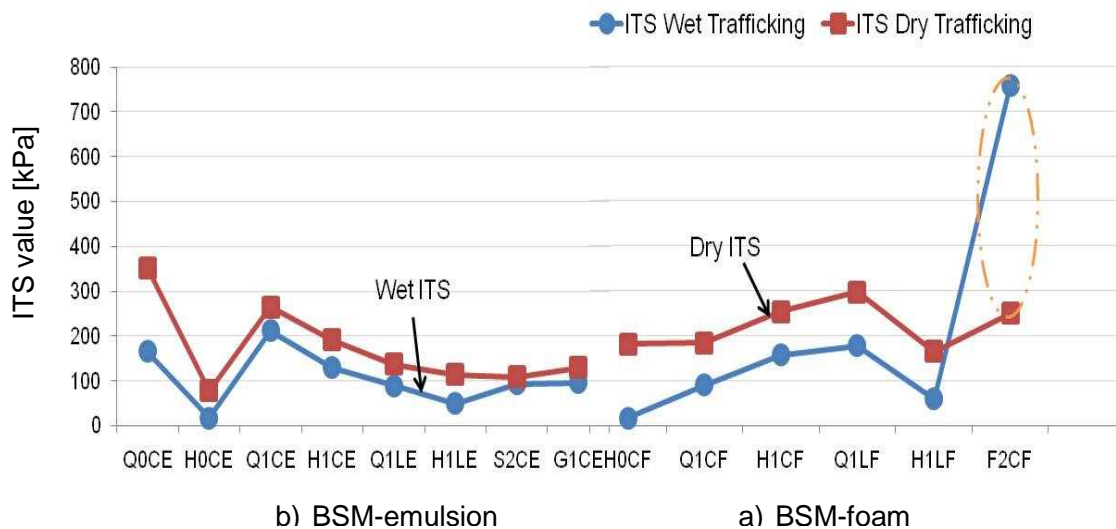


Figure 104: Superimposed values of wet ITS and dry ITS of different BSM mixes.

From Figure 104 and Figure 103, it is evident that the ITS of BSMs after dry MMLS3 trafficking is higher than the ITS after wet MMLS3 trafficking. However, the ITS results provide inconsistent results when isolating variables such as mix composition. A BSM without the addition of active filler, Q0CE (i.e. Quartzite stabilised with emulsion) has a higher ITS value than Hornfels-RAP stabilised with emulsion and additional active filler (H1CE) after dry trafficking. However, when these mixes are compared in terms of number of load applications or ravelling depth of wet MMLS3 trafficking, H1CE performs significantly better than Q0CE. Similar observation is noted for BSM mix (G1CE) cured in a long period (nine months) which shows lower ITS values

compared to significant performance in terms of ravelling depth (< 2mm) after 1 000 000 number of load applications.

Further, the evaluation of MMLS3 trafficking on the field cores stabilised with foamed bitumen (F2CF) yielded higher ITS values after wet trafficking than dry trafficking. This behaviour is contrary to the findings of the ravelling analysis after wet MMLS3 and dry trafficking and also when compared with field cores stabilised with bitumen emulsion (S2CE). These inconsistencies are expected from ITS testing. Therefore, these tests should be regarded as indicator tests for BSMs. Nevertheless, screening of BSMs for moisture susceptibility using TSR continues to be applied globally and is based on a performance limit of 75%. BSMs with a TSR value of higher than the performance limit are considered highly resistant to moisture damage (see Figure 105). Of the materials evaluated in this research, only Quartzite crushed stone stabilised with bitumen emulsion and 1% cement complied with such a criterion for moisture resistance. Yet, evaluating the depth of ravelling after wet MMLS3 trafficking, mixes such as BSM-emulsion Hornfels-RAP with 1% cement or lime rank as highly resistant to moisture damage. Therefore, the TSR criterion applied on its own can result in the exclusion of some acceptable BSMs. In this study, the developed MIST/triaxial testing shows a reliable ranking of BSM moisture susceptibility with good correlation to wet MMLS3 trafficking.



Figure 105: Tensile Strength Retained values for the BSMs after MMLS3 wet and dry trafficking at 25°C.

4.5.7 Classification of moisture damage

Evaluation of the ravelling behaviour of BSMs using MMLS3 has shown potential as a surrogate method for classifying BSMs in terms of their moisture resistance. The testing realistically simulates field conditions where moisture damage would occur and accelerates the rate of deterioration into an acceptable time frame. Nevertheless, the question remains: “where are the boundary limits for MMLS3 testing for classification of BSMs?”

The composite representation of different mixes of BSMs that have been evaluated using the MMLS3 provide insight into the determination of classification limits. The ravelling potential of different BSM mix combinations is shown in Figure 106. This range of BSM combinations has shown that the mixes can be classified into three categories: poor, moderate

and good in terms of moisture resistance. Some of these mixes are of known full-scale performance, which assists in validating these classes.

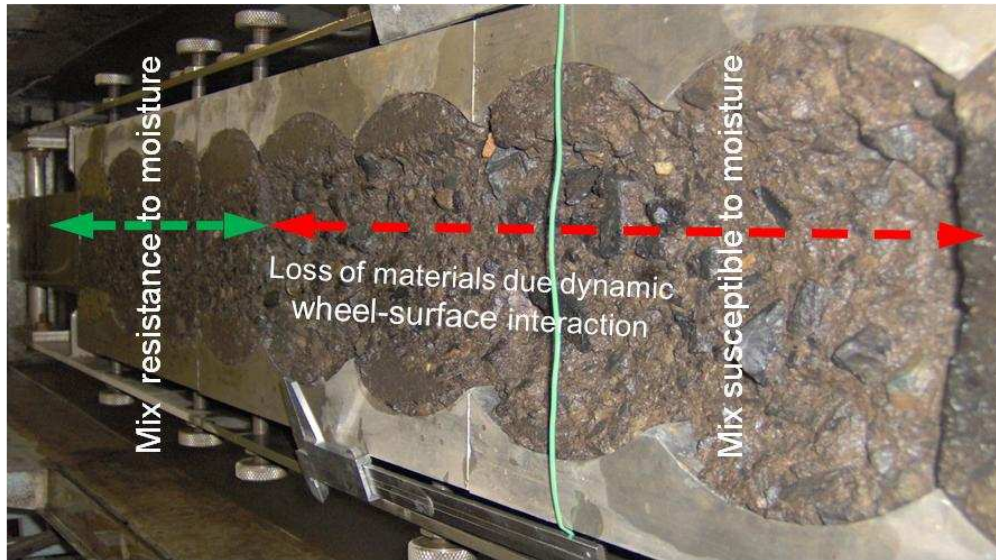


Figure 106: Ravelling behaviour of different BSM mixes (H1LE and H1CE) under wet MMLS3 trafficking after 45 000 load applications at 25°C

Wet MMLS3 trafficking is required to be run to a maximum of 50000 load cycles for BSMs classification. A depth of ravelling of 5mm appears to be a critical boundary between severe loss of cohesion in BSMs and moderate cohesion reduction (i.e. stiffness loss) (see Figure 107). BSM mix classification based on MMLS3 wheel load repetitions can be defined as:

- BSMs marked A and C with depth of ravelling greater than 5mm, after 3000 wet trafficking illustrate a POOR BSM classification and
- BSMs marked D with depth of ravelling greater than 2mm and less than 5mm, after 6000 wet MMLS3 trafficking illustrate a MODERATE BSM classification
- BSMs with depth of ravelling less than 2mm, after 15 000 wet MMLS3 trafficking illustrate a GOOD BSM classification

∴

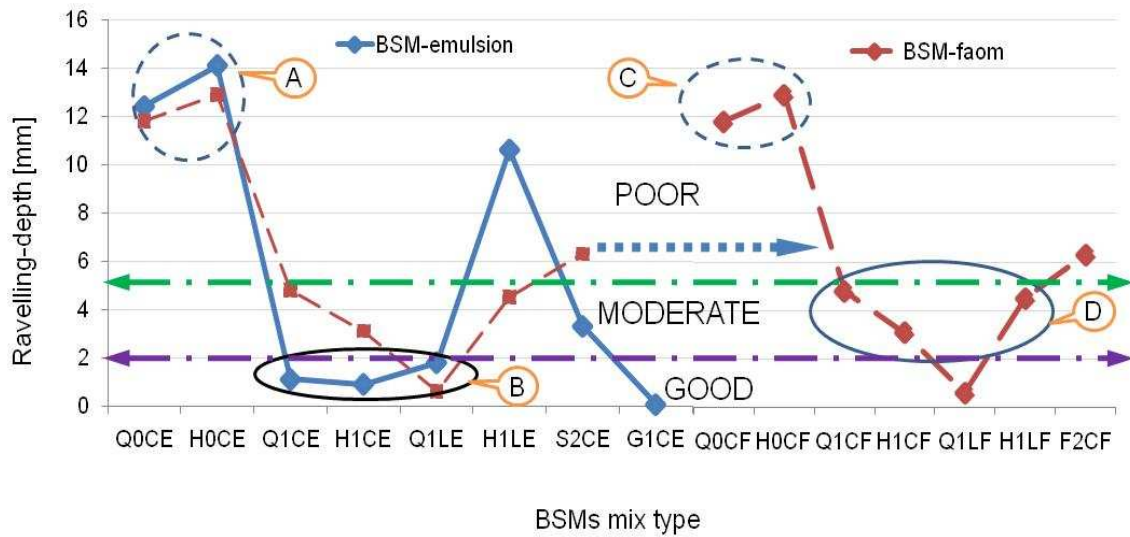


Figure 107: Potential classification of BSMs using ravelling depth after wet MMLS3 trafficking at 25°C

Although it is possible to discern some sub-groups, practically it is not helpful to use these classes. The comparative ravelling model for different BSM mixes is presented in Figure 108. The possible classifications of BSM-emulsion or BSM-foam, tested in this study in terms of ravelling potentials after wet MMLS3 trafficking, show that an accelerated MMLS3 testing procedure can be used to screen BSMs that have good to poor resistance to moisture damage.

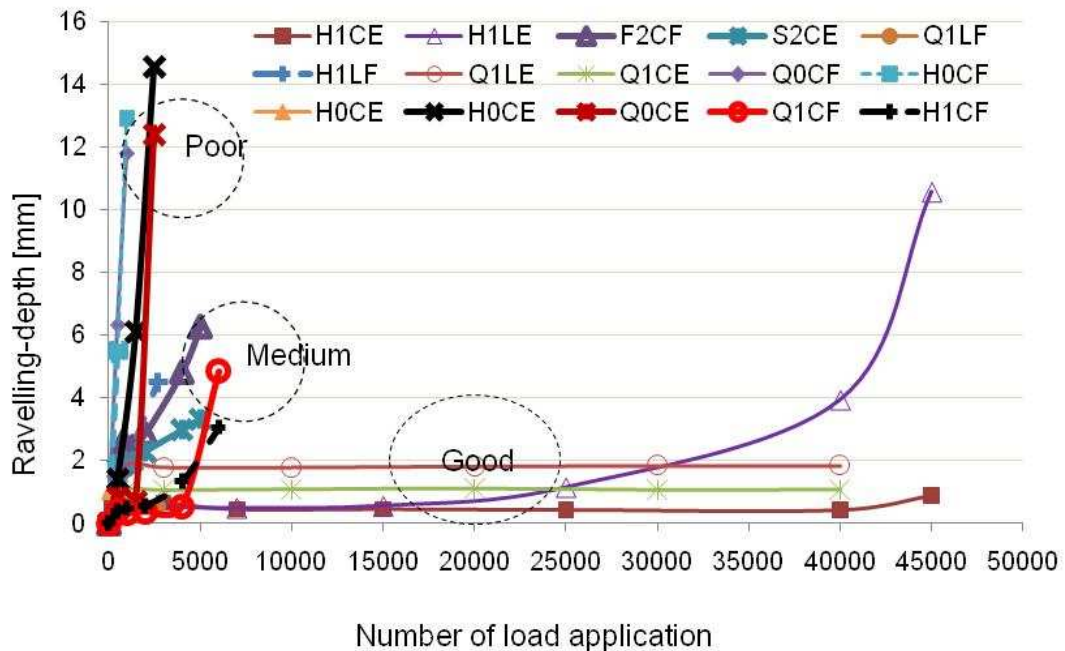


Figure 108: Ravelling model for wet MMLS3 trafficked BSMs at different number of MMLS3 wheel load applications at 25°C.

The ravelling model established during wet MMLS3 trafficking can be correlated with the laboratory triaxial permanent deformation. This provides a better understanding of the durability behaviour modelled in the laboratory compared to actual field environments. The influence of the addition of active filler (cement or lime) in BSMs in mitigating pavement distress, in particular shear properties, is substantial. That means that adhesion and cohesion are enhanced, which in turn significantly influences the durability properties and long-term performance.

4.6 CONCLUSIONS

The resistance of BSMs to moisture damage was investigated using the APT (MMLS3) device approach. The approach employed included trafficking of BSMs specimens under full saturated conditions to achieve the following objectives:

- Establish a laboratory APT test procedure that realistically simulates moisture exposure of BSMs through development of a new protocol for the MMLS3.
- Validate the performance of BSMs under MMLS3 trafficking to the change in mechanical properties, as assessed with ITS testing.
- Validate the moisture resistance of BSMs by selecting component materials of known field performance.
- Establish applicable limits for the BSMs classification in terms of moisture susceptibility.

Based on the findings of the study, the following conclusions can be drawn:

- The MMLS3 test procedure can be adapted from the HMA protocol to be used for BSMs so that representative wheel loads and tyre pressures can be applied to specimens under controlled moisture conditioning, to evaluate susceptibility to moisture related distress that has been induced in a realistic manner.
- The test setup variables that should be used for MMLS3 testing on BSMs briquettes, trafficked wet and dry, include tyre pressure = 420kPa, wheel load = 1.8kN and loading rate = 7200 wheel repetitions per hour. These settings provide acceptable number of load applications for suitable differentiation between levels of moisture resistance of BSMs.
- Vinite or reinforced rubber mat are suitable materials to apply to the surface of BSMs specimens in a wet MMLS3 test, as a protection against the direct abrasion of the wheels. The thinness and flexibility of the vinite layer does not compromise stress distribution of the briquettes nor the pore pressure induction during wheel trafficking.
- MMLS3 trafficking of BSMs specimens submersed in water, results in significant distress in terms of ravelling and reduction in tensile strength. This does not occur under dry trafficking conditions. It is apparent that the mixes lose cohesion (and most likely stiffness) due to moisture damage that is activated by dynamic pore pressures.
- The inclusion of active filler and especially cement in BSMs is vital for an improvement in moisture resistance. The results indicate that BSMs with the addition of 1% cement have significantly lower moisture susceptibility than BSMs with the addition of lime or no active filler.
- An attempted validation of Indirect Tensile Strength ITS, Tensile Strength Retained TSR and Ravelling-Depth highlights the uncertain nature of the TSR in measuring moisture related resistance of BSMs. TSR does assist in identifying moisture susceptible BSMs, but it also yields “false-positives” i.e. BSMs that would classify as moisture susceptible, but in reality would perform well. Therefore, TSR can be used as an indicator for further evaluation and classifications using other test methods, e.g. RvD or RC.

REFERENCES

- Asphalt Academy, 2009. A guideline for the design and construction of bitumen emulsion and foamed bitumen stabilised materials. TG2. Technical guideline: Second edition. Pretoria, South Africa.
- Bondiotti, M., Murphy, D., Jenkins, K. and Burger, R. 2004. Research on the stabilisation of two different materials using bitumen emulsion and cement, Proceedings of the 8th Conference on Asphalt Pavements for Southern Africa, Sun City, South Africa,
- Erkens S.M.J.G. 2002. Asphalt concrete response (ACRe)-Determination, modelling, and prediction. PhD Dissertation published at the Delft University of Technology, The Netherlands, pg 29.
- Hugo F. and Epps A.L. 2004. NCHRP Synthesis 325. Significant findings from full-scale accelerated pavement testing. TRB, National Research Council, Washington D.C.
- HMA Guidelines. 2001. Interim guidelines for the design of hot-mix asphalt in south Africa. prepared as part of the hot-mix asphalt design project. CSIR. Pretoria
- Jenkins KJ, van de Ven M.F.C., 1999. Investigation of the performance properties of the Vanguard drive pavement recycles with foamed bitumen and emulsion respectively and analysed using MMLS3. ITT Report 9-1999. University of Stellenbosch. South Africa.
- Maree J.H. Freeme C.R. and Kleyn E.G. 1982. Heavy vehicle simulator testing in South Africa. International colloquium full-scale pavement. Institute fur Eidgenossischen Hochschule, Zurich, Switzerland, pp 54-69.
- Nikajima Y., Seta E., Kamegawa T. and Ogawa H. 2000. Hydroplaning analysis by FEM and FVM: Effect of the rolling and tire pattern on hydroplaning. International journal of automotive technology, Vol. 1 no.1 pp 26-34.
- Stellenbosch University Institute of Transport Technology, 2008. DPG1 – Method for evaluation of permanent deformation and susceptibility to moisture damage of bituminous road paving mixtures using the *Model Mobile Load Simulator (MMLS3)*. First Draft Version 3 Rev1, South Africa.
- van der Riet J. 2007. Moisture resistance on recycled materials. BEng. Dissertation, Department of Civil Engineering, Stellenbosch University. South Africa
- Walubita L.F., Hugo F., and Epps A. 2000. Performance of rehabilitated lightweight aggregates asphalt concrete pavement under wet and heated model mobile load simulator trafficking: A comparative study with the TxMLS, Report no. 1814-3, Centre for transportation research at the University of Texas at Austin. USA.

CHAPTER 5

ADVANCED CHARACTERISATION OF MOISTURE DAMAGE

5.1 INTRODUCTION

Most publications about durability behaviour of BSMs provide procedures for the identification of moisture damage using empirical methods. These methods do not take cognisance of or attempt to account for the mode of failure found predominantly in BSMs. The material properties of BSMs are commonly derived from stress-strain behaviour. Stresses to which materials are subjected in a pavement are overlying weight, which is constantly vertical and horizontal at any point in the pavement area. In addition, the traffic-induced stresses that are vertical (σ_v), horizontal (σ_h) and shear (τ). This occurs in a pavement as a result of repeated applications of moving wheel loads. The horizontal and shear stresses normally develop as an element of the material is loaded and deformed against neighbouring materials. These stresses are thus a function of the applied vertical stress and of the material's response or behaviour. From the relationship of stress-strain (σ - ϵ) curves of failure, a distinctive aspect of the mechanical behaviour (i.e. static failure, resilient deformation or permanent deformation) can be related and analyzed for moisture damage. The σ - ϵ curves determined under both monotonic and repeated loading demonstrate that the response of BSMs is that of stress-dependent material. Stress-dependent materials can accurately be modelled using triaxial testing.

In a triaxial test, the applied vertical stress (σ_v) and horizontal confining stress (σ_h) are by definition principal stresses. To establish the mechanical behaviour of material accurately, it is necessary to measure specimen deformations under the applied stress directions and magnitudes. However, this requires measurement of the deformation on the specimen over the middle uniformly stressed part of the specimen. Therefore, the specimen should have a height to diameter ratio of 2 in order to account for the friction of the applied dead weight, and a specimen diameter to a maximum grainsize ratio of at least 5–7. These requirements dictate the dimension of the triaxial test specimen, for example 150mm x 300mm.

In this chapter, the fundamental factors that influence moisture damage behaviour of BSMs are investigated. Triaxial (static and repeated loading) testing under stresses and saturation was used in advance characterisation of the moisture damage from stress-strain behaviour. The selections of test variables for triaxial testing such as deviator stress and deviator stress ratio were based on the review of the analysis on similar BSMs reported in the past study. The monotonic loading test at different horizontal confined stress (σ_3) levels was performed to establish failure behaviour. The failure behaviour is described using the Mohr-Coulomb failure criterion (C and ϕ). Repeated loading tests (using single parameters) on various materials were performed to establish stiffness behaviour under different saturation conditions. A repeated long dynamic loading test was performed up to a high number of load applications ($N = 1$ million) on a limited number of different specimens at different stress ratios. This was done in order to establish the influence of moisture damage on the plasticstrain behaviour of BSMs with N and stress ratio.

5.2 DETERMINATION OF MOISTURE DAMAGE THROUGH TRIAXIAL TESTS

The change in material properties due to moisture ingress, coupled with traffic and the environment conditions, have been indicated to be primary causes of BSM failure. Triaxial tests have been identified to be the most appropriate method of determining BSM behaviour. However, it has not been perceived by practitioners as a tool for material selection during mix design. This is due to its complex nature in its application and data acquisition. However, in 2008 the development of the simple triaxial test (STT) device (Mulusa, 2009) at Stellenbosch University cleared this uncertainty. The research on STT has shown that BSM behaviour can be better understood and modelled accurately. This makes it possible to classify and select BSMs properly for mix design based on performance. Nevertheless, current setup of the STT is only applicable for static (monotonic) tests. In this study, not only monotonic tests were researched; additional procedures such as short and long dynamic tests were used for advanced moisture damage characterisation. In this regard, the research triaxial test (RTT) device was used for the fundamental understanding of BSM moisture susceptibility. The flow diagram in Figure 109 illustrates the testing method and selected parameters applied during triaxial testing.

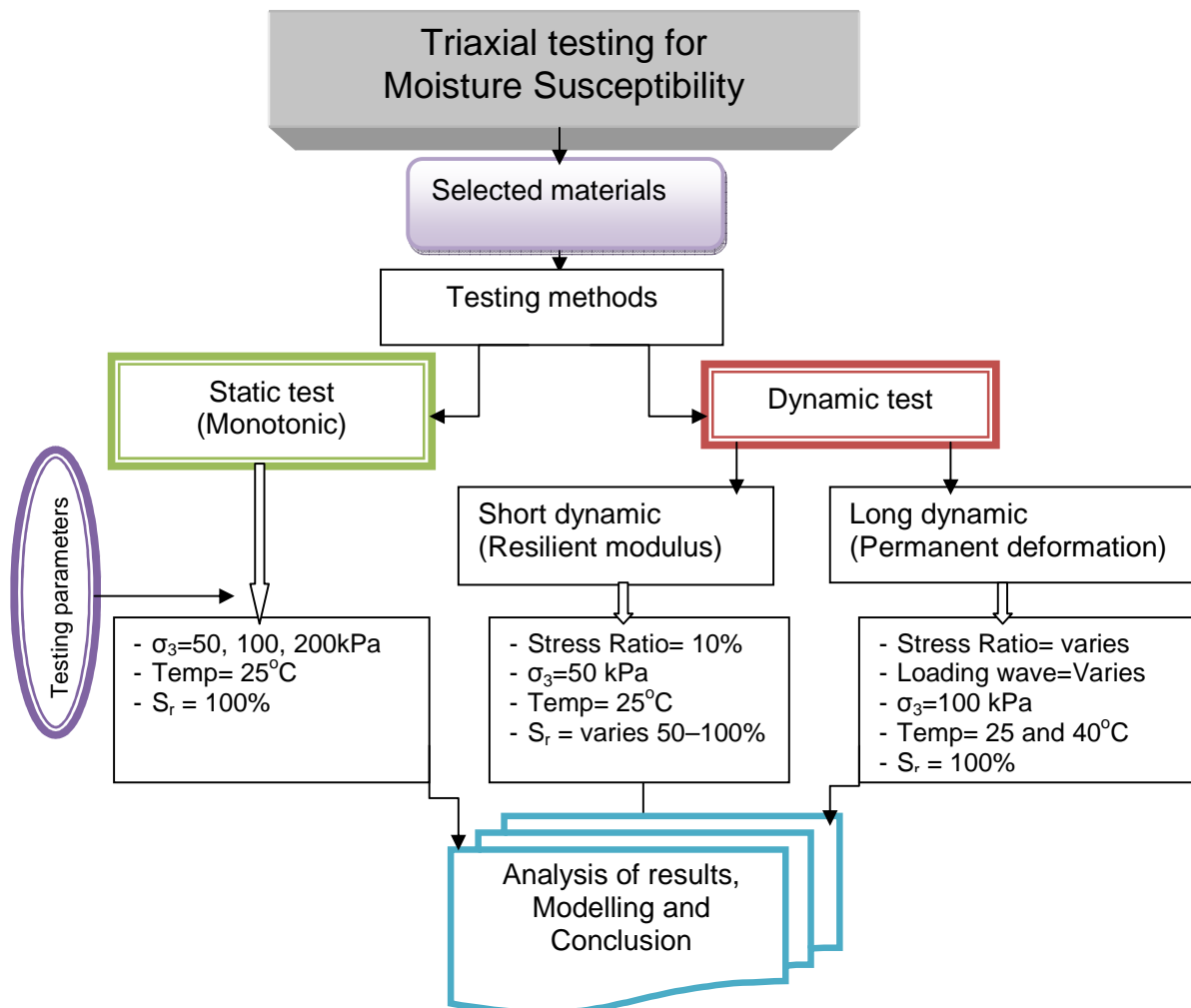


Figure 109: Flows diagram illustrating the triaxial testing methods for moisture susceptibility

5.2.1 Selection of mixes

The materials selected for triaxial testing were the same to the ones described in Chapter 3. Two different continuous graded materials, Hornfels-RAP and Quartzite crushed stone, were used in this study. The mixes, which include two binder types (foamed bitumen or bitumen emulsion) with or without the addition of active filler (1% cement and 1% lime), were prepared for triaxial testing. Material properties such as grading, compaction level and method, mixing methods, moisture content, curing method and void content are presented and discussed in detail in Chapters 3 and 6. Therefore, these are not repeated in this chapter.

The repeated long dynamic loading triaxial test or permanent deformation test, a limited number of mixes were investigated. These were the ones observed to have high and low resistance to moisture damage during MIST and monotonic triaxial testing, and also after MMLS3 wet trafficking. Mixes such as Hornfels-RAP stabilised with bitumen emulsion and 0% and 1% cement were selected for the permanent deformation test. This is because permanent deformation usually takes a long time before the specimen realises tertiary flow. Depending on specimen performance a test can run up to one million load repetitions or six days continuously until termination of the test. The available timeframe for completing laboratory testing did not allow a full matrix investigation of the testing variables mentioned in Chapter 3. For this reason, a limited number of variables were identified and investigated for advanced moisture damage characterisation.

5.2.2 Triaxial test methods

The triaxial test setup for this study utilised a hydraulic actuator and a closed feedback loop control system. The capacity of the load cell and actuator, including calibration and data acquisition systems has been described in Chapter 3, page 137. The triaxial testing method adopted for the characterisation of moisture susceptibility of BSMs includes static (monotonic), short dynamic [M_r] and long repeated dynamic [ϵ_p] testing. These tests measure the;

- Monotonic shear failure behaviour,
- Resilient deformation behaviour,
- Permanent deformation behaviour, described as follows:

5.2.2.1 Monotonic shear failure behaviour, (C and ϕ)

Monotonic shear failure tests were conducted on the materials studied to determine the fundamental shear properties (i.e. angle of internal friction ϕ and cohesion C) after the ingress of moisture. An envelope that is plotted in the Mohr-Coulomb space, that is normal stress and shear stress conditions, describes compression mode of failure of BSMs. From the monotonic failure tests, the angle of internal friction ϕ and cohesion C can be obtained using the Mohr-Coulomb model. The ratio of stresses within BSMs to the failure stresses have been related closely to the response of the materials in terms of resilient modulus and permanent strain (Jenkins, 2000; Ebels, 2008).

Mohr-Coulomb: According to the Mohr-Coulomb criterion, shear strength increases with increasing normal stress on the failure plane, as indicated in Equation 25.

$$\tau_f = C + \sigma_{1,f} \cdot \tan \phi \quad \text{Equation 25}$$

where τ_f = shear stress on the failure plane; $\sigma_{1,f}$ = major principle stress at failure; C = the cohesion of the material; ϕ = angle of internal friction.

A tangent line between two Mohr-Coulomb circles of stress, obtained from two monotonic failure tests at different confining stresses, is used to approximate the failure envelope for BSMs. A third test, conducted at a different confining pressure, creates more reliability to define the envelope shape. A regression line is usually fitted through the three data

circles to determine failure criteria. Such an approach to defining the shear parameters is considered applicable to BSMs with lower binder content (less than 4%) according to Jenkins, (2000). The major principal stress σ_1 in the Mohr-Coulomb circles is defined as the applied failure stress plus the confining pressure σ_3 , σ_2 and the stress of the dead weight on top of the specimen σ_{dw} (loading plate and piston).

$$\sigma_1 = \sigma_{a,f} + \sigma_3 + \sigma_{dw} \quad \text{Equation 26}$$

The major principal stress at failure condition $\sigma_{1,f}$ can be defined geometrically using a relationship between the failure parameters C and ϕ and the minor principal (confining) stress σ_3 , as described in Equation 26.

$$\sigma_{1,f} = \frac{(1 + \sin \phi) \cdot \sigma_3 + 2 \cdot C \cdot \cos \phi}{(1 - \sin \phi)} \quad \text{Equation 27}$$

The relationship between the major principal stress $\sigma_{1,f}$ and the minor principal stress σ_3 is considered to be linear, therefore expressed as shown in Equation 27 and Equation 28.

$$\sigma_{1,f} = A \sigma_3 + B \quad \text{Equation 28}$$

where A and B are defined as follows:

$$A = \frac{1 + \sin \phi}{1 - \sin \phi} \quad \text{and} \quad B = \frac{2 \cdot C \cdot \cos \phi}{(1 - \sin \phi)} \quad \text{Equation 29}$$

The Mohr-Coulomb criterion is expressed in terms of maximum and minimum principal stresses. Hence, it does not incorporate the effect of intermediate principal stresses. The shear parameters C and ϕ can be determined from laboratory tests. The failure line is fitted in the envelope of the Mohr-Coulomb circles and the values of C and ϕ could be determined as shown in Figure 110.

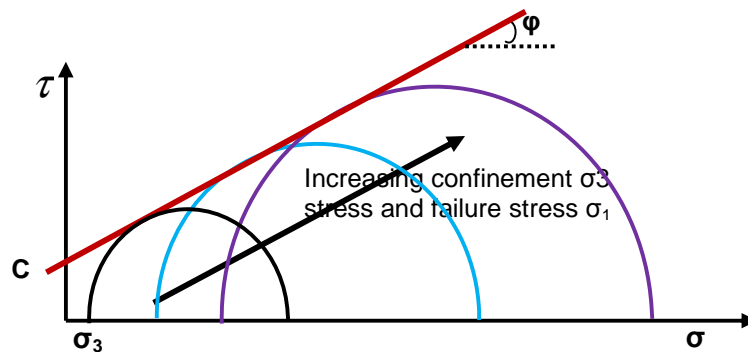


Figure 110: Stress (Mohr-Coulomb) circles at failure and determination of shear parameters

The monotonic triaxial tests in this study were conducted at 25°C in a displacement-controlled mode. The applied displacement rate was 5.25mm/min (strain rate of 2.1%/mm/minute at height of 250mm) and confining air pressure of 50kPa, 100kPa and 200kPa. The results of dry and conditioned (saturated) specimens are presented in section 5.4.1.

5.2.2.2 Resilient deformation failure behaviour (M_r)

The resilient behaviour of BSMs can be tested in a triaxial setup by applying relatively low stresses creating low strains so that the elastic range of materials is not exceeded. It is assumed that, within this elastic range, stress history does not affect the material's response. The selection of a range of stress magnitudes, in terms of a combination of deviator stress and confining stresses, allows the non-linear resilient deformation behaviour to be analyzed on one specimen. Because the number of load applications in resilient deformation is limited, that is permanent deformation is restricted, it was possible to test resilient modulus in one specimen at different saturation levels. Resilient modulus testing was carried out by using the failure parameters obtained in the monotonic results tested at a confining pressure of 50kPa. After the resilient modulus test, the same specimen was tested for the shear failure at an increased confinement of 100kPa. The resilient modulus was determined after 5 000 load cycles to allow for initial seating of axial strain as described in Figure 111.

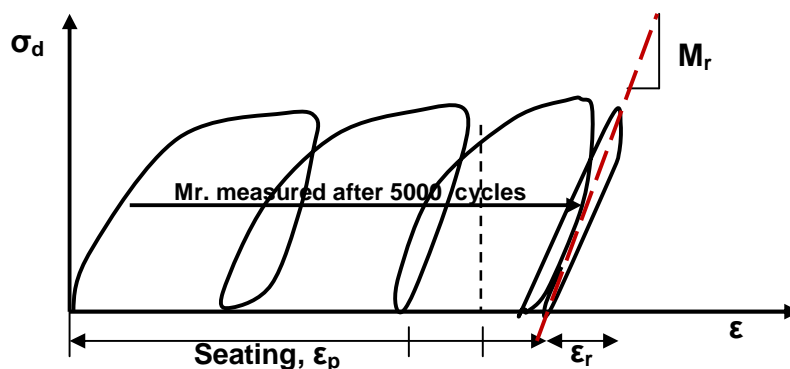


Figure 111: Descriptions of the resilient deformation test, showing seating axial strain

The short dynamic triaxial test was carried out at 25°C. The deformation in the specimen was measured by external LVDTs positioned under the triaxial cell. The applied load consisted of a haversine waveform and a pre-load (seating stress) of 20kPa. A test frequency of 2Hz and no rest period were included in the loading. The loading level was selected with care so as not to overstress the specimen under saturation. The stress ratio (deviator stress σ_a to deviator stresses at failure $\sigma_{d,f}$) of 10% and a confining pressure of 50kPa were applied. The intention of applying a single variable during short dynamic loading was to determine the influence of pulsing water pressure into a triaxial specimen on the stiffness properties. In that way, quantification and comparison of moisture damage mechanisms in different BSM mixes was possible.

The seating axial strain was subjected to 5 000 conditioning cycles prior to the measuring of the stiffness response (Figure 111). Load and displacement data were sampled using Spider 8 at a frequency of 800 Hz for a duration of 5 seconds. Figure 112 and Figure 113 show a sample of data collected during the test. The test results and discussion are presented in section. 5.4.2

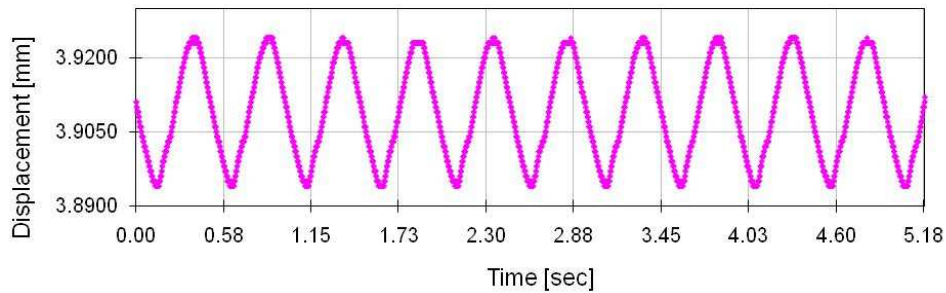


Figure 112: Typical LVD's displacement data captured at 800 Hz with 10% stress ratio and 50 kPa confining pressure at 25°C

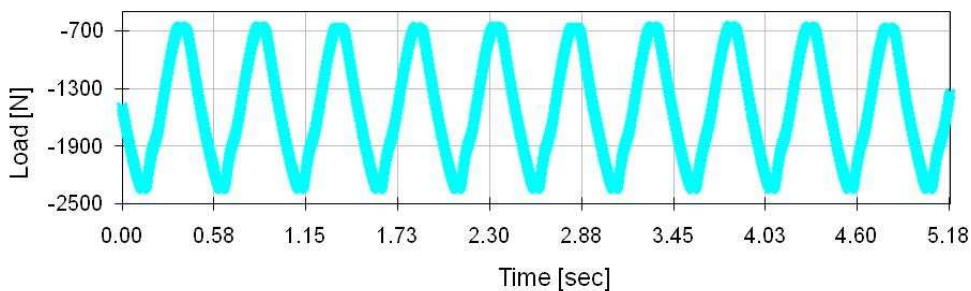


Figure 113: Typical loading data captured at 800 Hz with 10% stress ratio and 50 kPa confining pressure at 25°C

5.2.2.3 Permanent deformation failure behaviour (ϵ_p)

A permanent deformation test was performed in a triaxial setup by means of repeated load applications for the controlled deviator stress ratio. Tests were carried out on dry and wet (conditioned) specimens at the same deviator stress ratios and confining pressure. In that way, it was possible to understand the plastic strain behaviour of the mixes due to the effect of moisture damage. The quantification of permanent strain was aimed at investigating this behaviour at different loading waveforms and temperatures. The selected variables are presented as following:

- o Loading waveform = haversine no rest period and square wave
- o Frequency = 2Hz
- o Temperature = 25°C and 40°C
- o Mix type = H1CE and H0CE (resistant to moisture damage and susceptible to moisture damage respectively)
- o Stress ratio = 40%
- o Confining pressure = 100kPa

The failure criteria for the permanent deformation test were limited to total axial stain of 4% or 1 million load repetitions, whichever come first. The permanent deformation test on H1CE (saturated and dry) at stress ratio 40%, confining pressure 100kPa and temperature 25°C or 40°C did not reach flow state at 1 million load repetitions. Therefore, in order to determine the distinguishable failure behaviour under dry and wet conditions, step-up of deviator stresses criteria were applied. In a multi-stage permanent deformation test, a different stress ratio was selected starting from 40% then increased at intervals of 10% to 80%. The change in stress level was measured after each 50 000 load applications. The stress path numbers are indicated in Figure 114.

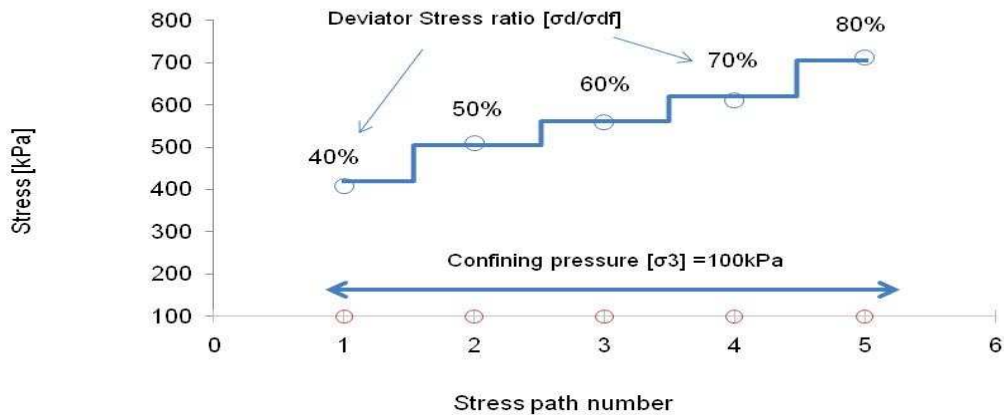


Figure 114: Sequence of deviator stress ratio in multi-stage permanent deformation testing at constant confining stress 100 kPa

The ϵ_p tests were performed based on a designated waveform at a frequency of 2Hz. Due to limitation in the triaxial set-up, testing at a higher frequency is not possible. The reason being, the loading piston in the MTS equipment is fixed and the triaxial cell is moving up and down from bottom against the fixed loading piston. The constant σ_3 value of 100kPa was applied in all tests. During testing, the total plastic strain was recorded manually by reading from a MTS controller. The axial deformation is measured over the entire height of the specimen by the vertical LVDT within the MTS actuator. At the early stage of the axial deformation, the measurement interval was short. However, as the rate of permanent deformation accumulation decreased, these intervals were increased. The typical measurement intervals were as follows: 0, 20, 50, 100, 200, 500, 1000, 2000, 5000, 10 000, 20 000 and 50 000. After the last measurement, the step-up stress ratio was applied and measurements recorded in the longer interval as no seating takes place. These longer interval measurements are 500, 1000, 2000, 5000 10000, 20000 50000, and so forth, until failure or reaching designed maximum stress ratio.

5.3 MOISTURE DAMAGE CHARACTERISATION USING TRIAXIAL PROPERTIES

Stress ratio in BSMs is used as an indicator of stress state's relationship to the failure envelope. Jenkins (2000) recommends the use of deviator stress ratio ($\sigma_d/\sigma_{d,f}$) in lieu of failure stress ratio ($\sigma_1/\sigma_{1,f}$). The advantage thereof is that the deviator stress ratio is not influenced by the confinement pressure levels while principal stress ratio is. At decreasing friction angle ϕ or where σ_3 is a tensile stress, the difference becomes more evident. Therefore, sensitivity in moisture susceptibility was compared between deviator stresses (at 50kPa or 100kPa) and retained cohesion (RC). The sensitivity analysis is presented in Figure 115 and Figure 116. It can be seen from the results that the deviator stresses after moisture ingress are less sensitive to moisture damage, at different confinement 50kPa and 100kPa the tests yields similar ranges of differences. That means, using the deviator stress ($\sigma_{d-dry}/\sigma_{d-wet}$) or deviator stress at failure ($\sigma_{d,f-dry}/\sigma_{d,f-wet}$) after MIST conditioning and triaxial testing, the BSM mixes cannot be clearly distinguished with respect to moisture susceptibility. The trend line for retained cohesion seems to be sensitive, with a significant shift for moisture-susceptible BSMs (e.g. H0CF and Q0CF)

compared to moisture-resistant mixes. For the mixes with high moisture resistance (e.g. Q1CF, H1CE and Q1CE) deviator stresses and RC show comparable results. Therefore, it can be recommended that moisture susceptibility in BSMs be determined using retained cohesion rather than deviator stress or deviator stress at failure.

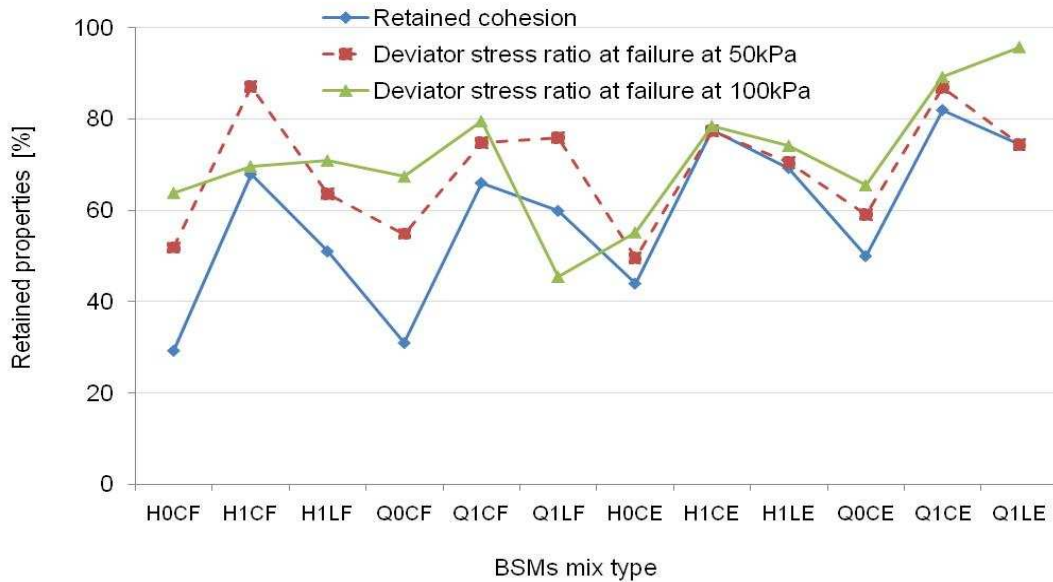


Figure 115: Comparison of moisture sensitivity of BSMs between retained cohesion (RC) and deviator stress ($\sigma_{d-dry}/\sigma_{d-wet}$) at 50kPa and 100kPa

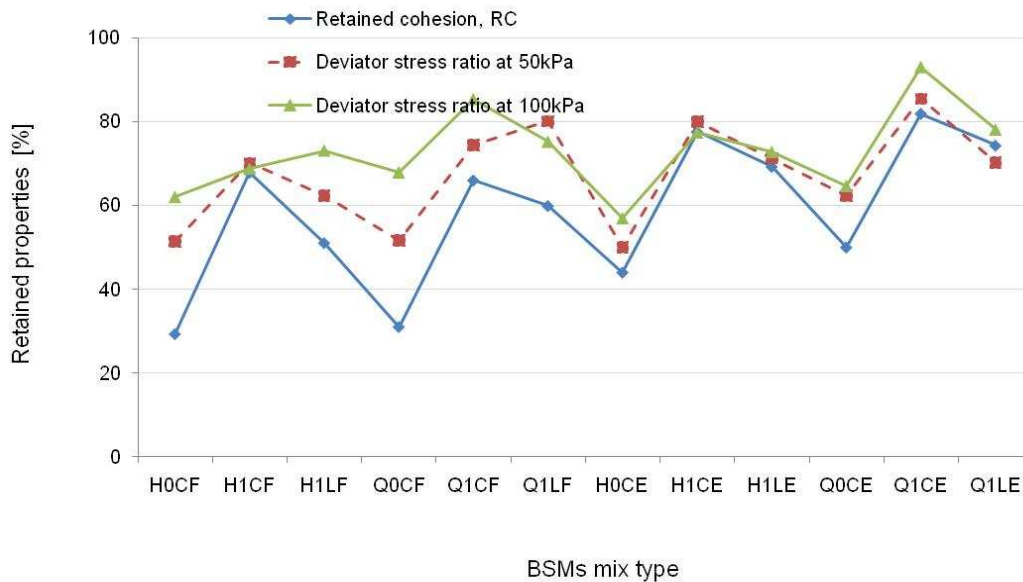


Figure 116: Comparison of moisture sensitivity of BSMs between retained cohesion (RC) and deviator stress at failure ($\sigma_{d,f-dry}/\sigma_{d,f-wet}$) at 50kPa or 100kPa

5.3.1 Behaviour of shear properties (C and ϕ)

The retained cohesion (RC) of BSMs is determined from shear properties of unconditioned and conditioned specimens to compare the influence of moisture damage on the studied materials. The applied stresses at failure, measured during monotonic triaxial testing, are used to calculate the fundamental shear properties of the mixes. The applied stress at failure measured at different confining pressures defines the failure conditions of the materials. The failure conditions (change in shear properties) provide an indication of the relative damage that will occur due to pulsing of moisture into a specimen. The shear strength parameters, angle of internal friction (ϕ) and cohesion (C), were determined by plotting a Mohr-Coulomb diagram using applied stress at failure and different confining pressures. A linear failure envelope was fitted to the circles such that the intercept of the line defines the cohesion and its slope defines the angle internal friction. A linear approximation of the failure model is considered sufficient to define the shear properties, although non-linear behaviour at lower applied stress levels generally occurred (Jenkins *et al.*, 2007; Gonzalez, 2009).

Selected results of the failure Mohr-Coulomb cycles for the mixes stabilised with bitumen emulsion, and with or without the addition of active filler, are presented in Figure 117 and Figure 118.

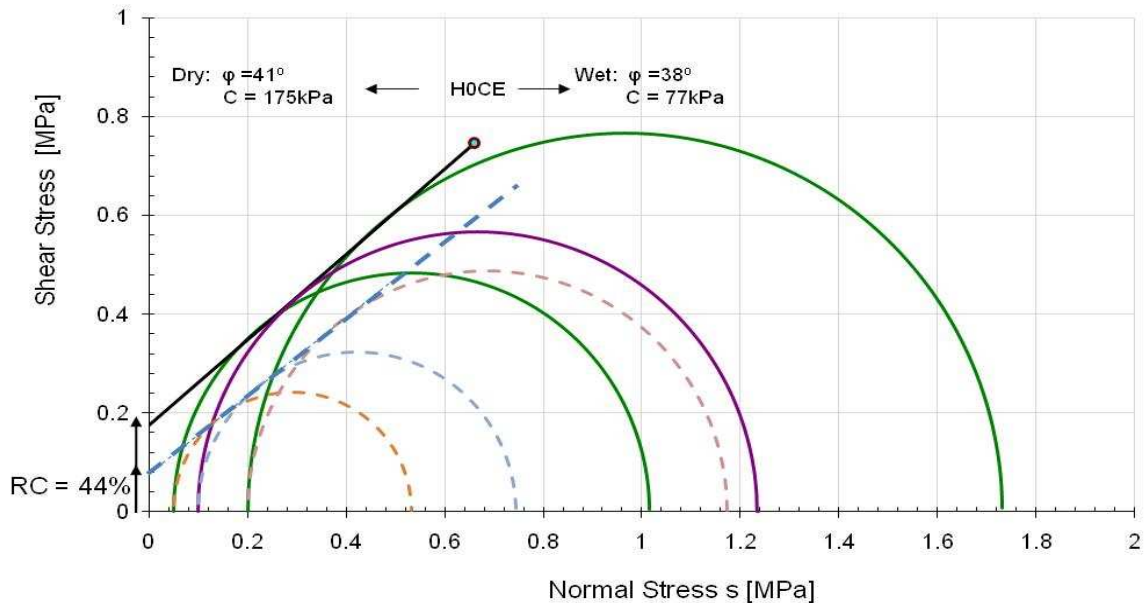


Figure 117: Effects of moisture damage on shear properties of BSM-emulsion mixes of Hornfels-RAP without the addition of cement (H0CE)

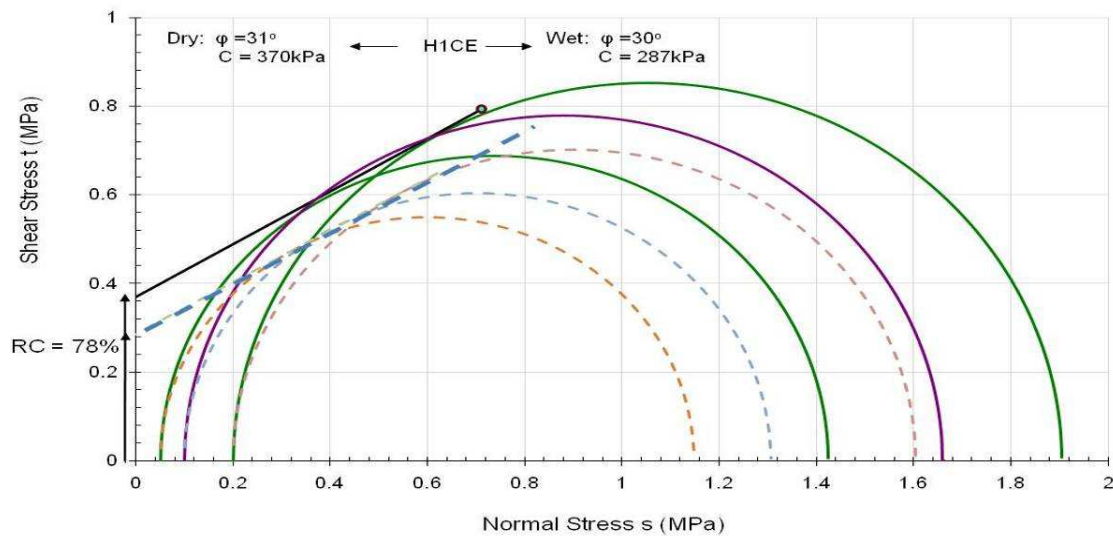


Figure 118: Effects of moisture damage on shear properties of BSM-emulsion mixes of Hornfels-RAP with 1% cement (H1CE)

Figure 117 and Figure 118 show shear parameters (C & ϕ) for the unconditioned (dry) and conditioned (wet) Hornfels-RAP mixes stabilised with bitumen emulsion, with or without the addition of active filler (cement). It is evident from the Mohr-Coulomb failure lines that changes in cohesion and internal angle of friction occurred due to moisture ingress in the mixes. The differences in retained cohesion for the mix with cement, is significant compared to the mix without cement. The mix with cement (H1CE) had retained cohesion of 78% compared to 44% in the mix without cement (H0CE). The change in shear properties due to pulsing water pressure into the mix can be applied to model structural behaviour of BSMs under the influence of the ingress of moisture. The shear properties results obtained from the studied mixes were used for the structural analysis of the BSM layer in a pavement structure as discussed further in section 5.4.

The internal angle of friction yields two observations: firstly, H0CE at equilibrium (dry) condition appeared to have a higher internal angle of friction compared to H1CE. However, after pulsing of water pressure into these mixes big change of internal angle of friction occurred in the H0CE than in H1CE. The ingress of moisture in the H0CE can result into a lubrication effect during triaxial testing, hence decreases the internal angle of friction. Secondly, it can be seen from the results that the addition of cement into Hornfels-RAP stabilised with bitumen emulsion reduces the internal angle of friction significantly (i.e. 41° – 31°). This behaviour is not clear, therefore needs further investigation. However, after pulsing water pressure in the H1CE a small reduction in the internal angles of friction occurred (i.e. 31° – 30°). This is due to the fact that the effect of water in damaging the integrity of the H1CE occurs at a lesser extent.

Further evaluation shows that the failure envelope for H1CE shifted upward relative to the H0CE, this is a result of an increase in the maximum principal stresses $\sigma_{1,f}$, and $\tau_{1,f}$ through the addition of cement. In conclusion, the observed behaviours show that the cohesion, adhesion and internal angle of friction in BSMs seem to be interdependent, with one influencing the other. However, further investigation is required to ascertain this behaviour.

Additional results from Mohr-Coulomb analysis of the monotonic triaxial test performed on materials stabilised with either bitumen emulsion or foamed bitumen and with or without active filler (cement or lime) are presented in Table 25. The corresponding Mohr-Coulomb failure diagrams are presented in Appendix E.

Table 25: Comparison of shear failure parameters of unconditioned (dry) and conditioned (wet) specimens of different studied BSMs mixes

Mix type	DRY				WET				RC [%]
	C [kPa]	ϕ [°]	$\sigma_{1,f}$ [MPa] at 200kPa	$\tau_{1,f}$ [MPa] at 200kPa	C [kPa]	ϕ [°]	$\sigma_{1,f}$ [MPa] at 200kPa	$\tau_{1,f}$ [MPa] at 200kPa	
Q0CE	132	41	1.86	0.84	66	44	1.44	0.63	50
Q1CE	260	40	2.03	0.92	213	41	1.90	0.86	82
H0CF	116	43	1.60	0.70	34	44	1.24	0.52	29
H1CF	221	40	2.36	1.12	150	44	1.84	0.82	68
Q0CF	158	50	2.34	1.08	49	52	1.90	0.87	31
Q1CF	297	52	3.34	1.60	196	53	2.95	1.40	66
H1LE	192	44	2.00	0.92	133	42	1.60	0.72	69
H1CE	370	31	1.90	0.88	287	30	1.60	0.70	78

Note: three test results were used to fit a linear failure envelope

The summary of results in Table 25 shows the comparative shear failure parameters for unconditioned and conditioned BSM mixes stabilised with bitumen emulsion or foamed bitumen and with or without active filler (cement). It is evident from the results that reduction in shear properties occurred due to pulsing water pressure into the mixes. In addition, a reduction in applied stresses (normal and shear) is noted for all studied mixes. However, irrespective of binder or aggregate type, the benefit of the addition of active filler (cement or lime) into BSM mixes is apparent with regard to resistance to moisture damage. It can be seen from the result of Q1CE that pulsing of water pressure had little effect on the change in cohesion properties of the mix, compared to a similar mix without cement (Q0CE): the retained cohesion of Q1CE is 82%, compared to 50% in Q0CE. This behaviour confirms the theory on physicochemical and mechanical interaction of binder and mineral aggregates, as discussed in Chapter 3 of this study.

Hornfels-RAP mixes stabilised with foamed bitumen without active filler (cement). H0CF, show a significant drop in cohesion due to the ingress of moisture. However, significant improvement occurred after the addition of 1% cement, with retained cohesion rising from 29% to 68%. H0CF could be rejected in mix design according to the new TG2 (Asphalt Academy, 2009) with a lower cohesion of 29% (i.e. <50%), but the addition of 1% cement allows the mix to be classified BSM3. The influence of the active filler in BSMs for moisture resistance is vital in durability and long-term performance.

A comparison of the shear properties of the mixes stabilised with bitumen emulsion and additional cement or lime is presented in Table 25. It has been reported in Chapter 3 that the addition of 1% lime did not give the same cohesive strength in the studied mixes as cement did. The reason provided was the physicochemical behaviour of lime in interaction with the mineral aggregates. Therefore, the results presented in Table 25 provide comparative differences in cohesion strength and applied stress at failure between lime and cement. This highlights the role of ICL prior to the application of lime as an active filler in BSM mix design. It is evident that 1% lime provides less resistance to moisture damage compared to 1% cement. This confirms the conclusion that the addition of lime as an active filler in BSMs greatly depends on the type of mineral aggregate; therefore its selection during mix design should take cognisance of its reactivity with mineral aggregates for a proper percentage application.

The internal angles of friction for the Quartzite crushed stone stabilised with bitumen emulsion are smaller than in similar mixes stabilised with foamed bitumen. In Hornfels-RAP, the internal angles of friction are relatively uniform in both bitumen emulsion and foamed bitumen stabilisation. This indicates that the use of bitumen emulsion or foamed bitumen has different influences on internal angle of friction, depending on the aggregate type. With bitumen emulsion

showing higher influence than foamed bitumen, this might be due to larger coating of the binder, which may have lubrication effect during triaxial testing.

The analysis of other parameters in the Mohr-Coulomb diagram, such as maximum stresses at failure ($\tau_{1,f}$ and $\sigma_{1,f}$), can give insight into the performance of BSMs in terms of moisture damage. The results for the maximum stresses at failure ($\tau_{1,f}$ and $\sigma_{1,f}$) for unconditioned and conditioned monotonic test at 200kPa are presented in Table 25 for comparison. The comparison is made on conditioned (wet) mixes with the addition of active filler (1% cement) tested at higher confinement. The higher confinement normally gives a better indication of shear failure than lower confinement. The results in Table 25 show that mixes stabilised with bitumen emulsion and with additional active filler (cement) less susceptible to moisture damage compared to foamed bitumen. Nevertheless, the mixes stabilised with foamed bitumen show higher maximum stresses at failure compared to bitumen emulsion. For example, maximum shear stress ($\tau_{1,f}$) of H1CE is 0.7MPa and normal stress ($\sigma_{1,f}$) is 1.6MPa while $\tau_{1,f}$ of H1CF is 0.85MPa and normal stress is 1.85MPa. Similar behaviour occurred in the Quartzite material stabilised with foamed bitumen. The higher stress at failure for the foamed bitumen mixes under dry or saturated conditions indicate that mastic in foamed bitumen mixes exhibit elastoviscoplastic behaviour, compared to the elastoplastic behaviour of mastic in bitumen emulsion mixes. Twagira (2006) reports similar behaviour of foamed bitumen in terms of fatigue analysis. His findings indicate that, bitumen emulsion had higher initial stiffness during fatigue test, but exhibit less number of load applications to failure than foamed bitumen.

5.3.3 Behaviour of stiffness properties (resilient modulus, M_r)

The short dynamic (resilient) triaxial tests carried out in this study intend to determine the influence of the new moisture conditioning method on the change of stiffness behaviour of the mix matrix. Modelling of the stiffness behaviour due to moisture susceptibility was not the main objective; therefore a limited variable was selected to analyze the response of materials to loading at a single stress level. The short dynamic test was performed at a confining pressure of 50kPa to reduce the effect of pore water pressure in the specimen and deviator stress ratio ($\sigma_d/\sigma_{d,f} = 10\%$). The results of resilient modulus at different saturation levels and retained modulus were presented and discussed in Chapter 3, section 3.6.3.2 page 146. It is evident from the results that resilient modulus decreases as saturation level increases. The determined stiffness behaviour indicates that ingress of moisture into BSMs damages both cohesion and adhesion and consequently a decrease in resilient modulus occurs at different saturation levels, with severe reduction at 100% saturation. The healing of stiffness reduction after the evaporation of water was not investigated; this is an area, which needs further investigation.

Modelling of the stiffness reduction due to moisture ingress is important, particularly for structural pavement design. However, challenges exist in collecting reliable resilient modulus data under saturation conditions. In Chapter 3 it was indicated that the setup method for capturing the resilient response on the entire specimen height was variable and unreliable. Therefore, the current triaxial setup and methodology of fixing on-specimen LVDTs at Stellenbosch University cannot be applied for testing saturated specimens. It is therefore necessary to review the mechanical setup and connection of on-specimen LVDTs to be able to model stiffness reduction due to moisture damage accurately.

5.3.4 Behaviour of permanent deformation (ϵ_p)

Two sets of specimens (i.e. dry and wet) were tested for ϵ_p on each of the variables indicated in section 5.3.3. The dry specimens were tested after curing while the wet specimens were tested after curing and MIST conditioning. For dry testing, after curing, the specimen is conditioned in the climate chamber at test temperature (i.e. 25°C or 40°C) for four hours to achieve a uniform

temperature. During conditioning, the specimen is sealed with a membrane to maintain its equilibrium moisture content prior to testing. For wet testing, after curing, the specimen is conditioned in a climate chamber at testing temperature for four hours. Thereafter, MIST conditioning (saturation) is done at the same test temperature. MIST conditioning is done by pulsing hot water at test temperature for 3.2min. After conditioning, the specimen is sealed with a membrane to maintain saturation level. Further conditioning is necessary in the climate chamber to ensure equilibrium temperature of the saturated material, followed by a permanent deformation test.

The results of permanent deformation of H1CE at different test variables during triaxial long dynamic testing are plotted as permanent axial strain (%) against number of load applications (N). Figure 119 presents the superimposed results of the tested variables. It can be seen from the results that the permanent axial strain remains below tertiary flow (i.e. <4% axial strain) for the lower temperature (25°C) and the higher temperature (40°C). Nevertheless, the multi-stage stress ratio shows significant influence in the axial strain accumulation. However, an increase of stress ratio from 40% to 80% did not raise total permanent axial strain to 4%. This behaviour of lower permanent axial strain in H1CE was similarly observed during wet MMLS3 trafficking. Minimal reduction in cohesion and adhesion was also observed during MIST and monotonic triaxial testing. The permanent axial strain of less than 4% at stress ratio of 80% and the test temperature of 40°C shows that 40°C is not a critical temperature to reach a tertiary flow for BSM emulsion with the addition of cement (see more results in Appendix F). To substantiate the influence of temperature and stresses in BSMs, comparison was made with permanent axial strain determined for the cores extracted from the pavement section, which was in service for 3 years (Shedgum Road). Permanent deformation of the cores was tested at different temperatures in dry conditions to determine the critical temperature during pavement in-service conditions. The results are discussed in section 5.3.4.1.

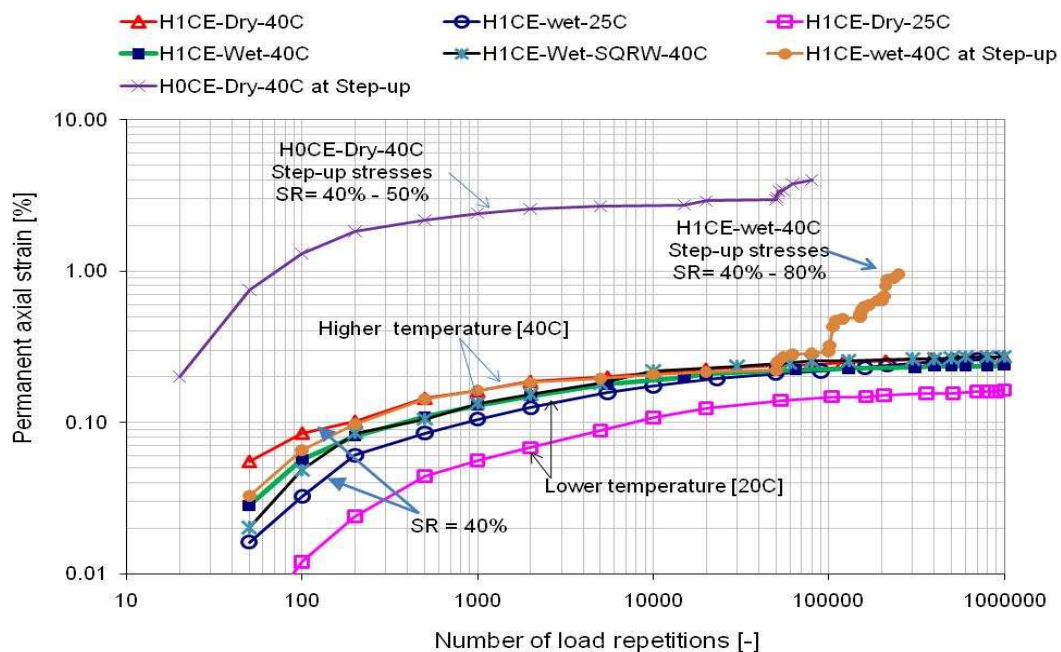


Figure 119: Permanent axial strain of H1CE and H0CE tested wet and dry at various parameters (i.e. havesine wave, square wave, 25°C, 40°C, 40% SR, multi-stage stresses 40%– 80% SR) at 100kPa and frequency of 2Hz

5.3.4.1 Critical temperature

The results in Figure 120 show that 40°C is not a critical temperature in order to reach tertiary flow in BSMs. The cores extracted from Shedgum Road were tested at different service temperatures ranging from 40°C to 60°C. It is evident from the results that the critical temperature of BSM mixes lies between 40°C and 50°C. However, the critical temperature is influenced by binder content, percentage of RAP and addition of active filler. The details of cores extracted from Shedgum Road are presented and discussed further in Chapters 6 and 7.

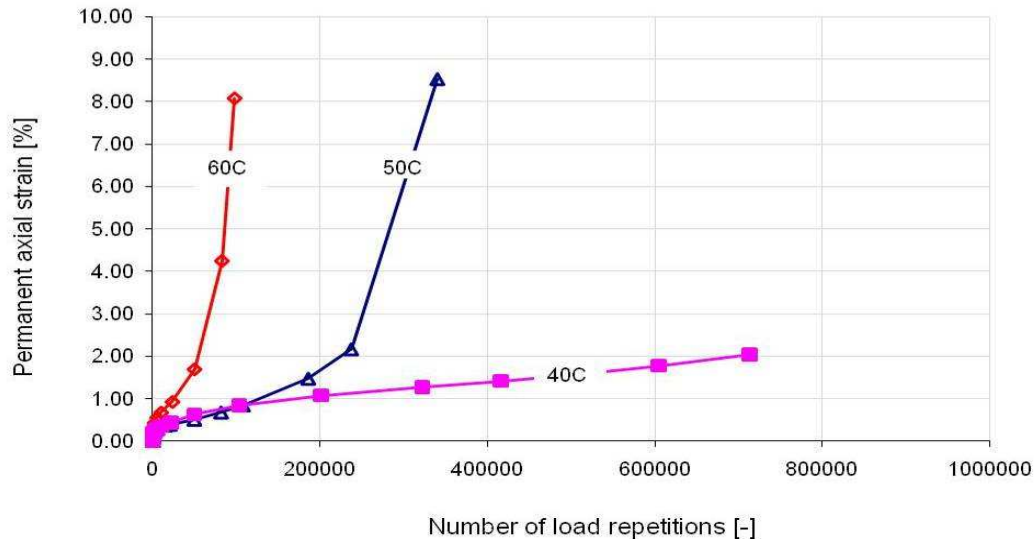


Figure 120: Permanent axial strain of field extracted cores (BSM-foam) with 100% RAP from Shedgum Road, tested at 40% SR, 100kPa and different temperatures of 40°C, 50°C and 60°C

5.3.4.2 Critical deviator stress ratio

The critical stress ratio in BSMs varies depending on material properties, applied confining stress and testing temperature. The multi-stage stress applied to H1CE at SR ranging from 40%–80% shows that the addition of cement significantly influences the critical stress ratio to reach tertiary flow at low temperatures. Fu *et al.* (2009) report similar results: they performed triaxial tests for permanent deformation and report that less than 0.5% axial strain at deviator stress of 700kPa was obtained after multi-stage stress analysis up to 250 000 load applications, (see Figure 43, Chapter 2, page 97).

5.3.4.3 Influence of loading wave

The influence of the loading wave was studied. The haversine and square wave were applied to the H1CE during the triaxial permanent deformation test. The application of square loading wave was expected to cause more severe, permanent axial strain due to its impact effect. However, the results of superimposed permanent axial strain in Figure 119 show that there was no significant effect on applying impact loading to H1CE at 40°C in wet conditions, compared to the haversine in the same tests conditions. The influence of loading wave in determining permanent axial strain accumulation is vital, particularly in urban areas. Pavement in urban areas experiences static as well as dynamic loading. Therefore, more research is warranted in this area to be able to model the durability properties of BSMs under these conditions for better selection of materials for mix design.

5.3.4.4 Influence of active filler

The results in Figure 119 compare the permanent axial strain for H1CE and H0CE at 40°C. It is evident from these results that the addition of cement in BSMs is absolutely necessary. Mixes without the addition of cement had significant shift in the flow path and reached tertiary flow at 60% stress ratio with 12 000 load applications. The benefits of the addition of cement in BSMs have been discussed in detail in Chapters 3 and 7 of this thesis.

5.4 ANALYSIS OF MOISTURE DAMAGE TO BSM LAYER IN PAVEMENT STRUCTURES

The modelling of pavement material durability is an important aspect in order to predict long-term pavement performance accurately. However, modelling the durability behaviour of BSMs is a complex task due to the diversity of materials that are needed to be accounted for during pavement design. The material properties and behaviours determined in this study are valid for quality aggregates and the tests conditions adopted. The controlled parameters in a laboratory test, such as temperature, loading, frequency and saturation levels, might differ from the actual pavement conditions experienced in the field. Therefore, the analysis of moisture damage in this section uses the linear elastic theory to determine the influence in the changes of material properties and the performance of pavement structures incorporating a BSM layer.

The type of pavement structure selected for analysis is the N7 expressway near Cape Town, which incorporates BSM-emulsion as a base layer. The BSM-emulsion layer in the N7 expressway consists of Hornfels-RAP stabilised with 2% bitumen and with 1% cement. The full pavement structure is made of UTFC (Ultra-thin friction layer), thin AC, BSM-emulsion and natural gravel.

The pavement response in terms of stress and strain is commonly evaluated using a linear or a non-linear elastic multi-layer program, such as BISAR (Shell, 1998), KENLAYER (Huang, 1993) or RUBICON (MAS, 2007). These programs, however, have certain limitations in predicting pavement response accurately. Therefore, the use of a finite element method is required for a better performance prediction in pavement structures. However, finite element analysis is a specialised area and therefore, was not formed as part of this study. The pavement response in terms of moisture sensitivity in this study was done using the linear elastic multi-layer BISAR 3.0 program.

5.4.1 Pavement structure analysis

The pavement analysed in this section is the N7 expressway pavement structure. The base layer of the structure is made of BSM-emulsion. The material properties of BSMs have been investigated in this study. The base layer (BSM-emulsion) material properties subjected to stress and strain analysis are listed in Table 26. These values were obtained from the monotonic and short dynamic triaxial tests performed in this study, see section 5.3.1 and Chapter 3 section 3.5.4.3 respectively.

Table 26: BSM-emulsion layer, material properties for BISAR analysis

Material type	Stiffness properties		Shear properties			
	Dry-Mr [MPa]	Wet- Mr [MPa]	Dry- C [kPa]	Wet- C [kPa]	Dry-φ [°]	Wet-φ [°]
H1CE	1400	1100	370	287	31	30

The overlaying material properties featured in the analysis were not investigated in this study, however, were selected from a range of values suggested in the SAMDM (Theyse et al., 1996). The typical stiffness properties of the surface layer, natural gravel as a subbase layer and soil

as subgrade (foundation) layer and the corresponding Poisson's ratio are presented in Table 27. The surface layer combines UTFAC and AC, because UTFAC is added to the AC to ensure skid resistance between the wheel surface and pavement.

Table 27: Material properties of layers analysed using BISAR 3.0 program.

Material type	Stiffness, M_r [MPa]	Poisson's ratio, ν
Asphalt surfacing	5000	0.44
Natural gravel	350	0.35
Subgrade	150	0.35

5.4.2 The BSM-emulsion analysis using BISAR 3.0 Program

Two pavement structures consisting of a BSM-emulsion layer at equilibrium moisture state and in a saturated state are analysed. The loading condition consists of a super single of 45kN and tyre pressure of 700kPa. The wheel load is modelled as a circular loading area with a radius of 143mm and a uniform contact pressure equal to the tyre pressure. The comparative pavement structures and loading conditions are presented in Figure 121.

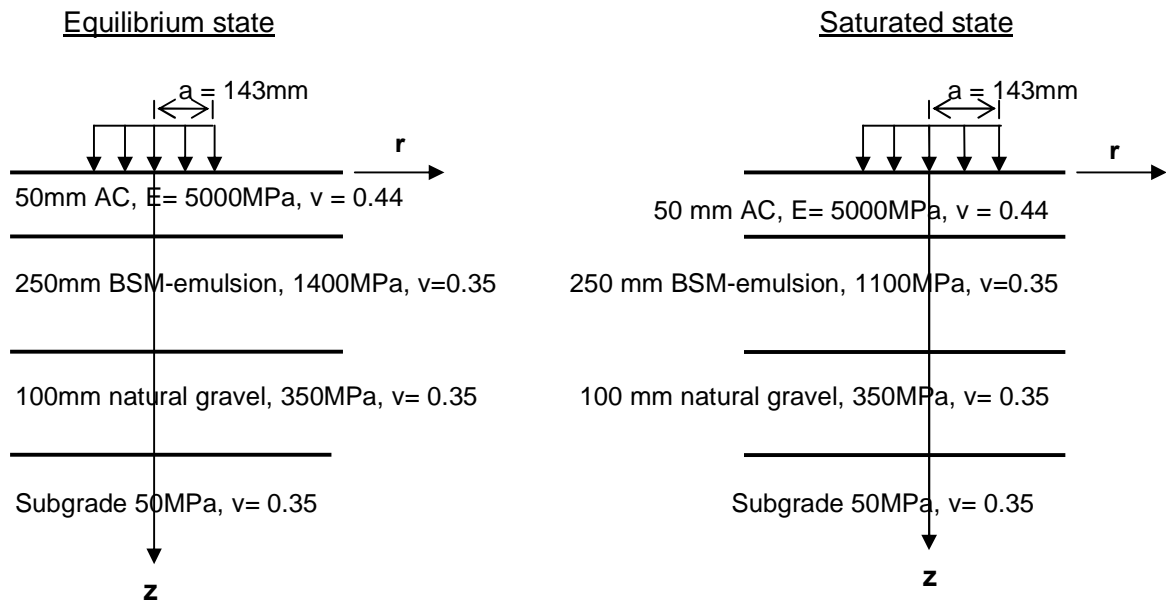


Figure 121: Comparative pavement structure comprising a BSM-emulsion layer at equilibrium state and in a saturated state, used in BISAR analysis

5.4.2.1 Comparison of stress distribution with depth

The calculated stress distributions σ_1 and σ_3 in a BSM-emulsion layer at equilibrium moisture content and saturated conditions are presented in Figure 122 and Figure 123. The vertical stress σ_1 in Figure 122 shows no difference in distribution at equilibrium and in saturated state. In addition, the influence of the vertical stress (wheel load) is minimal beyond the BSM-emulsion layer. This is an advantageous aspect of using BSMs as the load spreading layer. The uniform stress distributions between BSM-emulsion layer at equilibrium and in a saturated condition indicates that the mix design of BSM layer, which is less susceptible to moisture damage, is a beneficial for the durability behaviour and long-term performance of the pavement structure.

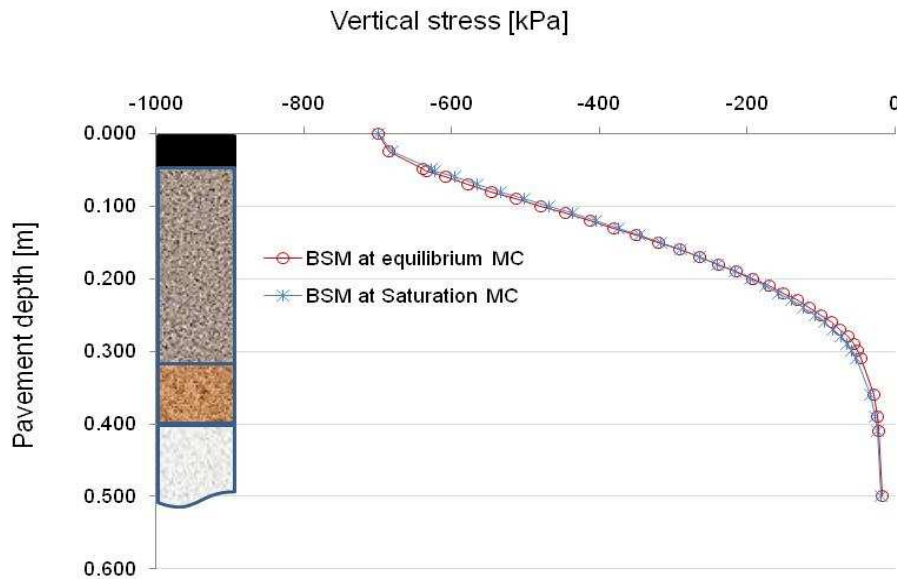


Figure 122: Comparison of vertical stress distribution in BSM-emulsion at equilibrium and in a saturated state, in a pavement structure

In Figure 123, the vertical and horizontal stresses are superimposed. The horizontal stress σ_3 distributions of the BSM-emulsion layer both at equilibrium moisture content and in saturated condition seem to shift from compression (top) to tension (bottom). However, at the bottom, BSM-emulsion in an equilibrium condition seems to have slightly higher horizontal stress. The changes in horizontal stress from compression to tension do not occur under triaxial testing. It should be noted that in any elastic multi-layer program, significant tensile stresses are calculated. The M_r - θ model used to predict the stiffness of a BSM-layer was developed from granular materials. Granular materials cannot take any significant tension as coarse grained materials have very low cohesion. Therefore, in order to avoid a negative bulk stress θ and subsequently imaginary predicted M_r values, the stress as calculated by the elastic multi-layer program needs to be modified. That means that tensile horizontal stresses σ_3 are set to 0 while maintaining the same deviator stresses σ_d . In doing so, the major principal stress σ_1 can be shifted further into compression. This type of adjustment by shifting principal stresses is also adopted in the SAMDM (Theyse *et al.*, 1996). Ebels (2008) comments that when shifting is not performed, the M_r - θ cannot be used because there is no solution for θ^{k_2} when $\theta < 0$ and $k_2 < 1$. When a negative bulk stress exists, it means $M_r < 0$ at the bottom of the layer, which is highly improbable for these materials. Alternatively, when the bulk stress is very low and the horizontal stress are in tension (not shifted), this leads to unrealistically low M_r values, which are not expected to occur in the BSM layer.

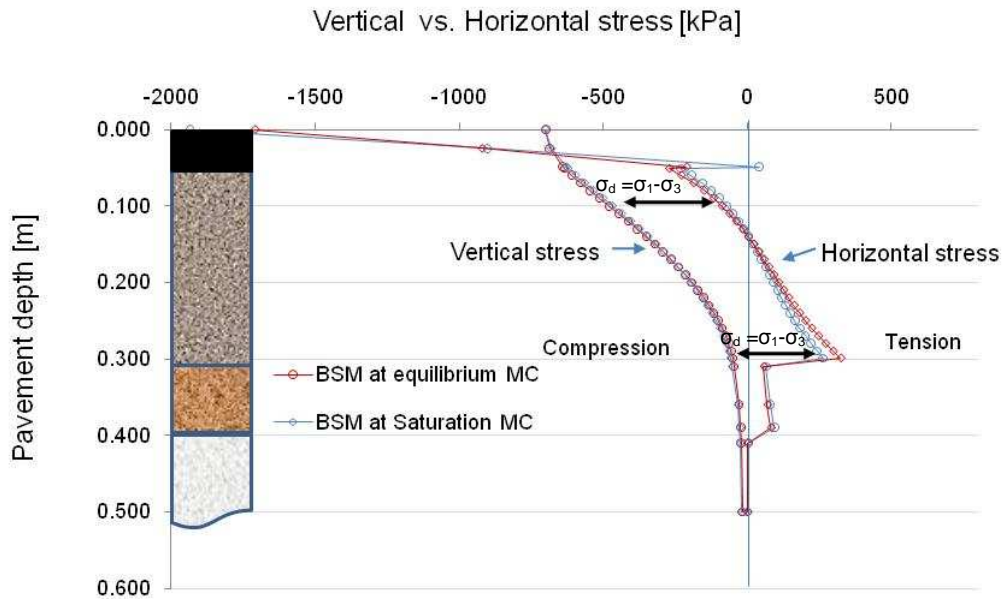


Figure 123: Comparison of vertical and horizontal stresses distribution in BSM-emulsion at equilibrium and in a saturated state, in a pavement structure

5.4.2.2 Comparison of strain distribution with depth

From Figure 124 it can be seen that the vertical strain in BSM layer is higher at the top than the bottom. In addition, BSM-emulsion at equilibrium moisture content and in saturated condition has a different vertical strain distribution, the difference is big at the top and small deeper in the layer. This shows that BSM-emulsion in saturated condition experiences higher permanent deformation at the top subsection (1/3) compared to a similar material at equilibrium moisture content. This is due to higher stress at the top layer compared to deeper in the layer, as indicated in Figure 122 as well as lower M_r than for equilibrium conditions. Similar behaviour was observed during MMLS3 trafficking. The decrease difference in the vertical strain at the bottom of the layer indicates that, either at equilibrium or in saturated condition, there will be minimal deformation of the underlying layer. Therefore, the selection of less moisture susceptible mix in BSM layer is vital for a long-term performance of the pavement structure.

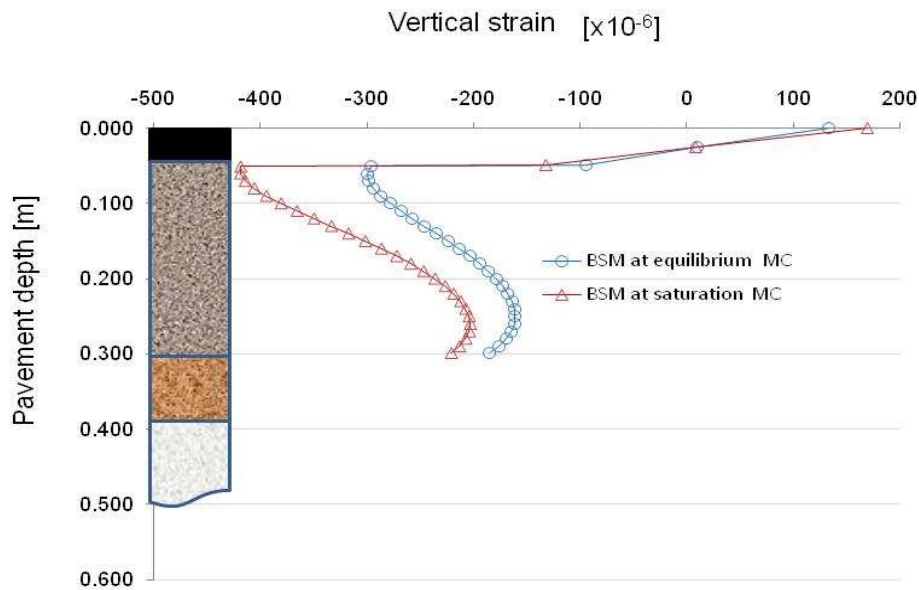


Figure 124: Comparison of vertical strain distribution in a BSM layer, at equilibrium and in saturated condition, in a pavement structure

The horizontal strain distribution calculated from linear elastic behaviour of BSM-emulsion layer is presented in Figure 125. The horizontal strain varies from top to bottom, with the bottom showing higher strain level. It can also be seen that the horizontal strain at the top subsection (1/3) of the BSM layer differs at equilibrium and in saturated condition, with the saturated condition showing higher horizontal strain. The horizontal strain level at the bottom of the BSM-emulsion layer is 180microstrain. Depend on support condition of a BSM layer and the amount of cement content, such magnitude of horizontal strain can be measured at the bottom of layer Brown *et al.* (2000). Nevertheless, such magnitude of horizontal strain can result in fatigue failure in a long-term in-service condition, which is not a predominant failure mode for BSM layer.

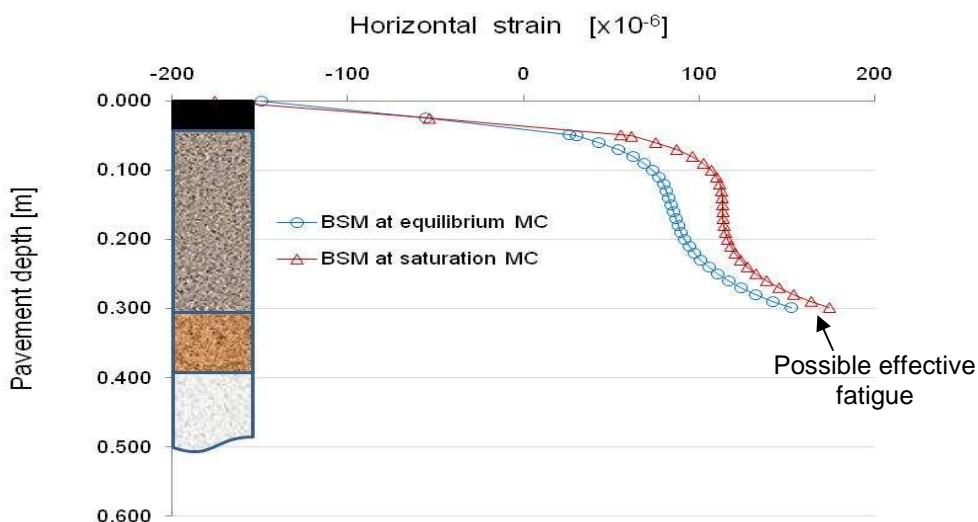


Figure 125: Comparison of horizontal strain distribution in BSM-emulsion, at equilibrium and in saturated condition, in a pavement structure

The vertical strain in the BSM layer results in horizontal strain; that means from the applied stresses and resultant strain, Poisson's ratio, ν , and the modulus can be determined. Jenkins (2000) indicates that a model for the change in Poisson's ratio with variation of stress conditions has been established for granular materials (Niekerk *et al.*, 2000a). The same model was found to be applicable to BSMs. The model indicates that Poisson's ratio is a function of principal stress ratio σ_1/σ_3 . This shows that disturbance of bonds through moisture damage or axial deformation results in an increase in Poisson's ratio. Therefore the change in Poisson's ratio is not only function of axial deformation but also the critical stress ratio $\sigma_d/\sigma_{d,f}$. The application of ν in the linear elastic analysis is therefore necessary for closer representation of field behaviour to determine the critical design stress ratio. The critical stress ratio determined using the linear elastic behaviour of BSMs is presented in Figure 126 and Figure 127.

5.4.2.3 Comparison of deviator stress distribution with depth (moisture sensitivity)

The principal stresses at various points in a BSM layer are used to calculate the critical deviator stress and deviator stress ratio. In that light, a large number of points were evaluated over the depth in order to sufficiently compare deviator stress at different points in the BSM at equilibrium moisture content and in saturated condition, as indicated in Figure 126. BSM-emulsion at equilibrium condition shows higher deviator stress at the bottom than in saturated condition. It can be seen from the deviator stress distribution that a critical deviator stress is calculated at the bottom where horizontal stress changed from compression to tension. The effect is twofold: firstly, when $\sigma_3 \leq 0$ it causes an increase in deviator stress: secondly, the calculated major principal stress at failure $\sigma_{1,f} = A\sigma_3 + B$ and subsequently the deviator stress at failure $\sigma_{d,f}$ reduces because of diminishing first term ($A\sigma_3$). However, once $\sigma_3 > 0$, deviator stress increases and deviator stress at failure also increases. These results in a rapid increase in deviator stress ratio (see Figure 127).

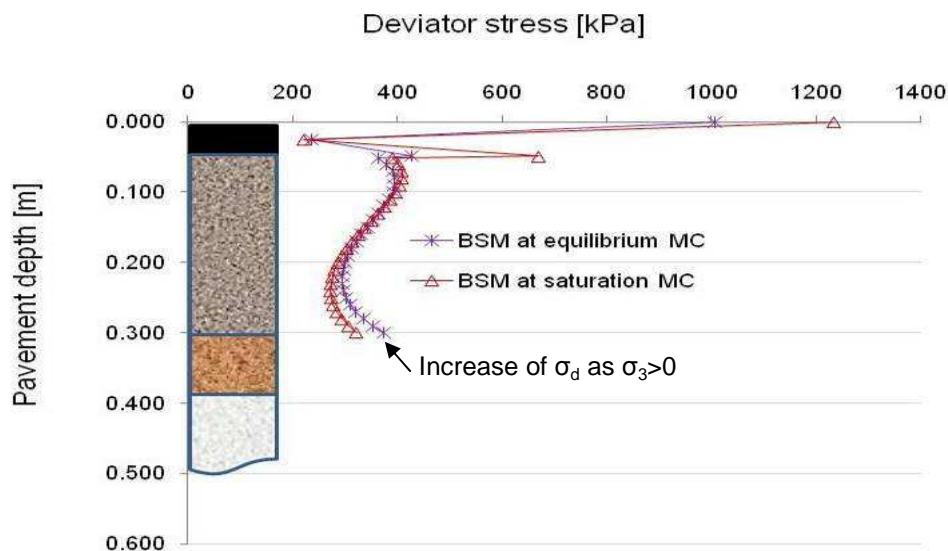


Figure 126: Comparison of deviator stress distribution in BSM-emulsion, at equilibrium and in saturated condition, in a pavement structure

Deviator stress ratio is calculated from deviator stress σ_d and deviator stress at failure $\sigma_{d,f}$. Deviator stress at failure is calculated based on the shear parameters of BSM materials. In a triaxial test, the σ_3 is always in compression, therefore $\sigma_{d,f}$ increases as the σ_3 increases. In a linear elastic analysis, the σ_3 changes from compression at the top to tension at the bottom. The

top subsection of a BSMS layer, which is in compression show a lower deviator stress ratio of 0.2 compared to a higher deviator stress ratio of 0.6 at the bottom subsection (see Figure 127). The deviator stress ratio for the BSM-emulsion at equilibrium is lower than in a saturated condition at the compression subsection. However, in the tension subsection the deviator stress ratio increases rapidly at the same level for both materials at equilibrium condition and in saturated condition. The effect on change of horizontal stress from top to bottom of the BSM layers indicates that the critical stress ratio therefore occurs at the bottom of the BSM emulsion layer. The magnitude of the critical deviator stress ratio for design purposes as well as the depth at which it occurs is therefore affected when the pavement is analysed using the linear elastic model.

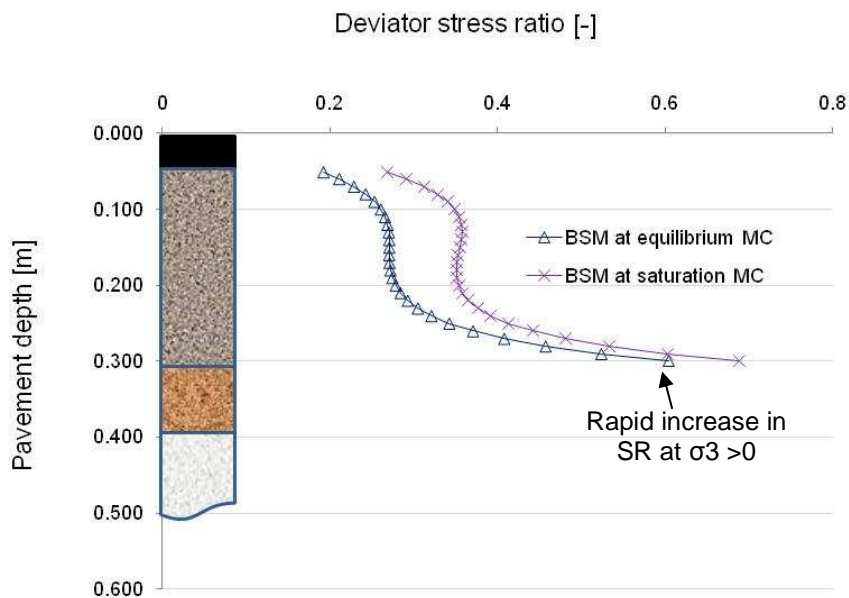


Figure 127: Comparison of deviator stress ratio in BSM-emulsion, at equilibrium and in saturated condition, in a pavement structure

The analysis using the BISAR program has shown that it is possible to model the influence of moisture damage in a pavement structure using stress-strain material characteristics. However, the magnitude of stress states calculated using BISAR are likely to be an overestimation of the actual stress states expected in the field. This is because the stress dependence behaviour of BSMs is to a certain extent not accurately modelled in the linear elastic model calculations. Therefore, one needs to take note of this shortfall when selecting design critical deviator stress ratios observed at the bottom of the BSM layer.

5.5 CONCLUSIONS

The stress-strain (σ - ϵ) relationship of the mechanical behaviour of BSMs was analysed in this chapter. From the stress-strain response, the durability behaviour of BSMs in terms of static failure, resilient deformation and permanent deformation were determined. The findings in this study lead to the following conclusions:

- The use of triaxial testing before and after moisture conditioning of a specimen can identify mechanical property changes in BSMs due to infiltration of excess moisture. In this way, it is possible to screen BSMs mixes in terms of moisture susceptibility.
- The σ - ϵ properties determined under both the monotonic and repeated loading triaxial testing demonstrated that the excess moisture in BSMs has influence on the reduction of cohesion and adhesion of the mix matrices. This is more pronounced for mixes without active filler (cement or lime), stabilised with either foamed bitumen or bitumen emulsion, compared to the mixes with active filler.
- The permanent axial strain determined for a BSMs mix that is resistant to moisture damage, e.g. Hornfels-RAP stabilised with emulsion and with 1% cement (H1CE), show that the axial strain accumulation cannot reach a tertiary flow at a temperature of 25°C and 40°C, after 250 000 number of load applications. Therefore, multi-stage stress ratio and elevated temperature of 50°C was found to be critical for BSM mix with 1% cement or that is less susceptible to moisture damage.
- The stress-strain analysis of a BSM emulsion (H1CE) incorporated into a pavement structure (N7 expressway) was done using a linear elastic model in the BISAR 3.0 program. The analysis indicates that significant tensile stress occurs at the bottom of the BSM emulsion layer. Care should be taken when critical design values are determined from these stress state calculations, as they are likely to be an overestimation.

REFERENCES

- Asphalt Academy TG2. (2009). Bitumen stabilised materials. Technical guideline "A guideline for the design and construction of bitumen emulsion and foamed bitumen stabilised materials. Second edition. Pretoria, South Africa.
- Brown S. and Needham A. 2000. A study of cement modified bitumen emulsion mixtures. Proceeding of the association of asphalt paving technologists. AAPT, vol. 69, Reno.
- Ebels. L.J. 2008. Characterisation of materials properties and rehabilitation of cold bituminous mixture for road pavements. PhD dissertation, published at the University of Stellenbosch, South Africa.
- Fu P. Jones D. Hervey J.T, Asce M. and Halles F. A. 2009. An investigation of the curing of foamed asphalt mixes based on micromechanics principles. Journal of materials in civil engineering. Submitted November 9, 2008; accepted May 8, 2009.
- Gonzalez A. 2009. An experimental study on deformation characteristics and performance of foam bitumen pavements. A Doctoral thesis. Presented at University of Canterbury. New Zealand.
- Huang Y.H 1993. Pavement analysis and design. Prentice hall, Englewood cliff, New Jersey. USA.
- Jenkins K, Long F, and Ebels L.J., 2007. Foamed bitumen mixes = shear performance?. International Journal of Pavement Engineering, Volume 8, Number 2, pp. 85-98(14). Taylor & Francis Ltd.
- Jenkins, K. J., 2000. Mix Design Considerations for Cold and Half-warm Bituminous Mixes with Emphasis on Foamed Bitumen. PhD Dissertation, University of Stellenbosch, South Africa
- MAS. 2007. Modelling and analysis Systems, <http://www.modsys1.com>
- Theyse H.L De Beer M. and Rust F.C. 1996. Overview of the South African mechanistic pavement design method. Transportation research record no. 1539. USA. pg 6-32.
- Twagira M.E. 2006. Characterisation of fatigue performance of selected cold bituminous mixes. MSc Thesis. University of Stellenbosch, South Africa
- Shell Global Solutions. 1998. BISAR 3.0 Software and user manual, CD_ROM, Shell International oil products, Amsterdam, the Netherlands.
- Mulusa W.K. 2009. Development of a simple triaxial test for characterising bitumen stabilised materials. MSc. Thesis. University of Stellenbosch. South Africa.
- van Niekerk A.A van Sheers J. and Galjaard P.J. 2000a. Resilient deformation behaviour of coarse grained mix granulate base course materials from testing scaled gradings at smaller specimen sizes. UNBAR 5 Conference, University of Nottingham.

CHAPTER 6

INFLUENCES OF TEMPERATURE DISTRIBUTION AND VOID CHARACTERISTICS ON DURABILITY BEHAVIOUR OF BSMs

6.1 INTRODUCTION

Temperature distribution in pavement structures has been studied in HMA design and construction to assess the stresses in a layer induced by temperature variation and its effects on material properties. In BSMs, less is known about temperature distribution. Nevertheless, literature reviews indicate that temperature distribution in the layer plays a significant role in both the ultimate gain in mix engineering properties and the exhibition of premature distress. Therefore, understanding the temperature distribution in BSMs is important in gaining an insight into behavioural changes in the mixes, performance at the three different stages, i.e. mixing, moisture loss and compaction, and in-service conditions. The recently released BSM guideline (TG2, 2009) categorically states that laboratory or in-situ recycling using BSM-foam or emulsion should not be done when aggregate temperature is lower than 10°C. Jenkins (2000) indicates that binder distribution and coating in the mineral aggregates in foamed bitumen mixes are significantly influenced by aggregate temperature. Loizos *et al.* (2007) found that the stiffness modulus gain of the foam mix in the field tends to occur within weeks or months of construction. Therefore, it is important that emphasis should be placed on the prediction of the field temperature variation and its influence on the curing period when adjudicating mix selection. The ultimate strength that a BSM layer develops after full curing does play a role in durability and long-term performance. The effect of curing and strength development for BSMs should be considered during mix design, while using environmental information applicable to a specific location. Several distinct climatic regions exist (Weinert, 1980). These regions are characterised by environmental conditions like relative humidity, temperature, wind and rainfall. It is therefore appropriate to apply a temperature distribution model to be able to account for the local environmental conditions in order to predict the temperature distribution in the layer and the related moisture evaporation during the curing process. A temperature prediction model has a benefit of understanding the curing period before the opening of BSM layer to traffic or application of surface layer (AC or seal). The current curing method in practice is empirical, largely based on 7–14 days of cure, which might not result in optimal performance of BSMs, as foamed bitumen cures differ slightly compared to bitumen emulsions.

Various studies have been carried out that included experimentation with the curing temperature and moisture to investigate the influence of these factors on the behaviour of BSM mixes (Moloto, 2008; Serfass *et al.*, 2003), but without consideration of the temperature distribution in the BSM layer under field conditions. Although simulating all field conditions under laboratory conditions might not be feasible and developing different procedures will not be realistic, understanding the coefficient of heat transfer of BSMs gives insight for simulation of the laboratory curing procedure more accurately. Temperature in the mixes is known to influence the following:

- Evaporation of moisture present in the mixes, enhancing breaking of emulsion and adhesion of the binder to the mineral aggregates;

- Development of bonding between the binder and mineral aggregate surfaces;
- Stiffening of the mastic, which in turn affects stiffness, shear properties, and ultimate strength of the mixes;
- Equilibrium moisture content in the mixes and
- Ultimate durability behaviour of the mixes and long-term performance.

BSMs are generally less susceptible to temperature variations (Jenkins, 2000; Loizos, *et al.*,2007). However, depending on mix composition, e.g. higher BC and RAP content, temperature distribution in the layer may adversely influence the performance of BSMs. The heat transfer coefficient of the surface layer, i.e. thin AC or seal, and its mix composition contribute to temperature distribution in BSMs. Loudon International (2008) investigated the excess deformation that occurred in full-depth in-situ recycled BSM-foam constructed in Saudi Arabia. The site inspection on the distressed area shows that during summer months the temperature distribution in the pavement layer was as is indicated in Figure 128.

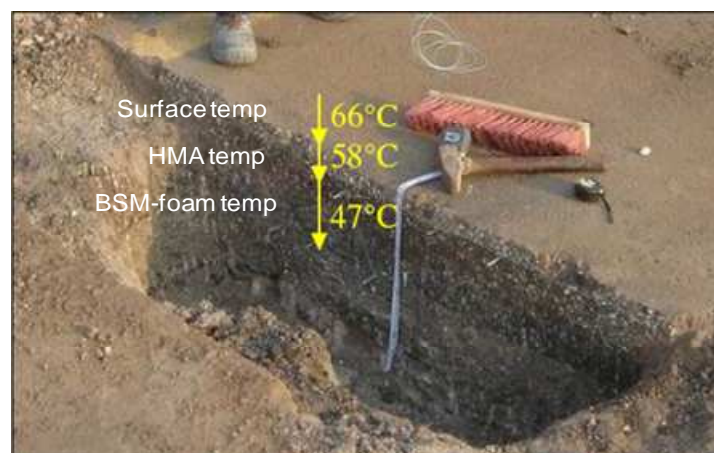


Figure 128: Temperature distribution of distressed pavement structure including BSM-foam as a base layer (Loudon International, 2008)

The temperature distribution observed in the pavement structure gives an insight into the performance of the BSM-foam layer. The higher temperature in the BSM layer coupled with the void content in the mixtures and higher the BC, result in deformation under heavy traffic loading. It is apparent from these observations that the determination of the temperature distribution in the BSM layer is vital. The influence of ambient temperatures and seasonal changes must be understood so that the effect of heating and cooling trends within the pavement structure can be quantified. Recently studies have shown that it is possible to model daily pavement maximum and minimum temperatures by knowing maximum and minimum ambient temperatures. The depth at which the pavement temperature is desired might be calculated using the daily solar radiation utilising a linear relationship.

The objective of this chapter is to present the results of the temperature distribution and relative humidity in a BSM layer measured under field environmental conditions. In addition, a model that can be used in predicting the temperature distribution in a pavement structure using climatic conditions of the location of the pavement construction is presented. The model was developed for HMA; nevertheless, it shows potential to be extended to BSMs. The analysis of the void content characteristics of BSMs using microscopic devices, such as CT-scan and SEMs, is presented and discussed. Lastly, the influence of these parameters (temperature, relative humidity and voids) in relation to durability behaviour of BSMs is discussed. The flow diagram illustrating the focus areas of this chapter is presented in Figure 129.

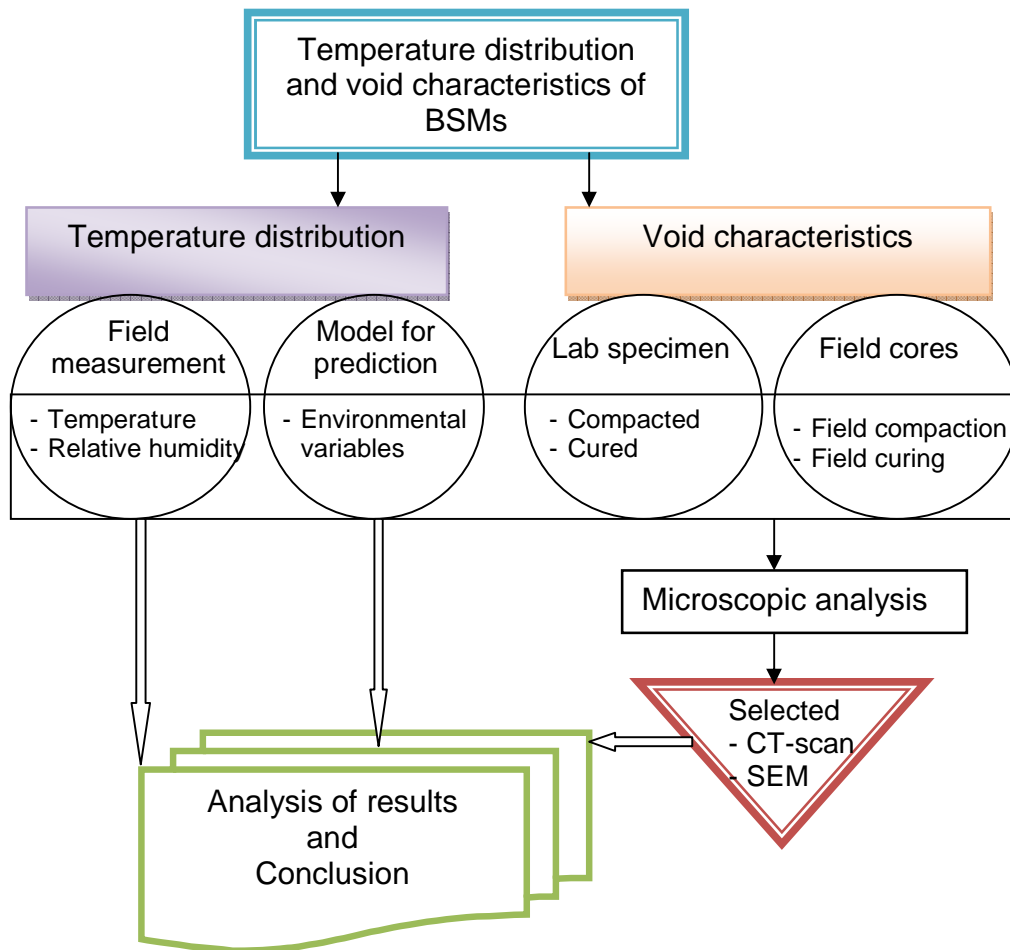


Figure 129: Flow diagram illustrating focus area of temperature distribution and void characteristics of BSMs

6.2 TEMPERATURE MONITORING AND EVALUATION

Monitoring of temperature and relative humidity in this study was done at different depths on BSM layers under field conditions. The aim was to gain holistic understanding on the link between the temperature gradient and age hardening and moisture loss (curing) in a complete cycle of climatic seasons. This includes monitoring of temperature and relative humidity in a BSM layer throughout a year (i.e. during all seasons winter to summer to winter).

The selected pavement structure for the case study was the N7 expressway near Cape Town. This pavement section was selected because the materials used in the recycling of this project cover the main part of research done in this study. The material properties have been discussed in Chapter 3. The constructed pavement structure after recycling with bitumen emulsion is presented in Figure 130.

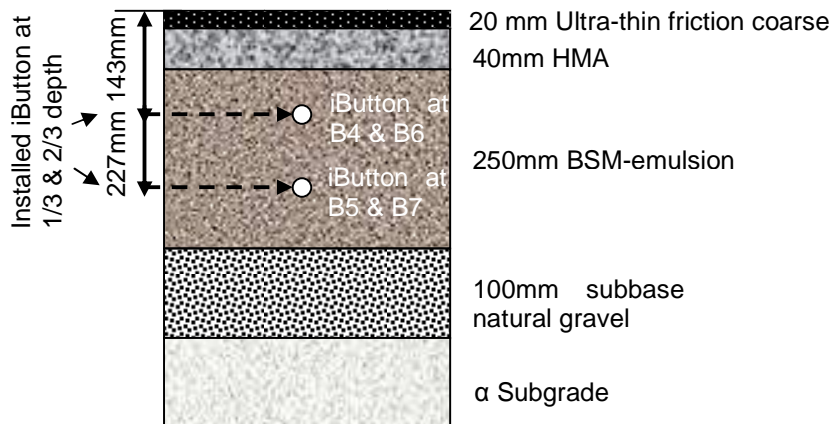


Figure 130: The section of N7 pavement structures after recycling with BSM-emulsion

6.2.1 Monitoring of temperature and relative humidity

The monitoring of the temperature and humidity in the BSM layer was done using a DS1921G iButton device, purchased from Fairbridge Technologies Ltd. The iButton is circular, made of stainless steel, with a diameter of 16mm and 6mm thick. The capacity of the iButton for temperature reading is between -20°C and 85°C, while the percentage relative humidity is from 0 to 100. Its accuracy is indicated to be $\pm 1^\circ\text{C}$ for temperature reading and 5% for the relative humidity. The iButton is supplied with a USB adaptor, blue dot receptor and software called ClimaStats. The blue dot receptor works like a landline telephone socket, where the iButton is inserted into the blue dot which is then plugged into the USB adaptor and the USB is connected to a laptop or desktop for transfer of information. The iButton dimensions and accessories i.e. one wire with two blue dot and USB are shown in Figure 131.

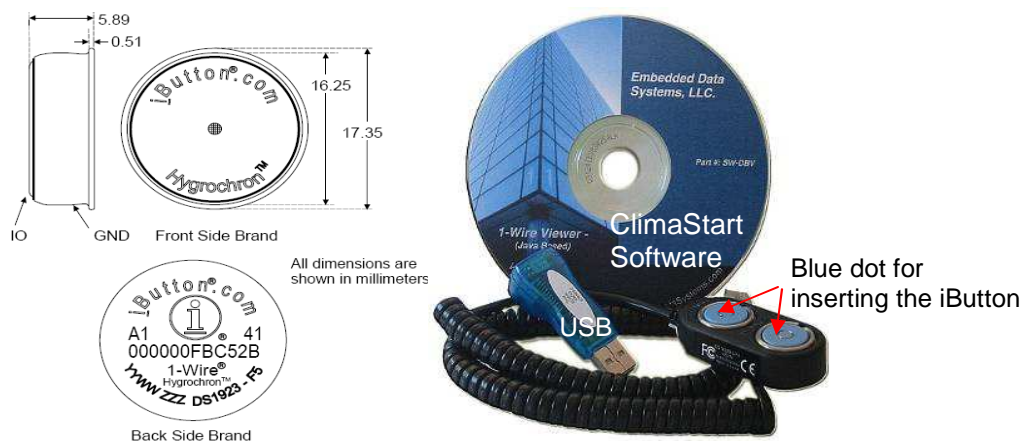


Figure 131: iButton, blue dots, USB and ClimaStats software used for retrieving temperature and RH measured in the BSM-emulsion layer

The layout for the installation of the iButtons along the BSM-emulsion section is shown in Figure 132. The points where iButtons were installed in a longitudinal direction are the flat section on

the crest alignment. In transverse direction, two iButtons were installed near the centreline or inner lane (IL) and two iButtons near the shoulder or yellow line, (YL).

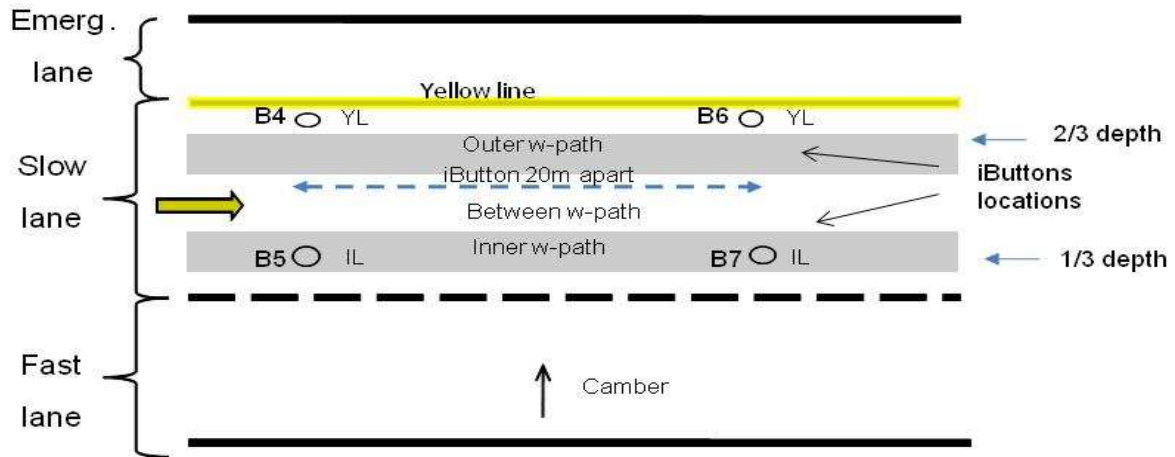


Figure 132: Layout and location of the installed iButtons in a BSM-emulsion pavement section of the N7 expressway

Before the instillation of the iButtons in the BSM-emulsion layer, configuration on the rate of sampling, the start time and date and total number of samples (or finishing time and date) are required. In this study, the mission started at 12:00 on 21 June 2007. The iButton installed at the yellow line (YL) location B4 was programmed with a sample rate of 18.2 hours for a period of 6 months (i.e. June 2007 until December 2007). The iButton installed at position B6 was programmed with a sample rate of 18.2 hours for a period of 2 years (i.e. June 2007 until July 2009). The iButton installed in the inner lane (IL) location B5 was programmed with a sample rate of 2.2 hours for a period of 6 months. The iButton in position B7 was programmed for the same sample rate but for a period of 2 years. The selection of sample rate and period was based on the amount of data and study period.

The installation of the iButtons was done after the completion of the pavement rehabilitation project. A hole of 50mm diameter was drilled using a heavy-duty chisel and the iButton was inserted. Similar material (i.e. bitumen emulsion mix) was placed and compacted into the hole to maintain the homogeneity of material on top of the iButton. The installation depth varied: in the yellow line location, the iButton was installed at 2/3 of the depth of base layer (i.e. approximately 167mm into the BSM emulsion layer). That is, from the top surface it is at a depth of approximately 227mm, see pavement structure Figure 130. The iButtons installed at the centreline near the inner wheel path, location B5 and B7, were placed at 1/3 of the depth of base layer (i.e. approximately 83mm into the BSM emulsion layer), approximately 143mm from the top surface. The selection of depths was based on the following facts: first, during winter RH will vary across the width of the pavement. The yellow line can have higher humidity, due to infiltration of water from the shoulder or the delay of surface water slopping from the inner lane camber, while the centreline near the inner lane will have less humidity due to fast draining at the start of the camber. Second, during summer the temperature distribution varies in pavement layers. The data collected by the iButtons was stored during the period of study. The iButtons were retrieved from the pavement by core extraction. The stored data was exported into an Excel spreadsheet for analysis. The measured data is presented and discussed in the following section.

6.2.2 Temperature distribution data and analysis

Previous studies (Jia *et al.*, 2007; Highter *et al.*, 1884 and Burger *et al.*, 2005) indicate that the temperature distribution in the pavement layer is influenced by the time of solar radiation and the heat transfer coefficient. This shows that pavement layer conductivity varies in the depth during the day and the night. Jia *et al.* (2007) indicate that temperature distribution in the pavement layer can be assumed adiabatic at a certain depth. That means deeper in the pavement layer, the temperature is constant and the effect on conductivity is negligible. A BSM layer in a South Africa pavement structure is positioned shallower, at less than 50mm deep. Therefore, the variation in the temperature distribution in a BSM layer needs to be understood. This involves observing critical temperatures at different depths and the difference between day and night time temperatures. In HMA, temperature gradient is studied at noon solar radiation, morning and night hours with no solar radiation. The analysis of the variation of solar time and its effect on moisture evaporation in a BSM layer is vital. It is common practice to carry out BSM construction during summer; therefore, indication of temperature distribution during summer was analysed in this study.

6.2.2.1 Temperature distribution in the BSM-emulsion layer

The installed iButtons recorded the temperature distribution in the BSM emulsion layer for different periods, at different locations and positions. The first iButton was installed near the yellow line (YL), position B4, and recorded the temperature 227mm below the pavement surface for a period of 6 months. The second iButton in a similar location near YL, position B6, recorded temperature for 2 years. The third iButton near the inner lane (IL), position B5, recorded temperature 143mm below the pavement surface for a period of 6 months. The fourth iButton installed on the centreline near the inner lane, position B7, was damaged during recovery using a core drill and the iButton was unable to retrieve the recorded data. Therefore, the data from only the iButtons in positions B4, B5 and B6 are presented in Figure 134, Figure 135 and Figure 135.

The temperature data in Figure 133 presents the extreme temperatures measured at 1/3 depth of the BSM-emulsion layer during the study period. In position B5 near the inner lane during the winter period, the BSM layer had a lower temperature, at 9.6°C, while toward the beginning of summer the layer experienced a maximum temperature of 37.6°C. The minimum winter temperature occurred on 28 June 2007 at 7:48 hours while the maximum at the beginning of summer occurred on 30 October 2007 at 16:36 hours. These extremes of temperature are compared to the temperature measured at position B4 near the yellow line at 2/3 depth of the BSM emulsion layer, as shown in Figure 134.

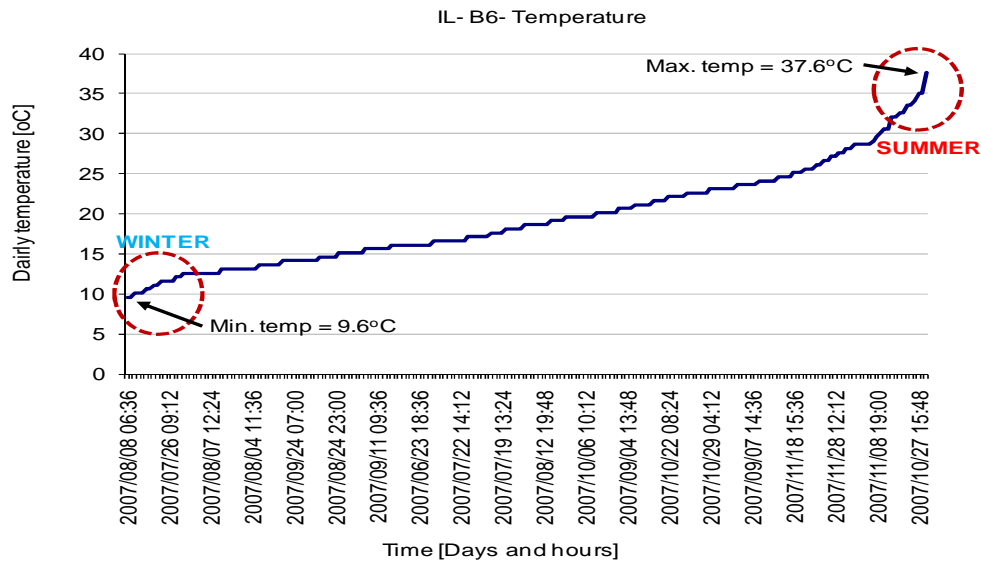


Figure 133: Daily temperature data near the inner lane (IL) at 1/3 depth of the BSM-emulsion layer of the N7 expressway near Cape Town

The measured temperature data in the BSM-emulsion layer at position B6 is indicated in Figure 134. The minimum winter temperature in the layer was found to be 10.7°C, while the maximum temperature measured at the beginning of the summer period was found to be 34.3°C. The minimum winter temperature occurred on 27 June 2007 at 10:12 hours while the maximum temperature at the beginning of the summer occurred on 30 October 2007 at 19.09 hours. The comparison of the temperature data in the BSM-emulsion layer at 1/3 and 2/3 depths during the winter period and the beginning of the summer shows that there is a temperature gradient in the BSM-emulsion layer. From the fact that the top 1/3 of the BSM-emulsion layer shows an overall higher temperature than the bottom 2/3, it is clear that the temperature distribution in a BSM layer is not uniform. Therefore, an understanding of the heat transfer coefficient (proposed in the Burger model) in BSMs is necessary to be able to quantify the temperature variation and its influence on moisture evaporation and other material behaviours affected by temperature variation.

The temperature data recorded in a full cycle of different seasons (i.e. from winter to summer and winter) is presented in Figure 135. The mission for all the iButtons started in June 2007. However, for the full cycle's measurement, the iButtons were left to continue taking temperature data for a period of 2 years, until July 2009.

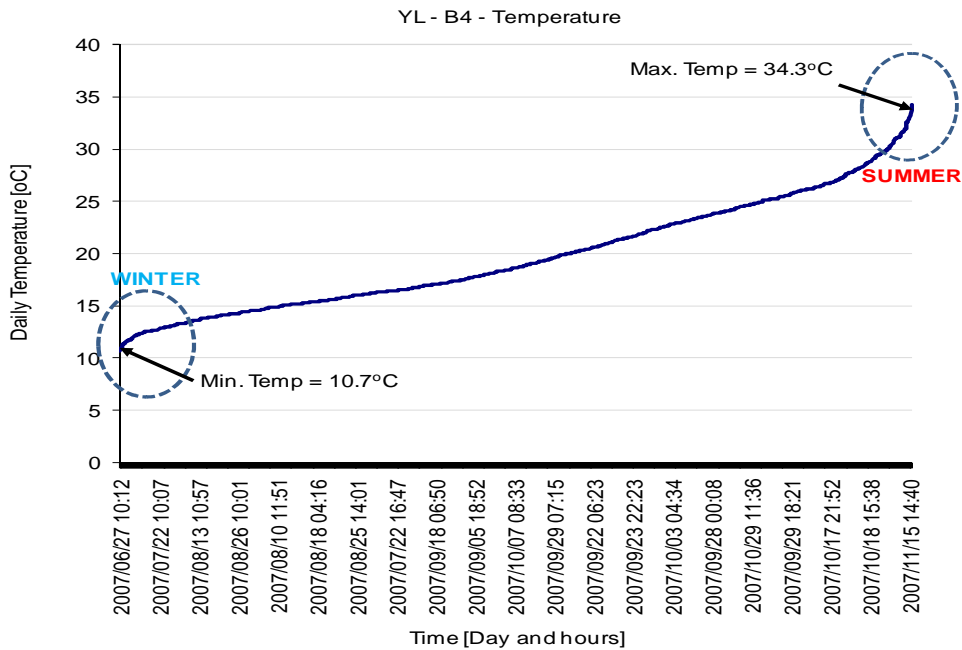


Figure 134: Daily temperature data near the yellow line at 2/3 depth of the BSM-emulsion layer of the N7 expressway near Cape Town

The temperature measured in the BSM-emulsion at position B6 indicates that the BSM layer can experience significant heat transfer during summer. The maximum measured temperature in the BSM-emulsion layer during summer was 49.6°C while the minimum during the winter period was 9.6°C. The maximum temperature in summer was recorded on 3 March 2009 at 12:00 while the minimum temperature in winter was recorded on 11 July 2008 at 11:48 hours. The hottest months in summer were found to be consistently in all years, i.e. 2007, 2008 and 2009, December to March. The extract of consecutive hot days in Figure 135 gives an indication of the summer maximum, minimum and average temperature in the BSM layer, as presented in Table 28.

Table 28: Extract of the hottest maximum daily temperatures in the BSM-emulsion layer at 2/3 depth during summer

Year	Month	Date	Time [hrs]	Temp. [°C]	
2007	Dec	22	18:36	39.6	Min. temp
2008	Jan	10	17:36	37.7	
2009	Jan	11	18:24	38.6	
2009	Feb	08	19.48	38.6	
2009	March	19	18:00	49.6	Max. temp
Average temperature				40.8	

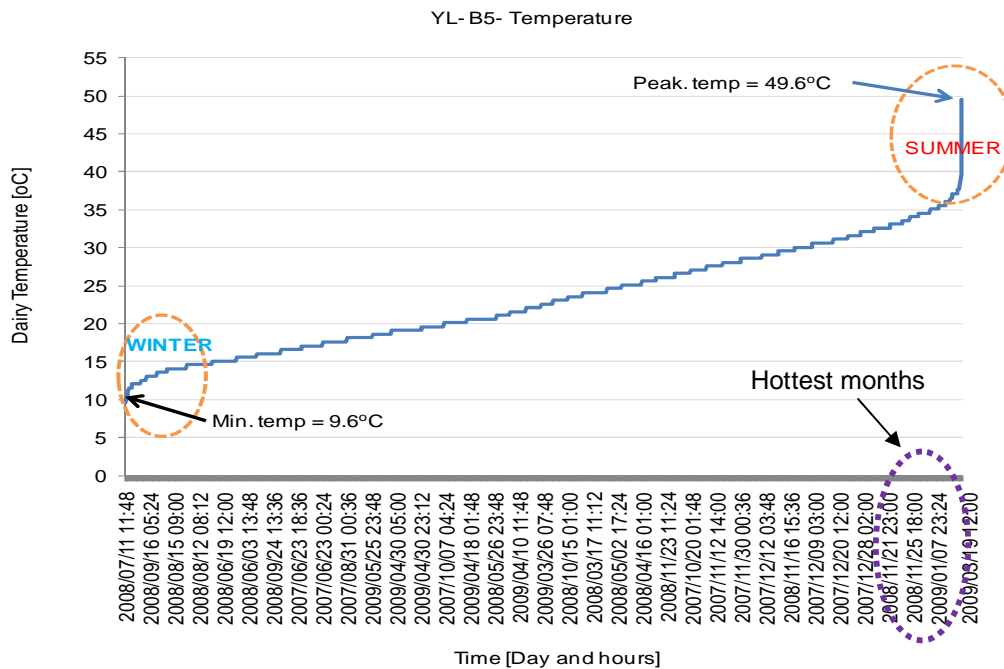


Figure 135: Daily temperature data near the yellow line at 2/3 depth of the BSM-emulsion layer of the N7 expressway near Cape Town

The maximum temperature, presented in Table 28 and Figure 135, for the BSM layer measured at 2/3 depth is 49.6°C. The trend observed in Figure 133 and Figure 134 shows that the maximum temperature is higher closer to the top surface than deeper in the layer. Although the temperature data from the iButton installed at position B7 was not retrieved, it is evident from the trend noted at B4 and B5 that a temperature of higher than 49.6°C can be expected at 1/3 depth. The temperatures are expected to be higher than measured in 2/3 depth at the YL during the hottest day. It is apparent from the field temperature results that modelling of temperature distribution in a BSM layer is vital for understanding the mechanism of material durability behaviour and long-term performance.

6.2.2.2 Temperature gradient observed in the BSM-emulsion layer

After the description of temperature variation in the BSM layer, it is important that the temperature gradient in a layer be defined. In practice, BSM construction is carried out during summer. The temperature distribution recorded during summer is used in the analysis of the temperature gradient in a BSM emulsion layer. The temperature gradient due to time of solar radiation can influence the moisture loss and strength development of the layer over time. The temperature gradient in BSM-emulsion is defined using the results of the iButtons installed in locations B4 and B5, at a depth of 1/3 and 2/3 respectively. It is anticipated that a similar temperature gradient trend will appear in the temperature data recorded for the full seasons.

The temperature results indicated in Figure 133, Figure 134 and Figure 135 show that solar radiation, air temperature, wind speed and heat transfer coefficient of pavement material play significant roles in the temperature gradient in the BSM-emulsion layer. The temperature gradient varies according to hourly temperature. At the top of the BSM-emulsion layer, the morning hours temperatures are lower, increase during the afternoon hours and later decrease during the night hours. On the other hand, at the bottom of BSM-emulsion layer, temperature is lower during morning hours and increases during the day but at a lower rate compared to the

top. At night, the bottom layer exhibits a higher temperature than during the daytime. This is due to rate of thermal conductivity of the absorbed heat. The top layer, however, cools down at a higher rate compared to the bottom due to the effect of wind and no solar radiation. Table 29 and Figure 136 show a typical hourly temperature variation in a BSM emulsion layer. Lower temperature is experienced in the morning for the top layer and this increases during the day and cools faster during the night. The recorded temperatures at the top and bottom of the layer (i.e. 1/3 and 2/3 depth) of BSM-emulsion on consecutive days in October 2007 are used as an example of the temperature gradient expected in the field conditions.

Table 29: Temperature gradient in the BSM-emulsion at different solar time

Depth [mm]	22-Oct-2007		21-Oct-2007		20-Oct-2007	
	Morning		Afternoon		Night	
	Time [hours]	Temp. [°C]	Time [hours]	Temp. [°C]	Time [hours]	Temp. [°C]
1/3 (143)	8:00-9:00	22.6	12:00-14:00	33.6	20:00-22:00	32.1
2/3 (227)		25.6		29.7		33.7
	16-Nov-2007		15-Nov-2007		14-Nov-2007	
1/3 (143)	8:00-9:00	22.1	12:00-14:00	34.1	20:00-22:00	28.6
2/3 (227)		24.9		31.0		33.2

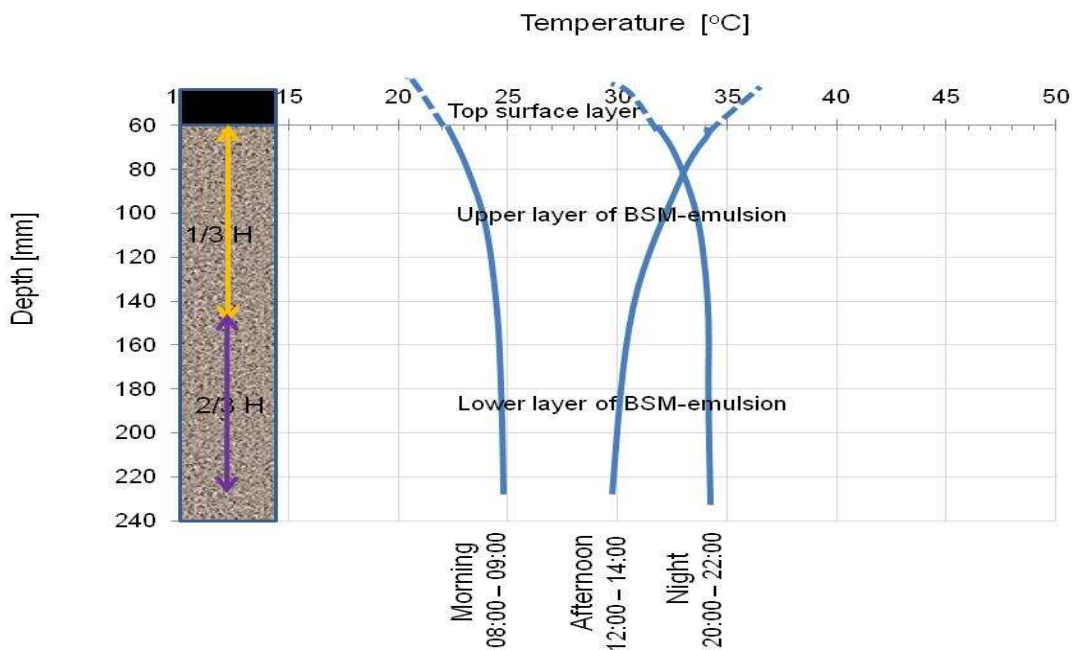


Figure 136: Temperature gradient through of N7 BSM-emulsion layer, with surface layer extrapolated

The temperature measured in the BSM-emulsion layer and presented in Table 29 and Figure 136 shows that temperature variation in the layer depends on solar time. Likewise, temperature variation is noted in the BSM layer, with the upper layer having higher temperatures compared to the lower layer at different time of a day. Nevertheless, it should be noted that the values indicated in Table 29 were taken from the maximum temperature at the beginning of summertime. This variation can be higher when considering the magnitude of maximum

temperature measured during peak summer months, for example January until March. Therefore, the observed temperature gradient in BSM needs to be modelled to predict this behaviour accurately. The accurate prediction of the temperature gradient will give a better understanding of the change of material properties through moisture evaporation during the day and night under various environmental conditions.

From these results, it is evident that understanding the temperature distribution in the BSM layer is important for predicting the long-term material performance based on environmental influences. However, this area has not been researched sufficiently to provide an accurate prediction of how materials develop strength based on temperature influence and evaporation of moisture during the curing period. The model for predicting temperature distribution presented in this section can be used as tool for judging the appropriate time (in hours or days) before a constructed BSM layer can be opened to traffic. Temperature distribution in HMA has been extensively studied in the past. In this study, a recent temperature distribution model developed by Burger and Kröger for HMA, which was found to be applicable to BSMs, is presented. This model addresses all the factors that influence the temperature variation seen in Table 29 and Figure 136. Although not validated due to a lack of some input variables obtained from field environmental conditions, this model needs to be researched further for BSMs.

6.3 TEMPERATURE DISTRIBUTION PREDICTION MODEL (Burger Model)

The temperature distribution in the pavement layer and its influence on materials performance depend on environmental conditions. In order to predict accurately, the moisture loss or engineering properties of the BSMs based on the influence of temperature, the following environmental factors need to be modelled. Air temperature, solar radiation, wind condition, and relative humidity, which differs according local environmental conditions. Other materials properties necessary as input parameters in the model include; density of materials in different layers, thermal conductivity, the specific heat capacity and thermal diffusivity. These parameters depend on binder and mineral aggregates composition. For BSMs these parameters are not know and therefore need to be determined experimentally as an input into the model. Whilst, the boundary layers such HMA, granular and cemented these parameters have been documented in the past studies. The usefulness of the model is the introduction of new parameters, which can provide a better understanding of the durability properties and long-term performance under the influence of temperature variation in the BSMs layer.

6.3.1 Heat transfer coefficient in the pavement layer

In a pavement structure, BSM is incorporated as a base layer. Therefore, understanding of the thermal properties of BSMs require good knowledge of the thermal properties of the surface layer e.g. HMA. The surface layer is exposed to adverse environmental conditions and transfers the heat to BSMs. Surface temperature can be measured or determined through the model below.

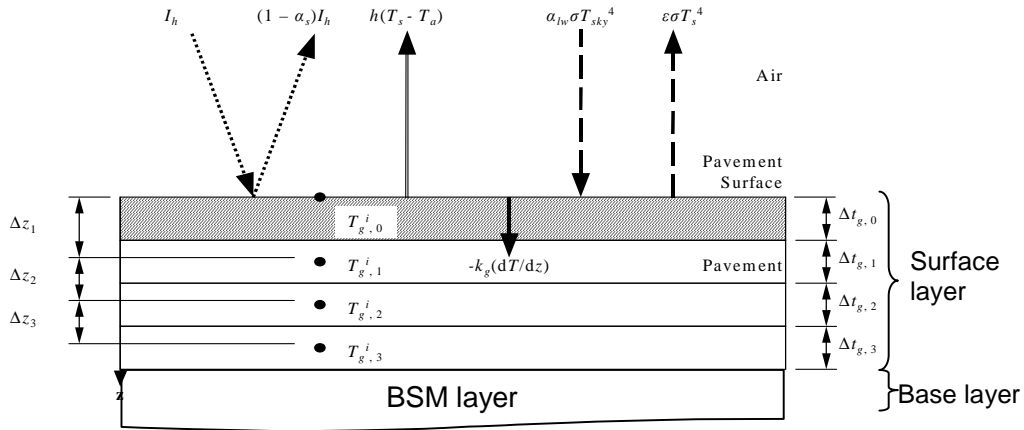


Figure 137: Models parameters on control volume for a unit layer of pavement surface exposed to the natural environmental conditions (Berger *et al.*, 2005)

The parameters presented in are expressed in the following relationship, Equation 30:

$$\begin{array}{ccccc}
 [1] & [2] & [3] & [4] & [5] \\
 I_h \alpha_s = h_d(T_s - T_a) + \epsilon \sigma T_s^4 - \alpha_{lw} \sigma T_{sky}^4 - k_g(dT / dz) & & & & \text{Equation 30}
 \end{array}$$

- The first term $I_h \alpha_s$ is net incident solar radiation absorbed per unit horizontal surface. Solar radiation is made up of two components namely diffused radiation, I_d and beam radiation I_b both are short wave radiation, i.e. $I_h = I_d + I_b$. The absorptivity, α_s of blacked surface is a function of the incidental angle, i.e. $I_h \alpha_s = I_b \alpha_z + I_d \alpha_d$
- The second term represents the convection heat transfer between the horizontal surface T_{surf} and air T_a with h_d , as the heat transfer coefficient.
- The third and fourth term represent the net sky emissivity, i.e. exchange in radiation between horizontal surface and the air due to long wave solar radiation and effect of dew point.
- The fifth (last) term represents conductivity in a discretised volume of the pavement layer, where k_g = thermal conductivity of a layer.

Burger *et al.*, recommend the heat transfer coefficient on the horizontal surface exposed to the natural environment be based on a distinction for daytime and nighttime. For nighttime, the first term in Equation 29 is negligible, because there is no solar radiation. Heat transfer coefficient h_d , during daytime is presented in Equation 30, and for nighttime, the heat transfer coefficient is presented in Equation 31.

$$h_d = \left[0.2106 + 0.0026 v_w \left[\frac{\rho T_m}{\mu g(T_s - T_a)} \right]^{1/3} \right] \left[\frac{g(T_s - T_a) c_p k^2 \rho^2}{\mu T_m} \right]^{1/3} \quad \text{Equation 31}$$

where the semi-empirical variables are defined by Burger *et al.* (2005) as:

- h_d = the daytime heat transfer coefficient.
- T_m = the mean temperature between surface, T_s and ambient T_a temperatures.
- ρ , μ and C_p = thermal properties of dry air, i.e. the density of air, dynamic viscosity and specific heat; these are determined empirically.
- v_w = the wind speed.

- k = thermal conductivity determined experimentally.
- g = gravitational force.

The heat transfer coefficient for nighttime is presented as follows:

$$h = 3.87 + 0.0022 \frac{v_w \rho c_p}{(\mu c_p / k)^{2/3}} \quad \text{Equation 32}$$

The suitability of these models is that they address all variables influencing environmental factors necessary to predict moisture evaporation and temperature gradient based on solar radiation, wind effect and relative humidity in the air.

6.4. RELATIVE HUMIDITY DISTRIBUTION IN THE BSM-EMULSION LAYER

The relative humidity (RH) is a measure of the amount of water vapour in the air (at a specific temperature) compared to the maximum amount of water vapour air could hold at that temperature; it is given as a percentage value. RH depends on the temperature of the air because warm air can hold more moisture than cold air. A RH of 100% indicates that the air is holding the maximum amount of water vapour it can at the current temperature and any additional moisture at that point will result in condensation. A RH of 50% means the air is holding half the amount of moisture it could. As the temperature decreases, the amount of moisture in the air does not change but the RH goes up (since the maximum amount of moisture that cooler air can hold is smaller).

In this study, RH in the BSM-emulsion layer was measured using the same iButtons installed for measuring temperature. The RH was measured at the same depths and locations as the temperature. The RH data is presented in Figure 138 Figure 139 and Figure 140. The RH measured by the iButtons has an accuracy of 5%. In addition, the RH measured in the BSM-emulsion layer represents a measure of the percentage of water vapour around the BSM-emulsion materials. It is anticipated that condensation occurred due to temperature gradient in the layer. However, the water vapour condensation measured with the iButtons i.e. over 100% RH does not truly represent the moisture content or saturation level of the BSMs. Therefore, further correlation needs to be established between RH and moisture content in the materials.

From Figure 138, it can be seen that the BSM layer at position B5 had an RH of approximately 90% during winter (at lower temperatures). However, as the air temperature increased during summer, the relative humidity in the layer fluctuated between 40% and 100%. This is due to the temperature variation in the layer, which influenced the evaporation of water vapour.

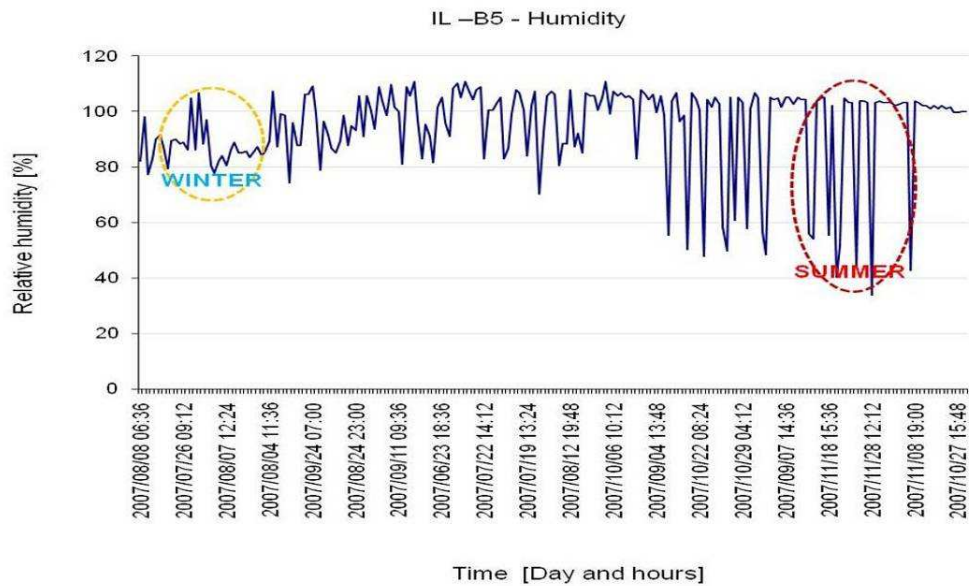


Figure 138: Daily RH data near the yellow line at 1/3 depth of the BSM-emulsion layer of the N7 expressway near Cape Town

The RH measured in the BSM layer at position B4 (Figure 139) was slightly higher than 100% during winter. An RH higher than 100% shows that condensation of water vapour occurred in the BSM material at lower temperatures. This may occur due to excess moisture diffused into a layer from the pavement. At the beginning of the summer, higher precipitation dominates resulting in a higher amount of moisture diffused in a BSM layer, therefore RH fluctuated due to moisture loss and air temperature increase.

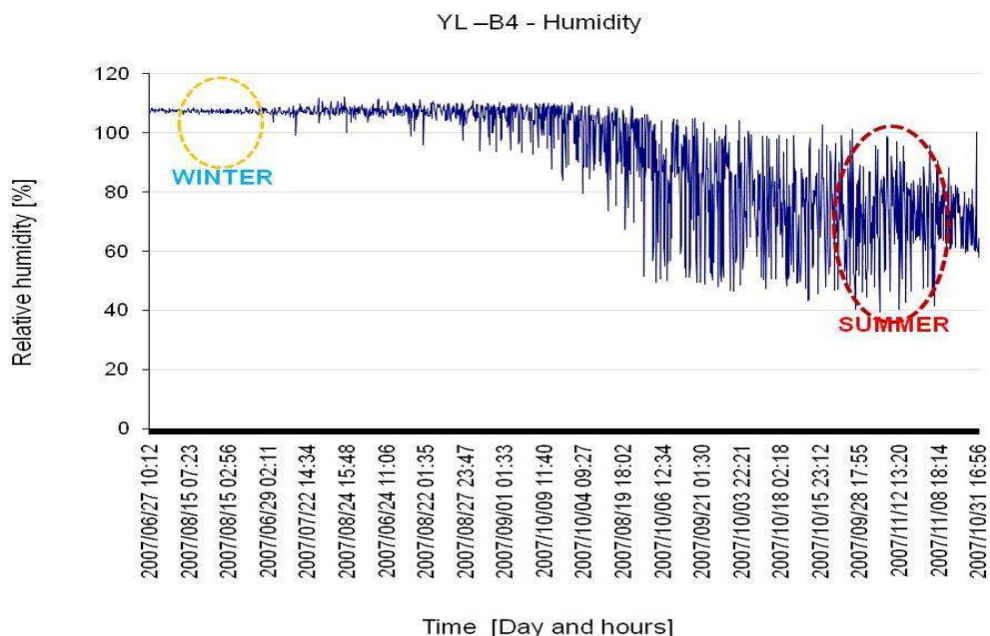


Figure 139: Daily RH data near the yellow line at 2/3 depth of the BSM-emulsion layer of the N7 expressway near Cape Town

The RH measured in a full cycle of seasons (winter to summer to winter) shows that the RH in the BSM layer can be predicted. It can be seen from Figure 140 that the measured RH at position B6 due to excess moisture diffused at the end of the surface camber, coupled with the lower temperature during winter, resulted in condensation. The effect of condensation in the BSM layer can be noted by the lower temperature of 9.6°C measured during this period. During the summer, it can be seen that the measured RH was uniformly at a range of 100%. This indicates that it is possible to predict the evaporation rate during summer, or dry, period using numeral formulation. However, the challenge remains as to how the relationship can be established between the measured RH and the actual moisture content in the BSMs. This is an area which needs further study in order to provide meaningful results in the performance of the BSM layer, due to variation in temperature and RH.

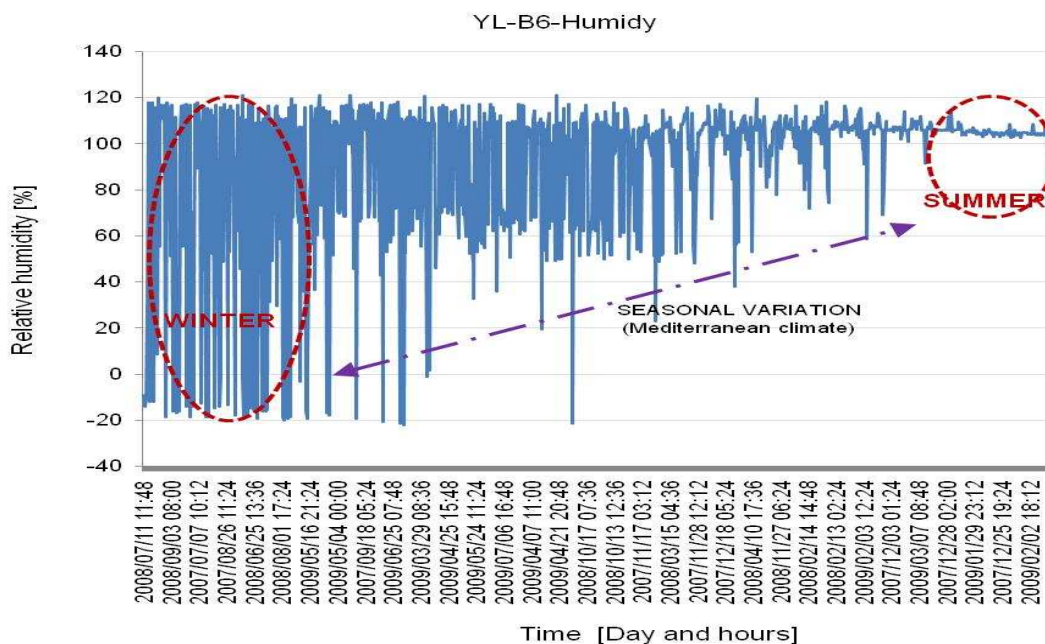


Figure 140: Daily RH data near the yellow line at 2/3 depth of the BSM-emulsion layer of the N7 expressway near Cape Town

From the limited results presented in this study, it can be seen that the measured temperature in the layer during peak summer went up to 49.6°C. This temperature range can adversely influence the durability behaviour and long-term performance of the BSM layer. Higher temperature coupled with excess moisture significantly influence moisture susceptibility of BSMs. In addition, this range of temperature variation in the long term significantly influences the age hardening of the binder in a BSM layer. Lower temperature, 9.6°C, can cause higher internal stresses in the layer and raise a concern about the strength behaviour of a BSM layer. It is therefore important that future studies explore more about the mastic adhesion characteristics at this range of temperature observed in the BSM layer. The lower and higher temperature study on the mastic-mineral aggregate interaction will give an insight into failure mechanisms due to the variation of temperature and RH in the BSM layer.

It is apparent from the results of temperature and relative humidity in BSMs that better understanding of BSM layer under field conditions can be achieved. Nevertheless, the application of thermal transfer and heat conductivity of materials is a multidisciplinary topic; therefore, experts from different fields need to be involved in the future research on this area.

6.5 VOID CHARACTERISTICS IN THE MIX MATRIX

The fundamental influence on age hardening and moisture damage in BSMs is linked with air void content. The void content characteristics in BSMs is a result of the nature of dispersion of binder into selective fractions in the mineral aggregates, binder thickness, mastic filler, addition of active filler and binder-mineral aggregate interaction. It is apparent from the literature that understanding age hardening and moisture damage in BSMs requires microscopic analysis. In this section, a detailed analysis of BSM volumetric properties is presented. The void content in BSMs is determined from a laboratory compacted specimen and cores extracted from the field pavement. The void content distributions are analysed using a CT-scan and voids in mineral aggregates are analysed using Scanning Electron Microscopy analysis (SEM). The results of analysis of different mix compositions are presented and discussed.

6.5.1 Void content determination

The air void content in a BSM mixture is highly dependent on grading, compaction level and filler/binder ratio. In addition, the physical properties of mineral aggregates, such as size and shape, also play a significant role in minimising the air voids in mixtures. Therefore, quantification of the void content in the material composition for BSM mixes used in this study was essential in order to relate the results with the influence on the change of rheological properties due to age hardening and moisture damage. The void content of the mixes was determined after carrying out the test on the relative bulk density (RBD) and maximum theoretical relative density (RICE) according to TRHM1 method C3 and C4, respectively. The calculation of the air void content was done according to the following relationship.

$$\text{Voids\%} = \frac{\text{RDm} - \text{RDv}}{\text{RDm}} \times 100 \quad \text{Equation 33}$$

where, RDm= maximum theoretical relative density RDv= bulk relative density.

6.5.1.1 Voids in laboratory compacted specimen

A vibratory BOSCH® compactor was used to compact laboratory-prepared specimens. Vibratory compactors normally pack the aggregate particles in a specimen closely, similar to field conditions. However, the inter-particle voids in BSMs are usually higher than in HMA. The attribute of higher void content in BSMs relates to lower binder content, higher viscosity (cold to warm) of the binder and the presence of moisture during mixing, which later evaporates. The determined inter-particle voids in BSM-foam and BSM-emulsion are presented in Table 30 and Figure 141. These results show that BSM-emulsion void contents fall in a range of 10% to 13% while BSM-foam shows higher inter-particle voids with a range of 13% to 16%. The influence of the voids difference and a link to moisture susceptibility in BSM-foam and BSM-emulsion is presented in Chapter 3. The influence of the variation of void content in BSM mixes is further related to age hardening behaviour and presented in Chapter 7.

Table 30: Bulk relative density, RICE density and void content in BSMs

Binder type	BSM mix type	Bulk relative density, BRD [kg/m ³]	RICE density [kg/m ³]	Void content [%]
BSM-foam	H0CF	2 177	2590	16.0
	H1CF	2 232	2593	13.9
	H1LF	2 241	2592	13.5
	Q0CF	2163	2553	15.3
	Q1CF	2196	2573	14.6
	Q1LF	2198	2561	14.2
BSM-emulsion	H0CE	2245	2566	12.5
	H1CE	2287	2564	10.8
	H1LE	2237	2694	13.0
	Q0CE	2289	2580	11.3
	Q1CE	2201	2516	12.5
	Q1LE	2273	2584	12.0

Note: Aggregates type, H=Hornfels-RAP, Q=Quartzite stone, C=cement, 0=No cement added

The analysis of the trends of the void properties in terms of binder and aggregate types are presented in Figure 141. The result shows that aggregate type, that is either Hornfels-RAP or Quartzite, has no particular influence (or trend) on different void contents measured in BSM mixes. However, there is a general trend of increase in the void content in BSMs without the addition of active filler compared with ones with the addition of active filler (i.e. lime or cement). The higher void content of the mix without active filler has a link to moisture susceptibility presented in Chapter 3.

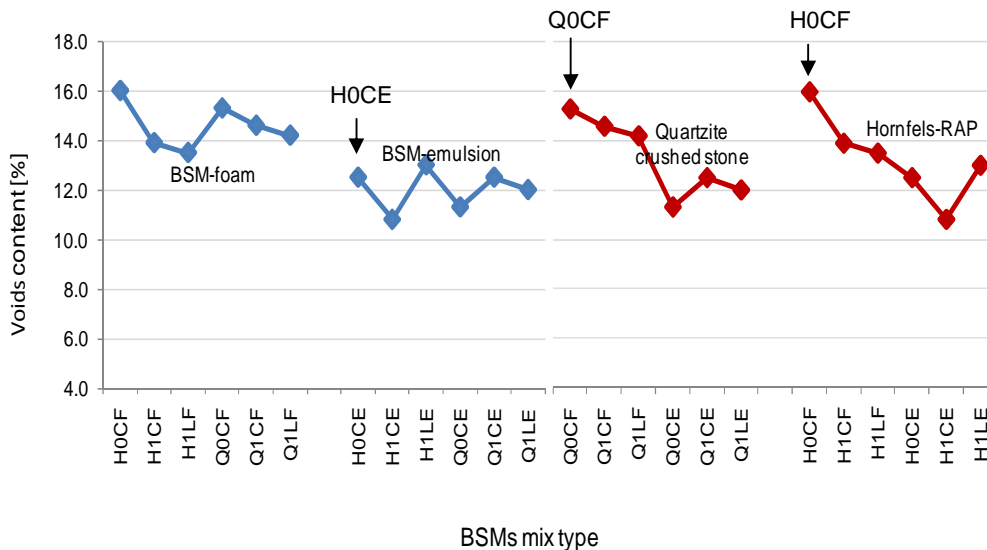


Figure 141: Void properties of BSMs and influence of mineral aggregates type

From the void properties results, it is evident that BSMs have a total higher void content in the mix matrix compared HMA. However, the void properties in different mix compositions, Quartzite aggregates or Hornfels-RAP, with different active filler content were found not to correspond to the moisture damage behaviour studied in Chapter 3. This shows that void content structure in the mix matrix is largely isolated and less interconnected. However, this behaviour needs further investigation. The isolated high void content in the mixes is generally

more damaging in the presence of pore pressure (more pronounced on less bound mixes without cement) than interconnected voids. This is due to less water, which might reside in the interconnected voids. The behaviour of the void structure distribution in BSM mixes is illustrated in Figure 142.

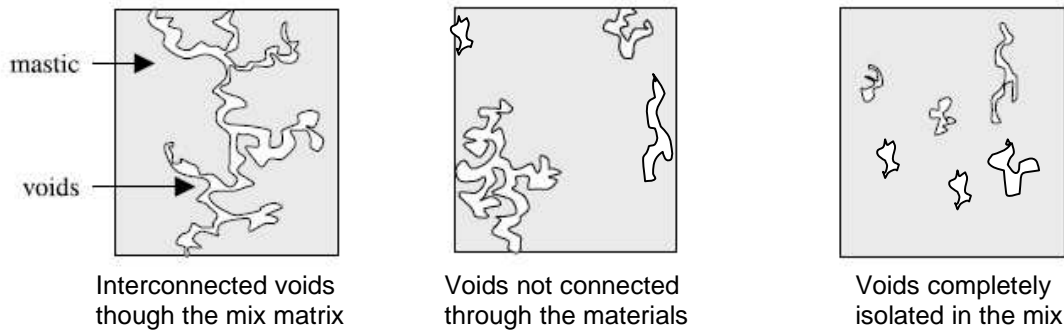


Figure 142: The different mode of voids structure present in BSMs

6.5.1.2 Voids in field extracted cores

The void characteristics of BSM mixes exposed to field conditions were analysed from cores extracted from an in-service pavement section. The cores from two different roads were analysed: P243/1 near Vereeniging in Gauteng and Shedgum Road in Saudi Arabia. The cores from these roads were extracted mainly to investigate the age hardening behaviour of the binder. However, prior to extraction of binder it was necessary to carry out void analysis for a better understanding of the relationship between void characteristics and age hardening of binder. The age hardening of binder is discussed further in Chapter 7 of this study. The cores from P243/1 were extracted from two different pavement sections, i.e. foamed bitumen and bitumen emulsion. The material composition during foamed bitumen recycling includes 40mm HMA and 200mm of cement-treated Ferricrete base material, while in the bitumen emulsion it includes 40mm HMA and 200mm of cement-treated Quartzite sandstone base. The binder content during stabilisation was 1.8% with 2% active filler (cement). 36 briquettes were extracted, 12 from the foamed bitumen section and 12 from the bitumen emulsion section, one briquette was extracted from YL, OWP and BWP from different stations along the road. The average moisture content and the void content of the cores from different positions are presented in Table 31.

Table 31: Volumetric properties of the field extracted cores from P243

Volumetric properties	Mixture type					
	Foamed bitumen			Bitumen emulsion		
	YL	OWP	BWP	YL	OWP	BWP
MC [%]	11.3	11	19.7	9.6	9.6	-
Voids [%]	16.4	16.0	15.2	24.9	25.9	23.7

Note: Aggregates type; Foam=Ferricrete, Emulsion= Sandstone

From the void content results in Table 31, it can be seen that bitumen emulsion mixes have high void contents compared to the laboratory compacted specimen (Table 30). This is because of a larger aggregate size of RAP content recycled with crushed cement treated material in the mix. The condition of cores extracted from the field shows that compactability of RAP aggregates

with sandstone leave large amount of voids in the mix (see picture of the cores' conditions presented in Chapter 3 section 3.7 pg 153).

The cores extracted from Shedgum Road came from full-depth in-place foam bitumen recycling. Full-depth recycling involves 100% RAP in the mix composition, i.e. pulverisation of 300–400mm distressed HMA and stabilisation of the top 150mm with 2.5% foamed bitumen, without active filler. However, it was noted that after opening to traffic within a short period of time, signs of distress with localised deformation and shoving were observed on the road. Progressive deformation occurred during the summer on the full length of the 12.8km road (Loudon International, 2008). This prompts investigation into the durability behaviour of the stabilised foamed bitumen base. The investigation was extended to void content determination, binder durability and mixture performance in terms of temperature and loading condition susceptibility. Stellenbosch University was assigned to undertake the investigation. Therefore, because the investigation is about the durability properties of foamed bitumen it was included in this study.

The premature failure investigation on Shedgum Road involves determination of void content in the cores extracted from different locations, the extraction and recovery of binder and determination of its durability properties. The calculated void content is related to binder content and rutting behaviour in different locations (i.e. OWP, IWP and BWP) of pavement structures, as presented in Table 32. In Chapter 7, the void content, rutting and age hardening behaviour are compared and discussed.

Table 32: The average rutting, bitumen content and percentage voids of the cores extracted from different stations and locations of Shedgum Road.

Volumetric properties, Top and bottom of core		Core extraction location and position on pavement					
		ST04 right	ST04 left	ST08 right	ST08 Right	ST09 left	ST09 left
		OWP	OWP	IWP	BWP	OWP	BWP
	Rut [mm]	10	20	0	0	20	0
	BC [%]	8.4	7.7	6.8	6.8	9	7.4
	Voids [%]	5.5	5.0	8.4	8.4	2.5	9.4
	BC [%]	8.4	7.1	6.8	6.8	9.5	7.5
	Voids [%]	10.2	10.9	11.6	12.8	5.4	13.3

Note: Aggregate type: recycled 100% Limestone-RAP

The extracted cores from different stations (ST04, ST08 and ST09) were sliced into two sections. The binder content from the top and bottom slices were extracted and later tested for age hardening, as presented in Chapter 7. However, prior to the extraction of binder, the void contents of the sliced top and bottom specimens were calculated from measured BRD and RICE properties. The binder content and calculated void contents were related to the rutting behaviour at that particular station, as presented in Table 32.

The binder content recovered from the top and bottom slices are relatively higher than the HMA; this is because 100% RAP was used in the mix with the addition of 2.5% foamed bitumen. Nevertheless, the binder content seemed consistently equal for the different locations (Table 32). The general trend shows that void content is related to binder content and rutting. The location with higher void content and lower binder content has lower rutting. Likewise, the location with lower void content and higher binder content has higher rutting. This behaviour is graphically presented in Figure 143. The top slice shows less air void content compared to the bottom slice. This is expected due to extra densification by traffic and the percentage of binder

content. The rutting behaviour is normally influenced by higher binder and less voids. According to the results presented in Table 32, this behaviour is more pronounced in Station 09 (OWP). Although Station 04 (OWP) shows similar rutting to Station 09 (OWP), the measured void and binder content do not show similar trends. Other parameters known to influence rutting behaviour are temperature and overloading, rather than void content in the mixes. The correlation between void content, rutting and age hardening are further presented and discussed in Chapter 7.

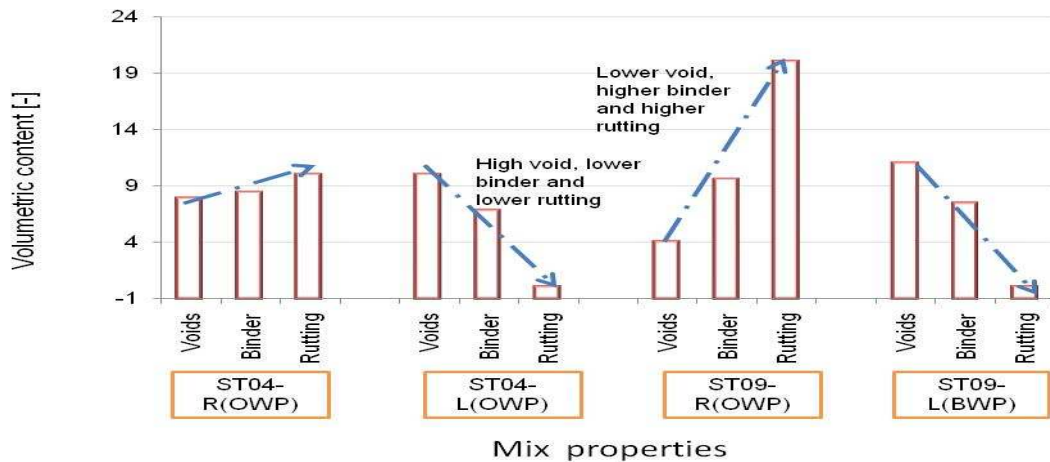


Figure 143: The relationship between void content, binder content and rutting behaviour in BSM mixes from Shedgum Road

6.5.2 Void distribution in the mix matrix

6.5.2.1 CT-scan analysis

The utilisation of advanced measurement techniques can assist in understanding, at microscopic level, the material properties that play a critical role in durability behaviour and long-term performance. In a recent research project into BSMs at the University of Stellenbosch, a number of laboratory investigations were involved: a CT-scan was used to investigate the volumetric distribution composition of the BSM mixture to understand the influence of the new compaction method developed for BSMs (Kelfkens, 2008). The main concern was to look at the density of the compacted specimen, void contents and possible crushing of stones. However, through the application of the CT-scan, critical analysis can be extended to gaining insight into the influence of the volumetric distribution composition on temperature gradient and moisture transport, thus understanding the influence on age hardening as well as moisture damage susceptibility in BSMs as presented in this study. Limited CT-scan analysis was performed on both foamed bitumen and bitumen emulsion. The CT-scan image analysis method known as x-ray tomography was used to study compacted briquettes with the aim of determining:

- the distribution of the air voids in the compacted specimen,
- the volume of the different mixture composition (mineral aggregate skeleton),
- the bitumen content in the compacted or field core briquette

The CT-scan analysis presented in this study was performed at Delft University of Technology in The Netherlands. The principle of the CT-scanner is based on the emission of x-rays. The absorption and radiation depends mainly on the atomic number and density of the material Hagos (2008). The images are taken at a specific interval and by combining a series of 2D images, a 3D image can be constructed, as shown in Figure 144.

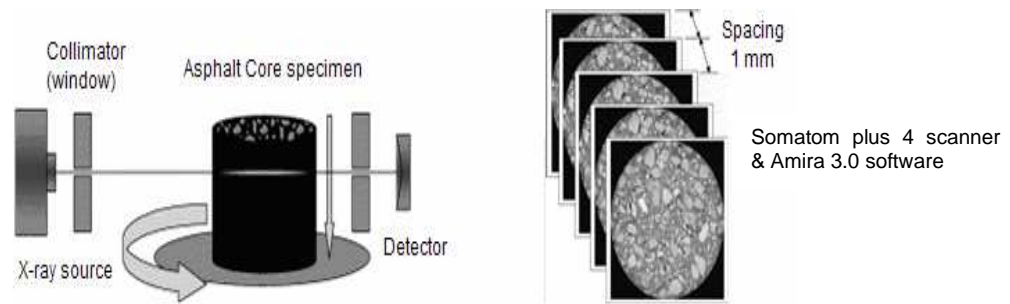


Figure 144: The CT-scan (x-ray tomography) technique, (Hagos, 2008)

The results of CT-scan image analysis of the laboratory compacted and cured specimens is presented in Figure 145 and Figure 146. However, it should be noted that the scanning was done using Siemens Somatom, which is applicable for scanning relatively large specimens. That means the accuracy for small specimens may be reduced due to small voids and the isolated void structures found in BSMs. In addition, because of the presence of moisture in the mix, CT-scanning cannot distinguish between water and bitumen. Therefore, the information on voids between the binder and water cannot accurately be analysed. It can be seen from the results in Figure 145 and Figure 146 that void content distribution in foamed bitumen and bitumen emulsion was not detected in the mix composition. Nevertheless, some valuable information can be obtained from the results. The distribution of mortar and aggregates in foamed bitumen and bitumen emulsion seem to be different. In foamed bitumen, there are distinctions between mortar and aggregate distributions. This confirms the affinity of dispersed binder to filler fractions and the occurrence of less coating on the larger aggregates. In bitumen emulsion mixes, it can be seen that mortar distribution is significantly non-uniform due to the fact that the breaking of emulsion does not only coat the filler particles but, instead, a thin film of bitumen also coats the large aggregates.

The distribution of mastic and mineral aggregates in BSMs gives an insight into durability properties when the mixes are exposed to the field conditions. The effect on binder ageing and moisture damage can be linked to the mix matrix distribution. Void structures being isolated or interconnected plays a significant role in durability properties, therefore further investigation into this area is required. Nano CT-scanners have been indicated to be applicable to scan accurately small specimens with small void contents. In addition, permeability using Darcy Law can be applied to supplement the investigation on void structure characteristics.

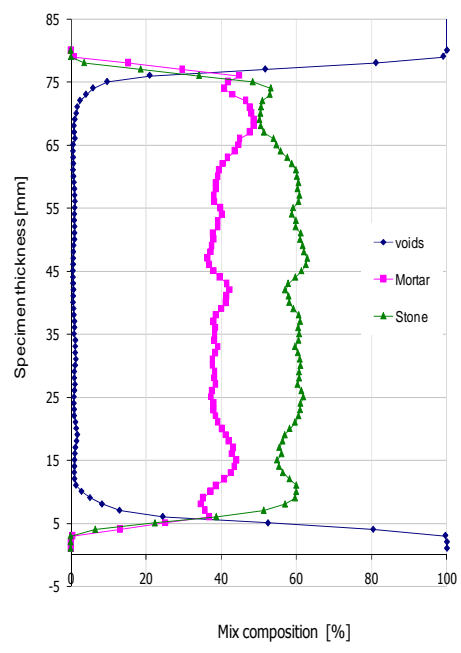
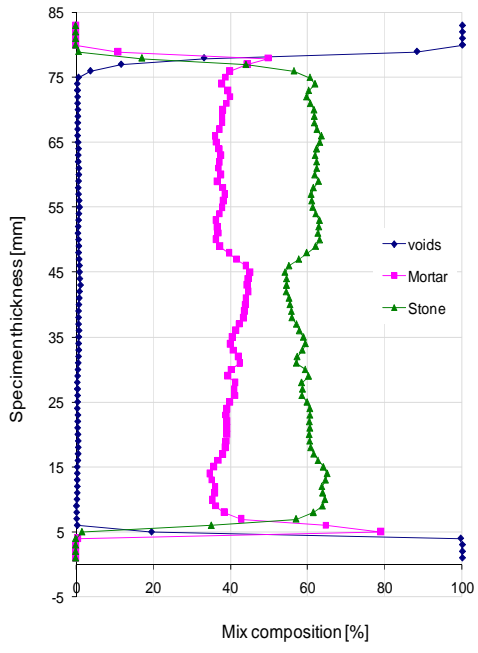


Figure 145: CT-scan analysis of the distribution of foamed bitumen mix composition of vibratory compacted specimens S3b and S3a

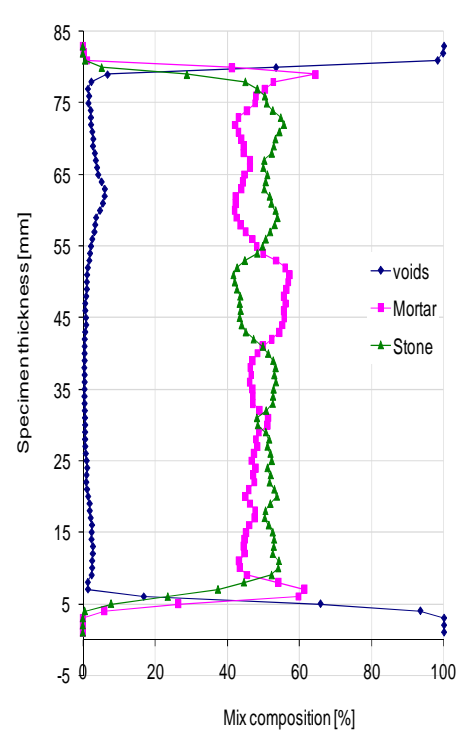
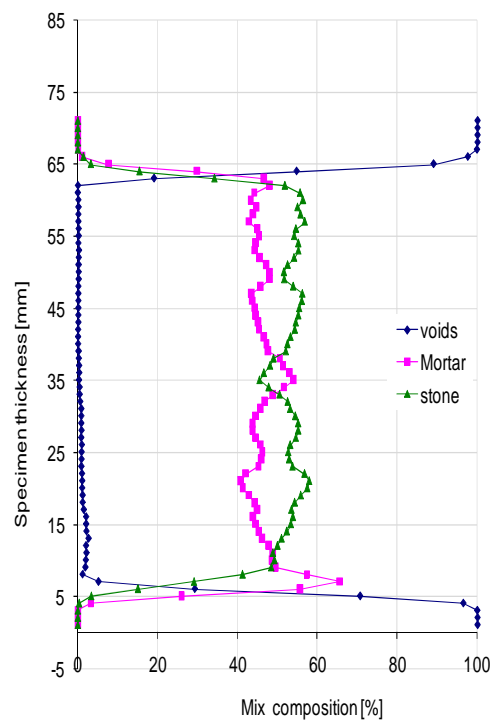


Figure 146: CT-scan analysis on the distribution of bitumen emulsion mix composition on vibratory compacted specimen S2 and S1

6.5.2.2 SEM analysis

Scanning Electron Microscopy (SEM) is another advanced measuring technique, which has been used by researchers for materials characterisation. Past studies examined samples of pavement materials at a micro-scale using the SEM technique for potential identification of the key elements that could provide the opportunity to understand the fundamental behaviour of pavement engineering materials (Mgangira, 2007; Mgangira and Paige-Green, 2006). In order to gain insight into the volumetric distribution composition, and particularly the influence of the addition of active filler (cement or lime) in BSMs at micro-scale, the SEM measuring technique was used in this study.

The SEM measuring technique is commonly applicable in the field of mineralogy; therefore, analysis of the BSM samples in this study were done at the Department of Geology, Stellenbosch University. Small size samples are needed for analysis so sample preparation, such as cutting BSM briquettes to 15mm x 50mm size, was necessary to be able to fit them into a scanner chamber. However, due to the spalling (brittle) behaviour of BSMs, it was necessary to apply epoxy to the sample prior to cutting into the required size (Figure 147). After cutting to size, polishing was done using different sandpaper sizes, ranging from coarse (no. 100) to fine (no. 1000). The polished sample needed to be electrically conductive or rendered so by being coated with gold, as backscatter, prior to SEM analysis. After gold coating, the sample was mounted on a stub and energised until an image was visible. Backscatter images show the compositional difference in the sample with the addition of topography. Energy dispersive analysis was used to detect x-rays generated from the sample surface to determine the elemental composition. The SEM device and the computer magnification during the analysis of the sample are shown in Figure 147.



Figure 147: The Scanning Electron Microscopy, SEM, device system and prepared polished samples

A microscope, model A LEO 1430 VP SEM was used with Oxford INCA software for the Energy Dispersive X-ray Spectrometer (EDS) analysis. The magnification level varied depending on the level of detail required. Particle size in the image can be determined by the scale bar shown on each image. Microanalysis was accomplished using the EDS coupled with the SEM.

The SEM image acquisition during analysis describes feature of volumetric composition and structures of the materials that were significant. Once the selected features of interest were identified on the images, they were marked and magnified to the required scale. A spot analysis was made to determine the elemental composition from which it was possible to identify the mineral or materials within a matrix. Each feature of interest was captured and stored in a file. EDS analysis was performed on some of these spots, as shown in the results presented.

Limited samples were analysed due to the availability of the equipment. The results of SEM analysis presented in this study are for the BSM-foam. The BSM-emulsion specimen took a long time (over 8 hours) to be energised. As a result, the test was terminated prematurely due to the tight schedule of the equipment. The results of the successful SEM analysis are presented in Figure 148, Figure 149 and Figure 150.

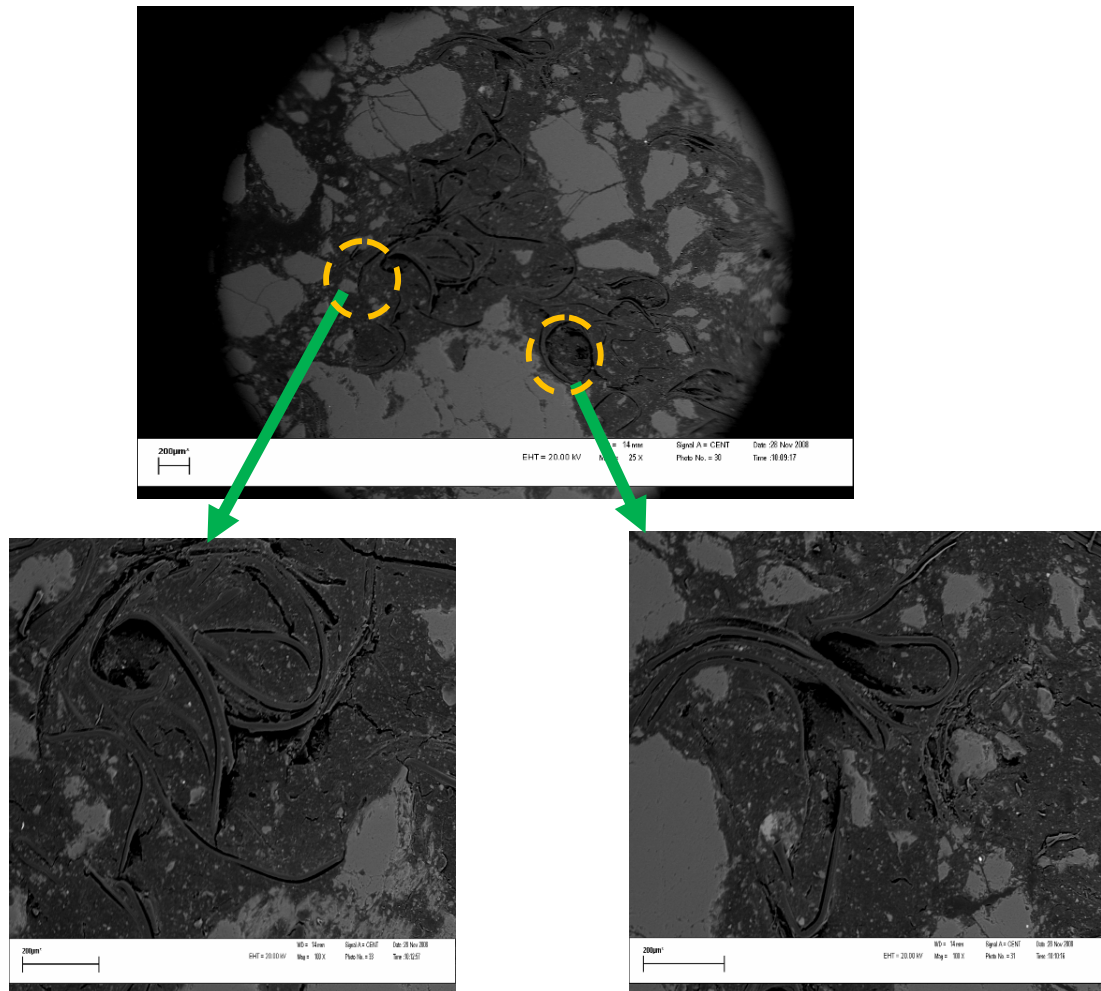


Figure 148: SEM analysis and magnification (200µm) of a selected part of Quartzite aggregates stabilised with foamed bitumen and added of cement (Q1CF)

Figure 148 presents a SEM images of Quartzite aggregates stabilised with foamed bitumen, magnified at 200µm. The images show that thread-like structures of bitumen mastic are present between coarse particles. This behaviour is not normally evident to the naked eye after foamed bitumen is applied during mixing in a laboratory. However, the electron microscopy analysis provides the means to observe the mastic structure, including the dispersion of the binder throughout the filler particles. Comparison of the selected scans reveals the pertinent findings of the differences in mastic structure between the Quartzite aggregates stabilised with foamed bitumen and added cement (Q1CF) and the Hornfels-RAP stabilised with foamed bitumen without cement (H0CF). Figure 149 presents the SEM images of the sample prepared from H0CF.

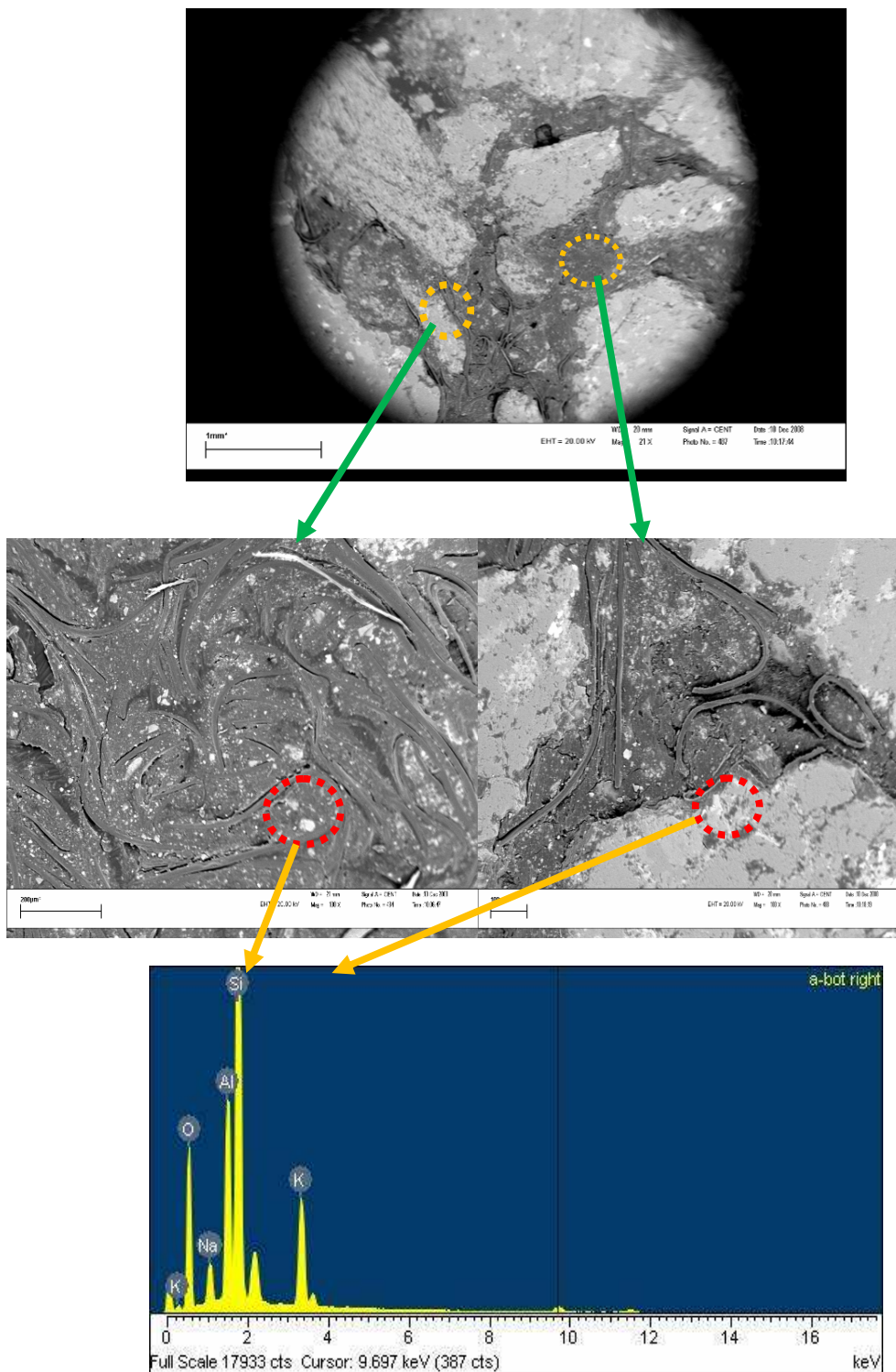


Figure 149: SEM analysis and magnification of selected parts of Hornfels-RAP aggregates stabilised with foamed bitumen and no cement (HOCF), further elemental analysis on the whitish part on the mastic was done by EDS

The SEM image of Q1CF mastic in Figure 148 shows a continuum of bitumen embedded with filler particles (rich in bitumen) and interconnected by threads of bitumen. Similar behaviour of bitumen thread structure is observed in the mix of Hornfels-RAP without cement (see Figure 149). However, it can be seen that the bitumen is lightly dispersed in the mineral due to lack of cement. The voids in the mastic are observed in the H0CF with cracking behaviour than in Q1CF. The cause of mastic cracking in Hornfels-RAP without cement is a result of a higher PI of 7.1 compared to Q1CF, which is non-plastic. The voids in the foamed bitumen mastic between the threads of bitumen can result in two detrimental effects on the mix matrices: 1) diffusion of air, which might result in oxidation and age hardening of the bitumen threads and thin film binder; 2) transport of moisture, causing cracks to be filled with water, consequently generating pore pressures under dynamic loading. The pore pressure affects cohesion within the mastic and adhesion to the large aggregates. However, at the equilibrium state of moisture content, the implication of thread foamed bitumen mastic might significantly improve both durability behaviour and long-term performance characteristics of BSMs. The bright spot noted on the mastic and on the large aggregate fraction of the Hornfels-RAP were further analysed using EDS (see Figure 150).

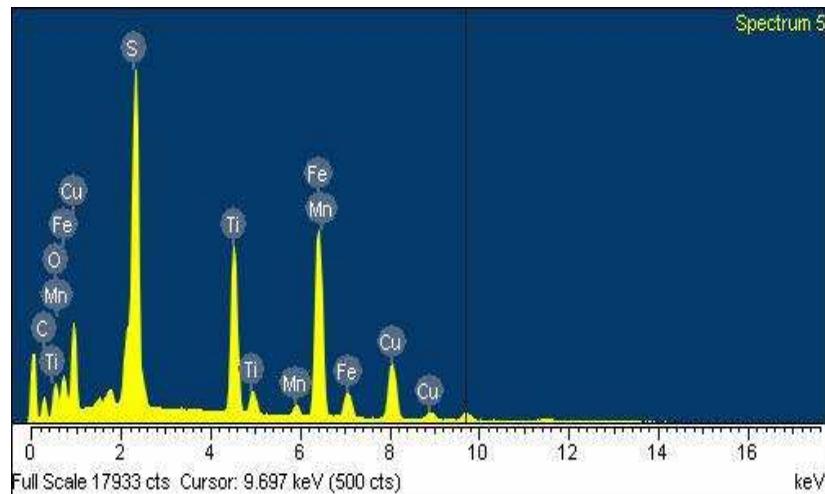


Figure 150: EDS elemental analysis of the thread structure of the mastic composition.

Figure 148 and Figure 149 show the elemental composition of the mineral aggregates and filler encapsulated in the thread structure of bitumen mastic, respectively. The large Si peak in Figure 149 shows that the materials are predominantly quartz, with moderate Al, and with the presence of K, Na and O. Figure 150 is the EDS scan of the thread structure of bitumen mastic observed in the SEM image. It can be seen that the elements detected in the mastic thread are S, and Fe, which dominate over Cu, Ti, Mn, and O. These elements might be part of the heteroatom present in the bitumen composition. These type of mineral element observed in the bitumen mastic and aggregate have been reported by Mgangira and Paige-Green (2006). They comment that the presence of K, Mg, Na, and Al, in the mineral aggregates indicates that there is a likely presence of soluble salts. Depending on the environmental condition, with these soluble salts in the presence of water, the formation of sodium sulphate, sodium chloride, magnesium sulphate, and sodium carbonate can occur. That means that any formation of soluble salt in the mix can result in no significant bonding between bitumen mastic thread and the large aggregate fractions.

From these observations, although limited, it may be demonstrated that the SEM technique is useful in understanding the mechanism of failure of BSMs and being able to

characterise materials at micro-scale level. Micro-structural characterisation of materials can help to identify key elements that contribute to the durability behaviour of BSMs and understanding the long-term performance. However, since certain aspects of chemistry fall into specialised areas, proper interpretation requires an experienced person in this field.

6.6. CONCLUSIONS

The influence of temperature and void characteristics on durability behaviour of BSMs were analysed in this Chapter. From the results presented, it can be seen that temperature and voids play a significant role in the durability and long-term performance of BSMs.

- Temperature is regarded as a powerful accelerating factor for evaporation and age hardening; void content significantly influences the moisture transport in the mix matrix and diffusion of air into the binder. It is apparent that understanding of these parameters gives an insight into the mechanisms influencing not only age hardening and moisture damage, but also evolution of adhesion and cohesion in the mix through evaporation and curing potential.
- Field investigation of BSM layer shows that the temperature and RH across the pavement section are not uniformly distributed over the layer. The trend observed show that maximum temperature is relatively higher on BSM depth closer to the top surface than deeper in layer. The temperature gradient in a layer significantly influences the moisture evaporation and curing behaviour. Therefore, understanding of this behaviour is important for judging the appropriate time (in hours or days) the constructed layer can be opened to traffic.
- The key factors that have been indicated to influence temperature and void characteristics in BSMs are: 1) heat transfer and 2) voids structure. The heat transfer in the BSM layer depends on the materials properties and local environmental factors such as solar radiation, wind speed and relative humidity. In this chapter, a Burger model developed for predicting heat transfer in pavement structure is proposed for application to BSMs. The void content determination in the BSM mix matrix is not sufficient to provide a conclusive answer about a link to mechanisms of moisture transport and the damaging effect in the BSM layer. In this light, more study needs to be directed into this area to be able to understand the contribution of the voids and failure mechanisms.
- The results from CT-scanning and SEM presented in this study shows that the fundamental failure mechanisms of BSM mixes can be properly defined through microscopic analysis. Therefore, further research on this area is required to provide a better understanding on the durability behaviour and long-term performance under field conditions.

REFERENCES

- Burger, M. and Kröger D.G. 2006. Experimental convection heat transfer coefficient between a horizontal surface and the natural environment, proceedings of the 17th International congress of chemical and process engineering, Prague, Czech Rep. pp. 1523 – 1524,
- Burger M. 2005. Prediction of the temperature distribution in asphalt pavement samples. Master thesis, Department of mechanical engineering, Stellenbosch University, South Africa.
- Hagos E.T. 2008. The effect of ageing on binder properties of porous asphalt concrete. PhD dissertation published at the Technical University of Delft. The Netherlands
- Highter W.H and Wall D.J 1984. Thermal properties of some asphaltic concrete mixes. TRB no. 969 pg. 38-45.
- Jenkins K.J. 2000. Mix design consideration for the cold and half-warm bituminous mixes with emphasis on fumed bitumen. PhD dissertation, University of Stellenbosch, South Africa
- Jenkins K.J., Ebels L.J, Twagira M.E, Kelfkens R.W, Moloto P and Mulusa W.K., 2008. Updating bitumen stabilised materials guideline: Mix desing report, phase II. Reseachr report, prepared for SABITA and Gautrans, Pretoria. South Afrca.
- Jia L and Sun L. 2007. Numerical prediction model and thermal properties for asphalt pavement. Journal of advanced characterisation of pavement and soil engineering materials. Taylor & Francis Group. London.
- Loudon International, 2008. Failure mechanism of in situ recycling with foamed bitumen stabilisation. Technical report on the investigated of distress on Shedgum Road in Saudi Arabia
- Kelfkens, R.W.C. 2008. Vibratory hemmer compactor of bitumen stabilised materials. MSc Thesis. University of Stellenbosch. South Africa.
- Moloto P. 2009. Curing protocol for the BSMs-Improving and validation. M.Sc. Thesis. To be submnitted at Stellenbosch University. South Africa
- Mgangira M. 2007. Use of scanning electron microscope in the road materials characterisation. CSIR BE report CSIR?BE/IE/2007/024/B. Pretoria South Africa.
- Mgangira M.B and Paige-Green. P. 2006. Scanning electron microscopy (SEM) internal technical report no. CSIR/BE/IE/IR/2006/0017/B. CSIR. Pretoria South Africa.
- Serfass, J. P., Poirier, J. E., Henrat, J. P. and Carbonneau, X., 2003. Influence of Curing on Cold Mix Mechanical Performance. Performance Testing and Evaluation of Bituminous Materials PTEBM'03, 6th International Rilem Symposium, Zurich, Switzerland
- Steyn W.J.vdM. 2006. Observation technique for pavement infrastructure. PG report CSIR/BE/IE/IR/2006/0007/B. Pretoria. South Africa.
- Weinert H.H. 1980. The natural road construction materials of Southern Africa. H & R Academia (Pty) Ltd. Cape Town. South Africa.

CHAPTER 7

AGE HARDENING AND ENGINEERING PROPERTIES

7.1 INTRODUCTION

In recent times, fundamental durability properties of bitumen stabilised materials, in terms of age hardening and moisture damage, have been of concern for practitioners. It is known from HMA that age hardening of bitumen occurs during in-plant mixing, construction and in the long-term under in-service conditions in the pavement. However, little is known about the age hardening of bitumen in BSMs and its influence on the durability properties and/or long-term performance of a pavement. The fact that BSM technology is evolving means a number of factors are still under investigation and a lot still needs to be done for practitioners to gain confidence during mix design and application of BSMs.

The age hardening of binder in HMA normally significantly influences the adhesion and cohesion of the mix. This results in stripping among other effects. This is unlike BSMs where the fundamental age hardening characteristics have a different influence on binder to filler behaviour and the effect on adhesion and cohesion is not as obvious. In the literature review, oxidation was identified as the main source of age hardening of bitumen. However, due to physicochemical interaction between colloidal particles of foamed bitumen and bitumen emulsion, modelling oxidation behaviour of BSMs is a challenging task both during short-term and long-term application. In this chapter, the fundamental characteristics of age hardening of BSMs will be explored. The aim is to provide a better understanding of how the colloids of foamed bitumen and bitumen emulsion interact with mineral aggregates and the influence on age hardening of BSMs. Further comparisons between age hardening potential of BSM-foam and BSM-emulsion are made during mixing or short-term ageing and during in-service pavement condition or long-term ageing.

7.1.1 Lessons from the literature review

From the literature review conducted on bituminous binder durability, the following points are regarded important for consideration in the study of age hardening behaviour of binder in BSMs and are presented in this chapter.

- Heating of bitumen above 150°C shows that a non-oxidative (non-chain free radical oxidation) reaction may begin to cause chemical changes in bitumen, even without the presence of oxygen. Thus there is a need to investigate short-term age hardening potential of foamed bitumen produced at an elevated temperature of between 160°C and 180°C.
- Temperature has been indicated to be a powerful accelerating factor in ageing by serving two purposes: 1) it softens the bitumen and increases the diffusion rate of oxygen, in presence of enough oxygen; and 2) it accelerates the chemical reaction even at the low temperatures encountered under the BSM layer in pavement field conditions. This important aspect needs to be understood in terms of the heat transfer and thermal conductivity of BSMs in a pavement layer.
- The change in rheological and chemical properties of the binder is used to characterise the effects of age hardening on binder durability properties. Therefore, in understanding

these behavioural changes, one needs to recover the binder from mixes and determine the ageing effect with respect to rheology (i.e. change in penetration, viscosity and softening point). The changes in chemical composition associated with oxidation are determined by studying the changes in molecular distribution and functional group due to the presence of sulfoxide and ketone molecules in the age-hardened bitumen.

- Physicochemical properties of binder-mineral aggregate interaction have a significant influence on the age hardening behaviour of the binder in BSMs. Depending on the adsorption properties (acidic or basic), mineral aggregates have a dual role in binder oxidation: 1) they absorb the highly polar fraction of bitumen and make them less oxidisable; and 2) they work as a catalyst when adsorption is not effective by promoting the formation of an oxidation product in the less polar generic fraction, such as saturates and naphthalene aromatics, and increase binder viscosity. In this regard, the effect of different mineral aggregate and binder interactions on age hardening need investigation.

The performance of mastic in BSMs is mainly dependent on the binder content and properties and the amount of filler. Therefore, mastic properties such as stiffening play an important role in adhesion and cohesion and the resulting durability behaviour of BSMs. In that light, the characterisation of binder and mastic in relation to age hardening and performance of BSMs needs investigation. The investigations require recovery of binder from BSM mixtures. The recovered bitumen can be analysed to understand the change in physical (rheological) and chemical properties of the binder. The change in physicochemical properties can be used as a fundamental tool in studying the age hardening behaviour of BSMs and aid better prediction of the long-term performance of BSMs.

7.1.2 Objectives and scope

Age hardening of binder influences adhesion and cohesion of the mix. Past studies indicate that poor adhesion is a major contributor to poor performance in HMA. The mechanism of failure due to embrittlement of the binder, particularly at low temperatures, is related to the environment and traffic conditions. In this state, the resistance of binder to stress and fatigue is reduced. In BSMs, less binder is dispersed in the mineral aggregates and the dispersed colloidal particles (foam or emulsion) have high affinity to the filler fraction. As such, the dispersed thin film of the binder encapsulates and interacts strongly with the filler. This behaviour results in graduating temperature susceptibility and hence the crack development mechanism and fatigue failure is different from HMA (Twagira, 2006).

The main objective of the study presented in this chapter is to provide an overview of binder durability in BSMs. The study was undertaken to understand the actual cause and degree of the age hardening effect on the physical (rheological) and chemical properties of binder in BSMs. In addition, this chapter aims to understand the difference in ageing behaviour between foamed bitumen and bitumen emulsion, if any. In that regard, further studies can be based on the findings of this study to investigate the effect of age hardening on the performance of BSMs, as well as simulating short-term and long-term behaviour. This may enable practitioners to understand the implication of the selection of the binder type during mix design and expected influence on the durability behaviour and long-term performance of BSMs.

The scope of this study is limited to the effect of age hardening on the rheological properties of binders used in BSMs, such as penetration, viscosity and softening point. No mechanical tests, such as Shear Rheometer (DSR) or PATTI test or age hardening simulation (RTFOT or PAV), were performed in this study. The rheological properties investigation includes both short- and long-term age hardening. Short-term age hardening involves two different sources of bitumen suppliers for the production of foamed bitumen commonly used in South Africa and one source of bitumen emulsion. For long-term age hardening, materials commonly used for pavement construction in the Western Cape in South Africa, such as Hornfels-RAP and Quartzite, were sourced and samples prepared in the laboratory. In addition, long-term ageing

of field extracted cores from BSM pavement sections were investigated. This involved the collection of cores from existing pavement sections, which had been in service for about 8–10 years. The extracted cores were from pavements located in different climatic regions to investigate the influence of climate on age hardening. The location and details of the tested material are presented in subsequent sections.

7.2 METHODOLOGY AND EXPERIMENTAL PROGRAM

It is known from HMA that age hardening occurs during in-plant mixing, construction and long-term in-service conditions in the pavement. The same principle has been used to investigate the age hardening behaviour of BSMs, but looking at the in-plant production and in-service conditions, which are critical for BSMs. To understand the effect of age hardening on rheological properties, short- and long-term behaviours need investigation. Short-term involves understanding the binder ageing during production, for instance, circulation of bitumen for an extended period of time before actual foaming. On the other hand, long-term entails understanding binder ageing for a period of 2–3 years during in-service life, which is achieved by making specimens and carrying out accelerated curing in an oven. For assessing long-term behaviour in service condition, over 8–10 years, field cores were extracted from different road conditions and climate and binder recovered and evaluated. The extraction of field cores was based on traffic consideration and the cores were extracted from different locations in the pavement section. In the emergency lane (or yellow line) and between wheel paths, the cores were extracted to investigate the influence of high void and moisture content due to less densification. The cores extracted from the slow lane were taken to investigate the influence of traffic loading and low void and moisture content. The flow chart in Figure 151 shows the approaches taken to studying age hardening of binder in BSMs, thus understanding the durability behaviour of binder in BSMs.

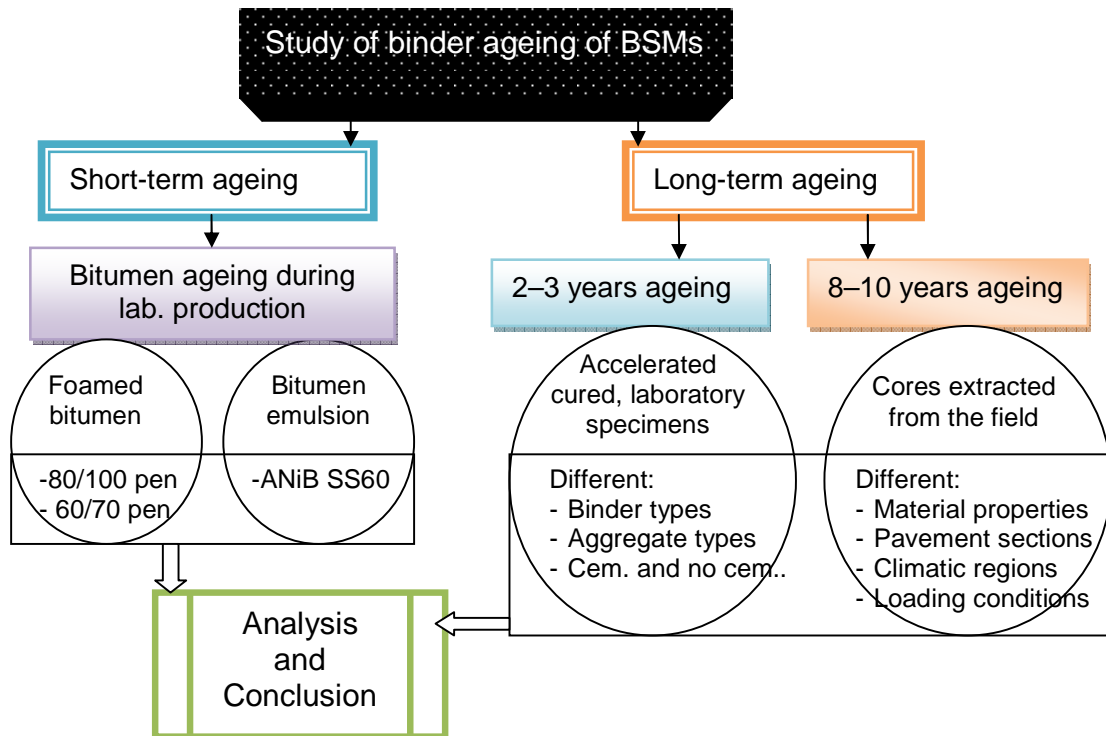


Figure 151: Flow chart describing the procedure for the study on binder ageing on the BSMs

7.2.1 Research method

The short-term age hardening of foamed bitumen was investigated, based on the circulation period. During in-place recycling in pavement construction or production of foamed bitumen mixes in the laboratory or in-plant, the bitumen is heated at a temperature of 160°C–180°C. A long period of circulation in the recycler or foam plant in the laboratory, for eight working hours, can result in age hardening. The circulation of bitumen at the indicated temperature and time can give insight into the effect on rheological properties and chemical compositional change. Likewise, testing of base bitumen and foamed bitumen at the same time will provide an understanding of whether the foaming process itself has influence on rheological property change during interaction with moist air or on expansion. Therefore, the bitumen was heated at a temperature of 170°C–180°C and circulated for a period of eight hours while taking samples after 1hr, 4hr and 8hr. The base bitumen was collected before the foaming process and foamed bitumen was collected after the total collapse. The foamed samples were conditioned in the oven at 100°C for 30 minutes to evaporate all the water prior to the rheological testing, that is penetration, viscosity and softening points following testing procedures prescribed in the ASTM (2003). Typical bitumen emulsion used for recycling was recovered from the water continuous phase by sufficiently heating the sample until no trace of water was seen prior to rheological testing.

The ageing behaviour of the field samples was divided into two categories, i.e. short ageing period of 2–3 years and long ageing period of 8–10 years. The short ageing period was determined from laboratory compacted, cured and recovered binder on specimens made of foam or emulsion. Laboratory accelerated curing (i.e. 30°C for 20 hours and 40°C for 72 hours) has been indicated to be equivalent to a field curing of period of 2–3 years (Jenkins, 2000 and Malubila, 2005). For long-term ageing, the cores were extracted from existing pavement sections and binder recovered prior to rheological properties testing. The extraction method is described further in subsequent sections. The extracted cores' location in the pavement section based on traffic conditions is presented in Figure 152.

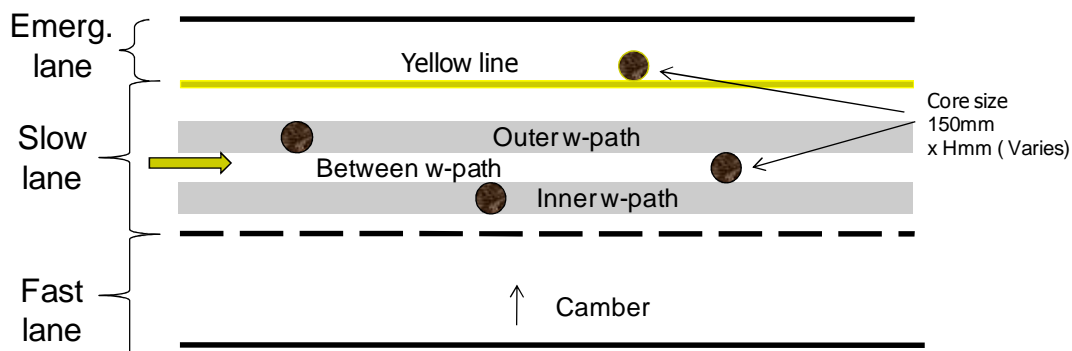


Figure 152: Locations of the field cores extracted from the pavement section

The extracted cores were taken from the pavement sections, which have been exposed to different traffic loading and climatic conditions. The climatic conditions varied from a Mediterranean-type climate in Western Cape Province in South Africa to a sub-tropical-type climate in Gauteng Province in South Africa and to desert-type of climates in Saudi Arabia.

7.2.2 Materials and test methods

The materials used in this study as well as the preparation of the specimens and the recovery methods are presented in this section. Further, the rheological tests that were conducted to determine the effect of ageing behaviour of the binder in BSMs are described. Finally, the results are presented and analysed in the subsequent section.

7.2.2.1 Short-term age hardening

The selection of materials was made to match the type of materials commonly used in previous recycling for pavement construction in South Africa. The sources and types of bitumen selected for this study are presented in Table 33.

Table 33: Source and type of binder for short-term ageing study

Source	Binder type	
	Foamed bitumen	Bitumen emulsion
NATREF	80/100 base bitumen	60/70 base bitumen
CALTEX	80/100 base bitumen	60/70 base bitumen
COLAS		Anionic stable grade 60/40 or ANi B SS-60

7.2.2.2 Long-term age hardening

The laboratory-prepared specimen was made from Quartzite crushed stones and Hornfels-RAP, stabilised with either foamed bitumen or bitumen emulsion, with or without the addition of active filler (cement). Table 34 presents the mix matrix prepared for this study.

Table 34: Mix matrix for the laboratory prepared specimen

Binder type	Mix type			
	Quartzite		Hornfels-RAP	
	No cem.	1% cem	No cem.	1% cem
Foamed bitumen	Q0CF	Q0CF	Q1CF	Q1CF
Bitumen emulsion	Q0CE	Q0CE	Q1CE	Q1CE

Note: Q = Quartzite, 0 = no cement, 1 = % cement, H = Hornfels-RAP, F = foam, E = Emulsion

Pavement sections constructed with either foamed bitumen or bitumen emulsion were listed for the field age hardening investigation. To be able to compare the effect of different environmental conditions, 28 cores were sourced from the Western Cape and 36 cores from Gauteng Province. An additional six cores were sourced from Saudi Arabia. The pavement sections included in this study are listed in Table 35.

Table 35: List of pavement section selected for field ageing studies

Bitumen emulsion	Foamed bitumen
N7 TR 11/1, Cape Town	P243/1, Vereeniging
Grassy Park, Cape Town	N7 TR11/1, Cape Town
	Grassy Park, Cape Town
	Shedgum Road, Saudi Arabia

Table 36 gives a summary of the sources of cores and pavement sections, mix types, core numbers and the locations of extractions in the pavements. Figure 153 presents the laboratory-prepared specimens and the cores extracted from the existing pavement sections for both emulsion and foam mixes.

Table 36: Summary of cores sourced for investigating BSMs field age hardening behaviour

Pavement section	Mix type	Core number	Location of cores	Age
Grassy Park - At the robot - Straight section - Straight section	Foam Foam Emulsion	4 6 6	OWP, BWP OWP, BWP, YL IWP, BWP, YL	8yrs
P243/1, Vereeniging - Straight section - Straight section	Foam Emulsion	18 18	OWP, BWP, YL OWP, BWP, YL	7yrs
Shedgum Road, Saudi Arabia - Straight section	Foam	6	OWP, IWP, BWP	3yrs

Note: OWP = outer wheel pass, BWP = between wheel pass, IWP = inner wheel pass, YL= yellow line



Figure 153: Laboratory- prepared specimen and cores extracted from the existing pavement sections for both emulsion and foam mixes

The ageing behaviour of pavement layers is known to differ between the top and the bottom. Therefore, bitumen in the extracted cores was recovered from the top and bottom halves. However, it was realised that, due to low binder content of the mix, top and bottom halves do not produce sufficient recovered bitumen to carry out penetration tests. Therefore, recovered bitumen was done per mix type.

7.2.3 Bitumen recovery

Bitumen extraction is a process necessary to regain binder from laboratory compacted and cured BSM mixture specimens as well as cores extracted from existing pavement sections. In preparation for the recovery of bitumen from BSM mixtures, the following activities were performed:

- Specimens were crushed into a loose mixture; three specimens were crushed for each mix type.
- Specimens of the same mix type were put together into a pan and dried in the oven at 110°C for a period of 1–2 hours to ensure that all water had been evaporated prior to extraction.
- The materials were left to cool and split into small amounts of 3–4kg and soaked with extraction solvent. In this study, trichloroethylene was used to dissolve and wash the binder from the mineral aggregates.

The extraction and recovery process was conducted in the privately-owned laboratory Soil Lab, located in Kraaifontein in the Western Cape and MUCH Asphalt central laboratory located in Eersterivier, Western Cape. At Soil Lab, the Abson method is commonly used for the recovery of bitumen after cold centrifuge extraction. At MUCH Asphalt, the rotary vapour method is used

after cold centrifuge. The reason for using these two methods was to establish whether they achieve the same results. The first batch of the recovered bitumen seemed to have high variability in penetration and softening point. This variability was either because of overheating of the bitumen or excess filler recovered with the bitumen. The conclusion is discussed with the results, below.

7.2.3.1 Extraction of binder from the mixture

The extraction of binder from loose mix was conducted in two steps during the centrifuging process. The loose mix was soaked in trichloroethylene (C_2HCl_3 -TCE) and left for 30 minutes to dissolve the bitumen from the mix (trichloroethylene was used due to its availability). However, precautions and safety measures were in place to minimise contact due to its carcinogenic effect. The soaked mixture was further stirred and the liquid with dissolved bitumen, filler and solvent was poured into a sieve pan of 0.075mm and placed on top of the centrifuge (see Figure 154). Super filler (<0.075mm) and dissolved bitumen were poured into the centrifuge. The centrifuge is a fast revolution device delivering a minimum of 3 000 times the force of gravity. The centrifuge cups were used to collect super filler separated from the dissolved bitumen by the centrifuge. It was revealed that three repeat processes were not adequate to separate the super filler from dissolved bitumen. Therefore, the complete extraction ended up with five to six cups and sometimes up to seven cups. The process was exhaustive to ensure all filler was removed to minimise the influence on the test results. Typical quantities of the super filler recovered in different cycles are presented in Table 37.

Two centrifuge machines were used in the extraction process. A complete wash of one mix type uses approximately 6-8 litres of trichloroethylene, with time spent of 2-3 hours.

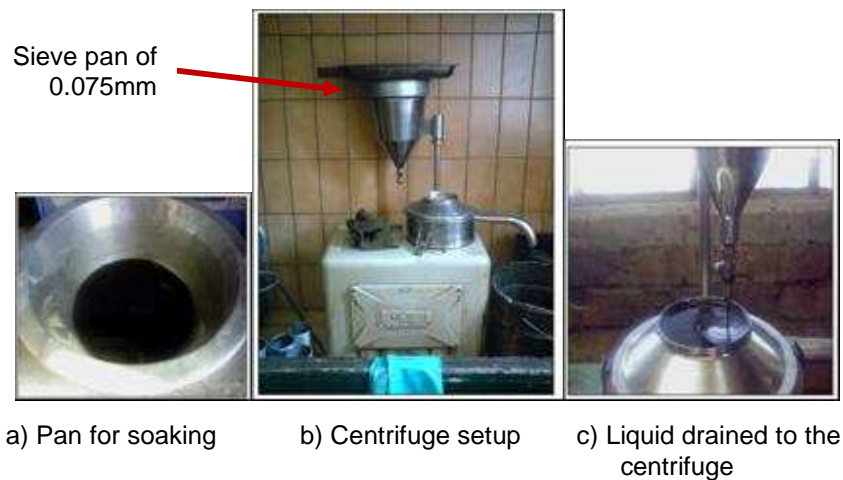


Figure 154: Cold centrifuge for washing bitumen from mineral aggregates

Table 37: Separated filler collected after each cycle on different cup.

Cycle or cup [no.]	Cup weight [g]	Cup +filler [g]	Filler [g]
M01+M02	391.1	785.9	394.8
M03	195.7	306.4	110.7
M04	196.1	295.5	99.4
M05	215	272.4	58.4
M06	194.7	198.1	3.4
M07	196.4	197.9	1.5
M08	209.9	211	1.1

7.2.3.2 Recovery of bitumen from the solvent

After extraction, the second step is to recover the bitumen from the solvent (separation of bitumen from the trichloroethylene). The separation process was done using the Abson method, according to the standard procedure described in ASTM D 1856-95a. The process involves pouring the liquid (bitumen plus solvent) into a flask, which is placed in the heating mantel. The temperature of the mantel is raised at a controlled rate, monitored using a thermometer, until the liquid boils. The initial temperature was set at 90°C. Foaming of the liquid is controlled by supplying carbon dioxide gas, which also speeds up the condensation of solvent from the boiling liquid. In order to facilitate the condensation of the evaporating solvent, cold water was continuously supplied from a water source during the entire period of distillation. Distillation is complete when there is no sign of further dripping of the solvent. Thereafter, the temperature was raised to 135°C–150°C to ensure all solvent has been distilled. The retained bitumen in the flask is immediately poured into the testing container while the bitumen still has low viscosity. Figure 155 shows the equipment utilised during the Abson method.

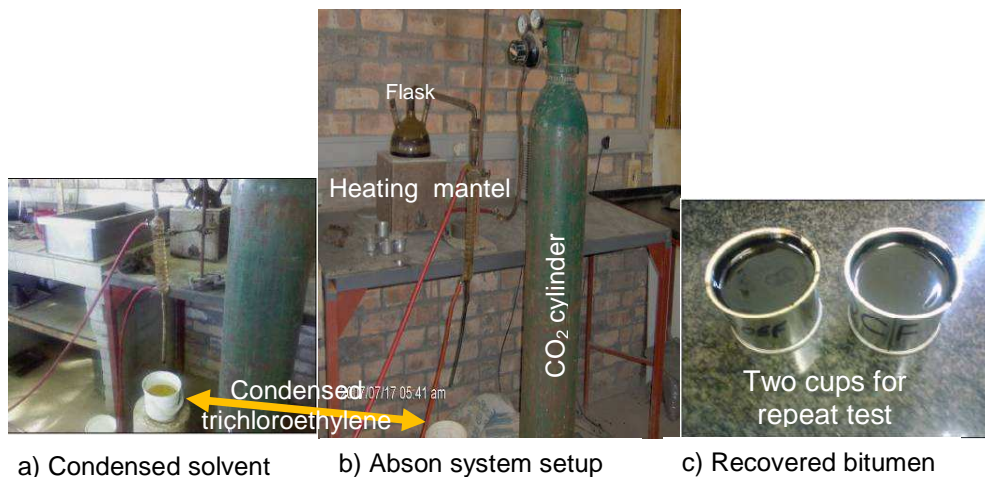
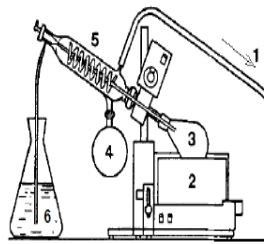


Figure 155: Abson method of bitumen recovery from the solvent (done at Soil Lab. Kraaifontein)

The second method of recovery was the use of a rotary vapour, according to the standard procedure DIN EN 126997/3. The recovery process involves the separation of the solvent from the bitumen by heating up the bitumen solution and collecting the evaporated solvent by condensation. At the start, an oil bath is heated to a temperature of 90°C and the suction pressure is set at 400kPa. The temperature and pressure are maintained while the solution is fed into the rotating flask covered with hot oil. In order to facilitate the condensation of the evaporating solvent, cold water is continuously supplied from the water source nearby. After all the bitumen solution is collected in the rotating flask, the system is kept running and the temperature is raised to 160°C. The suction pressure is also lowered to 200kPa and maintained for about 30 minutes to ensure that all solvent is completely removed from the bitumen. The retained bitumen is poured into the testing cups while in a lower viscosity state. Figure 156 shows the rotary vapour recovery system for separation of solvent from the bitumen.



1. To vacuum pump
2. Heating oil bath
3. Rotating evaporating flask
4. Receiving flask
5. Condenser column
6. Binder solution



Figure 156: A rotary vapour recovery system for separation of solvent from bitumen (done at MUCH Asphalt Eersterivier)

Table 38 shows the differences between the conventional methods of extraction and recovery for HMA and BSM mixtures.

Table 38: Difference in bitumen recovery from HMA and BSMs using conventional methods

Properties	HMA	BSMs
Binder content	Usually higher (4–5%)	Usually lower (1.5% –3%)
Binder dispersion	Coats all aggregate fractions	Selectively coat aggregate fractions, particularly filler fractions
Mineral aggregates	Clean and dry, with minimum size of sand fractions	Mist and coated with clays, minimum size fractions, super filler
Extraction with cold centrifuge	Possible to separate bitumen from sand fraction	Impossible to separate bitumen from super filler, some bitumen fractions will be discarded with the filler
Dissolving solvent	Small quantities (1–2L) required to wash bitumen (100g) from aggregates	Large quantity (5–7L) required to wash the material to obtain 100g of bitumen
Recovery method ABSON (ASTM D 1856-95a)	Applicable for distillation of solvent; care should be taken not to over heat the bitumen content	Applicable for distillation of solvent; due to large quantity of solvent, trace of solvent might stay with bitumen. Possible overheating due to long time of distillation
Rotary vapour (DIN EN 126997/3)	Applicable for distillation of solvent	Applicable for distillation of the solvent longer time is required with use of heavy oil. This method is recommended

7.3 EVALUATION AND ANALYSIS OF RESULTS

The short- and long-term durability behaviour of the recovered bitumen is evaluated. The analysis is based on the effect of the change of the physical (rheological) properties of the base bitumen due to the age hardening effect. In this respect, the test conditions of the rheological properties of the binder are presented. The short-term effect on the production of foamed bitumen and bitumen emulsion is evaluated. In addition, the long-term age hardening effect of the recovered bitumen from the lab-prepared specimen and cores extracted from the pavement sections are discussed.

7.3.1 Short-term age hardening behaviour

7.3.1.1 Penetration, softening point and viscosity test methods

Penetration, softening point (ring and ball temperature test) and dynamic viscosity are common test methods used to characterise bitumen properties. The age hardening of bitumen can be described from the change in the values obtained from these tests. The penetration test was performed after conditioning the specimen at 25°C for 2 hours. The testing procedure involves penetration of 100g weight needle into the bitumen content for 5 seconds, the process is repeated for three times (see Figure 157). The procedure is done according to ASTM D5-IP49. One set of tests was done per sample of recovered bitumen. The average of the two replicates was recorded and presented in Table 40 to Table 43.

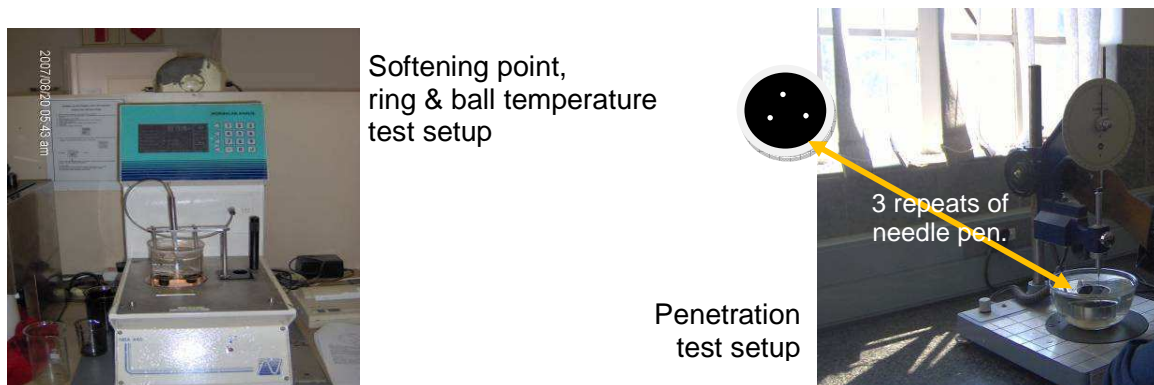


Figure 157: Penetration and softening point test setup

The *softening point test* was performed according to ASTM D36 (Figure 157). The sample and the ring and ball setup were placed in a 800ml flask and conditioned at 5°C for 15 minutes. The automatic heating mantel was used to heat the water at a constant rate of temperature change of 5°C per minute until the bitumen softened and moved with the ball bearing 25mm below the ring. The temperature of the water was recorded automatically when the balls touched the bottom plates. The difference in temperature between the two rings should not be more than 1°C.

The *dynamic viscosity test* was done according to ASTM D4402 using a Brookfield Model DV-I viscometer with a Thermocel temperature control system. The selected spindle was SC-29 for the 60°C and SC-21 for the 135°C. The temperature range was 60°C and 135°C to determine the viscosity of bitumen in field conditions and mixing temperature. The spindle was equilibrated in the clean Thermocel chamber for 15 minutes. 13g of sample for 60°C and 8g for 135°C was poured into the tube and placed in the Themorcel (with spindle temporarily removed). The spindle was hooked to the viscometer and inserted into the bitumen and left to

reach equilibrium for a further 15 minutes. The spindle and torque speed were selected from the digital panel and viscometer (Figure 158). The torque of the viscometer is between 2% to 98% of full scale, the reading with the higher torque percentage recommended as being more accurate. Three readings were recorded at intervals of 60 seconds and averaged. However, due to the sensitivity of the readings, the spindle was left to rotate for 15 minutes and the readings were taken thereafter. The unit of dynamic viscosity is the pascal-second (Pa·s) which is 1N·sec/m². The cgs (centimetre gram second) unit is gm/cm·s, or poise or centipoise (cP), at a given temperature; 1 Pa·s = 1 000 mPa·s = 10 Poise = 1 000cP. The kinematic viscosity (ν) is the ratio of the dynamic viscosity (η) to the density (δ) of a liquid such that;

$$\text{Kinematic viscosity} = \frac{\text{dynamic viscosity}}{\text{density}} \quad \text{Equation 34}$$

where ν = kinematic viscosity [mm²/s]; η = dynamic viscosity [Pa·s]; δ = density [kg/l] at the temperature under consideration. The unit of kinematic viscosity is mm²/s or cgs (cm²/s), stoke, which is conveniently converted (centistokes) as follows: 1 mm²/s = 0.001 cm²/s = 1 centistoke.



Figure 158: Dynamic viscosity test setup

The rheological test results obtained from this study were related to the South African Bureau of Standards. The SABS 307 standard specification for the penetration, softening point and viscosity of bitumen are indicated in Table 39.

Table 39: Specification for road bitumen in South Africa, SABS 307

Properties	Penetration grade			Test Method
	40/50	60/70	80/100	
Penetration at 25°C [dmm]	40–50	60–70	80–100	ASTM D5-IP49
Softening Point [°C]	49–59	46–56	42–51	ASTM D36
Viscosity at 60°C [Pa.s]	220–400	120–250	75–150	ASTM D4402
Viscosity at 135°C [Pa.s]	0.27–0.65	0.22–0.45	0.15–0.4	ASTM D4402

7.3.1.2. Rheological properties of base bitumen and foamed bitumen

The consistency of base bitumen and foamed bitumen after different periods of circulation (i.e. 1hr, 4hr, 8hr) was determined in order to understand its durability behaviour during mixing in recycling pavement construction or laboratory conditions. The change in rheological properties with respect to time is presented in Table 40 and Table 41.

Table 40: Base bitumen and foamed bitumen rheological properties of 80/100 pen grade from NATREF refinery with lab conditioning

Properties	Original Bit	Fresh Bit				Foamed Bit		
	Bitumen circulation time in WLB10							
	0hr	1hr	4hrs	8hrs	1hr	4hrs	8hrs	
Penetration 25°C [dmm]	95(96)	82(85)	74(76)	64(64)	86(87)	77(79)	66(67)	
(repeat)	95.5	83.5	75.0	64.0	86.5	78.0	66.5	
Softening point [°C]	47	48	49	50	47	48	50	
Viscosity at 60°C [Pa.s]	132.0	153.0	167.8	211.5	140.4	160.6	216.5	
Viscosity at 135°C [Pa.s]	0.306	0.310	0.331	0.352	0.308	0.326	0.398	
Penetration Index, PI	-0.324	-0.444	-0.458	-0.515	-0.620	-0.626	-0.358	

Supplied bitumen: Unit nr. 2900, Tank nr. F29317, Dec.2007.

Table 41: Base bitumen and foamed bitumen rheological properties of 80/100 pen from CALTEX refinery with lab conditioning

Properties	Base Bit	Fresh base bitumen				foamed Bitumen		
	Bitumen circulation time in WLB10							
	0hr	1hr	4hrs	8hrs	1hr	4hrs	8hrs	
Penetration 25°C [dmm]	82(85)	66(73)	62(64)	54(54)	76(76)	67(66)	58(58)	
(repeat)	83.5	69.5	63.0	54.0	76	66.5	58	
Softening point [°C]	47	48	49	51	48	49	50	
Viscosity at 60°C [Pa.s]	134.0	166.0	205.0	252.8	165	200.0	235.7	
Viscosity at 135°C [Pa.s]	0.342	0.370	0.395	0.434	0.361	0.384	0.431	
Penetration Index, PI	-0.721	-0.936	-0.915	-0.780	-0.698	-0.778	-0.859	

Supplied bitumen: Unit no. APP, Tank nr., Oct.2007

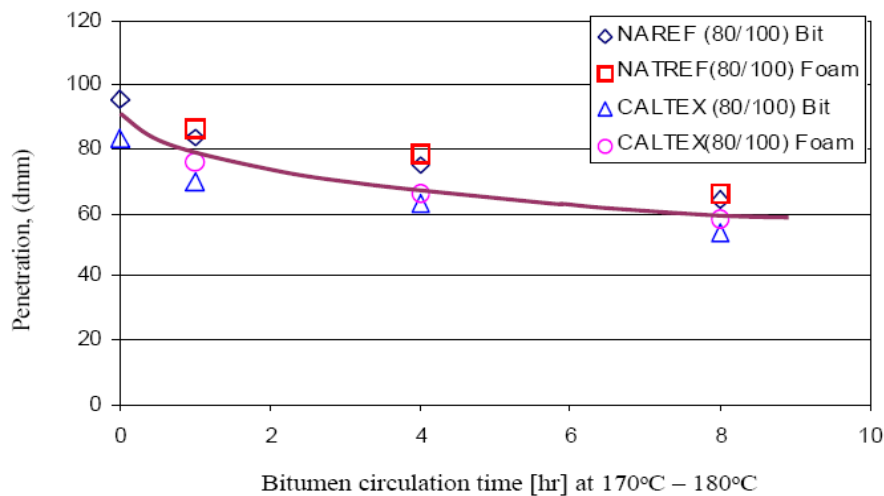


Figure 159: Penetration versus ageing time (hr) of base bitumen and foamed bitumen at 170°C–180°C

The relationship between penetration and circulation time of base bitumen and foamed bitumen for 80/100 from both NATREF and CALTEX is presented in Figure 159. It is clear from the relationship that base bitumen from both NATREF and CALTEX refineries undergoes age hardening of approximately 30% in the short term – a period of eight hours heated at 170°C–180°C. Similar behaviour occurs for foamed bitumen that is produced after ageing of the base bitumen, that is the foaming process does not alter this trend. The comparison between two refineries indicates that the higher the penetration of the base bitumen, the less the effect of age hardening: 96 penetration versus 83 penetration.

Further analysis of the results in Figure 159 shows that foamed bitumen age hardening follows the ageing of the base bitumen. This clearly shows that the foaming process itself does not have a significant effect on ageing of the base bitumen even when different sources of bitumen are used. The effect of age hardening of hard bitumen after circulation for eight hours is presented in Table 42 and Table 43.

Table 42: Base bitumen and foamed bitumen rheological properties of 60/100 pen from NATREF refinery with lab conditioning

Properties	Base Bit	Fresh base bitumen				Foamed bitumen		
	Bitumen circulation time in WBL10							
	0hr	1hr	4hrs	8hrs	1hr	4hrs	8hrs	
Penetration 25°C [dmm]	66(64)	66(67)	65(66)	53(55)	69(69)	68(66)	53(55)	
(repeat)	65	66.5	65.5	54.0	69	67	54	
Softening point [°C]	50	50	51	53	50	50	54	
Viscosity at 60C [Pa.s]	220.2	237.2	255.2	387.2	227.2	235.2	396.8	
Viscosity at 135C [Pa.s]	0.370	0.369	0.376	0.458	0.356	0.366	0.460	
Penetration Index, PI	-0.574	-0.515	-0.298	-0.299	-0.417	-0.495	-0.066	

Supplied bitumen: Unit nr. 2900, Tank nr. 29306, Dec.2007

Table 43: Base bitumen and foamed bitumen rheological properties of 60/70 pen from CALTEX refinery with lab conditioning

Properties	Base Bit	Fresh base bitumen				Foamed bitumen		
	Bitumen circulation time in WBL10							
	0hr	1hr	4hrs	8hrs	1hr	4hrs	8hrs	
Penetration 25°C [dmm]	71(74)	68(70)	67(66)	62(65)	77(77)	69(63)	64(64)	
(repeat)	72.5	69	66.5	63.5	77	66	64	
Softening point [°C]	50	50	50	53	49	51	52	
Viscosity at 60C [Pa.s]	202.0	207.0	267.2	328.8	198.0	259.6	324.0	
Viscosity at 135C [Pa.s]	0.361	0.396	0.439	0.483	0.356	0.432	0.477	
Penetration Index, PI	-0.284	-0.417	-0.515	-0.113	-0.385	-0.278	-0.109	

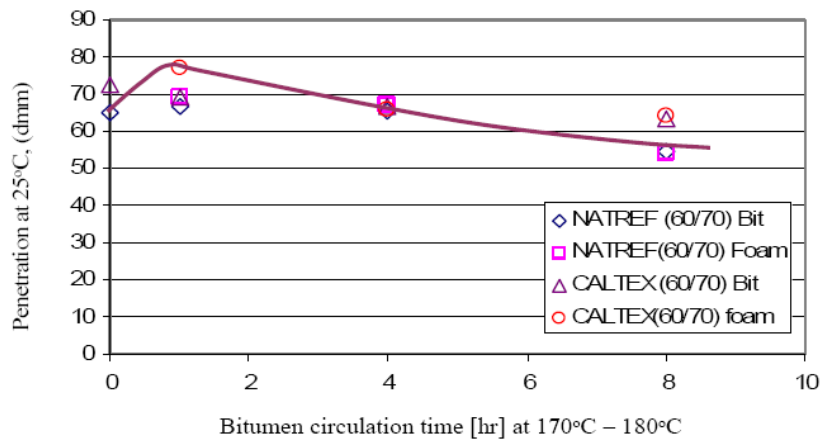


Figure 160: Penetration versus ageing time (hr) of base bitumen and foamed bitumen at 170°C-180°C

Figure 160 shows the ageing behaviour of base bitumen and foamed bitumen made from 60/70 penetration bitumen circulated at a temperature of 170°C–180°C. Both base bitumen and foamed bitumen show no ageing in the first four hours. However, after eight hours, age hardening resulted in a drop of penetration of 17% for the NATREF and 12% for the CALTEX binders. It can be seen from the results that the CALTEX 60/70 base bitumen used in the study does not comply with SABS 307 specification, with 73 maximum penetration tested as opposed to 70 maximum specified. The penetration of retain foamed bitumen circulated for one hour is higher than base bitumen.

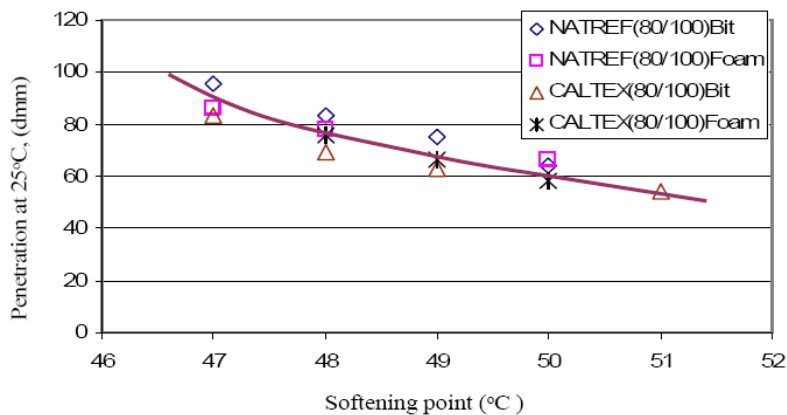


Figure 161: Penetration versus softening point of base bitumen and foamed bitumen at circulation temperature of 170°C -180°C for the 80/100 penetration.

The relationship between penetration and softening point is shown in Figure 161. This reveals an increase in binder hardness of 80/100 bitumen over the short-term. This behaviour gives an insight into the behaviour of BSM-foam. Foamed bitumen is recognised as having an affinity for fine particles with high surface area to mass ratio. This hardening of foamed bitumen could influence the cohesive behaviour of foam mastic, although this has not been investigated. In addition, it should be noted that the binder in BSM-foam is dispersed in a non-continuous manner. Figure 162 shows that the softening point of base bitumen and foamed bitumen increases as the penetration decreases. CALTEX bitumen shows a greater susceptibility to temperature effects during the ageing process than NATREF bitumen.

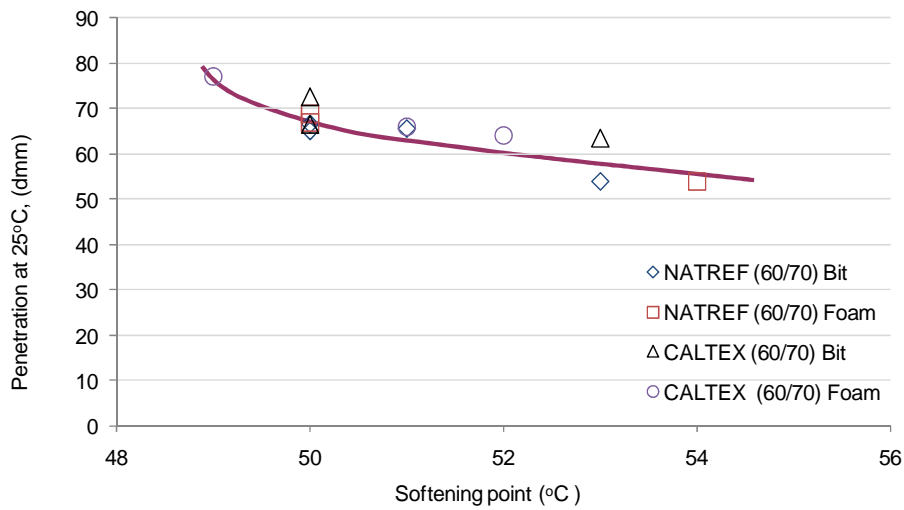


Figure 162: Penetration versus softening point of base bitumen and foamed bitumen at 170°C-180°C for 60/70 penetration

Figure 162 shows the ageing behaviour of base bitumen and foamed bitumen made from 60/70 pen binder. It can be seen that the rate of ageing of base bitumen and foamed bitumen is relatively small compared to 80/100 pen bitumen. Similarly, small differences are noted for bitumen from NATREF and CALTEX. The use of 60/70 penetration bitumen could have slight advantages in terms of short-term ageing. However, Wirtgen (2004) indicates that 60/70 pen bitumen has a problem of blocking the nozzles during the recycling process.

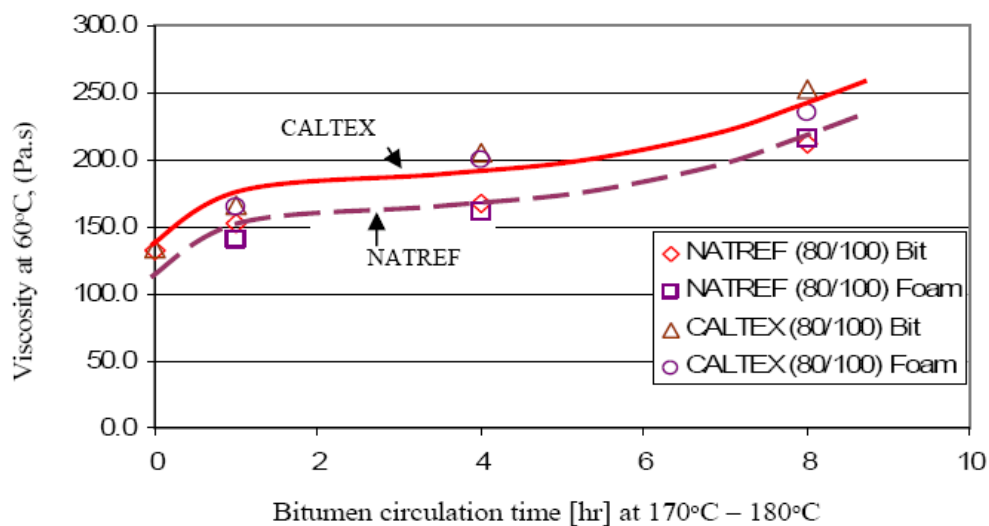


Figure 163: Viscosity versus mixing time (hr) of base bitumen and foamed bitumen at temp 170°C-180°C

Figure 163 shows the behaviour of the base bitumen in terms of viscosity and foamed bitumen at 60°C. It can be seen from the results that the viscosity increases as the bitumen hardens. CALTEX bitumen shows a higher rate of change of viscosity with time than NATREF bitumen.

However, NATREF bitumen and foamed bitumen show less ageing susceptibility for the first four hours and a sharp increase at eight hours in thermal ageing. It can be concluded from this behaviour that performance of foamed bitumen mixes produced with binder that has been circulated at high temperatures for a long time needs to be investigated. Further observations show that hardening differs for different refineries' products. This indicates that the behaviour of foamed bitumen mixes is dependent on the bitumen source. The bitumen characteristics should therefore be considered during mix design.

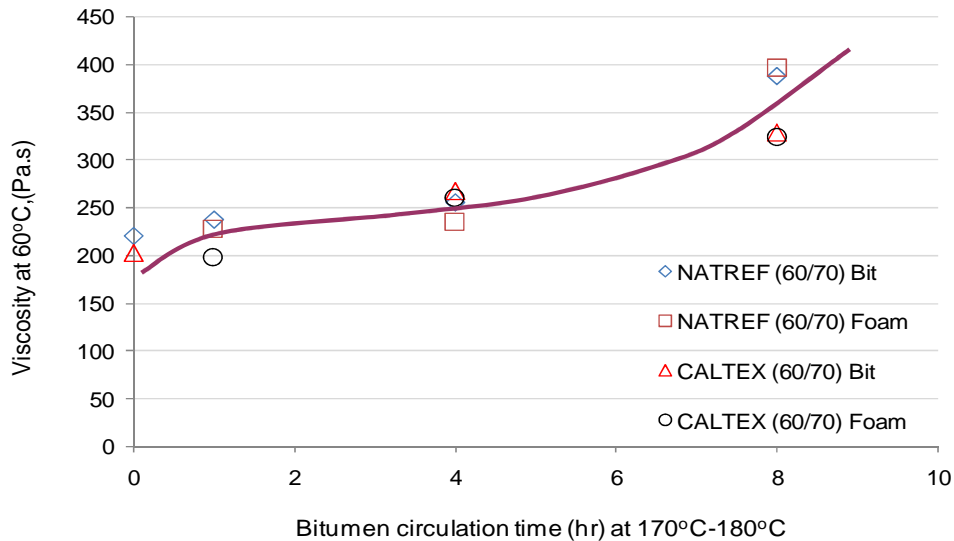


Figure 164: Viscosity versus mixing time (hr) of base bitumen and foamed bitumen at 170°C-180°C

The viscosity behaviour of base bitumen and foamed bitumen produced from 60/70 penetration bitumen exhibits a similar trend to 80/100 penetration bitumen (see Figure 164). However, after eight hours of circulation 60/70 pen bitumen shows relative higher viscosity than 80/100 pen bitumen. The NATREF bitumen shows higher susceptibility to ageing in terms of viscosity increase at longer circulation times than CALTEX bitumen. This confirms the findings of Wirtgen (2004) on the use 60/70 pen for the recycling process: higher viscosity binder than 60/70 pen bitumen can result in blockage of nozzles. However, if less time of circulation is allowed during mixing process, 60/70 pen bitumen can improve performance of BSMs.

7.3.1.3 Rheological properties of base bitumen and bitumen emulsion

The consistency of base bitumen and bitumen emulsion after separation of bitumen from a water-continuous base was measured in order to understand durability behaviour during mixing period in recycling pavement construction and laboratory conditions. The change in rheological properties of the retained bitumen is presented in Table 44.

Table 44: Recovered bitumen rheological properties from Emulsion, ANi B SS-60

Properties	80/100 pen CALTEX	
	Original bitumen	Recovered bitumen
Penetration at 25°C [dmm]	100	105
Softening point [°C]	44	44
Viscosity at 60°C [Pa.s]	94.4	95.8
Viscosity at 135°C [Pa.s]	0.27	0.265
Penetration Index, PI	-1.125	-0.976

The results of penetration, softening point and viscosity of the base bitumen and the residual bitumen from bitumen emulsion are more or less the same. This confirms that, at initial application, emulsification and addition of surfactant does not influence short-term age hardening of the residual bitumen during recycling in pavement construction. However, studies have indicated that improper storage or long duration of storage of bitumen emulsion has an influence on the initial ageing prior to application during pavement construction.

7.3.1.4 The influence of temperature susceptibility of ageing

The selection of bitumen type and source, prior to mix design, requires an understanding of the influence of bitumen on temperature susceptibility. Temperature-susceptible bitumen has a significant influence on ageing and results in premature failure of the pavement. From the results of this study, it is shown that bitumen from different sources have different ageing characteristics. The temperature susceptibility of bitumen can be determined from penetration and softening point tests. The slope of the line connecting the penetration at 25°C and the ring and ball temperature (equivalent to 800dmm) in the Heukelom Bitumen Test Data Chart (BTDC) characterise the temperature susceptibility of the binder (Heukelom, 1973). The temperature dependency of bitumen is described by the Penetration Index (PI) shown in Equation 34 (Shell Bitumen, 2003).

$$PI = \frac{1952 - 500 \cdot \log Pen - 20 \cdot SP}{50 \cdot \log Pen - SP - 120} \quad \text{Equation 35}$$

where SP = ring and ball softening temperature [°C]; pen = penetration at 25°C [dmm].

The penetration and softening point temperature test results for different types of bitumen and sources, presented in Table 40, Table 41, Table 42 and Table 43 above, are used to determine comparative temperature susceptibility. Temperature susceptibility is compared for bitumen type and source at different times of bitumen circulation in the plant before and after production of foamed bitumen. The foamed bitumen and bitumen emulsion are also compared in Figure 165.

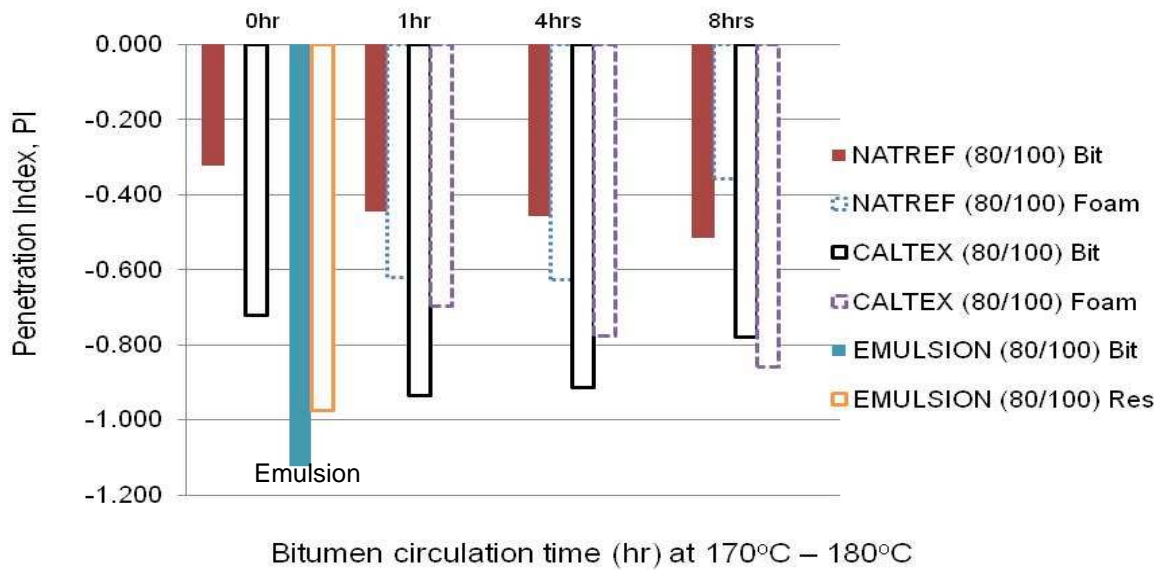


Figure 165: Penetration Index (PI) of base bitumen versus foamed bitumen and bitumen emulsion for 80/100 penetration bitumen

Figure 165 shows the relationship between PI and bitumen circulation time, for temperatures of between 170°C and 180°C. It can be seen that PI values are between -0.32 to -1.13. According to Shell Bitumen (2003), most paving binder has PI values ranging between +1 to -1. The ageing behaviour of the bitumen types have been analysed in terms of PI. From Figure 165 the tested emulsion (base bitumen and recovered bitumen) show higher temperature susceptibility than other base bitumen and foamed bitumen. Foamed bitumen and bitumen from NATREF lie within the limits of Shell Bitumen (2003). However, CALTEX base bitumen and foamed bitumen showed higher temperature susceptibility than NATREF binder.

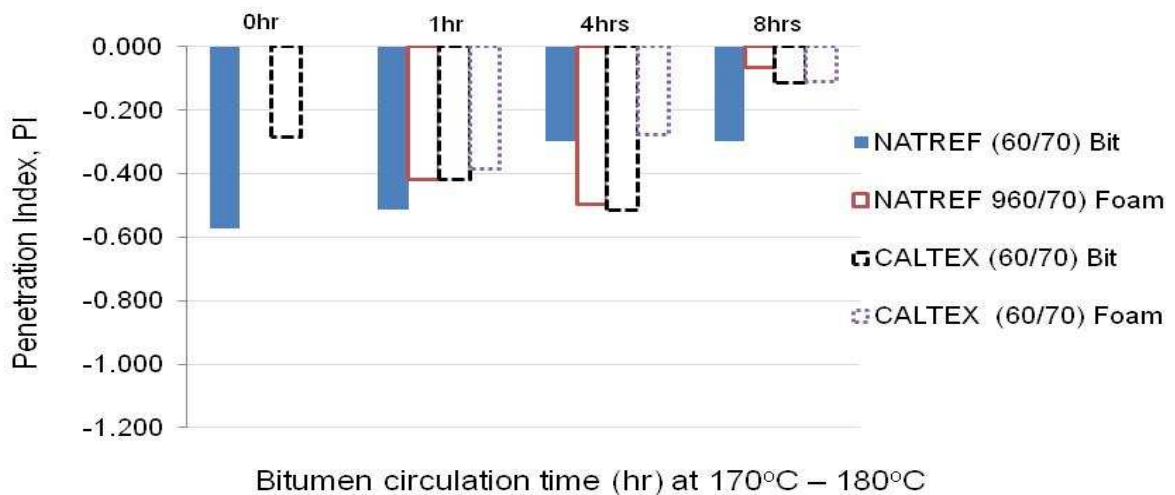


Figure 166: Penetration Index (PI) of base bitumen versus foamed bitumen and bitumen emulsion for 60/70 penetration bitumen

Hard bitumen (60/70) has lower temperature susceptibility compared to soft bitumen (80/100). The results in Figure 166 are typical for paving asphalt. As the binder ages, it becomes more resistant to softening at moderate temperatures. Therefore, the inclusion of higher contents of RAP aggregates (coated with aged bitumen) into BSMs can hinder rejuvenation by the new binder (foam or emulsion) which is applied at ambient temperature, hence poor adhesion. This is more pronounced in bitumen emulsion than foamed bitumen. Foamed bitumen may provide better adhesion because higher temperature (i.e. >35°C) of bubbles is induced to the RAP aggregates during mixing. Therefore, performance of BSMs at higher composition of RAP is a challenge and requires investigation to ensure durability and long-term performance.

7.3.2 Long-term age hardening behaviour

The consistency of the recovered bitumen from the laboratory-prepared specimens and the cores extracted from existing pavement are presented in this section. However, prior to presentation of the results, the material types, binder content and age of existing in-service pavements are summarised in Table 45.

Table 45: Summary of the laboratory and field cores material type, binder type, content and pavement age

Pavement section	Materials type	Binder type and content		Passing 0.075mm	Pavement age
		Foamed bitumen	Bitumen emulsion		
Lab compacted specimen	Hornfel-RAP	2% bitumen +1% cement	2% bitumen +1% cement	11%	2-3years
Lab compacted specimen	Quartzite crushed stone	2% bitumen +1% cement	2% bitumen +1% cement	6%	2-3years
Grassy Park	Recycled crushed hornfels G2	1.5% bitumen +1% cement	1.5% bitumen +1% cement	<10%	8 years
P243/1 near Vereeniging	Weathered dolerite and deco ferricrete	1.8% bitumen +2% cement		13%	7 years
P243/1 near Vereeniging	Weathered dolerite and quartzitic sandstone		1.8% bitumen +2% cement	<10%	7 years
Shedgum road	Limestone-RAP	2.5% bitumen		20%	3 years

7.3.2.1 Age hardening characteristics

The age hardening characteristics (change in rheological properties) of the recovered bitumen from different locations in the pavement are presented in Table 46 to Table 50.

Table 46: Recovered bitumen properties from Grassy Park BSM-foam and BSM-emulsion sections (Abson method)

Properties	Foamed bitumen				Bitumen emulsion			
	Robot		Straight section		Straight section			
	BWP	OWP	YL	OWP	BWP	YL	IWP	BWP
Penetration 25°C [dmm]	49	15	37	5	83	39	22	40
Softening point [°C]	55.8	80	51.2	70.7	44.6	56	63	54.4
Viscosity at 60°C [Pa.s]	810	N/A	411	NA	108.6	-	-	650
Viscosity at 135°C [Pa.s]	0.932	5.65	0.532	2.283	0.278	0.61	1.108	0.76

The Grassy Park road is an urban road, which has been in service since rehabilitation for the past eight years. During rehabilitation, the construction records show that base bitumen had 72 penetration and 45.5°C softening point. The change in rheological properties during the eight years shows a significant drop in pen on the trafficked sections (i.e. OWP and IWP) compared to un- trafficked sections (i.e. BWP and YL). The tendency of rheological change seems to be the same for the slow loading section (at the robot or intersection) and the faster loading section (on the straight section). In addition, there is no difference in age hardening behaviour between the foamed bitumen and the bitumen emulsion. Nevertheless, the recovered pen shows significant variability. The extreme penetration values of 5 and 83 and the increase in viscosity (no flow) at 60°C show the weakness of the convention extraction and recovery method adopted for BSM mixtures.

It was not clear exactly what caused this variability. However, close observation of the entire extraction and recovery process shows that either extraction was not done sufficiently enough to completely separate the filler and the bitumen, the Abson method from Soil Lab burns the bitumen during the recovery process or some trace of solvent remained in the bitumen resulting in softer bitumen. Therefore, additional measures were taken to minimise the speculated causes by carrying out the following procedures:

- Little dry mass of 2.5kg was dissolved in the trichloroethylene solvent and left soaking for 1–2 hours to ensure that all the binder adhered to the filler was dissolved before extraction.
- Several cycles of capturing filler from the centrifuge were performed to ensure all filler has been separated from the binder. The weight of the empty cup and the cup with filler after every cycle was taken and dried in the oven and the filler weight was determined. It was realised that six to seven cycles were needed to reduce filler from the bitumen liquid (bitumen and solvent) to 0.5–1.5%; a cycle means one time desiccation of filler from 2.5kg of materials.
- Apply a different recovery method, that is substantiate the initially applied Abson method with the newly installed rotary vapour method. MUCH Asphalt central laboratory in Eersterivier procured new recovery equipment and granted us access to the equipment for carrying out binder extraction and recovery.
- Carry out independent comparisons on similar samples using a commercial laboratory (SRT laboratory). Due to variability in results and disputable results, the specimen from Shedgum Road was taken to SRT laboratory for extraction and recovery for comparison with results obtained using Abson from the Soil Laboratory. SRT laboratory procedure

for recovery of bitumen involve cold centrifuge and rotary vapour. The comparative results are presented in Table 47.

Table 47 presents the rheological properties of the recovered bitumen from P243/1 near Vereeniging using either rotary vapour or Abson after the seven cycles of centrifuge.

Table 47: Recovered bitumen properties from P243/1 near Vereeniging BSM-foam and BSM-emulsion sections (Abson or rotary vapour method)

Properties	Foamed bitumen			Bitumen emulsion		
	Straight section			Straight section		
	YL	OWP	BWP	YL	OWP	BWP
Penetration 25°C [dmm]	>100	>100	>100	>100	>100	>100
Softening point [°C]	42	39	33	44	45	34
Viscosity at 60°C [Pa.s]	52	37	32	74	77	36
Recovery Method	ABSON			ROTARY VAPOUR		

Table 47 unexpectedly shows an increase in penetration (>100 dmm) and softening point of the binder rather than a decrease due age hardening. This behaviour is noted on both recovery processes, namely the rotary vapour and Abson methods. The understanding of this behaviour was not obvious due to the fact that more caution was taken in the extraction and recovery procedures. Therefore, it can be commented that the cause of softening of the binder is the incomplete recovery of all fractions of the bitumen. The highly diffused polar fractions to the filler aggregates, for instance asphaltene, were discarded with the super filler during extensive recovery. This led to the loss of the viscous component of the recovered bitumen. This is attributed to the higher filler content of the natural gravel of weathered dolomite and decomposed Ferricrete. The recovered bitumen properties for the extracted cores from Shedgum Road are presented in Table 48.

Table 48: Recovered bitumen properties from Shedgum Road BSM-foam section (Abson method)

Properties	Foamed bitumen							
	ST 02		ST 04		ST 08		ST 09	
	OWP		OWP		IWP		IWP	
	TOP	BOTTOM	TOP	BOTTOM	TOP	BOTTOM	TOP	BOTTOM
Penetration at 25C, [dmm]	3	2	5	4	8	12	12	11
Softening point, [°C]	90	90	91	88.5	77.3	84.7	79.4	83.8
Viscosity at 60C, [Pa.s]	N/A		N/A					
Viscosity at 135C, [Pa.s]	88.4	27.35	44.6	89.1	6.7	11.85	26.25	9.225

Table 48 shows severe age hardening behaviour in the recovered bitumen from the semi-arid Shedgum Road. The drop of the pen to a single digit with no flow at 60°C may lead into the following postulations being offered as causes:

- The grading of limestone-RAP used for stabilisation with foamed bitumen appears finer, with 20% passing sieves 0.075mm. Due to the fact that separation of this amount of filler with a centrifuging process is not possible, super filler (silt) can be recovered with bitumen coupled with aged bitumen resulting in a significant reduction in penetration and increase in softening point.
- The foamed bitumen stabilisation was carried out on full-depth HMA. The recovered bitumen from RAP had significant ageing (i.e. penetration of 10dmm). Therefore, bitumen recovered from the cores includes foam bitumen as well as aged bitumen. The combined bitumen negatively influences variability in the rheological properties of the recovered bitumen.
- Unlike virgin crushed aggregates, where diffusion of binder (foamed bitumen or bitumen emulsion) properly adhered to the mineral aggregate surface, the effect of the high percentage of RAP (100%) has a significantly negative influence on the diffusion (adhesion) or binder-aggregate interaction. The literature review indicated that aggregates coated with old bitumen make the surface inactive to the physicochemical interaction with the new bitumen at a lower temperature of mixing. This results in a reaction of bitumen to oxidation in the presence of air and high temperatures in the pavement layer. Therefore, a high percentage of RAP stabilised in BSMs is critical for age hardening of the additional binder.
- The trial pit inspection during coring indicates that the BSM-foam layer had a temperature of approximately 47°C during summer, depending on temperature susceptibility of the bitumen and the air void content of the mixes. That high a temperature is sufficient to cause age hardening of the BSM-foam in a long-term service condition.

There is no obvious explanation for the extent of the drop in bitumen properties of BSM-foam pavement layer in Shedgum Road after three years in service. In order to explore any possible causes, such as procedures or equipment factors, a different independent laboratory (STR, from Kwazulu Natal Province) was requested to perform a similar exercise. The comparative results are presented in Table 49.

Table 49: Recovered bitumen properties of Shedgum Road BSM-foam section from different laboratories for comparison

Properties	SRTLaboratory				Soil Laboratory				
	ST08	Layer 1 TOP	Layer 2	Layer 3	Layer 4 BOTTOM	Layer 1 TOP	Layer 2	Layer 3	Layer 4 BOTTOM
Penetration at 25C, [dmm]	22	24	22	21	16	18	15	17	
Softening point, [°C]	68.0	64.0	68.0	68.4	76.0	71.0	74.0	75	
Recovery method	ROTARY VAPOUR								

Cores from station km 8+000 and station km 6+000 were given to SRT laboratory for extraction and recovery. Four slices from each core were cut and bitumen was dissolved using

trichloroethylene. SRT used the rotary vapour method on recovery. From the results (Table 48, Table 49 and Table 50), there is no significant difference observed. The comparisons on of these results assuage the doubt that, extraction and recovery procedures are not the only factors that can influence a drop in bitumen properties. The implication is that age hardening behaviour of BSMs is as a result of a combination of a number of factors, indicated above, and needs further research.

7.3.2.2 Effect of active filler on age hardening behaviour

The influence of the addition of active filler on age hardening has not been reported. It was the objective of this study to look at the effect of active filler (cement) on age hardening in BSMs. Laboratory compacted and cured specimens, which represent similar ageing to pavement layers after 2–3 years in-service environmental conditions, were prepared. Typical material used for recycling on the N7 TR11/1 expressway near Cape Town and Quartzite from the Prima quarry were used for the laboratory research. The specimens were made of foamed bitumen or bitumen emulsion mix with or without addition of cement. The bitumen was recovered from the mixture and rheological properties tested. The results for both mixtures are presented in Table 50.

Table 50: Recovered bitumen properties of laboratory-prepared specimens

Properties	Foamed bitumen				Bitumen emulsion			
	HO CF	H1 CF	Q0 CF	Q1 CF	HO CE	H1 CE	Q0 CE	Q1 CE
Penetration 25°C [dmm]	>100	>100	67	>100	17	25	33	42
Softening point [°C]	32	26	48.1	38	78	61.1	53.9	39.8
Viscosity at 60°C [Pa.s]	2.730	0.430	146.1	-	N/A	N/A	788.3	424.8
Viscosity at 135°C [Pa.s]	0.056	0.030	0.333	0.0806	2.434	1.097	0.484	0.500
Recovery Method	ABSON / ROTARY VAPOUR				ABSON			

Note: H = Hornfels-RAP, Q = Quartzite, 0C = no cement, 1C cement, F= foam, E = emulsion

The results in Table 50 show a significant difference in the ageing behaviour between foamed bitumen and bitumen emulsion. Foamed bitumen shows softer bitumen instead of age hardening while bitumen emulsion shows age hardening behaviour similar to the field-extracted cores from a pavement which was in service for eight years (Grassy Park). The influence of the addition of active filler is not distinctive in age hardening. There is no clear trend in age hardening behaviour of the mixes, with or without age hardening. The extent of the drop in bitumen penetration grade in bitumen emulsion is severe. It is expected that accelerated curing cannot impact the change in rheological properties at the applied temperature and time of exposure. Although the literature review indicates that significant age hardening normally occurs during the first few years after exposure to environmental conditions, the extent of the drop in penetration and softening of BSM-foam need further investigation. The aggregate types indicate that Hornfels-RAP stabilised with emulsion has higher age hardening compared to Quartzite crushed aggregate. This is a result of the recovery of old bitumen within the RAP fractions. From the literature review, it has been reported that the softening behaviour of the recovered foamed bitumen might result from the extraction method or incomplete recovery of all composition of the bitumen fraction. In these mixes, base bitumen applied had pen of 72dmm

prior to foaming. The observed age hardening behaviour, both in the field-extracted cores and the laboratory compacted specimens, shows that understanding the age hardening characteristics of bitumen is still a challenge. As seen from this study, there is no simple explanation that gives an indication of the age hardening behaviour, as many factors have a significant influence on the outcome. Although BSM mixes age during field in-service conditions, a reliable extraction and recovery method for BSMs and quantification thereof needs further investigation.

The difference in age hardening potential of the pavement layer, depending on the location of the loading, was investigated. A comparison of the average ageing behaviour (change in bitumen pen) of the trafficked and untrafficked pavement layer is presented in Figure 167.

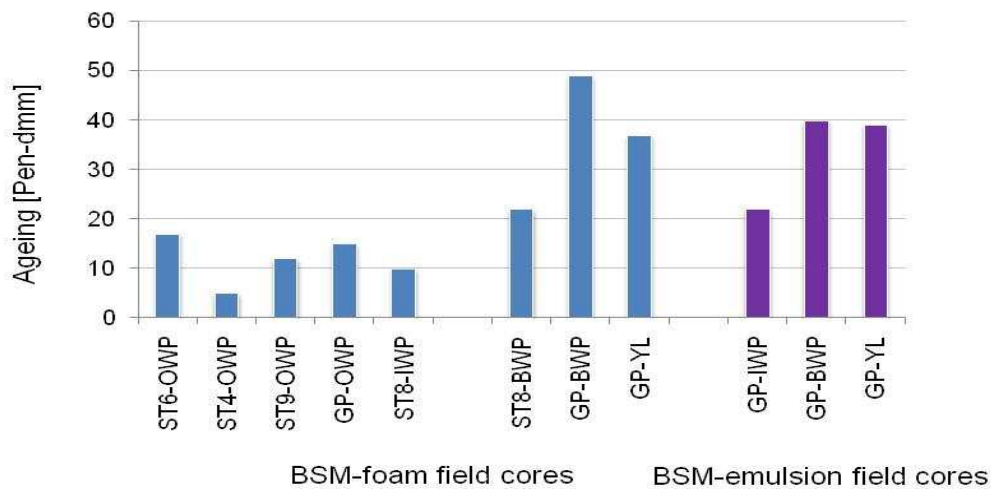


Figure 167: Comparison of age hardening behaviour of trafficked and untrafficked location on the pavement layer

The age hardening behaviour of the pavement layer differed for the trafficked and un-trafficked areas. The trafficked location (OWP and IWP) shows a higher drop in bitumen pen compared with the untrafficked location (BWP and YL) (see Figure 167). However, this behaviour contradicts the previous studies on HMA which indicated that age hardening is more pronounced in untrafficked locations than in trafficked locations. The reason being higher void contents occur at untrafficked locations compared to trafficked locations due to less densification by traffic. The relation between void content and age hardening potential is discussed in the subsequent section.

The results in this study indicate that BSMs can undergo short- and long-term age hardening. The short-term being more likely with foamed bitumen than bitumen emulsion, because higher temperature is applied during production foam. The combined behaviour in the short and long term is presented in Figure 168. The use of the Ageing Index (AI) method can clearly distinguish the age hardening behaviour of the foamed bitumen and bitumen emulsion. Shell Bitumen (2003) defines the Ageing Index as a ratio of the viscosity of the aged bitumen (η_a), measured at different times, to the viscosity of the base bitumen (η_o), both measured at the same temperature. This method was used to determine the ageing behaviour during production (short term) and in-service condition (long term). The viscosity at 135°C is used in calculating the ageing index of BSMs. The use of viscosity of aged bitumen at 60°C is inappropriate to understanding the ageing trend because most of the bitumen had no flow properties at 60°C. The combined age hardening behaviour (short and long term) could be determined for bitumen with known base bitumen properties. The initial bitumen properties used during recycling were

not known for all investigated mixes so the selected results show the age hardening trend, as shown in Figure 168.

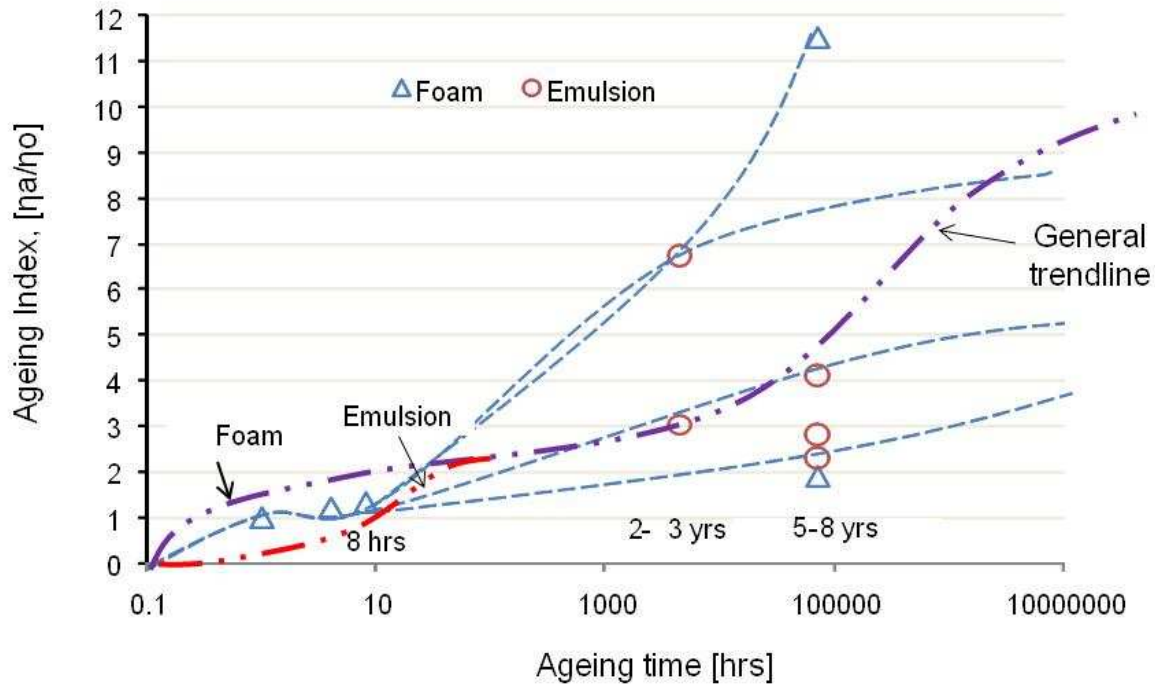


Figure 168: The combined (short and long-term) age hardening behaviour of BSMs

The ageing characteristics of bitumen-stabilised mixes can be classified into two major groups: short-term (during production) and long-term (during in-service conditions). The age hardening process of BSMs is affected by several factors, all operating at the same time. In assessing these factors, the most critical variables to consider are the characteristics of the BSM mixes themselves. Age hardening of HMA is different to BSMs due to the nature of binder distribution and the physicochemical interaction between the binder and mineral aggregates. The trend line for the short- and long-term age hardening behaviour of BSMs is presented in Figure 168.

The Ageing index (AI) during production of BSM-emulsion (short-term ageing) is low compared to BSM-foam. The results in this study indicate that, for periods of 2–3 and 5–8 years, age hardening rises to about 4%. This is due to the nature of binder-mineral interaction, where aggregates play a role in discriminating binder from immediate reaction. Therefore, oxidation continues after 5–8 years, but because of the possible stage of molecular structuring after 5–8 years, any oxidation can sharply increase the ageing behaviour and after complete molecular structuring, no more age hardening will be possible. Therefore, plateau trend line in Figure 168 indicates the terminal level of age hardening in the long-time in-service condition of BSMs.

7.5 ENGINEERING PROPERTIES

Past studies have indicated that short- and long-term age hardening of binder in HMA influences the durability properties and long-term performance of the pavement. The effect on age hardening is a change on the characteristics of the materials, such as stiffness, strength, fracture, toughness and relaxation. This results in changes to the adhesion and cohesion of the binder, which in turn leads to premature failures including fatigue and moisture damage.

Age hardening of binder in BSMs has different implications. The hardening of binder in the mastic implies proper adhesion and cohesion resulting in better durability behaviour and pavement performance. The extent of binder ageing in the mastic that negatively affects adhesion and cohesion is difficult to quantify. To unfold the complexity, comparison is made between the age hardening results and the engineering properties of similar mixes in terms of void content, moisture damage (ravelling) and field permanent deformation (rutting). In addition, the influence of the addition of active filler on ageing and BSM performance is discussed.

The average air voids content of the extracted field cores and laboratory compacted and cured specimens are placed side by side with their age hardening behaviour, to obtain an insight into their relationship in BSMs. The comparison is made for the mixes that show a relatively sound range of ageing expected in BSMs as indicated in Figure 169.

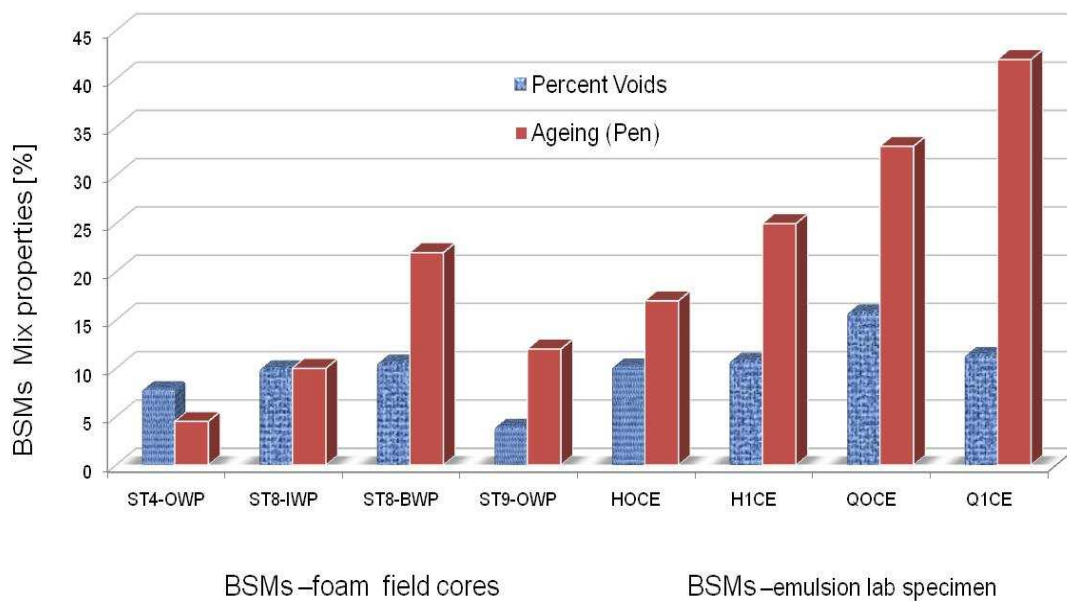


Figure 169: Comparison between air void content and age hardening behaviour in BSMs

It is known from the literature that the higher the air void content in the mixture, the higher the possibility that age hardening will occur. However, the results presented in Figure 169 show that air void content in some BSM mixes has no direct correlation with age hardening behaviour. The mix at ST8-BWP has a lower void content of 10% but higher ageing (pen 20dmm) compared to the mix from ST8 IWP, which has void content of 10% and ageing of the same magnitude (pen 10dmm). On the other hand, other mixes show a direct relationship. For instance, the mix at ST4-OWP has a higher void content and higher age hardening. The influence of the addition of cement also does not show a direct relation to the void content and age hardening behaviour. Hornfels-RAP and Quartzite stabilised with emulsion and with added cement (H1CE and Q1CE)

have similar ranges of air void content, but the ageing behaviour is significantly different. The Quartzite mixture has lower ageing behaviour compared to the Hornfels-RAP aggregates.

In order to compare the influence of age hardening on the engineering properties of BSMs, the relationship between ageing and permanent deformation was plotted. The distress on Shedgum Road indicates that different rutting behaviour occurs in different locations (trafficked and untrafficked) on the pavement layer. The investigation and the relationship between age hardening and rutting behaviour are presented in Figure 170.

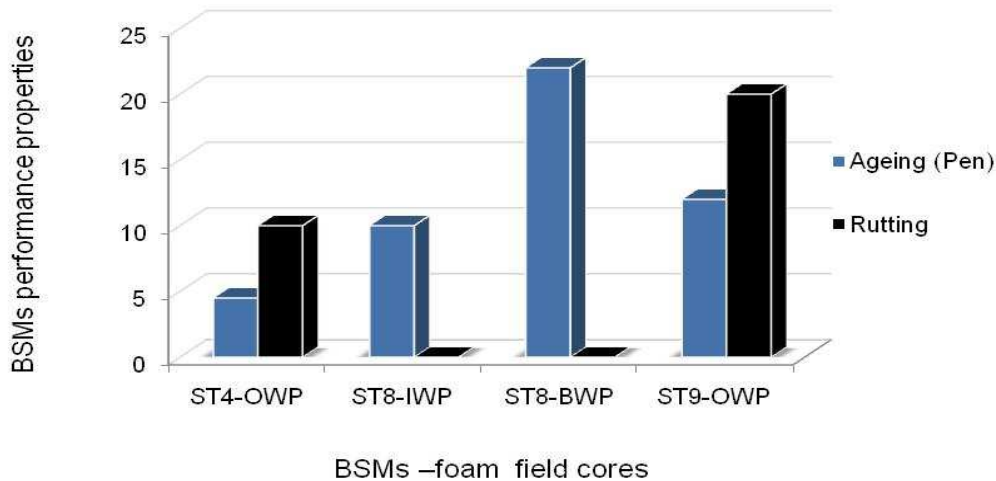


Figure 170: Comparison between age hardening and rutting behaviour of BSMs in the field

It is a general trend of HMA that higher rutting occurs in the less aged bitumen (softer) than age-hardened bitumen. In BSMs, the age hardening and rutting relationship is not consistent. The less aged binder at pavement location ST8-BWP has small rutting compared to the aged binder at pavement location ST4-OWP. This implies that the failure mechanism of BSMs is predominantly viscous flow. However, this behaviour can differ depending on binder content of the mix and temperature.

Additional analysis involves the relationship between age hardening and ravelling. Ravelling in BSMs is a failure mechanism that occurs due to disintegration of adhesion and cohesion within the mixture. It is common in BSMs that aged mastic will have better resistance to ravelling compared to unaged mastic. Nevertheless, ageing of binder in the mastic will result into higher ravelling due to reduction on the adhesion properties. To understand this phenomenon, the results of age hardening and ravelling behaviour in similar mixes were superimposed, as presented in Figure 171.

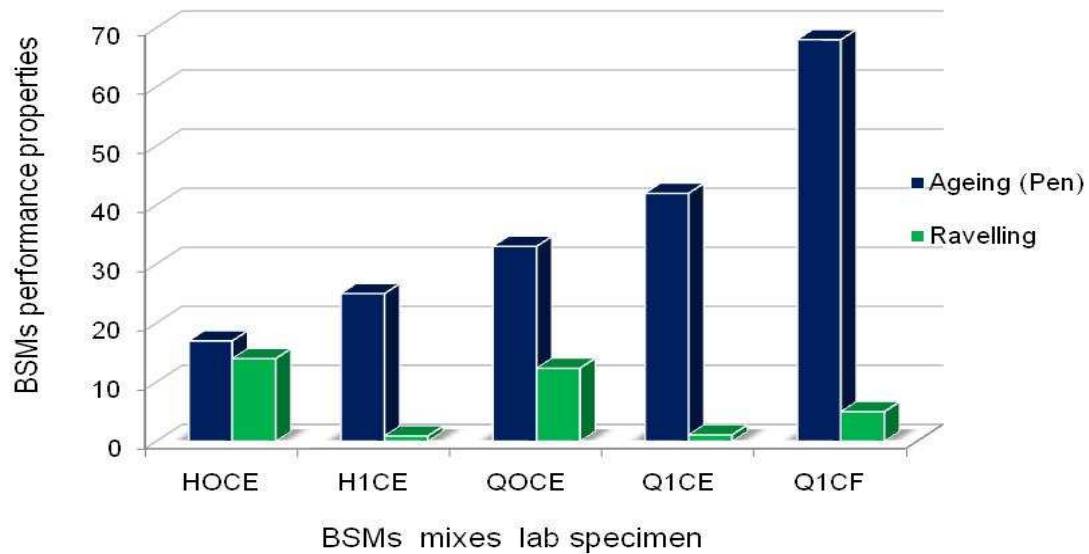


Figure 171: Comparison of age hardening and ravelling behaviour of BSM mixtures

The comparison between the age hardening and ravelling of BSMs (Figure 171) shows no defined trend. Instead, it is mix dependent. It is evident from the results that mixes with higher binder ageing (e.g. H1CE) have lower ravelling compared to mixes with less binder age hardening (Q1CF), but having higher ravelling. Mixes that show higher age hardening (HOCE) and higher ravelling, under microscopic analysis, show weaker initial bondage due to the physical chemical nature of the interaction between binder and mineral aggregates. Therefore, higher ravelling and age hardening occurred in this mix have no direct correlation.

In conclusion, it is apparent from these relationships that binder-mineral aggregate interaction is a complex phenomenon and no single parameter can describe BSM engineering properties or durability and long-term performance. In the long term, binder in BSMs undergoes age hardening; nevertheless, its contribution to the failure mechanism or impact on the engineering properties is a challenge to be accurately quantified. The fact that BSMs have been successfully applied with a wide range of mineral aggregates, which show significant differences in physicochemical properties, means that no single parameter can prove durability behaviour of BSMs. This confirms that microscopic analysis of the physicochemical behaviour of binder and mineral aggregates in BSMs is vital, as is mechanical testing. The findings in this study have not shown a method that can accurately define binder age hardening behaviour of BSMs. In addition, it has been proved that investigating binder ageing in isolation with filler is a complex and challenging task. In this light, an avenue is open for more research on a better method of recovery and extraction of binder from BSMs, rather than the conventional method applicable to HMA. It is further recommended that study of the influence of age hardening of binder in BSMs should take into account the higher affinity of filler and active filler to polar fraction of bitumen.

7.6 CONCLUSIONS

Age hardening in BSMs and the fundamental characteristics of BSMs associated with short-term and long-term age hardening have been investigated through laboratory testing. Based on the data of the study, the following conclusions are drawn:

The time bitumen is kept in circulation in the laboratory plant at an elevated temperature before the making of BSM-foam contributes to the ageing of the binder, especially after eight hours. The effects of ageing are more noticeable for softer bitumen (80/100) than hard bitumen (60/70), with a 30% drop in penetration for 80/100 bitumen compared to a drop of 12–17% in the 60/70 bitumen.

It is apparent from the study that some short-term age hardening of foamed bitumen during production occurs. However, the trend follows that of the age hardening of base bitumen. This shows that the foaming process in itself does not alter the bitumen properties. For bitumen emulsion, no age hardening occurred during production and mixing because elevated temperature is not used in the mixing process.

This study has also shown that bitumen from different sources (CALTEX or NATREF) age at different rates. This is consistent with other studies, as the compositional balance and chemistry of the binders vary even if they comply with the same classification requirements.

Ageing behaviour of foamed bitumen and bitumen emulsion has proven to be a point of consideration during mix design and long-term performance. In the short term, foamed bitumen has a drop in penetration by an estimated average of 30% during laboratory circulation. In the long term, both foamed bitumen and bitumen emulsion have a reduction in penetration of on average of 10–30dmm for trafficked sections, with an increase in viscosity at 60°C that leads to a reduction in flow. The impact of these changes in the binder on mix behaviour remains to be investigated.

The study has also indicated that age hardening of foamed bitumen and bitumen emulsion mixes in the field depends on the effects of traffic. Ageing occurs differently in trafficked versus untrafficked locations in the pavement (according to the limited data obtained). Trafficked locations (OWP and IWP) have higher ageing influence than untrafficked locations (YL and BWP). This tendency is contrary to previous studies. Other studies have indicated that air void content of the layer is the major factor in oxidative hardening. It is expected that untrafficked (BWP and YL) locations will have higher void contents than trafficked (OWP and IWP) locations, hence high ageing potential. However, these factors were not obvious and therefore need further investigation.

The extreme values measured for penetration of bitumen exposed to field ageing are questionable. This raises the concern that total separation of filler from bitumen during extraction and recovery was unsuccessful. Cold centrifuge extraction seems to be unable to separate all the fillers (super filler), which is a key component in mix design of BSMs. The use of the Abson method of recovery and rotary vapour method show consistent results of either higher or lower age hardening. Therefore, the whole process of extraction and recovery of binder needs to be reviewed critically. It is evident that the compositional change of the recovered bitumen and presence of super filler is vital in achieving a reliable conclusion.

The analytical method for the recovered binder, such as Gel Permeation Chromatography (GPC) and Fourier Transformation Infrared FTIR, can give an insight into the influence of super filler in the recovered bitumen. Any rheological test on the recovered bitumen should first investigate the chemical composition of recovered binder compared to the base bitumen. The findings showed that extensive use of solvent and number of repeat extractions can cause some binder compositional loss to occur. Therefore, a device such as Gel Permeation Chromatography (GPC) can be used to identify the age hardening behaviour of

binder recovered from BSMs because GPC (Gaestel Index, IC) is used to characterise the molecular weight distribution of binders. Therefore, it provides essential information on the molecular weight distribution of original and aged binders: normally ageing results in a shift towards a higher molecular weight. Thus, oxidative aging causes formation of more polar molecules at the expense of the lower weight molecules. This is a complex phenomenon in the binder-filler interaction in BSMs and needs to be identified and analysed critically.

The complex nature of the extraction and recovery of binder from BSMs, and the complex nature of the reactivity of the binder with mineral aggregates, might require a shift in the focus on the study of the influence of binder ageing in the mix matrix. In this regard, understanding the mastic behaviour due to changes in adhesion and cohesion with large particles will give a better understanding of binder behaviour rather than studying binder in isolation from the filler and active filler.

REFERENCES

- Loudon International. 2008. Failure mechanism of in situ recycling with foamed bitumen stabilisation. Technical report on the investigated of distress on Shedgum Road in Saudi Arabia.
- Domke C.H, Davison R.R. and Glover C.J. (1999). Effect of oxidation pressure on asphalt hardening susceptibility. TRB. Issue no. 1661. Pg 114-121.
- Hagos E.T. 2008. The effect of ageing on binder properties of porous asphalt concrete. PhD. Dissertation published at the Technical University of Delft. The Netherlands.
- Heukelom W. 1973. An Improved Method of Characterising Asphaltic Bitumen with Aid of their Mechanical Properties. Proceeding of Association of Asphalt Paving Technologist. Vol. 42, pg 67-84.
- Jenkins K. J. 2000. Mix Design Considerations for Cold and Half-warm Bituminous Mixes with Emphasis on Foamed Bitumen. PhD Dissertation, University of Stellenbosch, South Africa.
- Kelfkens R.W.C. 2008. Vibratory hemmer compactor of bitumen stabilised materials. MSc Thesis. University of Stellenbosch. South Africa.
- Loizos A and Papavasiliou V. 2007. Evaluation of foamed asphalt cold in-place pavement recycling using nondestructive technique. Journal of transport engineering (ASCE), 132(12) pg 970-978.
- Malubila S.M. 2005. Curing of foamed bitumen mixes. Masters thesis. University of Stellenbosch. South Africa.
- Mgangira, M.M 2008. Microstructural pavement material characterisation: some examples. Proceeding of the 27th Southern African transport conference, Pretoria.
- Mgangira M. 2007. Use of scanning electron microscope in the road materials characterisation. CSIR BE report CSIR/BE/IE/2007/024/B. Pretoria South Africa.
- Mgangira M.B and Paige-Green. P. 2006. Scanning electron microscopy (SEM) internal technical report no. CSIR/BE/IE/IR/2006/0017/B. CSIR. Pretoria South Africa.
- Shell Bitumen. 2003. Shell Bitumen Handbook. Shell bitumen UK .
- Steyn W.J.vdM. 2006. Observation technique for pavement infrastructure. PG report CSIR/BE/IE/IR/2006/0007/B. Pretoria. South Africa.
- Asphalt Academy. 2009. Bitumen stabilisation materials. A guideline for the design and construction of bitumen and foamed bitumen stabilised materials. TG2. Technical guideline. Pretoria. South Africa.
- Twagira M.E. 2006. Characterisation of fatigue performance of selected cold bituminous mixes. MSc. Thesis. University of Stellenbosch, South Africa.
- Weinert H.H. 1980. The natural road construction materials of Southern Africa. Academia. Cape Town
- Wirtgen .2004. Wirtgen cold recycling manual.Wirtgen GmbH. Germany.

CHAPTER 8

CONCLUSIONS AND RECOMMENDATIONS

The findings in this research have highlighted advances in the BSM mix design process by enabling the assessment of selected materials, based on their influence on durability behaviour and long-term performance. An important part of the scope of this research included a comprehensive literature review to understand the fundamental characterisation of bitumen and mineral aggregate interactions. To portray this understanding in a broader perspective, comprehensive laboratory testing was conducted for various BSMs. The quantification thereof in terms of moisture damage was developed and determined. In addition, age hardening behaviour was investigated and quantified through different test methods.

This chapter summarises the major findings on the fundamentals and mechanical characterisation of BSMs based on the influence on durability properties. Where applicable, recommendations for future research are provided.

8.1 MINERAL AGGREGATES DURABILITY

In the literature review on BSM material characteristics and investigation, this study reveals the need for research into the fundamentals of adhesion between mineral aggregates and binder. Theory of adhesion has significance influence in understanding the trends of long-term performance and durability properties of BSMs. The findings on the fundamental durability behaviour of mineral aggregates in BSMs are outlined as follows:

- o Weak bonding theory shows that the structure of mineral aggregates is important in surface characteristics and their potential interaction with adjacent phases such as binder and water. Studies on adsorption/desorption confirm that adhesion in the bitumen-mineral aggregate system cannot be adequately addressed without special assessment of the bonds in dry and wet states. The review indicates that physicochemical and mechanical properties dominate the bitumen-mineral aggregate adhesive bond strength.
- o Depending on the nature of the rock type (silicates or carbonates), bond formation and strengthening can be determined through thermodynamic, hydrodynamic and electrokinetic theories. Orientation of polar molecules at the interface occurs as part of the minimisation of surface free energy and consequently an intimate contact is achieved between binder and mineral aggregates.
- o In the pavement layer, aggregates age as the layer is exposed to the cycles of varying temperature, humidity, wind and dynamic loading. Therefore, during in-service period, their physicochemical properties might change. The rate of weathering depends on the stage of weathering of the rock at the time the material was removed from its source, and the length of time it has been in a pavement layer. To assess durability of these materials is therefore important prior to recycling them in BSMs. This study used a DMI device to test the durability of typical materials for BSM mix design. The tested materials were distinguishable in terms of disintegration and decomposition. This indicates that a DMI device can be applied for assessing mineral aggregate durability for BSM mix design.
- o The quantification of mechanical properties of mineral aggregates in BSMs is important. However, it does not satisfy the explanation of the fundamentals of physicochemical

properties of adhesion between binder and mineral aggregates. It is apparent that this phenomenon requires assessment with more fundamental testing at a microstructure level.

8.3 MOISTURE DAMAGE MECHANISM

- o The fundamentals of adhesion were applied to understanding the binder-mineral aggregate interaction and moisture damage mechanism in the context of BSMs. This was done by taking cognisance of specific aspects peculiar to BSM mixes, such as aqueous phase, colloidal nature of the binder, grading of aggregates and type, addition of active filler and bond development as a result of the curing process. The theories of thermodynamics, hydrodynamics and electrokinetics were then used to describe the steps governing the process and formulation of adhesive bonding and cohesion in BSMs. It was evident from the formulation that the main factors contributing to bond formation and strengthening are temperature and moisture evaporation. These parameters play a key role in the intimate contact of the binder and mineral aggregates, which result in full strength development in the BSM mix matrix.
- o Using the governing process on bond formation described in this study, it is possible to define the mechanisms influencing moisture damage. Proper understanding of bond formation in BSMs is a tool for effective and appropriate selection, combination and formulation of available materials for BSM mix design.
- o The mechanisms of moisture damage in BSMs have mainly been related to excess moisture in the mix matrices and dynamic applied loading. In this study, the main components of moisture damage mechanisms identified are: 1) change in internal condition due to moisture transport mechanisms; and 2) the response of the materials and loss of integrity due to deterioration of the cohesive and adhesive bonding. The reason for deterioration is associated with void properties (pore pressure), aggregate characteristics and change in moisture state (i.e. degree of saturation and mastic diffusion). The quantification of voids in the mixes cannot fully describe the performance of BSMs in terms of moisture damage mechanisms. However, understanding of void structure and distribution (i.e. size, connectivity and isolation) is important in explaining their relationship to the mode of moisture transport and damaging mechanisms.

8.4 CHARACTERISATION OF MOISTURE DAMAGE

- o The current approach for moisture damage simulation and thereafter quantification of mechanical performance does not simulate the field moisture infiltration condition and resulting performance behaviour peculiar to BSMs. In this study, the shortfalls of the current procedure were identified and fundamental factors influencing moisture damage in BSMs were reviewed. A new conditioning protocol using the MIST device was developed. Based on the findings of this study, the new MIST device has demonstrated the following:
 - It can be used to condition BSMs and screen mixes that are moisture susceptible and those that are resistant to moisture damage.
 - Established protocol that can be utilised by practitioners for the selection of mix composition in terms of moisture damage durability during mix design.
 - It is simple to use (repeatable and reproducible), cheap and it simulates pulsing of water pressure similar to field conditions.
 - The ratio of the performance parameters from the MIST conditioning and static triaxial test correspond well with ravelling behaviour observed during the MMLS3 wet trafficking test.

- The ranking and evaluation of BSM mixes based on retained cohesion (RC) shows good agreement with the ranking of similar BSM mixes using MMLS3 wet trafficking and ravelling behaviour.
- The influence of the addition of active filler on cohesion and adhesion in BSMs is apparent. Cement or lime plays a significant role in the early stiffening of the mastic and bond formation. This is beneficial for early trafficking of the layer for BSM mixes with less moisture content such as BSM-foam. In microstructure analysis, addition of active filler has shown the following influences: 1) accelerates hydration of water entrapped in the mastic and reduces moisture diffusion in and out of the mastic; 2) bond formation between binder and mineral aggregate interface; and 3) adhesion and cohesion of the mix matrices, resulting in high resistance to moisture damage and long-term durability behaviour. It was apparent from the benefits that the addition of 1% cement is sufficient to produce durable and long-term performing BSMs. On the contrary, application of 1% lime did not provide a similar benefit to cement. Therefore, determination of initial consumption of lime (ICL) is important prior to application of lime during bituminous stabilisation.
- The study of moisture damage characterisation presented in this study indicated that materials stabilised with bitumen emulsion with added active filler (1% cement), both Hornfels-RAP and Quartzite crushed stone, are less susceptible to moisture damage compared to similar materials stabilised with foamed bitumen. Nevertheless, mixes stabilised with foamed bitumen show higher maximum stress at failure compared to bitumen emulsion. The comparison is made for maximum shear and normal stress of both Hornfels-RAP and Quartzite materials. The higher stress at failure for the foamed bitumen under dry or saturated conditions shows that foamed bitumen mixes exhibit higher plasticstrain (elastoviscoplastic) behaviour, compared to the lower plasticstrain (elastoplastic) behaviour of bitumen emulsion.

8.5 AGEING BEHAVIOUR OF BSMs

The study of the short- and long-term age hardening of BSMs and their fundamental characteristics draws the following findings:

- The time bitumen is kept in circulation in the laboratory plant at elevated temperatures before production of BSM foam contributes to the ageing of the binder, especially after eight hours. The effects of ageing are more notable for softer bitumen (80/100) than hard bitumen (60/70), with a 30% drop of penetration for the former, compared to a drop of 12–17% in the latter. However, in both types of bitumen, the short-term ageing of foamed bitumen follows the trend of ageing of the base bitumen. Nonetheless, the foaming process in itself does not alter the bitumen rheological properties. Therefore, a temperature range of 160°C–165°C is appropriate for the production of foamed bitumen with softer bitumen while maintaining its quality. On the other hand, the time of circulation prior to production of foamed bitumen should not exceed three hours. The ageing effect of bitumen emulsion in the short term was not observed during production and mixing.
- The governing process and bond formation in BSMs presented in this study reiterate that physicochemical and mechanical interaction of binder with the mineral aggregates plays a significant role in the age hardening behaviour of BSMs. It is evident from the interaction of the filler and colloidal characteristics of the binder (foam and emulsion) that, depending on the filler to binder ratio in the mix, the filler-mastic has the effect of minimising temperature sensitivity of the mix. The benefit of this characteristic is to resist softening at relatively moderate temperatures in the pavement layer, which in turn minimises the oxidation reaction. However, depending on the physicochemical nature of

- the rock type or binder content in the mix (higher binder content), the mix can be temperature sensitive. This sensitivity can favour the exposed thin film binder to oxidise in the presence of high air content and moderate temperatures found in the pavement layer (i.e. 40°C–47°C).
- o The laboratory study on age hardening indicated that age hardening of foamed bitumen and bitumen emulsion during in-service life occurred. The ageing BSMs were found to be dependent on the effect of traffic. Ageing occurs differently in trafficked versus untrafficked locations in the pavement. Trafficked locations (OWP and IWP) have higher ageing influences than untrafficked locations (YL and BWP). This tendency is not expected because air void content of the layer is the major factor for oxidative ageing. It is expected that untrafficked locations will have higher void contents than trafficked locations, hence, higher ageing potential. However, this was not observed in the studied BSMs. Instead, the study shows no direct correlation between ageing and air voids. This implies that the air void distribution in BSMs is characterised by structures that are isolated, which results in inconsistency in the influence on oxidation.
 - o Extreme values were measured during the penetration test (i.e. very low, 2dmm to 5dmm, and very high, above 100dmm) and also an increase in viscosity at 60°C that leads to no flow of the recovery of bitumen from BSMs. These values make the whole process inconclusive in defining the age hardening behaviour of BSM mixes. However, this behaviour was related to the binder-mineral aggregate interaction discussed in this study, and the entire extraction and recovery process. It was evident for the measured values that extraction and recovery of binder from foamed bitumen and bitumen emulsion is a challenging and complex process. The conventional method of extraction and recovery of bitumen applied for HMA is uncertain for extracting and recovering all bitumen fractions from BSM mixes.
 - o BSM mixes with realistic values obtained from age hardening characteristics were compared in terms of the engineering properties investigated in this study. The engineering properties such as void percentage, rutting and ravelling were compared with age hardening behaviour (reduction in pen value). It was evident from these relationships that, although binder undergoes age hardening, its contribution to the failure mechanism or impact on the engineering properties is difficult to quantify.

8.6 CLIMATE AND ENGINEERING PROPERTIES

- o The recently released BSMs guideline TG2 (2009) categorically indicated that stabilisation (laboratory or in-situ recycling) using BSM-foam or BSM-emulsion should not be done with aggregates having a lower temperature than 10°C. It is evident from this study that binder distribution and coating of mineral aggregates is significantly influenced by aggregate temperature. The ultimate development of strength in a BSM layer is related to evaporation (full curing). However, the strength in early or intermediate cure represents the most critical time period during the service life of BSMs. Emphasis should therefore be placed on the prediction of the field temperature variation and its influence on the curing (evaporation) period when adjudicating mix selection. The availability of a model predicting temperature distribution and evaporation in a layer would enhance accurately the three phases of BSM application (i.e. mix design, construction and in-service life) under local environmental conditions (i.e. temperature, wind, relative humidity and rainfall).
- o The developed protocol for the moisture susceptibility of BSMs defined the classification of mixes based on resistance and susceptibility to moisture damage. These classifications can be appropriately linked to the climatic region for better selection and application of BSMs. Regions characterised with a high period of precipitation should

select mixes which are highly resistant to moisture damage ($RC > 75\%$), whereas regions with moderate to lower periods of precipitation can make use of mixes with $RC \geq 60\%$ and regions with lower or very little precipitation (arid or semi-arid climate) can use mixes with $RC \geq 50\%$.

8.7 RECOMMENDATIONS FOR FURTHER STUDY

- o A larger percentage of recycled materials in BSMs constitutes aggregates which have been exposed to the cycles of varying temperature, humidity, wind and dynamic loading. This might result in a change in physicochemical properties, influencing the performance of the stabilised materials. The tests on mineral aggregate durability (i.e. Hornfels-RAP, Ferricretes and Quartzite) carried out in this study have shown that DMI has potential to be used for screening mineral aggregates in terms of durability. However, the current DMI limits designated for natural granular materials cannot be directly applied to BSMs. It is therefore recommended that further research be carried out on a wide range of mix matrices commonly used for BSM recycling to provide reliable and applicable DMI limits for BSM mix design.
- o The quantification of mechanical properties of BSMs has been widely used to determine durability and long-term performance. The fact that BSMs have been successfully applied in a wide range of mineral aggregates with significant differences in physicochemical and mechanical properties, means that mechanical performance alone cannot stand to prove durability behaviour of BSMs. In this light, analysis of the physicochemical behaviour of binder and mineral aggregates in BSMs is vital. The understanding of this behaviour will provide confidence in determining the failure mechanisms and the ability to characterise the durability properties with a higher percentage of certainty during all phases of application of BSMs, that is mix design, construction and in-service condition.
- o In conjunction with research on physicochemical properties, the assessment of adhesion behaviour between the binder (foam or emulsion) and mineral aggregate surface using contact angle approach (wettability), force microscopy PATTI device and SEM device might provide an insight into BSM durability behaviour at microstructure levels.
- o The findings on age hardening provided in this study indicate that BSM-foam and BSM-emulsion can undergo age hardening after a long time during in-service life. However, quantification of this behaviour using the conventional methods of extraction (cold centrifuge) and recovery (Absorb or rotary vapour) applied to HMA raises concerns on their viability for BSMs. The complex recovery of all bitumen components, particularly asphaltenes and resins aromatic which are adsorbed into filler particles, and their separation from mineral aggregates need further research. In addition, it is recommended that, in any recovery of binder from BSMs, the compositional change and any trace of filler or super filler needs to be identified prior to rheological testing. The use of Gel Permeation Chromatography (GPC), Gaestel Index (IC) and/or FTIR offers appropriate methods of identify ageing in BSMs.
- o The complex nature of the extraction and recovery of binder from BSMs, and the complex nature of the reactivity of the binder with mineral aggregates, require a shift in focus in the study of the influence of binder ageing in the mix matrix. In this regard, it is recommended that the mastic behaviour due to changes in adhesion and cohesion with large particles needs further research to allow for an understanding of the binder behaviour rather than studying binder in isolation from the filler and active filler.
- o Currently, the field-curing techniques for BSMs are subjective, without any appropriate guideline. The model developed by Burger and Kröger (2005) is considered useful as a

curing technique in the BSMs. The model takes into account the curing factors related to local environmental conditions. These factors can be used to predict accurately the heat transfer in a BSM layer and related moisture evaporation. In addition, the temperature data presented in this study indicated that BSM layers experience significant temperature variation in different seasons from winter to summer (i.e. extremes of 9.6°C and 49.6°C). Temperature and RH variation influence full strength bonding, equilibrium moisture content, age hardening potential, physicochemical and mechanical properties in BSMs. It is apparent from temperature and RH distribution that the proposed models (evaporation and heat transfer coefficient) need further research into their applicability to BSM layers. However, heat transfer and thermal conductivity of BSMs is a multi-disciplinary topic, therefore input of specialised experts is required.

APPENDIX A

NEW MOISTURE CONDITIONING PROCEDURE FOR BITUMEN STABILISED MATERIALS (BSMs), USING MIST DEVICE

1. BACKGROUND

The study for investigating the moisture related damage of BSMs, highlighted the needs for the development of the laboratory-based moisture conditioning method. The aim was to accelerate the ingress of moisture into the mix, then evaluation of mechanical properties such as stiffness (M_r), and shear parameters (C & ϕ). The test method developed in this study has been adopted as part of draft TG2 (Asphalt Academy, 2009), applicable in South Africa for mix and pavement design guidelines aimed at distinguishing between different levels of resistance to moisture damage for BSMs.

2. SCOPE

This method covers the procedure for determining the moisture-related damage on cured or cored triaxial test specimens made of BSMs. The method employs cyclic pulsing of water pressure into a specimen to simulate moisture induction of the dynamic loading in the field condition.

3 APPARATUS

- 3.1 MIST device indicated in Figure 62 Chapter 3, consists of; 20 litres pressure tank, water pump, ON-OFF timer ranging from 0-60 seconds, Pressure regulator and pressure gauge, ON-OFF solenoid valves set by the timer, and hose pipe.
- 3.2 Three phase electrical supply for the water pump
- 3.3 Triaxial cell, capable to accommodate specimen of 300mm high and 150mm diameter, and top access to water pressure connection
- 3.4 Cylindrical container, (150mm diameter and 300mm high) with bottom outlet to drain water outflow
- 3.5 Water bath to accommodate overflow from triaxial cell
- 3.6 Steady water supply connected to the 20-litre pressure tank
- 3.7 A balance to weigh up to 15 Kg with accuracy of 0.5g
- 3.8 A drying oven capable of maintaining the temperature of $110^{\circ}\text{C} \pm 5^{\circ}\text{C}$

4.0 METHODS

4.1 Preparation of specimens

Prepare specimens in accordance with the procedure described in the Appendix to BOSCH® compaction procedure, in the TG2 (Asphalt Academy, 2009). Enough material should be mixed to produce at least twelve specimens on recommended binder.

4.2 Curing of Specimens

Cure the specimens in accordance with the procedure described in the TG 2 (Asphalt Academy, 2009)

4.3 Evaluation and grouping of specimens

After curing, remove the wet bag and let the specimens cool at ambient temperature (25°C) for about one hour. Cover the specimens immediately if delay occurs for conditioning.

After cooling, the following physical tests and measurements of each specimen must be carried-out:

- The average height (h) and average diameter (d)
 - Rice's density (G_{mm}) in accordance with THM1 Method C4
 - Bulk relative density (G_{mb}) in accordance with THM1 Method C3
 - The specimen volume (E) as a difference in specimen weighed in water and specimen saturated surface-dry weight.
 - Percentage air void (P_a) in accordance with THM1 Method C3.
- 4.3.1 Group the specimens into a set of two, with approximately equal void content (P_a). Separate these sets with six (6) specimens for wet conditioning and static (monotonic) test, and other six (6) for un-conditioning or dry static (monotonic) test.

5. CONDITIONING OF SPECIMENS

- 5.1 Setup the test variables on MIST device i.e. ON-OFF timer at 0.54sec load time, and 1.40sec rest period, and regulate pressure gauge so that 140kPa cyclic pulsing water pressure is achieved in the cell (i.e. cell pressured should be adjusted slightly higher by ± 30 kPa to accommodate for the water momentum).
- 5.2 Place specimen in a triaxial cell base and assemble the cell firmly. Then connect the top of the cell to the water pressure outlet, see Figure 62.
- 5.3 Start the MIST device and count 100 cycles, or time the haversine cyclic pulsing for 3.2 minutes then stop.
- 5.4 De-assemble the triaxial cell, and remove the specimen carefully. Take weight of saturated surface-dry specimen and transfer the specimen to the triaxial static (monotonic) test setup.

6. CALCULATION

Volume of air voids (V_a) in specimen [cm^3], $V_a = \frac{P_a \times E}{100}$

Volume of water absorbed (V_w) in specimen [cm^3], $V_w = B - A$

Degree of saturation (S_r) in specimen [%], $S_r = \frac{V_w}{V_a} \times 100$

Where:

B = Weight of saturated-surface dry specimen [g]

A = weight of dry specimen in air [g]

P_a = air void content in specimen [%]

E = volume of specimen [cm^3]

- 6.1 The degree of saturation should be at least 80% for accurate screening of the BSMs.
- 6.2 Determination of retained cohesion ratio
- 6.2.1 After conditioning, place the specimen into the simple triaxial device setup. Triaxial test is performed in accordance with the procedure described in the Chapter 5.
- 6.2.2 Two sets of six (6) specimens with predetermined height and an approximately equal void content, after conditioning are tested for static (monotonic) test at 50kPa, 100kPa, and 200kPa. Another two sets of six (6) specimens are tested unconditioned at 50kPa, 100kPa, and 200kPa, with displacement controlled rate of loading at 5.25mm/minutes (or strain rate of 2.1%mm/minute).
- 6.2.3 Shear properties (C and ϕ) of the conditioned and unconditioned sets of specimens are determined in accordance with the procedure described in Chapter 5..

Retained cohesion ratio is calculated as follows:

$$\text{Retained cohesion, (RC)} = \frac{\text{Cohesion of wet mix, (CoW)}}{\text{Cohesion of dry mix, (CoD)}} \times 100$$

where, cohesion of wet and dry mix calculated from Mohr-Coulomb cycle as per Equation.

$$\sigma_{1,f} = \frac{1 + \sin \phi}{1 - \sin \phi} \sigma_3 + \frac{2.C.\cos \phi}{1 - \sin \phi}$$

where,

- σ_{1f} = Maximum principal stress at failure [kPa]
- σ_3 = confining pressure [kPa]
- ϕ = internal angle of friction of the mix [deg]
- C = cohesion of the mix [kPa]

7 REFERENCES

- 7.1 MIST device features, setup, and connections (Chapter 3)
- 7.2 Bosch® vibratory compaction procedure (TG2, Asphalt Academy, 2009)
- 7.3 Appendix to Curing of BSMs procedure (TG2, Asphalt Academy, 2009)
- 7.4 Appendix to Simple triaxial testing procedure (TG2, Asphalt Academy, 2009)
- 7.5 THM1 Method C3, and C4 (CSIR, 1985)

APPENDIX B

MONOTONIC TRIAXIAL RESULTS FOR DRY AND MOISTURE CONDITIONED SPECIMENS USING MIST DEVICE

I: BSM-EMULSION

Table 51: Shear properties of BSM-emulsion at dry and wet (conditioned) state, tested at 25°C.

WET-MIST AND MONOTONIC					DRY-MONOTONIC TEST					Retained Cohesion
Specimen Type	σ_3 [kPa]	Fmax [kN]	C [kPa]	ϕ [deg]	Specimen Type	σ_3 [kPa]	Fmax [Kn]	C [kPa]	ϕ [deg]	RC [%]
Q0CE02	50	9.8			Q0CE07	50	15.7			
Q0CE04	100	13.4			Q0CE03	100	20.8			
Q0CE09	200	22.0	66	44	Q0CE08	200	29.3	132	46	50
H0CE07	50	8.5			H0CE02	50	17.1			
H0CE01	100	11.4			H0CE03	100	20.2			
H0CE09	200	17.4	77	38	H0CE04	200	27	175	41	44
Q1CE08	50	19.5			Q1CE08	50	22.8			
Q1CE01	100	24.2			Q1CE03	100	26.0			
Q1CE07	200	30.0	213	41	Q1CE06	200	32.3	260	40	82
H1CE07	50	19.4			H1CE01	50	24.3			
H1CE10	100	21.3			H1CE08	100	27.5			
H1CE05	200	24.8	287	30	H1CE09	200	30.1	370.0	31	78
Q1LE04	50	11.9			Q1LE07	50	12.9			
Q1LE09	100	15.7			Q1LE06	100	16.5			
Q1LE03	200	20.5	133	38	Q1LE05	200	26.7	179	40	74
H1LE07	50	14.0			H1LE01	50	19.7			
H1LE02	100	17.4			H1LE03	100	21.3			
H1LE04	200	24.5	133	42	H1LE05	200	24.8	192	44	69
S2CE19	50	14.2			S2CE26B	50	20.7			
S2CE20	100	25.6			S2CE28	100	28.3			
S2CE21	200	35.7	87	53	S2CE25B	200	45.3	108.0	55	81

II: BSM-Foam

Table 52: Shear properties of BSM-emulsion at dry and wet (conditioned) state, tested at 25°C.
WET-MIST AND MONOTONIC DRY-MONOTONIC TEST Retained Cohesion

Specimen Type	σ_3 [mm]	Fmax [kN]	C [kPa]	ϕ [deg]	Specimen Type	σ_3 [kPa]	Fmax [kN]	C [kPa]	ϕ [deg]	RC [%]
Q0CF08	50	10.5			Q0CF04	50	20.3			
Q0CF01	100	18.9			Q0CF06	100	27.8			
Q0CF07	200	30.0	49	52	Q0CF08	200	38.0	158	50	31
H0CF06	50	6.8			H0CF02	50	13.2			
H0CF09	100	10.5			H0CF05	100	16.9			
H0CF07	200	18.5	34	44	H0CF08	200	24.6	116	43	29
Q1CF06	50	26.8			Q1CF07	50	36			
Q1CF05	100	37.2			Q1CF02	100	43.6			
Q1CF01	200	49.1	196	53	Q1CF04	200	55.5	297.0	52	66
H1CF06	50	17.1			H1CF07	50	24.4			
H1CF05	100	19.8			H1CF02	100	28.8			
H1CF01	200	39.0	150	44	H1CF04	200	38.4	221.0	47	68
Q1LF06	50	18.9			Q1LF03	50	23.6			
Q1LF01	100	25.2			Q1LF05	100	33.5			
Q1LF07	200	39.5	112	53	Q1LF02	200	43.1	187.0	51	60
H1LF06	50	10.4			H1LF07	50	16.7			
H1LF09	100	15.4			H1LF02	100	20.8			
H1LF01	200	23.4	74	45	H1LF04	200	29.5	145	45	51
F2CF16	50	18.2			F2CF13	50	22.9			
F2CF17	100	33.6			F2CF14	100	51.9			
F2CF18	200	26.47	100	57	F2CF15	200	64.53	120.0	61	83

APPENDIX C

TRIAXIAL RESILIENT MODULUS RESULTS FOR DRY AND MOISTURE CONDITIONED SPECIMENS USING MIST DEVICE

Table 53: Resilient modulus of BSM-emulsion and BSM-foam at dry and wet (conditioned) state, tested at a confinement of 50kPa and SR of 10% at 25°C.

Mix type	DRY STATE RESILIENT MODULUS		WET STATE RESILIENT MODULUS		
	Specimen type	Equilibrium	S _r =50%	S _r =80%	S _r =100%
			Mr [MPa]		
BSM-emulsion	Q0CE	430	380	330	230
	H0CE	520	440	390	300
	Q1CE	1340	1200	1090	1020
	H1CE	1450	1340	1210	1100
	Q1LE	740	870	840	520
	H1LE	680	600	580	550
BSM-foam	Q0CF	680	660	560	340
	H0CF	880	660	560	400
	Q1CF	920	670	670	620
	H1CF	1160	1160	1000	720
	Q1LF	830	710	720	710
	H1LF	680	750	1060	520

APPENDIX D

RAVELLING RESULTS AFTER MMLS3 WET TRAFFICKING

1: Mix type = H1CE vs. H1LE

Table 54: Number of load application and ravelling depth after wet MMLS3 trafficking at 25°C on H1CE and H1LE trafficked together.

Wet test	BSM-emulsion	No. OF LOAD APPLICATIONS							
		0	200	3000	7000	15000	25000	40000	45000
Specimen Location	Specimen Type	RUTTING-DEPTH (mm)							
0100	H1CE02		0.75	0.69	0.22	0.13	0.11	0.12	1.27
0200	H1CE03		0.65	0.85	0.79	1.03	1.15	1.06	1.22
0300	H1CE06		0.40	0.43	0.30	0.18	-0.01	0.07	0.15
	AVERAGE	0	0.60	0.66	0.44	0.44	0.42	0.42	0.88
	STD		0.18	0.22	0.31	0.50	0.64	0.56	0.63
	COV		0.30	0.33	0.71	1.14	1.52	1.34	0.72
0400	H1LE08		0.25	0.09	0.07	-0.08	0.77	3.28	7.07
0500	H1LE05		0.92	0.64	0.61	0.88	2.55	3.39	8.45
0600	H1LE03		0.63	0.66	0.62	0.68	0.58	6.28	12.87
0700	H1LE02		0.67	0.71	0.65	0.74	0.68	2.78	13.86
	AVERAGE	0	0.62	0.52	0.49	0.56	1.14	3.93	10.56
	STD		0.27	0.29	0.28	0.43	0.94	1.59	3.31
	COV		0.44	0.56	0.58	0.78	0.82	0.40	0.31

2: Mix type = Q1LE vs. Q1CE

Table 55: Number of load application and ravelling depth after wet MMLS3 trafficking at 25°C on Q1LE and Q1CE trafficked together.

Wet test	BSM-emulsion	No. OF LOAD APPLICATIONS						
Specimen Location	Specimen Type	0	1000	3000	10000	20000	30000	40000
		RUTTING-DEPTH (mm)						
0100	Q1LE01		2.19	2.17	2.18	2.25	2.29	2.31
0200	Q1LE02		1.48	1.52	1.56	1.65	1.63	1.64
0300	Q1LE03		2.33	2.13	2.10	2.07	2.18	2.15
0400	Q1LE04		1.46	1.35	1.32	1.32	1.28	1.25
	AVERAGE	0	1.86	1.79	1.79	1.82	1.85	1.84
	STD		0.46	0.42	0.42	0.42	0.47	0.49
	COV		0.25	0.23	0.23	0.23	0.26	0.26
0500	Q1CE01		0.46	0.45	0.46	0.49	0.46	0.42
0600	Q1CE03		1.31	1.34	1.35	1.41	1.36	1.37
0700	Q1CE05		1.40	1.37	1.43	1.42	1.37	1.43
	AVERAGE	0	1.05	1.06	1.08	1.11	1.06	1.07
	STD		0.52	0.52	0.54	0.53	0.52	0.57
	COV		0.49	0.49	0.50	0.48	0.49	0.53

3: Mix type = H0CE vs. Q0CE

Table 56: Number of load application and ravelling depth after wet MMLS3 trafficking at 25°C on H0CE and Q0CE trafficked together

Wet test	BSM-emulsion	No. OF LOAD APPLICATIONS			
Specimen Location	Specimen Type	0	500	1500	2500
		RUTTING-DEPTH (mm)			
0100	H0CE01		1.98	6.75	14.37
0200	H0CE06		1.02	2.97	15.12
0300	H0CE07		1.14	8.55	14.14
	AVERAGE	0	1.38	6.09	14.54
	STD		0.52	2.85	0.51
	COV		0.38	0.47	0.04
0400	Q0CE08		0.55	0.32	12.77
0500	Q0CE06		0.73	0.75	12.16
0600	Q0CE05		0.64	0.60	12.20
0700	Q0CE04		1.30	1.18	12.39
	AVERAGE	0	0.80	0.71	12.38
	STD		0.34	0.36	0.28
	COV		0.42	0.50	0.02

4: Mix type = Q0CF vs. H0CF

Table 57: Number of load application and ravelling depth after wet MMLS3 trafficking at 25°C on Q0CF and H0CF trafficked together

Wet test Specimen Location	BSM-emulsion Specimen Type	No. OF LOAD APPLICATIONS		
		0	500	1000
		RUTTING-DEPTH (mm)		
0100	Q0CF02		11.18	13.74
0200	Q0CF03		8.04	13.87
0300	Q0CF04		2.52	11.17
0400	Q0CF07		3.54	8.39
	AVERAGE	0	6.32	11.79
	STD		4.03	2.59
	COV		0.64	0.22
0500	H0CF06		5.09	13.81
0600	H0CF05		3.79	12.99
0700	H0CF01		7.44	11.89
	AVERAGE	0	5.44	12.90
	STD		1.85	0.96
	COV		0.34	0.07

5: Mix type = Q1LF vs. H1LF

Table 58: Number of load application and ravelling depth after wet MMLS3 trafficking at 25°C on Q1LF and H1LF trafficked together

Wet test Specimen Location	BSM-emulsion Specimen Type	No. OF LOAD APPLICATIONS			
		0	500	1000	2700
		RUTTING-DEPTH (mm)			
0100	Q1LF01		0.89	0.72	0.59
0200	Q1LF04		0.62	0.38	0.22
0300	Q1LF06		0.93	0.63	0.43
0400	Q1LF07		1.06	1.05	0.96
	AVERAGE	0	0.87	0.70	0.55
	STD		0.19	0.28	0.31
	COV		0.21	0.40	0.56
0500	H1LF04		0.00	0.00	0.00
0600	H1LF03		2.30	3.76	10.41
0700	H1LF02		1.80	1.99	3.07
	AVERAGE	0	1.37	1.92	4.49
	STD		1.21	1.88	5.35
	COV		0.89	0.98	1.19

6: Mix type = Q1CF vs. H1CF

Table 59: Number of load application and ravelling depth after wet MMLS3 trafficking at 25°C on Q1CF and H1CF trafficked together

Wet test	BSM-emulsion	No. OF LOAD APPLICATIONS					
		0	500	1000	2000	4000	6000
Specimen Location	Specimen Type	RUTTING-DEPTH (mm)					
0100	Q1CF01		0.49	0.15	0.22	0.29	0.34
0200	Q1CF02		0.14	0.19	0.38	0.50	0.44
0300	Q1CF03		0.29	0.23	0.25	0.57	13.53
0400	Q1CF04		0.71	0.71	0.67	0.78	5.03
	AVERAGE	0	0.41	0.32	0.38	0.53	4.84
	STD		0.25	0.26	0.21	0.20	6.19
	COV		0.61	0.82	0.54	0.38	1.28
0500	H1CF01		0.50	0.58	0.53	0.66	1.48
0600	H1CF02		0.30	0.52	0.68	1.57	5.42
0700	H1CF04		0.32	0.34	0.42	1.74	2.27
	AVERAGE	0	0.38	0.48	0.54	1.33	3.06
	STD		0.11	0.13	0.13	0.58	2.08
	COV		0.30	0.27	0.24	0.44	0.68

6: Mix type =F2CF vs. S2CE

Table 60: Number of load application and ravelling depth after wet MMLS3 trafficking at 25°C on F2CF and S2CE trafficked together

Wet test	BSM-emulsion	No. OF LOAD APPLICATIONS						
		0	500	800	1300	2000	4000	5000
Specimen Location	Specimen type	RUTTING-DEPTH (mm)						
0100	F2CF09T		0.18	0.13	0.31	0.42	0.25	0.36
0200	F2CF04		1.04	7.27	6.29	7.37	13.59	17.82
0300	F2CF09B		0.60	0.45	0.72	0.74	0.58	0.56
	AVERAGE	0	0.61	2.62	2.44	2.84	4.81	6.25
	STD		0.43	4.04	3.34	3.93	7.61	10.02
	COV		0.71	1.54	1.37	1.38	1.58	1.60
0400	S2CE27		1.03	1.05	1.14	1.10	1.25	1.22
0500	S2CE27B		0.43	0.39	0.46	0.50	0.48	0.50
0600	S2CE26		3.36	3.69	3.77	4.71	6.20	7.03
0700	S2CE25		2.05	2.35	2.62	2.83	3.94	4.58
	AVERAGE	0	1.72	1.87	2.00	2.28	2.97	3.33
	STD		1.28	1.46	1.49	1.89	2.62	3.04
	COV		0.75	0.78	0.74	0.83	0.88	0.91

APPENDIX E

SHEAR PROPERTIES RESULTS FOR THE DRY AND CONDITIONED (WET) MIXES

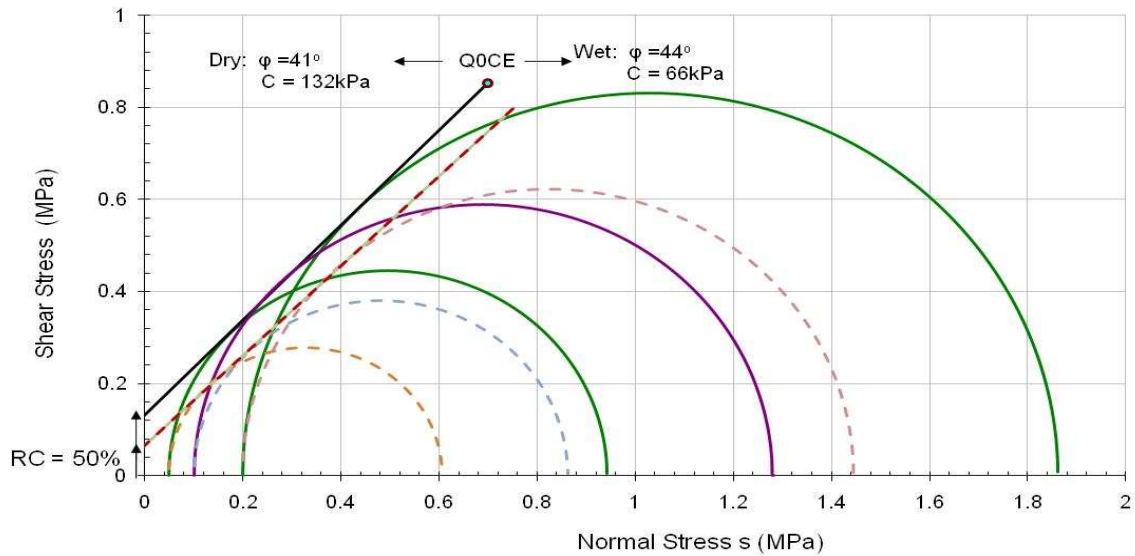


Figure 172: Effects of moisture damage on shear properties of BSM-emulsion mixes of Quartzite crushed stone without the addition of cement (Q0CE)

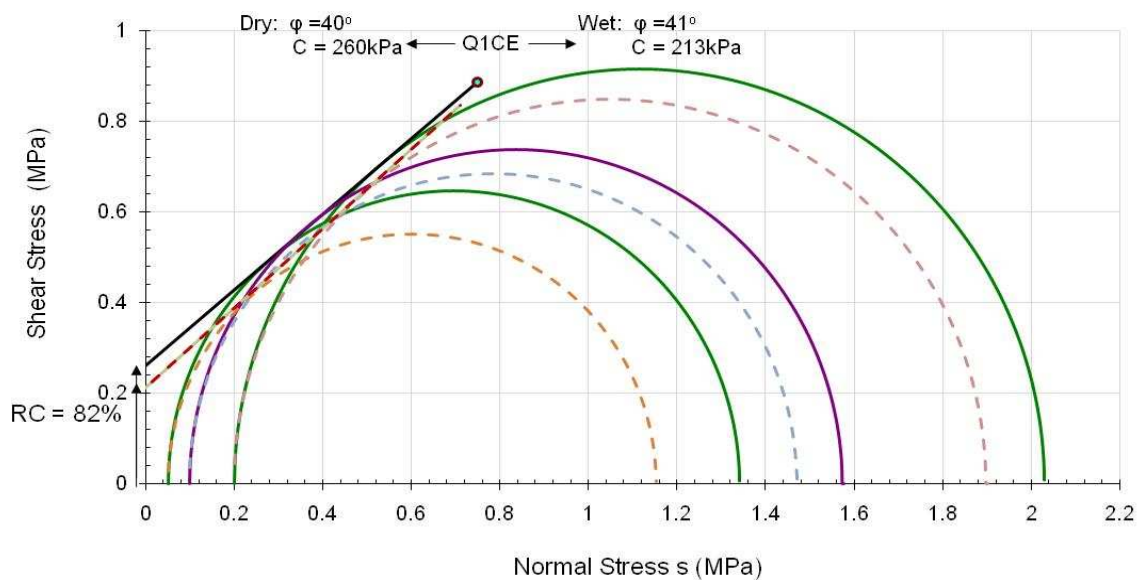


Figure 173: Effects of moisture damage on shear properties of BSM-emulsion mixes of Quartzite crushed stone with 1% cement (Q1CE)

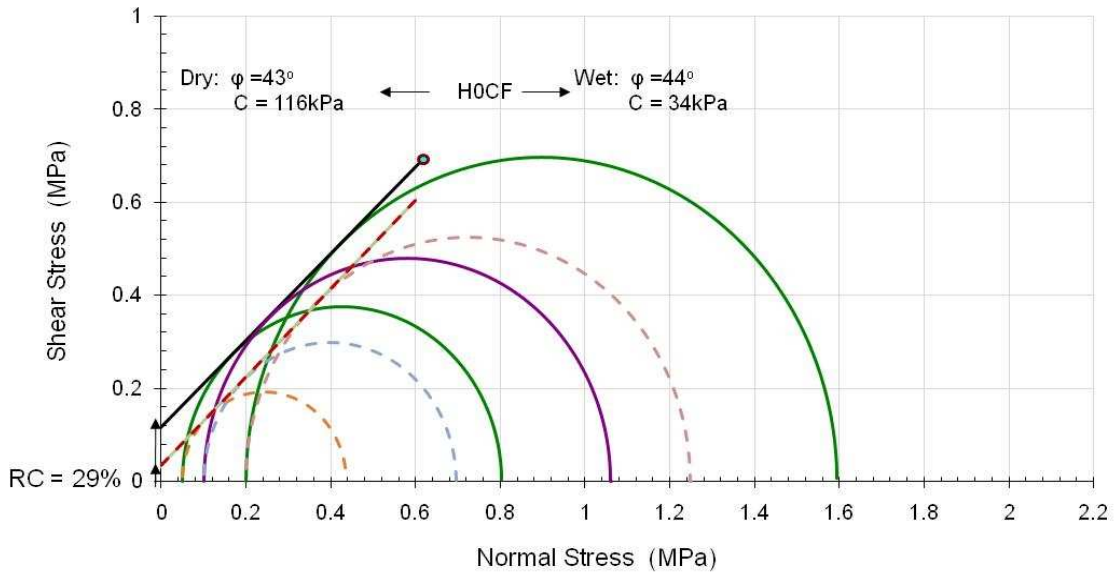


Figure 174: Effects of moisture damage on shear properties of BSM-foam mixes of Hornfels-RAP without the addition of cement (H0CF)

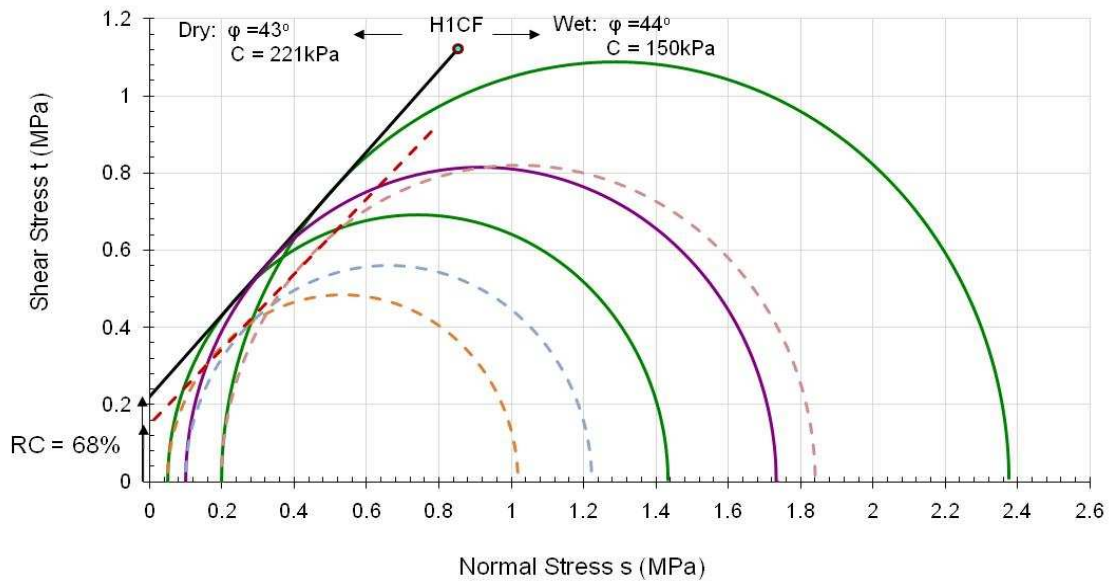


Figure 175: Effects of moisture damage on shear properties of BSM-foam mixes of Hornfels-RAP with 1% cement (H1CF)

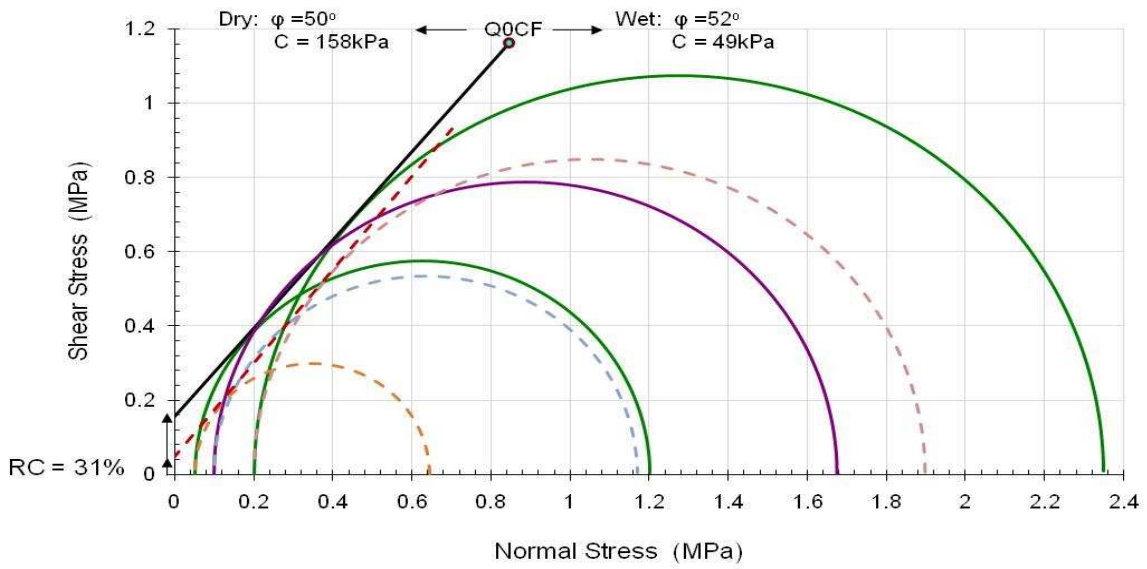


Figure 176: Effects of moisture damage on shear properties of BSM-foam mixes of Quartzites crushed stone without the addition of cement (Q0CF)

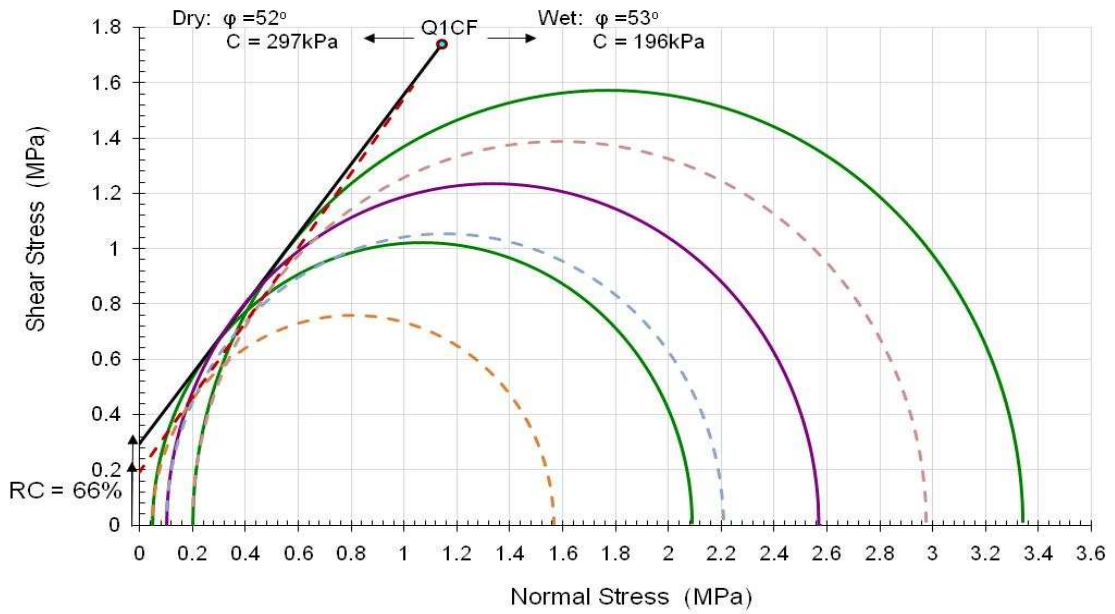


Figure 177: Effects of moisture damage on shear properties of BSM-foam mixes of Quartzite crushed stone with 1% cement (Q1CF)

APPENDIX F

TRIAXIAL PERMANENT DEFORMATION TEST RESULTS OF DRY AND CONDITIONED (WET) BSM MIXES

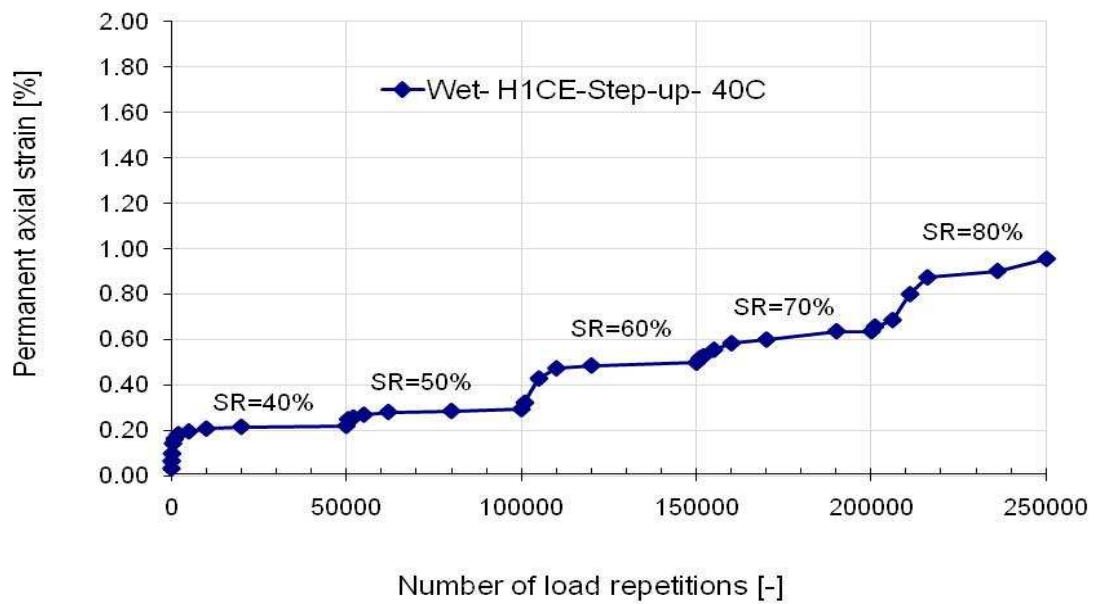


Figure 178: Multistage permanent deformation results on wet BSM-emulsion (H1CE) at 40°C and confinement of 100kPa and varying stress ratios

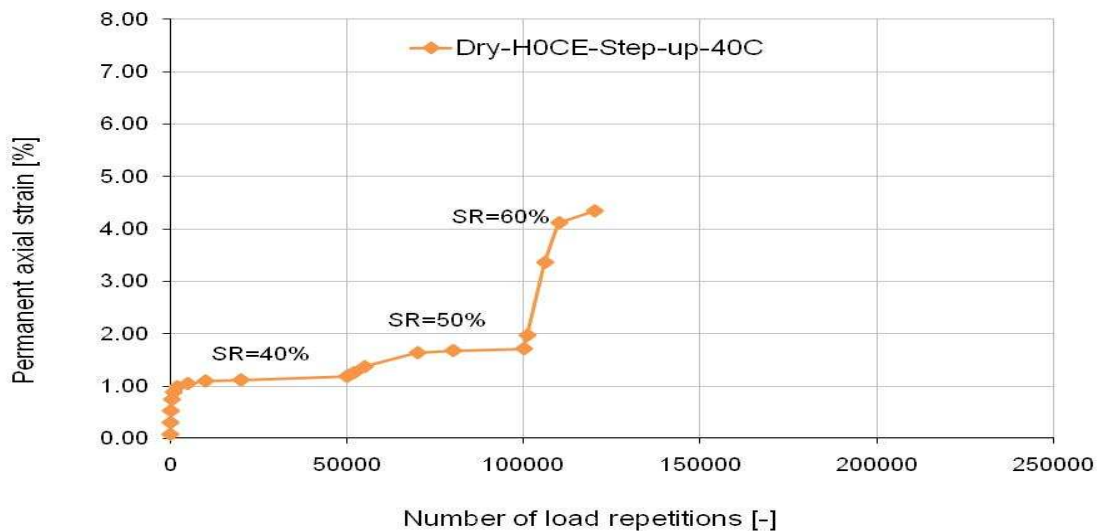


Figure 179: Multistage permanent deformation on dry BSM-emulsion (H0CE) at 40°C and confinement of 100kPa and varying stress ratios

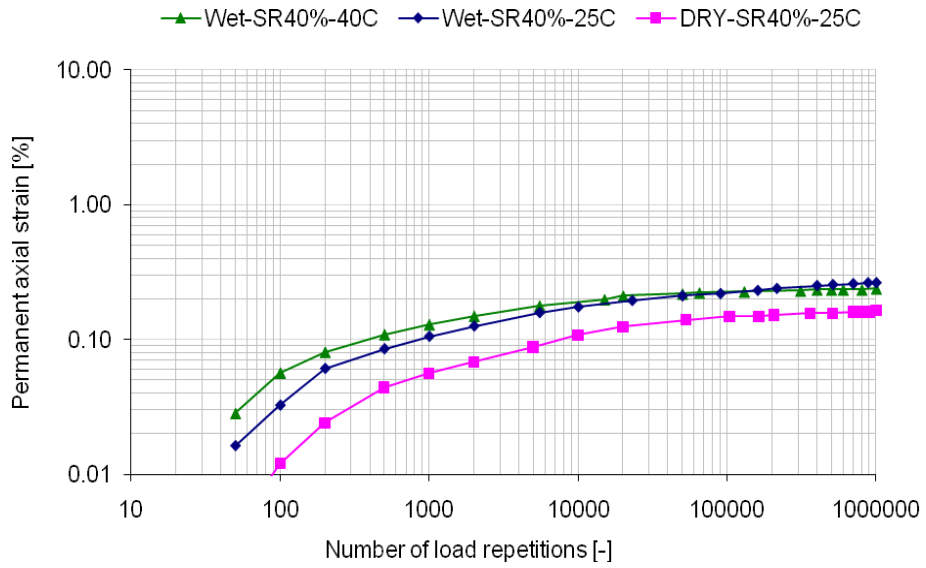


Figure 180: Permanent deformation results on wet and dry BSM-emulsion (H1CE) at 25°C and confinement of 100kPa and stress ratio of 0.4

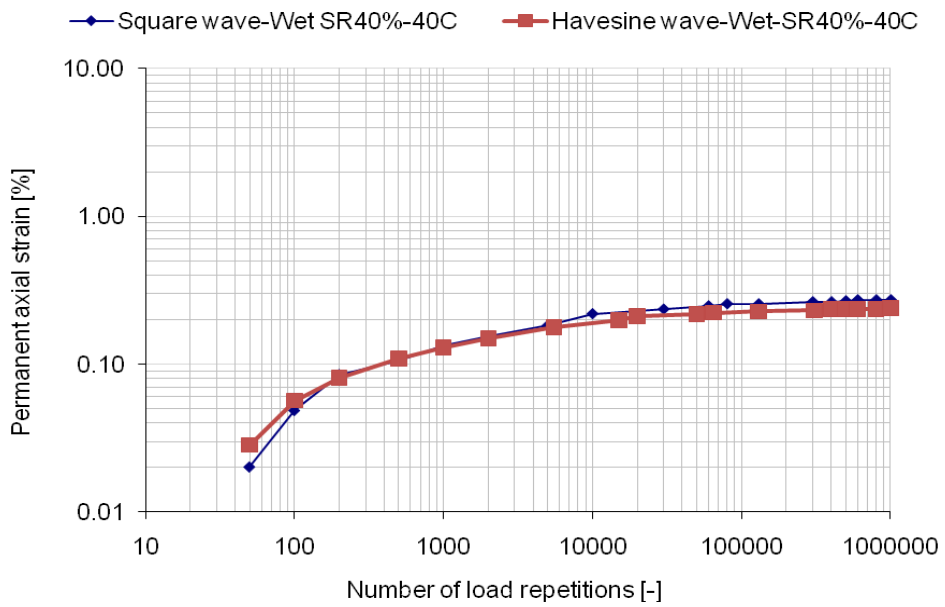


Figure 181: Comparison of square wave and haversine wave permanent deformation results on wet BSM-emulsion (H1CE) at 40°C and confinement of 100kPa and SR=0.4